Transitioning Power Distribution Grid into Nanostructured Ecosystem: Prosumer-Centric Sovereignty

Bin Mohamad Saifuddin, Muhammad Ramadan

School of Electrical & Electronic Engineering
Newcastle University, UK

A dissertation submitted to the Newcastle University for the degree of

Doctor of Philosophy
February 2021

Abstract

Growing acceptance for in-house Distributed Energy Resource (DER) installations at low-voltage level have gained much significance in recent years due to electricity market liberalisations and opportunities in reduced energy billings through personalised utilisation management for targeted business model. In consequence, modelling of passive customers' electric power system are progressively transitioned into Prosumer-based settings where presidency for Transactive Energy (TE) system framework is favoured. It amplifies Prosumers' commitments into annexing TE values during market participations and optimised energy management to earn larger rebates and incentives from TE programs. However, when dealing with mass Behind-The-Meter DER administrations, Utility foresee managerial challenges when dealing with distribution network analysis, planning, protection, and power quality security based on Prosumers' flexibility in optimising their energy needs.

This dissertation contributes prepositions into modelling Distributed Energy Resources Management System (DERMS) as an aggregator designed for Prosumer-centered cooperation, interoperating TE control and coordination as key parameters to market for both optimised energy trading and ancillary services in a Community setting. However, Prosumers are primarily driven to create a profitable business model when modelling their DERMS aggregator. Greedy-optimisation exploitations are negative concerns when decisions made resulted in detrimental-uncoordinated outcomes on Demand-Side Response (DSR) and capacity market engagements. This calls for policy decision makers to contract safe (*i.e.* cooperative yet competitive tendency) business models for Prosumers to maximise TE values while enhancing network's power quality metrics and reliability performances.

Firstly, digitalisation and nanostructuring of distribution network is suggested to identify Prosumer as a sole energy citizen while extending bilateral trading between Prosumer-to-Prosumer (PtP) with the involvements of other grid operators−TE system. Modelling of Nanogrid environment for DER integrations and establishment of local area network infrastructure for IoT security (*i.e.* personal computing solutions and data protection) are committed for communal engagements in a decentralise setting. Secondly, a multi-layered Distributed Control Framework (DCF) is proposed using Microsoft Azure cloud-edge platform that

cascades energy actors into respective layers of TE control and coordination. Furthermore, modelling of flexi-edge computing architecture is proposed, comprising of Contract-Oriented Sensor-based Application Platform (COSAP) employing Multi-Agent System (MAS) to enhance data-sharing privacy and contract coalition agreements during PtP engagements. Lastly, the Agents of MAS are programmed with cooperative yet competitive intelligences attributed to Reinforcement Learning (RL) and Neural Networks (NN) algorithms to solve multimodal socio-economical and uncertainty problems that corresponded to Prosumers' dynamic energy priorities within the TE framework. To verify the DERMS aggregator operations, three business models were proposed (*i.e.* greedy-profit margin, collegial-peak demand, reserved-standalone) to analyse comparative technical/physical and economic/social dimensions. Results showed that the proposed TE-valued DERMS aggregator provides participation versatility in the electricity market that enables competitive edginess when utilising Behind-The-Meter DERs in view of Prosumer's asset scheduling, bidding strategy, and corroborative ancillary services. Performance metrics were evaluated on both domestic and industrial NG environments against IEEE Standard 2030.7-2017 & 2030.8-2018 compliances to ensure deployment practicability.

Subsequently, proposed in-house protection system for DER installation serves as an add-on monitoring service which can be incorporated into existing Advance Distribution Management System (ADMS) for Distribution Service Operator (DSO) and field engineers use, ADMS aggregator. It provides early fault detections and isolation processes from allowing fault current to propagate upstream causing cascading power quality issues across the feeder line. In addition, ADMS aggregator also serves as islanding indicator that distinguishes Nanogrid's islanding state from unintentional or intentional operations. Therefore, a Overcurrent Current Relay (OCR) is proposed using Fuzzy Logic (FL) algorithm to detect, profile, and provide decisional isolation processes using specified OCRs. Moreover, the proposed expert knowledge in FL is programmed to detect fault crises despite insufficient fault current level contributed by DER (*i.e.* solar PV system) which conventional OCR fails to trigger.

Dedicate this thesis to my loving parents and comical siblings.

"My success is only by the will of Allah ﷿ . . . "

Declaration

I hereby declare that this dissertation has been written and composed based my own knowledge and has not been submitted anywhere else for other degree or qualification in this, or any other university. Citations and acknowledgements have been presented where transcribed statements of other author(s) were excerpted.

This dissertation contains fewer than 80,000 words inclusive of notes, footnotes, tables and equations, and has fewer than 150 figures, but excluding bibliography and appendices.

Bin Mohamad Saifuddin, Muhammad Ramadan
February 2021

Acknowledgements

Words cannot describe how much I am grateful to my parent and siblings who have prayed for my success and constantly looking out for my well-being. Humbly salute to all my supervisors, Assoc. Prof. R.T. Naayagi, Asst. Prof. T. Logenthiran, Assoc. Prof. K. Abidi , and Prof. W. Lok Woo for their contributions and guidances.

Dr. Naayagi for paving opportunities during my research years. Having me on-board as a Research Associate and working alongside with her on a Research Project Grant has moulded me to become a better researcher of tomorrow. I am blessed to have her seeing me get through the end of my PhD journey.

Dr. Logenthiran who had guided and believed in my research work. I am also thankful for giving me this rare opportunity to be part of the committee member in IEEE Power and Energy Society Singapore Chapter. I wish you success in University of Washington Tacoma, USA.

Dr. Lok Woo for his company till late evenings and initiate debatable discussions on current research trends. He has always inspire me to innovate trending solutions and I thank you for that. I wish you success in Northumbria University and congratulation in getting your Professorship.

Dr. Khalid for having me on-board as an Adjunct Lecturer with Newcastle University Singapore. Your support and confidence in me really means a lot.

Special thank goes to my classmate/buddy, Dr. Tiong Teck and Dr. L. Weixian who have invested hours of intense discussions. I thank them for their valuable feedbacks and motivations during those difficult times. Appreciations to Lee Yuzhen and LEW8 Max Tang for bringing laughter during our weekly coffee sessions.

To my beloved fiancée, Tan SzePei Torres, for her unconditionally love for me despite abandoning her on Christmas and New Year countdown celebrations, and many weekends for I was busy writing this dissertation. Am looking forward to grow old with you.

Publications, Awards, and Seminars

Dissertation Related Papers

1. B. M. S. Muhammad Ramadan, T. Logenthiran, R. T. Naayagi and W. L. Woo, "A Nano-Biased Energy Management Using Reinforced Learning Multi-Agent on Layered Coalition Model: Consumer Sovereignty," *IEEE Access*, vol. 7, pp. 52542-52564, 2019. doi: 10.1109/ACCESS.2019.2911543

2. B. M. S. Muhammad Ramadan, T. Logenthiran, R. T. Naayagi and W. L. Woo, "Apprehending Fault Crises for an Autogenous Nanogrid System: Sustainable Buildings," *IEEE Systems Journal*, vol. 13, no. 3, pp. 3254-3265, Sept. 2019. doi: 10.1109/JSYST.2018.2853078

3. W. P. Qi Tong, B. M. S. Muhammad Ramadan and T. Logenthiran, "Microgrid Management Encompassing AC & DC Renewable Generations with Energy Storages," *2018 IEEE Innovative Smart Grid Technologies - Asia (ISGT Asia)*, Singapore, 2018, pp. 1262-1267. doi: 10.1109/ISGT-Asia.2018.8467770

4. A. W. L. Lim, T. T. Teo, B. M. S. Muhammad Ramadan, T. Logenthiran and V. T. Phan, "Optimum long-term planning for microgrid," *TENCON 2017 - 2017 IEEE Region 10 Conference*, Penang, 2017, pp. 1457-1462. doi: 10.1109/TENCON.2017.8228087

5. B. M. S. Muhammad Ramadan, E. C. J. Hao, T. Logenthiran, R. T. Naayagi and W. L. Woo, "Islanding detection of distributed generation in presence of fault events," *TENCON 2017 - 2017 IEEE Region 10 Conference*, Penang, 2017, pp. 1919-1924. doi: 10.1109/TENCON.2017.8228172

6. B. M. S. Muhammad Ramadan, S. Raj, T. Logenthiran and R. T. Naayagi, "Self-healing network instigated by distributed energy resources," *2017 IEEE PES Asia-Pacific Power and Energy Engineering Conference (APPEEC)*, Bangalore, 2017, pp. 1-6. doi: 10.1109/APPEEC.2017.8308959

Other Papers

1. W. P. Qi Tong, B. M. S. Muhammad Ramadan, and R. T. Naayagi, “A Novel Self-Powered Dynamic System using Quasi-Z-Source Inverter Based Piezoelectric Vibration Energy Harvester,” *Electronics*, vol. 9, no. 2, pp. 265-285, Feb. 2020. doi: 10.3390/electronics9020265

2. B. M. S. Muhammad Ramadan, R. T. Naayagi, W. P. Qi Tong, "Design and Control of a DC Collection System for Modular-Based Direct Electromechanical Drive Turbines in High Voltage Direct Current Transmission," *Electronics*, vol. 9, no. 3, pp. 493-526, Mar. 2020. doi: 10.3390/electronics9030493

3. W. P. Q. Tong, B. M. S. Muhammad Ramadan, T. Logenthiran, R. T. Naayagi, W. L. Woo and V. Phan, "High-Performance CLL Resonant Multi-Channel LED Driver for Lighting Application," *2018 IEEE 4th Southern Power Electronics Conference (SPEC)*, Singapore, Singapore, 2018, pp. 1-6. doi: 10.1109/SPEC.2018.8635959

4. W. P. Q. Tong, B. M. S. Muhammad Ramadan and T. Logenthiran, "Design and Simulation of a Piezoelectric Cantilever Beam for Mechanical Vibration Energy Harvesting," *2018 IEEE Innovative Smart Grid Technologies - Asia (ISGT Asia)*, Singapore, 2018, pp. 1245-1250. doi: 10.1109/ISGT-Asia.2018.8467796

5. W. P. Qi Tong, B. M. S. Muhammad Ramadan and T. Logenthiran, "A Comparative Analysis between Z-Source and Quasi-Z-Source Inverters for Boost Operation," *2018 Asian Conference on Energy, Power and Transportation Electrification (ACEPT)*, Singapore, 2018, pp. 1-6. doi: 10.1109/ACEPT.2018.8610771

6. B. M. S. Muhammad Ramadan, R. T. Naayagi and Woo Li Yee, "Modelling, simulation and experimentation of grid tied inverter for wind energy conversion systems," *2017 International Conference on Green Energy and Applications (ICGEA)*, Singapore, 2017, pp. 52-56. doi: 10.1109/ICGEA.2017.7925454

7. D. L. Aparna, R. T. Naayagi and B. M. S. Muhammad Ramadan, "CFD analysis of tidal turbine blades," *TENCON 2017 - 2017 IEEE Region 10 Conference*, Penang, 2017, pp. 2708-2711. doi: 10.1109/TENCON.2017.8228321

8. B. M. S. Muhammad Ramadan, T. Logenthiran, R. T. Naayagi and C. Su, "Hybridization of Genetic Algorithm and Priority List to solve Economic Dispatch problems,"

2016 IEEE Region 10 Conference (TENCON), Singapore, 2016, pp. 1467-1470. doi: 10.1109/TENCON.2016.7848258

9. B. M. S. Muhammad Ramadan, T. Logenthiran, R. T. Naayagi and C. Su, "Accelerated Lambda Iteration Method for solving economic dispatch with transmission line losses management," *2016 IEEE Innovative Smart Grid Technologies - Asia (ISGT-Asia), Melbourne*, VIC, 2016, pp. 138-143. doi: 10.1109/ISGT-Asia.2016.7796375

Accepted Paper

1. B. M. S. Muhammad Ramadan and R. T. Naayagi, “Impedance Source Inverter Wind Turbine and DC Collection System: Fault Ride-Through Analysis,” *3rd International Conference on Energy, Power and Environment 2021*, accepted.

Symposiums & Workshops

1. One-day workshop exchange with University of Strathclyde, National University of Singapore, Newcastle University in Singapore, organized by School of Electrical and Electronic Engineering, Nanyang Technological University 2018.

2. Poster presentation, "Non-convex Economic Dispatch with Alternative Transmission Line loss Management", at IEEE Symposium on Emerging Topics in Smart and Sustainable Grids, Singapore, 2016.

3. Poster presentation, "Advance Active Network Management," Singapore International Energy Week, Singapore, 2016.

Awards & Scholarships

1. Scholarship Recipient for Doctor of Philosophy, Newcastle University Upon Tyne, UK.

2. IEEE Student Travel Grant Award (AUS 300) by Innovation Smart Grid Technologies-ISGT Asia, Melbourne 2016.

3. Conference Support Grant Award (SGD 400) from IEEE PES Singapore Chapter 2016.

4. Best Presentation at International Conference on Green Energy and Applications-ICGEA Singapore 2017.

Involvements

1. Committee Member of IEEE Power and Energy Society Singapore Chapter. (Jan 2019−Present)
2. Adjunct Faculty in Newcastle University in Singapore (NUIS) with the Department of Electrical Power Engineering. (Jan 2019−Jun 2019, Sept 2019−Jan 2020)
3. Research Assistant and Publication with Newcastle University in Singapore (NUIS); Research Grant awarded by Global Excellence Fund. (RA:June 2016−Feb 2017 ; RP:Nov 2018−Apr 2019)
4. Technical programme sub-committee of IEEE PES ISGT Asia 2018 Conference. (May 2019)
5. Adjunct Faculty in Singapore Institute of Technology (SIT) with the Department of Electrical Power Engineering. (Sept 2017−May 2018)

Table of Contents

List of Figures

List of Tables

Nomenclature

Acronyms / Abbreviations

ADMS	Advance Distribution Management System
AMI	Advance Metering Infrastructure
BTM	Behind-The-Meter
DCF	Distributed Control Framework
DER	Distributed Energy Resources
DERMS	Distributed Energy Resource Management System
DSO	Distribution System Operator
DSR	Demand-Side Response
EMS	Energy Management System
EPS	Electric Power System
ESS	Energy Storage System
IoT	Internet of Things
LCOE	Levelised Cost Of Energy
MAS	MultiAgent System
NAN	Nanogrid Area Network
PCC	Point of Common Coupling
PMP	Prosumer Market Platform

PSPG	Personal-owned Sustainable Power Generation
PtP	Prosumer-to-Prosumer
RES	Renewable Energy System
SCADA	Supervisory Control and Data Acquisition
SOC	State-of-Charge
TE	Transactive Energy
TSO	Transmission System Operator
Volt/VAR	Voltage/Reactive Power
VPP	Virtual Power Plant

Chapter 1

Introduction

Operational modelling for today's electric power system have proved to be highly complex where holistic/cooperative managerial solutions are somehow conjugated with nonlinearity relationship factors (*i.e.* human behavioural interventions, transient-stability constrained optimal power flow). For instances, having high penetration of Distributed Energy Resource (DER) especially at the low-voltage level and liberation in Retail Electricity Market (REM), Distribution and Transmission System Operator (DSO-TSO) are forced to strengthen utility-customer reciprocal engagements in view of Transactive Energy (TE) values; grid-tied flexibility and reconfigurable (plug-and-play), resilient in self-healing executions and reliable interoperability (power quality efficiency), convergence of Internet of Things (IoT), and synchronised participation in energy market. Hence, research investments and industrial synthesisation for decentralised yet cohesive Distribution Management System (DMS) solutions have exponentially inclined involving new and multiple energy actors perspectives. It incentivise operational reliability, performance, and overall productivity for sustainable economical and societal benefits across all energy actors. Hence, this chapter reveals revolution towards decentralised managerial trends where consumer(s) are empowered with greater stake in directing energy regulatory outcomes with favourable participating policies; top-down and bilateral energy/market legislations.

1.1 Primitive Energy Security and Management Systems

The primitive configured Electric Power System (EPS) seen in Fig. 1.1 is conventionally divided into three regions; generating station, transmission lines/feeders, and distribution network comprising residential and commercial customers. The EPS is modelled such that it has a single localised coupling point for all online/offline thermal generating units, and

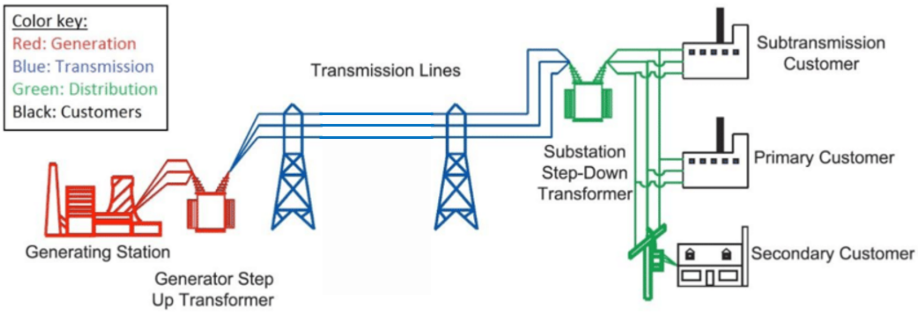

(a) Electric power system high-level layout.

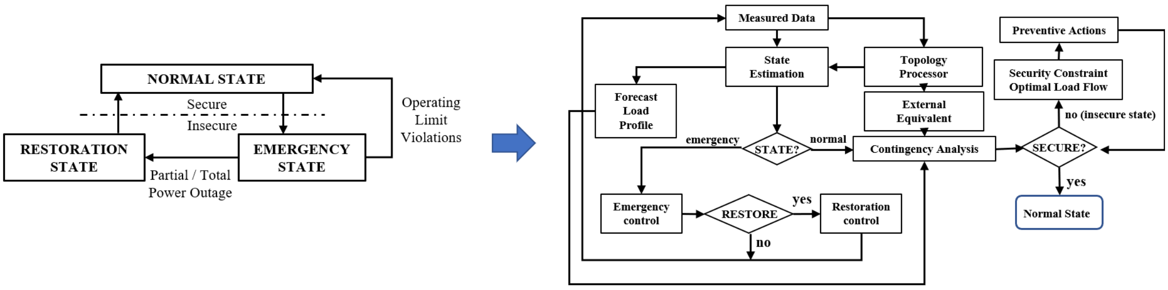

(b) State diagram for EPS control operation.

Fig. 1.1 First generation of electric power system and its operational management sequences.

customers' were only to receive electrification at the receiving-end of transmission lines operating as a load entity. In this sense, modelling of energy managerial proceeding for distribution grid planning was unambiguous as the network operational were passive (*i.e.* top-down administrations); power generation uses unit commitment algorithm to balance demand-supply equilibrium, routing strategy to ensure transmission lines are not overloaded with minimised power losses, intelligent energy distribution during peak demand loading, outage management services, and optimise voltage level compensation planning during both peak and non-peak demand periods [1–3]. In that sense, several key energy actors were introduced:

1. Transmission System Operator (TSO)—focuses on voltage and frequency level reliability through supply and demand equilibrium, robust and resilient in providing recovery solutions when faced with unexpected low impact crises or outage vulnerability, and dynamically adapts to normal changes in system conditions or potential line congestion. Comprehensively, they are responsible in managing the reliability and management processes in transporting electrifications from the contracted generation capacities and ensure customers have constant access to electricity.

2. Distribution Network Operator (DNO)−anticipates customers' Demand-Side Response (DSR) expectancies and incentivise cost effective solutions when dispatching scheduling available generations and loads. It comprises interoperable intelligent systems to coordinate new integrated technology devices/generation for sustainable yet profitable engagements at low-voltage level.

3. Energy Market Authority (EMA)−responsible in regulating effective competition in the non-discriminatory wholesale and Retail Energy Market (REM) while enforcing compliance activities. Work closely with TSO to create greater market flexibility and price transparency that would satisfy customers' expectancy.

Nevertheless, among the selected operators listed above, TSO holds a major stake in the power grid operational and planning domains, whose objectives involved ramping robust-reliable performance and optimise generation availability under both abnormal and normal conditions including transient responses (*i.e.* motor start-up, loads' nonlinearity, and generator losses) [4–7]. Much research efforts were contributed into solving optimum transmission planning also known as $n-1$ contingency; using collected measuring data to perform load flow analysis based on current operating state, and predict future demand capacity in the next window timeframe $(t+1)$, to better schedule generation availability using state estimation approach. For instances; *(i)* finding the optimum surge impedance loading to meet the required transmission operating limit from voltage or transient instability (*i.e.* classic $P-V$ curve, Power−Angle curve) [8], *(ii)* regulating energy prices based on market limit that discerns transmission constraints and congestion [9, 10], *(iii)* security and resiliency for protection system automations during overcurrent crises or power outage (*i.e.* scaling down the affected area through re-routing strategy of transmission feeders) [11–14], *(iv)* perform load flow analysis to identify areas for improvement based on different loading conditions, and *(v)* model low-variance with maximum likelihood state estimation for profitable operation planning in future timestamps.

1.1.1 Introducing Renewable Energy Resources in Transmission

As EPS enters into early technology modernisation, deployment of large-scaled Renewable Energy Resource (RES) technologies (*i.e.* windfarms and solar farms) coupled at transmission level gained recognitions as DNO-TSO foresees befitting potentials towards security planning and power quality. Hence, centralised Virtual Power Plant (VPP) were introduced mainly addressing solutions for economical operation during peak demand loading, increase

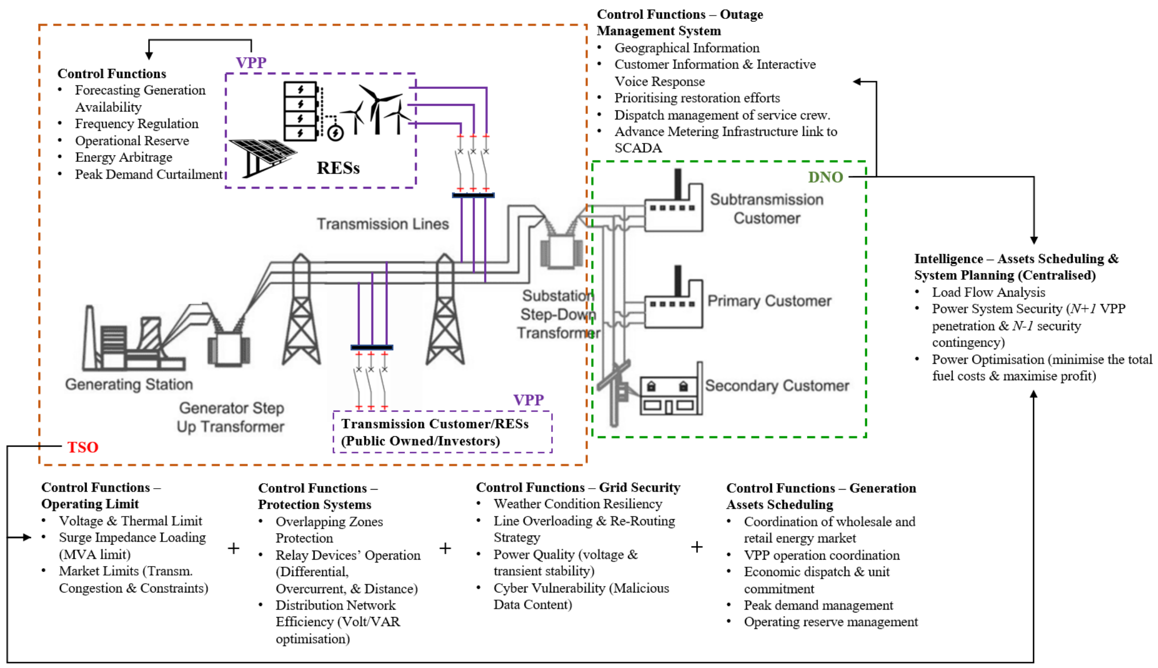

Fig. 1.2 Summary of critical TSO-DNO control managements with integration of RES technologies at transmission level.

contingency efficiency, and provide intuitive risk-based distribution network planning. The VPP controls active power generation across a group of integrated RESs to provide several grid services that are not dependent on feeder's location [15, 16]. Hence, typically, the operations of VPP provides system wide regularities with respect to increase or decrease of generation capacity or load size for regional transmission system areas. The grid services includes supporting DSR [17], frequency compensation [18], reserve generation pooling [19], energy arbitrages [20], and curtailment during peak demand crises [21]. Nevertheless, in the transmission planning for grid services, TSO-DNO regards integrated VPP (public/investor owned) as an auxiliary asset where contracted energy bidding agreements are ordered to render support in securing the distribution network reliability, wholesale electricity prices, and large energy demand deviation episodes. Fig. 1.2 illustrates the integration of VPPs at transmission and corresponding control functionalities rendered by respective operators.

Research efforts in identifying challenges/opportunities when adopting generation mix are trending, assessing operational impacts when unloading dependency on power plants and divert to RES-based VPP. Listed below were several open discussions in view of addressing a balanced and unbiased operations of RES penetrations [22]:

1. *Essential reliability services (frequency response, ramping, and voltage support)*—as the generation resource mixes continue to evolve, what measures were taken to ensure

power quality reliability is secured? are there specific beneficiaries or risks posed by generation variability from RES-based resources and what are the roles of these transmission customers (energy retailers) can do for reserve margin or in the market despite operation irregularities?

2. *RES integration does impose high risks*−lessons drawn from August 2016 Blue Cut Fire and October 2017 Canyon Fire events, inverter-connected and non-synchronous technologies do impose reliability and resiliency issues hence, what measures should Standard regulators impose and how industry are preparing solutions in their responds (reliability and resiliency)? are there still potentials toward improving power quality metrics with such technologies?

3. *Optimal planning adaptations*−what real-time monitoring data and energy management system application requires, or changes in Reliability Standards, would better enhance grid operations and resiliency anticipations? what is considered best practices when planning transmission system with VPPs? How does it impact the wholesale and retail electricity market policies?

Contrastively, addressing its socio-economical impacts in adopting RES-based VPP as part of bulk power generation sources, realisations in system's return on investments and customers' flexible participation in the revised energy market must be considered. RES installations and, operation and maintenances costs have high-risk return on investments hence, it will only be successful if partnering power generation companies and state governments provide supportive programmes (*i.e.* incentives, rebates) for market penetration. Therefore, VPP operators need to find emerging business models that will maximise VPP potentials in supporting TSO-DNO managements through grid service augmentations or increase credibility in the reserve market (*i.e.* ancillary services).

Studies in [23–27] have present holistic solutions between system's integration and operational responses when addressing or prioritising challenges/risks associated to VPP penetrations. Identified from these studies, two common application functions were often mentioned; Energy Management System (EMS) and VPP control managements. They represent key managerial drivers in securing optimal power flow with VPP participations to secure power quality and customer connectivity in the distribution network.

1.1.2 Energy Management Control System

EMS is defined as a scalable computer-aided system [28–30] that provides monitoring, automated control, and scheduling services that optimises geographical operations of generation customers, transmission, and dispersed distribution substation in real-time. It is designed with modular based managerial functions/applications that are typically fused with distribution Supervisory Control and Data Acquisition (SCADA), generation dispatch and control, energy scheduling and accounting, and transmission security management [31–33].

In practice, EMS is a collective suite system that optimally manages transmission grid and energy generation to increase customers' network performance; resilient towards either curtailing or preventing power outages, observes constrained security requirements respectively based on electricity market prices and Standard compliance rulings, and fuel-operation management cost and transmission loss reductions [29, 34, 35]. In this sense, EMS are programmed to provision *(i)* operating system that is comprehensive, unified, and free from malicious invasion/corruption, *(ii)* industrial deployable transmission security applications and generation control, *(iii)* synchronised platform independent graphical user interface, *(iv)* accessible backup control center options during malfunction episodes, *(v)* sustainable decision-making processes, *(vi)* provide training simulation for dispatcher/operator.

Supervisory Control and Data Acquisition System

Computer-based control and monitoring platforms serves as the most ciritical medium that can support operators in system visualisation for cost effective solutions where realisations in reliability or optimum operation can be augmented in real-time. SCADA [36] is common referred as solution for data acquisition, monitor, and control system that has bi-directional communication infrastructure; portable and scalable. In the context of SCADA in power system application, the major components in SCADA system comprises Remote Terminal Units (RTUs), Master Terminal Units (MTUs), Information and Communications Technology (ICT), and Human Machine Interface (HMI). The deployment of SCADA system architecture can be viewed as two categories [37]; transmission and distribution network management. They have similar monitoring and control capabilities however, differs from the equipment devises (*i.e.* sensors, actuators, meter) used.

RTU serves as the main devise in SCADA system that physically connects with various sensors, meters and control actuators. It is a real-time programmable logic controller that converts measured data into digital format for transmitting. It communicate closely with MTUs where operators can remotely send out control command and pilot actuators and switchboxes operations. Meanwhile, MTU is a central host server(s) that networked with other RTUs, also known as SCADA center, performing read and write functions during scheduled scanning. It is a GUI platform that programmed with alarm management and notifications during abnormal events and suggest possible restoration processes. Whereas, in normal condition, optimum supervisory control schemes can be deployed remotely and perform predictive or state estimation for security planning. It uses conventional ICT infrastructure mainly to perform data/command transfers from field interface devices to central host computer servers and vice versa. Lastly, HMI is a platform comprising of multiple software from request-receive applications to intelligent computing for control and protection solutions based on the gathered data from the remote field parameters.

Transmission Security Management

Discussed in [38–43], actual case studies and results were contributed into network topology analyses focusing in optimising utilisation of transmission assets and security-constrained optimal power flow. Following reviews several sub-components/attributes when deal with transmission security management:

Suggested in [40], it elaborates recommended practice when conducting modern *load flow studies* using computer-aided computing system on existing transmission network, considering optimal power flow calculation techniques for steady-state power flow and voltage transient analysis. It aims to navigate power-oriented operators with limited experience to conduct load flow analyses and quantify sufficient generation in real-time (5*mins* intervals) while observing minimised operating costs.

Additionally, [41] explains the importance in extending load flow studies with *state estimation observability analysis* using standard normal equation (triangular factorisation) to a orthogonal transformation-based approach. It eliminates numerical ill-condition in the gain matrix by combining sparsity from the normal equations method and orthogonal transformation numerical robustness. It aims to solve normal equation using orthogonal transformation on the Jacobian matrix to render hybrid state estimator that performs observability analysis.

Meanwhile, interoperation of *contingency analysis* is required where it provides operator(s) with major information on static security when planning transmission operations discussed in [42]. It assess vulnerability where one or multiple contingencies occur (*i.e.* transmission line fault, transformer overloaded, voltage rise/fall), contingency analysis calculates violations and suggest real-time remedial actions to bring normality in the transmission's operations. Correctional solutions provided are much dependant on the quality of state estimator and computational speed as required by the operating Standard; violations to be cleared within 30*mins*.

Lastly, [43] provide optimal solution in *solving security management using successive linear programming* when allocating reactive and active power generation to relieve violations based on control action time constraints. It aims to minimise active and reactive power losses while maximising reactive power reserve absorbed by generating units to compensate system voltage dip crises during high interconnected load capacity subjected to power flow constraints. These algorithms comprehend that active and reactive power are non-separable and largely nonlinear, generators' cost-rate curves were considered to discourage near limit operation, and piecewise linearisation techniques are employed which iterates with fast convergence towards minimal variance of AC power flow.

Dispatch Control for Generating Assets

In relations to fuel driven generating units, the term Economic Dispatch (ED) and Unit Commitment (UC) optimisation are commonly associated to solve generation capacity for individual generating units and, select which and when a generation units to start-up or shut-down for a short-term period respectively. Its global objective is to search for the minimised total fuel costs based on real-time demand load capacity, subjected to transmission line and generating unit operating constraints. Primitively, the two mentioned optimiser functions are modelled as piecewise linear problems and are solved individually in a sequential order. However, with the advancement in computing intelligence technology today, ED and UC can be solved simultaneously as a single statement problem using nested loop approach incorporating robust operating constraints and relative fuel costs with no prior assumptions. Its goal is to solve minimised operating costs by selecting which thermal generating unit(s) has the lowest marginal costs (*i.e.* locational marginal prices due to transmission constraints) that can satisfy the demand load capacity at time, t.

There are two popular optimisation approaches when solving UC and ED problems; integer programming algorithm involving Mixed Integer Linear Programming (MILP) or Mixed Integer Quadratic Programming (MIQP), and any methods from heuristic algorithms. In [44] and [45], they proposed similar two-stage MILP approach when solving minimised ED-UC problem considering quadratic fuel cost, transmission line loss, and valve-point functions. Here, the quadratic objective function is converted into a linear approximation problem statement using piecewise linearisation method. Meanwhile, [46] addresses possible linear approximation errors in MILP due to the non-linearity in objective cost function which dissatisfies the power balance constraints. Thus, MIQP was proposed where it suggests a combined warm start technique and range restriction scheme with MIQP to eliminate convergence stagnancy and increase computation efficiency during optimisation process.

On the contrary, [47] and [48] proposed a heuristic approach when solving UC-ED. Heuristic algorithm is best used to solve nonlinear multi-objective optimisation problems within a search space. It is known for its reduced computational processing time and proves close to optimal solution based on the search jump greediness intensity (*i.e.* computation speed proportional to solution accuracy). Therefore, given a quadratic fuel cost and other operating constraint functions, the iteration process (gradient descent) in finding optimal solution may not be the global minimum. Nevertheless, heuristic approach is sufficient to solve fast and feasible short-term solutions such as ED-UC problem verified in [47]. It suggests nested Particle Swarm Optimization (PSO) while comparing to other optimisation programming approach where the minimised costs differences were $< \pm 2\%$ and, the computation stress and time improves by 50%. However, PSO may suffer computation divergence due to operating limit constraints. Therefore, [48] suggest hybrid solution approach, optimisation-based heuristics, where it infuses priority list optimiser to localise initial starting point in the vast search space based on generator's and transmission inequality constraints before gradient descending towards the optimal solution using Genetic Algorithm (GA) approach.

Energy Scheduling and Accounting

TSO control center or or Independent System Operator (ISO) keeps track of regional area energy production costs and transactions at specific evaluating periods. The energy scheduling and accounting software has the capability to compile electricity production costs comprising the physical transfer of energy through transmission lines and operation & maintenance committed by generating units. It schedules energy exchange and actual power flow based on NERC Reliability Standards that will authorised user-defined parameters when formatting power transfer against electricity marketplace as shown in Fig. 1.3. Here, it involves more in-depth towards policy modelling and Standard compliances where they set operational requirements for generating assets to meet balanced market transactions and quality electrification for customers.

An example case study implementing hourly based energy scheduling and accounting architecture can be seen in [49] where it uses 49 historical days data using SCADA and Automatic Generation Control (AGC) systems to generate an economical/profitable business model for seven future days. It also suggest regulation in limiting net schedule interchange, congestion settlement credits, and basepoint generation capacity.

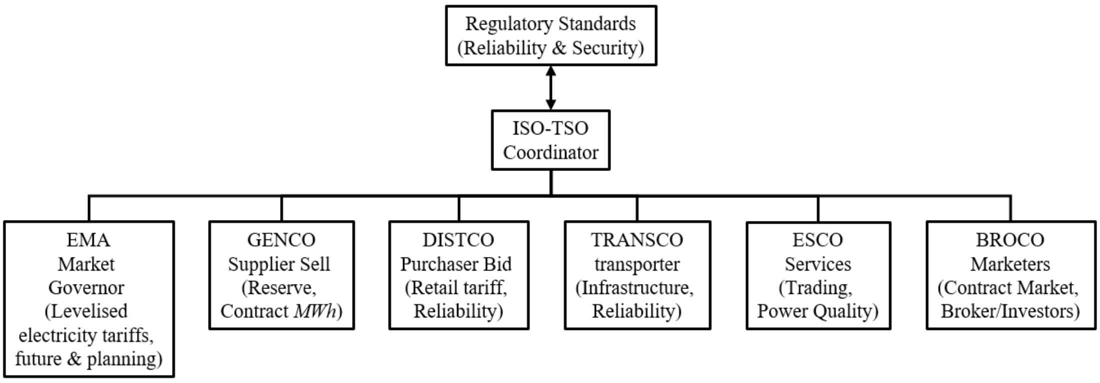

Fig. 1.3 Energy marketplace−horizontally integrated business model between energy actors.

1.1.3 Distribution Management Control System

Primitively, DMS is designed to govern electrification in the distribution network to meet customers' quality requirements which later known as Advance DMS (ADMS) which suggests operational integrations with other featured applications discussed in Chapter 1.2.4. As a base, DMS serves as a dynamic decisional support system comprising collective suite of applications that can assist operator (*i.e.* Distribution Network Operator (DNO)) with monitoring (*i.e.* SCADA, smart meter) and control functions to resolve abnormal/outage events. It is also commonly referred as Outage Management System (OMS) as it key deliverables improve; *(i)* outage duration, *(ii)* minimise and isolate outage affected area, and *(iii)* restore/compensate frequency-voltage level to prevent outage crisis. Minimally, DNOs have their OMS equipped with comprehensive IT framework that integrates Geographical Information System (GIS), Customer Information System (CIS), and Interactive Voice Response System (IVRS) [50, 51]. From its networked communication infrastructure, its uses information received from customers regarding power outage and knowledge of protection devices location (*i.e.* circuit breakers) to localise and isolate the outage affected area. With this information, DNO will proceed with restoration activities and dispatch ground crews to physically access the cause of outage. Correspondingly, DMS can also be employed for scheduling maintenance and network expansion works in the distribution, or profile DSR (*i.e.* energy consumption) trends for better transmission security planning.

A comprehensive review on DMS is presented in [52] where it explained customer service and reliability are key drivers into modelling OMS functionalities while considering complexity when distribution system expands and operational knowledge base starts to erode without the aid of IoT-based framework. Thus, considering cost effective solutions, DNO turned to process automation technology imbued with decision-making features where parallel communications can generate faster service restoration and accurate reporting of outage information. It also highlight other areas of enterprise integrating business process, information systems, and users' feedback data for effective with cost-efficient OMS. Meanwhile, [53] proposed distribution network protection and restoration control algorithms where it exploit IoT framework with automated controlled equipments in distribution. The algorithm uses MultiAgent system architecture to communicate and coordinate switching controllers in circuit breakers along the distribution network to isolate and restore service to customer during an outage event. The results have shown advantages in self-management trajectory where self-healing and adaptive (*i.e.* learning) re-routing capabilities procured faster fault interjections resulting in minimised loss margin. Uniquely in [54], it highlights the importance in hybridising EMS with DMS functionality to gain higher level security analysis; state estimations and security contingency for EMS and voltage level in feeders and loss optimisation for DMS. Such hybrid systems was proposed to encapsulate extended real-time and study mode functions that administer corresponding operational aids for network reliability-security while dispatching optimum economic operation. Neither a pure EMS nor DMS would fulfil distribution network operation requirements.

1.1.4 Virtual Power Plant Control System

In corporation with EMS operations, how does VPP services fit in? What are the necessary control functions or managerial features when governing VPP?

The operational objectives of VPP management is much dependant on the market environment specified by users. In general, it aims to concatenate RES or Sustainable Power Generation (SPG) and Energy Storage System (ESS) with flexible power consumers with the ability to forecast and monitor uncertainty, and dispatch generation or consumption capacity optimally. It is viewed and traded as a single power plant [55] into the existing markets where it brings forth flexibility in terms of VPP readiness to be deployed instantaneously during grid balance crisis as compared to those thermal generating units.

Asset Dispatch and Control

As the demand for energy at distribution level grows considering charging of electric vehicles, consumers have took much interests into profiling retail market price fluctuations in correspond to different time intervals [56]. In consequence, TSO-DNO suffers anticipation crises when levelling supply-demand equilibrium and scheduling of thermal generating units would take on greater ED-UC dispatch losses due to ramping or start-up issues in order to meet large power deviations within smaller timeframe intervals (*i.e.* overgeneration spinning reserve). Therefore, VPP can provide solutions into handling large power fluctuation in real-time while thermal units operate as baseload power plants. It would maximise utilisation of RES-based generation units and compensate using controllable units (*i.e.* hydro, biogas) during shortage and store surplus into ESS. A comprehensive study in VPP economic short-term scheduling and joint profit distribution problem is discussed in [57] where it proposes an operation scheduling model. The results attained from the case study proves to provide optimal decision-making solutions when piloting generation assets in VPP with maximised profit return. In addition, the cooperative decision-making process exploits market policy incentives to further gain greater profit margin.

Likewise, the operation of VPP can be market driven and steer consumers to have a predictable energy consumption profile. It can react quickly to changes in the exchanged electricity prices and thus, execute shorter time interval trades [58]. In turn, it triggers DSR flexibility for grid support and overturn additional revenue affecting power exchanges. VPP takes advantage of the changes in wholesale energy prices by contracting larger generation when tariff is high and conserve/store during low. In [59], analyses on interactive dispatch and bidding strategy models of VPP based on DSR against locational marginal market prices (wholesale) using game theory were presented. It proposed a VPP dispatch model that coordinates time-of-use pricing mechanism against DSR. In addition, the VPP dispatch controller incorporate multi-time scale rolling scheduling strategy to gain approximate generation certainty when operating RESs. To comprehend the operations of VPPs in a multi-actor environment, the authors introduced game theory approach where individual VPP will optimally compete and bid in the wholesale market based on maximised profit margin.

Forecasting Generation Availability

When dealing with RESs in VPP (*i.e.* solar PV farm, windfarm), generation uncertainty which results to UC scheduling errors at time, $(t+1)$, are inevitable. In addition, it creates security-constraint complexity when planning for optimal $N-1$ contingency which often resorted to deployment redundancy (RESs under-utilised) or power quality reliability issues mentioned in [60]. Therefore, renewable energy forecasting is a crucial and cost effective tool that aids VPP operators to up- or down-ramps those controllable generation assets in VPP to achieve cost-effective UC-ED and meet demand equilibrium for intra-day or day ahead scheduling with minimised RESs generation curtailment. The influencing factor when profiling RESs' generation is mainly contributed by weather conditions thus, weather prediction model is key to gain high forecasting accuracy. Depending on the scheduling operation required, the learning algorithm for accuracy can be attuned to adapt long-term relaxed criterion (errors $<30\%$) to short-term high precision and fast convergence rate criterion (errors $<12\%$).

Commonly, forecasting tools are modelled based on two categories; Physical and Statistical methods. Physical approach focuses in creating a numerical weather prediction (NWP) using weather-related parameters (*i.e.* temperature, atmospheric pressure, humidity, precipitation) as input to create terrain-specific weather conditions. With those information, it is converted into energy production. Whereas, statistical method uses historical data of real-time power generation to statistically correct results derived from NWP models. To evaluate the performance index of the modelled forecasting tool, three forecast accuracy metrics can be employed to weigh prediction deviation between the forecasted and actual data; mean bias error, mean absolute error, and root mean square error. The mentioned metrics help the adopted forecasting model to better attune it learning algorithm and minimised forecast error. A comprehensive literature review [61] on NWP explained the importance in hybridising forecasting approach to increase accuracy. Likewise, [62] presents possibilities in using deterministic input parameters in NWP when forecasting output power generation. It also explained that by hybridising both physical and statistical methods can improve performance accuracy as they compliment each others' limitations at different time horizon. Meanwhile, it highlights that persistence model presents the worst forecasting approach with large spread of errors when compared to others.

Utilisation of forecasting tools is not limited only to power generation from RES whereas, industries have proved that it serves better in transmission $N-1$ security-constraint planning which involved DSR profiling, and electricity tariffs [63].

Ancillary Services for Transmission Security Planning

VPP fits very well in the spinning reserve and reactive power market [64] where supporting services during power quality crises in the transmission network (*i.e.* voltage-frequency dip/swell, thermal generator unit failure, malicious power transformer tripping) can be compensated instantaneously. In addition, it is frequent that the transmission system ought to experience momentary voltage dip/swell crises due to sudden increase/decrease in energy demand during peak/off-peak periods. Therefore, VPP can serve as a power quality compensator that can be deployed instantaneously by injecting or absorbing real/reactive power into the distribution network to regulate the voltage/frequency level. Thus, introducing VPP into the transmission security constraint planning as $N+1$ redundancy can increases system's resiliency [65]. Likewise, VPP can also provide solution for weak $N-1$ contingency planning that often resorted to reserving large spinning generation as relief. Having energy demand demographic to expand with unanticipated capacity trajectory (*i.e.* energy ramp-up and down during peak- and off-periods), TSOs were resorted in having multiple thermal generators in spinning reserve mode at time, $(t-1)$, to counter unforeseen large energy demand deviations while observing generator's operating time-domain limitations(*i.e.* cold-start, ramp-rate limit, prohibited zones).

Explained in [66], research investigations on VPP deployments serving as a self-healing, physical resilient, and energy efficient services were presented. It models corresponding loci control features for new emerging operations in relations to electricity market participation, DSR, and ESS solutions. In addition, studies involving economics, sociology, and psychology interactions were considered implicating evolutionary challenges/opportunities from current practice dealing with generators to consumers and planning real-time operation. Meanwhile, [67] schedules VPP dispatch for optimal bidding, and spot arbitrage opportunities in the electricity market environment through spinning reserve and reactive power services. It employs security-constrained price-based unit commitment model that maximises operational profit margin from arbitrage ancillary opportunities. The results offers single optimal bidding profile and schedules active-reactive power under market participation. The proposed model produces minimised reactive power costs through strategic allocation and secures voltage level at transmission feeder. In view of transmission security planning, [68] suggested a day-ahead self-scheduling model for VPP as a single entity to trade both energy and reserve electricity market based on optimised asset dispatch. It also considered uncertainty operation rendered by RES-based generations in VPP when called upon to partake as reserve hence, it the problem statement is modelled as a stochastic adaptive robust optimization. The results showed advantage when characterising certainty in lieu of market prices and available generation capacity from RES to accommodate reserve deployment upon request. Low values uncertainty budget produces less conservative solutions while high value increases robustness. In addition, having flexibility in DSR operation can be useful to arbitrage leverage in different market participations against inflexible energy consumption over the scheduled horizon.

1.2 Power System Turning into Grid Edge Technologies

The concept in Grid Edge has become the center of next generation utilities. Having decentralised installation of generation resources in the distribution network, also referred as DER, the edge has become the focus [69]. It promotes the concept of decentralised and active management between TSO and DNO to address DSR requirements and increase credibility in DMS during system abnormal events in the distribution network. Primarily, the ideology was to bring DERs as a single entity closer to demand shifting from transmission to distribution installations regulated by DNO using centralised VPP management approach that aims to relief TSO's shortfalls during DSR, voltage dip/swell, or transmission line failure crises. Its operations are biased towards providing ancillary services for DMS [70] management as these installed DERs (*incl.* ESS) are typically modelled with small-scaled power generation capacity ($<500kW$ system).

However, it was found that DERs were economically underutilised when employed only for DMS purposes and feeder congestion crises were often observed due non-strategic distribution of DER installation to ill-defined optimisation constraints in ED-UC problem [71]. Whereas, DERs have greater potentials if they are strategically allocated providing grid services that are highly dependant on the specific location (*i.e.* feeder oriented). It aims to resolve locational voltage management, optimal power flow, and energy capacity relief of a specific feeder that has critical demand loads or high intense energy consumptions. Therefore, the concept of Distributed Energy Resource Management System (DERMS) was proposed governing multiple DERs in a single feeder bridging TSO and DNO operating alongside to meet customers' demand along that peculiar feeder as seen in Fig. 1.4. In this sense, DNOs were bestowed with system operator functions, transitioning DNO to Distribution Service Operator (DSO) that accounts for multiple points of generation variability against energy consumptions in addition to DERMS requirements in a decentralised environment.

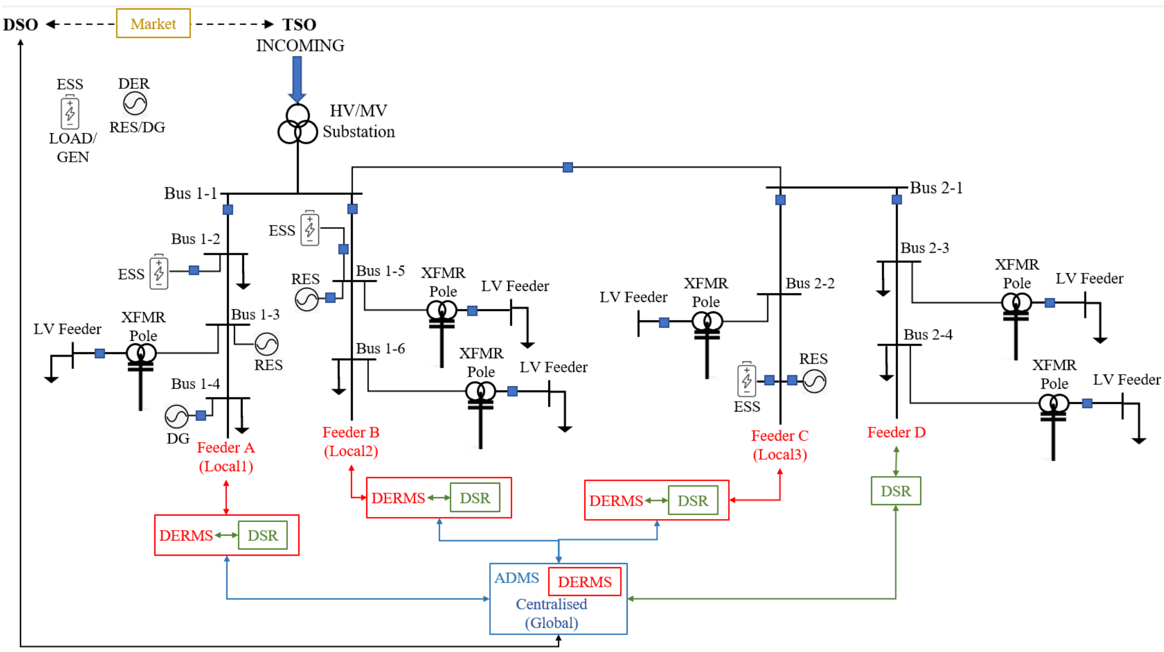

Fig. 1.4 Integrating feeder-oriented DER systems in distribution network.

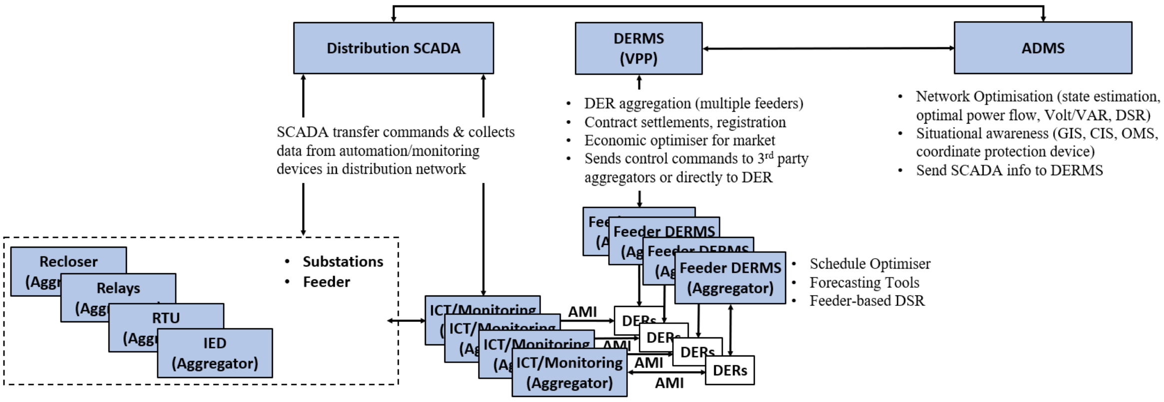

(a) DERMS interaction layers with SCADA and ADMS.

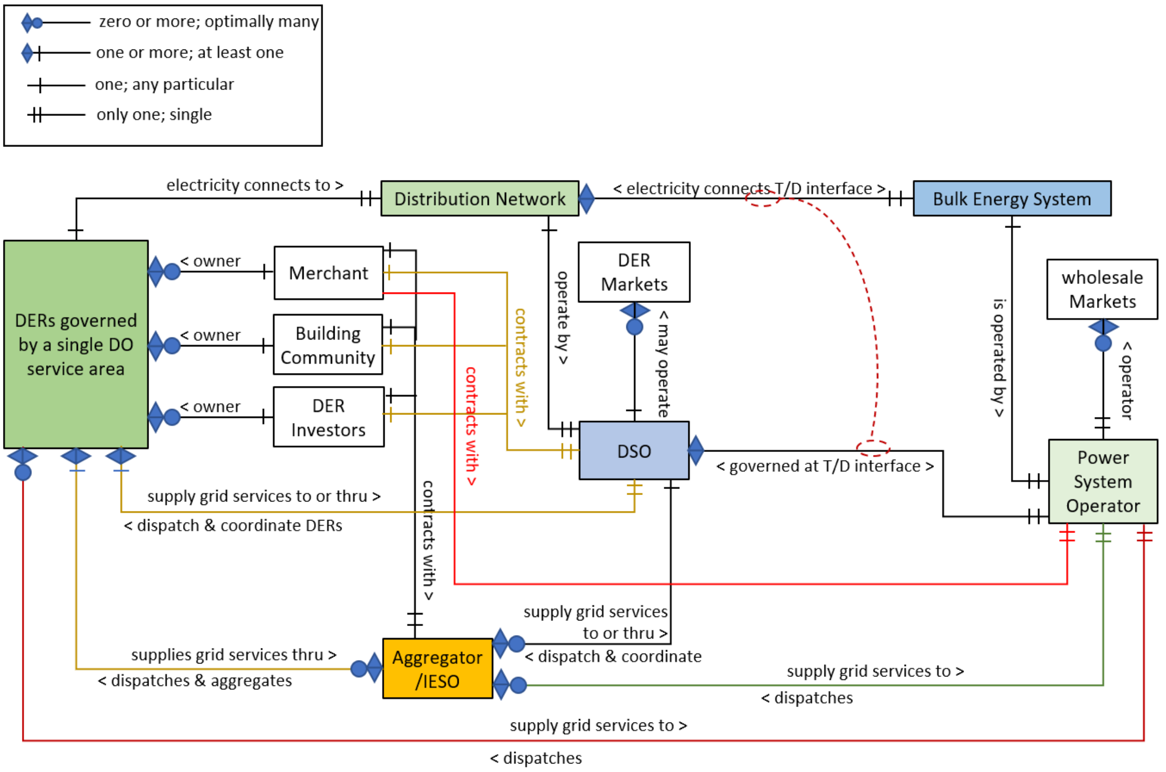

(b) Hybrid DSO-TSO control architecture with DER operations.

Fig. 1.5 Distributed governing regimes and interactions for DER penetrations in distribution network; enabling bi-directional energy transactions.

1.2.1 Distributed Energy Resources in Distribution Network

When mentioned about DERs penetrations in distribution level, association with DERMS architecture modelled for DSO is favoured. DERMS [72] comprises of combined managerial systems designed to optimally coordinate and automate business processes for DERs in a decentralised environment at individual feeder; DSR planning-optimisation, schedule VPP generation and storage, load management to satisfy demand-supply equilibrium, ancillary services, and short-term forecasting ability to gain certainty (*i.e.* load capacity, weather, spot price in wholesale market). Likewise, DERMS also has the ability to support DERs from multiple feeders grouping them into a single VPP to maximise DERs' value by selling excess into the energy capacity markets thus, enabling flexibility-availability price market [73].

The modelling of DERMS functions variates from one energy provider to another depending on mandated requirements for regulatory and market environments. Therefore, there is no common definition agreed upon for DERMS industrial operations, and it is often confused with other similar systems accomplished from utilising DERs. Nevertheless, the value of DERMS addresses three specific business models; *(i)* operating as a DER aggregator platform for Advance DMS (ADMS) operations, *(ii)* generate optimised solution for generation dispatch, charging/discharging ESS, and load shedding/scheduling in local or cohesive domain influencing wholesale price market (*i.e.* clearing, spot), and *(iii)* ancillary services focusing at individual feeder (*i.e.* Volt/VAR support, peak load management).

Despite having DERMS operating as VPP or feeder-based stability and control, the sum of managed feeders in the distribution network might not be optimised for overall efficiency-reliability. Hence, ADMS is introduced to enable energy aggregation so that DSO can plan and optimise DERs in a unified problem statement with TSO's objectives; hybrid DSO-TSO interactions. In this sense, integrated DERMS and ADMS serves as the next key intelligent platform for distribution utility [74]. Apart from aggregated DERMS, ADMS architecture also links with other components such as distribution SCADA [75] designed with distributed-based IoT interface for big data computing, data storage, and monitor DER energy exchange, and ICT infrastructure to command operations for automation devices as seen in Fig. 1.5.

1.2.2 Feeder-based DERMS (Local)

Table 1.1 lists the typical localised (feeder-based) DERMS use case functionalities; not all additional cases were mentioned as the platform is still evolving and proliferating. Here, the cases focuses in utilising DERs installed along an individual feeder to service connected customers at low-voltage as seen in Fig. 1.4.

Many research studies have proved positive performances in using DERs to optimise decentralised DERMS cases mentioned in Table 1.1 at individual feeder; highlighting from reduced operating costs through strategic dispatch of forecasted RES-ESS [76] against peak demand to securing feeder head voltage using Volt/VAR optimiser [77] to other short-term ancillary services [78]. In addition, investigations into selection of which distribution feeder and sizing of DER capacity implementations also require greater attention to better utilise non-dispatchable renewable resources in sync with dispatchable DER technologies against feeder's demand load profile. In [79, 80], both articles reviewed and suggest an optimised approach when selecting which feeder and DER size based on several performance indexes that helped to quantify the relationship between feeder load and stochastic nature of RESs. The algorithm ranks utility feeder for DER system installation based on performance index of peak-load reduction and feeder load growth while DER capacity uses increased system capacity and load-generation correlation indexes. The comparative results have shown redundancies for some feeder to install DERs as higher operating costs were incurred. The ranking algorithm is greatly steered towards Volt/VAR crises due to large peak demand deviation and line congestions, indicating reliance on DER system is greatly recommended for instantaneous response. Meanwhile, [81] suggested introducing a feeder-based market platform for DER as players to partake in the clearing market by trading energy with neighbouring feeders and redeem incentives. The decentralised control algorithm adopted two-step clearing price mechanism; first, local market is cleared independently and second, DERs can trade energy with neighbouring feeders.

1.2.3 VPP-based DERMS (Global)

Table 1.2 lists the full spectrum of DERMS use cases serving for the whole distribution network. Here, the cases are driven to support mostly in the grid services domain and their impact in the electricity spot market. The optimisation control algorithms focus in technical and financial aspects using centralized decision-making protocols that aggregate independent DER operations and interacts closely with the bulk power system operators to gain optimal

Table 1.1 Spectrum of decentralised DERMS (aggregator) use cases based on short-term planning.

Beyond the Meter *Feeder Optimiser*	T&D *Grid Services*	System *Market Application*
-schedule RES-ESS -operating costs reduction -forecasting tools -islanded with resiliency -%shifting load vs AVAIL. generation	-peak load management -relief line congestion -enhance power quality (*i.e.* Volt/VAR)	-ancillary services (*i.e.* voltage support, reserve, frequency regulation)

power flow. In [82, 83], a proof-of-concept illustrating interactive protocols between DERMS and stakeholders interactions were presented highlighting predictive decision-making tool performances on reduced operating costs and support distribution network optimisation (*i.e.* optimal power flow, line congestion & unbalanced load management, switching and Volt/VAR optimisation, optimal DER placement, FISR & outage management). In addition, through optimal allocation of available DER resources and its flexibility, it aimed to solve optimal match local supply and global demand while flattening the remaining net exchange over time.

Apart from supporting grid services, the electricity spot and contract market serves as an influential component that can steer VPP-based DERMS to match desired market signals despite operating in a decentralised environment [84]. In addition, an energy sharing market platform was proposed to reinforce coordination between operators' of DERs using crowdsourcing approach. Each DER participant undergoes revenue-based operation based on it inherent characters and develop risk preferences while the energy sharing market governs the crowdsourced DER energy supplies with ESS. In addition, through revenue analysis, DER aggregator can cipher investment decision and appropriate DER sizing. In lieu of energy clearing market, [85] proposed an optimised day-ahead Distribution Locational Marginal Pricing (DLMP) for line congestion management and voltage support. It comprised of marginal costs for active and reactive power, line congestion, substation and feeder losses,

Table 1.2 Full spectrum of centralised DERMS use cases for distribution network application.

Beyond the Meter *Feeder Optimiser*	T&D *Grid Services*	System *Market Application*
-shifting time-of-use -reduce demand charges -Microgrid operation	-situational awareness (*i.e.* DER monitoring, generation forecasting) -peak load management -reroute line congestion (*i.e.* AVAIL. feeder, upgrade deferral) -load shaping -coupling renewable system -power quality optimisation (*i.e.* Volt/VAR) -ADMS support (*i.e.* Outage management, FLISR) -distribution interconnection (*i.e.* IEEE 1547, Rule 21)	-VPP management -contract capacity & trading -spot market & clearing price -ancillary services (*i.e.* reserve pooling, freq. regulation, voltage support)

and voltage support to steer price signals. The overall DLMP decreased proportionally with DER penetration level, procuring financial benefits for spot market, and contribute balance and loss reduction in distribution network.

1.2.4 Advance Distribution Management System

Promoting DER penetrations in distribution network, DSOs are much reliant on ADMS, a comprehensive power distribution intelligent system designed to provide situational intelligence for planning and reliable grid analyses management during rapid change in network state. ADMS is commonly referred as a modular-based intelligent computing and monitoring system equipped with five operating features; GIS, SCADA, DMS, Distribution Network Applications (DNA), and OMS. It is an improved version from previously designed DMS where it boost technological advancement in remote automations, enhanced quality of data acquisition, precise prediction/forecasting for network resiliency, and initiate DNA that optimises distribution state estimation processes for unbalanced load allocation and non-technical losses. Figure 1.6 summaries the control functionalities and framework of ADMS incorporation with DERMS to support DSO in grid-following operations. Despite decentralised computing for DERMS to regulate individual DERs, the operation of ADMS adopts centralised-based optimisation processes to secure benefiting unified objectives seen in Fig. 1.6b. Here, it is assumed that all DERs are regarded as Beyond-The-Meter installation where regional DSOs are granted with full access control and data transparency while engaging diversified government registered operating policies/programs preferred by owners.

A comprehensive review on ADMS functionalities cooperating with DERs were reviewed in [86]. It suggested four critical management features for ADMS; *(i)* model dynamic state estimation to monitors each component and perform protection functions, *(ii)* synthesise distribution network feeders in real-time using DMS from the estimated states, *(iii)* perform time sensitive optimisation for both upper (operations planning) and lower (instantaneous control) levels using hierarchical structured processes, and lastly *(iv)* design control feedbacks that search for global optimum operating point. Findings have showed unified solutions in integrating emerging technology/devices in the distribution network with intelligent optimisation tools to support operation competency in a closed-loop environment. Flexible grid-management platform without compromising operating costs effectiveness is key to accommodate emerging demands from customers, investors, and regulator.

As ADMS is a data-driven, probabilistic system that is highly dependant on statistical trends and data quality for state estimation likelihood, [87] highlights the importance in

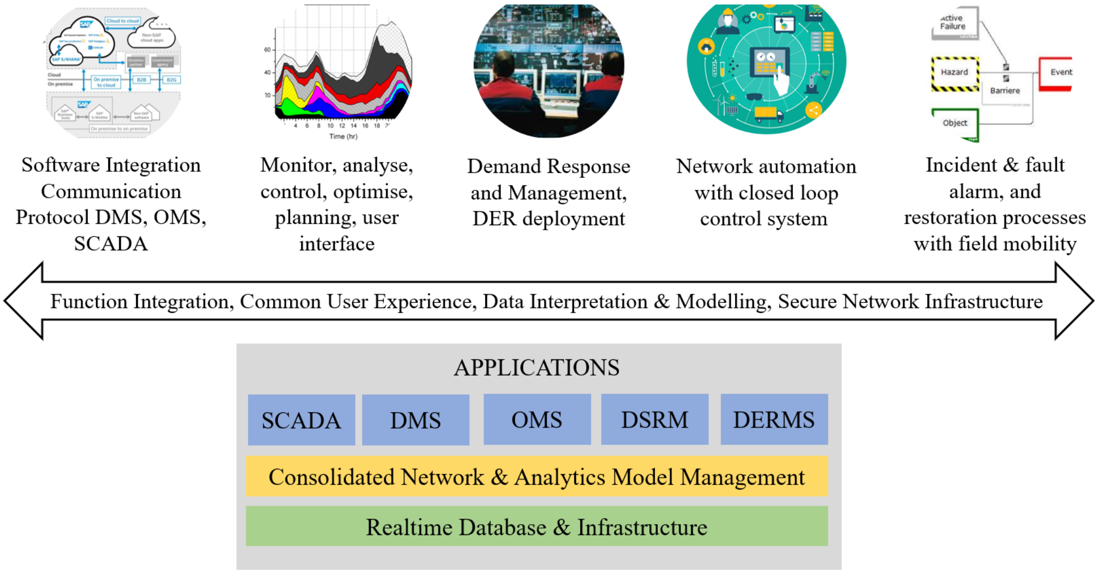

(a) Unified architecture.

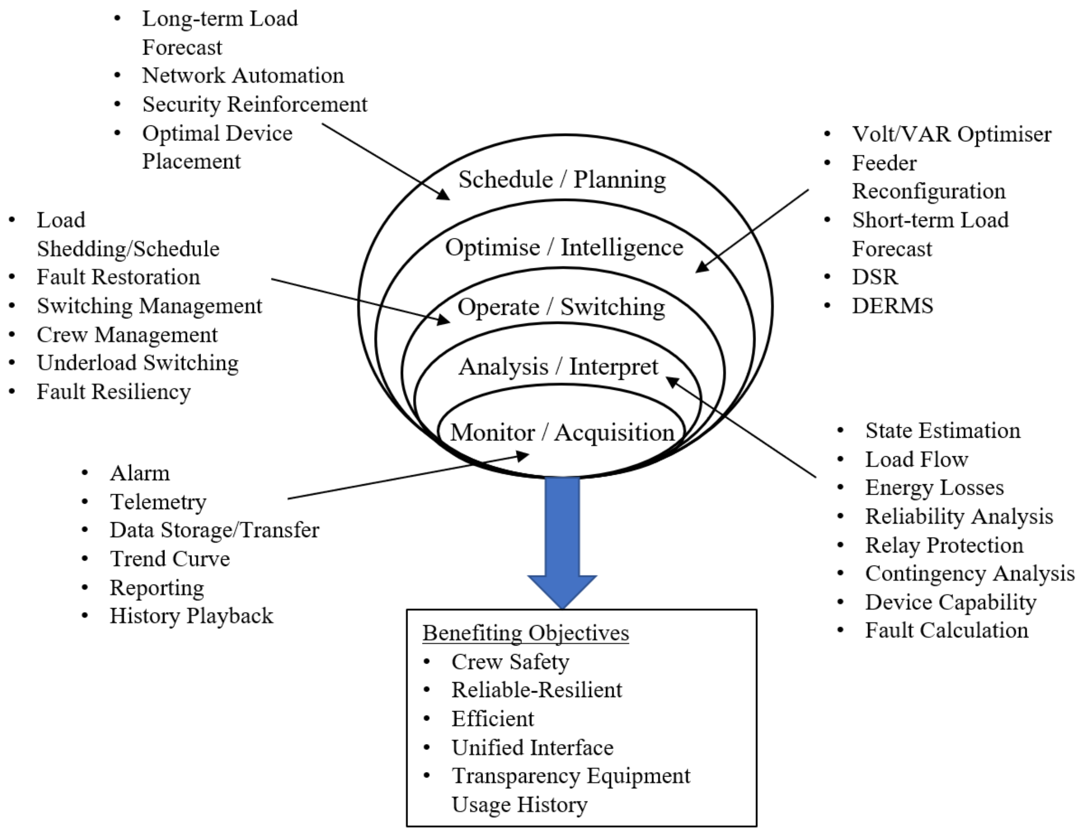

(b) Operation functionalities.

Fig. 1.6 Modelling of ADMS in response to DER penetrations in distribution network.

pseudomeasurements, placement of metering instruments, and cyber-security along the distribution network. Hence, modelling of SCADA is pivotal, eradicate vulnerability in data misinterpretations for situational awareness. [88] provide solutions in SCADA deployment using cloud-based networking infrastructure mapping as a virtual machine, focusing on ADMS functional blocks performances using four metric evaluations; processor, memory, network, and storage utilisation. The cloud platform serves as the data concentrator and middleware interoperability for interactive metering devices operating at low-level protocols. Moreover, cloud services is a big data oriented software modules that solves scalability-portability issues in cooperative settings and has competency in generating virtual solutions without comprising system efficiency.

1.3 Problem Descriptions: Distributed Energy Resources Behind-The-Meter

Advancing into the Fourth Industrial Revolution, research and industrial interests for DER installation Behind-The-Meter (BTM) progresses beyond its timeline trajectory. Public access for technological and IoT solutions in low-powered DER technologies become economically adequate, and liberalisation in the retail energy market have steered demands for DER installations at low-voltage level [89]. In this sense, penetration of Personal-owned Sustainable Power Generation (PSPG) system (*i.e.* solar PV, CHP, diesel-driven generators, HVAC, ESS, PHEV) are taking much fame for their potentials in bringing generation closer to demand load devices shown in Fig. 1.7a. Additionally, modelling of PSPGs are not limited to bulk generation system which includes offshore technologies that can be coupled directly to the low-voltage network. Such positive trends expose energy customers (*i.e.* residential and building owners) and RES-based generation investors to take greater ownership in electrification, seeking opportunities in owning in-house VPP system with an objective to reduce energy billing and partake in market trading (peer-to-peer) against retail prices.

1.3.1 Behind-The-Meter DER for Distribution System Planning

Modelling of customers' electrical power system has evolved into Prosumer environment [90]: to produce and consume electricity seen in Fig. 1.7b. Such configuration rises concerns for DSO as the location and operation of DERs are left up to Prosumer adoptions which provoke; *(i)* detrimental effects on distribution power quality and reliability, *(ii)* unpredicted DSR which complicate unit commitment scheduling (baseload) and state estimations, *(iii)*

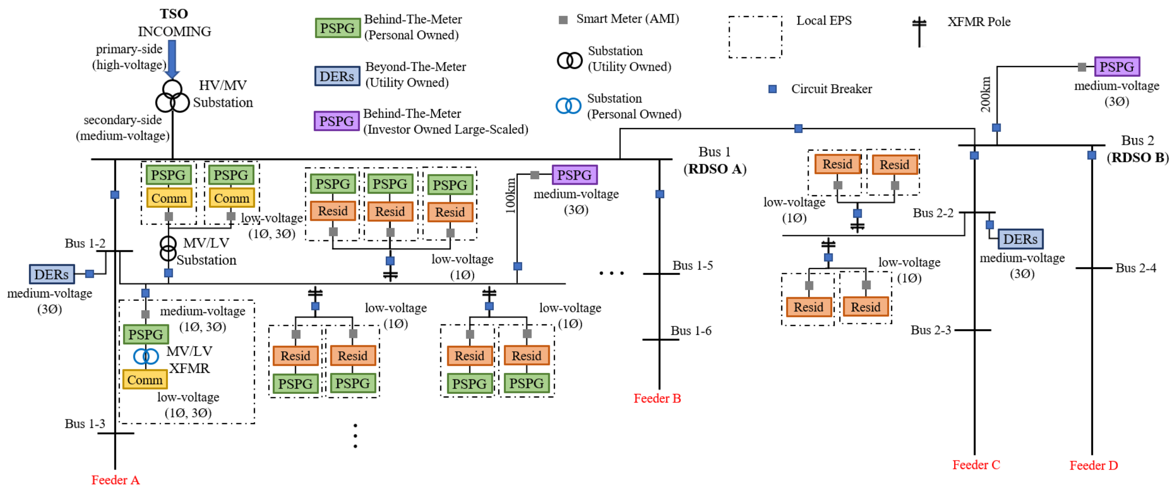

(a) A simplified one line drawing of distribution network with DER installations at low-voltage level.

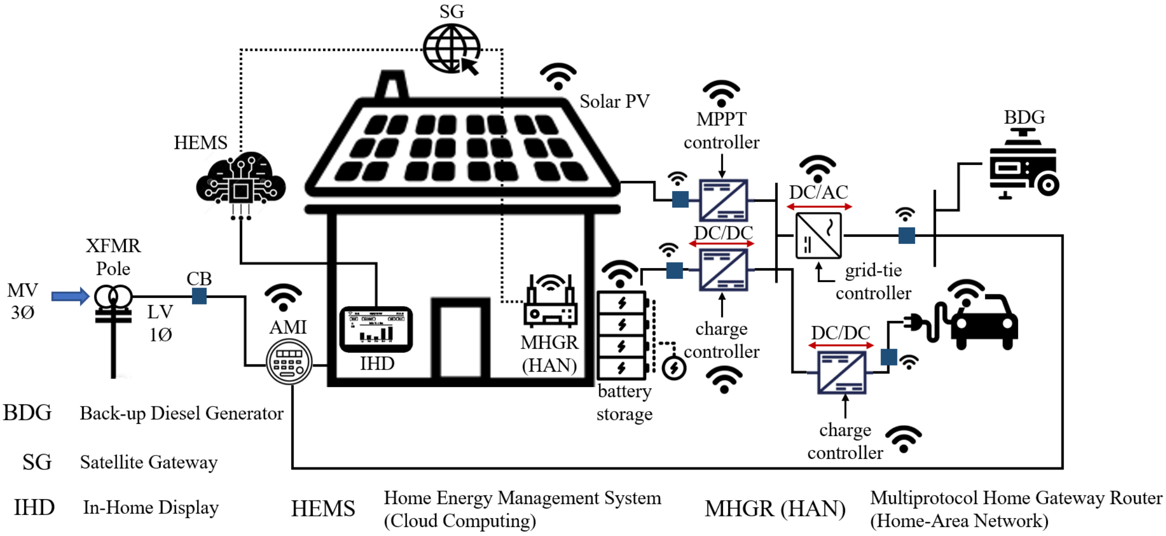

(b) Example of DER components in a local electrical power system of Prosumer: Residential.

Fig. 1.7 Customers demand for Behind-The-Meter DER system installations: Prosumer Community.

high volume participants in the spot market and peer-to-peer energy trading, and *(iv)* multi-tenant decentralise ADMS-DERMS coordination (*i.e.* diverged management interests based on business model options) thus, optimisation problem exponentially increases. Furthermore, regional DSOs need to find value contributions when implementing Utility owned feeder- or VPP-based DERMS against Prosumer Community. How these PSPGs can serve as an aggregator in DERMS to improve operations in the distribution network that is cooperative yet competitive.

Till to date, DSOs are working closely with International Energy and Renewable Agencies, customising Prosumer's roles in delivering new electrification policies and standards that synchronise with ADMS and DERMS interoperability [91]. Due to large penetration of PSPGs, primary innovation was to anatomise distribution network into Microgrid settings governed by respective Regional Distribution System Operators (RDSO). It comprises of decentralised aggregators (Prosumer Community) and DERs (Utility) into a single centralised DERMS with ADMS functionalities to meet optimised regional DSR and operating costs requirements while performing global market trading (bid/sell) with neighbouring DSOs. Nevertheless, there are still many open issues when planning for desired DERMS-ADMS operations against realism as; *(i)* Prosumers are out to exploit spot and retail market to gain higher return on investment without considering 'duck curve' or unit commitment crises, *(ii)* undetected islanded operations which can expose field engineers with live wires, *(iii)* synchronising individual Advance Metering Infrastructure (AMI) with DSO or other Prosumers without comprising data security and sharing, *(iv)* Programs and incentives for DERMS (aggregator) that adopts cooperative optimisation with decentralised intelligences, *(v)* contracting Prosumers' bilateral energy trading (*i.e.*peer-to-peer or back to grid) and transmission, distribution, and administrative (TD&A) costs, *(vi)* the layered control hierarchy of ADMS is structured in a bottom-up-lateral order (low-voltage level), and *(vii)* PSPGs will have stronger coupling impact on voltage and frequency level over grid due to larger stake in serving demand load capacity (*incl.* generation intermittency and inertia responses).

1.3.2 Empower Prosumer as the Major Energy and Market Stakeholder

Policy Officer Gerd Schönwälder, a member of European Commission in Accelerating Clean Energy Innovation, in his recent paper [92] questioned, "*Is power really seeping away from the giant energy behemoths of the past to the nimble, green-energy Prosumers and cooperatives of the future?*". How successful it will be if Prosumer Community are empowered to take greater authoritarian in shaping operations/managements in the distribution network?

A comprehensive review in [92] explained empowering to the people really meant and how future's energy landscape should be redefined, relieving electricity poverty and intensify alternatives for carbon-intensive regions. The term 'empowering' demonstrates three prepositions; *(i)* grant full data access and transparency on electricity usage billings and flexibility to interchange energy contract inbetween retailers in real-time, *(ii)* wide-range of incentive programs for Home or Building Energy Management System, also known as DERMS aggregator, that serves as a catalyst for business model innovations while reducing dependency on Utility, and *(iii)* establish data privacy and public access to AMI-ICTI for personal area network digitalisation. Substantially, to empower bestow liberations in positioning individual Prosumer as sole energy citizen that orchestrates operation and market choices. However, obligations are not to be compromised, safeguarding power quality integrity at global level and block discriminatory against retail energy providers.

Understanding the motivations behind Prosumers' energy-related choices and behaviour can influence DERMS aggregator competency when making optimum decisions. For an instance, the declining cost and accessibility in owning PSPG system has put into a position where energy trading instincts have leverage ways in which energies are produced. It has become a pivotal drivers for DERMS aggregator modelling in which Prosumers are expecting high investment returns. In consequence, energy transactions may largely divert away from retail markets and monopolism in wholesale tariffs (*i.e.* spot market) for Prosumers that have superiority over its geographical location or PSPG system capacity. In general, [92] urged researchers to innovate benefitting management strategies, devising ways to reach co-existing operating objectives. Demand for DER interoperability services (*e.g.* installing, maintaining, power quality of DER) will incline hence, initiation for new operator is recommended as part of DSO's grid service chain.

1.3.3 Negative Impacts on Power Quality and System Reliability

Predicaments on malicious reliability incidents generated by BTM PSPGs at low-voltage level present coordination challenges (*i.e.* unintended system tripping) due to several technical issues (*e.g.* ride-through capability, unintentional islanding, low inertia synchronisation) as the primitive electric power system was not designed to carry generation upstream [93, 94]. RDSOs are constantly challenged with unsighted BTM fault interruptions, having fault currents to propagate upstream which can result to line feeder failure if PSPG is not isolated instantaneously. Likewise, the grid's ride-through requirements needs larger timespan tolerance that allows PSPG to remain connected within a specified voltage-frequency level thresholds. Meanwhile, unintentional and intentional islanding is viewed as the utmost challenge in distribution planning and feeder protection. In unintentional islanding, transient overvoltage or undervoltage crises will transpire due to rapid change in demand loading capacity; oversupply or insufficient respectively. It can also resulted in large transient torque forced onto prime-moving generators which can damage mechanical parts. In view of protection system, islanded settings generate insufficient fault current level to trigger fuses or overcurrent relay protection devices (undetected). On the contrary, unscheduled intentional islanding could cause negative reciprocal effects on distribution security planning, $N-1$ contingency, and state estimation as provisioning for ancillary services to other feeders are blocked out. Likewise, in the context of Prosumer's EPS, it may not have access to gain external support during power quality issues which results to constant system tripping.

On the contrary, data misinterpretation and weak short-term forecasting tools can be burdensome in securing DERMS and gratifying the supposed contracted energy trading. Having power generation uncertainty from RES-based PSPGs, security in supply-demand equilibrium from scheduled unit-commitment and Volt/VAR optimisation can be a challenge as the transmission system has weaker power quality coupling than PSPGs' inverters [95]. Likewise, weak forecasting algorithms in predicting energy market tariff and DERs' available power generation capacity can drive cooperative participation of Prosumers to diverge thus, leading to an uncoordinated DSR management (*i.e.* duck curve, baseload, or large power deviation crises) [96]. Typically, accuracy of forecasting model is much dependant on historical data and quality. Thus, data misinterpretations due to package loss during transmitting or low sampling intervals can cause negative and propagating impact on system state estimation planning or optimisation of DERMS.

1.4 Motivations

DERMS and ADMS of yesterday are forced to maturate into contracting idiocentric yet cooperative managements as costumers at low-voltage level are indeed ready to be Prosumers. On the surface, energy trading has transitioned from a rigid top-down management structure with centralised optimisation approach to a mixed-oriented (*i.e.* centralised and decentralised) with multi-layered transactive control framework that enables Prosumer-centric BTM administrations; Home or Building Energy Management System. In this sense, modelling of DERMS and ADMS as an aggregator in a single operating platform for in-house automated governance needs recognition. It is programmed to comprehend standards and policy compliances that can be useful to Prosumer individually or as a Community when providing grid services and market participations based on RDSO requirements. Likewise, convergence in game-theory mathematical modelling and decentralisation in DERMS aggregator are fundamental additives for Prosumer when creating cost efficient billing experience [97] to habituate; *(i)* optimal integration of PSPGs considering cyber-physical architecture and operational constraints, *(ii)* competitive yet cooperative peer-to-peer business models and value realisation, and *(iii)* self-optimised incentive-driven energy management that is flexible in supporting roles (*i.e.* ancillary and DSR services). Meanwhile, ADMS aggregator focuses in local protection system and feeder-based reliability optimisations to support RDSO in power flow and outage security in distribution network. The local protection system ensure fault generation from PSPG does not propagate upstream causing deficiency to other feeder-connected customers. In this sense, preposition for advance overcurrent relays that are equipped with better malicious tripping tolerance towards RES ride-through transients and immediate fault diagnose rectifications to isolate fault current with restoration capability. Whereas, reliability optimisations involves Volt/VAR compensation, peak demand management, over-generated baseload due to high PSPG penetration, and large power deviation in UC.

Meanwhile, despite having an optimised Prosumer-centric DERMS and ADMS aggregator, realisation in transforming Prosumer's electrical infrastructure into Nanogrid identifies the operating habitat for a single energy citizen. It comprises from local area network that connects with local PSPG devices and loads to cloud system framework for computational needs when ciphering optimise control solutions to establishment of communications beyond the meter. Its goal is to create a secured yet public accessible nano-scaled SCADA platform designed for Nanogrid system, bridging AMI and ICTI with cloud computing services to orchestrate data-driven functionalities in DERMS and ADMS aggregator. It also addresses concerns for data privacy and quality suitable in peer-to-peer sharing platform where cyber-attack vulnerability and operation BTM transparency must meet in the middle to navigate RDSO with necessary security planning and resiliency.

1.4.1 Fitting Prosumer into Transactive Energy Framework

The pivotal driver when conceptualising the control/management features for DERMS and ADMS aggregator lies within the Transactive Energy (TE) framework [98]. TE was popularised by Grid-Wise Architecture Council back in 2011 where growing discussion originated from the realisation in high demand for DER penetration at low-voltage level [99]. In view of TE system applicability to emerging challenge in DER integrations, it aims to built a community set of economic and control practices that promotes dynamic balance between supply-demand in the distribution infrastructure using value as key operational parameter. It can be viewed as two parts definition of TE; using value as key operational parameter for 'transactive' decision-making processes made through value-based exchanged information captured during transactions between Prosumers that is feasible across the entire power grid, from transmission system level to variety of Prosumers at low-voltage level.

In addition, involvement of governments initiatives in TE framework promoting market signal rebates for better investment returns can steer Prosumers to subscribe for cost-

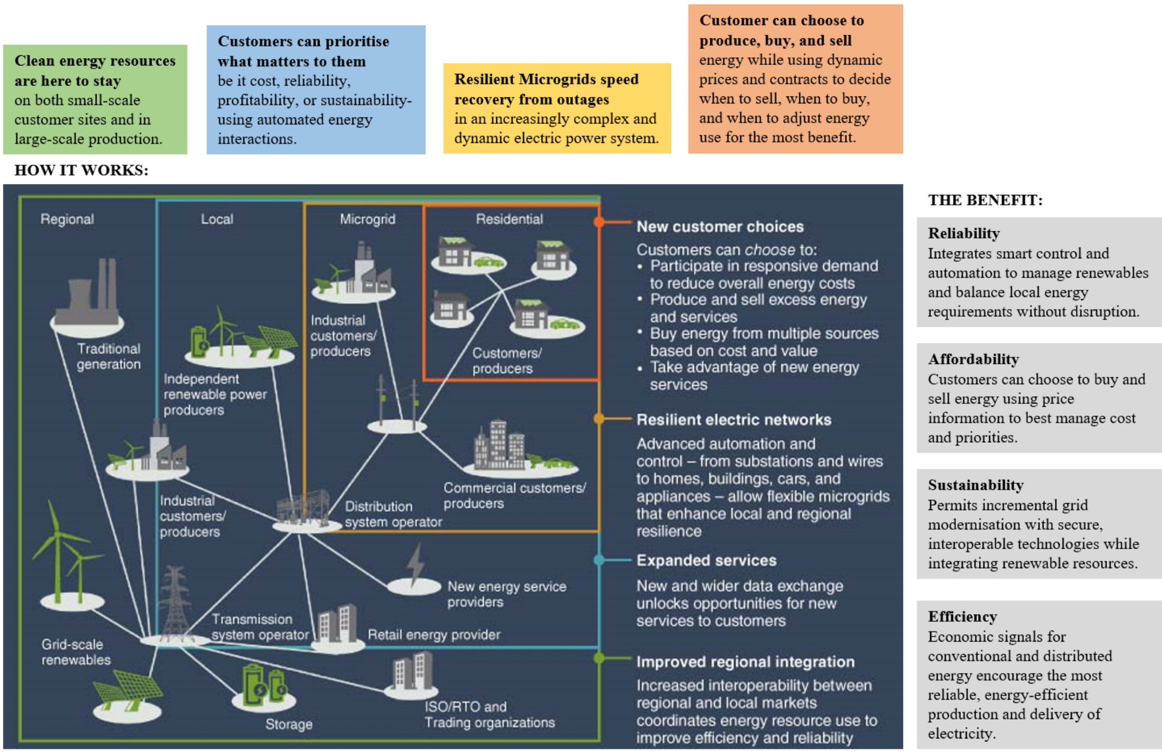

Fig. 1.8 TE values across all levels of the grid.

benefitting models on a levelled playing field. This includes bidding and selling of excess energy in spot market to long-term PSPG resource planning for capacity market. Fig. 1.8 [99] illustrates an overview of TE defined by Grid-Wise council and how values are assigned across all energy actors respectively. It advocates transparent energy prices that enables Prosumers to join traditional energy providers in producing, buying, and selling electricity using personalised automated control system that prioritises network reliability and operating cost-efficient.

1.4.2 Prosumer Communication and Monitoring Interdependency

The constitution of nano-scaled SCADA comprises AMI and ICTI setups, providing bidirectional IoT platform that preprocess metering information at Nanogrid's point of common coupling (PCC) for broadcasting and monitors PSPG, demand load, and other interactive devices status in real-time [100, 101]. The utilisation of AMI provides visibility into understanding social-centered analytics that enabled Prosumer to prioritise programs for optimal decisions/actions in a Community settings. The security of data transportation/management will only guarantee the success in gaining optimal solution as decision-making processes

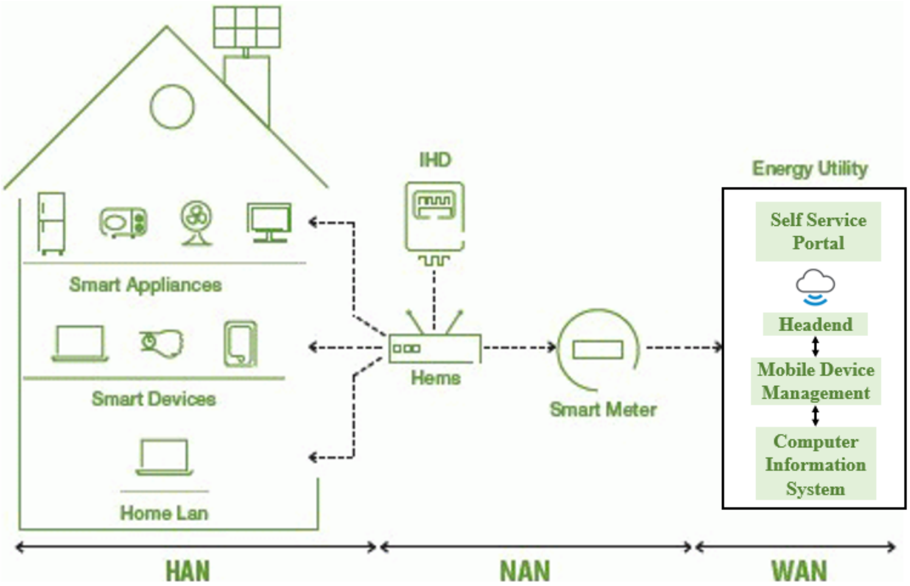

Fig. 1.9 Nano-scaled SCADA system using Nanogrid area network architecture for Prosumer empowerment.

are generally data-oriented. Meanwhile, ICTI provides interoperability of multiprotocol communication from diversified devices and data acquisition services [102]. Its focal functionality is to interoperate all communication devices under a single mainframe where remote automation commands are encrypted and decrypted for user access. Fig. 1.9 [103] presents AMI and ICTI set-up in Nanogrid for Community engagements, connecting local devices to other energy actors.

1.4.3 Sole Assigned Cloud Framework for Prosumer Use

Accompanied with nano-scaled SCADA, virtualisation on data structuring (*i.e.* storage, sharing) and computing platform using IoT cloud-edge services is key in imparting intelligences into any operating system. Using edge computing settings, also known as fog computing, provides Prosumers with improved response time and save bandwidth as computation and data storage are brought closer to operating sites, Nanogrid. It ensures measured data commitments are organised peripherally, curtailing network congestions or falsified data content transfer crises. Moreover, subscription cost and maintenances significantly reduced as physical machines are not dependant on network size; quick scaling of provisioned instances, data mapping, storage automation, and reserving more leeway for high-computing server capacity as compared to centralised cloud system connecting to millions of devices [102].

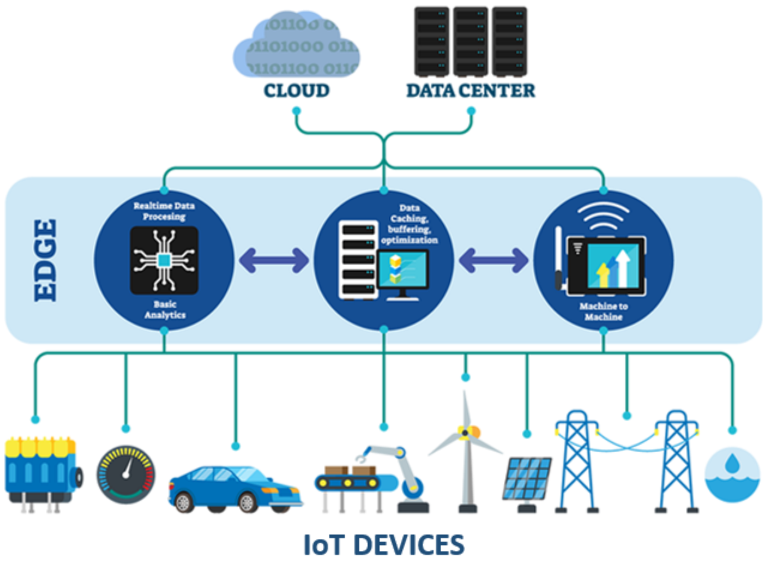

Fig. 1.10 Cloud-edge computing architecture.

Figure 1.10 [104] presents the architecture of edge computing that be applied for Prosumer use, connecting IoT devices with computing intelligences.

1.4.4 Consideration for Highly-Coordinated Intelligences

These monitored data from IoT devices will then used to perform reliability and resiliency assessments using learning-based computing algorithms (*i.e.* either off- or on-line) to generate optimised solution, schedule, actions (actuator) during normal or abnormal Nanogrid operations. Decision processes such as heuristic search, knowledge-based, and probabilistic machine learning are no stranger towards Community-based optimisation; minimising search space, increase operation certainty, and cooperative yet competitive. Moreover, decentralised computing will be ideal to accommodate growth in Prosumers and avoid high order functions when using centralised approach. Thus, research efforts into constructing time-critical big-data engine architectures and costs minimisation data processing are in trend to justify reduced convergence response time using parallel and hierarchical computing approach while endorsing joint optimisation to limit storage and computation resources as proposed in [105–107].

1.5 Research Aims and Objectives

This dissertation explores into nanotechnology innovations, transitioning distribution energy security planning into Prosumer-biased flexible management that responses towards cooperative yet competitive energy services based on TE values. It provides autonomous authoritarian in DERMS and ADMS aggregator catered for Prosumer(s) to personalise and reap beneficiaries from TE-based framework operations as shown in Fig. 1.11. Prosumers' short-term planning expectancy will be reviewed in grid-tied engagements based on both spot and ancillary market opportunities. The suggested problem statements and propositions are formulated based on Nanogrid EPS, peer-to-peer electrification that recognises Prosumer(s) as sole energy citizen.

Novel intelligent systems are proposed to advance Prosumer Community energy hub for aggregatable Nanogrids. Modelled in a Prosumer-centric domain, the proposed decentralised DERMS and ADMS aggregator modular systems will act as the primary regulator. Its ideology is to promote TE values and relief DSO-TSO from; *(i)* BTM complexity for whole system DERMS optimisation and DSR managements at low-voltage, *(ii)* centralised to

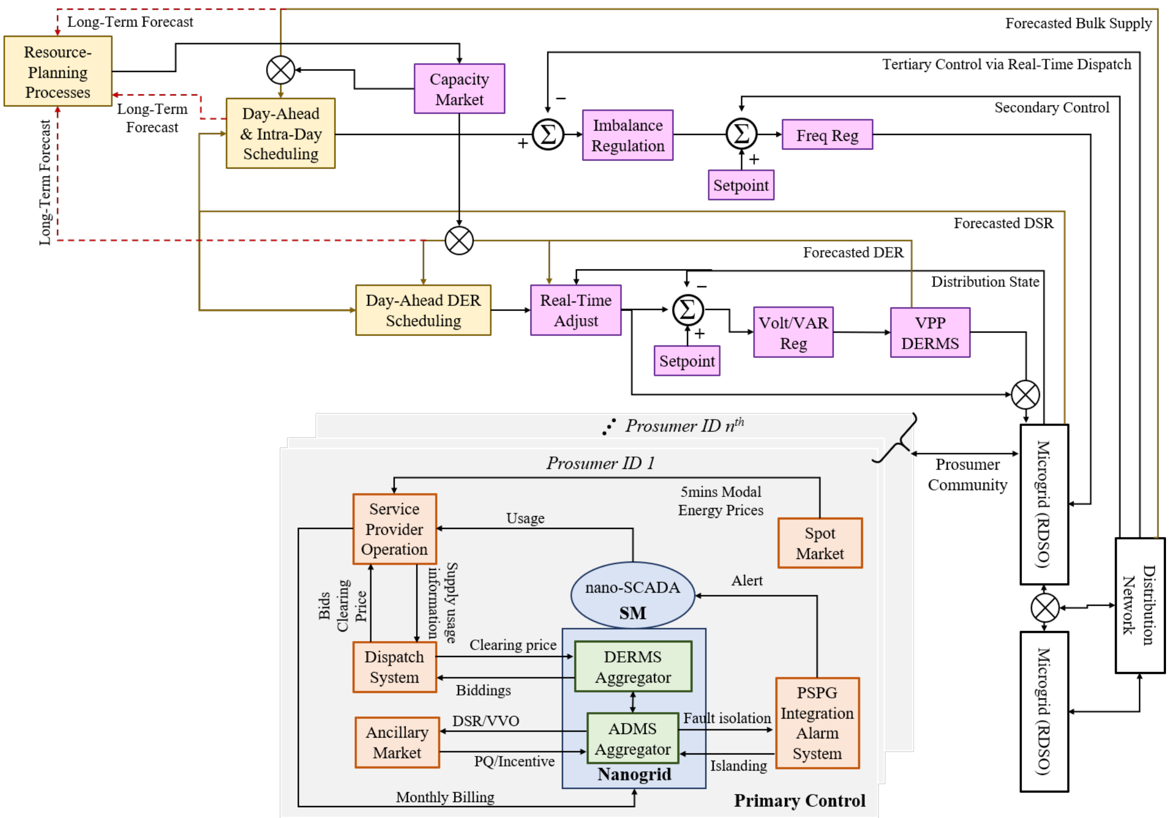

Fig. 1.11 Distribution network TE model; Prosumer Community engagements.

distributed ADMS support for systematised OMS (*incl.* islanding) with reduced fault-isolated customers, and schedule load shedding/shifting during supply-demand crises, *(iii)* scalability for millions of IoT devices and data management bottlenecks, and *(iv)* multi-participant chaos in the biding/selling of energy trading in the spot and ancillary market. Meanwhile, RDSOs focuses more on peer-to-peer, regional distribution network analysis facilitating $N-1$ contingency planning and day-ahead or long-term scheduling for levelled, reliable, and resilient power distribution. It also operate as a policy maker that steers Prosumer Community into incentive-based business models that support grid's stability and efficiency.

Bounded in a Nanogrid-based EPS, this research aims to validate the feasibility of:

1. *Prosumer-centric DERMS aggregator* controlled by MultiAgent reinforcement learning swarm intelligence using Q-learning algorithm and other subsidiary machine learning techniques under various operating environmental parameters involving local DER resource planning and load scheduling, cooperative yet competitive energy trading (sell/bid) in capacity-spot-ancillary market, and relief DSR crises through incentive programs. Thus, organisational structure of *involving energy actors' responsibility and roles are redefined* to fit in the TE framework along with its respective values.

2. *Prosumer-centric ADMS aggregator* targeted for in-house protection system which provides decisive isolation from possible fault interruptions transpire from PSPG and load shedding/scheduling intelligences. In addition, provide safe monitoring for *islanded operations*.

3. *Cloud-edge computing and nano-scaled SCADA platform* for decentralised and personalised data computing, storage, monitoring system immuned to quantity/latency limitations and computation divergences. It suggests to unload computational and storage stresses on main cloud interface with greater latency tolerance.

4. A *BTM full-suite modular platform* that hybridises DERMS and ADMS aggregator with TE value functions for an autonomous *in-house energy manager* unique to Prosumer's interests.

The objectives are to:

i model *Nanogrid EPS* comprising PSPG technologies and establish *nano-SCADA* using AMI in smart meter and ICTI for meshed-based area network. They are bridged with bilateral communications, control commands, computing intelligence, and data acquisition under a *single cloud-edge layer* that is equipped with data privacy protocols and high resolution low latency data exchange processes.

ii define control functions of DERMS and ADMS aggregator in *the layered decentralised optimisation for peer-to-peer TE operation modes*. Here, Prosumer Community takes greater roles in dictating energy security in distribution network while Utility focuses in secondary and tertiary control layers involving network contingency analysis and market participation respectively to ensure *energy monopolism or price discrimination are levelled* as not to obsolete or bypass existing energy retailers.

iii introduce acceptable error percentage trade-off for high computing speed *forecasting techniques* to solve renewable uncertainty operations, load consumption capacity curve, and profiling meta-relations that influence energy usage patterns. Hence, managerial proceedings can be attuned to achieve *optimal scheduling of available generation, ESS, and controllable loads* against electricity tariffs and incentives in real-time to solve DSR commitments/equilibrium.

iv formulate *computing intelligences based on Prosumer's business model interest* that provide optimum DERMS and ADMS aggregator solutions for cooperative yet competitive in Community environment. Strategic scheduling of BTM renewable, ESS, and controllable load capacity in response to *DSR constraints and peak load management, and TE markets*. In addition, arbitrate *bidding-abled competency* market participation (*i.e.* spot, capacity, ancillary) to yield high return on investment through bidding/selling optimisation based on incentive payout and electricity retail prices.

v administrate accurate *BTM point detection for fault interferences and perform autonomous isolation* protocols on PSPG to prevent cascading catastrophe on distribution network and malicious tripping of circuit breaker. Furthermore, cooperation of *intentional islanding operation* is incorporated.

1.6 Main Research Contributions

The main contribution is to devise a Prosumer-centric energy manger "platform" that highlights TE values, employing plug-and-play modular system that is equipped with nano-scaled SCADA and execute DERMS and ADMS as an aggregator in relations to RDSO's operational requirements. Despite having their control intelligences designed for Prosumer's Nanogrid EPS engagements, it should not be limited to Community (peer-to-peer) settings. It is expected that Prosumer Community will take larger presidency being the primary regulator in shaping DSR demographics, securing energy efficiency, and level the market economics as a cumulative creation, *"the power grid is only as smart as its consumers"*.

Subsequently, stimulus-response system is modelled based on IoT edge device cloud network with intelligent-embed Multi-Agent System (MAS) at respective Nanogrid for decentralised Community engagements. Agent of MAS are then modelled with TE values and organised based on level of importances decision-making processes for assembled DERMS and ADMS operations. Using data collected from nano-SCADA system, data-driven intelligence map inherent knowledges using artificial neural network considering model-reality mismatch when quantifying uncertainty and Prosumers energy usage behaviour. It then deploys dynamic programming technique for individual Nanogrid, employing MultiAgent Deep Deterministic Policy Gradient (MADDPG) reinforcement learning in DERMS and ADMS aggregator to create a cooperative yet competitive TE-based business model. The proposed reinforce Q-learning algorithm reasons decisive actions (policy) to meet Prosumer's energy usage interests from the joined critics (Prosumer Community) attained from MADDPG. The optimised DERMS dictate Prosumers' energy management strategies which includes scheduling of short-term forecasted RES and ESS against load consumption capacities in view of real-time retail prices.

Meanwhile, in view on ADMS aggregator operations, a fuzzy logic controlled Overcurrent Current Relay (OCR) device is proposed to serve as a BTM protection mechanism for PSPG. The proposed controller feature profiling and detecting fault direction attributes, locating fault origin and perform isolation processes. The algorithm is designed using expert knowledge characterisation reference to Nanogrid fault level and short-circuit current suitable for any type of RES integration at low-voltage where conventional OCR operation would failed to detect or maliciously triggered. In addition, it serve and an indicator for islanded operation, indicating upstream directional current flow reference at Nanogrid's PCC.

Detailed contributions of this research are as follows:

1. **Modelling comprehensive Nanogrid environment and formatting decentralised organisational structure for Prosumer Community and RDSO commitments.**

   i Decomposing distribution network into Nanogrid EPS with corresponding IoT infrastructure that will identify Prosumer as a sole energy citizen. The decentralised managerial operations of power distribution system is retrofitted, mapping Prosumer(s) as the primary regulator in provisioning TE values through personalised energy business model while DSO provides tertiary control dispatch focusing network analysis (*i.e.* distribution network optimization, protective device coordination). Meanwhile, RDSOs operates in a peer-to-peer domicile managing regional VPP-based DERMS and feeder-based ADMS to built community of practice in the area of transactive control and coordination.

ii Develop nano-SCADA using AMI and ICTI for local area network connecting BTM IoT devices and adopt flexi-edge cloud topology for decentralised data storage management and fog computing processes. Here, Microsoft Azure Cloud Platform is employed as the IoT base station system (close to end-user), accelerating computational processes using flexible/stackable modular structured drop-and-drag algorithm block functions from container registry. In a sense, to create an organised data-oriented environment efficient for data-driven intelligent system attached with data-sharing privacy protocols during peer-to-peer information broadcasting or hidden away for personal use.

2. **Modelling of Prosumer-centric DERMS aggregator based on various business models in view of TE values.**

i Establish a multi-layered Distributed Control Framework (DCF) that defines roles and responsibility of energy actors in their respective layer. It focuses in creating Prosumer-centric DERMS as an aggregator to RDSO in securing DSR and peak demand managements. The primary control in DERMS ciphers short-term forecast of BTM RES and optimum scheduling of ESS against retail electricity prices. It also characterises demand load and shed/schedule controllable loads corresponding to available generation resources and retail prices using demand load metrics (*i.e.* load factor, demand factor). The secondary control provides optimised portfolio management, solutions in peer-to-peer or upstream energy trading (sell/bid) to level market signals and reap economic benefits in Prosumer's energy billing. At tertiary level, the DERMS aggregator operates in a Community settings for long-term resource planning to support RDSO in optimising power flow and $N-1$ contingency planning. Here, MADDPG algorithm is employed to render cooperative yet competitive learning nature induced by it decentralised critic function and centralised state-action policy well suited for Community settings. From the bid energy capacity and price, the Q-learning algorithm transacts maximum TE values in relations to Prosumer's business model.

ii Provide Prosumers with forecasting tools to gain PSPG generation certainty for better scheduling plans in response to load demand capacity. A supervised Extreme Learning Machine (ELM) is employed to forecast PSPG energy generation and demand load consumptions. It is modelled based on qualitative technique with flexible forecast bias responses (*i.e.* generation: under-forecast, demand load: over-forecast) that uses less historical data with fairly reasonable percentage error (<15%) suitable for short- to medium-term forecasting. Here, it traded off percentage error with computational speed to meet 5-15mins forecasting intervals requirements. The need for high accuracy is not necessary as compensations can be rendered from ESS and controllable load management. Meanwhile, in market participation, Utility-owned DERs can compensate contracted generation capacity shortfalls in real-time. It is cheap to operate and maintain, and adaptable to changes in PSPG system responses (*i.e.* size, seasonal) as the forecast does not require large historical data; suitable for first launch product.

iii Provide clustering tool to weigh demand load consumption contribution/awareness for individual Prosumer among Community and add-on resilient in DSR services. Using data collected at AMIs, Nanogrids are clustered using Expectation Maximisation-Gaussian Mixture model (EM-GMM) to assign Prosumers into respective consumption attributed based Community. This allows RDSO to better plan long-term DSR operations, evaluating their energy trading attributes and participation in the market. In addition to EM-GMM, K-Nearest Neighbors Algorithm (KNN) and K-means clustering algorithms are integrated to characterise local demand loads into respective classes (*i.e.* fixed, shiftable, throttleable, instantaneous loads). It helps Prosumers to optimally schedule online loads (peak load management) to meet the desired demand load curve at respective time intervals.

3. **Modelling of Prosumer-centric ADMS aggregator for BTM protection system and support ancillary services in Community setting.**

i It focuses on accurate fault security assessments on PSPG, provisioning BTM protection, profiling, and isolation capabilities. An OCR with fault directional current detection is proposed to replace conventional OCR that often trigger maliciously due to renewable generation voltage-current transient profiles. Thus, using fuzzy logic system and defining its expert knowledge (*i.e.* membership functions, fuzzy rules), the proposed OCR is equipped with ride-through tolerance understanding operations of respective renewable system which strengthen accurate triggering of relay during fault interruptions or intentional/unintentional islanded operations. Based on the Nanogrid's maximum fault current level against PSPG operating current and current phase angle, it determines switching operation of OCR and provide comprehensive analysis for exact rectification. Such implementation prevent fault current to travel upstream and create a cascading power quality detrimental effect on the distribution network.

ii In Community settings, it provide ancillary services such as Duck curve and unit commitment crises for baseload and peak demand management. Participation in capacity market is primary objective and reap incentives to reduce Prosumer's energy billing. Meanwhile, it also provide feeder-based Volt/VAR optimisation to increase power quality and ride-through issues generated from renewable system integration.

The proposed DCF and corresponding algorithms have shown successful TE valued operations and gaps. Several proposed testbed systems were modelled representing various types of Prosumer's EPS environment and its business model using industrial and commercially available product specifications to view operational practicability in energy trading and distribution network stability. Several test cases were simulated to view comparative operational performances against other existing Prosumer-centric EMS methodologies, highlighting decision-making superiority for end-to-end operation of TE system and market commitments.

1.7 Dissertation Outline

The dissertation is divided into 6 chapters. The outlines of each chapter are as follows:

1. Chapter 2 - proposes digitalisation of Nanogrid EPS as a sole energy citizen (Prosumer). It modernises distribution network with PSPG system BTM integrations and nano-scaled SCADA implementation for local area network in cloud-edge computing system that establishes interconnection between local IoT devices and AMI with other energy actors. Case studies were proposed to view Prosumer Community energy trading engagements using greedy-oriented DERMS and their impacts on DSR managements without considering TE framework. Here, the obtained results will serve as the pivotal driver to recognise TE values and contributions as the prime energy actor in securing optimum power distribution systems.

2. Chapter 3 - explores into designing Multi-Agent intelligent systems using decentralized computing infrastructure, flexi-edge computing, correspond to TE control and coordination at respective layers of proposed DCF. Modelling of Agents' intelligent

functions is presented using Coopeception (Cooperative and Deception) Reinforcement Learning algorithm to view potential bidding capability in Community setting, suitable for Prosumer-centric DERMS aggregator engagements in DSR and markets operations. Mathematical modelling of Coopeception learning is discussed and tested.

3. Chapter 4 - models the Prosumer-centric DERMS aggregator in TE framework and evaluate operating performances in both Prosumer and Community setting using different business models as case studies. Here, the Coopeception (Cooperative and Deception) Reinforcement Learning algorithm is defined along with Agents' characterisation mapping TE control and coordination functions, and system constraints. In addition, demand load clustering program is deployed to comprehend Prosumers' socio-economic attributes in DSR and group them into Community classifications. The Agents' intelligent system were then tested on three case studies to validate the cooperative yet competitive learning regression of Agent's in view of TE values against DSR performances.

4. Chapter 5 - models Prosumer-centric ADMS aggregator that provides BTM fault protection for PSPG integrations and Nanogrid islanding indicator. Using centralised fuzzy logic system on deployed OCRs, the expert knowledge algorithm is modelled with fault current inferences to detect and perform characterisation. Moreover, fault current directional flow membership is also incorporated, providing decisional isolation processes using specified OCRs. The fuzzy logic system is then tested against momentary fault interruptions (symmetrical and asymmetrical) typically transpired during RES operations and refrained from malicious tripping of PSPG system.

5. Chapter 6 - concludes the dissertation, and provides future research directions that progresses further into power converter ride-through controller design that can improve integration/coupling security of PSPG.

Chapter 2

Nanostructuring Distribution Network into Prosumer-based Ecosystem

This chapter discusses on nanostructuring the distribution network into Nanogrid EPS to pave way for Prosumer engagements at low-voltage level as sole energy citizen. The Nanogrid comprises of BTM DER system integrations, PSPG, and digitalise local area network, Nanogrid Area Network (NAN), to extend communications, data management, and connectivity of IoT devices. Subsequently, explorations into hierarchical structuring of new service providers/operators into their respective operating boundary as an aggregator within the power distribution operation framework is presented to accommodate scalable penetration of Prosumers. Understanding Prosumers' socio-economical energy interests and possible market exploitations serves as a basis in defining respective independent aggregator's roles and responsibilities so that Prosumers are levelled on the same playing ground in community setting.

To visualise operational impacts on distribution network optimisation against uncoordinated Prosumers' DERMS aggregator and RDSO absence, simulation-based case studies of a 2-feeder distribution network testbed system involving 27 Nanogrid units is proposed. Investigations on DSR performances, Prosumers' energy billing, market participation, and distribution system state estimations against uncertain BTM DERs penetrations were evaluated. Moreover, review on power quality metrics and stability were presented to comprehend issues between high penetration of BTM DERs and performance of ADMS (*i.e.* Volt/VAR optimisation, unintentional islanding, fault isolation & service restoration).

2.1 Prosumer Existence as Sole Energy Citizen

Adaptations of Nanogrid-based distribution network involving smart homes/buildings operating at low-voltage level as sole energy citizen is only valuable to DSO if planned energy services from Prosumer Community can increase distribution optimisation globally. Dependency on grid-centric managements, centralised EMS and ADMS, regulated by DSO-TSO remains critical as existing modelled EPS infrastructure was designed not to carry power generation upstream from low-voltage level, a passive distribution network. It introduces regulatory impairments on network's stability as DERs in distribution network will have stronger power quality coupling due to inferior upstream power generation capacity, from grid-following to grid-forming. Table 2.1 [108] gives a perspective of BTM PSPG installation and energy usage in a Prosumer's EPS (Nanogrid), it being household or commercial building setting.

Thus, DSO-TSO needs to rethink new aggregative solutions that are decentralised and scalable to promote active administrations in view of Prosumers' energy subscriptions in liberalised markets. This call for organisational restructuring in the distribution network interlinked directives and introduce new energy service providers/actors as independent aggregator to set-up and contract regional settlements on behalf of Prosumer Community in the domain of market functioning which includes ancillary services, PtP cross-region energy trading cooperation, and high level of digitalisation protections. It aims to relief DSO-TSO from EMS and ADMS bottleneck complications when treating millions of Prosumers' energy behavioural interests and constraints while securing distribution system analysis, planning and optimisation in a centralised intelligent environment.

However, there are still many open questions to what are the control and coordination boundaries for respective aggregators in view of Prosumer Community participation limitations and billing compensations. How would aggregators retrofit into existing EMS and ADMS functionalities, providing add-on services to relief DSO-TSO engagements in relations to PtP energy trading and participation in liberalised market? What are the ruling measures when defining policies and regulations that can strengthen Prosumers' trusts in subscribing these aggregators; responsibility in protecting Prosumers from penalty fees while endorsing switching of service provider freely? Critically, what are the protective measures in ensuring communication between Prosumers and aggregator are digitally secured from external malicious threads (*i.e.* data-sharing privacy, data tempering)? In this sense, realisations in Prosumers' energy interests; business model choices and consumption trends are

Table 2.1 Power usage & BTM PSPG generation capacity of Prosumer during summer (estimated trajectory).

Home (24Hrs)	Usage (Appliances)	EV Charging	PV 5kW (rooftop)	Energy Storage	Other SPG
Rating ($\approx kWh$)	15.0−20.8	16.0−30.0 (Make Models & Mileage,km)	14.0−22.0 ($\propto$ capacity & weather)	13.2kWh,48V (2 sets)	Diesel Gen. (back-up)
Costs ($\approx \$/day$)	2.7−4.5	3.2−6.0 (O&M)	1.4−2.7 (O&M)	0.8−1.7 (O&M)	nil
Upstream ($\approx kW/day$)	nil.	1.4	6.1	3.8	nil
($/monthly) Gross Billing:160∼230, Savings:50∼100, Rebates:15∼40					
Comm. Building (24Hrs)	Usage (Machines & Appliances)	EV Charging	PV 100kW (rooftop)	Battery Size Storage	Other SPGs
Rating ($\approx MWh$)	0.214−0.336	0.16−0.24 (20 Charge Pt.)	0.23−0.28 ($\propto$ capacity weather)	0.35−0.67 (Container based)	0.1−0.3 (CHP, HVAC, μTurbine)
Costs ($\approx \$/day$)	42.7-67.2	32.5-65.0 (O&M)	75.0−140.0 (O&M)	40.0−80.0 (O&M)	65.0−140.0 (O&M)
Upstream ($\approx MW/day$)	nil.	nil	0.152	0.488	0.242
($/monthly) Gross Billing:6000∼8000, Savings:280∼500, Rebates:120∼300					

pivotal drivers in defining operation boundaries of independent aggregators as a new energy service provider in-line with TE framework and values.

2.1.1 Building a Community of Practices in Transactive Energy

Inclination interests for both BTM DER installation at the low-voltage and bulk DER integrations at medium-voltage have led compelling variability in demand-side planning. Furthermore, liberalisation in energy markets and digitalisation for Nanogrid infrastructure have forced operators to adopt stackable-ecotechnological offset mechanisms when securing power distribution system operations (*i.e.* distribution network analysis, planning, protection, and resources management). Since the rise of TE in the year 2011 till to date, research and industrial developments are still focused on strengthening TE's perspective framework and

Table 2.2 Operation attributes and principles in TE framework.

Attribute	Principle
-Objectives alignment -Socio-economical	implement high-level of self-optimisation coordination.
-Effectuate commodities -Fair mechanism & value	ensure non-discriminatory participation for qualified Prosumers.
-Extendable architecture	the geographic boundary must be adaptable, scalable, and portable for device-participant connectivity.
-Interoperability -Operation stability	reliable control features for system resiliency & reliability for optimal DER integrations.
-Spatial & temporal variability -Transaction data	system interfaces must be observable & auditable.
-Value assignment & discovery	transacting parties must held accountable for policy & standard compliance.

its credibility for future distribution network engagements [99]. Several pilot demonstrations have been initiated to serve as a learning experience program that views varying degrees and propositions that will benefit both sides of the meter, Behind- and Beyond-The-Meter [109]. In-line with organising of community practices and synchronising different TE values, the TE framework also interprets attributes and principles of TE system as a shown in Table 2.2.

Prosumers are constantly seeking for business opportunities that transcend full ownership in scheduling use of PSPG and demand loads. It includes having participation privileges during two-sided market clearing; assent PtP energy trading and auxiliary services. However, such propositions propagate DSO predicaments when Prosumer engagements increases exponentially; *(i)* monopolism in the electricity market and possible obsoletion from upstream generation; generation capacity from DERs have larger significance than Utility, *(ii)* provoke unsighted reliability issues due to stronger power quality coupling rendered by DERs, *(iii)* uncertainty in demand-side planning-optimisation and high volume market participants, and *(iv)* complex data management bottleneck in SCADA system for IoT device visualisations. Therefore, TE framework serves as a useful intersystem catalyst in preserving an interactive electric system that promotes decentralised BTM DER installation interests while securing DSO and market operating boundaries through high-level coordination from new energy service providers (*i.e.* independent aggregator). It serves as a mediator in collaborating multiple stakeholders; regulators, vendors, asset owners, policy & decision makers, developers, and customers in driving communal revitalisation and economic growth for reliable and cost effective distribution network.

2.1.2 Independent Aggregator as Energy Service Provider in Transactive Energy Framework

As an independent energy and market aggregator, it creates managerial gateways that interlink optimisation objectives between decentralised Prosumers' energy interests and centralised DSO security in view of transactive DERMS, ADMS, and market participations. Hence, Fig. 2.1 proposes two independent aggregators; feeder-based RDSO aggregator that contracts Prosumer Community engagements in-line with DSO operating boundary and, hybridised DERMS and ADMS aggregator only for Prosumer use. Following discusses the overview governing boundary of individual aggregators at their respective operating layer.

RDSO Aggregator

The proposed RDSO provides five feeder-based services for Prosumer Community connecting at a peculiar feeder:

1. *Promote cooperative yet competitive energy market*—participation for both aggregators and Prosumers in the market should be made easy. Moreover, Prosumers must have the flexibility and freedom to change energy supplier or transactive value programs-incentives of choice in real-time without facing contractual penalties.

2. *Participations are voluntary and provide diverse business model options for Prosumers*—Prosumer engagement with aggregators should be voluntary, that includes se-

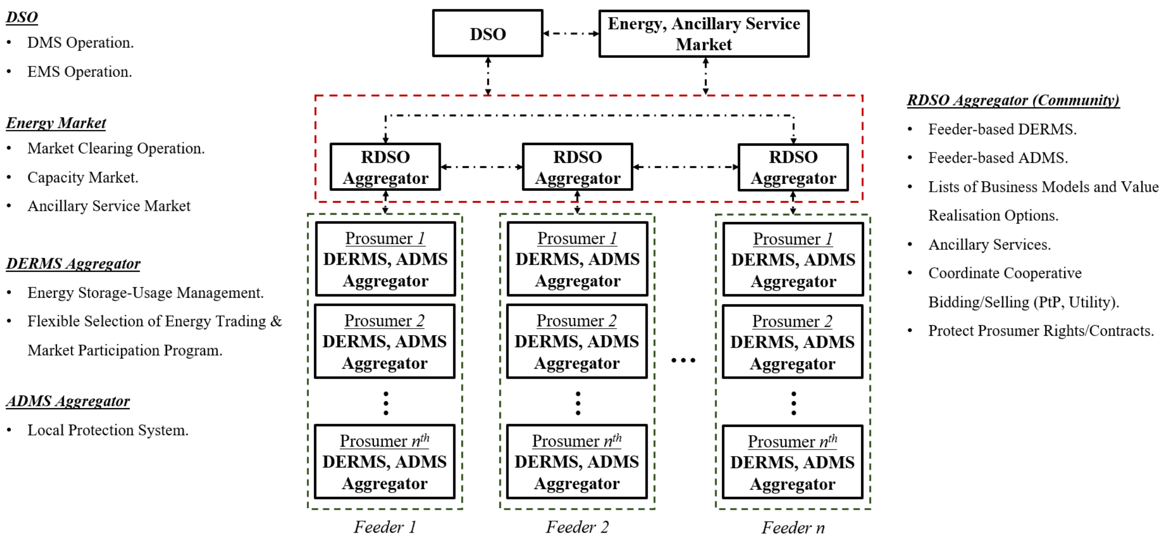

Fig. 2.1 Re-structuring distribution network management architecture with independent aggregators: Prosumer hierarchy of priorities in-line with DSO services.

lection from wide range of affordable and non-variable prices electricity offers/programs. Aggregators must able to contract tailorable offers that matches Prosumer's energy consumptions and lifestyles with clear, transparent, and agreeable to early termination of fixed-term contracts under strict terms and conditions. Lastly, EMA should be updated on aggregators entry into the market to facilitate market monitoring and intervene when there are indications of malicious in aggregator offers.

3. *Prosumers are only to reap benefits and flexibility*−Prosumers are to be financially remunerated for their flexibility in energy consumptions and savings claims must be reasonably awarded in lieu to the services rendered. Moreover, Prosumers should not be penalised for costs of compensation between market operator. In the case if required financial arrangements, it will be financed through the benefits collected by all market operators. Likewise, overall benefits from using flexible electricity consumption in view of lower system costs must be disseminated to all Prosumers through lower network costs.

4. *Policymakers and Regulators must co-exist across policy areas*−Security and liability policies should be updated, addressing possible threads/risks from aggregators when participating digital-sharing technologies in the energy sector. Collaborations with regulators across sectors address new complexities in what flexible electricity services will offer.

5. *Prosumers and aggregators should enjoy the same level of protection*−constant monitoring of personal data collection and processing should be subject to participant explicit concern and General Data Protection Regulation. In addition, Product Liability Directive must be extended to all products, digital content, and other services (*i.e.* message command & control). By default, connected IoT devices are protected by design and IoT PtP communications are legislated across sectors. Any product in the IoT chain should be liable for defects when product's activities have breached the market safety, including software applications.

Hybridised DERMS-ADMS Aggregator

The proposed hybridised DERMS-ADMS aggregator provides local services for Prosumer:

1. *DERMS: Participate in responsive demand*−take advantage of available business model options from aggregator's TE programs and execute scheduling algorithm for

BTM PSPG generations and consumptions according to contracted agreement, reduce energy billing.

2. *DERMS: establish nano-scaled SCADA system*−Prosumer will have access to a centralised monitoring and communication platform that connects local IoT devices with data security features installed. Prosumer also have the ability to remotely send commands and perform billing comparisons against other business models offered by aggregators.
3. *DERMS: facilitate participation in the energy market*−Prosumer has the flexibility to sell excess energy to selected aggregator or render available grid services in real-time to gain incentives. Likewise, buy energy from multiple sources based on costs and value.
4. *ADMS: BTM PSPG integration protection*−secure system integrity to avoid cascading upstream fault interruptions.

2.1.3 Realisation of Transactive Values for Prosumers' Demands

Energy identification of Prosumer involvements as a standalone EPS system or cooperative settings as Prosumer Community are initial process in creating operating environment for independent aggregator. Prosumer(s) is regarded as an electric customer that produces local power generation and consumes energy within the boundary of his/her domestic EPS, Nanogrid. It also includes an Energy Storage System (ESS) that stores excess generation or discharge for consumptions locally. Therefore, independent aggregators need to realise respective transactive values to promote Prosumer's participations in the TE framework, an operating platform where Prosumers' are authorised and rewarded for their value-based

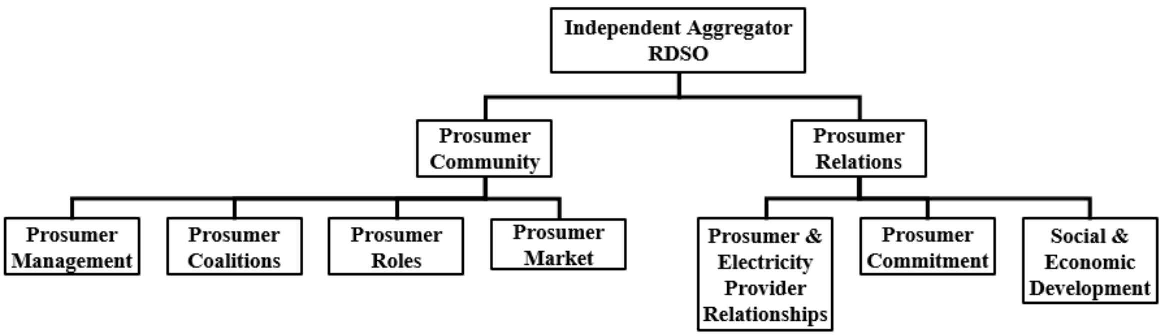

Fig. 2.2 Energy service provider appreciating transactive values of Prosumer's relationships and expectations.

approach in domestic energy usage and supply. Thus, Prosumer's relationships and expectations are divided into two categories Electricity Prosumer Community (EPC) and Electricity Prosumer Relation (EPR) as shown in Fig. 2.2, comprehending collaborative solution based on shared objectives while regarded as a value-adding actors in the energy value network.

Prosumer Community

There are four sub-branches under the Prosumer Community tree; (i) Prosumer's roles as a value-added proposition that drives sustainable and receptive energy system, (ii) effective asset management and resources planning to optimise local and global objectives, (iii) market design and prosumption schemas that evaluates respective Prosumer's involvements across the distribution network, and (iv) promote coalition legislation to render cooperative energy transactions based on global reliability interests. Following explains in correspondences:

(i) As an RDSO provisioning for global sustainable energy administrations, it has the ability to influence early stages of smart grid implementations employing peculiar intelligent control system, and business model opportunities [110]. It too serves as digitalisation aggregator in energy value chain that contributes co-creational managements [111–113].

Hypotheses developed for Prosumer roles need more attention in quantification validation on human behavioural factors [114, 110, 112]. Influencing elements such as billing rebates due to incentives, constitution percentage of consumer versus Prosumer, and flexibility to co-create cooperative solutions for long-term sustainability by compromising local commitments.

(ii) Prosumers' energy consumption demographics, behavioural organisation of lifestyle preferences, and motives for market participation are pivotal drivers for effective coordination in reinforcing unbiased ethics when jointing energy trading processes [115]. Formulating goal-oriented management programs, it being individual [116] or simple-group integration approach [117], can steer stronger synchronicity across independent aggregators through mutual business model offers on a levelised playing field [118].

Management schemes for Prosumer communities need more attention [115, 119]; considering passive consumer into the energy sharing equation, employ analytical techniques when grouping Prosumer's risk management induced by unfavourable behaviours, recognise energy efficiency programmes and incentives that reward Prosumers, and literate towards non-financial aspects when modelling business model.

(iii) Introduce Prosumer Market Platform (PMP) in the energy value chain using market-based prosumption schemas [120]. The PMP models facilitate PtP, Prosumer-to-Utility (PtU), Prosumer-to-Microgrid (PtM), and hybrid of both PtP and PtU [121]. On the basis, PMP adopts four transactive layers (*i.e.* Prosumer activities, value-adding services, ICT digitalisation, energy) to bind diversified intelligent processes which bring forth ecological community success [111–113].

Suggested in [113, 122], incorporating economic, politic, and social dependence elements into designing PMP can avoid risks of market monopolism or biased energy trading thereby advocating initiatives for continual improvements. In addition, aggregators must consider emerging algorithms that identify communities with the ability to transcend multi-player energy distribution within the same time frame.

(iv) Employing intelligent community gateway for wide-area communication, optimal coalition formation for Prosumer Community setting, can offer emerging socio-economic settlements using object-oriented problem solving regime [123]. It aims to globally facilitate balanced TE across actors while maximising Prosumer's interests. In this sense, historical data of Prosumers' energy behaviour and geographic profiles provide insights on formalising distributed optimisation problems into hierarchical framework based on high influential factors [122].

Common research direction mentioned in [116, 122] was assessing dependant intensity and reputation effectiveness in building sustainable Prosumer community groups. In this sense, data driven approach for decentralised energy trading strategies using Agent-based modelling scheme can gain deeper comprehension of Prosumers' strengths and weaknesses for a more robust coalition energy engagements.

Prosumer Relationships

On the contrary, under the Prosumer relationships has three sub-branches; *(i)* investigates Prosumer commitments that define participation enabling elements and promote acceptances, *(ii)* hybridising socio-eco-tech drivers for effective management/interaction in community operations, and *(iii)* healthy relationship establishment between aggregators and Prosumers in a circular process. Following explains their correspondences:

(i) Using PMP to generate market objectives and profile Prosumer's level of commitment in community [124, 125]. Support and increase Prosumers' confidences in subscribing aggregators. Transparencies in critical economical risks and compensations must be publish to give Prosumers commitment options. Thus, trusted and competitive business models tailored for Prosumer's energy lifestyle bring forth benefitting awareness and prevent stakeholder resistances [126].

Identifying social-economic commitment catalyst, long-term funding policies to boost sustainable community energy system, and decentralised regulatory qualitative approach, are key drivers to strengthen cohesive business relationships based on endogenous and exogenous functions [127, 128].

(ii) Endorse holistic thinking in view of economic, technological, and socialism impacts are significant drivers that can either serves as an enabler or barrier on Prosumers' participations [129–131]. It can steer social values, forcing trading or utilising electricity leaning towards billing security and even resort to islanded operation mode.

Resolving social-economic acceptability to educate Prosumers with high costs incurment due to technological advancement does not imply negative business decision. Hence, convincing collaborative propositions using holistic approach is suitable to heighten the communal relationship, entrusting aggregators to uphold fair play in the name of sustainability [131].

(iii) Establishment of aggregator-Prosumer relationship provides influential impact on demand-side security (*i.e.* DSR, DERMS, ADMS, SCADA). It is a reciprocal relation that contracts incentive and risk sharing to avoid biasness or objective conflicts therefore, deviating managerial perspectives from a linear ordering to a circular process of production. Realisations on agreed expectations from aggregator-Prosumer interests must align to gain "bilateral monopoly" [132].

Demand for participatory approaches [133] can mitigate biased decision-making processes reflected from retrospective interviews poised from provider-consumer relationship. Retaliation and compensation factors conspired from communal interactions can actuate unfavourable energy sharing patterns from Prosumers. Hence, joint production business models needs higher order of scrutiny that considers underlying behavioural risk evaluations.

2.1.4 Transactive Energy Policies and Standards

Primarily, the development of an ideal independent aggregator in TE framework revolves around the engagements of operation policies and standards, and recognising requirements/viewpoints that synchronises objectives statements for high Prosumer penetrations at low-voltage level. Likewise, it creates awareness in lieu of limitations and compliances for customer to voluntarily operate as a Prosumer. Through establishment of TE policies and preferred energy programs, aggregators can steer Prosumer(s) into a accountable course of actions with respect to DERMS and ADMS optimisations at demand-side (Behind- and Beyond-The-Meter). It aims to progressively update supply and demand demographics based on optimised DSR ruling while considering open market pricing and trading scheme in real-time. Policy setters has to indulge Prosumers' behavioural trends into the equation on how policies/incentives can influence confidence despite having to bear large investment costs on what is still remained uncertain. Serving as a guideline, there are four dominant pillars of state policy design based on the learning experiences gained from New York State Energy Plan [134]:

1. Mandate Utility to welcome new service provider and endorse TE management framework to mediate Prosumer penetration. Envisioned installation of DER systems in distribution network to take its presidency by year 2030 in gratifying 70% of national electricity consumptions. Thus, an aggressive $34billion funding (spread across 10 years) was approved to accelerate the economics for clean energy involving research and development, safe system integrations, subsidiary for private sector investment, and customer accessibility to own affordable renewable systems at low-voltage level.

   Policies: Clean Energy Standards (CES) [135] & Fund (CEF) [136]−Integrating Large Scale Renewables, DERs Oversight [137].

2. Prosumers have the liberation to select a list of independent aggregators (*i.e.* demand-side business proposal) to facilitate bidding-abled services, coordination and control functionality of local BTM DERs, and long-term investment assessments. In a sense, envisioning communal transactive values, Prosumers will be guided to contract tailorable business model offer while boosting their confidences in reduced energy billing and faster return on investments. Such program will attune operation obligatory namely; optimum consumption scheduler based on local PSPG status (*e.g.* ES availability either for storage or distribution), market trade tracking analyser and energy bill reduction, identifying online load patterns (*e.g.* shiftable energy loads or peak demand shaving), and comfortability (*i.e.* electricity usage lifestyle habits).

   Policies: Community Choice Aggregated Programs [138], Community Distributed Generation [139], Benefits of Net Metering [140].

3. Open up a hybridised market between energy retailers and Prosumer by extending wholesale into retail market region. Assignment of incentives and financial support from the governments must be made aware to Prosumers, setting a community-based business practices in retail market design that prevents biasness and monopolism. Subsequently, modelling of DER market that considers liquidity and social equity plans to boost general affordability can serve as a pivotal driver to transform consumer into Prosumer setting. Likewise, exploiting DER to assist in the capacity market is another avenue to provide ancillary services for Prosumer to earn rebates or limiting reliance on the Utility during time of energy crises.

   Policies: Benefit-Cost Analysis and Distributed System Implementation Plan [141], Utility Energy Efficiency Budget and Targets [142], Eligibility Requirements for Energy Service Companies [143].

4. Comprehending that RDSO aggregator are to be operated in a community transactive energy framework, initiatives in providing Prosumer with protective measures are vital to maintain trusting relationship between third-party services and participants. Protective measures against passive managed decisions and data sharing threads, notifying and consenting Prosumers' agreements in real-time. Hence, customer support services and transparencies on energy billing/trading needs greater accessibility for Prosumer to attune decision-making tools by interchanging objectives from time-to-time.

   Policies: Cyber-Physical Privacy and Autonomy Issues [144], Utility Rate and Pricing Structure to Respond to Customer Technology [145].

2.2 Problem Descriptions

Contrarily, the mathematical definition of a Prosumer must not be limited by its power generation capability but instead, functioning as a proactive energy consumer. Any customer at the low-voltage level who has the capability to extend communications and legislate active energy management at Nanogrid PCC based on TE-driven managerial proceedings needs to be labelled as a Prosumer; ability to contribute in the operation at demand-side reliability and efficiency [146, 114]. In this sense, customer as Prosumer includes either; *(i)* subscribe to a business model offer introduced by independent aggregator to achieve reduced billing and communal energy sharing experiences, *(ii)* optimise load scheduling operations (*i.e.* PHEV, ES, shiftable loads) based on energy market tariffs or shaving peak demand crisis, *(iii)* ability to operate in islanding mode, and *(iv)* secure load matching and Volt/VAR optimisation to prevent network failure. Furthermore, aggregator must consider all the customers connected to that particular feeder to meet communal optimisation problems regardless of the generation assets availability in respective Nanogrid. It calls for TE managerial schemes that consider Prosumers' energy attributes in clustered formation to render viable community services; *(i)* ability to sustain as an islanded Microgrid, *(ii)* optimise operation resiliency and DSR management using DERs for non-generation customers without burdening the bidding process in wholesale or capacity market, and *(iii)* render ancillary services to neighbouring Prosumer communities to gain higher profit margin.

Hypothetically, re-visitation into devising a TE system model for independent aggregator that fits mass operational perturbation induced by Prosumers' management options requires further reasoning into behavioural economics. Aggregators need to offer optimum supportive roles, commitments, and market functioning that will empower Prosumers' as independent manager. This includes issuing "mandatory" notices to all customers at low-voltage level to subscribe as Prosumers without intimidating economic discrimination despite minimal participation with aggregators. However, in view of Prosumers' expectations in deregulated REM and decentralise TE operations, aggregators are constantly challenged with entity identification reconciliation in big and open data that views distributed constraint optimisation in problem centralisation. Meanwhile, wide-area telecommunication system that uses centralised cloud computing architecture will face scalability predicaments and conflicts in data synchronisation due to bottleneck-latency bandwidth issues [104, 147, 148] and cyber attack vulnerability [149, 150].

Thus, scaling the distribution network into Nanogrid system creates stackable-based EPS that recognises scalable Prosumer penetration with encased nanotech-energy assets and independent governing jurisdictions. Innovations in layered middleware architecture that extends decentralised cloud computing are in-demand to breaks beyond limitations imposed by centralised cloud networks. Portability, device-to-software cloud service, and latency efficiency are key features that can bring cloud closer to Prosumers' smart devices and allow independent ruling of intelligent services. How will Nanogrid system influences in macro-managing and defining set of problems against Microgrid environment, developing stackable control structure with much greater application potentials? Will there be power system interoperability issues when coupled with Nanogrids?

2.3 Visualisation of Nanogrid Environment as Sole and Community Deployment

As consumer's EPS are no longer passive, viewing distribution network as a single management entity has been ruled out. Thus, Nanogrid planning was introduced in the early 2010s to synthesise smaller EPS jurisdiction [151, 152]. Pilot projects and research efforts exposed promising impacts on addressing grid-edge complexities into smaller analytical approach suitable for decentralise optimisation avenues. Bruce Nordman [151] popularised Nanogrid system as a solution to empower Prosumer's voice as new energy actor, *"Nanogrids offer the possibility of attaining a critical mass of technology, affordability, and familiarity to enable Nanogrids(Prosumers), and then Microgrids, to flourish".*

2.3.1 Defining Prosumer BTM Energy Mix Environment

Explorations into mathematical modelling of a Prosumer is proposed to comprehend respective interests environment defined in (2.1)-(2.10). Three peculiar combinations are proposed; full-pledge, load-only, and Prosumer.

$$Prosumer_{(full\text{-}pledge)} = PG \cup LD \tag{2.1}$$

sets are defined as:

$$\begin{gathered} PG \setminus LD = \{\sum_{i=1}^{n} renewable_i^t\} \cup \{\sum_{i=1}^{n} fuel\text{-}driven_i^t\} \\ LD \setminus PG = \{\sum_{i=1}^{n} appliances_i^t\} \\ (PG \cap LD) = BESS = \{\sum_{i=1}^{n} battery_i^t\} \end{gathered} \tag{2.2}$$

constraints $s.t.$

$$\min PG = \begin{cases} deny, & \{renewable_i : i \in I\} \\ deny, & \{battery_i : i \in I\} \\ allow, & \text{otherwise} \end{cases} \tag{2.3}$$

and $if\ renewable$ is a proper subset of PG then:

$$\min LD = \begin{cases} deny, & \{appliance_i : i \in I\} \\ allow, & \text{otherwise} \end{cases} \tag{2.4}$$

(2.1)-(2.4) denotes a full-pledge Prosumer's characteristics where PG refers to PSPG system with size-up battery energy storage system, $BESS$, and typical load appliances as demand loads, LD along the timeline, t. Full-pledge configuration gives Prosumer larger energy trading and utilisation options to facilitate optimisation of individual interests. Nevertheless, its risks in cost investments are high but greater dominance in enjoying incentives/rebates from DSO. Uniquely, constraints given in (2.3) and (2.4) dictates ESS element as mandatory for renewable energy mix to harness full potential of intermittent generation and maintain efficient flow of power.

Meanwhile, load-only Prosumer solely fixate on load and purchase scheduling management for reduced electricity billing defined in (2.5)-(2.7). Prosumer may experience lifestyle discomfort due to tense optimisation load management (*e.g.* shifting ,shaving) in DSR participation. Billing outcome is proportional to Prosumer's operational comfort level.

$$Prosumer_{(load\text{-}only)} = LD \setminus PG \tag{2.5}$$

$sets$ are defined as:

$$LD \setminus PG = \{\sum_{i=1}^{n} appliances_i^t\} \tag{2.6}$$

hence,

$$\begin{gathered} PG = \{\emptyset\} \\ PG \cap LD = \{\emptyset\} \end{gathered} \tag{2.7}$$

Subsequently, (2.8)-(2.11) defines storage-load Prosumer that reaps maximum benefits of ESS installations without PSPG. It aims to exhaust stored energy capacity and exploit electricity tariff versus demand demographics to optimise participation incentives and increase local supply-demand resiliency. According to (2.1), $Prosumer_{(storage\text{-}load)}$ is rewritten:

$$Prosumer_{(storage\text{-}load)} = (LD \setminus PG) \cup (LD \cap PG) \tag{2.8}$$

sets are defined as:

$$\begin{aligned} PG \setminus LD &= \{\emptyset\} \\ LD \setminus PG &= \{\sum_{i=1}^{n} appliances_i^t\} \\ (PG \cap LD) = BESS &= \{\sum_{i=1}^{n} battery_i^t\} \end{aligned} \tag{2.9}$$

constraint $s.t.$

$$\min,\max PG = \begin{cases} allow, & \{battery_i : i \in I\} \\ deny, & \text{otherwise} \end{cases} \tag{2.10}$$

and

$$\min,\max LD = \begin{cases} allow, & \{\cup_{i=1}^{n} battery_i, \cup_{i=1}^{n} appliances_i\} \\ deny, & \text{otherwise} \end{cases} \tag{2.11}$$

2.3.2 Defining Prosumer in Community Environment

Recognising Prosumers' diversified operational mix interests, (2.12) defines existence of clustered Prosumers into respective Community setting recognise by aggregators along the distribution network. Indeed, engagement of clustering formation approaches [153, 154] can provide optimal resiliency in DSR long-term planning for aggregators when piloting these communities based on their energy attributes. Fig. 2.3 illustrates a simplified example in demarcating Prosumer Communities, (2.12), using feeder line and clustering of Prosumer Community, (2.13)-(2.14), separated by substation across a typical radial-connected distribution network.

Assume: $A = Prosumer_{(full\text{-}pledge)}$; $B = Prosumer_{(load\text{-}only)}$; $C = Prosumer_{(storage\text{-}load)}$.

$$Communities_{(Prosumer)} = \{community_i : i \in I\} \tag{2.12}$$

$$\begin{aligned} community_{(Prosumer)} &= A \cup B \cup C \\ community_{(Prosumer)} &= \{\forall j \in \{A_1, ..., J\}, \forall k \in \{B_1, ..., K\}, \forall l \in \{C_1, ..., L\}\}_{jkl} \end{aligned} \tag{2.13}$$

not limited to:

$$community_{(Prosumer)} = \begin{cases} deny, & \{\ \} = \emptyset \\ allow, & \{A\} or \{A, B\} or ... \text{ any combi} \end{cases} \tag{2.14}$$

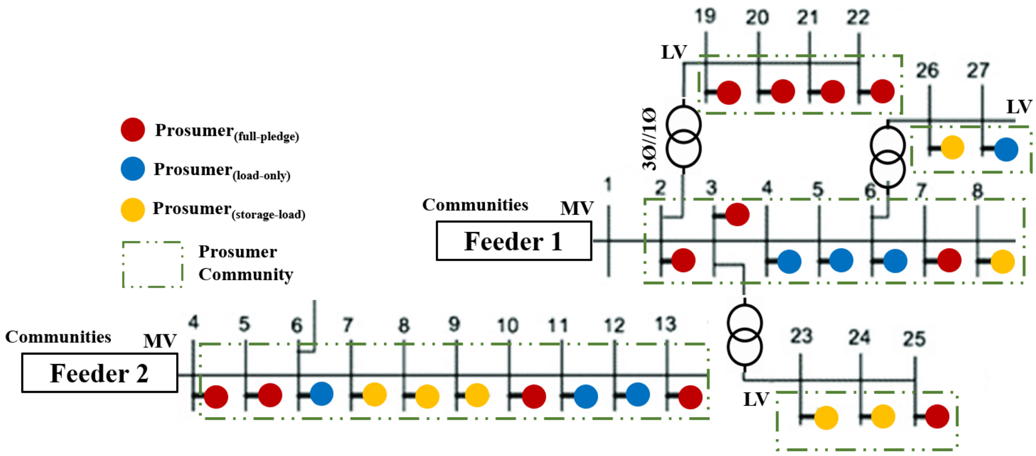

Fig. 2.3 Example of Prosumer environment mix in community setting clustered into respective energy attributes.

2.3.3 Modelling Distribution Network into Nanogrid Community

Unlike Microgrid, Nanogrid is devised to procure idiosyncratic-bounded EPS suitable to demarcate Prosumer's BTM grid connected assets. Nanogrid is best described as an electrical installation behind a single meter (*i.e.* AMI) while Microgrid aggregates Nanogrids under a single or multiple feeder together. Uniquely, it creates an environment for local DERMS and ADMS designed by Prosumer without the dependencies on central entity. Moreover, Nanogrid setting is not only limited to low-voltage level Prosumers but it broaden into medium-voltage DER owner (*i.e.* VPP investor, Independent Power Producer (IPP)) that

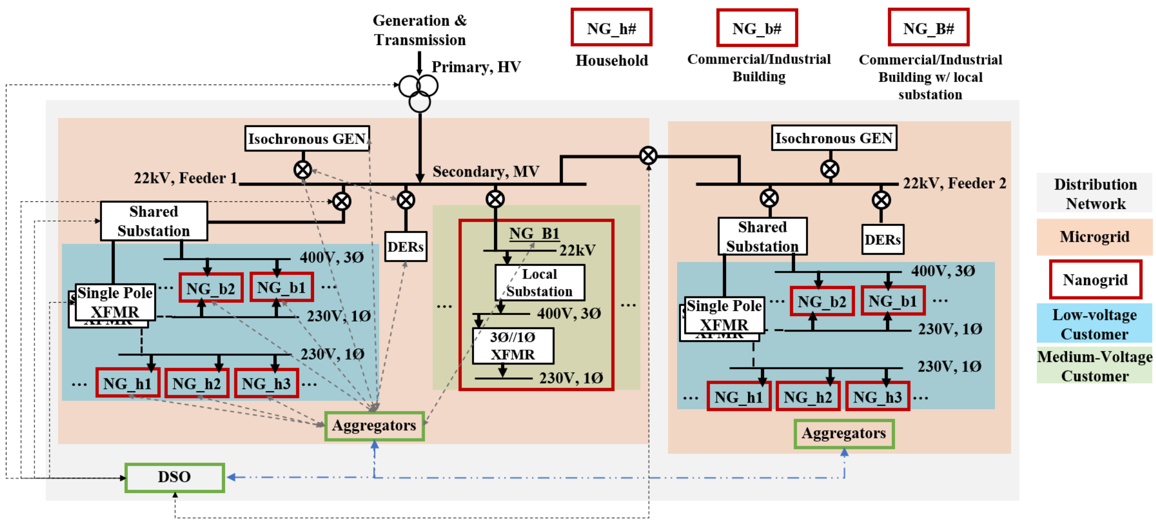

Fig. 2.4 Sectorising distribution network into Nano- and Micro-grid jurisdictions, feeder-oriented.

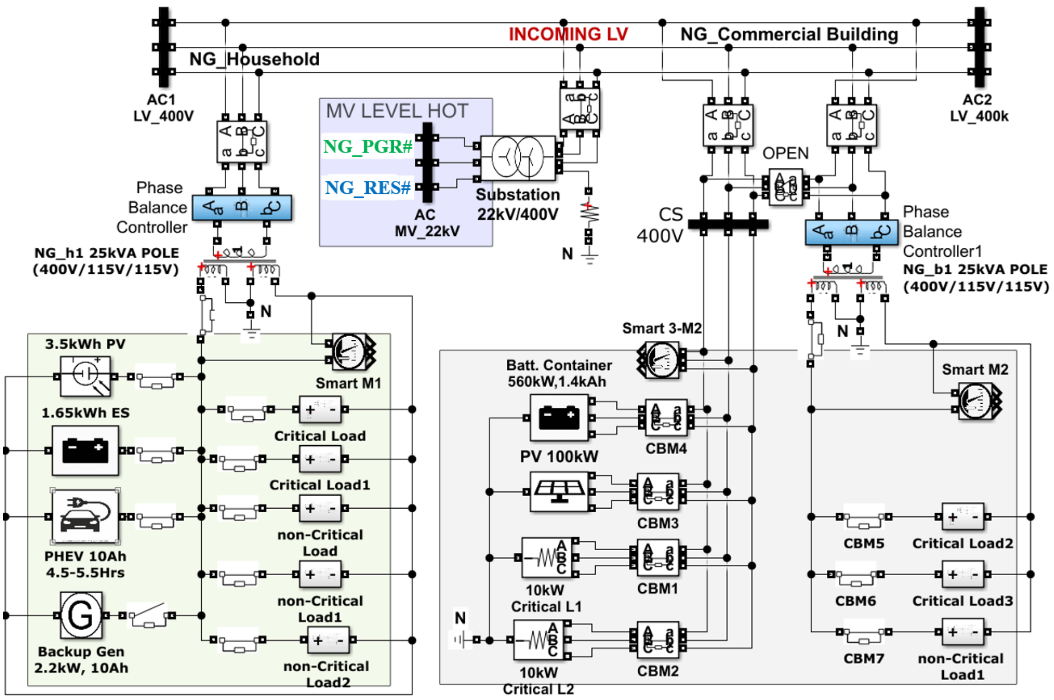

(a) Connecting household and building Nanogrid to distribution network; Prosumer-configured.

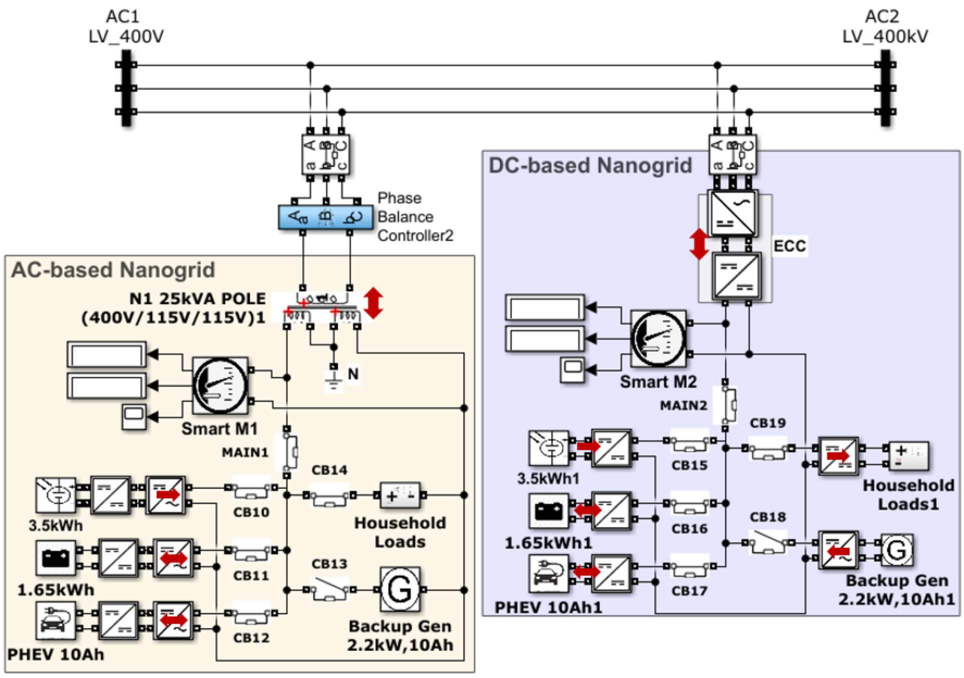

(b) (cream)AC- and (purple)DC-based configured electrical wiring for a Nanogrid.

Fig. 2.5 Definition and visualisation of Nanogrid implementations.

partakes in TE. Fig. 2.4 presents a multiple integrations of Nanogrids to form Prosumer Communities. Fig. 2.5a provides structural visualisation in Nanogrid BTM DERs integration where it comprises at least one load/sink of power, PSPGs, and AMI. While Fig. 2.5b presents two operating electrical system when designing Nanogrid EPS; AC- or DC-based wiring installation. (2.15)-(2.20) mathematically defines Nanogrid composition. Firstly, distinguishment between Microgrid and Nanogrid environment must be established as specified from (2.15)-(2.17).

$$NG_i = Prosumer_{IDi} = Single\ Electricity\ Meter \tag{2.15}$$

Initialise Microgrid = empty set, ∅,

$$Microgrid = \{NG_1, NG_2, NG_3, ...\} = \{NG_i : i \in I\} \tag{2.16}$$

$s.t.$

$$\begin{aligned} NG_i &\subseteq Microgrid \\ Microgrid &\nsubseteq NG_i \\ \therefore Microgrid &\neq Nanogrid_i \end{aligned} \tag{2.17}$$

where NG_i is identified as Nanogrid system behind an electricity meter representing a single Prosumer, $Prosumer_{IDi}$. Whereas $NG_1, NG_2, ...$ is a proper superset of $Microgrid$ acknowledging that every set of NG_i is a subset of itself, ($NG_1 \subseteq NG_1$), and every element of $Microgrid$ is not $\{NG_1\}$. Therefore, we can conclude categorisation of $Microgrid$ and NG_i are contrary. Subsequently, mathematical modelling of Nanogrid to represent IPP, Prosumer, and consumer EPS set-up are defined. Using (2.18)-(2.19) as the base components for a Nanogrid environment, (2.20) assigns Prosumer to respective Nanogrid based on configured operating interests.

$$NG_i = DER \cup LD \tag{2.18}$$

$sets$ are defined as:

$$\begin{aligned} ER = DER \setminus LD &= \{\sum_{i=1}^{n} RES_i, \sum_{j=1}^{n} TG_j\} \\ BESS = DER \cap LD &= \{\sum_{i=1}^{n} battery_i\} \\ LD \setminus DER &= \{\sum_{i=1}^{n} appliance_i\} \end{aligned} \tag{2.19}$$

Nanogrid assignments based on Prosumer operating classification:

$$\begin{aligned}
NG_{i(IPP)} &= ER + BESS \neq Prosumer \\
NG_{i(ProX)} &= LD \setminus DER = Prosumer_{(load\text{-}only)} \\
NG_{i(ProA)} &= DER \cap LD = Prosumer_{(full\text{-}pledge)} \\
NG_{i(ProS)} &= BESS + LD \setminus DER = Prosumer_{(storage\text{-}load)}
\end{aligned} \tag{2.20}$$

$_{(IPP)}$ denotes independent power provider that entails only generation and energy storage system. $_{(ProX)}$ represents a typical consumer EPS that omits out DER and ESS installations whereas, $_{(ProA)}$ connects DER, ESS, and load appliances. $_{(ProS)}$ describes a typical consumer EPS with an additional ESS operating as load and generation.

2.3.4 Advance Metering and Communication Infrastructure

Pairing IoT technologies with decentralised computing/communication network into tomorrow's distribution operations are indeed critical for Prosumer-Aggregator-DSO to perform transactive electrifications. The engagement of decentralised IoT Hub applications hold great influence into recognising unique business functions at each node with separate authority for independent decision-making power while constituting global interactions with other systems. In this sense, the IoT network able to distribute processing power and workload functions across multiple independent machines to provide a pool of resources. Moreover, scaling of network becomes easier due to it modular integrated stackable layers that increases decentralized computing resources. The issues with centralised IoT Hub or network in view of Nanogrid deployment are; *(i)* problems with future scalability plan to accommodate network expansion against bandwidth bottlenecks, latency response time, and bias in the estimation of parameters [155, 156], *(ii)* unable to create autonomy and control over local resources and computing process needs [157], *(iii)* risks of single point failure and less possibility of data backup which serves as critical information for historical data-driven computation requests [158], and *(iv)* higher risk in security and privacy breech with complex solutions in finding the source of thread [159]. There are instances where it is debatable to use distributed configured network over decentralised. However, in the context of proposed feeder-based Nanogrid Community configuration, decentralised IoT application will be suitable as it provides sole edge computing for Nanogrid(s) that corresponds to a centralised multi-layered IoT Hub synchronised by independent aggregators. Contrarily, predicaments such as vulnerability from third-party cyber intrusions and protocol authentications breech

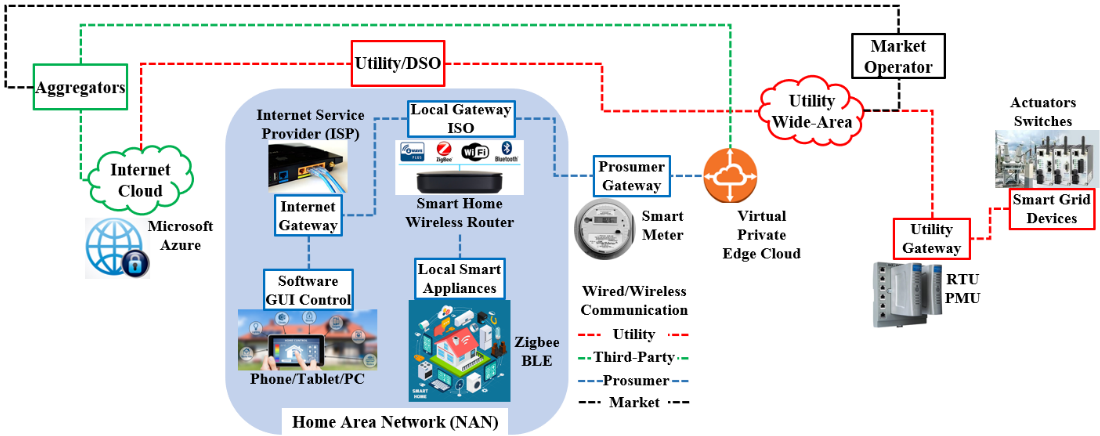

Fig. 2.6 IoT in AMI, extending communication gateways to external energy actors.

exposing non-authorised accessibility are critical malicious adversaries that require special attention for decentralised network as compared to centralised setting.

Here, the IoT infrastructure is incorporated into AMI for each Nanogrid system. AMI is a hybridised ICT-SCADA system that handles data storage and sharing gateways, computing and operating platform, and establish bilateral wide-area communication/command services integrated under a collective suite [103, 160]. It extends Nanogrid Area Network (NAN) communication gateway with independent aggregator and serves as a dedicated telecommunication layer that connects BTM IoT devices into a single metering system for smart function features. Its applications involve network encryptions, remote control commands, and dynamic information routing; a data aggregator that profiles Nanogrid's energy activities. Fig. 2.6 presents an overview of wide-area AMI that connects Nanogrid to external energy actors' internet gateways.

As the contribution of this dissertation were not focused on internet protocol suite, explorations into technical aspects of network protocol design is neglected. It assumes that all connecting appliances are meshed within a single network and interoperability compliances were observed using client-server or peer-to-peer networking model. However, this dissertation will briefly delve into big-data management and data flow traffics to facilitate cloud-based computing services. In this sense, distributed edge computing architecture and data acquisition point selections with low latency disruptions are reviewed to facilitate peak computational resources for intelligent system.

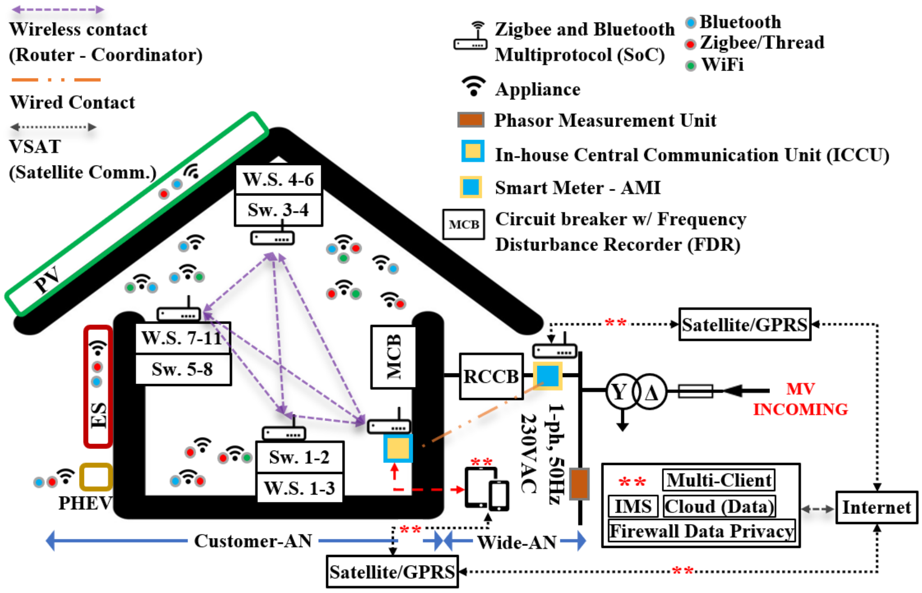

(a) Creating NAN, connecting IoT devices.

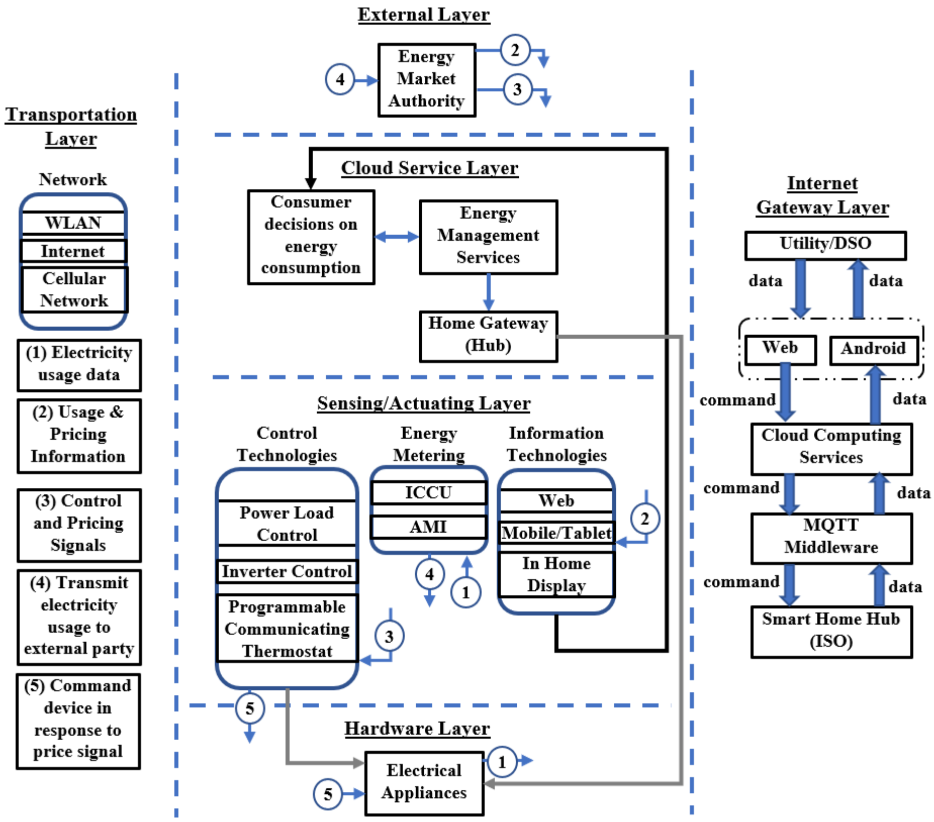

(b) Structural flow of data communication and device automation for ISO.

Fig. 2.7 Establishing IoT framework of NAN with independent aggregator gateway.

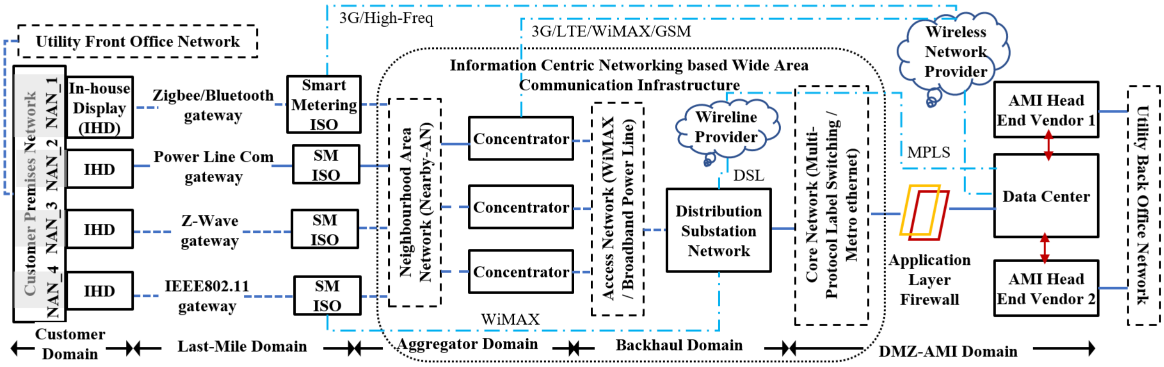

Fig. 2.8 AMI for wide-area Communication across EPS.

2.3.5 Modelling Nanogrid Area Network

Fig. 2.7a presents the proposed NAN system, creating layered networking domains to mesh Prosumer's IoT devices (*i.e.* BTM DERs and load appliances). The IoT devices uses dynamic multi-protocol Bluetooth Low Energy (BLE) and Zigbee connectivity, a new technology developed by *Silicon Labs* in meshing multiple wireless protocol for device-to-user-to-device communication & automation, and provide distant control via gateway [161]. It uses a wireless stack architecture that schedules prioritise-BLE beacons and Zigbee transmission to ensure simultaneous execution of multiple protocols within a shared radio access. All interactive appliances including smart meter are then synchronised to an In-house Central Communication Unit (ICCU) which collects monitoring data and processes real-time transactive energy solutions before sending decisional control commands using wireless-enabled handheld devices. Correspondingly, Fig. 2.7b illustrates proposed data flow and decentralise IoT edge framework interacting with aggregator's fog server node [162] to incentivise Prosumer-centric energy governance.

On the contrary, wide-area communication architecture of AMI interconnecting energy actors' gateways is shown in Fig. 2.8. Here, respective Nanogrid's fog computing server (*i.e.* edge computing) is then aggregated by Data Concentrator Unit (DCU) attached at strategic transformer poles or individual substations for DSO to extend data accessibility on a region of Prosumer Community.

2.3.6 MultiCloud Fogging for Coalition Computing

In view of big data transportations and analytics, on-demand availability of computer system resources are crucial in providing central remote servers for centralising storage, processing applications, and intelligences over the internet - "the cloud". Cloud computing have gained

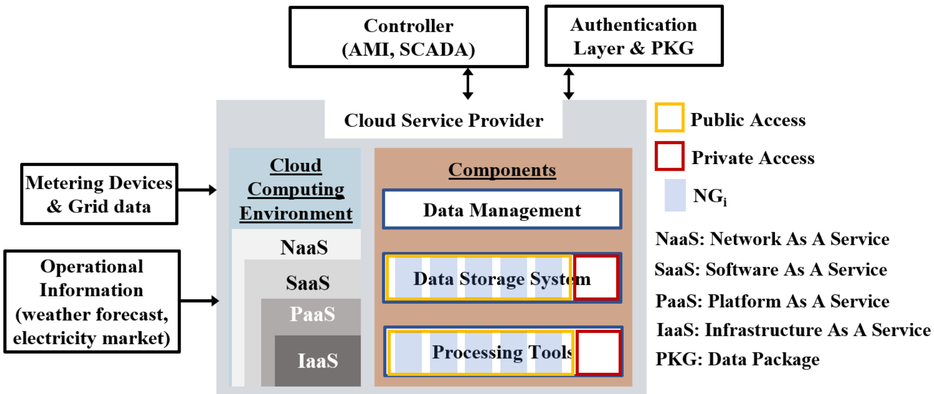

Fig. 2.9 Cloud computing architecture for hybrid data access.

full recognition in smart grid applications, designed as a service to give public the accessibility on computing resources.

Literatures [158, 159] highlighted advantages in adopting cloud computing technology; *(i)* govern data storage allotment, *(ii)* computational tools accessibility, *(iii)* data privacy with identity-based cryptography, and *(iv)* ability to pre-process data in offline or online computing. A high-level cloud computing platform that hybridises private and public is proposed in [158]. It is programmed with four cloud models as service option that allow cloud visitor(s) the freedom to share data/information space and processing tools; software, platform, infrastructure, and network as shown in Fig. 2.9. Nevertheless, complications such as data privacy and leakage can expose vulnerability to negative threads. Thus, [159] introduces Smart-Frame cloud computing framework that provides security features in parallel to client scalability. The key security feature employs identity-based encryption and proxy re-encryption schemes as shown in Fig. 2.10.

Fog or fogging computing is designed to perform analytic and management processes nearer to the point of data origin (metering devices and sensors) suitable for decentralised

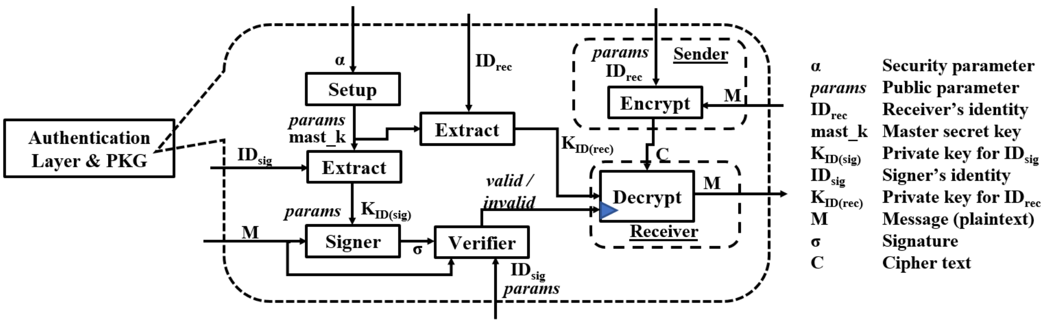

Fig. 2.10 Cloud data package authentication security.

systematisation; enabling accelerated data streaming, reduce bandwidth usage, and boost time-sensitivity [155, 156]. It opposes to a centralised cloud network where intricacy in data traffic coordination, single point security or outage failure, and latency versus scalability impairment are inevitable. Hence, one can view fogging as an extension of cloud that mediates collective integration of both data sources and devices to boost processing latencies and security efficiency. [155, 156] emphasised benefits in deploying fog computing nodes in the IoT mix to perform parallel computing, knowledge processes, and design data storage assembly at NAN's edge. As shown in Fig. 2.11, Fig. 2.11a presents the integration of edge computing in IoT. Meanwhile, Fig. 2.11b proposes fog computing framework that combines hardware devices and software operating systems for Nanogrid before merging into cloud.

Despite engaging decentralise fog computing for respective Nanogrid EPS, shortest-reliable data transferring path between fogging-to-DCU-to-cloud or determining optimised geographical location to place DCU (acquisition point) when serving Prosumer community require further analyses to address multi-hop communication processes in AMI. [163, 164] addressed the importance in deploying DCU nodes at effective places across the wide-area network. It employs optimisation model using near-optimal heuristic algorithm to access more remote devices with smaller quantity of DCUs considering quality of service requirements associated to mission critical and non-critical traffic. Similarly, [164] proposed an optimisation platform for DCU placement considering reliability requirement for data traffic and also minimised installation cost. Notably, when engaging matters on data transference

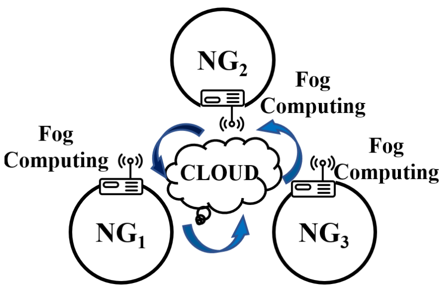

(a) Deploying edge computing for IoT-based Nanogrid.

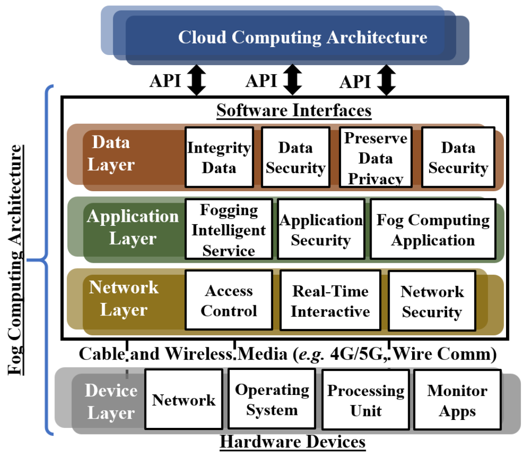

(b) Integrating fog and cloud computing reference architecture.

Fig. 2.11 Edge of IoT: Integrating distributed cloud computing environment.

latency in AMI, [164] addresses latency issues derived from power line communication network when communicating with AMI.

2.3.7 Modelling Community Cloud for Decentralise AMI

The deployment of multicloud computing in decentralised AMI is proposed in Fig. 2.12, employing three layered cloud architectural models servicing Prosumers, independent aggregators, and DSO respectively. Each group of hybrid fog computing is separated into primary (multiple) and secondary (single) cloud domains where the difference lies on accessibility features (refer to Fig. 2.9). The Primary Fogging (PF) is a dedicated public cloud assign for individual Prosumer use in designing personal edge computing algorithms to automate smart services in NAN. Intelligent service library and computational algorithms are made available for public access however, critical data sharing remains encrypted between PtP. Hence, cloud connectivity between Prosumers is not established to prevent data privacy breech and gain visibility in detecting cloud intrusion. Conclusively, PF cloud computing is integrated with NAN gateway to direct personalise transactive energy management govern by respective Prosumer's subscribed aggregator.

Contrarily, Secondary Fogging (SF) is a private cloud owned by the Utility that communally monitor and abstract data from respective NANs. The SF computing is interoperated in parallel with DCU, connecting substation's monitoring and control devices. It aims to administrate TE operations and market trading floor overseen by all aggregators, aggregator-to-aggregator cloud configuration. Ultimately, all fog computing clouds are collected at DSO

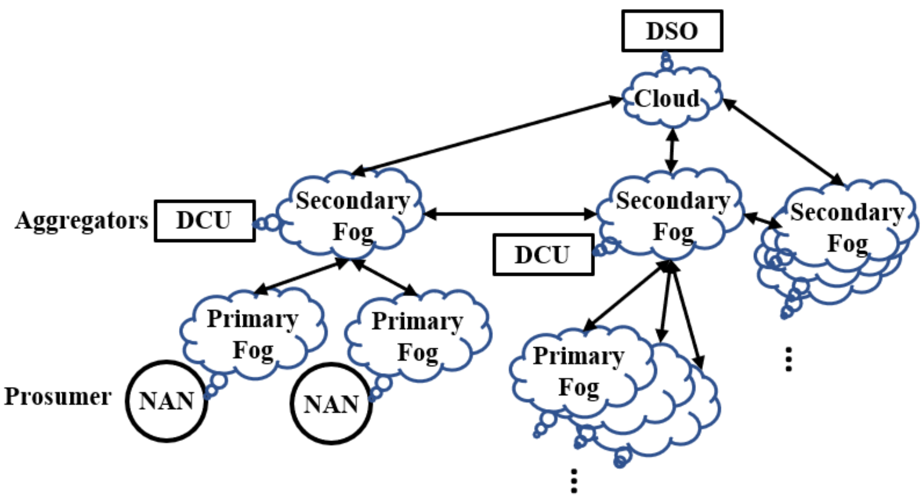

Fig. 2.12 Proposed edge cloud computing architecture in decentralised network setting.

centralise cloud. It is the only cloud service that endorses bilateral data source exchange with aggregators to procure global optimisation across the distribution network, ciphering solutions in Prosumer Communities domain.

2.4 Distribution System Assessments and Case Studies: Problem Identification

The distribution system analysis is divided into three assessments, investigating demand-side planning between DSO and Prosumers with the absence of independent aggregator. Proposed testbed Nanogird systems shown in Fig. 2.13a−2.13b for household and commercial building respectively, and small-scaled distribution network seen in 2.13c (2-feeder system serving 27 Nanogrid Communities with medium-voltage DERs). Each assessment evaluates TE economics and operational reliability-efficiency, and social consumption behaviour that steers DSO's EMS scheduling for DSR and ADMS resiliency when responding to both passive and active consumers.

1. Supply-demand (*i.e* load flow) analysis−review Prosumer's energy transactions in contra to BTM DERMS augmentation and electricity consumptions. Additionally, estimating Prosumer's daily operating costs to discern gross profit index without the support from incentive policies. Evaluating impacts on DSO's scheduling EMS and DSR management in securing supply-demand equilibrium based on respective operation constraints.

2. System's power quality and stability−steady-state, transient, and dynamic analyses were performed to view impacts of BTM DER penetrations on network's reliability and efficiency; DSO's ADMS operation. Determine consequences in voltage or frequency droop/swell and identify corresponding mitigation to regain voltage-frequency synchronisation. Operation of Nanogrid in islanding mode was also analysed to view its impacts on local and grid stability under grid-tied configuration.

3. Fault analysis−Investigate upstream and downstream fault interruption crises and how BTM DER (*i.e.* PSPG) operates under such conditions. Subsequently, operation under temporary fault interruption was also introduced to analyse PSPG fault ride-through transient against new power inverter standard for DER operation, IEEE1457-2018.

The following test case evaluations were discussed solely to address Prosumer's DERMS operations and their corresponding contribution towards DSO's EMS, ADMS, and DSR

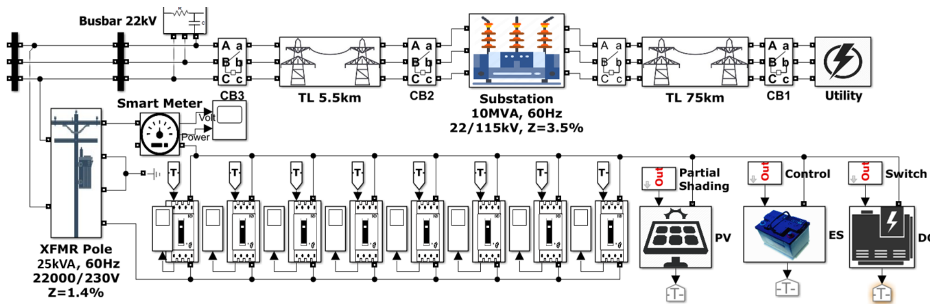

(a) Full-pledge Prosumer—domestic household.

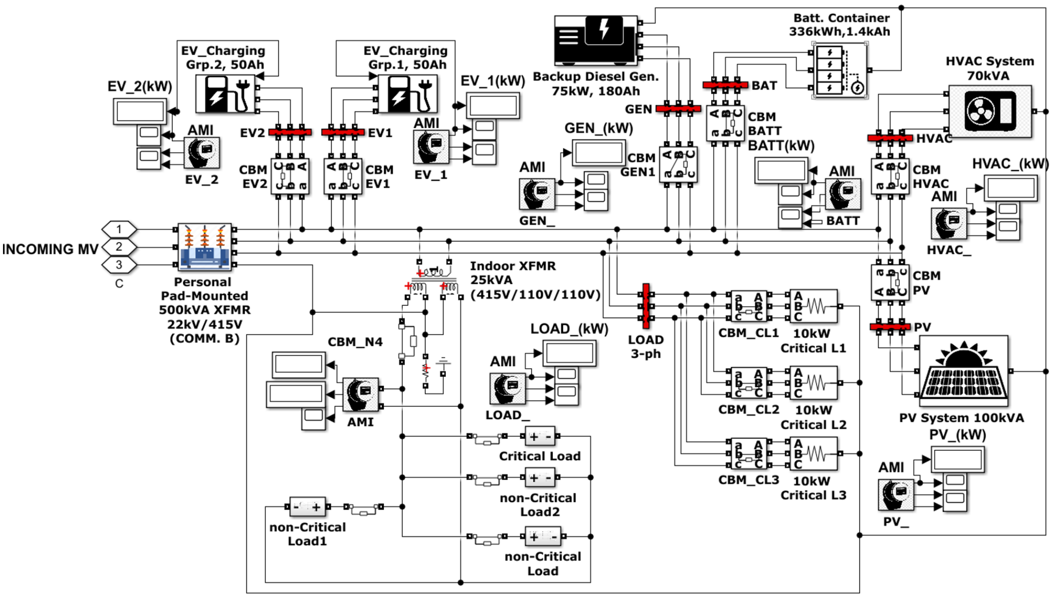

(b) Full-pledge Prosumer—commercial building.

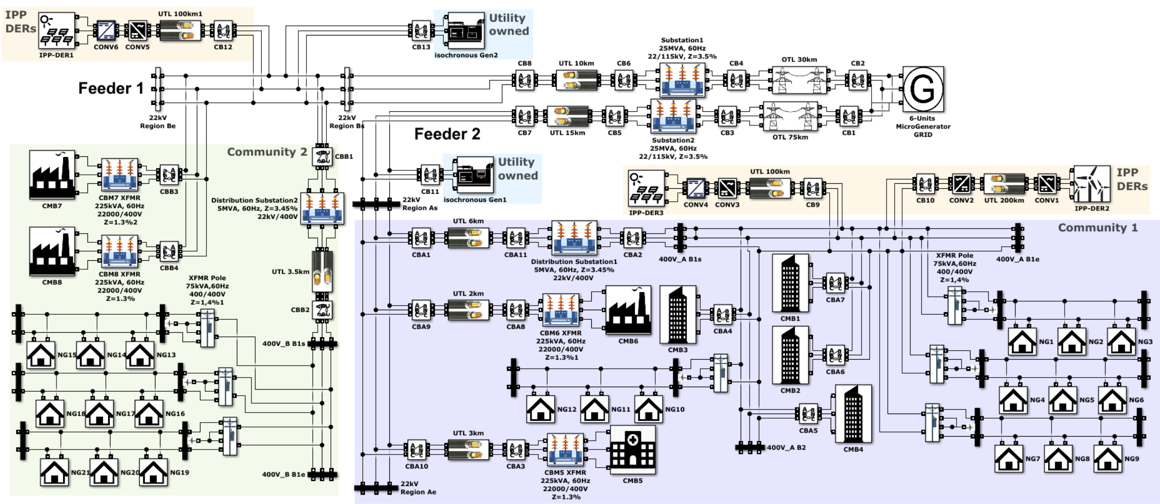

(c) Prosumer communities— joining 27 units of commercial buildings and homes.

Fig. 2.13 Proposed Nanogrid EPS testbed systems for test case studies in MATLAB.

regulatory-planning. In addition, implementations of non-optimised control intelligences were adopted to apprehend raw results that can be used for reinforced purposes. The modelled Nanogrid models in MATLAB were based on popular choice of PSPG systems (*i.e.* solar PV, ESS, PHEV, and back-up diesel generator). The simulations were conducted in phasor analyses domain defined at $60Hz$.

2.4.1 Energy Supply-Demand Analysis

Fig. 2.14 serves as the base energy consumption knowledge (24 hours sampling−12am to 12am) of passive customer in both single and community engagements. It provides DSOs with decisive information to schedule day-ahead unit commitment and anticipates peak or large demand shift crisis while levelling minimum loading of generation capacity to meet baseline demand. The data of demand load consumptions can be found in [141].

In view of load consumption profile in household environment shown in Fig. 2.14a, two peak and lull demand instances are recorded. An incremental of P_{demand} shift $\approx +\Delta 0.5kW/h$ was seen at 6am and $\approx +\Delta 0.38kW/h$ at 4pm, rising to its peak (four times greater) since $(t-1) \to t$. Likewise, there are also two demand dip instances that followed closely after every peak crisis, $t \to (t+1)$. It was recorded at $\max .P_{demand}$ decremental shift $\approx -\Delta 0.75kW/h$. In consequence, the grid's voltage experienced dipping and swelling due to abrupt increase and decrease loading of demand capacity respectively. However, the voltage level deviates within the safe "stay connected" region of $\pm 10\%$ mandated by IEEE Std 1547. It also brings forth no negative impacts when scheduling generation in parallel to generator unit operating constraints despite unregulated ΔP_{demand}, based on the impression of a single Nanogrid operations against unit-commitment ramping constraints.

$$P_{demand}\, shift = \frac{\Delta P}{\Delta t} = \frac{P_{(t_0+1)} - P_{(t_0)}}{(t_0+1) - t_0} \tag{2.21}$$

where rate of change in power generation or demand shift due time can be expressed as non-absolute delta. $+\Delta P_{shift}$ denotes incremental change and $-\Delta P_{shift}$ is decremental.

Typically in Community operations, DSOs will perform distribution network optimisation involving optimal power flow and DSR management based on optimum operating costs while balancing grid's constraints through cohesive scheduling of unit commitment and economical dispatch planning [165–168]. Hence, algorithms like heuristic or stochastic optimization functions to solve non-convex objective statements are typical avenues to better administrate demand-side EMS against operating constraints. Fig. 2.14b profiles Community demand load consumptions for 2 feeders distribution network. In comparisons to single Nanogrid demand

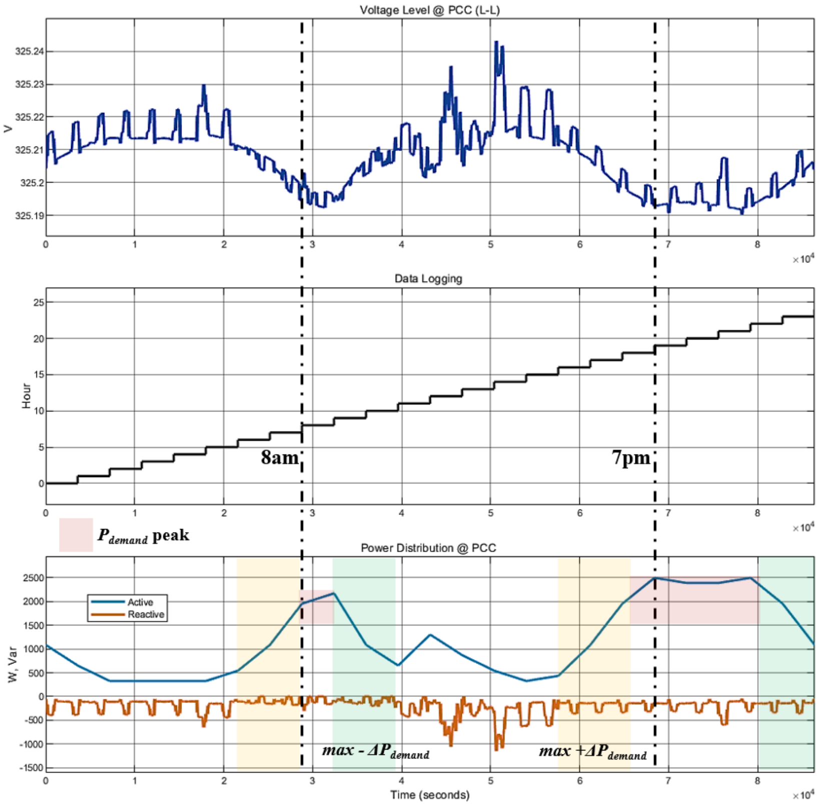

(a) Single domestic household.

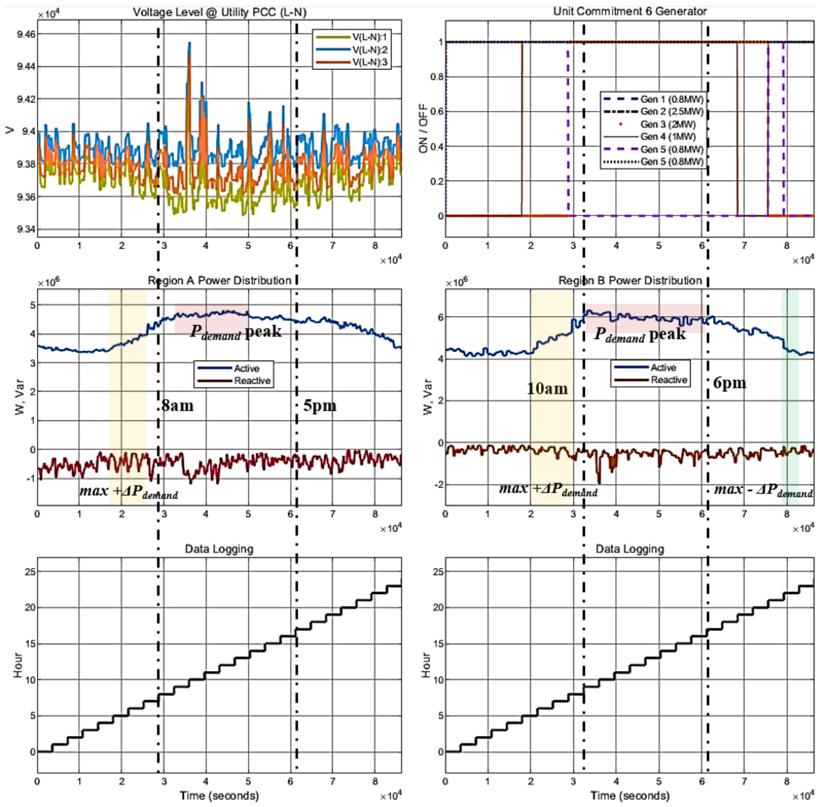

(b) Unit commitment for both Community 1 (Region A) and Community 2 (Region B).

Fig. 2.14 24-hours energy consumption profiles based on load-only (passive) Nanogrid system.

curve, Community provoked smaller slew rate index for $-\Delta P_{shift}$ and have better jurisdiction in scheduling baseline or energy shifts against ramp rate limitations. However, exposure to one instance peak crisis was recorded in the morning measured at $+\Delta P_{demand}$ >$0.735MW/h$. In consequence, DSO suffered major supply-demand imbalance where ordering of large demand shift at (t_0+1) intervals could not match generator's ramp rate limits. To overcome such issue, DSO adopts overforecast biasing on unit commitment that comfortably commits to large $\pm\Delta P_{shift}$. It sets to mobilise respective generators on standby, $(t-1)$, operating at spinning reserve to overcome ramp rate limitations during peak demand however, it has negative impact on operating costs. It can be seen that generator loading activities were seen at lull demand periods; generating unit 4 had an hour early start-up (operating in spinning reserve mode) contributing excess generation index of $\min.\ 102W/s \approx -\$2.33$.

Contrastively, in the case studies where full-pledge configured Prosumers were engaged, profiling energy demand trends have turned ambiguous. Based on direct control intelligence in directing DERMS for Prosumer's BTM PSPG and demand load, Fig 2.15 illustrates power exchange activities in both single and Community engagements. Here, the controller is deliberately programmed to maximise utilisation of battery energy storage charging and discharging rates. It exhausts maximum stored charge in battery contributed only by solar PV to serve local demand load while stores remaining generation available into battery within the State-Of-Charge (SOC) constraint boundaries [169, 170]. In the case if battery has reached its maximum SOC level, the excess generation will be distributed upstream towards Utility after meeting the full demand load capacity at time, t. Control algorithm:

$$P_{Utility} = P_{load} - P_{ESS} - P_{PV} \tag{2.22}$$

s.t.

$$P_{ESS} = \begin{cases} idle, & SOC \leq 20\% \\ idle, & SOC \geq 80\% \\ ON, & otherwise \end{cases} \tag{2.23}$$

AND *if SOC* $\leq$ *20; remain charge state until SOC = 40%* before activating discharging mode. $+P_{ESS}$ denotes charging and vice versa. Meanwhile, $+P_{Utility}$ represents energy flow downstream and upstream is negative.

Fig. 2.15a justifies Nanogrid's power exchange activities at PCC based on (2.22)-(2.23) employing $5kW$ solar PV system and $8.4kWh$ ESS ($240V$-$35Ah$ cascaded battery cells). Importantly, a negative power ratings was recorded approximately at 3pm to 6pm which exhibits that ESS have reached maximum SOC and excess generation will be distributed

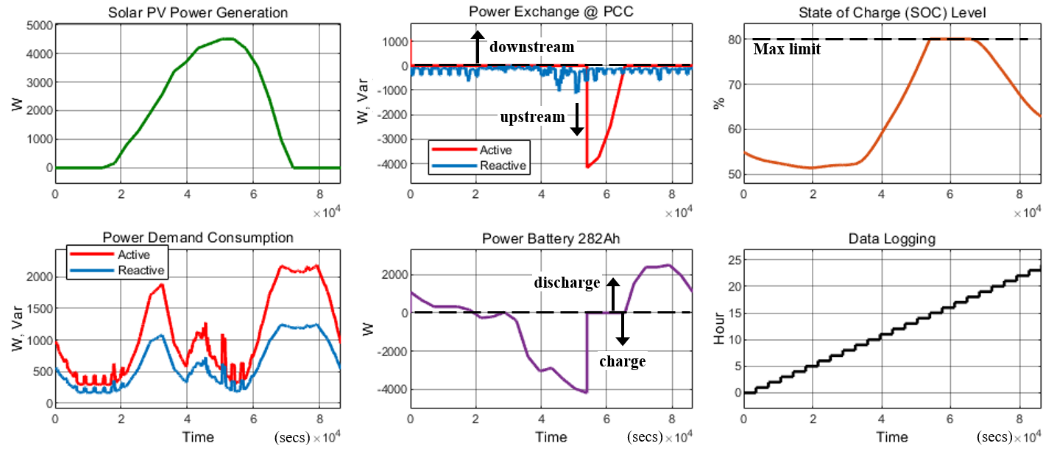

(a) Single domestic household.

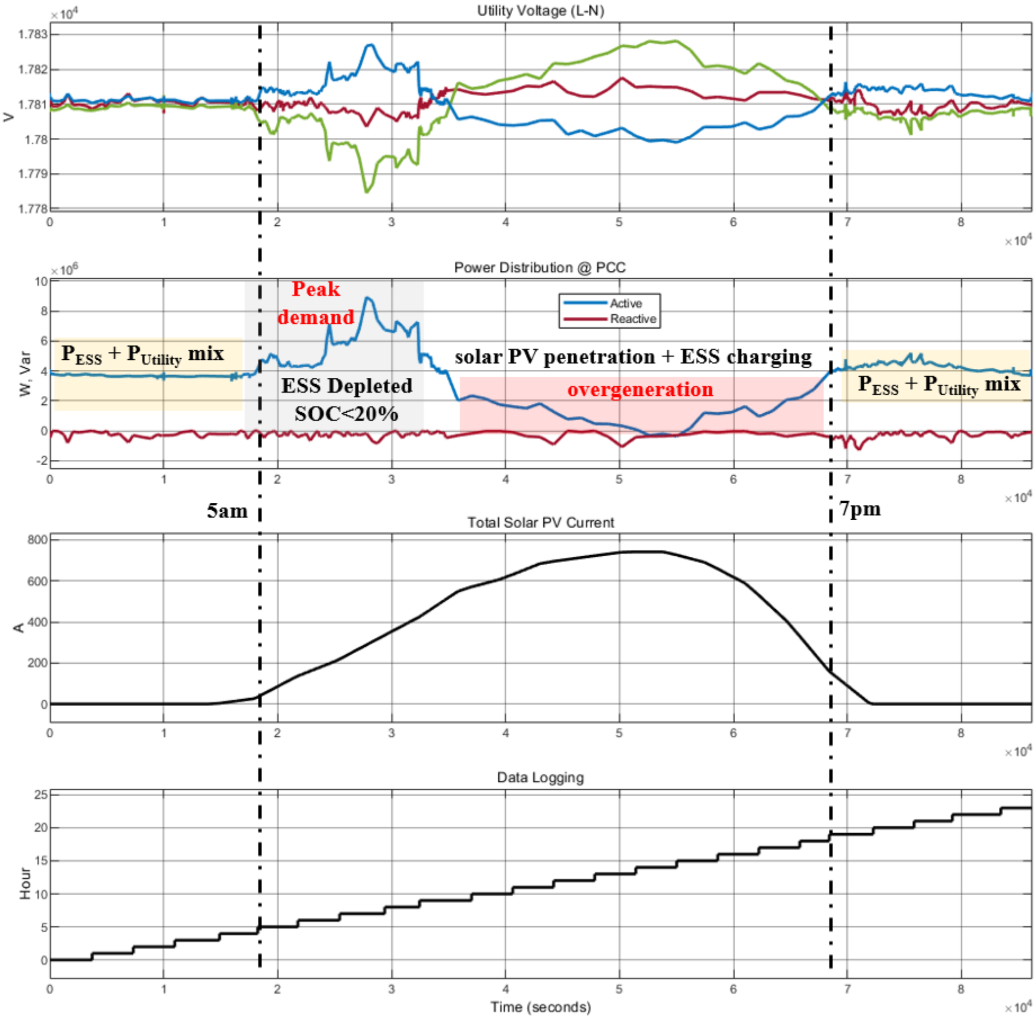

(b) Prosumer Communities.

Fig. 2.15 24-hours energy consumption profiles based on Prosumer (full-pledge) Nanogrid.

upstream. Meanwhile, the remaining timespan was measured at $0W$ downstream which entails Nanogrid managed to sustain supply-demand equilibrium without purchasing energy from external source.

In that sense, DSOs are faced with demand-side EMS predicaments where unit commitment for baseload and DSR becomes unregulated when legislating Prosumer in Community setting. Presented in Fig. 2.15b, the demand curve profile mimics a "duck curve" phenomenon [171] due to upstream overgeneration from solar PV. The term overgeneration also expresses baseload commitment crisis where power demand drops below base generation threshold capacity. Provided that all Prosumer's DERMS adopt similar control intelligences and ESS sizes in parallel to solar PV generation capacity, the downstream demand demographics becomes predictable. It imposes larger $+\Delta P_{shift}$ in the morning when compared to passive customer as stored energy in ESS has depleted. Likewise, during solar PV penetration, large $-\Delta P_{shift}$ and inferior baseline were presented. Such crises raised alarming concerns in possible collapse of grid due to generator's ramp rate limitations and failure to secure supply-demand equilibrium on time. Furthermore, more possible demand-side setbacks are yet to be incorporated involving; *(i)* surpass upstream intrusion where overall system's demand is smaller (*i.e.* generators at swing bus operating as motor or induce more reactive power), *(ii)* uncertainty in solar PV generation which resulted in misaligned scheduling of unit commitment to meet baseload capacity (unperceived day-ahead planning), and *(iii)* shifting of peak demand into indefinite time region due to contrasting scheduling of ESS's charging and discharging operations, commanding downstream or upstream power exchange with Utility.

The impact on energy economics reflecting on customer's consumption billing and PSPG investments also serves as an influential index when shaping supply-demand demographics. Events of peak demand or overgeneration could be closely related to electricity tariff patterns. There are three major electricity pricing categories in contestable/open market; fixed, peak & non-peak, and market clearing price (wholesale) contracts [173]. Table 2.3 compares customer's 24-hours energy consumption against electricity price to view economic benefits between active and passive consumer without incorporating motivations from government's incentive and subsidiary support. Hence, Prosumers are driven to formulate better DERMS controller to schedule charging and discharging of battery that correlates with electricity tariffs.

Table 2.3 24Hrs energy billing comparisons between active and passive customer without policy incentives.

Fixed Price 17.98c/kWh	Passive	Active
Billing Costs ($)	6.34	-0.88
Investments@10yrs ($)	-	4.28
O&M Billing ($)	-	2.91
Profit Margin ($)	-	-0.03
Peak/Off-Peak Price 7am-7pm:18.87c/kWh **7am-7pm:13.48**c/kWh		
Billing Costs ($)	6.27	-1.06
Investments@10yrs ($)	-	4.28
O&M Billing ($)	-	2.91
Profit Margin ($)	0.07	0.14
Wholesale Price [172]	Passive	Active
Billing Costs ($)	6.18	-1.62
Investments@10yrs ($)	-	4.28
O&M Billing ($)	-	3.32
Profit Margin ($)	0.16	0.2

2.4.2 Power Quality and Stability Analysis

Steady-state, transient, and dynamic stability analyses were conducted closer to individual Nanogrid, analysing impacts of upstream generation from BTM PSPG and its integrations. It aims to access Prosumer's feedback in securing power quality and weigh system reliability index at PCC. Fig. 2.16 illustrates typical transient responses at PCC for downstream power exchange. Here, DSO-ADMS governs the power quality supported by Utility (*i.e.* isochronous generators) performing Volt/VAR and switching optimisations by injecting or absorbing reactive power and feeder balancing with minimal power loss respectively. Such events occur when there is an abrupt shift in demand load capacity (*i.e.* weak DSR management) causing voltage to sag/swell or feeder-line overloading . Hence, Volt/VAR compensation controller and balanced feeder load transfer seen in Fig. 2.16 provide efficient restoration securing frequency deviation <0.0189 while voltage $<10\%$ from nominal level.

Conversely, with BTM PSPG penetrations, the power quality operation shifts towards the distribution network. In this sense, depending on the percentage of demand load capacity served by PSPG, the power quality coupling strength in regulating voltage and frequency level from Utility decreases as DER generation increases higher. Thus, power quality regulating system transit from grid-following to grid-forming, load following and compensation

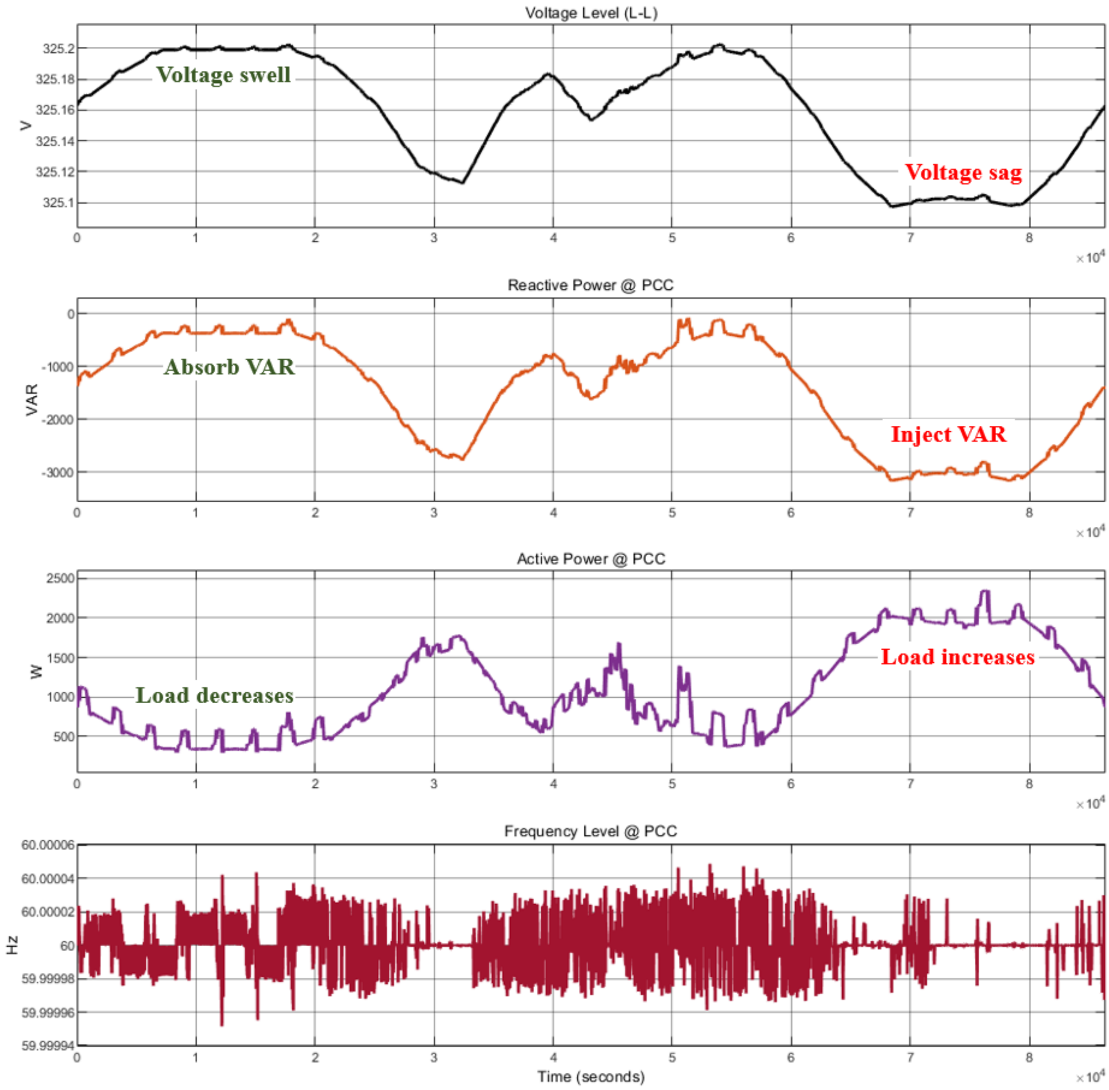

Fig. 2.16 Transient responses of Nanogrid directing passive-based customer.

responses from solar PV's inverter have a greater role in maintaining operational stability and quality. Fig. 2.17 provide visual validations in realising the importance of Volt/VAR control render by Nanogrid's solar PV inverter against Utility in relation to demand load capacity. The analyses were separated into 5 regions where different hosting capacity of solar PV, ESS and grid were initiated. In addition, the solar PV's inverter adopts PV-Static Synchronous Compensator (STATCOM) controller [174, 175] for Volt/VAR compensation control. To view comparative impacts on system stability, weak grid-forming Volt/VAR control was employed.

The results concluded that if Utility serves more than 70% of the demand load capacity, the Volt/VAR compensation uses grid-following operation otherwise employ grid-forming

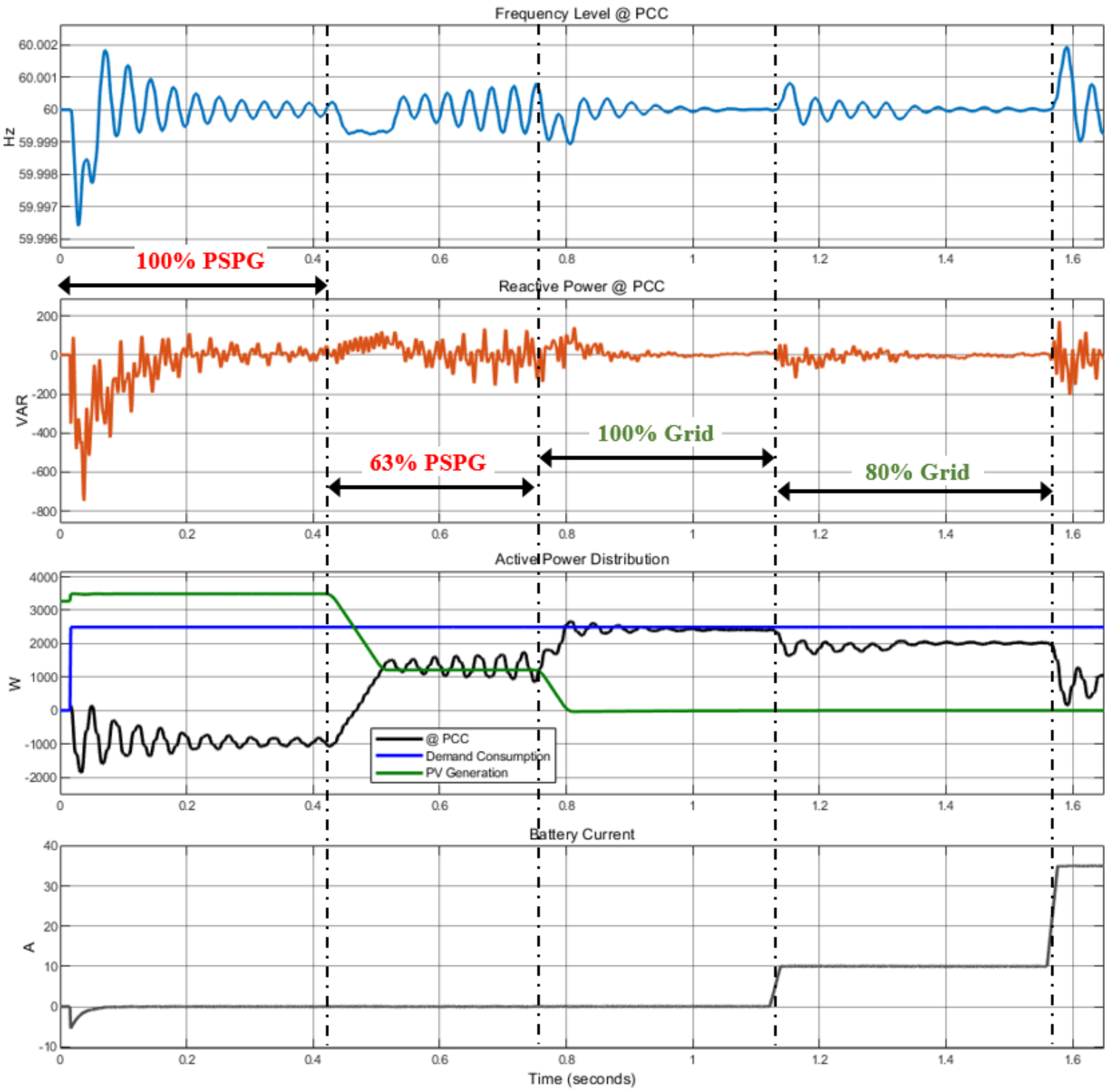

Fig. 2.17 Volt/VAR transient responses against demand load capacity in a Nanogrid: BTM PSPG and Utility hosting dependencies.

Volt/VAR controller (*i.e.* PV-STATCOM). Fig. 2.17 showed region 3 (100% Utility) and 4 (80% Utility), the active and reactive power transients converges with small settling time and minimal overshoot responses as compared to other regions. In this sense, higher DER generation distributed on demand load expanses inverter's role in securing voltage-frequency quality. Indeed, the voltage and frequency levels are oscillating within the safe region however, the results only demonstrate engagements of a single Nanogrid operation which yet to conclude for big-scale deployments. Further investigation showed that negative impact on system stability was recorded when deploying all 27 Nanogrids (Prosumer Communities). Moreover, power quality performances dramatically increases on PSPG's inverter in off-grid setting (*i.e.* islanding mode). Thus, BTM inverter's role changes into a grid-forming control operation where the design of Volt/VAR controller adopts droop control mode for load sharing in parallel-configured generation and existence of isochronous generator is mandatory which independently held constant with zero generator droop.

Diversely, in view of Prosumer interests for self-sustain electrification through optimum DERMS scheduling of BTM PSPG and local demand load capacity, Nanogrid can afford to switch into islanded mode (off-grid configuration) [176]. Islanding mode can be viewed in two categorises; intentional [177] and unintentional [178]. Intentional islanding serves as a viable solution during power quality crisis generated upstream which then can propagate into a prolonged power outage disruptions. Whereas, unintentional islanding are unplanned forming of Microgrid where power lines are still energised by BTM DERs despite network being disengaged from the Utility. Unintentional islanding rises much complications in voltage-frequency control or protection coordination which results in out of phase synchronisation with grid. Furthermore, with DER inverter's fault ride-through capability during recloser operation in circuit breaker can impose risk field personnels working with energised power lines. Thus, DER inverters must able to reflect formation of an islanding (anti-islanding) for operators to acknowledge that the feeder is de-energised.

Fig. 2.18 presents voltage-power behaviours of Nanogrid in islanding mode, shutting down all upstream generators at $0.55secs$. As expected, the Volt/VAR support from the grid has been isolated forcing PV-STATCOM (voltage-oriented control method) to take full responsibility in compensating both voltage and frequency droop/surge in parallel to demand load capacity. It manipulates current in the quadratic axis to order reactive power injection or absorption while direct axis controls the Maximum Power Point Tracking (MPPT). Alternatively, compensation of frequency droop can be stabilised using Freq/Watt function by increasing active power using ESS coupled at DC-link and vice versa. However, the PV-STATCOM has failed to perform full restoration on both voltage and frequency, generating high index of fluctuation due to larger demand load capacity against available power generation. The frequency level sags below permissible limit ($0.95p.u.$) and the voltage sags by 14% as it losses 30% of power demand capacity. Such phenomenon proved that in Microgrid setting, DER inverters are able to generate continual power generation while the demand load continuous to sag further. This rises much concerns for field personnels to perform power line servicing as excess power generation are distributing upstream.

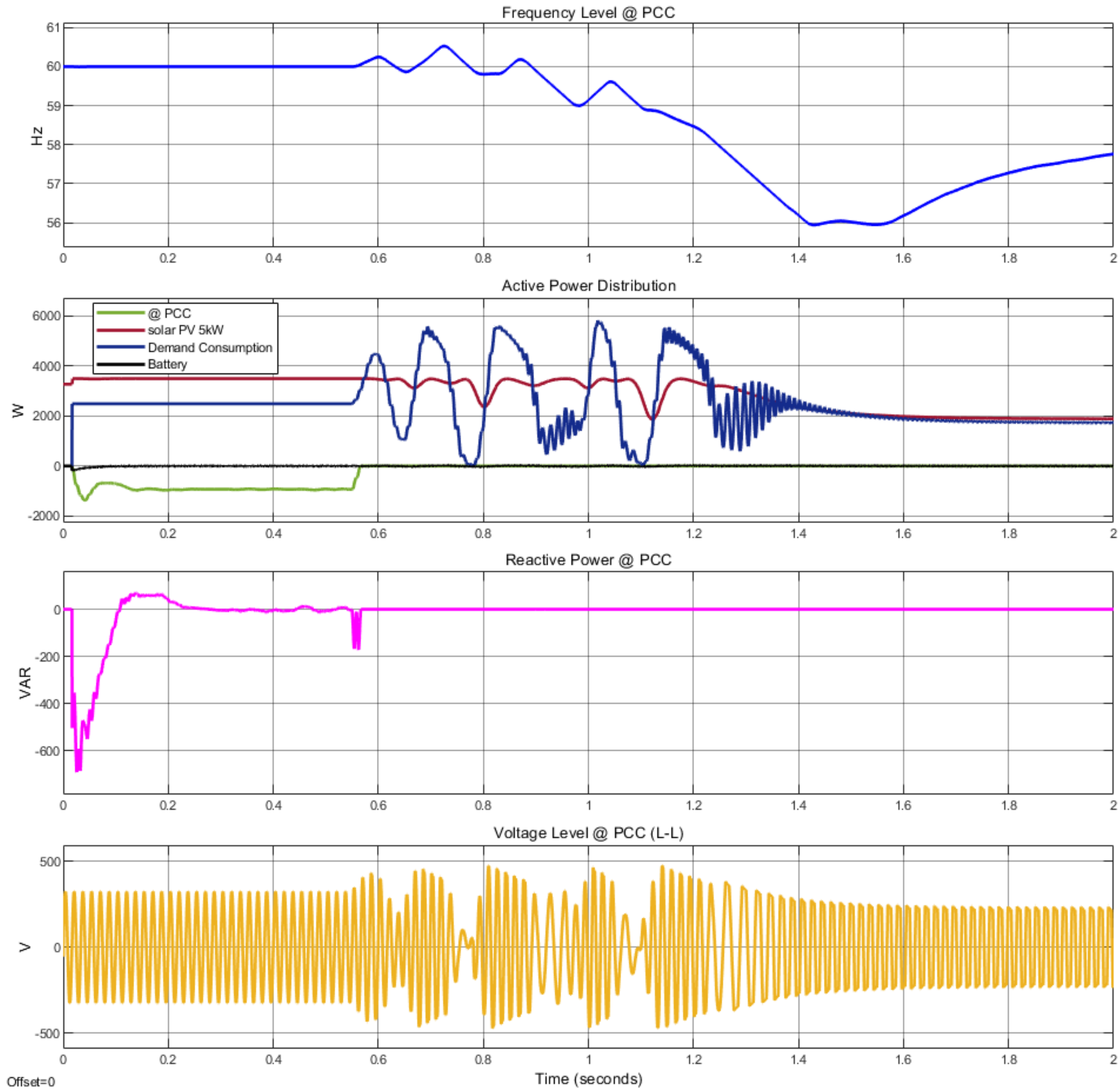

Fig. 2.18 Transient responses when Nanogrid operating in islanding mode.

2.4.3 Fault Interruption and Ride-through Analysis

The risks in propagating upstream fault interruptions by BTM PSPG system is inevitable, inducing power quality issues which can result to distribution network failure. Therefore, Prosumers need to take greater role in profiling and isolating BTM fault crises that transpires locally. Conventional circuit breakers are no longer suitable due to high-impedance blind spot ground faults in solar PV inverter at DC-side hence, new innovation for BTM PSPG protection coordination is important to detect low current ground faults and likelihood of nuisance tripping events from leakage current [144]. In addition, cases of temporary fault

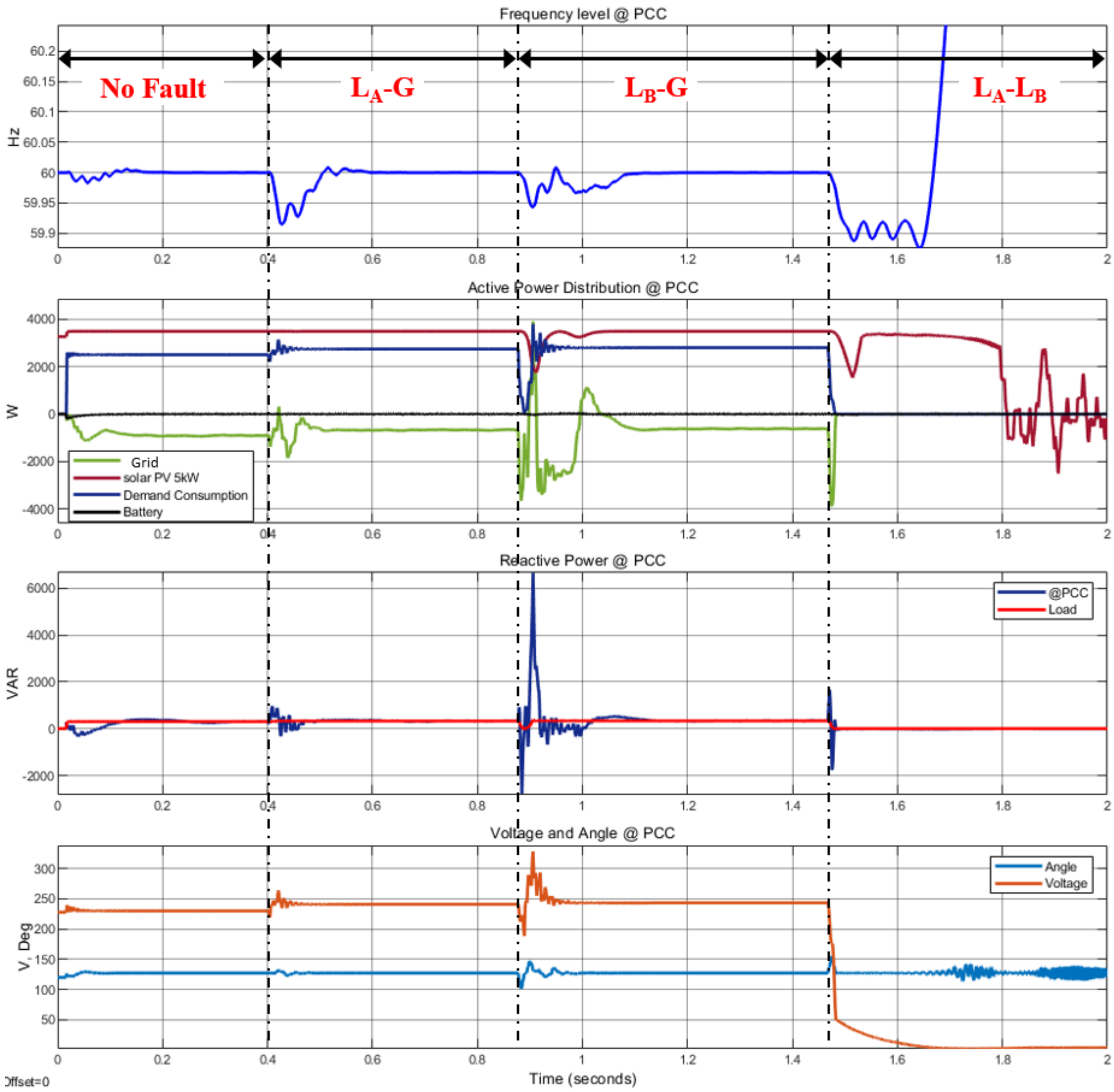

Fig. 2.19 Fault transients in Nanogrid during fault interruptions at primary distribution transmission.

interruptions [179] can also cause malicious tripping of PSPG due to rigid Low Voltage Ride-Through (LVRT) requirements.

Fault transient analyses were simulated based on down and upstream, symmetrical and unsymmetrical, fault current injections to simulate momentary fault interruptions from primary distribution level and in Nanogrid EPS respectively. Only line-to-ground and line-to-line fault characteristics were selected as they present suitable corresponding fault attributes in single phase operations. Fig. 2.19 presents fault transient activities in Nanogrid with inductive load based on downstream fault current while upstream shown in Fig. 2.20.

Employment of inductive load in the demand mix presents critical element when analysing fault transients. It responses closely to phase shift loading in relations to three phase wye-connected fault angle during single line-to-ground fault. It aims to comprehend phase shift synchronisation during reactive power compensation. The Nanogrid connects line A ($\angle 0°$) and B ($\angle +120°$) of the three phase transmission to create single phase coupling with grid. Results in Fig. 2.19 depict 3 types of fault interrupted at primary distribution level; *(i)* Line A-to-ground, *(ii)* Line B-to-ground, and *(iii)* Line A-to-Line B.

i Line A-to-ground−the fault current in phase A introduces hike in other healthy phase voltages as it finds a return path through the ground leakage capacitances. Thus, potential of appliance malfunction could surfaced where power at load increases by 17.8%. Power deviation of 11.34 was observed from grid before it settles within $0.1secs$. Nevertheless, the Nanogrid able to restore frequency balance rendered by the grid-following Volt/VAR compensator in PV-STATCOM. The power generation from solar PV did not suffer any abnormality as the DC-link voltage remains stable.

ii Line B-to-ground−the results should mimic Line A-to-ground fault however, it noticed further hike in voltage level and greater Volt/VAR compensation response. Such phenomenon was caused due to prior fault event not being cleared and thus, creating resonance and ferroresonance effects [180] in the leakage ground capacitances. Therefore swinging the power exchange at PCC to suffer greater deviation index and propagate back at solar PV's DC-link which resultant power generation dip. Overall, the system regained stability with the help from PV-STATCOM Volt/VAR controller.

iii Line A-to-Line B−where both lines are shorted together with low impedance. Comprehending that the power generation source is closer to the fault location, solar PV generation, larger fault current magnitude is expected due to greater impedance between source and fault which resultant to sudden voltage drop. Likewise, both faulted voltage's angles were also affected based on reactance and resistance ratio of 7. The Nanogrid system collapsed and did not recover.

Contrarily, Fig. 2.20 demonstrates transient responses of Nanogrid based on faulted solar PV. The analyses focused on the impacts of fault current at DC-link and how it will affect grid's stability. Two types of fault were employed; line-to-line (short-circuit) and line-to-ground (ground fault).

i Line-to-Line−in event of short-circuit at DC-link, the voltage collapsed and thus solar PV being isolated from inverter. The inverter becomes highly inductive due to high

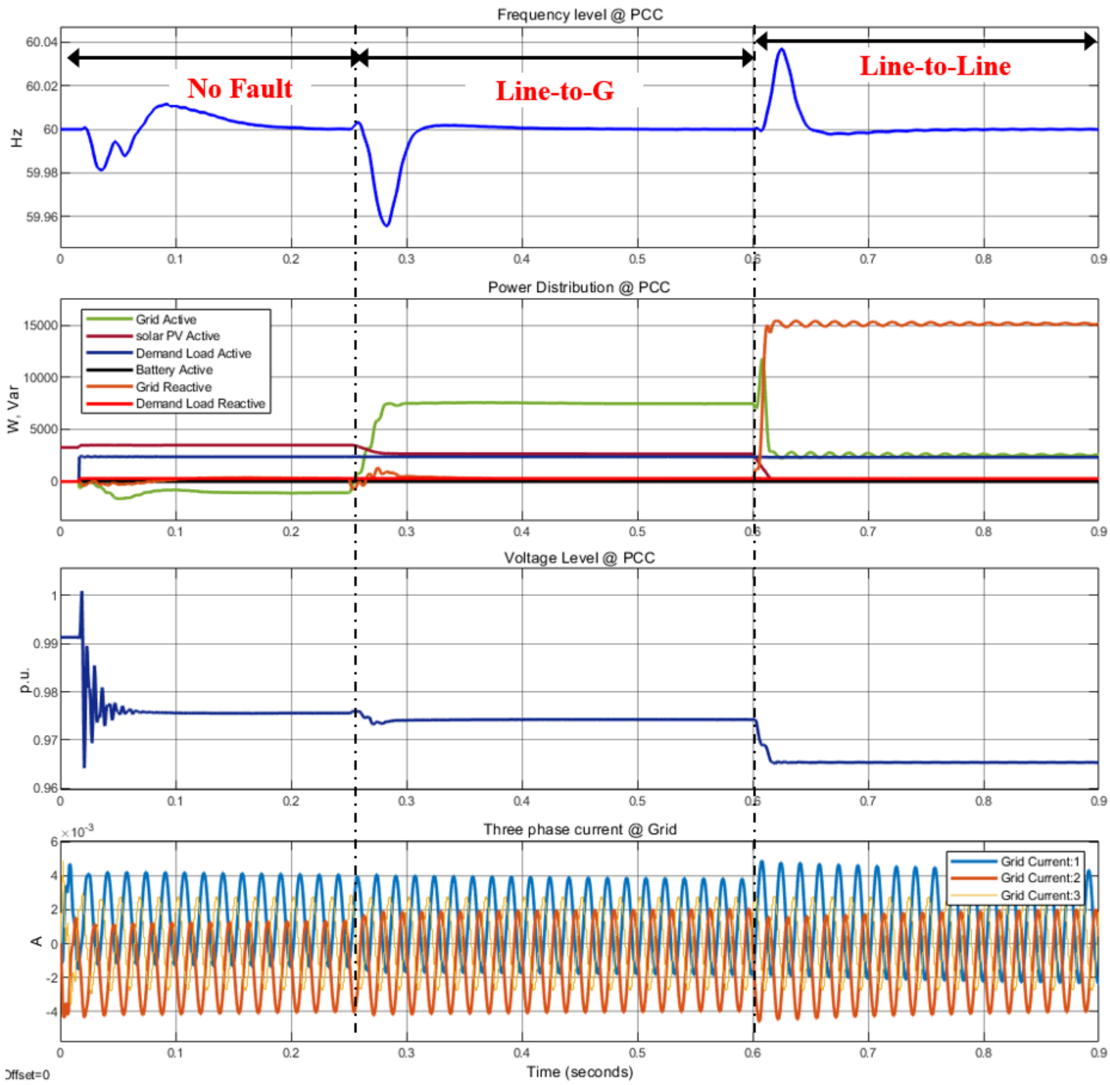

Fig. 2.20 Fault transients of Nanogrid during fault interruptions in local PSPG.

fault current consumed by the inverter's filter. The grid takes control over Volt/VAR compensation and hike in current was noticed at grid however, it was not sufficient to trigger tripping sequence. Overall, the system regained stability with a voltage dip of 0.03p.u.

ii Line-to-ground—the operations of solar PV under high fault current went undetected as abnormality in Nanogrid or at grid were not seen. Typically, due to weak grounding detection system (<1A), solar PV will remain connected to the grid as DC-link did retained at least 70% of voltage charge creating a fault current path into PV-STATCOM inverter. The grid did not suffer any voltage (insignificant) or frequency abnormality.

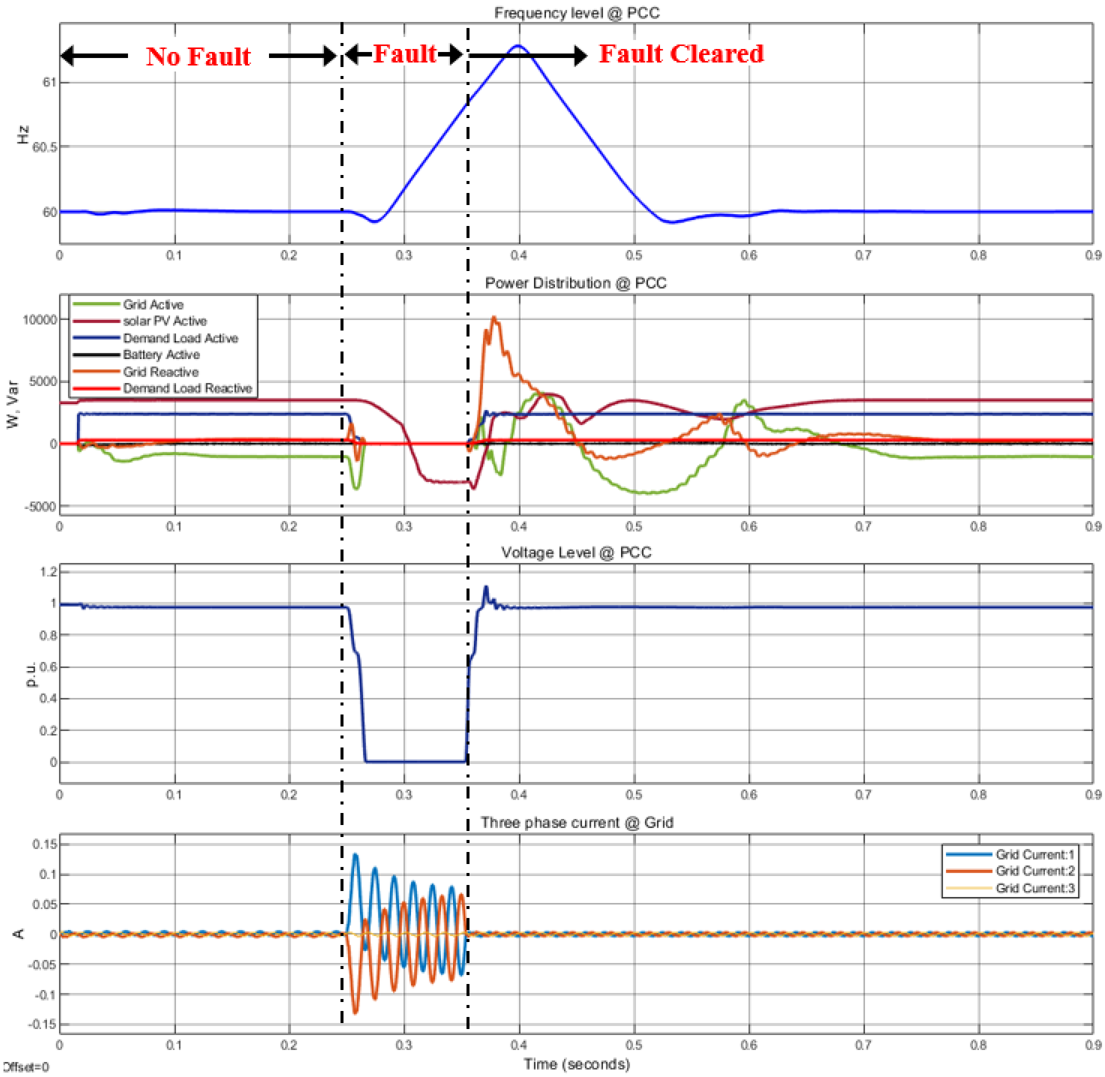

Fig. 2.21 Solar PV's ride-through operation during temporary fault interruption.

Based on new fault ride-through requirements suggested in IEEE Std.1547-2018, tripping thresholds of local PSPG-ESS was redefined in relations to voltage, frequency and phase angle during abnormal feedbacks. It defines mandatory LVRT boundaries and disconnection duration during voltage sag or swell crises. LVRT testing was visualised though inducing momentary fault from grid and activate autorecloser to clear the fault. Fig. 2.21 presents PV-STATCOM capability during 100*millisecs* of Line-to-Line fault at primary-side of distribution network.

Analyses of voltage and frequency ride-through performances were measured against LVRT requirements mandated in IEEE Std. 1547-2018 report. During the faulted period and may ride-through or trip ruling, solar PV was remain connected to the grid despite having voltage to dip at $0V$. Subsequently, after fault being cleared, the voltage level enters into the permissive region ($0.3-0.65p.u.$) within $0.16secs$ and continuously hike with large slew rate piercing into mandatory region ($0.65-0.88p.u.$) before the $2secs$ mark. With the support of grid-following Volt/VAR control rendered by PV-STATCOM, the system voltage and frequency transient did not enter into shall or must trip regions and regained stability in $0.45secs$. Frequency continuous operation region−within $0.98p.u.$ to $1.02p.u.$ and voltage $0.88p.u.$ to $1.1p.u.$

2.4.4 Findings

Learned from the proposed case studies, operative impacts were analysed with respect to demand-side energy management and how penetration of Prosumers can influences DSO's planning in the domain of EMS and ADMS without the engagements of TE framework nor independent aggregators. It highlights DSR issues at global level due to poor control intelligence in Prosumer's DERMS. Likewise, penetrations of DERs at medium-voltage level (IPP) serves no impact in mitigating DSR or network power quality issues as its market-driven DERMS is optimised based on high return in investments without factoring in incentives rendered by government bodies. On the contrary, issues in system interoperability was investigated to view dynamic stability responses of BTM PSPG integration against Utility support in power quality coupling (*i.e.* Volt/VAR optimisation, network loss minimisation due to fault interruptions). Following discusses more on the technical and operational impacts in relation to DSO perspective when liberalising network to accommodate Prosumer penetration:

i Long- and short-term scheduling of unit commitment becomes uncertain due to Prosumers' ambiguity in BTM DERMS and PSPG generation capacities. Moreover, generation variability from DERs in distribution network and unique control of ESS utilisation against market prices will provoke high ramping rate in demand shift. DSOs are constantly challenged to balance between peak demand and baseload where predictions in profiling consumption curve on daily basis requires advance considerations with regards to Prosumers' influential elements. DSO needs to find a socio-economic solution that can optimally steer power exchange at Prosumer(s) as a Community to support DSR and power quality management while benefitting their energy billings. Concerns in Prosumers participation in the wholesale energy market also bring forth coordination and monopolism challenges between retail energy provider and the clearing prices.

ii Prosumers must take bigger role in securing BTM PSPG integration to enhance upstream fault current resiliency and grid-forming capability to reduce propagative risks in malicious tripping/outage interruptions and support compensation for network's power quality respectively. Critical design of Volt/VAR controller in DER inverter can support/compensate voltage and frequency synchronisation with grid. Fault transient analyses were investigated by introducing momentary fault interruptions from both upstream and downstream with reference to Nanogrid PCC. Results verified that ground fault interruptions were often left undetected especially during solar PV operations and frequency of malicious tripping are high. Utility requires better ride-through requirement to accommodate DERs' initial voltage-current transients and events of voltage sag/swell during large demand load shift. Likewise, the role in securing power quality during grid-following and -forming (existence of isochronous generator), and must be considered when designing DER inverter against regulation standard mandated by IEEE 1547-2018.

2.5 Summary

From the learned case studies, comparing passive energy customer against Prosumer engagements, they highlight critical demand-side impacts on DSO planning towards reliable EMS and ADMS. Thus, the concept of grid-edge TE framework is introduced to optimise distribution managerial structure of Prosumers' idiosyncratic BTM-DERMS and medium-voltage DERs (*i.e.* IPP) into a communal and transactive demand-side coordination. Acknowledging TE values and their respective beneficiaries, it steers Prosumers with better DSR prognosis that supports DSO in contingency security planning (*i.e.* OPF, scheduling unit-commitment, feeder-balancing). However, direct synchronisation between millions of Prosumer participations into a centralised DSO sole governance arises coordination issues. Moreover, Prosumers energy trading interests must be protected and should not bear penalty/compensation fees that may conflict with DSO's whole system optimisation requirements. Therefore, the proposed TE framework introduces independent aggregators to operate on behalf of those subscribed Prosumers in securing optimal DERMS based on tailored socio-economic business models based on energy consumption lifestyle. In addition, between aggregators, they are to coordinate and collaborate with DSO to manage potential demand-side conflicts generated by Prosumer Communities while facilitating Prosumers' participations in the energy market (cooperative yet competitive).

In that sense, Prosumer Nanogrid environment comprising BTM DERs, NAN, nano-scaled ADMS, and controllable loads are mathematically defined to give aggregators better planning towards proposing TE business models and system identification for decentralised optimisation. In subsequent chapters, modelling of cooperative yet competitive intelligent system is reviewed for both DERMS in the domain of aggregator and asset-oriented Prosumer based on TE values.

Chapter 3

Cloud Computing Architecture and Intelligent System for Smart Grid Control

This chapter seeks to extend further discussion into advance metering and communication infrastructures mentioned in Chapter 2.3.4, conceptualising power distribution control software on a decentralised Cloud computing architecture that synchronises collaborative learning intelligences between system operators and Prosumer energy needs in the proposed TE framework. It aims to impart a holistic environment across the distribution network that is sustainable, cooperative yet competitive, and hospitable towards IoT advancements.

Thus, prepositions were laid upon to push grid computing platform into Cloud based technology, Smart Grid Cyber-Physical System (SGCPS), unlocking Cloud services for automation and decision support needs in distribution grid control/management. SGCPS operates on the basis of AMI and SCADA, extending communication from BTM and provide the needed interfaces to other energy actor services. It also observes guarantee, efficient, and low costs data transportation and computing bandwidth based on the intended applications. However, in a computational grid environment over a single Cloud infrastructure, it demands for high computational power on the central processing unit to perform calculation over millions of data streams from participants/IoT devices. Thus, SGCPS expands into a decentralised and scalable Cloud infrastructure placing computing analytics and data storage closer to where data are created. A user-oriented MultiAgent System (MAS) on flexi-edge Cloud framework is proposed to establish decentralised computing platforms assigned to individual energy actors when synchronises with central Cloud processing unit, managed by DSO or independent aggregators. Furthermore, Agents of MAS adopts flat organisational structure to perform collaborative tasks executed by smart devices/appliances in response to environment changes.

The objectives are to implement a data-driven Cloud-edge formatted system that employs MAS suitable for TE-based distribution management−bridging Prosumers, aggregators, and DSO into a single communal Cloud framework. Subsequently, modelling of intelligent function modules are fused into Agents of MAS with respective controller bandwidth to execute smart grid operations in view of TE-values and electricity market optimisation. It focuses in defining Agent's learning behaviour that can autonomously attune its competitive yet cooperative actions against respective operating environment reactions.

3.1 Problem Descriptions

In many literature reviews, the concept of Cloud computing and Agent-based modelling for modern power distribution operations have been well established due to its natural decentralised settings suited for large-scale data-driven optimisation operations [181–184]. Agents of MAS in Cloud act as a portable virtual operator that provides full-scale observability on integrated devices' performances and electrification interactions, evade from scalability constraint (flexible towards system's variability) [185]. Likewise, addressed in the referred literatures, efforts in modelling device-to-network protocol standardisation and compliance, creation Cloud platforms, computing intelligence deployment, and MAS content ontology accelerate interaction securities between device's responses and user's control interests. Fig. 3.1 depicts the simplified centralised IoT Cloud architecture and MAS deployment as the operation coordinator for smart grid applications.

However, revisitation into transitioning grid management platform from wired or secure private network to public access Cloud network poses cyber-security and controller bandwidth synchronisation concerns for system operators to guarantee power quality and management efficiencies at distribution level. Globally, open issues in relation to SGCPS involving [186]; *(i)* cost-efficient in merging public to private Cloud for exchanging communication and data in heterogeneous architecture, *(ii)* delay-free synchronisation of data traffic and controller bandwidth while adhering to users' data privacy requirements, *(iii)* integrating multiple DERs/participants using Cloud services for large–scale interactive coalition, and *(iv)* grid collapse vulnerability and cascading consequences due to single protocol failure (internet as the weakest link). Meanwhile, locally, existing Long Term Evolution (LTE) in SGCPS also poses concerns in view of [187]; *(i)* comprehensive surveillance of physical infrastructure supported by on–demand virtual data centers, *(ii)* synchronising functions of virtual SCADA,

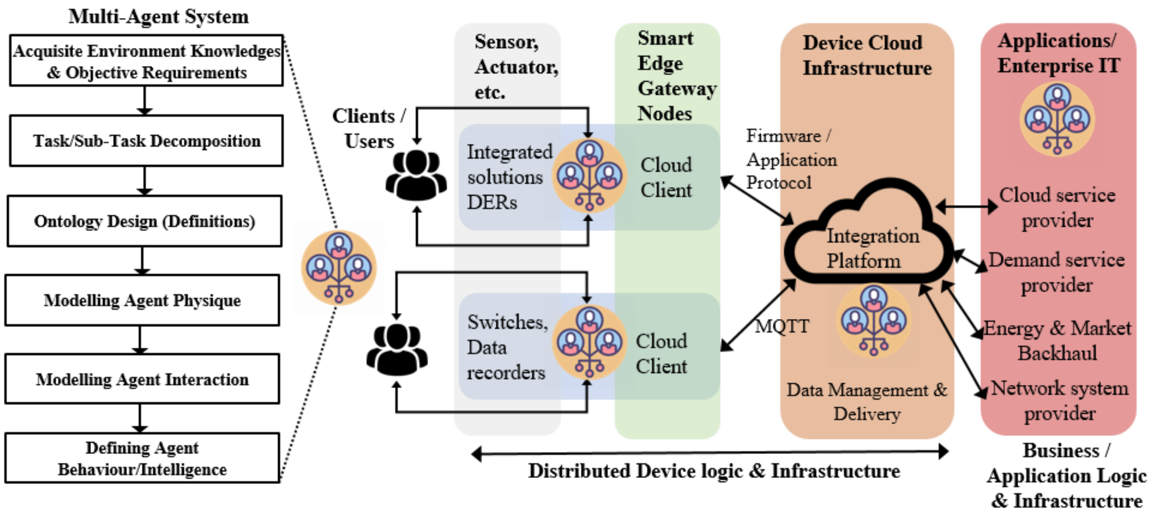

Fig. 3.1 IoT Cloud infrastructure coordinated by Agent of MAS connecting devices and users.

and controller bandwidth infrastructure in virtual machine, and *(iii)* coordinating user-privacy requirements, various Cloud gateway interfaces (*i.e.* pre–processing, data distribution and storage, analysis metrics), and self–service portal in a unified computing platform. In this sense, practicability in utilising Cloud-based smart metering infrastructure (*i.e.* AMI) for transmission-distribution services and automation is an unpopular choice yet alone suggesting edge computing. However, development advancements in Cloud computing technology has been very well established from Web-based search engines to home automation services thus, progressive innovation can be well fitted for Cloud-based SGCPS [188].

Despite acknowledging the credibility in Cloud-based SGCPS for power distribution management, it poses predicaments for big-data scalability/mobility and computational power limitations with respect to various controller bandwidth in a single Cloud infrastructure. Moreover, complications in provisioning data policy between multi-Cloud and generating optimal solution in coalition environment remained a challenge as operating costs increase exponentially in lieu of data trafficking and privacy optimisation, decreases usefulness for decentralised grid management. Hence, decisions in selecting suitable end-to-end Cloud services for SGCPS explores into edge computing in Cloud environment setting where it partitions the data storage, and the processing between public and private Cloud instances; offloading data concentration at central Cloud and safeguards direct communication between private Cloud (system operators) and public Cloud (customers). It deals with personalised IoT gateway servers for edge computing and contract data sharing platform in hybrid Cloud environment.

3.2 Cloud-based Smart Grid Cyber-Physical System

There are still many open questions to what extend Cloud services can serve the demand-side managements [189]. With the penetrations of independent aggregators as energy service operator for Prosumers and installation of DERs at both medium- and low-voltage levels, DSO are challenge with immense societal impact on energy mix security and sustainability. Existing demand-side management requires human-in-the-loop interventions due to DER unreliable generation and coupling effects on network's efficiency and ambiguous Prosumers' consumption profile. Hence, grid management platform must seek modern solutions to keep pace with the IoT needs modelled by energy actors at distribution network for better participation/experience in the liberalised energy market. Without computational and visualisation analytic support from smart meters for automated decision, distribution operators are ill-equipped to draw insights into the system behaviour and automate optimise control due weak comprehension of energy pattern dynamics.

Hence, introducing cyber-physical system in Cloud for smart grid applications, SGCPS, is on-demand; bridging Prosumers, aggregators, and DSO in a unified physical and computational infrastructure for "Big Data" to generate efficient and resilient demand-side management. It is supported by deployment of measurement infrastructure (*i.e.* SCADA, AMI) as the base components, enabling advanced informatics processing and cyber augmentation for complex control and management schemes. Data streaming from millions of smart meters provide historical and pattern matching between generation and demand curve within a service area, curtailing management ambiguity and incentivise Prosumer in a collaborative actions for optimal solution. Moreover, the proposed SGCPS is not only limited to grid management but also participation in the energy market. A platform where multi-participant can sell and bid excess energy from local-owned DERs in the wholesale market and attune local energy consumption based on electricity dynamic and clearing pricing signals at different time interval. The Cloud-based SGCPS is modelled based on edge computing in hybrid Cloud environment [190] that links Cloud services (*i.e.* Software as a Service (SaaS), Infrastructure as a Service (IaaS), and Platform as a Service (PaaS)) with independent AMIs to control data-driven demand-side management.

3.2.1 Edge Computing in Hybrid Cloud Environment

On the surface, Cloud computing is an on-demand network access that offers facilities and shared pool configurable computing resources (*i.e.* storage, communications, applications, services, and server gateways). It can be rapidly provisioned and deploy computing resources with minimal intervention from service provider. In conventional IoT implementation standards [157–159], Cloud computing is structured into multiple functional partitions serving as a reference interface model between IoT device and user interconnectivity as shown in Fig. 3.2a. Commonly, it involves three to five sequential core function layers focusing in data management and broadcasting ability between operating environment and decisional reaction-action states. Nevertheless, centralised Cloud-based management introduces complications in network degradation services, single point failure due to Cloud periodic interruption and data transfer congestions, transmission bandwidth limitations in computation and control feedback responses proportional to storage used, and data mining affliction when handling sensitive information. In this sense, penetration of edge Cloud services serves as a viable solution in bringing data processing (*e.g.* collection, filtering, feedback computations) closer to sources or control object in decentralised organisation.

Edge server gateway serves as an intermediate layer that interoperates device and Cloud physical domain shown in Fig. 3.2b. It improves network bandwidth crises and enhance response feedback performances for local optimisation purposes. However, positioning all computing processes at the edge Cloud may also induce vertical flooding at central Cloud [155, 156]. The function of Cloud is much dependent on the resources and system responses from edge thus, problems such as uniformity can surface due to unsynchronised performances.

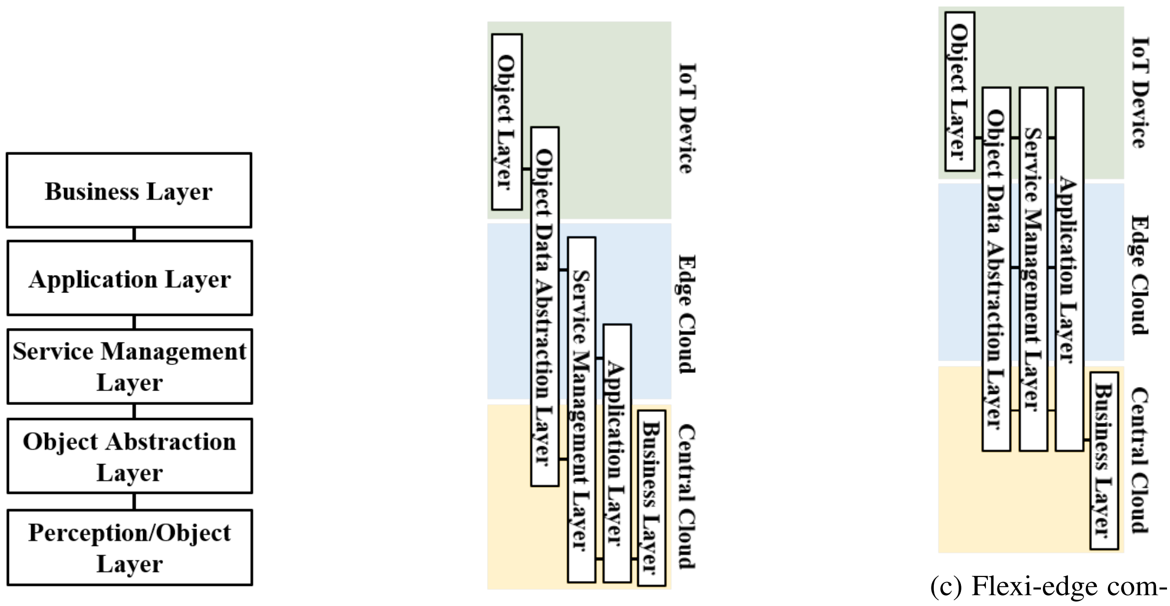

(a) Cloud computing. (b) Edge computing. (c) Flexi-edge computing.

Fig. 3.2 Application and service layer allocation comparisons, linking from IoT devices to centralised Cloud.

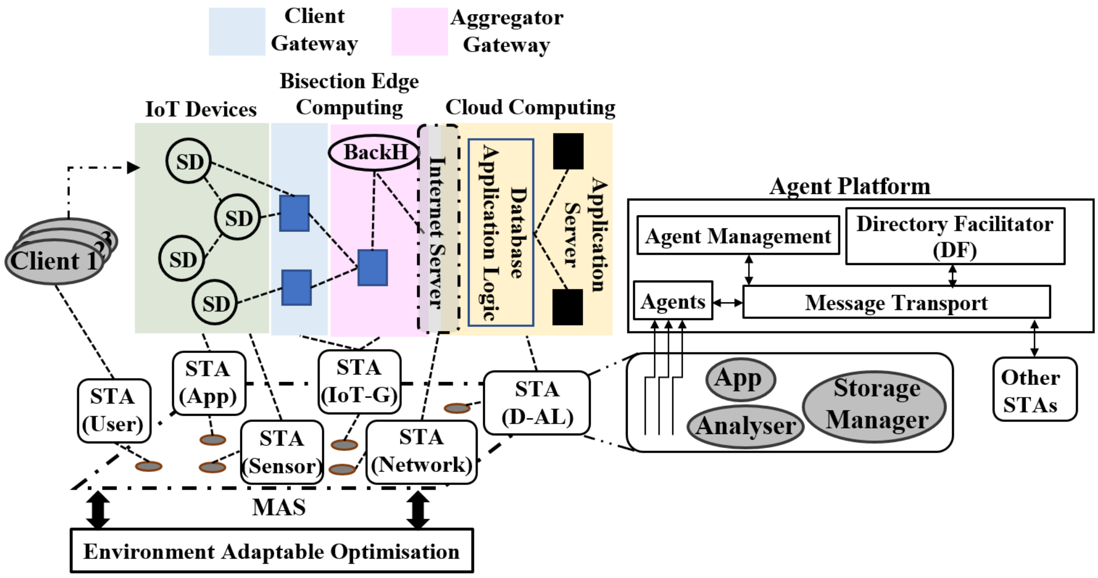

Fig. 3.3 Proposed Flexi-Edge computing infrastructure using MAS-based framework.

In such, Cloud is resorted to execute proxy functions presuming edge Cloud executions. Likewise, in the case where insufficient communication bandwidth available between a Cloud and an edge, the processing duty of Cloud will be taken over by edge temporarily. In consequence, it is necessary to optimise assignment of computing tasks and roles at Cloud and respective edge's domains in response to the dynamic resources based on environmental situations. However, due to its rigid edge Cloud architecture, it ignores fail-safe design addressing performance degradation, scalability and latency issues, inhospitable to functional development, and hostile towards user requests [191].

Taking points from Cloud and edge computing setbacks, improvements were focused in optimising Cloud and edge tasks assignment by extending candidacy's autonomy-adaptability across IoT domains [192, 193]. Fig. 3.2c depicts that the core function, service management layer, has integrated control regulatory in all three domains (*i.e* device, edge, Cloud) simultaneously. Likewise, the object data abstraction and application layers have broaden its data visualisation from device sensory to real-time control applications and platforms to network observability supporting overall response performances, scalability, and user's quality of experiences. The proposed flexi-edge architecture adopts user orientation ability system where it provides real-time computing services suitable for user intervention driven by detailed data information shared across IoT. It pays attention to managerial and autonomous control behaviours on the operating environment to comprehend user's intentions and preferences.

Fig. 3.3 illustrates the proposed flexi-edge computing infrastructure that uses Microsoft Azure IoT edge device framework to implement full-scale IoT implementation. Deployment

Agents of MultiAgent System (MAS) contract advance coordination between device and IoT layers, utilising Cloud computing services that can reflect user's intention and system responses based on Decentralised Control Framework (DCF) ruling. It aids to broadcast and exchange optimisation interests and negotiation expectation commands of energy actors across the distribution network.

User Orientation Ability Environment

User orientation refers to human factor interventions as the prime feedback objective to provide accordance for user's quality of experiences. It attunes loop control responses based on the information generated by user's IoT devices to embed indeterministic behavioural into computing processes. In this sense, high consistency of societal cooperative protocols is imperative to built communal trusts between decision-making tools and users when commanding state position changes that adapts stimulating environment. Fig. 3.4 illustrates IoT computing trajectory towards user-oriented processing and system environment adaptability responses. The two-plane axis (edge and Cloud) describes the potential adaptability deviation when balancing between Cloud's stability as edge computing variation increases. Thus, user-oriented computing reflects segregated autonomous control services based on user behaviour without distressing computation scalability and adaptability.

Each STA comprises of multiple Agents classified into respective IoT domain carrying idiosyncratic control applications. They comply to cooperative protocol and Agent's privity contract organisation that dynamically reconfigure to accommodate environment change. Having a flat organisational structure for MAS, Agents can adapt to any user's service

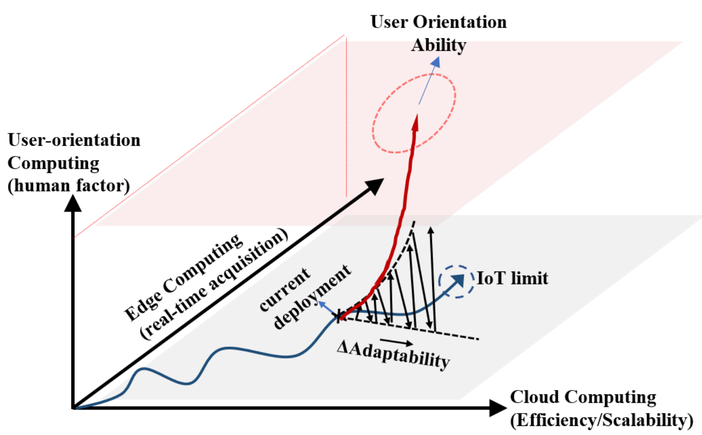

Fig. 3.4 IoT environment computing adaptability trajectory: Introducing user-oriented computing.

requests regardless of edge computing interactions. The user-based Agent in STA acts as a mediator between user's objective interests and system's executions that are closely obliged to closed-human-loop orientation concept.

Data-Sharing Privacy using COSAP Model

Suggested by Takuo Suganuma and *et. al.* in [194, 195], Contract-Oriented Sensor-based Application Platform (COSAP) was proposed to overcome distribution of data privacy-sensitive provisioning in conventional service configuration models [196]. The risk of data distribution determined by device owner's policy is not sufficiently reflected due to task acquisition conflicts when considering Cloud provider's policy. As a result, realisation of an application is limited and data provisioning could be omitted due to mismatch of policies and changes in environment settings:

- *Difficulty in adopting distributed data sensing based on Cloud provider policies*−providers are burdened to defend/protect quality of privacy-sensitive data sharing between users from accidental exposure that could discriminate user's identity. On the other hand, limiting the scope of disclosure can lead to malicious data-sharing processes offering impotent information leading to peripheral sharing platform.
- *Non-adaptive control service based on provider's policy*−it is important to have a flexible distribution of control services responding to provider's policy. The quality of service must meet user's requests when changing the protocol of distributed data.

COSAP utilises Contract-oriented Information Flow Protocol (CIFP) model that automates negotiation of Agents to contract distribution of data requests from users to synchronise with provider's privacy policy. Participants can freely register personal sensor devices onto COSAP and create policy instructions (disclosure capacity) as data provider and invoke sensor-based applications as consumer, transacting fair data sharing and optimising quality of service in view of user's interchangeable policies.

In this sense, Cloud service provider can fully block and secure risks of information leakage exposed to external parties while COSAP extends peer-to-peer data sharing platform among cooperative devices connected with contracts regulated by users themselves as displayed in Fig. 3.5.

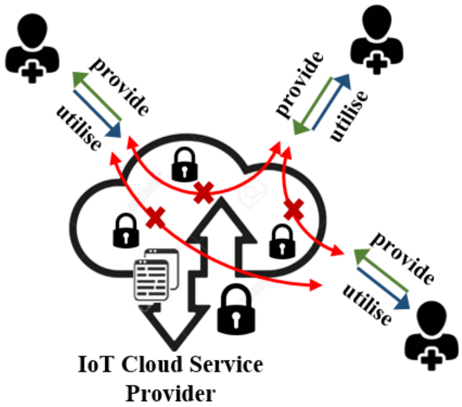

(a) IoT Cloud model.

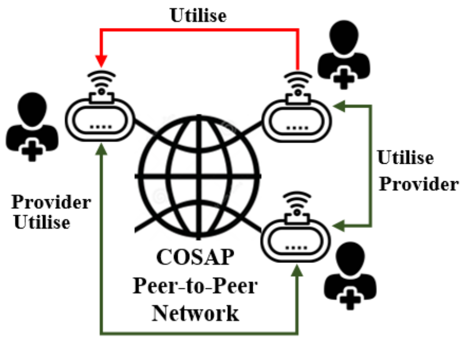

(b) COSAP model.

Fig. 3.5 Distinguishment of sensor-based data sharing sequence between IoT Cloud and COSAP to maintain privacy-sensitive contracts.

Hybrid Cloud Setting

There are three services provided by Cloud; Service as a Service (SaaS), Infrastructure as a Service (IaaS),and Platform as a Service (PaaS) and its architecture can be modelled into private, public or hybrid Cloud environment instances. Here it is proposed to adopt edge computing in hybrid Cloud environment due to it flexibility, shared metering and communication applications, and standardisation of data collection. Its unique ability to partition data and processing between public and private Cloud instances gives superior in creating energy data management, reporting, and analytics in a standardised, approved, and reliable for multiple stakeholders. Moreover, it restricts cross access of data and services between Cloud instances as it mandate security access controls and end-user authentication. Figure 3.6 presents the proposed Cloud-based SGCPS for demand-side control and management where it highlights use of hybrid Cloud environment and assigning Cloud setting for respective energy actors and its corresponding computing services. DSO and independent aggregator uses private Cloud setting equipped with IaaS and PaaS services, and extend communication through the hybrid Cloud environment. Meanwhile, a public Cloud is created by aggregators linking to edge Cloud where it provides SaaS for customer to utilise. The edge Cloud serves as the master to public Cloud where it has full jurisdiction in running applications and data collection closer to IoT devices while public supports with function modules and performs interrupt polling data to minimise traffic congestion, computing latency, and storage limitations.

In view of flexible scaling for DER penetrations and Prosumer participations in Cloud computing architecture, edge services provides an optimal solution where it relief both networking pressure and service response time where computing processes and data storage

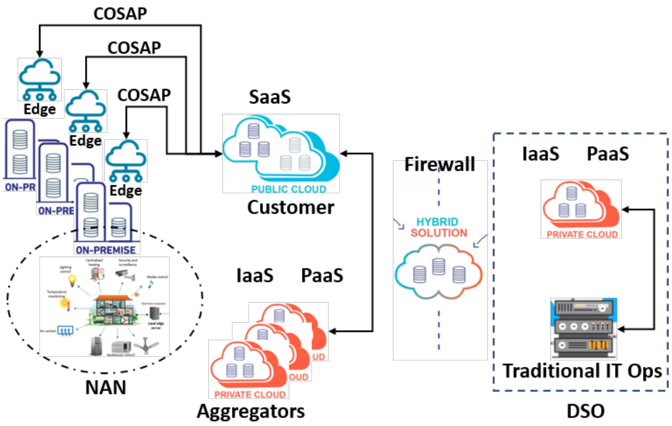

(a) Edge computing in hybrid Cloud architecture linking DSO, aggregators, and customers.

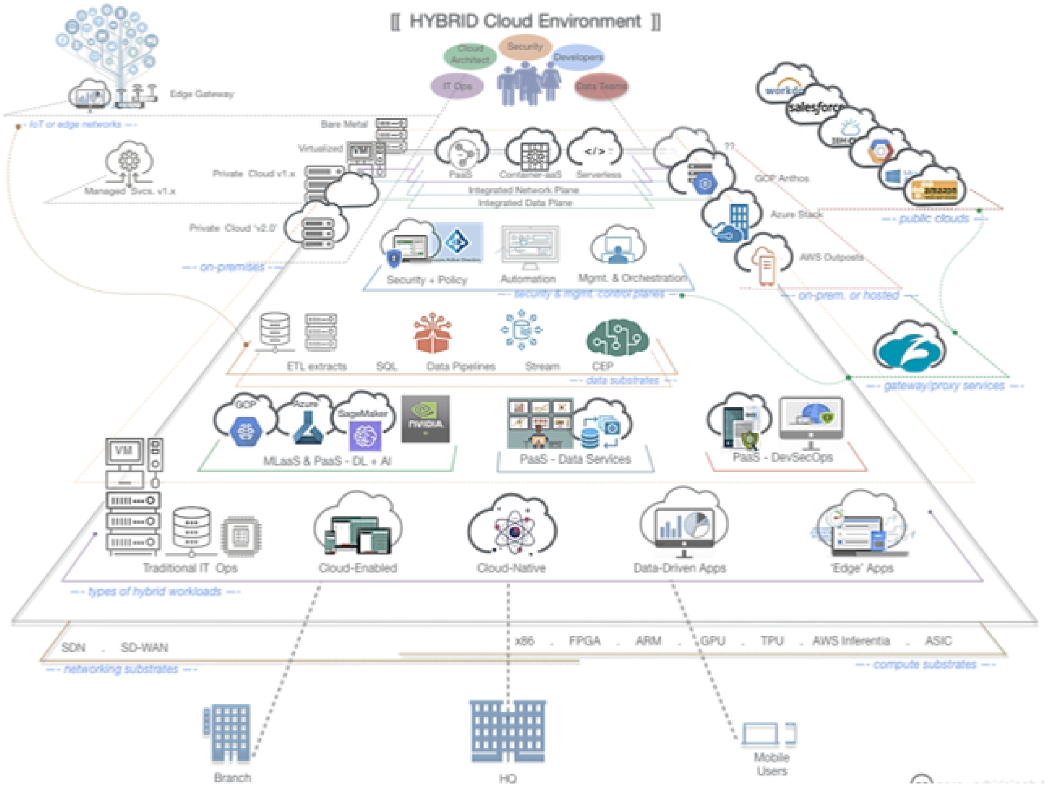

(b) Cloud computing services, providers, and applications in hybrid Cloud environment. Adapted from 'Thoughts on The Future of Hybrid Cloud IT' by Zorawar Biri Singh, 2019, Medium Blog. Retrieved from https://medium.com/@zbirisingh/thoughts-on-the-future-of-hybrid-cloud-it-1bc0716ae82

Fig. 3.6 Proposed hybrid Cloud-based Smart Grid Cyber-Physical System, SGCPS, for demand-side control and management.

is not done at centralised Cloud, but rather at the local edge Cloud of network (closer to IoT devices). Afterwhich, post-process data will be exchanged to the centralised Cloud at a lower bandwidth with smaller data package. In this sense, edge Cloud services fit the purpose in connecting local network area with computing and storage capability, and provide aggregators with Cloud identification of respective subscribed Prosumers for motoring purposes. Table 3.1 provides a brief summary of respective energy actors' computing services and applications in a hybrid Cloud environment for SGCPS.

3.2.2 Computational Power Needs

Big Data computing plays a key part in securing SGCPS services for smart grid applications. Following discusses existing computing platform and how it fits in SGCPS towards demand-side managements:

1. *Decentralisation*−It is ideal to unload computational stress from a centralised domain and pushing them into edge Cloud where storage and computation processes are closer to devices/user. Moreover, it eliminates latency and data misinterpretation issues when performing computation at the edge as compared to over the Cloud; complications in data traffic congestion and loss of data package may be suffered during transmission. It uses interrupt polling approach to send selected/compiled data from the edge Cloud to centralised Cloud using strategic time scheduler to avoid data overlapping with larger data transfer bandwidth. However, modelling cybersecurity system will be a challenge for data management and computation glitches where operators has to maintain edge to Cloud cohesiveness while privatising sensitive information away from public access.

2. *Scalability*−Increase Cloud flexibility to accommodate large-scale of participant and connect millions of devices with full visualisation (*i.e.* SCADA-AMI) and control

Table 3.1 Edge computing in Hybrid Cloud SGCPS model for respective energy actors.

Layers	Access	Services	Management	Infrastructure
Delivery	User Authenticate Common API Service Register	Data Analytic Stability Analysis Performance Simulate/Model	Security Framework Monitor Resources Manage SLA Load Balancing	Storage Computing Network
DSO	Private	Private	Public	Hybrid
Aggregator	Public	Hybrid	Public	Public
Prosumer (Edge)	Hybrid	Private	NIL	Private

during operation. Despite employing autonomous management at the edge, data dynamic provided by energy provider must be tapped to increase global awareness such as energy pricing and DSR participation. This includes DERs owned by IPP integrating into grid operation that requires non-trivial control to keep demand-side supply and demand equilibrium. In this sense, scalability serves a crucial component when modelling Cloud application and services for new computational approaches.

3. *Time Critical*−optimised computational sequence are orchestrated to gain synchronised loading and unloading of data across the Clouds. Some applications requires real-time data (*i.e.* load shedding, storage state) even during momentary offline with Cloud. Hence, it is best that computation are done at the edge Cloud connecting to wired controller (*i.e.* inverter control, VVO) where prediction model can be employed using existing stored data to estimate the next state. Some studies have shown that SCADA-AMI malfunction is inevitable despite having stable data or secured Internet standard like TCP/IP protocols due to unprecedented TCP delays in control flow and data losses.

4. *System Virtualisation Consistency*−communication consistency in SCADA-AMI system is critical when sharing of data across multiple IoT devices within the same bandwidth. Here, consistency refers to the levelled communication protocol where command languages and control across measuring devices and data acquisition are synchronised. It is key to search for bandwidth consistency and real-time guarantees between edge and Cloud during data replications. The risks of system operator when momentarily loses their control layers suffered coordination failure thus, SCADA-AMI solution for the future smart grid needs to have high reliable and maintain communication consistency.

5. *Data Security & Tolerance*−exposure to data breech or ill-modified computation thread events gives a lot of tractions to system operator when operating demand-side management over the Cloud. Cyber terrorists seek to take advantage of weak firewalls, seeking opportunities to monopoly the power commodities market. In this sense, computing power needs at edge and public Clouds will require to reserve greater resources for security and encryption processes. In addition, computing and data processing must operate while facing security breech or server malfunction hence, alternative measures must act upon to secure consistency for time critical services. Byzantine Fault Tolerance is one of the common solution during such incident due to it decentralised nature in reaching consensus despite some of the server nodes failed to respond or responded with falsified information.

Discussed in [197], it presents case studies on analytic performances of edge computing processing in hybrid Cloud involving workload parameters, input and output data size ratio representation, and speed up parameter accessing loading time in Cloud against edge by measuring communication-to-computation ratio. Comparative results presents quantification of computational power and speed comparison when using edge computing in hybrid Cloud against centralised Cloud architecture. Key distinguishment suggested that application characteristics (*i.e.* selectivity and edge bandwidth) affect data processing performances. Bandwidth measurement between local edge Cloud and centralised were analysed based on minimum and maximum thresholds to validate communication and computing processing power. Despite acknowledging that Cloud computing is 2 to 5 times faster than edge Cloud, it is limited due to poor data time transfer which affects the overall performance when dealing with large data inputs. Moreover, the computation speed may differ subjected to the application or running services required on the processor where results proved that edge Cloud have faster processing time than centralised Cloud using similar large-scaled data set even at greater bandwidth rate. Nevertheless, edge Cloud speed-up have better processing management despite small bandwidth rate between hardware and software design where it deviates from system bottleneck. Subsequently, similar processing performance comparisons between hybrid edge Cloud setups, single and separate cluster configuration, were analysed using the four *MapReduce* applications [198]. The results exposes a balanced time performance tradeoffs due to inter-cluster networking link structures. In single cluster, establishment of peer-to-peer connection across nodes thus, dissemination of data is intermediate and running of computing tasks is closer to data (reduces shuffling of data). Meanwhile in separate cluster, it is limited to a maximum bandwidth threshold due to single link connectivity per edge cluster. The bandwidth limit can be improved by creating more linkage between Cloud and edge Cloud if there is availability in creating more links and bandwidth increase proportionally to links employed. However, deployment practicability is questionable and unstable.

3.2.3 Smart Metering Infrastructure Requirements

Distributed software framework equipped in AMI serves as a medium in facilitating optimum data and control access for demand-side visualisation across multiple energy actor environment. It aims to foster competitive marketplace in distributed setting, providing new services to better manage demand-side requirements influenced by Prosumers' BTM DERs and private-owned IPP. Hence, coupling emerging IoT technologies with SCADA system and AMI software design enables geospatial knowledge on; *(i)* local energy awareness, *(ii)* state estimation, and *(iii)* demand-side engagements in lieu to distribution power quality and operation resiliency. Hardware-Software interoperability is key, developing standardise middleware protocols for communication/data processes across heterogeneous actuator and sensor devices. It is suggested that SCADA-AMI system is linked to the edge Cloud, enabling real-time data collection and computation through asynchronous communication (*i.e.* publish/subscribe activity). The publish/subscribe communication paradigm removes information interdependencies between operator and consumer which allows developers to create a distributed and bilateral micro-services that perform send/retrieve data to/from multiple entities (*i.e.* software or hardware) respectively. Therefore, employment of REpresentational State Transfer (REST) design principles is proposed to provision micro-services in data access using open and web-based standard formats that is easy-to-use interfaces and loosely coupled to IoT devices.

Proposed in [199], a Flexmeter platform is fused into smart metering infrastructure which integrates diversified technologies and devices with sensitive monitoring and management for demand-side operations. It is designed with three-layered services in edge Cloud: *(i)* device integration layer, *(ii)* middleware layer and *(iii)* application layer. In device integration layer, it uses Device Integration Adapter (DIA) to create a unified communication interoperability between different default language protocols from wired and wireless IoT devices (*i.e.* IEEE 802.11, Z-Wave, BLE, or 6LowPan). DIA is a software module that converts measuring data from devices into Flexmeter formatted data, transcending standard protocols and data sources of connected hardware technologies which is then pinged to the edge Cloud using message queuing telemetry transport protocol. In addition, DIA can also integrate real-time digital simulators into the Flexmeter to gain simulation processes for state estimation purposes. In middleware later, it consists of stackable software modules operating in asynchronous; *(i)* establish active communication with DIAs using MQTT publish/subscribe protocol, *(ii)* perform data exchange management (*i.e.* command instruction, storage, bandwidth), and *(iii)* render REST web services for access authentication. It routes all data events and send command messages to and from the device integration layer managed by inbound and outbound data traffic pipeline manager. Lastly, the application layer contains communication protocols that connects to the edge Cloud server gateway and service application for data interrupt pooling from device to edge Cloud in view of available bandwidth. It offers tools and APIs, designed for distributed services between edge Cloud gateway and IoT measuring devices. In addition, cohesive Transport Layer Security (TLS) services for secure communication channel and access authentication is introduced to enhance data integrity during transmission from device to only local edge Cloud. Note that, gateway/data sharing or scalability is only done through the edge Cloud hence, SCADA-AMI does need multi-tenancy software infrastructure.

3.3 Modelling Layered Control Concentrator in Edge Computing Hybrid Cloud for Transactive Energy

This sub-chapter reviews the use of edge computing hybrid Cloud environment to impart layered control features that synchronises for modern demand-side operations. It aims to facilitate device-to-user interactions at the edge and execute intelligent control services for demand-side interoperability based on assigned TE functionality at respective layer domain offered by independent energy aggregators.

A Distributed Control Framework (DCF) is proposed to categorise distribution network into three layered managerial zones as seen in Fig. 3.7. Each layer is assigned with selected TE regulatory features to satisfy distributed EMS and ADMS objective functions at global perspective, which uses Cloud services driven by Agents of MAS to cooperatively interact/reason and execute optimal local actions based on compounded system reactions. In addition, a bisection edge computing framework is suggested to separate IoT edge device runtime and IoT Hub gateway; endorsing continual computations and bidirectional com-

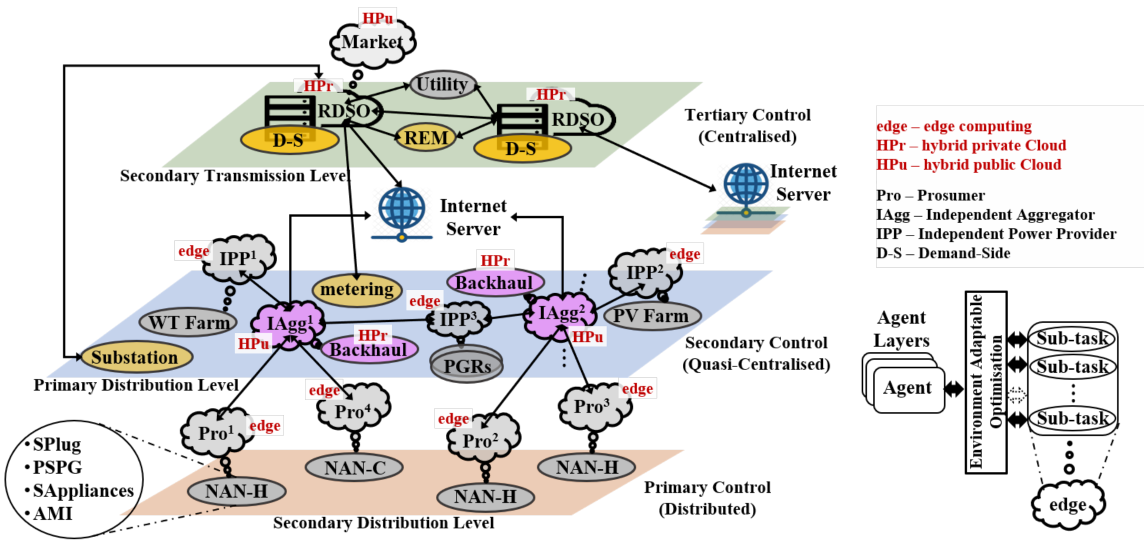

Fig. 3.7 Proposed multi-layered DCF interoperating SCADA-AMI and MAS in edge computing hybrid Cloud environment; linking energy actors for demand-side management and operations.

munication that are free from centralised Cloud connection issues (*i.e.* operable in offline setting).

Modelling includes; *(i)* assigning control functions and develop computing intelligence in relation to energy actor's governing domain to achieve optimum DERMS (*i.e.* aggregator-Prosumer), EMS (*i.e.* DSO), and ADMS operations, *(ii)* establishing edge-based IoT architecture with bisection edge gateway component emphasising user-oriented ability system and edgeHub-to-Cloud connectivity, and *(iii)* deploy contract-oriented sensor-based application platform (COSAP) [194] for data-privacy sharing policy specified by user.

3.3.1 Core Control Functions in Distributed Control Framework

The proposed DCF comprises; primary, secondary, and tertiary layers. They perform independent computation processes with parallel executions based on synchronised optimisation.

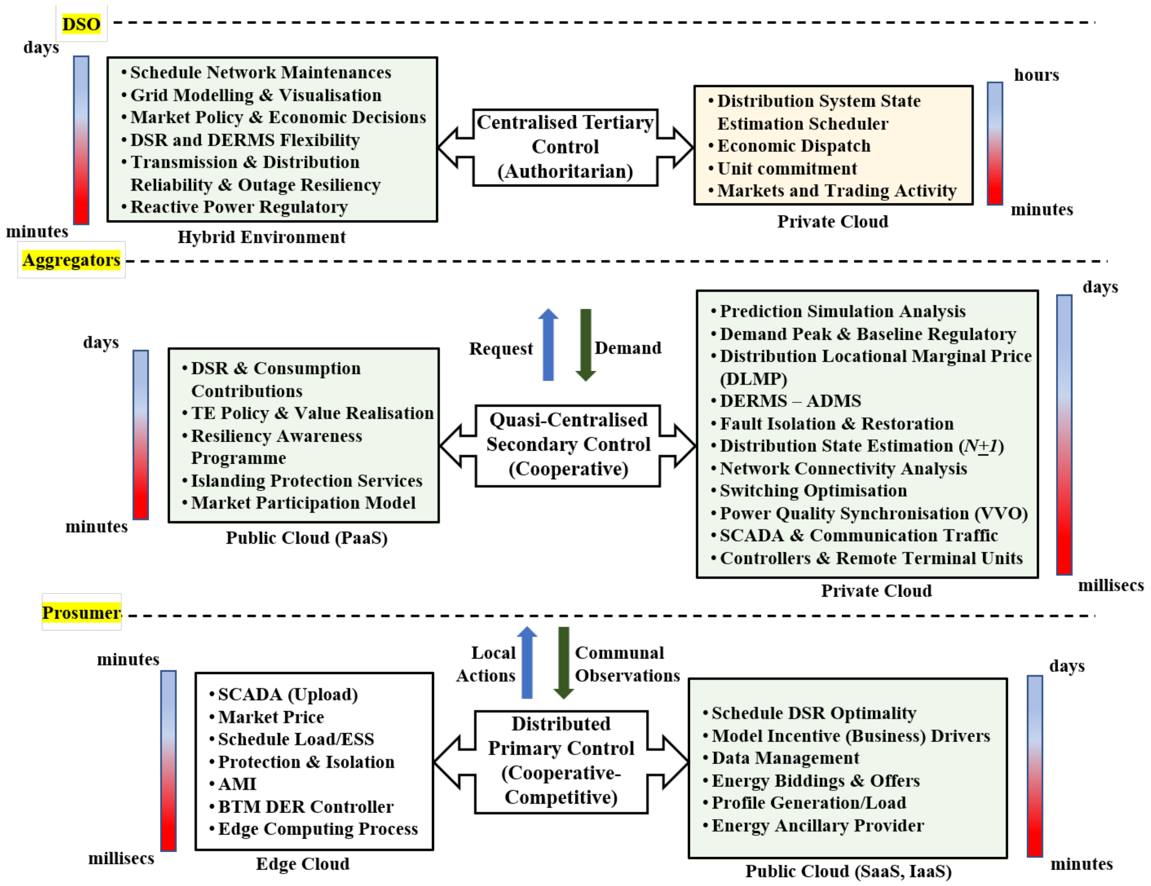

Fig. 3.8 Overview of TE values in DCF against controller bandwidth using edge computing hybrid Cloud environment.

Respectively, each layer is defined with unique control characteristics that highlight leading objective function before establishing a joined maximisation or minimisation expectation of a state function−increases resiliency and efficiency as a whole system.

The modelled managerial orientation of DCF defines; *(i)* primary layer focuses on selecting desired TE services made available for Prosumer in coordinating ESS charging-discharging operations, energy trading at PCC, and wholesale market participation in real-time, piloted by the subscribed TE-biased business model proposed by aggregator. Prosumers will benefit from a reduced energy billing influenced by the clearing price reaction approach and incentives from DSR contributions, *(ii)* secondary layer is governed by aggregators providing options for TE services and Cloud infrastructure that relays operational response/request to make necessary projectile corrections at respective scheduled time intervals for global demand-side optimisation (*i.e.* DERMS, ADMS, DSR), and *(iii)* tertiary layer for DSO which oversees the overall power delivery transaction across the distribution network, governing Utility-side EMS and energy market policies that can steer aggregators to observe fair-play, cooperative yet competitive environment for Prosumer Community.

The structured objective statement assignments at respective control layers were defined such that distribution network state estimation optimisations and dynamic security assessments are brought closer to aggregators while DSO focuses in managing grid's assets (*e.g.*transmission line loading, unit commitment, electricity market) and ordering network equilibrium and efficiency. Fig. 3.8 exhibits control functions in DCF accordance to respective Cloud layers during networked demand-side management.

Distributed Primary Control Layer

The modelled primary control layer operates as a responsive TE economic mechanisms based on two-sided market clearing model (energy demand vs. price) and local generation availability. Correspondingly, decentralised elements remain as focal action-reaction observation taking policy and TE values [200] as key decisional parameters. The decentralised elements refer to Prosumers' unique energy and economic management interests that are intended for multiple stakeholders to reach common interoperability objectives. The primary control BTM DER matrix shown in Fig. 3.9 illustrates classification of coordination approach trends shifting towards emerging distributed decision-making autonomy and yet gained global optimality.

Primitively, classic top-down switching approach [201] has served to be the simplest and effective DSR program that focuses on strategic switching of one device group (*e.g.* air-condition, thermostats, water heaters) during peak demand crises. However, the control

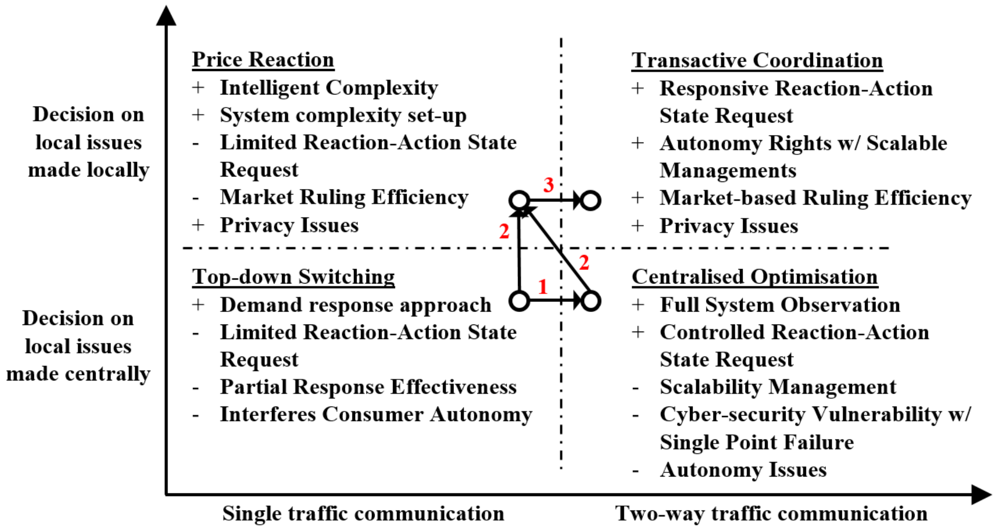

Fig. 3.9 Identifying pros and cons in demand-side management using four region matrix.

algorithm executions are much dependant on statistic evaluations where the states of devices and their responsiveness were unknown. Furthermore, it fails to interoperate human-factor anatomy and often interrupt consumers' usage preferences. Ideally, the control function evaluations are biased towards worst case scenario assumptions to compensate state estimation errors—lacks in unlocking full potential performances from IoT devices.

In response, AMI was proposed to gain managerial visibility of consumers' demand and supply demographics, and issue optimising dynamics for global executions. Having the luxury of local information and full device interactions, centralised optimisation control scheme unlocks direct reaction-action performances of individual devices with high operational transparencies. However, autonomy issues prevail as top-down switching approach is still key in directing device's state-action responses and privacy threads will surface as local informations are broadly communicated. The centralised data-driven controller is at risks of single point failure and scalability response issues as network aggrandises.

Emphasis in providing Prosumers' liberations in making local decisions to transact personalised power exchange at PCC is admirable in future's electrifications. Endorsing precedent price-reaction accession forces local energy management controller to constantly attune demand load capacities in parallel with wholesale electricity prices to gain economic optimality. It has greater advantage in providing consumers' with managerial options when steering respective reaction-action state responses of online devices. However, due to its limitation in communication infrastructure, utilities have troubled in profiling suitable price reaction within the demand-response pool without acknowledging device's state and Prosumers' energy usage preferences.

Conclusively, the primary control layer aims to coordinate TE values where BTM DER operations are communicated in a two-way negotiation model based on electricity price dynamics that are deeply influenced by Prosumers' energy exchange quantities. Due to its unique market-based control features [202] that drive uncertain demand responses into collaborative actions with derived auctioned prices, it somehow triggers a predictable reaction system. Comprehensively, the primary control layer provides rudimentary coordination for:

1. self-optimisation management between PSPG utilisations and demand load capacity against distribution locational marginal price for reduced electricity billing (market-based control response).

2. comprehend ride-through requirements when integrating PSPG at PCC and observe grid following power quality regulatory functions.

3. non-monopolist electricity market participation and energy sharing schemes (incl. ancillary services).

4. comprehend operating standards and restoration protocols at respective transacting elements. In addition, response to peak demand curtailment, load shedding or other similar programs (*e.g.* outage, interruptions) that supports feeder-based ADMS operations.

5. interface observable and auditable AMI (plug-and-play) that can encapsulates interactive devices, broadcast participant identification with data privacy measures, and extends geographical status that can influence demand demographics.

6. Partnering with EMA or demand response service providers to formulate a TE value proposition programs, incentive offerings, and partnership contracts.

Quasi-Centralised Secondary Control Layer

The secondary control layer mimics similar operating functionality when piloting a Microgrid system, serving as an aggregator for Prosumer Community, and IPPs in response to DSO demand-side requirements. Here, the control features are separated into two intelligence domains; relay ADMS and market functions initiated by DSO, and classifying Prosumers into community formation for optimal DERMS-ADMS. It targets four diversified Prosumers transactive mode operations and aims to strike operational balance in power exchange demographics using market-based model [203]; *(i)* appreciate distributed energy managerial preferences and concoct global optimisation executions, *(ii)* facilitate in bilateral wholesale market price signal (*inclu.* price clearing) engagements in response to DSR and available energy reserve pooling, *(iii)* offer optimum and flexible TE business models, and *(iv)* proactive towards operation resiliency and power quality (feeder-based).

The primary regulatory concept in quasi-centralised facilitates centralised managerial solutions based on distributed reaction-action responses (regional/community), addressing compensation or restoration strategies to secure ADMS criterion. Its control features prioritise scheduling and dispatching of Prosumer Community BTM DERs for the provision of grid services in compliance with network constraints or operating requirements (*e.g.* transmission congestion, load dynamics Volt/VAR compensation, spinning reserve capacity for peak demand and outage crises). Critically, to facilitate optimal market-based pool strategy and Prosumers' controller intelligences, decentralised locational marginal prices (DLMP) mechanism is employed to allocate energy pricing, payment, and cost settlements in wholesale market taking distribution losses and operation costs into consideration. Furthermore, innovations for real-time incentive policy schemes can encourage Prosumers to assist DSO in improving DSR and interruption resiliency.

Lastly, decentralised edge Cloud infrastructure regulated by aggregator is established to interconnect online devices and wide-area operation visuality between communities.

Centralised Tertiary Control Layer

The tertiary control layer focuses on DSO's operating EMS and ADMS functions, and serves as the energy market regulator and policy maker while minimally overlooking DERMS operative status/analysis as a subsidiary governor. In addition, close collaborations with Cloud service provider to establish networking infrastructure for AMI and communication with interactive devices. Primitively, adopting centralised computing approaches (top-down switching), DSOs were burdened with both EMS and DMS roles in both distribution systems and its affiliated subsystems; not limited to emergency control planning and full coordination with TSOs to minimise energy losses. However, with DER penetrations and Prosumer engagements, real-time managerial of DERMS and ADMS have been lifted and disseminated into primary and secondary control layer. Nevertheless, DSOs of today are required to cope with Prosumers' energy interests by modelling new functionalities that can increase system wide efficiency.

DSO is also responsible in conducting reliability and security analyses to increase operational resiliency against power outage threads based on interconnecting requests. It too involves in scheduling of unit commitments with economic dispatch settlements based on forecasted net load and dispatchable generation trajectories. Conjointly, as a regional market-based operator, it secures fair-play environment in buying and selling prices of electricity (spot-on and clearing), generate incentive and policy programmes for TE engagements, and market for reserve services. It has an important role in brokering wholesale and retail energy price signals between Prosumer-IPP and aggregators.

3.3.2 Implementation & Testing of Edge Computing with COSAP

The realisation of proposed multi-layered DCF is broken down into two phases;

1. Modelling of hybrid Cloud environment based on edge computing gateways configuration−employs a third-party Cloud service by Microsoft, Azure IoT Edge, that provides on-premise and offline analytics to drive business logic against local online devices. Here, it aims to use hybrid Cloud infrastructure to correspond with the proposed multi-layered DCF.

2. Employing COSAP-based MAS for peer-to-peer data sharing−using third-party distributed multi-agent framework, PIAX (peer-to-peer interactive Agent extensions), to implement data sharing application of sensor-based devices information using CIFP. Agents of MAS are modelled with contract protocol functions to perform data exchange management between users and devices.

Developing Flexi-Edge Hybrid Cloud in Microsoft Azure

Using Microsoft's Azure virtual machine and guidance from Azure IoT Edge documentation, a simulated IoT services were established to represent the proposed Cloud edge environment shown in Fig. 3.7. Using the in-built virtual machine tester, it allows users to create multiple IoT edge devices, IoT Hubs, start the IoT edge runtime on the virtual devices, and remotely send telemetry information from device modules to IoT Hub. Fig. 3.10 illustrates the deployment of edge computing hybrid Cloud using Microsoft Azure IoT Edge platform to built the proposed multi-layered DCF that offers personal computing and data storage domain that synchronises communication across aggregators.

The concept of edge runtime provides fundamental real-time services in managing constant connectivity and security for all connected smart devices (local) isolated from the internet despite various adopted communication protocols. It also have multiplexing capabilities that creates individual device identity for Cloud and leverage that edge device to store and forward if the connectivity to Cloud is disrupted. Besides offering these services, the runtime itself is designed to manage modules which contains chain of instructional actions and data processing pipeline to solve end-to-end scenario (*e.g.* converting & filtering

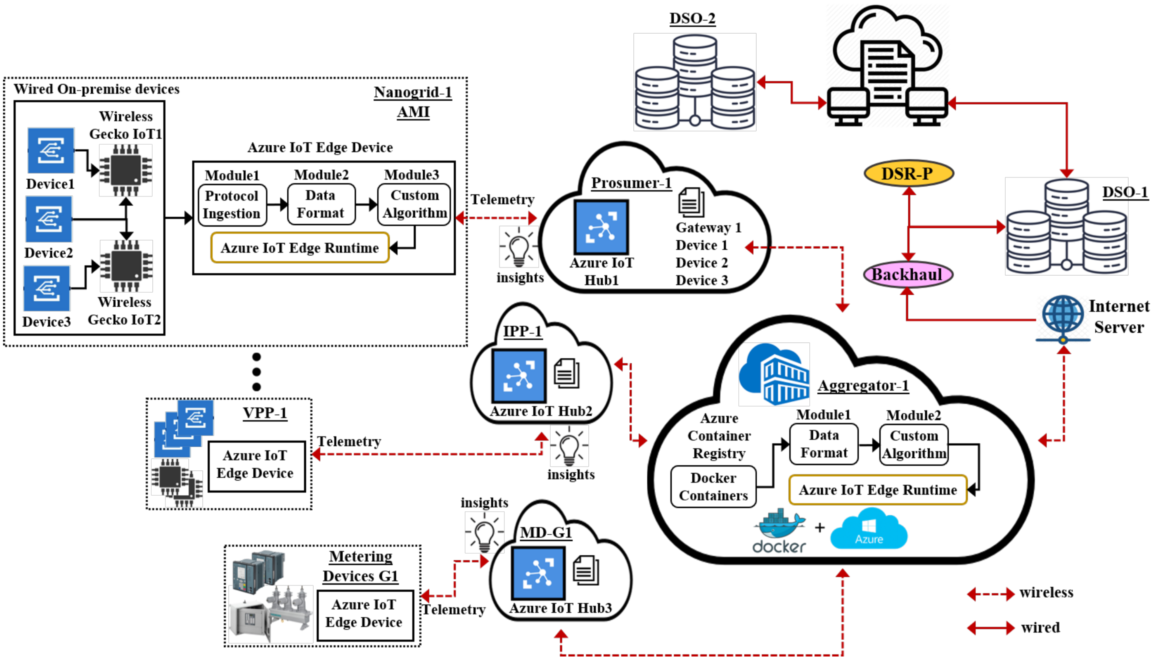

Fig. 3.10 Implementation of proposed multi-layered DCF environment using Azure IoT Edge.

of data, built customise algorithms). These modules are then packed by Docker containers in Azure container registry and distribute across Cloud on various computing operating system.

The Azure IoT edge device processing pipeline is broken down into five sequential data transactions employing various in-built modules:

1. *Protocol ingestion* module talks a protocol with unique devices which are not internet compatible. It ingests data from respective device, translating protocol into a synchronisable language for devices. It also provide data routing information within the Cloud environment that points to targeted IoT edge.

2. *Data formatting* module does conversion of the data into binary message for transportation, establishing interaction between Cloud services. The IoT edge runtime is used to connect distributed clouds and send data up to Azure.

3. *Custom algorithm* module is established through a process called Cloud offload, running the Cloud compute services onto the edge. These services are available in the Cloud (library) which provide various optimisation functions in near real-time analytics given to solve individual problem statements.

4. *Azure IoT Hub* configure and monitor each device lifecycle from the Cloud with IoT edge runtime to gain full control configurability. It configures a workflow from the

Azure container registry calling specific modules and disseminate them on a targeted device and run Cloud intelligence on the edge (reducing computational burden on the Cloud).

5. *Azure Container Registry* serves as the centralised Cloud system that acts as a container repository using Docker engine platform where IoT Hub can fetch functional modules and send insights of edge. It serves as a library that stores various customise computational intelligence algorithms and data formatting solutions either provided locally by the Cloud provider or external parties for mass sharing.

For testing purposes, a singular Azure IoT Edge environment is developed simulating a single Nanogrid system connecting to a household thermostat simulator device and communicate with IoT Hub and Azure container registry. The thermostat device reads temperature, pressure, and humidity of the room. Fig.3.11a demonstrates the creation of Azure IoT platform with subscribed edge modules, extending communication from thermostat sensor to the Cloud. Subsequently, both data filter and device modules with dependencies were compiled into an IoT edge docker image by adding *.esco* extension and published to the docker registry container shown in Fig. 3.11b. It is also necessary to prepare the routing configuration for the actual edge runtime in Azure IoT Edge Device to transport output real-time temperature data reading from sensor module to input filter module which then sends messages upstream to IoT Hub.

Finally, initiate runtime which connects device's ID and credentials to the IoT Hub and start the IoT edge runtime at the local machine. Fig. 3.12 presents the internal communication logs in Azure IoT portal with command lines. The logs shown in Fig. 3.12a is reading the configuration, calling the three modules; sensor, filter and edgeHub module. Internally, it is getting the docker containers from the various configuration registries and execute them. Fig. 3.12b presents the lists of existing modules running; agent, sensor, filter and the fourth module, edgeHub−responsible in establishing communication with IoT Hub and does the routing. Fig. 3.12c displays the real-time data logging traces between temperature sensor module and messages arriving in the Cloud (flags instances when temperature is above 25 degrees).

Fig.3.13 presents computing performance comparisons on two different Cloud environment; over the centralised Cloud against decentralised edge architecture (singular IoT Hub). Performance analytics on data management-transportation and bottleneck computations were evaluated to comprehend tradeoffs and superiority operations, suited for TE-based NAN deployments (high penetration of smart appliances/devices). The performance matrices

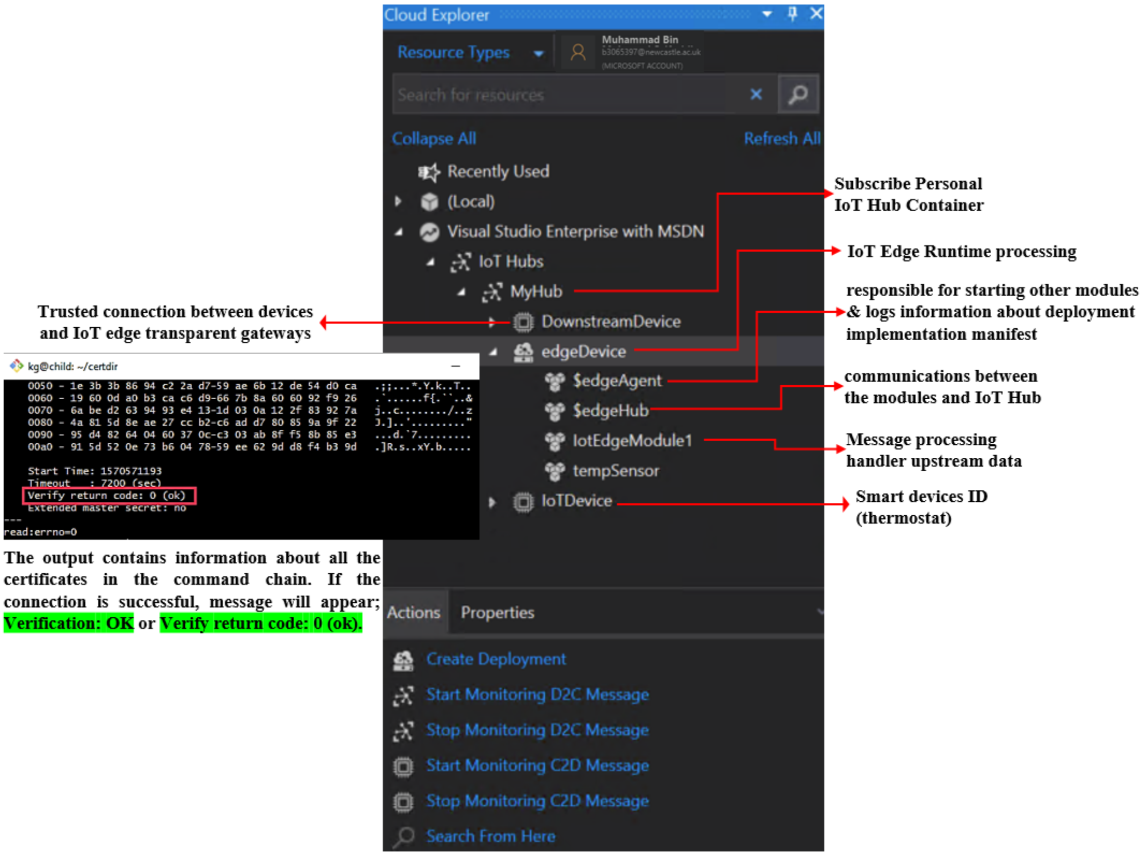

(a) Creating IoT Hub and Edge device runtime environment.

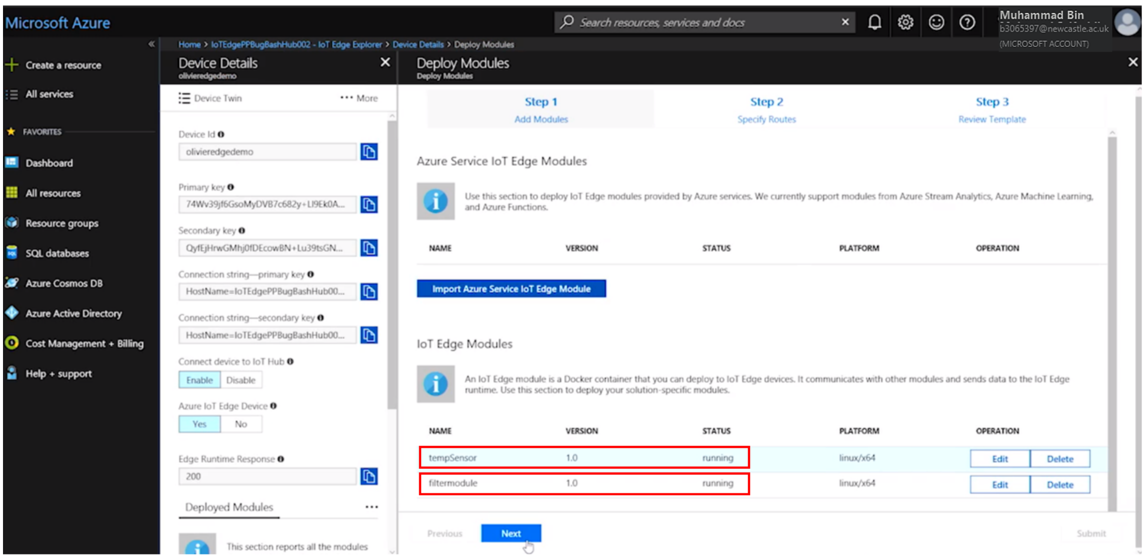

(b) Creating data filter module.

Fig. 3.11 Employing Azure IoT edge Cloud services to establish decentralised computing ability in local environment; closer to device.

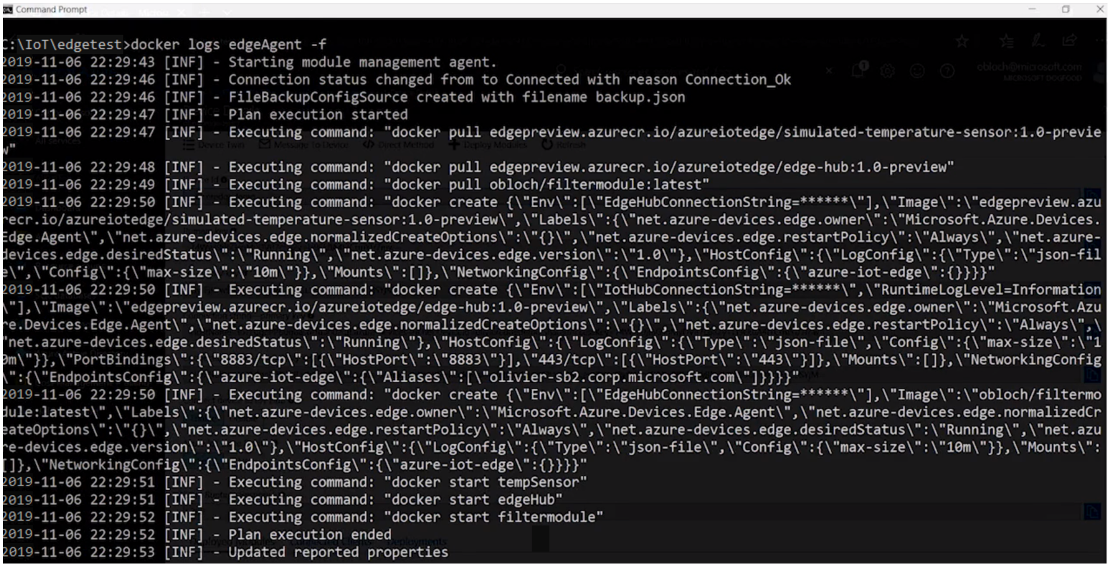

(a) Set-up and start IoT edge device on local machine, creating a docker container to hold all the necessary function modules.

(b) Lists of modules running/activated in IoT edge device runtime.

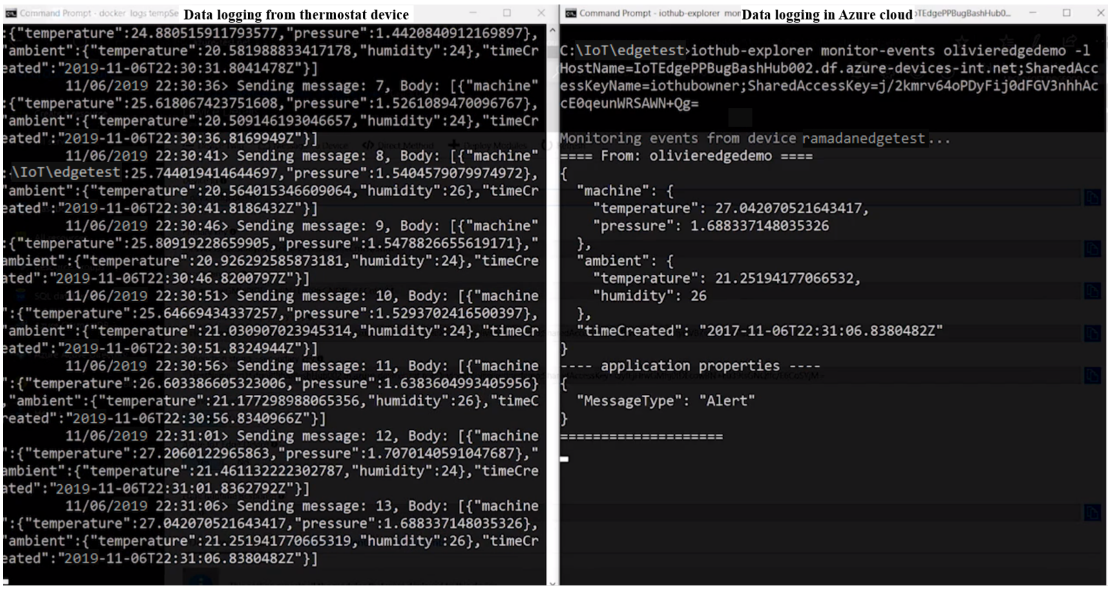

(c) Data logs between temperature sensor module and messages retrieved by Cloud.

Fig. 3.12 Bringing Azure IoT edge device online and test communicating system.

were measured using; *(i)* Processing delay−time taken to execute and complete the task assigned including processing element against data load or task length capacity, *(ii)* Processing costs−the costs incurred for requested computation capacity in CPU per hour rated by the Azure IoT Cloud services, and *(iii)* Processing capability−CPU data processing power required for the Cloud service entity based on millions of instruction per gigahertz. The size of task length is measured in billions of instructions (*BI*) packages.

Fig.3.13a reveals that IoT edge device configuration had a superior processing delay in relation to task length ranges within 10*BI* to 1000*BI* ($<$15 devices) however, deteriorates as it exponentially increases. Indeed, it is inevitable that the processing delay will increase in relations to the task length loaded into the Cloud system. However, a distinct delay curve response was recorded for edge system in case number 11 and above as it enters in the bottleneck threshold region forcing to consume large task length. Whereas, in Cloud settings, it managed to keep a small incremental deviations due to its natural large processing capacities.

In addition, Fig.3.13b investigates into computation delay and data management efficiency to further verify the results attained in Fig.3.13a. It presents a cascading effect in edge processing delay as computation time required increases due to decremental in data management efficiency. Hence, concluded that edge architectures are designed to cater personalised Cloud environment that proffers portability solutions when connecting local devices with computation processes at edge. Nevertheless, to mitigate processing delay when assigned with large task length, edge system will require to subscribe multiple IoT Hubs and divide IoT devices into smaller cluster. However, higher operating costs will be incurred as shown in Fig. 3.13c.

Fig. 3.13c demonstrates that edge has greater processing power and reduced processing delay at the expense of higher operating costs to maintain the Cloud services (inclusive of upstream Cloud container registry). A summarised comparisons between Cloud and edge computing settings is presented in Table. 3.2.

Extending COSAP for Privacy-Sensitive Data Sharing

The contract-service model proposes three negotiation protocols; basic contract, contract observation, and contract management. The basic contract protocol governs device sensors to submit unbiased data flow contracts based on provider's policy and users relationship. It also handles data privacy, masking provider's personal information attached to the sensor data. Contract observation protocol monitors execution of Agent's contracts and user's context arrangements. Contract management protocol manages modification, establishing

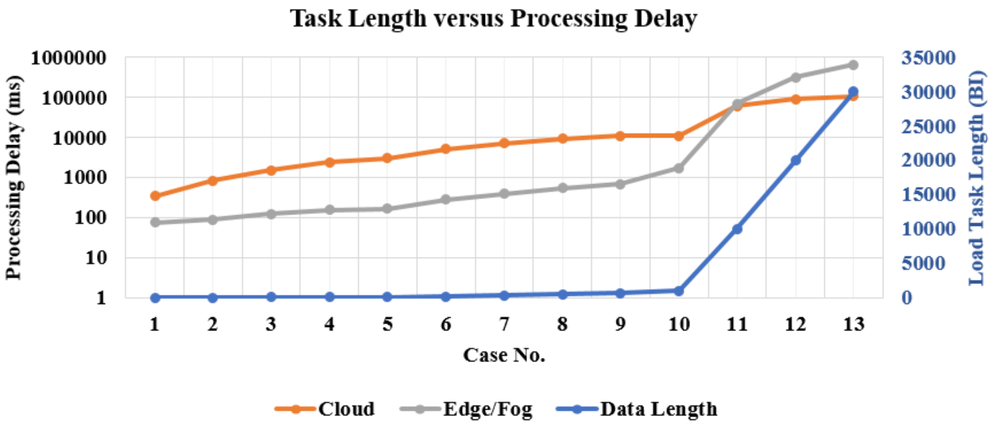

(a) Comparison of processing delay response between Cloud and edge applications.

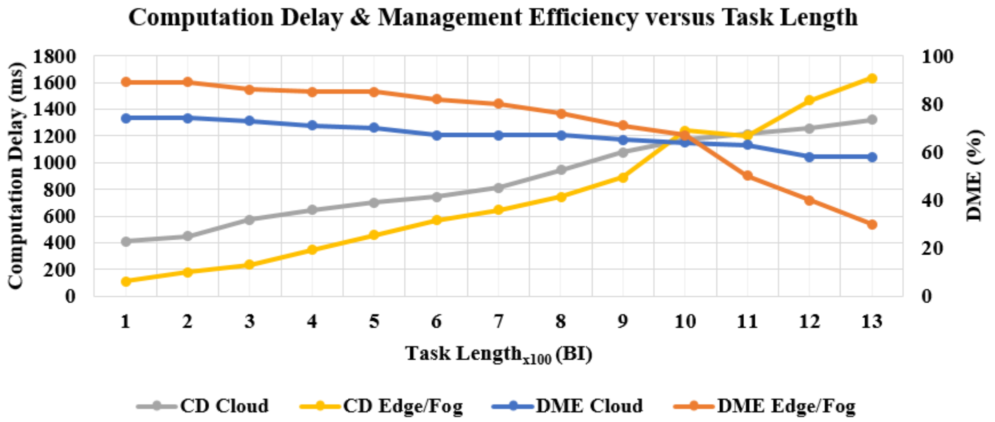

(b) Cloud and edge computing comparisons against data management efficiency (DME) in relations to task length.

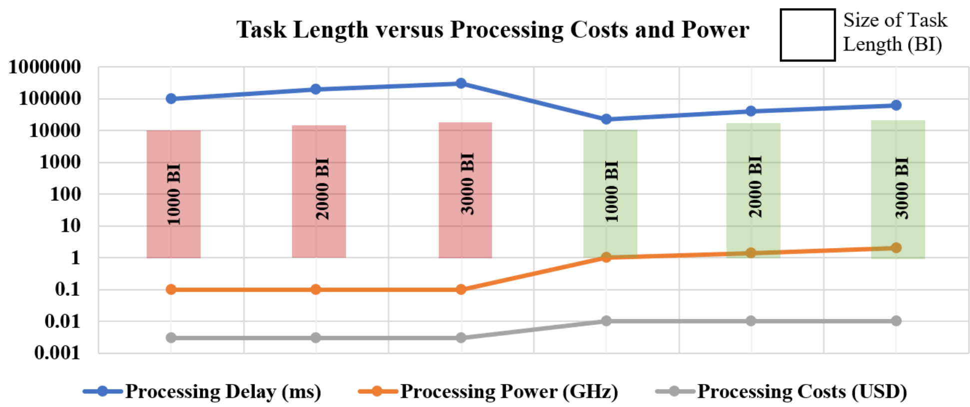

(c) Service costs and processing power consumption comparisons in Cloud and edge configuration (red:Cloud, green:edge Cloud).

Fig. 3.13 Performance comparisons between Cloud and edge computing services.

re-contract of other sensor devices, and cancellations of Agent's contracts. It also oversees optimisation of data flow in relations to the changes made in user's context (requirements).

Table 3.2 Summary of performance bottleneck between Cloud service efficiency and computation overhead.

Parameter	Cloud	Edge
Service Scale & Operation	Global-based resource planning.	local directive w/ custom implementations.
Data & Communication Security	service provider dependency.	stackable encryption layers at local.
Nodes & Bandwidth requirement	internet speed reliance (high traffic & latency).	wireless gateway/access point (refined communication to core hence low latency).
Service Model	provides the IoT infrastructure as a platform & software services	offload content & event processing, virtualisation of network function & accelerator, device management.
Operating expenses (device per server)	High (\$1500−3000)	Low (\$50−200 local gateway & \$1000 for Cloud container registry)

Hence, automation of function deployment is rearranged to maintain quality of exchange service.

There are four types of Agent functions modelled in COSAP environment; user, manager, application, and sensor. The user Agent create an interface and display processed results between users and device with notifications of provider's policy and consumer's specifications. As a contract governor, manager Agent perform validation of contract and generate privacy data protocol when sharing information. The application Agent serves as an application manager controlling sensing data stream, exchanging selected data of user's components. The sensor Agent identifies registered devices and makes contracts with application components based on provider's policy.

Fig. 3.14 illustrates the COSAP architecture and Agents relationships when creating the outline contracting policies to ensure privacy-sensitive is achieved when exchanging sensor data. The COSAP architecture is implemented in *PIAX*, a third-party multi-agent platform, utilising the peer-to-peer location aware network system and defining virtual Agent as users or devices with respective functions. In addition, these Agents must comply with the proposed contract-service protocols and its contract contents/policies.

Fig. 3.15 describes all three contract-service protocols sequence chart, comprehending creation of CIFP models delivered by respective Agents in COSAP environment. Fig. 3.15a demonstrates Agent's sequence in creating basic contract for consumers to send data request message to provider. The provider will then validate the contract in comparisons with its own performance requirements. The contract contains data type information, sensor performance, and consumer's policy. Once all contract are synchronised and agreed upon, the provider's content will be sent to manager Agent for publishing. Fig. 3.15b presents the contract observation protocols for both policy and network change. Here, the manager Agent takes a leading role in detecting any changes in the requested policy and proceed with necessary modification to the contract. Fig. 3.15c defines the contract management protocol sequences for three possible cases; modification, cancellation, and recontract. In component modifications of contract, the manager Agent send an offer to it corresponding partner (provider) highlighting intended changes (*i.e* data quality) in the contract. Sensing data will only start publishing once the contract is agreed between both manager Agents. Likewise, in contract cancellation, both manager Agents will remove the contract and exchanging of data finishes. However, in recontract management, the process restarts from creating the proposed basic contract and offering to other corresponding Agents. Upon agreeing with the new contract parameters, manager Agents from both parties will cancel the old contract and starts exchanging sensing data with its partner based on the specified data quality and sensor.

Using *PIAX* platform, the proposed COSAP is integrated to view Agents' responses to CIFP and sharing of sensing data. By default, the initialisation of contract content and policy are shown in Fig. 3.16; initialise ApplicationAgent101 and ApplicationAgent102 using

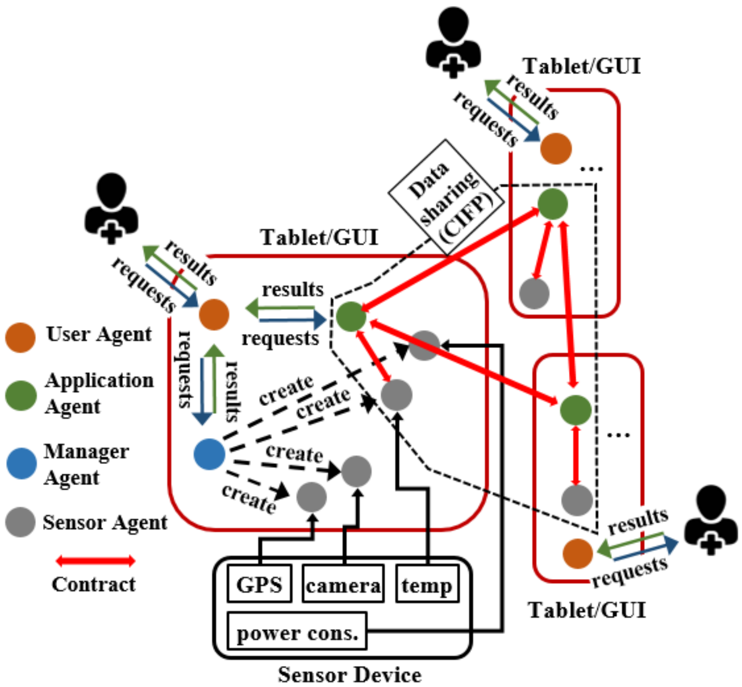

Fig. 3.14 COSAP architecture and Agent components.

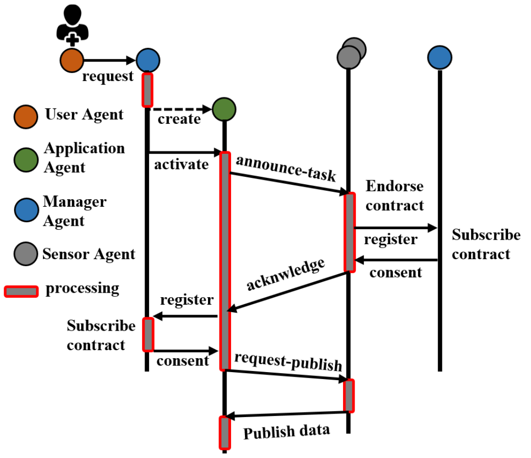

(a) Basic contract protocol sequences.

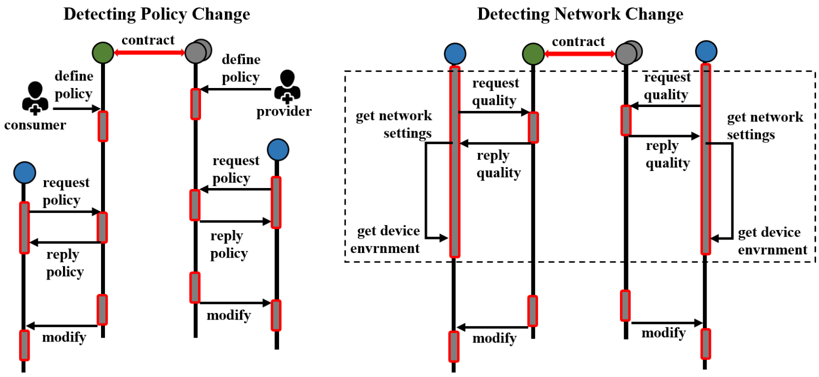

(b) Contract observation on policy and network change sequences.

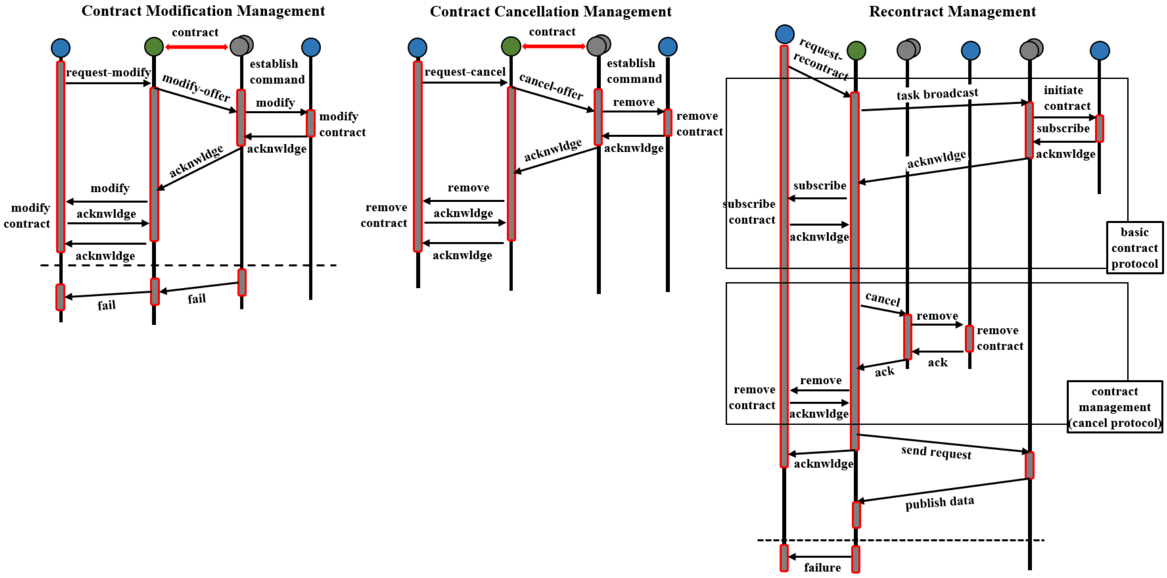

(c) Contract management sequences on modification, cancellation, and recontract.

Fig. 3.15 Modelling sequence of contract-oriented information flow protocols.

(a) Defining Agents and two sensor device units for two participants (users).

```
ManagerAgent101::policy=accuracy:MIDDLE
Contract::id=1674557768; sender=SnsAgent101; receiver=AppAgent201; policy=accuracy: MIDDLE
Contract::id=9824754571; sender=SnsAgent102; receiver=AppAgent202; policy=accuracy: MIDDLE
Contract::id=3685657955; sender=SnsAgent201; receiver=AppAgent101; policy=accuracy: MIDDLE
Contract::id=8568485688; sender=SnsAgent202; receiver=AppAgent102; policy=accuracy: MIDDLE
ApplicationAgent101::policy=accuracy:MIDDLE
Contract::id=3685657955; sender=SnsAgent201; receiver=AppAgent101; policy=accuracy: MIDDLE
ApplicationAgent102::policy=accuracy:MIDDLE
Contract::id=8568485688; sender=SnsAgent202; receiver=AppAgent102; policy=accuracy: MIDDLE
SensorAgent101::policy=accuracy:MIDDLE
Contract::id=1674557768; sender=SnsAgent101; receiver=AppAgent201; policy=accuracy: MIDDLE
SensorAgent102::policy=accuracy:MIDDLE
Contract::id=9824754571; sender=SnsAgent102; receiver=AppAgent202; policy=accuracy: MIDDLE
ManagerAgent201::policy=accuracy:MIDDLE
Contract::id=1674557768; sender=SnsAgent101; receiver=AppAgent201; policy=accuracy: MIDDLE
Contract::id=9824754571; sender=SnsAgent102; receiver=AppAgent202; policy=accuracy: MIDDLE
Contract::id=3685657955; sender=SnsAgent201; receiver=AppAgent101; policy=accuracy: MIDDLE
Contract::id=8568485688; sender=SnsAgent202; receiver=AppAgent102; policy=accuracy: MIDDLE
ApplicationAgent201::policy=accuracy:MIDDLE
Contract::id=1674557768; sender=SnsAgent101; receiver=AppAgent201; policy=accuracy: MIDDLE
ApplicationAgent202::policy=accuracy:MIDDLE
Contract::id=9824754571; sender=SnsAgent102; receiver=AppAgent202; policy=accuracy: MIDDLE
SensorAgent201::policy=accuracy:MIDDLE
Contract::id=3685657955; sender=SnsAgent201; receiver=AppAgent101; policy=accuracy: MIDDLE
SensorAgent202::policy=accuracy:MIDDLE
Contract::id=8568485688; sender=SnsAgent202; receiver=AppAgent102; policy=accuracy: MIDDLE
```

(b) Register contracts between Agents and sensor devices.

Fig. 3.16 Registering contracts and initialisation of Agents in *PIAX* environment based on two connected sensor devices.

ManagerAgent101, create contract with SensorAgent201 and SensorAgent202. Likewise, ManagerAgent201 initialise ApplicationAgent201 and ApplicationAgent202 and create contract with SensorAgent101 or SensorAgent102. Fig. 3.16b verifies that all Agents have established basic contracts with corresponding partners and both ManagerAgent comprehend policies managed by contract management.

```
ManagerAgent101::policy=accuracy:MIDDLE
Contract::id=8568485688; sender=SnsAgent202; receiver=AppAgent102; policy=accuracy: MIDDLE
Contract::id=3685657955; sender=SnsAgent101; receiver=AppAgent101; policy=accuracy: HIGH
Contract::id=1674557768; sender=SnsAgent101; receiver=AppAgent201; policy=accuracy: HIGH
ApplicationAgent101::policy=accuracy:HIGH
Contract::id=3685657955; sender=SnsAgent101; receiver=AppAgent101; policy=accuracy: HIGH
ApplicationAgent102::policy=accuracy:LOW
Contract::id=8568485688; sender=SnsAgent202; receiver=AppAgent102; policy=accuracy: MIDDLE
SensorAgent101::policy=accuracy:HIGH
Contract::id=3685657955; sender=SnsAgent101; receiver=AppAgent101; policy=accuracy: HIGH
Contract::id=1674557768; sender=SnsAgent101; receiver=AppAgent201; policy=accuracy: HIGH
SensorAgent101::policy=accuracy:LOW
ManagerAgent201::policy=accuracy:MIDDLE
Contract::id=8568485688; sender=SnsAgent202; receiver=AppAgent102; policy=accuracy: MIDDLE
Contract::id=1674557768; sender=SnsAgent101; receiver=AppAgent201; policy=accuracy: HIGH
ApplicationAgent201::policy=accuracy:MIDDLE
Contract::id=1674557768; sender=SnsAgent101; receiver=AppAgent201; policy=accuracy: HIGH
ApplicationAgent202::policy=accuracy:MIDDLE
SensorAgent201::policy=accuracy:MIDDLE
SensorAgent202::policy=accuracy:MIDDLE
Contract::id=8568485688; sender=SnsAgent202; receiver=AppAgent102; policy=accuracy: MIDDLE
```

Fig. 3.17 Change in contracts.

Subsequently, ApplicationAgent101 and 102 changes its contract policy by requesting high or low data accuracy. Likewise, SensorAgent101 and 102 also changes its content definition targeting the data accuracy; high−SensorAgent101 and low−SensorAgent102. Fig. 3.17 displays the processes of Agents changing the contract observation and management protocols. In contract 1 (id:1674557768), the policy was changed to data quality HIGH using modify protocol defined by ManagerAgent101. Contract 2 (id:9824754571) protocol was cancelled and no longer executed by the provider as ApplicationAgent102 changes its policy to LOW data accuracy. Whereas, contract 3 (id:3685657955) undergone recontract protocol as the user's requirement has changed to HIGH data quality from MIDDLE and it synchronised with SensorAgent101 policy content defined as HIGH. Contract 4 (id:8568485688) remains unchanged as the user's contracted protocol requested a LOW quality data sensing and the established policy contract remains at MIDDLE.

3.4 Multi-Agent System Intelligence

Agents of MAS are programmed with data-driven intelligence, modelling customise computational algorithm modules into Azure container registry Cloud (using Azure artificial intelligence toolkit as the base function model). Personalised function modules are programmed to solve holistic energy management solutions and deployed at respective DCF control layers. The intelligences adhere to cooperative yet competitive executions in electricity market or DSR operations across participating energy actors.

An Agent is only as intelligent as its knowledge. Hence, the key in edge computing lies within Agent's ability to autonomously acclimate and learn from its hosting environment. Through data analyses measurements, intelligent Agents provide close-to estimations on operational uncertainties and host strategic resolutions in securing either global or local objectives. Nevertheless, implementations of Agents' learning behaviours are typically leaned towards cooperative settings to gain operation equilibrium in real-time (biased management/business models) [183, 185]. The importance in providing Agents with deceptive behaviour are often neglected in multi-agent environment, adding hereditary pressure on Agents to generate policies that are collaborative but yet competitive.

3.4.1 Agent Learning Behaviour

Learning refers to the computational strength in enabling Agents to learn from experience and adapt autonomously in parallel to its parent environment before making absolute decision. Importantly, its learning curve is very much dependent on the feedback received from the computed performance of a system−misaligned data interpretation will only corrupt Agents' efficiency converging into viable solutions.

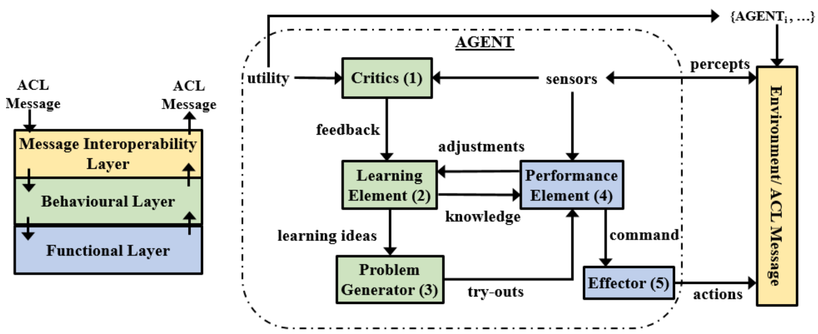

Fig. 3.18 Coopeception Learning Agent in layered architecture.

In addition to learning ability, the concept of deception mechanism [204] proofs to be an admirable supplement when modelling Agent's learning behaviour. Deception allows an Agent to increase its probability of success when competing with others or, instances where the outcome is interfered, compromise and act cooperatively to earn negotiable outcomes. In deception operation, Agent will hide its actions, utilities function (level of satisfaction), and provide decoy actions hoping to deceive overall utility of competing Agents. Hence, alleviating Agent's success rate during cooperative bidding processes.

3.4.2 Blending Cooperative and Deceptive Learning Strategy in Agent

Unfortunately, in smart grid applications, implementation of deception approaches were not favoured as Agents are always resorted to cooperative contracts when propagating global optimality. In consequence, Agents' learning elements are constantly resorted to sub-optimal optimisation at local in distributed environment−limiting Agent's utility from being competitive in order to achieve global objectives. Therefore, Coopeception Learning (CDL) is proposed to blend cooperative and deception attributes into Agent's learning processes. It suggests; *(i)* maintain adaptations of Q-learning [205] strategy to gain best action policy, *(ii)* incorporating Nash equilibrium [206] with relaxed decoy actions, *(iii)* partially disclose local utility to impart blind evaluation for competing Agents, and *(iv)* Agent can hide its actions to minimise competitor's utility expectations.

Fig. 3.18 presents anatomy of the proposed CDL Agent into three layered framework, sectorising Agent's elements. The message interoperability layer includes communication and networking protocols where incoming and outgoing messages of interacting Agents are decrypted and encrypted. It coordinates conversations between Agents during exchange of sensor data or disclose Agent's performances for knowledge purposes. It also extends communication with hardware's control interface to send action commands. The functional layer consolidates action commands based on the decisional information concluded by Agent to drive hardware actuators (effector). The actuator will then influence changes on the environment. Finally, the behavioural layer represents Agent's intelligences. It closely liaise with functional layer for new data so as the Agent's learning and knowledge are constantly updated.

Following describes working principles of respective element in learning Agent anatomy:

1. Critics−evaluates the environment's performance based on the previous determined actions rendered by Agent. The critics uses combination of reward/penalty system against utility's ranking list to provide feedback on Agent's learning process. Accord-

ingly, critics can suggest new coopeception rate to increase Agent competitive edge in a cooperative environment (using gradient descent technique to find optimum solution based on the current environment state).

2. Learning Element−it is responsible in deriving new possible alternatives that may or may not improve the quality of learning based on the critics given. It updates knowledge in performance element and collect advisable adjustments for further computations in an iterative manner. Here, the learning processes will weigh consequences based on the critic's decoy intensity and information from knowledge to avoid sub-optimal solution in global engagements (increase Nash equilibria).
3. Problem Generator−to assist learning element with new possible decoy renditions, focusing on Agent's commitments to share actions or utility with others. The objective is to manipulate contents of percepts and actions to steer other Agents in minimising their utility. It then submit to performance element for computation.
4. Performance Element−contains Agent's function that aids in selecting external actions. Based on the computed solution, it broadcasts a definite action without the consideration of problem generator's feedbacks and feed to learning element as knowledge.
5. Effector−refers to the control features of the actuator. The actions provided from performance element will be ciphered into execution commands readable for connected hardware devices.

3.5 Problem Descriptions in Coopeception Learning

In smart grid operations, cooperative management and adhering to operational constraints serves as vital components in ensuring reliable and balanced network. Rooms for Agents to generate coy actions would lead to constant uncompromise resolutions and hence, it imposes operational risks in finding electrification equilibrium between Prosumer and DSO Agents. Exposure of critics, knowledges, and problem generations element in CDL Agent are blinded within its learning domain (*i.e.* centralised training and policy evaluation). Hence, CDL lacks in the ability to accentuate collaborative behaviours and act incompetently in coalition environment.

Q-learning is an off policy learning algorithm that matures from past action experiences, seeking for superior reward by generating new policy outside the boundary of current ones. Agents' policies will change as training progresses which resultant in indeterministic environment. This imposes learning process of CDL to constantly deviate away from adhering new changes in grid operation constraints.

Despite having Nash equilibrium to increase cooperativeness, it creates inferiority on Q-learning function to search for superior policy as learning and problem generator element provides knowledges that are Nash equilibria biased (generating sub-optimal reward). In this sense, the vision is to create centralised learning but optimised execution of actions in decentralised settings where policies of external Agents can influence Q-learning processing.

3.6 Modelling Reinforcement Learning: Cooperative yet Competitive Multi-Agent System

Indeed, it is uncommon to infuse information into Q-function during learning process. The approach in imparting extra useful information into policy design will not be ideal as it creates ambiguity effects on Q-learning's initial purpose in searching max. reward and randomness. Thus, exploiting CDL Agent's critic element, a reinforced-CDL was proposed by augmenting policies of other participating Agent into critic element using off-policy gradient methods, Agent-critic. The objective is to collect percepts and actions of other competing Agent's and feed into local critics element to broaden policy options, providing feedbacks in view of decentralised evaluations. The Agent-critic element is entrusted to conceal policies of competing Agent from local and create its own policy learning based on the decentralised learned critics and local knowledges. Subsequently, to improve stability of multi-agent policies, ensemble approach is employed in the learning process. Fig. 3.19 presents anatomy of reinforced-CDL Agents incorporating Agent-critic to impart cooperative yet competitive decisional behaviour and abstained from deceptive consequences.

Subsequent sub-chapters provides preliminary mathematical derivations that defines reinforced-CDL processes/behaviour. It selects and fused several supervised reinforcement learning algorithms to create centralised training with decentralised learning designed specially for multi-agent engagements; *(i)* Markov Game (MG) to define Agent environment, *(ii)* Q-learning as the base learning tool, and *(iii)* Deep Deterministic Policy Gradient (DDPG) to procure optimal searching mechanism for best policy. It aims to model reinforcement learning behaviour framework for multi-agent based on deterministic policy that search for optimum action-state pair in decentralised settings, Multi-Agent DDPG (MADDPG).

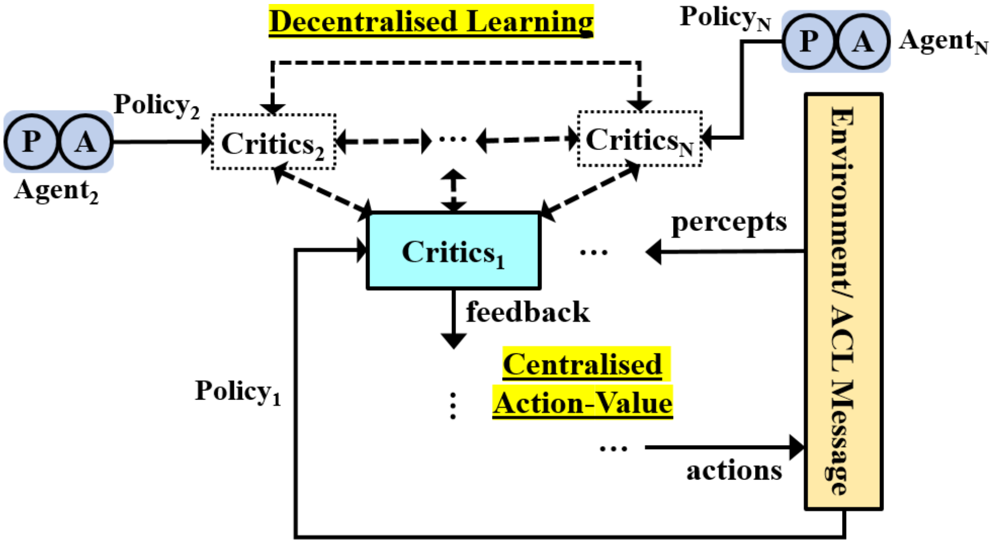

Fig. 3.19 Adds Agent-critic into CDL to create reinforced-CDL Agent anatomy.

3.6.1 Markov Game

MG is an extension of Markov Decision Process (MDP) that expands from single probabilistic transition function to multiple adaptive Agents with interacting or competing goals [207]. MG, also known as stochastic game, is defined by a set of states, $s \in S$, correspondent to set of actions, $a \in A$ and percepts, $p \in P$ which describes all possible configuration of each Agent for N Agents. In the process of choosing action, each Agent i uses stochastic policy (3.1) to estimate the next s controlled by state transition function (3.2) (current s and one a from each Agent) where $PD(s)$ refers to the set of discrete probability distribution over set s. Each Agent will then be assigned with reward as a function of s and Agent's action (3.3) and receives private observation correlated to state (3.4). Respective Agent aims to maximise its total discounted reward (3.5) where $r_{i,t+j}$ refers to the reward awarded to Agent in the future, t, using j increment and α is the discount factor, $\alpha \mapsto [0,1]$.

$$\pi_{\theta_i} \mapsto [0,1] : p_i \times a_i \tag{3.1}$$

$$T : S \times a_1 \times a_2 \times ... \times a_N \mapsto PD(s) \tag{3.2}$$

$$r_i : S \times a_i \mapsto R \tag{3.3}$$

$$o_i : S \mapsto p_i \tag{3.4}$$

$$TDR_t = r_{t+1} + \alpha r_{t+2} + \alpha^2 r_{t+2} ... = \sum_{j=0}^{\infty} \alpha^j r_{t+j+1} \tag{3.5}$$

3.6.2 Q-learning

Q-learning is a model-free algorithm that employs trial and error approach to update learning knowledge [208]. Its dependent on previous state and action is minimal as it uses off-policy learning to counter actions obtained from another policy, a^*. The Q-learning algorithm is modelled based on Bellman equation where optimal decision is concluded by using state-value function of policy π:

$$V^{\pi}(s) = E_{\pi}[TDR_t | s_t = S] \tag{3.6}$$

The symbol π seen in (3.6) denotes Agent policy function where Agent specify its action, a, taken in the current state, s, environment while $\mathbb{E}$ refers to the probabilistic expectation of random variable. Representation on how good the state is for the Agent is referred as V^{π} based on the expected total reward weightage gained from respective states. Depending on the policy assigned, Agent will perform corresponding actions. The policy function describes an action to be taken by Agent under specified environment/state. It represents Agent's learning behaviour that commands action-state pair at each time intervals, $t \in T$.

$$\begin{aligned} \pi(s) &: S \to A \\ \pi(s) &= a; \quad deterministic \\ \pi(a|s) &= P_{\pi}[a = A | s = S]; \quad stochastic \end{aligned} \tag{3.7}$$

To model the dynamics of Agent's environment and predicts its next state, it uses transition probability state function, $P^a_{ss'}$. Its affiliated reward gained is calculated using rewards function, R^a_s:

$$\begin{aligned} P^a_{ss'} &= P[s_{t+1} = s' | s_t = S, a_t = A] \\ R^a_{ss'} &= \mathbb{E}[r_{t+1} | s_t = S, s_{t+1}, a_t = A] \end{aligned} \tag{3.8}$$

hence the policy function is rewritten as:

$$\begin{aligned} P^{\pi}_{ss'} &= \sum_{a \in A} \pi(a|s) P^a_{ss'} \\ R^{\pi}_{ss'} &= \sum_{a \in A} \pi(a|s) R^a_{ss'} \end{aligned} \tag{3.9}$$

where P symbolises probability and s' refers to the next state after performing action (S':$S \to A$). Value function in (3.6) is rewritten where the first reward is taken out from the sum:

$$V^{\pi}(s) = \mathbb{E}_{\pi}[r_{t+1} + \alpha \sum_{j=0}^{\infty} \alpha^{j} r_{t+j+2} | s_t = S] \tag{3.10}$$

and combining (3.8)− (3.10), the state-value function correspond to Agent policy is expressed as:

$$V^{\pi}(s) = \sum_{a \in A} \pi_{\theta}(a|s) \sum_{s' \in S} P^{a}_{ss'}[R^{a}_{ss'} + \alpha V^{\pi}(s')] \tag{3.11}$$

Appendix B proof of value-state function. derivation

Similarly, employing Bellman's value function, (3.10) can be rewritten as action-value function that defines Q-value, $Q_{\pi}(s,a)$, in Q-learning based on Agent policy, π:

$$\begin{aligned} Q^{\pi}(s,a) &= \mathbb{E}_{\pi}[\sum_{j=0}^{\infty} \alpha^{j} t_{t+j+1} | s_t = S, a_t = A] \\ Q^{\pi}(s,a) &= \sum_{s' \in S} P^{a}_{ss'}[R^{a}_{ss'} + \alpha \sum_{a' \in A} \pi_{\theta}(a'|s') Q^{\pi}(s',a')] \end{aligned} \tag{3.12}$$

However, (3.11) & (3.12) does not depict value function optimality. Among all possible states and policies, there exist an optimal value function. To determine optimal Agent policy, apply argument *max*. function for all states.

$$\begin{aligned} V^{\pi^*}(s) &= \max_{\pi} V^{\pi}(s) \;\; \forall s \in S \\ \pi^*(s) &= \arg\max_{\pi} V^{\pi}(s) \;\; \forall \in S \end{aligned} \tag{3.13}$$

and similarly for optimal Q-value function yielding $Q : S \times A \rightarrow \Re$ thus,

$$\begin{aligned} Q^{\pi^*}(s,a) &\doteq \max_{\pi} Q^{\pi}(s,a) \\ \pi^*(a|s) &= \arg\max_{\pi} Q^{\pi}(s,a) \end{aligned} \tag{3.14}$$

Using (3.11)−(3.14) and recursive dynamic programming operation on Q-value function, it computes the optimal Q-value, $Q^*(s,a)$.Recognising optimal Q-value is probably the maximum value hence, the action performed, a', must the largest Q-value (Q-value on the right-side of equation):

$$\begin{aligned} Q^*(s,a) &= R^{a}_{s} + \alpha \sum_{s' \in S} P^{a}_{ss''} V^{\pi^*}(s') \\ Q^*(s,a) &= R^{a}_{s} + \alpha \sum_{s' \in S} P^{a}_{ss'} \max_{a'} Q^{\pi^*}(s',a') \end{aligned} \tag{3.15}$$

since,

$$V^{\pi^*}(s) = \max_{a \in A}[R(s,a) + \alpha \sum_{s' \in S} P^a_{ss'} V^{\pi^*}(s')] \tag{3.16}$$

Appendix B proof of optimal value-state function. derivation

Finally, using iterative dynamic programming, it performs either value or policy iteration [209] and updates new improved Q-value until it converges with a deviation error. Once iteration is terminated, apply $\arg\max$ function for all states to cipher optimal policy. However, both iteration method requires knowledge of transition probability function, P, which typically used only in model-based algorithm. Furthermore, model-based algorithm suffers scalability problem [209, 210] due to exponential action and state space for learning (more sample for efficiency).

Intuitively, reverting back to given Q action-value function in (3.12), it rates the learning quality based on the state-action pair used in the current state. Subsequently, the objective is to compute the next possible state-action pair and assign reward to improve Q-value and repeat the sequence until max Q-value is found.

Theoretically, employing value iteration computing method can serve as an alternative to converge Q-value using optimal action-value function. Hence, value iteration updates Q-value using all states and action to generate sufficient series of samples that progressively descents (gradient descent approach) into small deviation error by introducing learning rate, β (rate of learning approaching goal). In relations to (3.14), updating Q-value:
new Q-value = curr Q-value + LR [R + DF*maxQ'- curr Q-value].

$$\begin{aligned} Q_{i+1}(s,a) &= \mathbb{E}_{s'}[r + \alpha \max_{a'} Q_i(s',a')|s,a] \\ Q(s_t,a_t) &\leftarrow Q(s_t,a_t) + \beta[r_{t+1} + \alpha \max_{a} Q(s_{t+1},a) - Q(s_t,a_t)] \end{aligned} \tag{3.17}$$

where the next action, a' is selected to maximise Q-value in the next state instead of using current policy. Here a greedy approach as a function of $Q(s,a)$ is adopted to indicate improvement in policy based on action taken in corresponding state:

$$\pi(s,a) = \begin{cases} 1, & if\ a = \arg\max_{a} Q(s,a) \\ 0, & otherwise \end{cases} \tag{3.18}$$

Pseudo of Q-learning function $Q : S \times A \rightarrow \Re$:

declarations:

State = {1,2,...,N$_s$}

Action = {1,2,...,N$_a$}
Reward = R: S$\times A \rightarrow \Re$
Probabilistic transition function = P: S$\times A \rightarrow S$
$\beta \mapsto [0,1]$, typically $\beta = 0.1$
Discount factor = $\alpha \mapsto [0,1]$
MDP:(S,A,R,T,α,β)
initialise: Q: S $\times$ A $\rightarrow \Re$
while_loop Q-value not converge (error > tolerance)
Assign state $s \in S$
while_loop s is not complete
Calculate π_θ based on current Q, $\pi_\theta(s) \leftarrow \arg\max_a Q(s,a)$
$a \leftarrow \pi_\theta(s)$
$r \leftarrow R(s,a)$
$s' \leftarrow P(s,a)$
$Q(s',a) \leftarrow (1-\beta) * Q(s,a) + \beta(r + \alpha \max_{a'} Q(s',a'))$
s$\leftarrow s'$
end while
err = |Q(s,a)-Q(s',a)|
end while

The deployment of Q-learning will be allocated in critics element of Agent's anatomy and update knowledge to learning element.

3.6.3 Actor-Critic & Off-Policy Gradient

Policy gradient [208] approach is designed to explicit optimise Agent's policy, π_θ, at modelling directly. It is defined with a parametrised function with respect to θ, $\pi_\theta(s|a)$. Comprehending that performance of Agent's policy influences the reward function hence, optimising θ can attune Agent's actions in a more strategic manner as compared to Q-learning. In policy gradient method, it defines:

$$J(\theta) = \sum_{s\in S} d^{\pi_\theta}(s) V^{\pi_\theta}(s) = \sum_{s\in S} d^{\pi_\theta}(s) \sum_{a\in A} \pi_\theta(a|s) Q^{\pi_\theta}(s,a) \tag{3.19}$$

where $d^\gamma(s)$ refers to the stationary distribution of Markov chain [208] for on-policy state distribution under π_θ. As time progresses where the policy reaches a state where it is unchanged, it becomes a stationary probability for π_θ:

$$d^{\pi_\theta}(s) = \lim_{t\to\infty} P(s_t = S|s_0, \pi_\theta) \tag{3.20}$$

where probability that $s_t = S$ starting from s_0 follows policy, π_θ, for t step intervals. In theory, policy based approach yields better search optimality optimum in continuous domain as there are infinite number of actions and/or states. However, in generalized policy iteration, $\pi_0 \xrightarrow{\text{evaluation}} Q^{\pi_0} \xrightarrow{\text{improve}} \pi_1 \xrightarrow{\text{evaluation}} Q^{\pi_1} ... \xrightarrow{\text{improve}} \pi_* \xrightarrow{\text{evaluation}} Q^{\pi_*}$, the policy improvement, $\arg\max_{a\in A} Q^{\pi_\theta}(s,a)$, requires to compute and scan all action spaces which definitely resultant to "curse of dimensionality".

In this sense, using policy gradient theorem [208], θ can be steered in the direction suggested by $\nabla_\theta J(\theta)$ to search for optimal θ based on highest return policy, π_θ. It reforms the derivative objective function without involving state distribution, $d^\pi(.)$, as compared to computing gradient of $\nabla_\theta J(\theta)$ where both the action selection (ordained by policy π_θ) and stationary distribution of states follows the target selection behaviour (indirectly defined by policy π_θ):

$$\begin{aligned} \nabla_\theta J(\theta) &= \nabla_\theta \sum_{s\in S} d^{\pi_\theta}(s) \sum_{a\in A} Q^{\pi_\theta}(s,a)\pi_\theta(a|s) \\ \nabla_\theta J(\theta) &\propto \sum_{s\in S} d^{\pi_\theta}(s) \sum_{a\in A} Q^{\pi_\theta}(s,a)\nabla\theta\pi_\theta(a|s) \end{aligned} \tag{3.21}$$

Gradient is further written to incorporate episodic and continuing cases of learning trial tasks proportionality [211]:

$$\begin{aligned} \nabla_\theta J(\theta) &= \sum_{s\in S} d^{\pi_\theta}(s) \sum_{a\in A} \pi_\theta(a|s) Q^{\pi_\theta}(s,a) \frac{\nabla_\theta \pi_\theta(a|s)}{\pi_\theta(a|s)} \\ \nabla_\theta J(\theta) &= \mathbb{E}_{s\sim d_\pi, a\sim\pi_\theta}[Q^{\pi_\theta}(s,a)\nabla_\theta \ln \pi_\theta(a|s)] \end{aligned} \tag{3.22}$$

Refer Appendix B proof of policy gradient theorem. derivation
where $\mathbb{E}$ performs the distribution of both state and action following on-policy.

Unfortunately, conventional policy gradient algorithm (Monte-Carlo or REINFORCE [212]) suffers high gradient variance. Monte Carlo projects the full trajectory policy distribution and documents corresponding rewards attained. It has no value function and high in variance due to stochastic policy that have unsynchronised actions and episodes (resets back to initial state). Hence, in an event where action performed is deviated from planned policy trajectory, potential divergence can arise due to conflict in awarding rewards (increase and decrease the log likelihood for same action). Indeed, [212] has proposed baseline approach to update gradient ascent by subtracting state-value from Q action-value function to reduce variance of gradient estimation.

$$\begin{aligned}\nabla_\theta J(\theta) &= \mathbb{E}_{s\sim d_\pi, a\sim\pi_\theta}[Q^\pi(s,a)\nabla_\theta \ln \pi_\theta(a|s)] \\ \nabla_\theta J(\theta) &= E_\pi[G_{traj}\nabla_\theta \ln \pi_\theta(a_t|s_t)]\end{aligned} \tag{3.23}$$

since

$$Q^\pi(s_t,a_t) = \mathbb{E}_\pi[TDR_t|s_t = S, a_t = A] = G_{traj} \tag{3.24}$$

where expectation sample is equal to actual gradient and used to update the policy gradient.

Pseudo of Monte-Carlo Policy Gradient function:

initialise policy: Set θ at random.

Compute initial policy trajectory, $\pi_\theta : s_1, a_1, r_2, s_2, a_2, r_3, ..., s_T$.

for_loop t++ *neq* T

compute $G_{traj} -= V(s)$

Update policy $\theta \leftarrow \theta + \beta\alpha_t G_{traj}\nabla_\theta \ln \pi_\theta(a_t|s_t)$

end for

Alternatively, actor-critic proves to provide better control on the policy's gradient ascent as it considers both state-value function and action policy learned [213]. The actor updates policy parameter, θ, for $\pi_\theta(a|s)$ in the gradient direction suggested by critic. While critic updates the action-value function parameter, ac, in, $Q_{ac}(s,a)$.

Pseudo of Actor-Critic Policy Gradient function:

initialise: Set θ,s,w at random. Set both learning rate β_θ, β_{ac}

Sample initial policy over action distribution: $a \sim \pi_\theta(a|s)$

for_loop t++ $\neq$ T

Sample $r_t \sim \sum_{r\in R} r_t \sum_{s'\in S} P^a_{ss'}$ and $s' \sim P^a_{ss'}$

Sample next action $a' \sim \pi_\theta(a'|s')$

Update policy parameter: $\theta \leftarrow \theta + \beta_\theta Q_a c(s,a)\nabla_\theta \ln \pi_\theta(a|s)$

Compute TD error for action-value: $ERR_t = r_t + \alpha Q_{ac}(s',a') - Q_{ac}(s,a)$

Update action-value function: $ac \leftarrow ac + \beta_{ac} ERR_t \nabla_{ac} Q_{ac}(s,a)$

Update action, state: $a \leftarrow a'$; $s \leftarrow s'$

end for

Nevertheless, the proposed critic element of reinforced-CDL Agent requires off-policy approach to generate feedbacks based on decentralised environment. As compared to on-policy, Off-Policy Gradient (OPG) neglects dependent on full targeted trajectories and uses experience replay (*i.e.* samples are drawn randomly in memory and can be reused). In this sense, it improves data efficiency, smoother changes in data distribution, and sequence correlated observations are removed. In addition, unrestricted exploration of behaviour policy is attained from sample collection.

OPG adopts known behaviour policy, $\gamma(a|s)$, that collects predefined samples under prior distribution. The objective function defines the behaviour policy by summing the reward over state, s, distribution. recognising from (3.21):

$$J(\theta) = \sum_{s \in S} d^{\gamma_\theta}(s) \sum_{a \in A} Q^{\pi_\theta}(s,a)\pi_\theta(a|s) \tag{3.25}$$

hence:

$$J(\theta) = E_{s \sim d^\gamma}[\sum_{a \in A} Q^\pi(s,a)\pi_\theta(a|s)] \tag{3.26}$$

where $d^\gamma(s)$ refers to the stationary distribution of Markov chain for behaviour policy γ. (3.23) depicts that expectation reward state distribution follows the behaviour policy, π_γ. Recall that Q^π is the Q-value function corresponds to action-state pair that relates to target policy π_θ. And $d_\pi(s) = \lim_{t \to \infty} P(s_t = s|s_0, \pi_\theta)$ is the probability where $s_t = s$ in the initial state,s_0, and follows policy π_θ for t steps ($\neq$ behaviour policy). Having training observations sampled by $a \sim \gamma(a|s)$, from (3.23) & (3.26), the gradient is rewritten as:

$$\begin{aligned} \nabla_\theta J(\theta) &= \nabla_\theta \mathbb{E}_{s \sim d^\gamma}[\sum_{a \in A} Q^\pi(s,a)\pi_\theta(a|s)] \\ \nabla_\theta J(\theta) &= \mathbb{E}_\gamma[\frac{\pi_\theta(a|s)}{\gamma(a|s)} Q^\pi(s,a)\nabla_\theta \ln \pi_\theta(a|s)] \end{aligned} \tag{3.27}$$

where $\frac{\pi_\theta(a|s)}{\gamma(a|s)}$ refers to the importance weight biasness [214]. Given in OPG setting, adjustment to the policy gradient can be done by introducing weighted sum ratio (importance weight) to the behaviour policy.

From the algorithms described above, preposition of Agent's learning behaviour policy, π, has evolved from indeterministic (random) in Q-learning to on-policy ascent gradient (directly searching for policy optimality) to off-policy for sampling efficiency with larger action-state search space. However, the modelled policy function, $\pi(.|s)$, is always referred as a probabilistic distribution under action at a given state. To advance further, the policy exploration for optimality can be shifted from stochastic to deterministic decision.

3.6.4 Deep Deterministic Policy Gradient

Deep Deterministic Policy Gradient (DDPG) [215] aggregates Deep-Q network (DQN) with Deterministic Policy Gradient (DPG) to form an off-policy actor-critic algorithm. It performs using actor-critic framework in a continuous space with deterministic policy.

DPG [216] models the Agent's policy as deterministic decision defined in (3.7). It aims to estimate the policy gradient function based on a single action. To distinguish deterministic from stochastic policy, subsequent notation for policy is denoted as: $a = \mu(s)$.
To recall:
Describing the iterative probability of k steps transitioning from state, s, to next state, s', with policy, μ_θ, the visitation probability function at s' is $\rho^\mu(s \to s', k)$ after moving k steps by policy μ. Therefore, in a recursive procedure travelling to the next state is: $s \xrightarrow{a \sim \mu_\theta(.|s)} s' \xrightarrow{a \sim \mu_\theta(.|s')} s''$... and when $k = 0$, then, $\rho^\mu(s \to s, k = 0) = 1$. If $k = 1$, the transition probabilities are summed up based on all possible actions, $\rho^\mu(s \to s', k = 1) = \sum_{a \in A} \mu_\theta(a|s) P^a_{ss'}$. The objective is to travel from state $s \to s'$ after $k+1$ step and update iterative visitation probability $\rho^\mu(s \to x, k+1) = \sum_{s' \in S} \rho^\mu(s \to s', k) \rho^\mu(s' \to x, 1)$. Lastly, $\rho^\mu(s')$ denotes the improper discounted state distribution and it is expressed as $\int_S \sum_{k=1}^{\infty} \alpha^{k-1} \rho_0(s) \rho^\mu(s \to s', k) ds$. To optimise objective function for deterministic policy:

$$J(\theta) = \int_S \rho^\mu(s) Q(s, \mu_\theta(s)) ds \tag{3.28}$$

and DPG gradient theorem (using chain rule differentiation, $\int da$, $\int d\theta$):

$$\begin{aligned}\nabla_\theta J(\theta) &= \int_S \rho^\mu(s) Q^\mu(s,a) \nabla_\theta \mu_\theta(s)|_{a=\mu_\theta(s)} ds \\ \nabla_\theta J(\theta) &= \mathbb{E}_{s \sim \rho^\mu}[\nabla_a Q^\mu(s,a) \nabla_\theta \mu_\theta(s)|_{a=\mu_\theta(s)}]\end{aligned} \tag{3.29}$$

On the other hand, DQN [215] transforms Q-learning from linear to nonlinear function approximation. It counters Q-learning's weakness in gaining convergence and policy loss issues due to restricted action-state pair experiences. The key in DQN's learning performances that stabilises Q-learning is governed by two mechanisms: experience reply memory and target network that periodically updates and freezes. It uses neural network [215] to perform end-to-end learning that increases search space environment for state-action pair possibilities and help organise historic $Q(s,a)$ that reduces risks of correlation effect [217]. Hence, it introduces element of replay memory that stores experience tuples over many episodes, $e_t = (s_t, a_t, r_t, s_{t+1}, a_{t+1}, r_{t+1}, ..., s_T, a_T, r_T) \to D_t = e_1, ..., e_t$.

Hence, reverting back to Q-learning action-value iterative function (3.17) that uses stochastic policy:

$$Q_{i+1}(s,a) = \mathbb{E}_{s'}[r + \alpha \max_{a'} Q_i(s',a')|s,a] \tag{3.30}$$

Rewritten to incorporate weight matrix, w, for neural network's learning process (interconnecting neurons that influences output performance):

$$Q(s,a,w) \approx Q^{\pi}(s,a) \tag{3.31}$$

and the objective function that defines the Q-value error (mean-square error) and redefined Q-learning stochastic gradient descent:

$$\begin{aligned} \mathscr{L}(w) &= \mathbb{E}[(r + \alpha \max_{a'} Q(s',a',w) - Q(s,a,w))^2] \\ \frac{\partial \mathscr{L}(w)}{\partial w} &= E\big[(r + \alpha \max_{a'} Q(s',a',w) - Q(s,a,w))\frac{\partial Q(s,a,w)}{\partial w}\big] \end{aligned} \tag{3.32}$$

where $\Delta(w)$ denotes the change in neural network weights. Subsequently, infusing the Q-value error (loss) function into Q-learning:

$$\mathscr{L}(w) = \mathbb{E}_{s,a,r,s' \sim U(D)}[r + \alpha \max_{a'} Q(s',a',w) - Q(s,a,w)^2] \tag{3.33}$$

where $U(D)$ refers to the uniform distribution over replay memory and Q-learning. In addition, to avoid policy oscillation, Q-learning fixes parameter w with old value, w^-:

$$\mathscr{L}(w) = \mathbb{E}_{s,a,r,s' \sim U(D)}[(r + \alpha \max_{a'} Q(s',a',w^-) - Q(s,a,w))^2] \tag{3.34}$$

where every t interval, fixed parameter, w^-, is updated $w- \leftarrow w$. Furthermore, DQN limits the rewarding system to $[-1,+1]$ to prevent Q-value from aggrandising to large from uncoordinated policy gradient and misinterpretations.

Since DQN operates with stochastic policy in discrete action space, hybridising DPG's can extend its policy into deterministic and learning gradient into continuous domain. Following breakdowns the process for DDPG conversion where the neural network parameter are defined as; $\theta^Q -$Q network, $\theta^\mu -$deterministic policy network, $\theta^{Q'} -$target Q network, and $\theta^{\mu'} -$target policy network:

1. Deterministic policy representation: $a = \mu(S)$ with random parameter values θ^μ.

2. Critic estimates action-value of current policy:
$\frac{\partial \mathscr{L}(\theta^Q)}{\partial \theta^Q} = \mathbb{E}[(r + \alpha Q(s', \mu(s')|\theta^Q) - Q(s,a|\theta^Q))\frac{\partial Q(s,a|\theta^Q)}{\partial \theta^Q}]$.

3. Actor updates policy to improve Q-value: $\frac{\partial J(\theta^\mu)}{\partial \theta^\mu} = \mathbb{E}_s[\frac{\partial Q(s,a|\theta^\mu)}{\partial a}\frac{\partial \mu(s|\theta^\mu)}{\partial \theta^\mu}]$.

4. Critic adds experience replay memory, D, and target network, $\theta^{Q'}$, in Q action-value function: $\frac{\partial \mathscr{L}(\theta^Q)}{\partial \theta^Q} = \mathbb{E}_{s,a,r,s' \sim U(D)}[r + \alpha Q(s', \mu(s')|\theta^{Q'}) - Q(s,a|\theta^Q)\frac{\partial Q(s,a|\theta^Q)}{\partial \theta^Q}]$.

5. Actor adds experience replay memory for actor's policy function:
$\frac{\partial J(\theta^\mu)}{\partial \theta^\mu} = \mathbb{E}_{s,a,r,s' \sim U(D)}[\frac{\partial Q(s,a|\theta^Q)}{\partial a}\frac{\partial \mu(s|\theta^\mu)}{\partial \theta^\mu}]$.

6. Add noise, $\mathscr{N}$, to construct better policy exploration: $\mu'(s_t) = \mu_(s_t|\theta_t^\mu) + \mathscr{N}$.

7. introduce interpolation factor,τ, when updating weights for each time interval:
$\theta_{t+1}^{\mu,Q} \leftarrow \tau\theta_t^{\mu,Q} + (1-\tau)\theta_t^{\mu,Q}$

Pseudo for DDPG:

Initialise: Random Q-value & policy: $Q(s,a|\theta^Q)$, $\mu(s|\theta^\mu)$, and weight matrix θ^Q, θ^μ.

Assign initial target network Q' and μ' with weights $\theta^{Q'} \leftarrow \theta^Q$, $\theta^{\mu'} \leftarrow \theta^\mu$.

Declare buffer replay size, MBR, ($1e^5$).

for_loop episode++ $\neq$ EPI

Random generate $\mathscr{N}$ for action exploration.

Store observation for initial state, $s = \{o_1, ..., o_N\}$.

for_loop t++ $\neq$ T

Compute action,a_t, based on current policy with noise, $a_t = \mu(s_t|\theta^\mu) + \mathscr{N}_t$.

Store in MBR, (s_t, a_t, r_t, s_{t+1}).

Randomly sample a batch of N(64) transition from MBR: (s_i, a_i, r_i, s_{i+1})

(Begin backpropagation neural network, one t step):

Compute Q-value based on target network: $q_i = r_i + \alpha Q'(s_{i+1}, \mu'(s_{i+1}|\theta^{\mu'})|\theta^{Q'})$

Update critic gradient to minimise loss (distribution over batch):

$loss = \frac{1}{N}\sum_i(q_i - Q(s_i, a_i|\theta^Q))^2$

Using the sampled policy gradient, update actor's policy (distribution over batch):

(off-policy) $\nabla_{\theta_i^\mu} J \approx \frac{1}{N}\sum_i[\nabla_a Q(s,a|\theta^Q)|_{s=s_i, a=\mu(s_i)} \nabla_{\theta^\mu}\mu(s|\theta^\mu)|_{s=s_i}]$

Update weights for critic and actor:

$\theta^{Q',\mu'} \leftarrow \tau\theta^{Q,\mu} + (1-\tau)\theta^{Q',\mu'}$ where $\tau << 1$

(End backpropagation neural network):

end for

end for

3.6.5 Multi-Agent DDPG

Despite formulating Agent's model-free learning behaviour to perform action-state value function that updates policy (deterministic off-policy based) feedback in continuous space, it lacks the ability to procure emergent behaviour that co-exists with other interacting Agents. Behavioural elements such as social environment dilemmas, decentralised yet globally cooperative based on dynamic competitor policies can extend learning pattern optimisation to better suite environment settings.

In this sense, Multi-Agent DDPG (MADDPG) [218] is an end-to-end learning environment where it extends Q-learning into incorporating policies of other Agents. Exploiting actor-critic algorithm, MADDPG endorses centralised learning for critic from decentralised execution paradigm deduced from actor. Interacting Agents can only share critic (action-observation) during training while critics will randomly access memory buffer to cipher local Q action-value, avoiding correlations in action-state pair when learning. Fig. 3.20 presents the architecture of MADDPG, illustrating how joined policies aids in Agent learning behaviour towards environment.

The problem formulation of MADDPG can be conceptualised using MG in multi-agent domain. Instantaneously, there are N number of interacting Agents within a set of states, $s \in S$. A set of joined Agents' actions and state observations, $\{a_1, \ldots, a_N\}$ and $\vec{so} = \{so_1, \ldots, so_N\}$ respectively. Each Agent chooses action based on deterministic policy, $\mu_{\theta_i} : so_i \to a_i = \{\mu_{\theta_1}, \ldots, \mu_{\theta_N}\}$ where θ_i is the policy parameter. Centralised critic (Q action-value) function for the i^{th} Agent is defined as $Q_i^{\vec{\mu}_\theta}(\vec{so}, a_1, \ldots, a_N)$ taking actions of all Agents,$a_1 \in A_1, \ldots, a_n \in A_N$, but learns separately. Therefore, each Q-value from respective Agents will have arbitrary

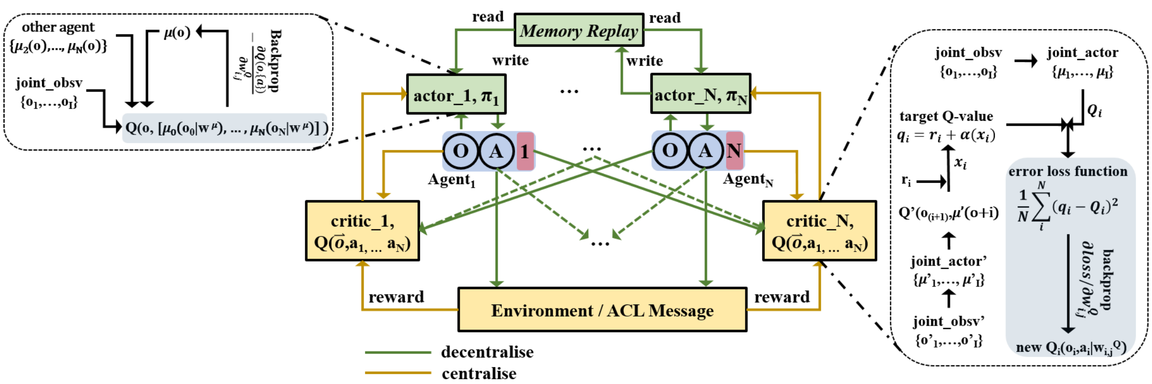

Fig. 3.20 MADDPG learning architecture.

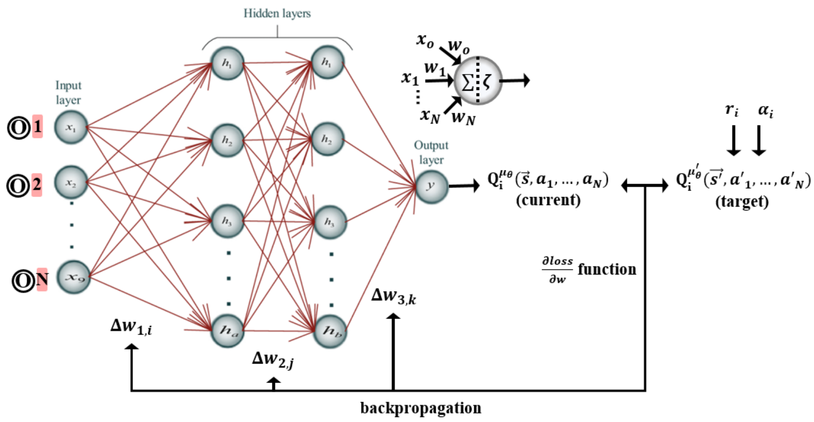

Fig. 3.21 Neural network for MADDPG's learning gradient.

and adverse reward system in competitive perspective, $Q_i^{\vec{\mu}_\theta}$ where $i = 1, \ldots, N$. The actor updates its deterministic policy gradient:

$$\nabla_{\theta_i} J(\theta_i) = \mathbb{E}_{\vec{so}, a \sim U(D)}[\nabla_{a_i} Q_i^{\vec{\mu}_\theta}(\vec{so}, a_1, \ldots, a_N) \nabla_{\theta_i} \mu_{\theta_i}(\vec{so})|_{a_i = \mu_{\theta_i}(\vec{so})}] \tag{3.35}$$

where $U(D)$ contains tuples abstracted from memory replay buffer, $(\vec{s}, a_1, \ldots, a_N, r_1, \ldots, r_N, \vec{s}')$. Based on Agents, actions, $\{a_1, \ldots, a_N\}$, and corresponding reward in current observations, $\vec{s}$, before heading to the next observation state, $\vec{s}'$. On the other hand, the centralised critic Q action-value is updated based on the minimised loss function:

$$\begin{aligned} target\ Q\text{-}value &= r_i + \alpha Q_i^{\vec{\mu}_\theta'}(\vec{so}', a'_1, \ldots, a'_N)|_{a_i = \mu_{\theta_i}(\vec{so})} \\ \mathscr{L}(\theta_i) &= \mathbb{E}_{\vec{so}, a_1, \ldots, a_n, r_1, \ldots, r_N, \vec{so}'}[(Q_i^{\vec{\mu}_\theta}(\vec{so}, a_1, \ldots, a_N) - target\ Q\text{-}value)^2] \end{aligned} \tag{3.36}$$

As MADDPG uses perceptron-based neural network, it expands learning behaviour in continuous domain and predicts gradient policies to enhance future' Q action-value as shown in Fig. 3.21. The input for critic element comprises of joined observations to predict Q action-value and uses minimised loss function to adjust the weight's gradient (backpropagation). While actor predicts the policy loss using observations and policy gradient as input. The neuron uses sigmoid as activation function to restrict output limit to [0,1].

MADDPG for N Agents Pseudo:

for_loop episode++ $\neq$ EPI

Random generate $\mathscr{N}$ for action exploration.

Store observation for initial state, $\vec{s} = \{o_1, \ldots, o_N\}$.

for_loop t++ $\neq$ T

Assign action for each agent i w.r.t current policy and noise exploration, $a_i = \mu_{\theta_i}(o_i) + \mathcal{N}_t$.
Execute actions $a_1, ..., a_N$ and monitor reward $r_1, ..., r_N)$ and new state, $\vec{s'}$.
Store in *MBR*, $(\vec{s}, \vec{a}, \vec{r}, \vec{s'})$.
$\vec{s} \leftarrow \vec{s'}$.
for_loop i++ $\neq N$ Agent
Abstract random S samples batch from *MBR*, $(\vec{s^j}, \vec{a^j}, \vec{r^j}, \vec{s'^j})$.
Compute $q^j = r_i^j + \alpha Q_i^{\mu'}(\vec{s'^j}, a'_1, ..., a'_N)|_{a'_i = \mu'_i(o_i^j)}$.
Update critic from the minimised loss function:$\mathscr{L}(\theta_i) = \frac{1}{S}\sum_j (q^j - Q_i^{\mu}(\vec{s^j}, a_1^j, ..., a_N^j))^2$.
Update policy gradient:
$\nabla_{\theta_i} J \approx \frac{1}{S}\sum_j \nabla_{\theta_i}\mu_i(o_i^j)\nabla_{a_i} Q_i^{\mu}(\vec{s^j}, a_1^j, ..., a_i^j, ..., a_N^j)|_{a_i = \mu_i(o_i^j)}$.
end for
Update target network:$\theta'_i \leftarrow \tau\theta_i + (1-\tau)\theta'_i$.
end for
end for

3.6.6 Implementation & Testing and of Reinforcement Learning Agents

In the testing phase, MADDPG reinforcement learning algorithm is modelled using Azure artificial intelligence module before transferring computational functions to the edge Cloud. The proposed function module was developed using Azure's embedded machine learning tools, utilising *Tensorflow* callback function in python's deep learning neural network library. Having resource (device) deployment limitations, Azure's advance IoT device simulator provides a platform to simulate customise device and environment instances. These simulated device instances uses real-time data sets as input behaviour to represent a realistic operating environment for testing. Furthermore, creation of other reinforcement learning (*i.e.* DDPG) was employed to provide analytical benchmarking of Agents' learning behaviours.

To analyse Agents' behaviours towards cooperative and deceptive decorum, a constrained space/environment representing the playing area with multiple Agents represented as players were created to execute three distinct tasks and evaluate Agents' learning experiences. The investigations involve; *(i)* analysing Agents' learning performances and how actor-critic deterministic policies are autonomously attuned based only on local information (*i.e.* observation) at run time, *(ii)* taking a non-differentiable function model that comprehends environment's dynamics without any means of communication between Agents, and *(iii)* impart cooperative-competitive mixes in decision making processes (action-state values) based on a centralised policy training in continuous space with decentralised actions/execution in discrete time.

The environment set-up in Azure IoT Cloud system is as follows:

- the IoT edge device will perform as an Agent, operating as a player with reinforced learning computing ability at the edge. The IoT Hub will then broadcast the real-time computed coordinates in a single way communication traffic to Azure container registry to render players' position in the playing area.

- The Azure container registry creates the playing area environment with specified coordinates; x-axis: -10 to 10 and y-axis: 10 to -10 (*cm*) and rendering of other required object instances. Based on the coordinates provided by IoT Hubs, Agents are placed in the play area.

- Using COSAP platform, IoT edge device will receive Agents' aggregated action-value function, landmark coordinates, actions, and rewards. Respective IoT Hubs will then compile and synchronises experience replay buffer tuples.

The Agents' policy set is modelled as a parametrised function with respect to θ_i, $\{\mu_{\theta_1}, \mu_{\theta_2}, \mu_{\theta_3}\}$. Its expected policy gradient of each Agent under the probabilistic distribution of memory buffer experience replay, $a \sim U(D)$, returns:

$$\nabla_{\theta_i} J(\mu_{\theta_i}) = \mathbb{E}_{\vec{so}, a \sim U(D)}[\nabla_{\theta_i} \mu_{\theta_i}(a_i|so_i) \nabla_{a_i} Q_i^{\mu_\theta}(\vec{so}, a_1, a_2, a_3)|_{a_i = \mu_{\theta_i}(so_i)}] \ \forall i = 1,2,3 \quad (3.37)$$

while the centralised action-value function is updated using the Lagrangian approach considering the targeted temporal difference:

$$\begin{gathered} \mathscr{L}(\theta_i) = \mathbb{E}_{\vec{so}, a_1, a_2, a_3, r_1, r_2, r_3, \vec{so}'}[(Q_i^{\mu_\theta}(\vec{so}, a_1, a_2, a_3) - y)^2] \ \forall i = 1,2,3 \\ y = r_i + \alpha Q_i^{\vec{\mu_\theta}'}(\vec{so}', a_1', a_2', a_3')|_{a_i = \mu_{\theta_i}(\vec{so})} \end{gathered} \quad (3.38)$$

where the state environment, s, remains stationary despite any changes in Agents' policies since; $P(s'|s, a_1, a_2, a_3, \mu_{\theta_1}, \mu_{\theta_2}, \mu_{\theta_3}) = P(s'|s, a_1, a_2, a_3) = P(s'|s, a_1, a_2, a_3, \mu'_{\theta_1}, \mu'_{\theta_2}, \mu'_{\theta_3})$ for any given $\mu_{\theta_i} \neq \mu_{\theta'_i}$. In order to gain high communicative responses from Agents, it is assumed that respective Agent's state observation and policies are made available instantaneously for other Agents during the training phase. However, to consider latency issues in Cloud or COSAP during data sharing, assumptions on those parameters can be relaxed by inferring policies based on other observations.

In the case where Agents' lacks in conceiving other policies required in (3.38), each Agent can maintain additional policy approximation factor, $\mu_{\Psi_i^j}$, where Ψ is the approximation parameter of Agent's true policy μ^j. It maximises the *log* probability of Agent j's actions with an entropy regularisation[219]:

$$\mathscr{L}(\Psi_i^j) = -\mathbb{E}_{so_j,a_j}[log\mu_{\Psi_i^j}(a_j|so_j) + \lambda H(\mu_{\Psi_i^j})]\ \forall i = 1,2,3;\ \ j = true\ policy \tag{3.39}$$

where H denotes to the entropy in policy distribution and λ refers the Lagrangian multiplier. In each iterative process, each agent j updates the gradient step Ψ_{ij} from the experience replay buffer before updating the centralised $Q_i^{\mu_\Psi}$. Referring to y in (3.38), it can be replaced by an approximated policy defined as:

$$y_\Psi = r_i + \alpha Q_i^{\mu'_\Psi}(\vec{so}', \mu'_{\Psi_i^1}(o_1), \mu'_{\Psi_i^2}(o_2), \mu'_{\Psi_i^3}(o_3)) \tag{3.40}$$

where $\mu'_{\Psi_i^j}$ refers to the targeted network of approximation policy, $\mu_{\Psi_i^j}$. Rather of using sampling, the *log* probability actions of each Agent is directly infuse into Q function.

Testing of Agent's Collaborative and Adversarial Learning Behaviours: Case Study

Respectively, Agents are to broadcast its landmark coordinates in the playing area environment based on its unique computed policies and observations. All Agents share a maximise Q-value return to gain high cooperative margin through commutative actions while observing competitiveness to execute physical behaviour defined by its policies. To test the learning behaviours responses of Agents, observation cases are as follows:

1. *Cooperative communication*–it involves an additional Agent serving as a speaker while the remaining three cooperative Agents acts as listeners. Set-up of the environment involves two sub-test scenarios distinguished by Agents' conditions when navigating towards the targeted objectives; *(i)* three colour-coded object instances placed in the playing area and Agents (listeners) are to cooperatively navigate towards each of them according to the paired sequences dictated by speaker's communication output. Here, the listeners has access to the location and colour of the object instances, *(ii)* Agents are tasked to cover all three neutral-coloured object instances by taking the shortest route and restrain from colliding with each other, neglecting speaker's command. At each episode, listeners will receive commutative rewards based on the distance covered to reach its destination.

2. *Cooperative Deception*−all three Agents will perform cohesively to accomplish a common goal (landing on a single targeted landmark). The rule states that only one of the Agents is required to meet the objective (correct colour-coded object instance) and receive collective weighted reward value. Hence, Agents are constantly updating its coordinates from the targeted landmark as reward is proportional to the distance covered (minimised). To view Agents' versatility, the environment introduces an adversary which has similar objective however, does not know the target's colour code. In this sense, Agents are spread out attending to all created object instances (regardless of colour) to deceive Opposer's intuition on which is the correct targeted instance. Agents will receive same penalty value relative to Opposer's distance from target.

3. *Chaser versus Evader*−the environment adopts a classic tagging game where cooperating Agents require to chase and tag a single Evader Agent who has higher speed velocity. The environment installs obstacles to hinder freedom of manoeuvring. Cooperative Agents receive a commutative reward whenever the Evader is being tagged (Evader receives penalty). Agents monitors each other relative position-velocity and strategically position in the playing area.

Performance comparisons and verifications were analysed between Agents adopting MADDPG and DDPG for all three test cases mentioned above. The primary objective is to appreciate the superiority in adopting centralised action-value function where Q-values of all participating Agents are incorporated during training phase. The employed neural network uses three-layered multilayer perceptions with rectified linear unit as activation function; depth: 3-layers; width: 128 neurons hidden layer, 4 neuron output layer. It uses the Adam optimiser function to perform first-order gradient-stochastic optimisation with learning rate (β) of 0.05, discount factor (γ) set to 0.9, and interpolation factor (τ) updating network weights 0.01. The experience memory buffer replay storage module in Azure container registry is sized at $1x10^6$ and continually stores experience tuples for every 100 samples. The batch size of each episode is set to 1024 samples and the weights are trained with random seed of 10. The neural network was let to train until it reaches convergence (coordinate error tolerance$\leq 0.4cm$).

In *cooperative communication*, the first scenario dictates that all three Agents are to comply speaker's command, specifying pairing sequences between Agent and colour-coded Landmark, L, (object instance) at each episode. With DDPG, the Agents fails to comply with speaker's command and constantly moves to the center of all the observed landmarks and occasionally reach the targeted landmark by chance. Primarily, such learning behaviour responses caused by inconsistency in the Agent's policy gradient signal. For an instant, as the listener Agents failed to meet the objective, speaker will receive penalty and it continues to aggrandise proportional to the number of time steps. Furthermore, at every time step, the policy gradient of listener Agents learned to reconstruct speaker's observation which only implies if initial positioning of Agents and landmarks are fixed. In this sense, deployment of DDPG involving multi-agents in instantaneous settings are not generalise when dealing with tasks complexity. Conversely, for MADDPG implementation, listener Agents learned

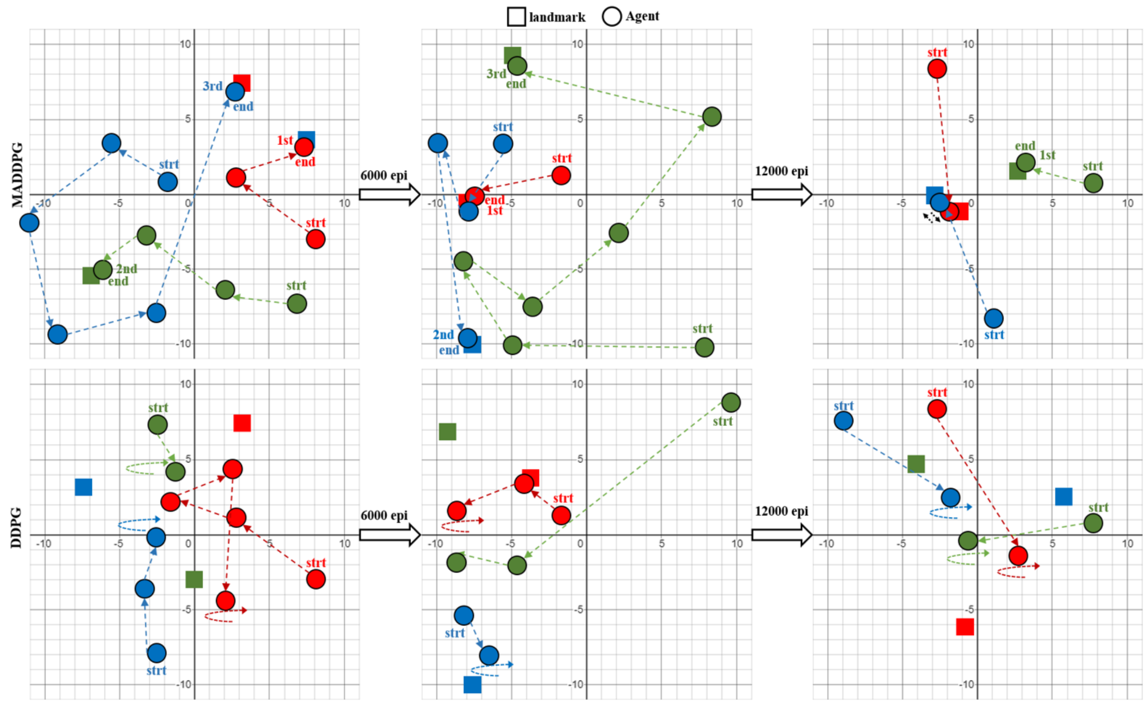

(a) Agents' navigation sequences to reach respective landmark.

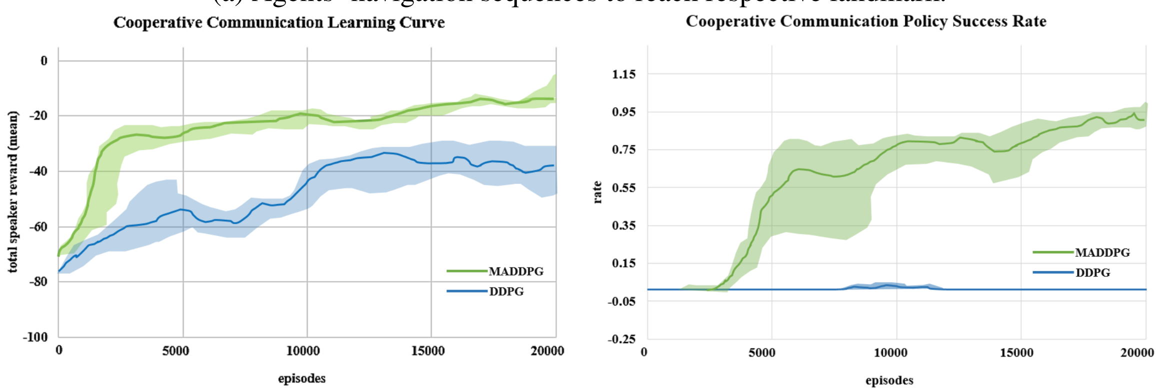

(b) Agents' learning curve: reward gained and policy success rate.

Fig. 3.22 Test Case 1: Agents' comparative performances in cooperative communication between MADDPG and DDPG.

to coordinate cohesively due to centralised critic. From the minimised critic loss function, Agents are able to update respective learning policy gradients and also comprehend speaker's policies. Fig. 3.22 validates Agents' learning performances in cooperative communication environment in ≤20000 episodes. Fig. 3.22a provides visualisation of Agents' responding towards paired landmarks based on speaker's policies while Fig. 3.22b records the speaker's total reward at each episode and Agents' policies success rate in both MADDPG and DDPG learning algorithms. Significantly, Agents' in MADDPG able to hit a minimum of 90% success rate after 25000 episodes, speaker and listeners are able to contrive cooperative policy gradient from centralised Q-value at which observations were attuned to match landmark locations, and Agents are thriving to gain maximum reward by taking shortest path to desired landmarks (reward exponentially increases ≤18760 episodes).

Contrarily, investigations in the second scenario only focuses on MADDPG implementation as shown in Fig. 3.23. Recording of distance covered to reach target and Agents' collision index are presented in Table 3.3 per episode. Agents in MADDPG learned to compromise with each other by prioritising landmark which is closest to Agent (shortest path) while other moves away to avoid collision. Agents that were interrupted during the course of its navigation, will manoeuvre to the closest landmark that is not attended. Whereas, in DDPG, Agents are frequently to collide with each other; navigating the same landmark (closest) as Agents are deliberately clustered together at initial position. Correspondingly,

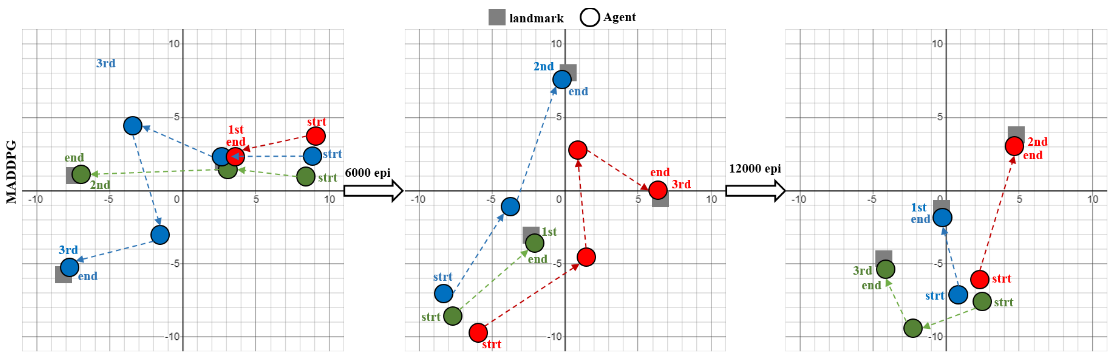

Fig. 3.23 Neural network for MADDPG's learning gradient.

Table 3.3 Comparison summary of MADDPG versus DDPG in cooperative communication and navigation.

Agent	Reach Target	N=3; L=3		N=6; L=6	
(μ_θ)	(%)	Travel Dist.(avg.)	Collide(#)	Travel Dist.(avg.)	Collide(#)
MADDPG	83.35	1.546	0.184	3.174	1.387
DDPG	35.18	1.971	0.325	3.577	1.893

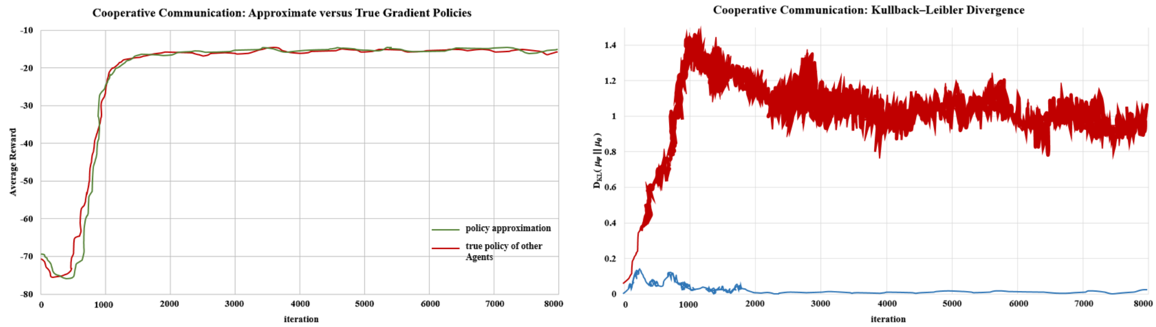

Fig. 3.24 Approximation and true policies: KL divergence index.

analysis on the effects of approximation policy gradient is presented in Fig. 3.24. It presents that despite lacking in learning listener Agents' policies by speaker, large Kullback–Leibler (KL) divergence against true policy, the approximated policies produces consistent success rate using true policies without comprising rate of convergence.

Subsequently, in *cooperative deception* settings, the objective is to lure opposing Agent (blind) towards the decoy landmark while Opposer Agent tries to tail other Agents hoping to hit targeted landmark by chance. Fig. 3.25 illustrates partial results attained from the analyses performed. Here, to appreciate the Agents' policy gradient signal in rendering deception on the Opposer, Table 3.4 quantifies the Agents' learning policy success rate performing as either roles (Agent-Opposer) considering all possible combinations. Likewise, MADDPG shows superior learning processes regardless in Agents or Opposer role. Despite operating as a lone Agent, it still able to avoid decoy landmarks due to its centralised training for Q-value absorbed by other Agents. Unlike DDPG, Agents have weak cooperative behaviour thus, unable to effectively lure/deceive opposing Agent away from targeted landmark. However, in the case where both Agents and Opposer adopts MADDPG learning policy gradient, the success rate being an Opposer hitting the targeted landmark exponentially increases after 17000 episodes and the deceive factor deteriorates. This cycle repeats where the trend for success rate (higher) will toggle between Agents and Opposer.

Table 3.4 Performance comparisons of MADDPG and DDPG in cooperative deception environment $\approx\leq$17000 episodes.

N=3 Agents (μ_θ)	Avg. success (%)	N=1 Opposer (μ_θ)	Avg. success (%)
MADDPG	91.05	DDPG	44.71
DDPG	63.67	MADDPG	74.80
MADDPG	92.24	MADDPG	66.98
DDPG	54.56	DDPG	66.82

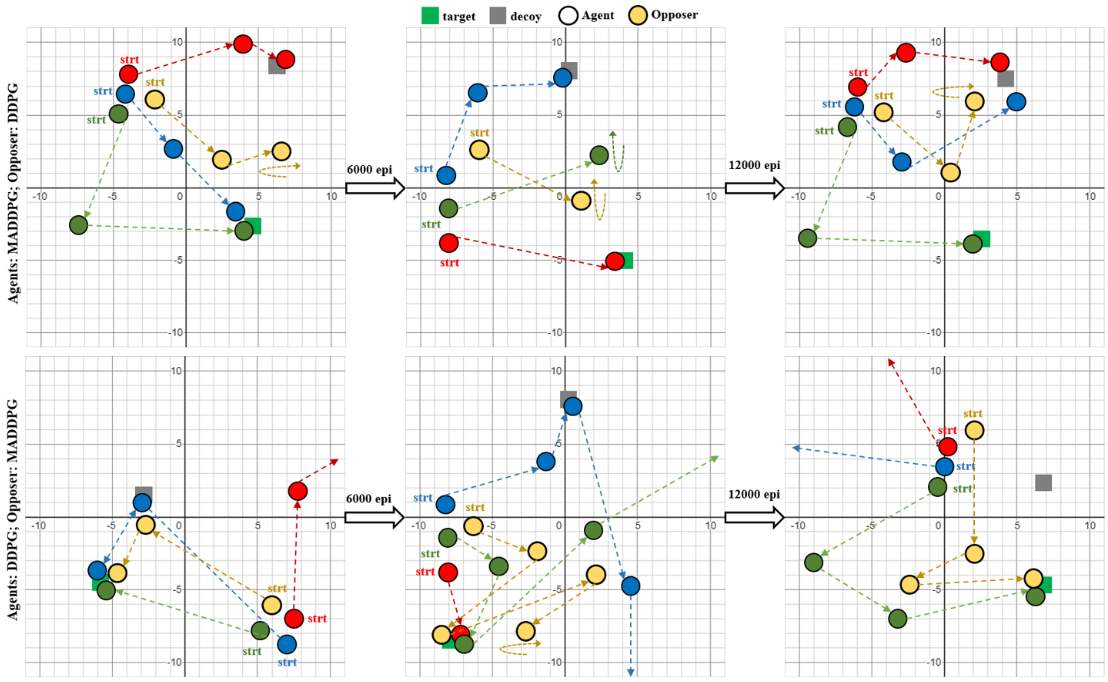

Fig. 3.25 Effects of Agents learning policy on cooperative deception environment: vice-versa roles.

Finally, in *Chaser versus Evader* observations, the results shown in Table. 3.5 has verified that MADDPG has better policy gradient in mapping Agents' navigation trajectories within the playing area. Simulations also displayed MADDPG Agents interoperates deception learning behaviour which tempers policy loss minimisation in DDPG-based Agent. Furthermore, in the case where DDPG Agent operates as the Evader, it has a higher tendency of navigating outside the playing area as the penalty awarded was lesser than being tagged. Nevertheless, a relatively small observable success and failure rates between MADDPG and DDPG were recoded and the impact on applying two-speed setting on Evader Agent is rather proportional to the number of touches attained (insignificant impact on learning policy gradient). The success and failure rate in-between MADDPG and DDPG becomes less apparent as the number of Agent, N, increases.

3.6.7 Findings

The technologies rendered by Azure IoT edge Cloud has proved that traditional centralised based Cloud system is no longer viable in supporting decentralised and transactive energy operations, endorsing large-scale penetration of participants and sovereignty at low-voltage level. Furthermore, computational stress and latency issues contribute high impairment

Table 3.5 Chaser versus Evader: average number of touches made by Chaser per episode based on Evader's two-speed setting (vector scaling), decrease 50% and increase 25%.

Chaser Agent (N=3; μ_θ)	Evader Agent (N=1; μ_θ)	avg. tagged # $\downarrow$ 50%	avg. tagged # $\uparrow$ 25%
MADDPG	DDPG	13.520	0.614
DDPG	MADDPG	11.227	0.389
MADDPG	MADDPG	9.268	0.296
DDPG	DDPG	6.975	0.523

on managerial efficiencies and thus, costs in maintaining large storage Cloud services exponentially increases. Hence, Azure IoT edge device (scalable, portable) provides users' with monitoring and control solutions at respective Cloud domain (edge gateway) suitable for administrating personalised energy utilisation and computing innovations to curb operating costs. Correspondingly, DCF was introduced to pave way for cooperative and active responses in which Prosumer Community, aggregators, and DSO can benefit from (*i.e.* incentives, market, DERMS, ADMS) while observing DSR and ADMS administrations.

In addition, COSAP was introduced to serve as a sensor data sharing (peer-to-peer) platform that adheres to providers' privacy policies. It is modelled based on serverless service configuration model that utilises CIFP to negotiate data sharing contract and content policy between providers. Data distribution path are automated, reflecting both party policies and data resolutions, to prevent malicious motivations and burden on Cloud providers when securing data privacy settings. However, solutions in integrating COSAP into Azure IoT edge Cloud is still an open discussion as Azure has an in-built IoT security architecture. The proposal involves assigning Azure to focus on hybrid Cloud-to-Cloud security services while COSAP governs device-to-device sensing paradigm.

Succeedingly, utilising Azure's artificial intelligence platform, reinforced-CDL reinforced learning was modelled as a module for edge computing. Its designed algorithm is based on MADDPG configuration that embraces cooperative and competitive learning behaviour suitable for decentralised decision-making processes. Agent used a centralised policy gradient algorithm that considers other Agents' actions and observations in the training phase. Results have outperformed other conventional reinforcement learning algorithms however, the approach introduces curse of dimensionality as Q-function grows linearly with respect to number of Agents deployed. Such crisis can be remedied by disseminating Q-function into modular, grouping Agents into clusters.

3.7 Summary

This chapter analyses proof of concept in establishing edge computing hybrid Cloud environment linking with AMI and system intelligences dedicated to solve decentralised coordination in future's distribution network operations. Testing of proposed system was investigated using several exemplar cases to view their employability for power distribution applications which will be discussed in subsequent chapters. It focuses on four interdependent solutions; exploiting IoT hybrid Cloud and edge computing applications, securing data-sharing platform, and imparting system intelligence in Agents of MAS when building suitable transactive energy environment. Following describes implementation details for sustainable 5G commercialisation suitable for demand-side management:

1. connecting a household thermostat device to Azure IoT Edge Cloud system to visualise and explore edge computing capabilities. It provides a total Cloud solution when developing personalised connectivity for local devices and programming customise intelligences (control features) based on users' preferences. Such platform serves as an applicable solution to support large-scale Nanogrid penetrations and administrate TE values; assigning dedicated edge gateway for local devices connectivity and empowers local decision-making processes. It also resolves latency, computational stress, and storage sizing issues when employing conventional centralised Cloud system.

2. using layer-structured IoT architecture to model DCF. Each layer is defined with interdependent objective statement and functions that transforms passive energy actors into authoritative figures while maintaining demand-side efficiency and reliability. DCF layered objective functions are defined in modules of Azure IoT edge Cloud and deployed at respective IoT Hub to execute decentralised control transactions as shown in Fig. 3.8.

3. flexible data sharing platform (COSAP) to eradicate provider's dilemmas in provisioning privacy/policies for data distribution and also reduces service control stress in aligning policy changes (data content and sharing contracts) between consumer and provider. Here, owners can exchange and monitor sensor-based devices with neighbouring Nanogrids without relying on the Cloud services.

4. imparting computational intelligences into Agents of MAS at edge. Hence, reinforcement machine learning algorithm is employed to impart cooperative yet competitive decisional-making behaviour suitable for decentralised settlements. Several reinforcement learning algorithms were proposed (*i.e.* DDPG, MADDPG, Q-learning,) and

simulated. The objective is to view Agents' learning behaviour and policy gradient relevant for TE control system.

Chapter 4

Realisation of Demand-Side Operations Governed by Transactive Energy

This chapter explores into deployment realisations of TE structured demand-side management using the proposed methodologies and design configurations discussed in Chapter 2 (*i.e.* nanostruturing the distribution network and introducing aggregators as new energy service provider), and Chapter 3 (*i.e.* integrate smart metering and edge computing hybrid Cloud infrastructure for control intelligence and analysis visualisation in the domain of network planning and optimisation processes). A proposed Testbed system is simulated to view Prosumer Community performances in a decentralised TE environment and their contributions towards power quality and PtP energy trading.

It focuses in creating a TE environment for aggregators when legislating Prosumer-centric energy management solutions using Multi-Agent Deep Deterministic Policy Gradient (MADDPG) reinforce learning for joint decision-making processes. Its intelligent system provides cooperative yet competitive solutions for Prosumer when scheduling PSPG utilisations and load shedding in response to clearing prices with strategic bidding capability in the wholesale market−securing minimised local billing while observing DSR and power quality dynamics globally. Moreover, it identifies the impacts on Prosumers' energy trading interests at PCC influenced by TE control mechanisms/policies as key operational parameters when meeting supply and demand dynamics against subscribed business offers. In this sense, despite employing diversified DERMS controller that is biased towards high payout incentives and fast return on investment trajectory, aggregators must gratify optimised core services (*e.g.* peak demand & baseload limit prohibitions, Duck-Curve & unit-commitment crises, and feeder congestions) in support of DSO's objectives.

4.1 Intelligences for Transactive Energy Management

In view of the transactive four-quadrant control sequences illustrated in Fig. 3.9, it offers governing boundaries when scheduling PSPGs and market participations in support of TE operations. In this sense, aggregators can use these guidelines to model diversified business offers to steer power exchange demographic (*i.e.* excess generation capacity and agreed contracted quantity in real-time) at respective PCC with cooperative yet competitive attributes during the two-way wholesale market bidding and trading for Prosumer Community engagements. Moreover, contribution towards reserve/ancillary market opportunities must not be neglected to enhance ADMS core services which further influence scheduling strategies for installed DERs at both low- and medium-voltage levels. Attributed to clearing price information, state of IoT devices, and user billing preferences, modelled controllers are to react cohesively in generating optimised demand-side solutions and yet allowing personalised governing of BTM DERs. Hence, price-reaction approach serves as a pivotal mechanism for aggregators in modelling DERMS options, respond correspondingly in the electricity marketplace based on price-quantity bidding transactions—communication between Prosumer and aggregator in their willingness to pay and produce, respectively. It also provides collaborative market-based price dynamics as control signal to shift demand responses from uncertainty to predictable system reaction at a global level while locally, assists Prosumers to strategically schedule bidding of excess generation capacity in the wholesale. Fig. 4.1 illustrates how

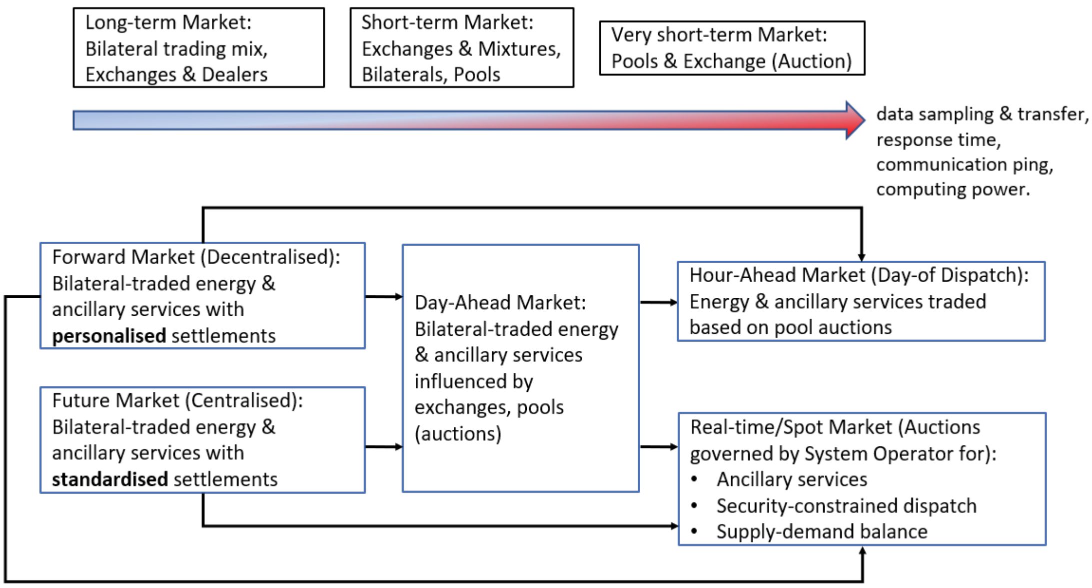

Fig. 4.1 Auction design in power market: Market-based control functions.

commitments and relationships of electricity market architecture serves as a pivotal driver when modelling intelligences for DERMS and changing Prosumers' energy usage behaviour.

When properly implemented, the market bids sent by end users' can be aggregated together, and the resulting bid represents preferences of both devices. The message size of the aggregated bid curve is a simple combination of the individual device bid curves. Using this property, a highly scalable system can be obtained when bids are aggregated together in a response cluster. The processing and communication time scaled with height of the aggregation tree instead of participating device quantity. Furthermore, the approach protects end users' privacy as the bidding process communicate only information about energy quantities and prices. When these bids are aggregated on the level of Prosumer Community, the information exchanged is comparable to that of a metering system collecting near-real-time data as described for the price-reaction approach above. And unlike the centralised optimisation approach, no complicated models of the devices, Prosumer behaviour, or preferences are exchanged or maintained. In summary, TE provides an avenue to access full response potential of flexible devices, provide greater certainty about the momentary system reaction, realize an efficient market with proper incentives payouts, and protect privacy of the end user whose devices participated in the energy management tasks.

4.1.1 Transactive Values Influenced by Market Operations

The terminology "transactive" implicates that the decisions made are based on a value that can be analogous to agreements or literally for economic contracts. It uses sequence of economic and control techniques to enhance operation reliability and efficiency through optimum scheduling of DERMS and Prosumers' participation in the market. Hence, development in market-based alternatives and competitive energy retailing serves as a common physical coordination (*i.e.* hourly-ahead or 5mins) between aggregators and DSO for balancing longer term (*i.e.* months-ahead) supply-demand matching services that comfortably accommodate bid and offer auction transactions. It formulates new business and management solutions that promote BTM integration of energy resource diversities and facilitate new intelligent load devices at the low-voltage level in response to inadequate grid control crisis when generation resource variability surpass more than 30% of the total demand load capacity. When transactive mechanisms are properly aligned to its value streams across all energy participants, it extends greater proliferation of DERs in rendering service options and custom solutions for Prosumers in scheduling optimum use of BTM DERs.

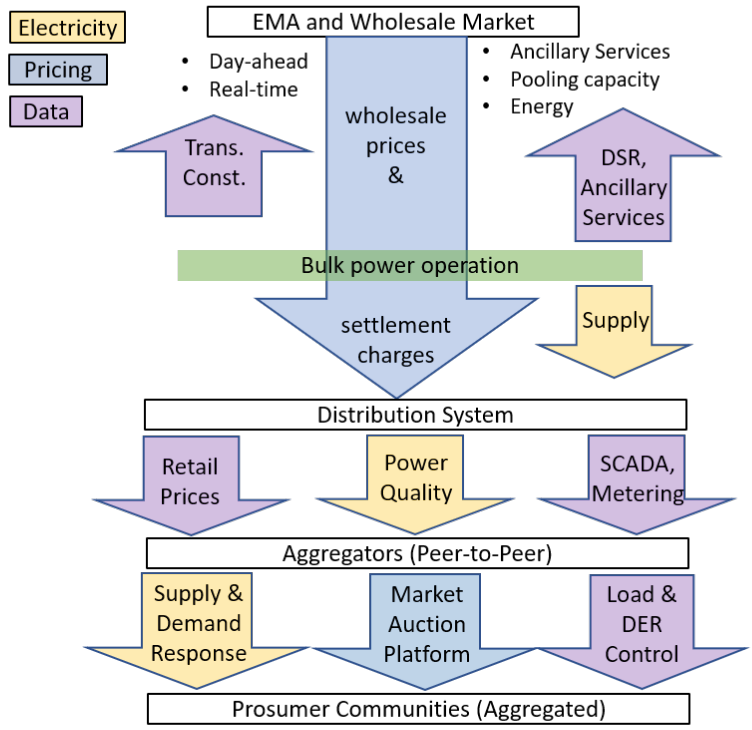

Fig. 4.2 End-to-end market-driven distribution network operations under TE values.

There are two types of organisational model for DSO development currently in the market; distributed system platform (DSP) and RDSO where both involve in functioning of market operations and distribution grid management. Here, DSP-configured model is selected as it is favourable to retain all distribution grid operations within a single unified environment as compared to RDSO ruling and is responsible for; *(i)* grid operations, *(ii)* stimulate market environment for multi-players, *(iii)* support in establishing DER integration platform, and *(iv)* perform holistic and integrated planning processes. In this sense, DSO has a role in brokering wholesale and retail, capacity, and reliable energy transactions from any number of aggregators and independent owners. Effective operations are greatly influence by the incentives payouts and regulatory framework ruled by Utility, making DSP indifferent to either traditional or distributed in ensuring distribution network needs. Overall, DSO is tasked to enhance system reliability focusing on "dynamic" or "adaptive" Microgrid formation assembled by aggregator (*i.e.* islanding feeder based on where fault has occurred and monitor available pooled generation capacity from DERs to serve online loads) and rendering services from third parties to support voltage level deviations or loading relief. Meanwhile, aggregators are tasked to empower Prosumers' BTM DER engagements; broadcast visibility (communications), and access full control of DER production using contracted business offer in real-time to secure integrity of the grid, and facilitate bidding in the wholesale market for better clearing price (*i.e.* distribution locational marginal price (DLMP)) thus higher return on investments.

4.1.2 Monetary Incentive Additive in Market Operations

Aggregators of today are responsible in guiding Prosumers into a holistic yet optimised scheduling of BTM DERs (PSPG) and energy usage through attractive business offers that discerns socio-economical aspects. Incentive payouts serves as a critical component in changing Prosumers' behaviour towards energy usage in real-time and it was found that it can be categorised into two energy usage behaviours; efficiency and curtailment. Efficiency behaviour is referred to a group of Prosumers that focused in financing one-time-off investment for technologies that can aid in reducing percentage of local demand capacity and dependency on upstream power generation (*i.e.* install solar PV, well-insulated premises to maintain temperature, energy-efficient appliances). It typically produce a long-term effect and larger energy savings due to one focused effort. Meanwhile, curtailment behaviour involves consistent commitment and vigilance (*i.e.* appliances are switched off after use instead of leaving it on standby) and switching high energy usage when penetration of surplus renewable resources is abundant to gain reduced energy billing. However, investments on energy-saving appliances or PSPG installation is limited as compared to efficiency behaviour Prosumer thus leading to lower energy savings. In this sense, Utility introduces monetary incentives to motivate aggregators in designing levelled market participation that responses well to either efficiency or curtailment behaviour change in view of energy usage lifestyle and billing benefits (*i.e.* rebound effect [220], intrinsic motivation, undeserving monetary saving).

The establishment of monetary incentives by policy makers and practitioners serve an additive in encouraging local creation of sustainable EPS. Subsidy payouts are offered to customers as financial aid for PSPG investments and appreciation when using electricity efficiently through competitive scheduling of assets in view of tariff against monetary rewards. Although respective monetary incentives do have its limitations and negative impacts on customers behaviour towards payouts exploitations and demand capacity demographics, some studies [221] have proved to gain greater benefitting outcomes at a global perspective and serves as an influential optimising tool to reduce fossil-energy consumption at low-voltage level. It also extend competitive edginess for third-party providers (*i.e.* aggregator) when modelling programs that can incentivise customer engagements and PSPG installation

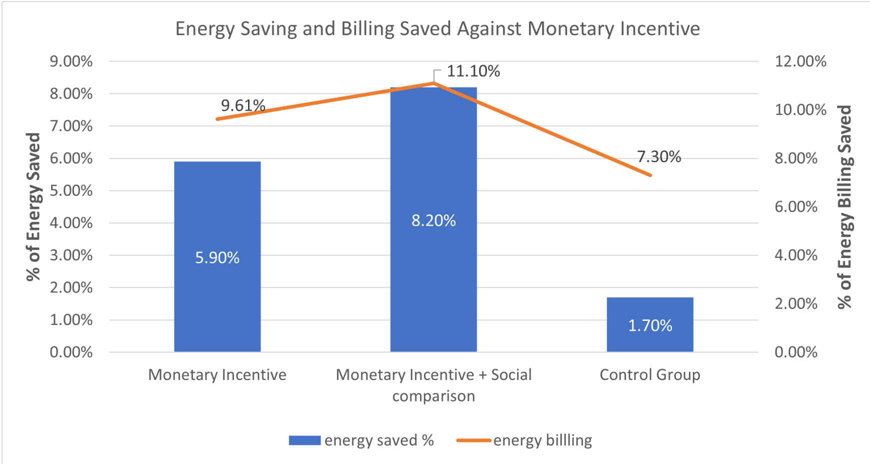

Fig. 4.3 Studies analysed on the impact of energy and billing saved by different group of customers who observed monetary incentives and social comparison components.

security for higher incentive payouts. In this sense, aggregators are to find solutions that can benefit both Prosumer and itself from higher payout issued by Utility and share the profit margin effectively (*i.e.* exploit time of use during high payout incentives and portioned out for maintenance costs and Prosumer's energy billing).

Contrarily, social comparison feedbacks in Prosumer Community energy usage can add value in steering curtailment behaviour as seen in Fig. 4.3, a study initiated in Japan [222]. Prosumers were subscribed into three different programs and view their contributions towards energy savings; *(i)* monetary incentive—reward payout of £1.70 for every 1% energy reduction, *(ii)* monetary incentive with social comparisons—similar reward payout agreement and provide energy usage indications against their neighbour to evaluate how they fair in the efforts toward reduced energy usage, and *(iii)* no information—serve as a control group that receives no information on how much they have saved on their energy usage and corresponding reward payouts.

4.1.3 Negative Impacts of Monetary Incentives

A few studies on practical deployment of monetary incentives packages suggests positive impact in reducing energy dependency at low-voltage from upstream generation for instant; monetary incentive combines with full technical support and installation of PSPGs (*i.e.* automations, suggest optimum solutions), and monetary incentives in combination with social comparison feedback regarding energy usage in a Community. However, these package of supplementary strategies often appears to generate small impact or even negligible as it undermines the effectiveness of monetary incentives in reducing energy use. Following present case studies in which monetary incentives can also deviate Prosumers at low-voltage from the initial objectives of reducing energy usage as compared to operation benefits (*i.e.* investments incurred) and discomfort (*i.e.* lifestyle).

Rebound Effects

One of the major setback in providing monetary incentive for energy savings is that it the money saved could be invested on other energy consuming behaviour. For an instant, investing on energy efficient appliances that leads to lower consumptions gives the intuition that these equipments can be operated for a longer period. Hence, compelling energy curtailment behaviour may lead to monetary savings that can spent elsewhere which results in rebound effect due to increase in energy consumption. Report summarised in [223] revealed that there is no difference and effectiveness in residential energy consumption savings despite installing energy-efficient appliances or supporting conservation technology set-ups in homes. The collected data shows detrimental outcomes where it was estimated to be 13% below the targeted or potential energy savings during non-summer while in summer deficit by 8-12%. Lower savings trend was reported due to participants' behaviour in wanting to gain better comfortability during seasonal changes with the conception that energy-efficient appliances can operate at higher operating thresholds to offset with those non-efficient appliances, assuming that the energy consumptions could be levelled or even reduced.

Efforts Is Not Worth the Incentive Earned

As energy customers' mindset focuses on the repercussion in investing much money, effort, and discomfort when subscribing to become Prosumer, the money saved through monetary incentives requires significant impact on individual energy billings. Small incentive payouts may not engage customers' behaviour to partake in such efforts despite realisation on the benefits they would offer at the global perspective. For instant, installation of the solar PV would need 8 or more years before Prosumer can earn a profit margins or breakeven investment and this is only the case if proper regime of energy utilisation is followed. Research have shown that investors are attracted to fast return on investment (receiving money now) as compared to the same amount of returns in the far future. Hence, curtailment behaviour seen as too costly compared to benefits and will be perceived as not worth the effort even with monetary savings. Conclusively, when quantifying monetary incentive payout that promotes cost-benefit thinking, consideration on private costs and benefits must be justifiable against Prosumers' lifestyle trade-offs and heavily subsidised monthly subscriptions (*i.e.* attractive service packages, unique electricity tariff from non-Prosumer, lifestyle discounts).

Incentive Payout Depresses Positive Intrinsic Motivations

Contrastively, providing substantial monetary incentive payouts for reducing energy consumptions may crowd-out or felt undermined to customers with intrinsic motivations for sustainable energy behaviour. These group of people are very motivated to save the environment without receiving monetary incentives thus, pro-active in subscribing for energy saving programs or switching to green energy providers. On the other hand, monetary incentive can generate spillover effects on peoples' behaviour towards being pro-environmental. Meaning, people are more money driven and motivated to be climate-friendly and has no intentions if efforts are not incentivised. Hence, to overcome such predicaments, large saving efforts are required to gain large incentive payouts, deserving at its maximum energy saving capability.

4.2 Contributions

It aims to unveil realisations in bringing demand-side management to Prosumers, preceding grassroot-based (bottom-up and bilateral) ruling, transacting in-house EMS (TE value) that allows either idiosyncratic or interdependent assessments. Primarily, it aims to position aggregators as the neutral market facilitator during energy trading transactions at low-voltage and response autonomously towards DERMS settlements. The reversed obligatory role accredit Prosumer(s) to constitute joined scheduling- and bidding-abled decision-making processes based on resource availability, shaping/shifting demand load profiles, and participate in the two-way market clearing to bias wholesale electricity tariffs in real-time. In this sense, control intelligences must be cooperative yet competitive, optimally schedules BTM DERMS operations and controllable loads at low-voltage to meet individual energy interest (*i.e.* high return on investment, reduced energy billing) which prepares aggregators with greater certainty in planning DSR and resilient towards power quality issues at a Community level.

The contributions of this chapter is separated into three categorise:

1. to define a small central grid by clustering Nanogrids into Prosumer Community using Expectation Maximisation-Gaussian Mixture Model (EM-GMM). Identifying diverseness of Nanogrid's energy needs/attributes based on socio-economic terms and distribution priorities. From structured Prosumer Community, complications in

MADDPG's policy gradient issues (linear Q-function) and large data stream can be eradicated.

2. contributing elements and influencing factors that affects local energy billing. In Prosumer decentralised modus operandi, observation on maximum contracted electrical demand is observed by scheduling local use of shiftable appliances and power exchange activities at PCC (utilisation of PSPG). It incorporates constraint relaxations to accommodate human lifestyle usage factor during intervals of peak demand instances. In addition, relative to leading consequences on centralised demand-side management (*i.e.* Duck-Curve crises, market bidding, unit commitment constraints/competence), scheduling Prosumer's PSPG shifts into a cooperative approach to gain larger incentive payout.

3. modelling of 'one-size-fits-all' TE management intelligences using MADDPG learning algorithm to manage local asset utilisations that bridges Prosumer-to-Prosumer (PtP) in energy trading and market operations across the distribution network. Communication and hierarchical control functions of MADDPG Agents are directed by the proposed DCF seen in Fig. 3.7, prioritising parent exigencies while considering other neighbouring Nanogrids' constraints. Primary tasked to manage power flow exchanges at PCC are based on in-house engagements to curb operating costs while maximising competencies in energy usage (*i.e.* auxiliary for operating reserve, market clearing price). In addition, implementations of Extreme Learning Machine (ELM) is employed to assist in forecasting processes to minimise uncertainty, it being power generation or demand profiles.

The operation control features in Agents of MAS interoperate *IEEE 2030.7-2017*−IEEE Standard for the Specification of Microgrid Controller, *IEEE 2030-2011*−IEEE Guide for Smart Grid Interoperability of Energy Technology and Information Technology Operation with the Electric Power System (EPS), End-Use Applications, and Loads, and *IEEE 1818-2017*−IEEE Guide for the Design of Low-Voltage Auxiliary Systems for Electric Power Substations. To test implementations of control functions, a proposed nanostructured distribution network (in Prosumer Community format) comprising four Communities with random distribution of Prosumer settings (*i.e.* residential, commercial, and industrial) is modelled in MATLAB on IoT Azure reference architecture to exploit Azure's artificial intelligence platform and machine learning modules.

4.3 Identification of Prosumer Community: Clustering

Prerequisite in clustering Prosumers into cluster-based structure requires bootstrapping of data acquired from NAN (Fig. 2.7a) to identify PSPG generation and load demand capacities. These data are then characterised into Nanogrid's energy exchange profile at PCC to represent its social attributes incorporating other meta-data relations (*e.g.* size of family, average age of family, nature of commercial/industrial operations). Succeedingly, in the holistic clustering approach, Prosumer(s) with no access to PSPG is also considered into modelling of Nanogrid system. Hence, it is separated into two Nanogrid domain−Prosumer type-I (w/ PSPG, consumer & producer) and Prosumer type-II (w/o PSPG, typical consumer). The Prosumer Community comprises a group of Prosumer type-I ($PT\text{-}I$) and type-II ($PT\text{-}II$):

$$\{PC\} = \{Cl_1, Cl_2, ..., Cl_n\} \tag{4.1}$$

where

$$\begin{aligned} \{Cl_i\} &= \{PT\text{-}I_1, PT\text{-}I_2, ..., PT\text{-}I_I\} \\ \{Cl_j\} &= \{PT\text{-}II_1, PT\text{-}II_2, ..., PT\text{-}II_J\} \end{aligned} \tag{4.2}$$

$s.t.$

$$\{Cl\} \neq \{PT\text{-}II_j, ..., PT\text{-}II_{j+n}, PT\text{-}I_i, ..., PT\text{-}I_{i+n}\} \tag{4.3}$$

In the case when PSPG could not meet the local demand, the deficit will be drawn downstream with reference to PCC while excess generation transferred upstream. Negotiation of energy transfer cannot be exchanged directly between $PT\text{-}I$ and $PT\text{-}II$ as it would generate exponential formulation and policy complexities for each pairing transactions. In this sense, any required communication schemes rendered by Prosumer(s) within a Community will pass to the Quasi-Centralised Secondary Control Layer (Fig. 3.7-3.8) of DCF managed by aggregator. Nevertheless, power exchange between aggregator to aggregator is allowed.

4.3.1 Clustering Paradigm & Profiling Prosumer Attributes

The clustering paradigm describes pairing assignments of $PT\text{-}I$'s excess generation with $PT\text{-}II$ in a Community. It relates to the allocation of excess energy generation pool generated by respective $PT\text{-}I$s during a predefined time interval, $\{E_{EXS}^{PT\text{-}I}\} = \{E_{EXS}^{PT\text{-}I_1}, E_{EXS}^{PT\text{-}I_2}, ..., E_{EXS}^{PT\text{-}I_n}\}$ and analysing energy acceptance capacity, $E_{EXC}^{PT\text{-}II_i}$, ordered from $PT\text{-}II$s to satisfy percentage of individual energy demand capacity, $\{E_{DMD}^{PT\text{-}II}\} = \{E_{DMD}^{PT\text{-}II_1}, E_{DMD}^{PT\text{-}II_2}, ..., E_{DMD}^{PT\text{-}II_n}\}$. Here, the accepted energy capacity may or may not equate to $E_{DMD}^{PT\text{-}II_i}$ requirement as allocation priority policy dictates assignment protocols (*i.e.* $E_{EXC}^{PT\text{-}II_i} < E_{DMD}^{PT\text{-}II_j}$ or $E_{EXC}^{PT\text{-}II_i} = E_{DMD}^{PT\text{-}II_j}$).

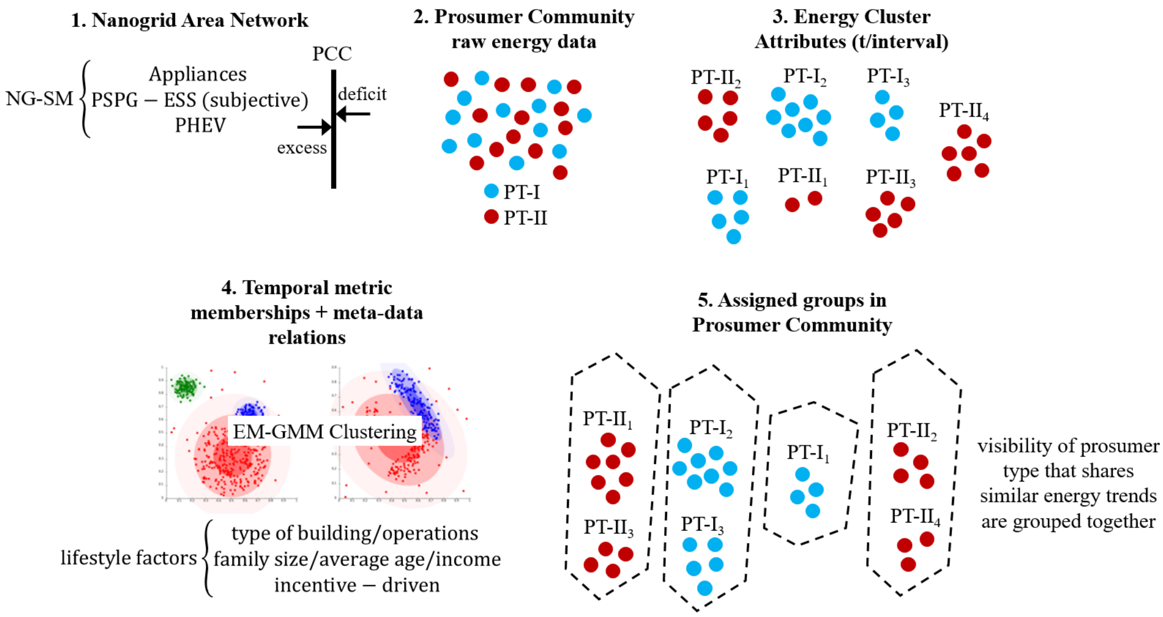

Fig. 4.4 Characterisation of Prosumer Community into clusters ($PT\text{-}I$ and $PT\text{-}II$) based on energy attributes.

The relations in assigning $E_{EXS}^{PT\text{-}I_i}$ to $E_{EXC}^{PT\text{-}II_i}$ depends on $PT\text{-}II$'s energy attributes and contribution status in the Community. For an instant, a predefined $E_{EXS}^{PT\text{-}I_i}$ is to be assigned into $E_{DMD}^{PT\text{-}II_n}$ under a policy which prioritises certain attribute. In the case if Community is not characterised in view of this attribute then, the status of $PT\text{-}II$ is not created. Consequently, the priority relations among $PT\text{-}II$ is left uncertain and the corresponding $E_{EXC}^{PT\text{-}II_i}$ attribute will not be tallied (*i.e.* large $E_{DMD}^{PT\text{-}II_i}$ can receive large amount of excess during low inferior-priority policy).

NGs are characterised into respective clusters which entails unique Prosumer-type and similar energy attribute trends. The characterisation processes also perform allocation of $E_{EXS}^{PT\text{-}I_i}$ to designate $PT\text{-}II$ based on priority policy (hierarchical) that describes sharing relations between the pairing clusters. Conclusively, it translates a Prosumer Community into homogeneous member (cluster) with low energy attribute variance that adheres to priority policy. The proposed characterisation approach will not mix both $PT\text{-}I$ and $PT\text{-}II$ in a cluster but instead clustering were done based on same Prosumer type and attributes as shown in Fig. 4.4 and defined in (4.1)-(4.3).

To create Prosumer Community homogeneity environment, profiling of energy usage trends from both $PT\text{-}I$ and $PT\text{-}II$ are utilised. Preliminarily, the initial categorisation starts with quantifying $PT\text{-}I$'s potentials in generating energy upstream (excess generations) and will be segregated from the rest. In continuous domain at time t, the energy deficient and excess capacities of individual $PT\text{-}I$s are monitored at Nanogrid PCC defined as $E^{PT\text{-}I_i}_{EXS_{(t)}}$ and $E^{PT\text{-}I_i}_{DMD_{(t)}}$ respectively. Subsequently, to gain close-to estimations of available energy allocation, considering irregularities in consumption behaviours (*e.g.* energy usage demographic deviates from weekday to weekend), $PT\text{-}I$ interoperates lifestyle factors (meta-data relations). It aims to recover convergence (stabilise) in calibrating energy allocations by averaging the energy attribute over a predefine duration (*i.e.* weekly, monthly), T, for a single $NG_{PT\text{-}I_i}$ given in (4.4) to minimise large demand shift/deviation episodes.

$$\{\overline{E^{PT\text{-}I_i}_{Att}}\} = \frac{\sum_{t=1}^{T} E^{PT\text{-}I_i}_{DMD_t;GEN_t;EXS_t}}{T} \tag{4.4}$$

where T denotes the total time taken based on the predefined time interval (*e.g.* $T = 168$, $t = 1$; hourly interval for a week). The average energy attribute itself will not define any insights neither on its consumptions nor generations behaviour. Hence, comparisons with other $\overline{E^{NG_i}_{Att}}$ within the Prosumer Community using clustering approach aids in determining Nanogrid's energy deficiency level with respect to others.

4.3.2 Proposed Clustering Analysis & Coordination

Employing Azure Machine Learning Studio, an EM-GMM based clustering module was created in Azure registry container to classify NGs into affiliated clusters based on respective Nanogrid's energy attributes. EM-GMM is an unsupervised machine learning algorithm that organises each data point into respective unique cluster that has similar properties/features. In this sense, the clustering distribution defined by EM-GMM algorithm is based on $\{\overline{E^{PT\text{-}I}_{Att}}\}$, $\overline{E^{PT\text{-}II}_{Att}}$, and the number of created clusters. Each cluster is characterised by a unique localise centroids, congregating NGs of the same proximity to the central value. For an instant, assuming the computed average energy attribute across all NG_i over period T is $\{\overline{E^{PT\text{-}I_1}_{Att}}^T\},\ldots,\{\overline{E^{PT\text{-}I_n}_{Att}}^T\},\overline{E^{PT\text{-}II_1}_{Att}}^T,\ldots,\overline{E^{PT\text{-}II_n}_{Att}}^T$. After clustering, the Prosumer Community is define as:

$$\begin{aligned} &\left\{\{\overline{E^{Cl\text{-}1,1}_{Att}}^T\},\{\overline{E^{Cl\text{-}1,2}_{Att}}^T\},\ldots,\{\overline{E^{Cl\text{-}1,N}_{Att}}^T\}\right\} \subset \overline{E^{PC}_{Att}}^T \quad ;\forall\ PT\text{-}I \\ &\left\{\overline{E^{Cl\text{-}2,1}_{Att}}^T,\overline{E^{Cl\text{-}2,2}_{Att}}^T,\ldots,\overline{E^{Cl\text{-}2,M}_{Att}}^T\right\} \subset \overline{E^{PC}_{Att}}^T \quad ;\forall\ PT\text{-}II \end{aligned} \tag{4.5}$$

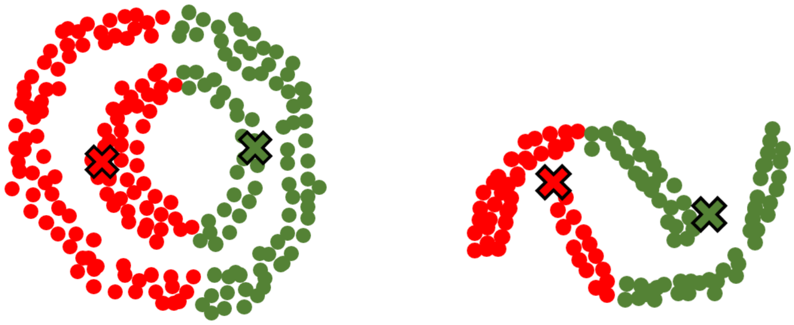

(a) Two circular cluster of different radius have same mean value.

(b) Interception clustering shapes causing deceptive mean value.

Fig. 4.5 Failure cases when identifying cluster centroid (mean value) using K-Means approach.

where

$$
\begin{aligned}
\overline{E^{Cl\text{-}2,m}_{Att}}^{T} &= \{\overline{E^{NG_i}_{DMD}}^{T}, \ldots, \overline{E^{NG_I}_{DMD}}^{T}\} \ ; \ of\ same\ CAT_m\text{-}Att \\
\left\{\overline{E^{Cl\text{-}1,n}_{Att}}^{T}\right\} &= \left\{\overline{E^{NG_i}_{DMD}}^{T}, \overline{E^{NG_i}_{GEN}}^{T}, \overline{E^{NG_i}_{EXS}}^{T}, \ldots, \overline{E^{NG_I}_{DMD}}^{T}, \overline{E^{NG_I}_{GEN}}^{T}, \overline{E^{NG_I}_{EXS}}^{T}\right\} \ ; \ of\ same\ CAT_n\text{-}Att
\end{aligned}
\tag{4.6}
$$

Note that clustering configuration for $PT\text{-}I$ is a set of 3 components, E_{DMD}, E_{GEN}, and E_{EXS}, while $CAT\text{-}Att$ refers to the attribute categories defined by user.

Typically, adaptations of K-Means technique deemed to be a popular avenue to perform clustering. However, drawback in K-Means is its naive approach in determining mean value for cluster centroid. Fig. 4.5 illustrates the confusions in K-Means technique when localising mean value of two groups that are placed close together and also cases where the groups are not clustered in an uniformed shape. Therefore, EM-GMM provides flexibility than of K-Means as it distributes data point in Gaussian function. In this sense, it avoids rigid visualisation of circular-based geometry assumptions when localising mean value; taking mean and standard deviation parameters to describe the cluster's shape. Given in the two dimensional axis (x-y) directions, a single cluster can take an elliptical shape based on the Gaussian distribution. To find the mean and standard deviation of the Gaussian parameters for each cluster, Expectation–Maximisation optimisation algorithm is employed. Fig. 4.6 displays the Gaussian distribution being fitted to form respective clusters.

The computing conceptualisation of EM-GMM is as follows;

1. It begins with predefining the number of cluster and randomly initialise the Gaussian distribution parameters. Comparably, these parameters can also be estimated based on

the data trends. Nevertheless, both approaches begin with a poor Gaussian inception but converged quickly.

2. From the Gaussian distribution, compute the probability of each data to which cluster it belongs to. Those data points that are closer to the respective Gaussian centroid will be clustered together. Intuitively, employing Gaussian distribution, it is assumed that most of the data points exist closer to the cluster's centre.

3. Based on the data probabilities, new set of Gaussian distribution parameters are computed to maximise likelihood estimation of data points within clusters. Those new parameters uses mixture weighted sum on the position of data point; where the weights denote probability assignments of data points to a particular cluster. To visualise the transition of distribution, refer to the green data points and cluster in Fig. 4.6. Initially, in first iteration, the distribution is generated randomly despite having the green data points spreading in the direction of 'top-right'. It then compute the mixture weighted sum from the probabilities, acknowledging that some green data points are near the centre while a densely populated data on the right. Hence, naturally the mean distribution shifts closer to the right forcing to create an ellipse that is fitted by the data standard deviations (maximising mixture weight sum probability).

4. Repeat Step 2 and 3 iteratively until the distribution converges from one iteration to the next.

Accordingly, EM-GMM algorithm aids in clustering respective NGs to a cluster member for every time interval t. Assuming that the cluster members are organised based on energy attributes exchange at PCC in a hierarchical order of their centroid ($e.g.$ $\overline{E_{Att}^{NG_m}}^{T}$ $<50kWh$,

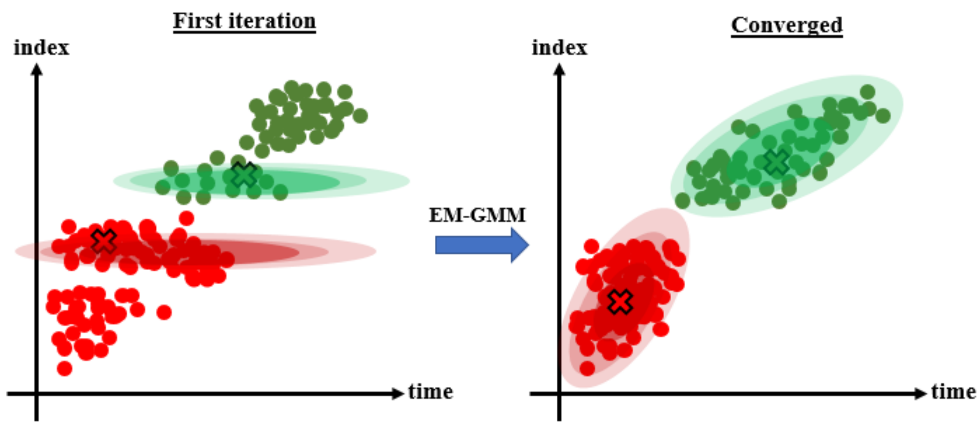

Fig. 4.6 Expectation-Maximisation clustering using Gaussian distribution model.

$T = 168$, $t = 1$, assign to cluster-consumption 1 and subsequent cluster-consumption has its energy attribute increases in value). The absolute difference in distribution between cluster members and their centroids defines clustering variances. Clusters that attained low variance depicts close proximity positioning among data points in relations to cluster's centroid.

4.3.3 Expectation-Maximisation Gaussian Mixture Model Algorithm

The prerequisite in employing EM-GMM assumes familiarity with mixture model, probability theory (defined in Appendix C), and maximum likelihood estimation (MLE). Taking the observations of X_i and K components derived from mixture model, (4.7) defines the marginal probability distribution of X_i:

$$P(X_i = x) = \sum_{k=1}^{K} \pi_k P(X_i = x|Z_i = k) \tag{4.7}$$

where the mixture proportion,π_k, represents the probability in which X_i associates to the mixture component of k^{th}. While, the latent variable, $Z_i \in \{1,..,K\}$, denotes the mixture component ($P(X_i|Z_i)$) for X_i.

Maximum Likelihood Estimation: Normal Distribution

Reviewing on MLE in normal distribution, suppose n number of observations $X_1,...,X_n$ are sampled from the Gaussian distribution with unknown mean(μ) and variance(σ^2). Hence, finding the MLE for mean requires log-likelihood, $\ell(\mu)$, by taking the derivative in relations to μ and equates it to zero. (4.8) defines the expression for MLE in normal distribution:

$$L(\mu) = \prod_{n}^{i=1} \frac{1}{\sqrt{2\pi\sigma^2}} exp^{-\frac{(x_i-\mu)^2}{2\sigma^2}} \tag{4.8}$$

By applying logarithmic function to the likelihood, it decomposes the product function and inverses exponential function so that MLE can be solve easily:

$$\ell(\mu) = \sum_{i=1}^{n} \left[\log\left(\frac{1}{\sqrt{2\pi\sigma^2}}\right) - \frac{(x_i-\mu)^2}{2\sigma^2} \right] \tag{4.9}$$

and taking the log-likelihood derivative, equate it to zero to achieve MLE, and solve for μ:

$$\begin{aligned} \frac{d}{d\mu}\ell(\mu) &= \sum_{i=1}^{n} \frac{x_i - \mu}{\sigma^2} = 0 \\ \mu_{MLE} &= \frac{1}{n}\sum_{i=1}^{n} x_i \end{aligned} \tag{4.10}$$

Mixture Model for Gaussian Mixture Model: Expectation-Maximisation

From the mixture model concept, Expectation-maximisation (EM) algorithm is defined in the context of Gaussian Mixture Model (GMM) implementation−hence contrived EM-GMM. Let $N(mean(\mu), variance(\sigma^2))$ denotes the distribution probability function for normal random variable. Here, the conditional distribution, $X_i|Z_i = k \sim N(\mu_k.\sigma_k^2)$, so that the distribution margin of X_i is expressed as:

$$P(X_i = x) = \sum_{k=1}^{K} P(Z_i = k)P(X_i = x|Z_i = k) = \sum_{k=1}^{K} \pi_k N(x;\mu_k,\sigma_k^2) \tag{4.11}$$

Likewise, the joint observation probability of $X_i = \{X_1, X_2, ..., X_n\}$ is:

$$P(X_1 = x_1, X_2 = x_2, ..., X_n = x_n) = \prod_{i=1}^{n}\sum_{k=1}^{K} \pi_k N(x_i;\mu_k,\sigma_k^2) \tag{4.12}$$

It describes EM algorithm in gaining MLE of $\pi_k, \mu_k, and \sigma_k^2$ when given a set of observation data, $\{x_1, x_2, ..., x_n\}$

Maximum Likelihood Estimation: Gaussian Mixture Model

Using the same concept as normal distribution MLE, subsequent defines MLE in Gaussian mixture model. Similarly, the unknown parameters; $\theta = \{\mu_1, ..., \mu_k, \sigma_1, ..., \sigma_k, \pi_1, ..., \pi_k\}$ and the likelihood is defined as:

$$L(\theta|X_1, ..., X_n) = \prod_{i=1}^{n}\sum_{k=1}^{K} \pi_k N(x_i;\mu_k,\sigma_k^2) \tag{4.13}$$

Hence, the log-likelihood is defined as:

$$\ell(\theta) = \sum_{i=1}^{n} \log\left(\sum_{k=1}^{K} \pi_k N(x_i;\mu_k,\sigma_k^2)\right) \tag{4.14}$$

However the expression in (4.14) shows that the summation of K components impede the log function from applying normal distribution. Hence assign the derivative of log-likelihood with respect to μ_k and equate it to zero:

$$\frac{d}{d\theta}\ell(\theta) = \sum_{i=1}^{n} \frac{\pi_k N(x_i;\mu_k,\sigma_k)}{\sum_{k=1}^{K}\pi_k N(x_i;\mu_k,\sigma_k)} \frac{x_i-\mu_k}{\sigma_k^2} = 0 \tag{4.15}$$

It can be seen that solving for μ_k will not be analytically possible as for the latent variables, Z_i, are still unknown. In this sense, if Z_i are known, gathered from the sampled X_i such that $k = Z_i$ then, estimation of μ_k can be done by using (4.10).

Estimating Expectation-Maximisation for Latent Variable (GMM) MLE

Intuitively, the latent variables, Z_i, guides in determining MLEs. Hence, initial attempt to compute posterior probability distribution of Z_i given in EM observations is as follows:

$$P(Z_i = k|X_i) = \frac{P(X_i|Z_i = k)P(Z_i = k)}{P(X_i)} = \frac{\pi_k N(\mu_k,\sigma_k^2)}{\sum_{k=1}^{K}\pi_k N(\mu_k,\sigma_k)} = \gamma_{Z_i}(k) \tag{4.16}$$

Substitute (4.16) into (4.15) and perform derivative of log-likelihood and solve for μ_k. Despite having μ_k-dependent for $\gamma_{Z_i}(k)$, it can be attuned to subconsciously neglect its relationship and 'approximately/predictively' solve for μ_k:

$$\begin{gathered}\sum_{i=1}^{n}\gamma_{Z_i}(k)\frac{x_i-\mu_k}{\sigma_k^2} = 0\\ \frac{\sum_{i=1}^{n}\gamma_{z_i}(k)x_i}{\sum_{i=1}^{n}\gamma_{z_i}(k)} = \hat{\mu}_k = \frac{1}{N_k}\sum_{i=1}^{n}\gamma_{z_i}(k)x_i\end{gathered} \tag{4.17}$$

$s.t.$

$$N_k = \sum_{i=1}^{n}\gamma_{z_i}(k) \tag{4.18}$$

where N_k refers to the number of effective points assigned to k component and $\hat{\mu}_k$ is the average weighted data with $\gamma_{z_i}(k)$ weights. Likewise, $\hat{\pi}_k$ and $\hat{\sigma_k^2}$ can be similarly computed using (4.17):

$$\begin{gathered}\hat{\pi}_k = \frac{N_k}{n}\\ \hat{\sigma_k^2} = \frac{1}{N}\sum_{i=1}^{n}\gamma_{z_i}(k)(x_i-\mu_k)^2\end{gathered} \tag{4.19}$$

Conditionally, derivations for finding MLE in GMM domain requires two specific observations; (i) posterior probabilities, $\gamma_{Z_i}(k)$, can only be computed if parameter θ are known, and (ii) solving for parameter, θ, requires $\gamma_{Z_i}(k)$. Motivated by the above mentioned observations, the EM algorithm pseudo is as follow:

Pseudo of EM:

---

initialise parameters, θ: μ_k, σ_k, π_k, ε=1.
compute initial log-likelihood function.
while_loop(ε>1e-5)
  Calculate γ_{Z_i}(k) using (4.16).
  Calculate estimation of $\hat{\mu}_k$, $\hat{\sigma_k^2}$, $\hat{\pi}_k$ using (4.17)–(4.19).
  Assign: $\pi_k \leftarrow \hat{\pi}_k$; $\mu_k \leftarrow \hat{\mu}_k$; $\sigma_k \leftarrow \sqrt{\hat{\sigma_k^2}}$.
  Assign: log-likelihood$_{old}$←log-likelihood and recalculate log-likelihood before assigning to →log-likelihood$_{new}$.
  if log-likelihood$_{new}$ < log-likelihood$_{old}$
    re-initialise parameter θ
    set tolerance: ε=1
    else
      tolerance: ε=|log-likelihood$_{new}$-log-likelihood$_{old}$|
 end while

It is critical to observe sensitivity when declaring the initial parameters, θ, deeming them to be 'valid'. This can be verified by monitoring log-likelihood if its value increases after every iteration.

EM-GMM

Conclusively, relevant quantities of estimate-based EM algorithm is fused into Gaussian mixture model. The absolute likelihood is expressed as follows:

$$P(X,Z|\mu,\sigma,\pi) = \prod_{i=1}^{n}\prod_{k=1}^{K}\pi_k^{I(Z_i=k)}N(x_i|\mu_k,\sigma_k)^{I(Z_i=k)} \tag{4.20}$$

where I denotes the identity matrix of covariance and the log-likelihood:

$$\log(P(X,Z|\mu,\sigma,\pi)) = \sum_{i=1}^{n}\sum_{k=1}^{K} I(Z_i=k)(\log(\pi_k)+\log(N(x_i|\mu_k,\sigma_k))) \tag{4.21}$$

The log function acts directly on the standard normal density, leading to non-complex solution for MLE. As the estimated EM function does not observe latent variables hence, expectation of log-likelihood with respect to posterior probability of latent variables were considered. In consequence, the expected (E) log-likelihood value is expressed in (4.22).

$$
\begin{aligned}
E_{Z|X}[\log(P(X,Z|\mu,\sigma,\pi))] &= E_{Z|X}\left[\sum_{i=1}^{n}\sum_{k=1}^{K} I(Z_i=k)(log(\pi_k)+\log(N(x_i|\mu_k,\sigma_k)))\right] \\
E_{Z|X}[\log(P(X,Z|\mu,\sigma,\pi))] &= \left[\sum_{i=1}^{n}\sum_{k=1}^{K} E_{Z|X}[I(Z_i=k)](log(\pi_k)+\log(N(x_i|\mu_k,\sigma_k)))\right] \\
E_{Z|X}[\log(P(X,Z|\mu,\sigma,\pi))] &= \left[\sum_{i=1}^{n}\sum_{k=1}^{K} \gamma_{Z_i}(k)(log(\pi_k)+\log(N(x_i|\mu_k,\sigma_k)))\right]
\end{aligned}
\tag{4.22}
$$

where $E_{Z|X}[I(Z_i=k)]$=$P(Z_i=k|X)$ and can be defined as $\gamma_{Z_i}(k)$ given in (4.16). Here, maximisation of expected log-likelihood with respect to μ_k, σ_k, and π_k are based on fixed $\gamma_{Z_i}(k)$ in order to achieve closed-form resolution.

4.3.4 Integrating Temporal Clustering: Membership & Adaptability

The proposed EM-GMM clustering approach holds characterisation for each Nanogrid's energy attribute at a predefined time interval, T. However, based on the expected energy means and variances during clustering, they are unable to describe energy behaviour for a longer period of time. For an instant, assuming time interval taken is rated at T =24 and the clusters offer insights on Nanogrid's energy exchange at PCC hourly basis for a day. However, if considering an ideal energy characterisation for a year that observes seasonal changes and festive periods then, taking the average energy attribute values (T=24hrs) and perform clustering will not comprehend temporal transition of energy behaviour. In this sense, temporal changes in profiling energy exchange activities at PCC could not be reproduce during clustering with shorter time intervals. Hence, clustering adopts weekly basis to smooth the energy variability across weekday and weekend, and employ temporal metrics involving temporal membership and adaptability to gain perspective on Nanogrid's energy attributes over a year.

Temporal Metrics

The temporal metrics comprises of two characterisations; (i) cluster membership−a label that defines Nanogrid's associated cluster based on specific energy attribute, (ii) cluster adaptability−where clustered NGs of the same energy attribute transitioned into another cluster at consecutive T intervals (during clustering periods). Hence, the peripherals of temporal membership and adaptability provides clustering identity for individual NGs and observes permutation in Nanogrid's energy attributes for definite clustering respectively. For an example, in week n, $NG_1^{PT\text{-}I}$ was assigned to cluster-consumption 1 however, in week $(n+1)$ it transitioned into cluster-consumption 2; transition adaptability: $\{\overline{E_{Att}^{Cl\text{-}1,1\Rightarrow 2}}^T\}$, cluster membership: from $\{\overline{E_{Att}^{Cl\text{-}1,\mathbf{1}}}^T\}$ to $\{\overline{E_{Att}^{Cl\text{-}1,\mathbf{2}}}^T\}$.

Using percentage as the reference quantifier, the frequency of NGs undergone cluster transitioning over a year can be monitored. For a specific clustering scheme, Cl, for NG_i (in general), its temporal membership identity, u, for a year is expressed as follows:

$$\begin{aligned} Cl_{Att,u}^{NG_i} &= \frac{\sum_{T=1}^{T_{max}} {Cl_{Att,u}^{NG_i}}^T}{T_{max}} * 100\% \\ {Cl_{Att,u}^{NG_i}}^T &= \begin{cases} 1, & \textbf{if } i \text{ member of } Cl_{Att,u} \\ 0, & otherwise \end{cases} \end{aligned} \tag{4.23}$$

where T_{max} refers to the total sampled duration while T denotes the time intervals, in this case is weekly. Contrarily, the annual temporal adaptability of NG_i transitioning from cluster to cluster $u \Rightarrow (u \underline{+} n)$ is defined:

$$\begin{aligned} \left[Cl_{Att,u}^{NG_i} \Rightarrow ... \Rightarrow Cl_{Att,(u\pm n)}^{NG_i}\right]_z &= \frac{\sum_{T=1}^{T_{max}} \left({Cl_{Att,u}^{NG_i}}^{(T-z)} \Rightarrow ... \Rightarrow {Cl_{Att,(u\pm n)}^{NG_i}}^{(T)} \right)}{T_{max} - z} * 100\% \\ \left[{Cl_{Att,u}^{NG_i}}^{(T-z)} \Rightarrow ... \Rightarrow {Cl_{Att,(u\pm n)}^{NG_i}}^{(T)}\right] &= \begin{cases} 1, & \textbf{if } \text{transition(s) exist} \\ 0, & otherwise \end{cases} \end{aligned} \tag{4.24}$$

$s.t.$

$$\left[Cl_{Att,u}^{NG_i} \Rightarrow Cl_{Att,v}^{NG_i}\right]^{\boldsymbol{T}} = \begin{cases} 1, & \textbf{if } u \neq v \\ 0, & otherwise \end{cases} \tag{4.25}$$

where z represents the number of transition occurred, relocating to consecutive clusters during T intervals. The interpretation of temporal adaptability is appraised by z value or its cluster hop-count−where $z = 2$ depicts $Cl_{Att,3}^{NG_i\,T} \Rightarrow Cl_{Att,2}^{NG_i\,(T+1)} \Rightarrow Cl_{Att,1}^{NG_i\,(T+2)}$.

Moreover, the primary interests in monitoring temporal adaptability suggests how individual Nanogrid, in terms of energy deficiency and consumptions, is rated among other NGs. Through cluster membership hierarchical indications, u, the transition from high to low index regarded as a favourable energy usage outcome that relates reduction in Nanogrid's electricity billing. Contrarily, in relations to excess generations from local PSPG, low to high cluster transition index is considered benefiting as Prosumer have the ability to gain greater profit margin from. Using both temporal membership and adaptability percentage metrics over a year, defined as θ_{mem} and θ_{adpt} limits, NGs are distributed into four regions based on respective energy attribute and reference to (4.23)−(4.25):

$$\theta_{mem}, \theta_{adpt} = \begin{cases} \theta \leq 25\% & \text{low} \\ 25\% < \theta \leq 50\% & \text{moderate low} \\ 50\% < \theta \leq 75\% & \text{moderate high} \\ 75\% < \theta & \text{high} \end{cases} \tag{4.26}$$

Social & Economic Attributes

To comprehend a factual characterisation of Nanogrid's energy attributes in a Community, the temporal metric performances are fused with meta-data relations to increase attribute sensitivity and reduce consumption variability. Meta-data relations represent social/human-factor aspects that can influence utilisation of excess generations and consumptions in Nanogrid based on economical trajectory. For an example, size of Nanogrid's building structure, nature of building's operations (*i.e.* industrial machineries, office spaces/shopping centre, hospital), installation of smart devices that helps to manage energy distribution, occupant's average income, number of pax residing. Moreover, government efforts in providing incentive programmes have driven Prosumer's behaviour to redesign energy management strategies and gain monetary incentives. Hence, the above mentioned influencing attributes can be used as meta-data relations, revealing social impacts and energy behaviour aspects of individual NGs.

Connecting the meta-data relation factors with the results attained from clustering, the Prosumer is fully characterised driven by its socio-economic circumstances against other Prosumers within the Community.

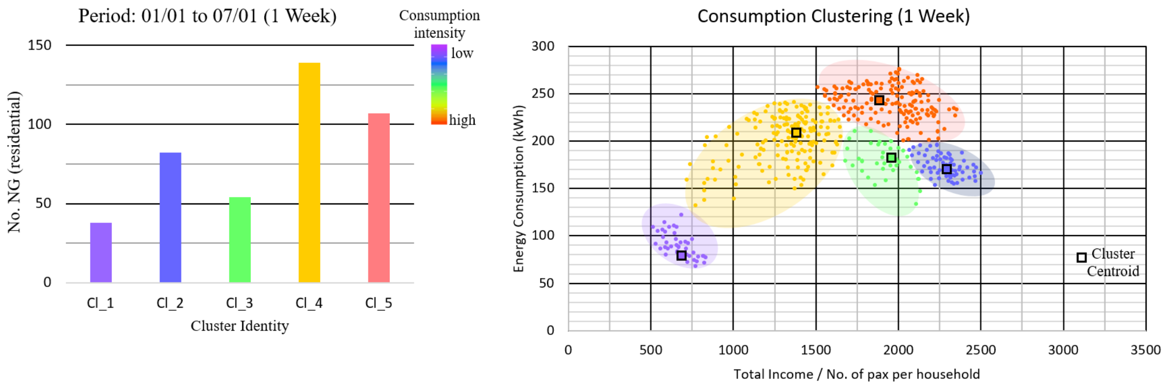

Fig. 4.7 Clustering of PT-IIs based on 1 week energy consumptions against average income.

4.3.5 Findings and Results for Clustering Prosumer in Community

Using energy profile data collected from [224] and [108], clustering analyses were performed to create a clustered-based Community. These data sets represent an annual compilation of energy consumptions and generations from both $PT-I$ and $PT-II$, a 'living lab' testbed Microgrid system in Pecan Street involving more than 1000 volunteered participants (typical household environment). Among these data, the clustering evaluations select only 180 of PT-I and 420 PT-II within close proximity (geographical location) to symbolise a Community. Based on respective Nanogrid's energy attributes, clustering algorithm with temporal metrics were applied to view Nanogrid's allocation into respective clusters. Note that both Prosumer-type has each set of clusters as PT-I and PT-II are not mixed together hence, two independent clustering analyses were performed.

Firstly, it involves clustering of 420 PT-IIs where creation of clusters are more apparent; energy attribute variable deals only in consumption demographics. From the consumption-based clusters, temporal membership and adaptability metrics are applied to rate Prosumer's energy consumptions and contributions over an extended time period. The temporal metrics are categorised into 4 regions based on (4.26). Fig. 4.7 illustrates households being clustered into respective cluster (Cl_1 to Cl_5) based on only energy consumption attributes gathered for a week. The clusters are ranked from lowest energy consumption, Cl_1, and to the highest clustered in Cl_5 while Fig. 4.8 presents effects of temporal metrics, $\theta_{mem,adpt}$, attributes; T=1 week, T_{max}=24 weeks.

In Fig. 4.7, the result illustrates that energy consumption distribution of PT-IIs in week 1 are levelled at high−majority of NGs are clustered in Cl_4 and Cl_5. The formed clusters were identified using EM-GMM clustering algorithm where the computed centroids describes level of consumption in relations to Nanogrid's average income. Fig. 4.8a presents the cluster's

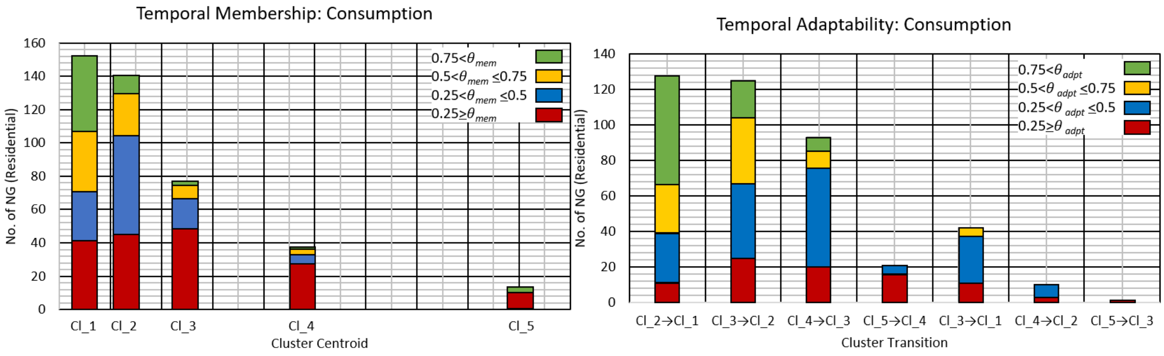

(a) Temporal membership of NGs retained within the same cluster member.

(b) Temporal adaptability of NGs transitioning into other cluster member.

Fig. 4.8 Temporal metrics on *PT-II* consumption attribute based on T=1 week, T_{max}=24 weeks.

consumption temporal memberships, θ_{mem}, for 24 weeks with an interval of 1 week. Similarly, Cl_1 denotes low energy consumption level and increases proportionately to cluster's index. In addition, the position of clusters along the x-axis defines their consumption centroids. The result shows that 151 *PT-I*s were clustered in Cl_1 with 21 out of which were abled to maintain its cluster membership throughout T_{max}, green coded area securing $\theta_{mem} >75\%$. Contrarily, Cl_3 has the largest number of NGs to be assigned with low temporal membership ($\theta_{mem} <25\%$). This indicates that NGs clustered in Cl_3 will transition out into other cluster index; an episode where Prosumers experience high energy consumptions for a particular week and subsequently regained normality. Likewise, Cl_4 also experienced the same temporal membership effects as Cl_3. Notably, in cluster Cl_5, there were 2 NGs maintained in the highest energy consumption usage region. Fig 4.8b presents temporal adaptability, θ_{adpt}, results describing transitioning activities of NGs into different clusters. The x-axis exhibits favourable cluster transition processes where NGs are transferred from high to low cluster index. The analyses present that the probability of NGs transitioning more than two clusters (*e.g.* $Cl_5 \rightarrow Cl_2$) are uncommon as such instances demand intense regulation potentials from *PT-II*s. However, 41 NGs have experienced an exceptional case of transitioning from Cl_3 to Cl_1 with mass rated at $\theta_{adpt} \leq 50\%$. Survey showed that the household's average income has increased and the energy consumption was reduced (*i.e.* unoccupied during the day). Most of the NGs had their energy consumptions regulated between clusters 1 to 3 which explains large assignment of NGs in those clusters as shown in Fig. 4.8a.

Upon analysing *PT-II*s' energy consumption behaviours across 24 week period, interoperation of meta-data relations were analysed considering only building structure/size variable to enhance characterisation accuracy. In Fig. 4.9, three building types/structures were studied

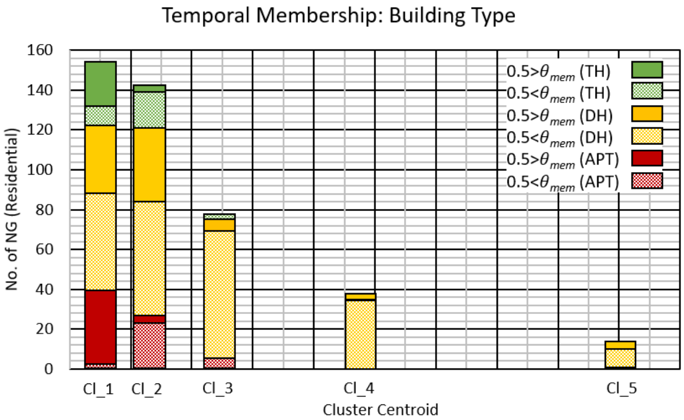

Fig. 4.9 Meta-data relation involving building type.

in response to their energy consumption in respective temporal membership; townhome (TH), detached home (DH), and apartment (APT). The results inferred that townhomes and apartments are typically characterised as low energy consumption habitat, clustered within Cl_1 to Cl_3. Surpassing, smaller type buildings (*i.e.* apartment) deemed to have greater advantage over consumption level as majority were clustered and preserve in Cl_1 rated at $\theta_{mem} > 0.5$.

Subsequently, investigations into profiling energy attribute across 180 PT-Is were analysed based on comparable timespan, interval of 1 week throughout 24 weeks. In relations to PT-I's energy attributes, they involved clustering of available excess generations and energy deficiency exchanged at Nanogrid PCC. The processes in clustering PT-Is avoid dealing with energy consumption and generation levels as they provide insignificant relations on DSR contributions as compared to energy exchanged levels at Nanogrid PCC gateways. Furthermore, it also provides better representation of individual PT-I energy attributes when compared other Prosumers in the Community (*i.e.* PT-II) and quantification of ESS's variables can be neglected.

Fig. 4.10 illustrates clustering outcomes of PT-Is in relation to excess generations (upstream) generated from PV system against its size and energy deficiency (downstream), and household's average income for 168 hours ($T_{max} = 168$) with an hour interval ($T = 1$). The x-axis demarcates cluster's centroids which correspond to the intensity level in respective domains (*i.e.* Cl_1 – lowest and Cl_5 – highest). For an example, for clustering excess generations, NGs grouped in Cl_5 gained the highest beneficiary in view of energy attribute whereas in the same cluster index for energy deficiency domain, NGs have suffered the worst due to dominant consumption capacity despite having PSPG. As seen in Fig. 4.10a, benefitting excess generation clusters, Cl_4 and Cl_5, comprises of PV systems that are larger

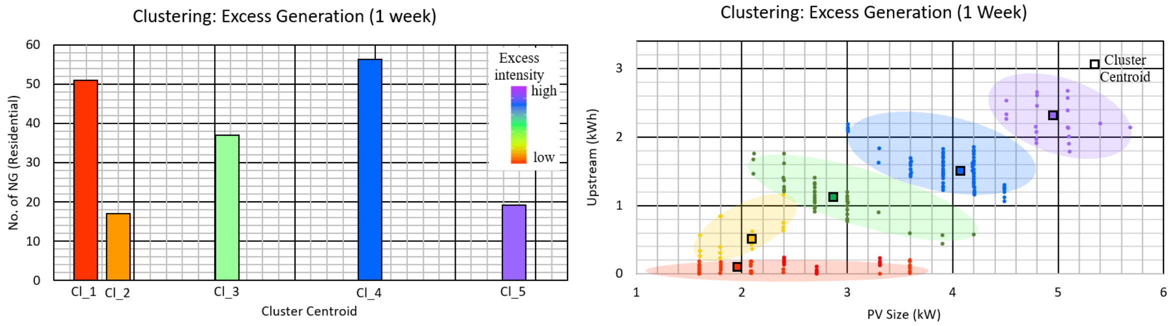

(a) Excess generation generated by PVs flowing upstream.

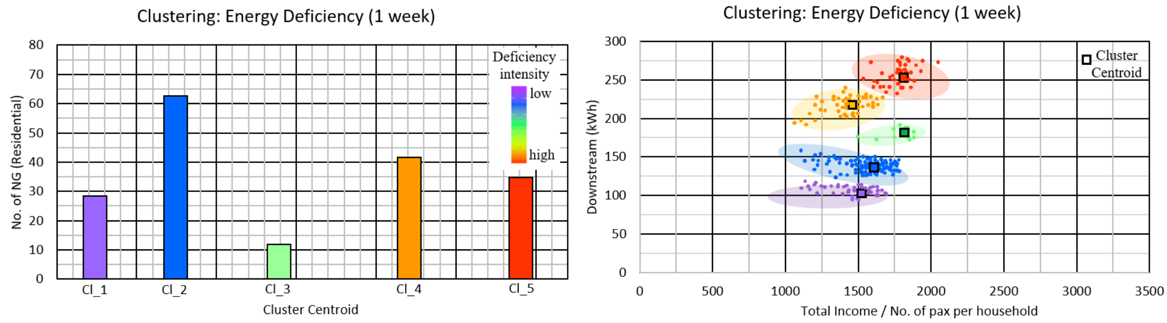

(b) Energy deficiency (energy demand flowing downstream).

Fig. 4.10 Clustering of *PT-I*s based on excess and energy deficiency in view of installed PV and ESS sizes.

than $3.9kW$ where the centroid difference from lower tier clusters are rated at $1kWh$ apart. In contrast, approximately 68-unit of NGs were clustered in the lower tier, $C1_1$ and Cl_2, where their centroids are measured at $<500Wh$ for a week and majority of NGs clustered in Cl_1 have zero excess generation availability. Such indication reflects that 40% of *PT-I* are still dependent on the grid to balance energy deficiencies due to dominant consumption capacity on a daily basis. It also signifies that they do not have significant contributions within the Prosumer Community; by means of supporting *PT-II* energy demands. In view of clustering *PT-I*'s energy deficiency attributes, Fig. 4.10b supports the cluster outcome seen in Fig. 4.10a by having close to half of *PT-I* population in Cl_4 and Cl_5. Such phenomenon indicates a possibility of poor energy management in utilising maximum potential of PV generation and optimum scheduling of ESS.

Investigating forward into temporal metrics for *PT-I*s, Fig. 4.11 presents both temporal membership and adaptability respectively for duration of 24 weeks with 1 week intervals. For temporal membership shown in Fig. 4.11a, more than 60% of *PT-I* managed to generate adequate capacity of excess generation, Cl_3 to Cl_5, and 30 NGs were able to retained their cluster membership in Cl_3 and Cl_4 (yellow regions). The dominant red regions seen in Cl_2

and Cl_5, θ_{mem} <0.25, describes that most NGs were rarely clustered in those two clusters which concludes most Nanogrids' excess generation falls between Cl_3 and Cl_4. Importantly, despite having 7 NGs clustered in Cl_1, the Cl_1's centroid value is rated at $1.27kWh$ per week which is better than the results attained in Fig. 4.10a. Likewise, the temporal adaptability shown in Fig. 4.11b, interprets that most NGs transitioned from Cl_2 to Cl_3 and CL_3 to Cl_4 which justifies the results attained for temporal membership seen in Fig. 4.11a.

Subsequently, Fig. 4.12 displays the temporal metrics for energy deficiency which will ultimately synchronises with PT-I's excess generation attributes given in Fig. 4.11. The Cl_1 energy deficiency centroid is close to zero where Nanogrids' are able to sustain and balance between generation and consumption capacities. Furthermore, 10-unit NGs were able to regain high temporal membership, θ_{mem}> 0.75 proving to have optimum energy management in ensuring less dependency on the grid (curtailing downstream exchange at PCC). Overall, all PT-Is had shown low energy deficiency level as there were less clustering occurrences in Cl_4 and Cl_5. It also can be validated by Fig. 4.12b where NGs were generally transitioned into cluster Cl_1, Cl_2, and Cl_3; green portions, θ_{adpt} >0.75.

Lastly, investigations into incorporating socio-economic attributes by introducing meta-data relations such as building size against energy consumption membership and incentive program enrolment for excess generation were analysed. Fig. 4.13a describes the temporal membership of energy consumption in view of building size where the result indeed justifies that the electricity demand grew proportionately to the building size. In comparison with the energy deficiency seen in Fig. 4.12a, installation of PV system does aid in curtailing DSR (downstream) and reduces PT-I's electricity billing, especially those staying in detached homes that are generally greater than 10k ft^2. Having installation of PV system, PT-Is

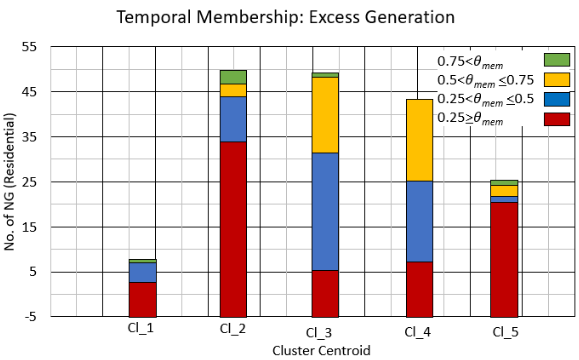

(a) Nanogrid temporal membership index.

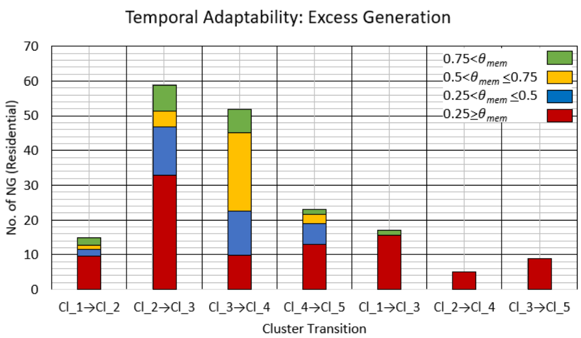

(b) Nanogrid temporal adaptability index; cluster transition.

Fig. 4.11 Temporal metrics of PT-I's excess generation attributes based on $T_{max} = 24weeks$, $T = 1week$.

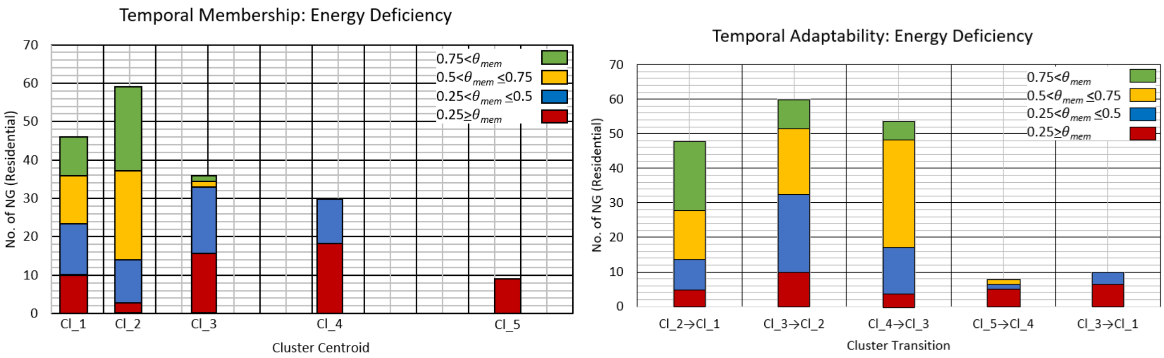

(a) Nanogrid temporal membership index. (b) Nanogrid temporal adaptability index.

Fig. 4.12 Temporal metrics of $PT\text{-}I$'s energy deficiency attributes based on $T_{max} = 24weeks$, $T = 1week$.

have the liberty to enrol into incentive programmes/policies provided by the government to promote effective DSR managements and sustainable efforts. Fig. 4.13b exhibits the responses in enrolling into different type of incentive programmes and how it does influence generation of excess energy capacities. Currently, there are 6 type of incentive programmes adopted by $PT\text{-}I$s; *(i)* Verizon−program for low-income families in which none were eligible due to high average income ceiling, *(ii)* Pricing−focuses on lowering energy consumption and minimise use of ESS to advocate sharing avenues, *(iii)* Control−emphasizes on self-sustaining solutions, *(iv)* Portal−similar to Pricing plan however, rated at a higher premium subscription fee with better customer relation reviews, *(v)* UT Text−regulates and controls energy consumption levels through penalty fees. In addition, monthly excess generation capacities must be met based on the contracted policy, and lastly *(vi)* TextMess−offers better incentive payouts as compared to others however, the total energy baseline level for fixed load appliances are capped within a certain threshold. The result has shown that Pricing program gained much popularity and many benefited by having greater excess generation capacities due to its energy management efficiency. Following behind it is TextMess program however, the temporal adaptability of excess generation is mostly less than 0.5 where NGs rarely crossover to other benefiting clusters. Control program received the least attention as it focuses much on maximising PV generation for self-sustain solutions which does not guarantee low energy deficiency level. Hence, it results in less energy exchange (upstream) for sharing and the incentive gained are at minimal.

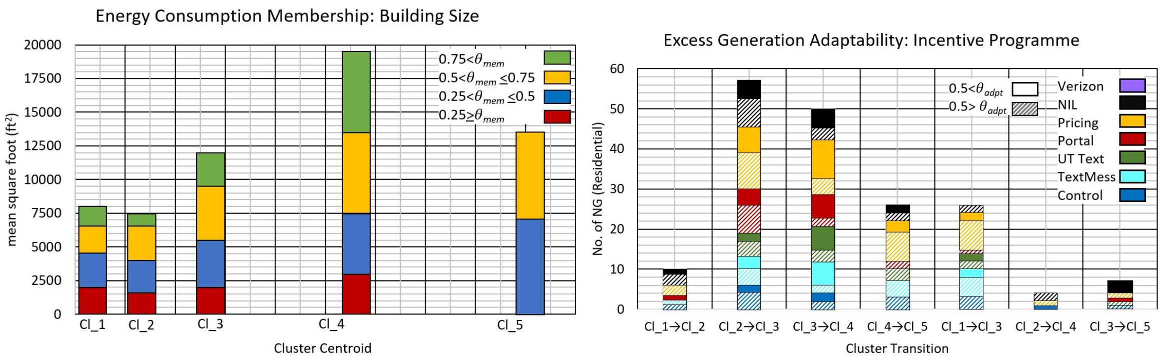

(a) Temporal membership of energy consumption against Nanogrid building size (sqft).

(b) Excess generation adaptability against incentive programme enrolment.

Fig. 4.13 Temporal metrics of *PT-I*' socio-economic behaviour based on $T_{max} = 24weeks$, $T = 1week$.

4.3.6 Performance Review on Clustering Prosumer Community

The results attained in Chapter 4.3.5 has shown its advantage in applying clustering algorithm to characterise Prosumers based on respective energy attributes and contribution domains. It ciphers excess generation availability against consumption level in a Prosumer Community, making scheduling of DSR management and modelling REM for bidding more apparent for DSOs. Utilising clustering algorithm with temporal metrics and meta-data relations, a complete decentralised energy profile characterisation is created. Furthermore, it also reflects certainty in Community's energy needs making DSR jurisdictions more apparent when allocating excess generation.

Predominantly, collected analyses have shown that socio-economic attributes (*i.e.* incentive programmes, lifestyles) are pivotal elements in steering Prosumers toward a cooperative energy sharing paradigm (not limited to consumption curtailments) hoping to achieve reduced electricity billing while maximising incentive payouts. Despite having such offered programmes, Prosumers are not well equipped with optimum EMS solutions and their involvements in the real-time REM are premature. *PT-I*s and *PT-II*s must co-exist to successfully attune the electricity market clearing price and also preserve network reliability against DSR problems.

Hence, in subsequent sub-chapters, investigations into modelling intelligent transactive EMS for individual Nanogrid is proposed, programmed to coordinate both DSR objectives (global) while securing individual interests (decentralised) within the Community.

4.4 Transactive Energy Management

With the recent liberalisation in the electricity market and integral digitalisation for decentralised energy management infrastructure, scientific communities are constantly resynthesising stackable-ecotechnological solutions that can radically address Prosumers' expectations in maximising PSPG potentials [225, 226]. At the global perspectives, distribution management methodologies have indeed become a pivotal topic driver for proactive energy business opportunities where standalone obligations/legislations are endorsed to sanction individualism while observing levelised administrations across all energy actors. However, as local management intelligences for greedy executions heightened to meet sole social objectives, cooperative functionalities such as stabilising clearing price market, commandeering DSR coordination between transmission and distribution network, and managing of fault isolation and service restoration due to DER integrations suffer periodic divergences. In this sense, ill-defined non-linear objective functions and large optimisation search space due to unconstrained variability becomes fragmented in global framework as local implementation of standards neglect foreign jurisdictions.

Therefore, TE management is introduced to comprehend the existence of personal owned DER penetrations and participation in the REM at low-voltage level. Its management proceeding focuses in ciphering Prosumer-centric solutions that interoperate technical, business, and social engagements in cooperative-competitive domain.

4.4.1 Related Work and Gaps

Research efforts in decentralised energy management systems at low-voltage level have focused much dependency on DSOs administrations, limiting Prosumers' options in purchasing or selling electricity in real-time. Such restrictions allow DSOs to have better accessibility and certainty towards supply-demand coordination at distribution level as compared to peer-to-peer transactions. Its core services addressing unit commitment (economic dispatch) scheduled for peak demand crises, anticipate uncertainty in DER penetrations and "duck-curve" effect, and inferior REM participations are critical elements that DSOs-TSOs are not willing to detach from. They justified that having a reversal role (*i.e.* low-voltage actors cooperatively govern DSR management) would compromise the reliability, security, and safety of the overall network. In this sense, DSOs-TSOs are yet placed as an energy transaction mediator that determines engagements of Prosumer-Retailer-REM where management solutions could be biased and may not be the greatest value for Prosumers.

H. Habib and et al. proposed an optimum strategy in coordinating local DER utilisations based on electricity market price guidance [227]. The management algorithm suggests hierarchical control framework coordinated by intelligent Agents of MAS in decentralised domain. It highlights the impacts on instantaneous scheduling of flexible load capacity and ESS based on real-time electricity tariff. In addition, mathematical evaluation index in quantifying energy management merits was proposed to distinguish different engagements in distributed or centralised control schemes. Correspondingly in [228], P. Almeida and et. al feature recent innovative projects involving DSO-TSO engagements in optimising peer-to-peer energy trading. Hence, new business model was proposed, presenting a generic market/trading platform that has complete optimisation tools in providing joined solution. It comprises of line congestion management, optimal power flow, use of market flexibility, and real-time control and supervision dedicated for DSO employment in TE commitments. Learning pointers were comprehended from the proposed test case studies; *(i)* modular-based/stackable−ability to expand decision-making protocols and search space based on learned energy management experiences, *(ii)* potability−adaptable towards environment in accommodate participants' domain. Other than managerial processes that affiliate with operating costs optimisation, [229] offers real-time scheduling of available generation resources with uncertainties to attune safe demand load demographics. Saint-Pierre and Mancarella proposed a novel dual-horizon rolling framework that regulates optimum power dynamics generated by DER penetration (upstream). It uses nonlinear programming algorithm to facilitate excess upstream generation to plan for reserve operation and treat voltage sag crises during large switching of demand load capacities at different time horizon.

A common decentralised managerial aspect was seen from the above mentioned methodologies where it is trivial for those proposed control algorithms to revolve around a centralised policy that is favourable for energy actors at top of the hierarchical chain but detrimental for Prosumer(s) as energy traders. Prosumers are seeking new business model (return on investment) options by taking full potential and ownership when dealing with upstream and downstream energy transactions at individual Nanogrid PCC. Network operators must realise that created electricity programmes and incentive policies may not maximise the potentials of individual interests especially retrofitting local social attributes. Network operators need to function as a secondary regulator that allows Prosumers to have greater liberation in conceding utilisation flexibility and PMP participations along the time horizon. Indeed, such undertakings can propagate predicaments when Prosumer participations starts to escalates; *(i)* endangering unsighted operations in times of energy crises for DSOs hence, complex restoration processes, *(ii)* monopolism episodes in the energy clearing price (greedy strategy) and possible obsoletion of energy Retailer(s) due to PtP dependency, *(iii)* competitive aggression between Prosumers which overshadow cooperative anatomy thus, jeopardises distribution network reliability, and (iv) power quality issue expands as higher integration of DERs beget stronger coupling between grid and inverters, and intermittent intentional islanding operations.

4.4.2 Significance of Transactive Energy on Demand-side Response Management

In this sub-chapters, it highlights a list of operational factors that can influence DSR at global (*i.e.* distribution network) and local (*i.e.* Nanogrid) levels. These variables and constraints will be fused into modelling of multi-objective statements for Prosumer-centric TE management at low-voltage level.

Estimating Demand Load Demographic

To gain full appreciation of online load profiles in a single Nanogrid, characterisation of domestic load appliances serves as an indication on Prosumers' demand capacity baseline. Considerations in load profile defers based on Nanogrid environment; $PT\text{-}I$ and $PT\text{-}II$ which also attributed to $full\text{-}pledge$, $storage\text{-}load$, and $load\text{-}only$ operating classification defined in (2.18)−(2.20).

The load demographics for $full\text{-}pledge$ and $load\text{-}only$ environment are relatively straightforward. However, uniquely for $storage\text{-}load$ based Prosumer is further divided into two classifications either operating as $PT\text{-}I$ or $PT\text{-}II$. As $PT\text{-}II$, it advocates islanding mode operations periodically and does not schedule to produce any generations upstream. It aims to utilise ESS for personal gain against real-time electricity tariff and time of energy crises (*e.g.* power outage, charging of PHEV).

Projecting the total energy consumptions can be distributed using Gaussian function to express Prosumer's lifestyles periodically across the day; partitioning morning and evening peak loading, midday base loading, and midnight loading as shown in Fig. 4.14. The Gaussian function for each time period is expressed as:

$$f(x) = a\exp(-\frac{(X-b)^2}{2c^2}) + d \tag{4.27}$$

where the peak height of the curve is denoted as a. It represents the estimated peak load magnitude in that particular time period based on the Nanogrid environmental dimension

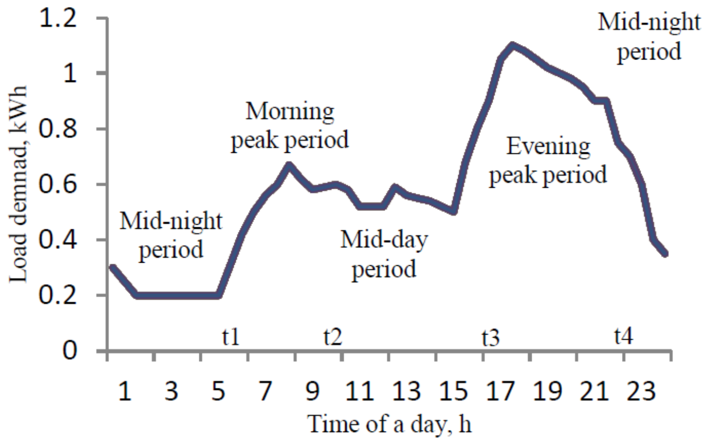

Fig. 4.14 Hourly load profile of domestic household separated into 4 time periods. The labelled time demarcations from $t1$ to $t4$ describe; $t1$—first activity (occupant awakes), $t2$—vacant (occupants goes off to work), $t3$—back home (occupants return home), and $t4$—no activity (occupants off to bed).

(*e.g.* square feet size of the building). b refers to the center of peak's position by averaging the event where consumption start and end (*e.g.* occupants wakes up and when they leave the vicinity). The width factor, c, control the Gaussian bell curve which relates to the number of occupants and rooms. d specify the function asymptotic converge far from peak, and X ascribes the time allocation along x-axis. The relations of parameter a, b, c, d, and $f(x)$ can be viewed in Fig. 4.15.

Using Fig. 4.14 as reference and Gaussian distribution function, Fig. 4.16 verifies the estimated load demand curve by adding all the Gaussian curve at respective time period together:

$$LD_{t\to 24} = \overset{M}{f}(x) + \overset{E1}{f}(x) + \overset{E2}{f}(x) + \overset{E3}{f}(x) + \overset{A}{f}(x) \tag{4.28}$$

where M refers to morning peak, $E1$ to $E3$ represents the three peak during evening, and A is the afternoon peak. However, in cases where parameters a, b, and c are unknown, (4.29)−(4.31) express the mathematical definition in quantifying respective parameter in relations to Nanogrid energy consumption attributes.

Defining the average peak magnitude parameter a at respective time period of the day will defer and commonly corresponds to the number of occupants and building size (*i.e.* number of rooms). Based on energy consumption behaviour generality reviewed in [230], discoveries present that; *(i)* evening peak load is 1.4 times greater than morning load, *(ii)* the average evening peak will last for 6 hours whereas morning peak lasted not more than 2 hours, *(iii)* The average morning peak magnitude is proportional to the number of rooms in Nanogrid as shown in Table 4.1, and *(iv)* The peak loading ratio in the afternoon increases with number of occupant(s) and room(s).

The peak magnitude in the morning, $\overset{M}{a}$ equitable to the number of rooms given in Table 4.1. Whereas in midday/afternoon, the peak magnitude, $\overset{A}{a}$, fluctuates between a minimum and maximum scalar of 0.3 and 0.86 times $\overset{M}{a}$ respectively to denotes weekday and weekend representation [231, 232]. In addition, $\overset{A}{a}$ decreases as the number of rooms increases defined as follow:

$$\overset{A}{a} = (0.3 + (0.7 - 0.14NR)) * \overset{M}{a} \tag{4.29}$$

where NR is the number of rooms in a Nanogrid, limited to 5. The value 0.14 is derived from taking the maximum variation of $0.7\overset{A}{a}$ divide by 5 (maximum rooms). Diversely, the peak magnitude for evening, $\overset{E}{a}$ is typically $1.4\overset{M}{a}$. Based on meta-data lifestyle relations, commonly, it can be seen that there are 3 peaks spread across the duration of 6 hours. The

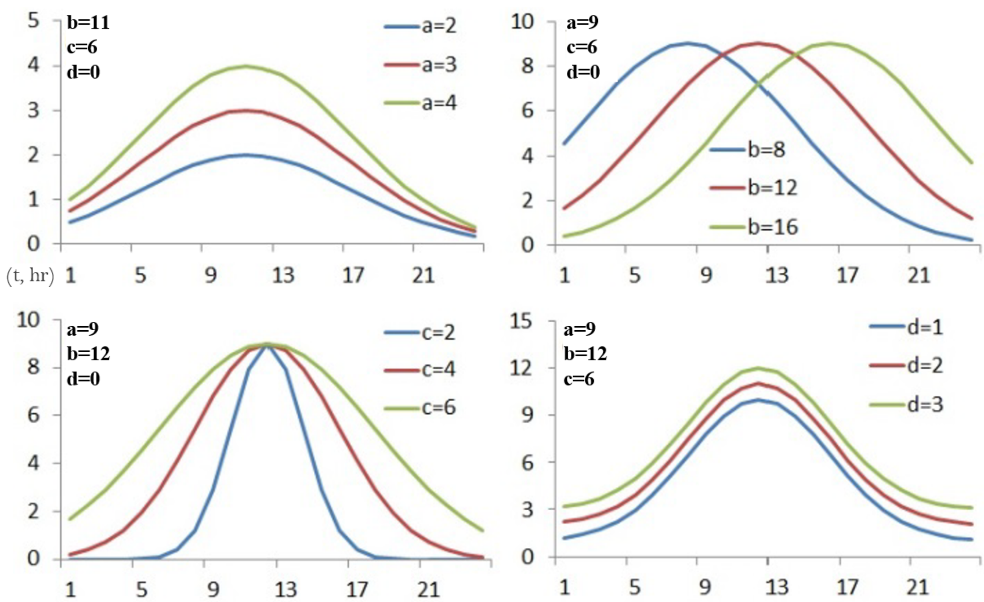

Fig. 4.15 The effects on Gaussian distribution curve from specifying parameters a, b, c, and d.

Table 4.1 Number of rooms in Nanogrid versus average morning peak demand magnitude.

No. of Room(s)	1	2	3	4	5
Average consumption rating (kW)	1	1.5	4.5	5.5	6.5

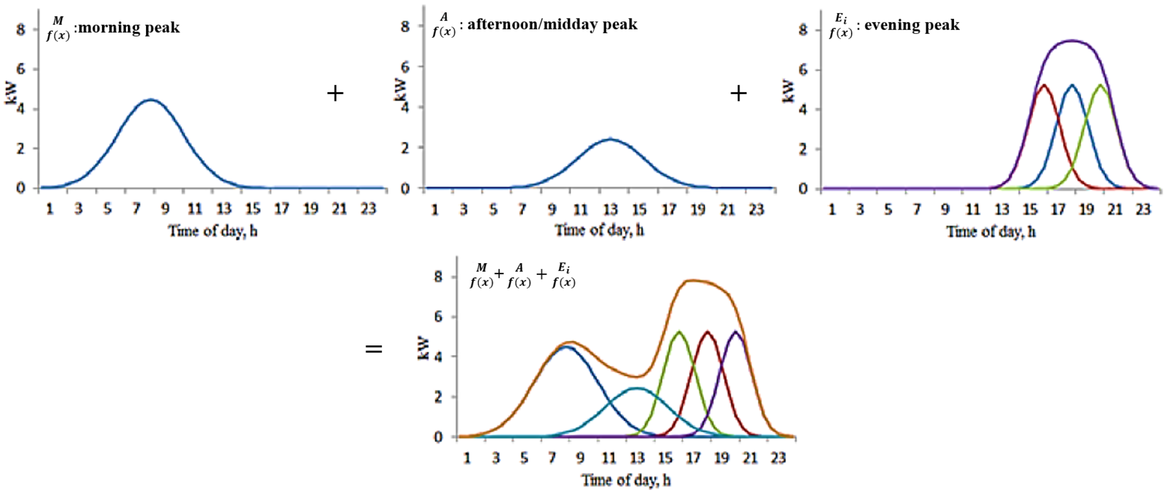

Fig. 4.16 Modelling of 24 hours demand load profile using Gaussian distribution based on known parameters.

relationships between peak magnitudes is dependant on number of occupant(s) at respective time instances.

$$\overset{E}{a}_i = \frac{\overset{E}{a}\sqrt{NO+NR}}{\sqrt{10}} \tag{4.30}$$

where NO denotes number of occupants and the total $NO+NR$ is limited to 10.

Subsequently, the positioning of peak magnitude parameter b along the time horizon describes the daily trends in consumption usage; $t1$—detecting the first activity in the morning, $t2$—last morning activity before occupant(s) vacates the vicinity, $t3$—resurface of first activity when occupant returns to vicinity (evening), and $t4$—signifies occupants goes to bed. Using Gaussian distribution function as the model, parameter b can be estimated by taking the center of time period, $t1$ to $t4$:

$$\begin{aligned}
\overset{M}{b} &= \frac{t1+t2}{2} \\
\overset{A}{b} &= \frac{t3+t4}{2} \\
\overset{E}{b}_1 &= \frac{t3+t4}{2} \\
\overset{E}{b}_2 &= \overset{E}{b}_1 - 2 \\
\overset{E}{b}_3 &= \overset{E}{b}_1 + 2
\end{aligned} \tag{4.31}$$

Lastly, the width factor parameter c correlates to the number of occupants (NO) and rooms (NR). The value c is limited within 2 to 8 to achieve smooth bell shaped Gaussian function curve. The width factor parameter for $\overset{M}{c}$ and $\overset{A}{c}$ are similar however, $\overset{E}{c}$ is reduced by half to maintain decrease/increase rate of evening average peak as shown in Fig. 4.16. (4.32) expresses the performance of c in relations to consumption attributes and Gaussian function.

$$\begin{aligned} \overset{M}{c} = \overset{A}{c} &= \frac{12}{\sqrt{NO+NP}} \\ \overset{E}{c_i} &= \frac{\overset{M}{c}}{2} \end{aligned} \tag{4.32}$$

Demand Load Characterisations

Based on the estimated demand load profile using Gaussian distribution function, the load is further characterised into 4 classification elements described in (4.33)−(4.34); *(i)* $FX-$load denotes appliances that are critical (*e.g.* refrigerator, devices for pet living) and needed to be online throughout the day/year. Due to its fixed consumption profile, it serves as a baseline load capacity for individual Nanogrid. *(ii)* $SHFT-$refers to shiftable loads (*e.g.* washing machine, dryer, dish washer). They have the greatest influence in achieving reduced electricity billing due to flexible ordering of utilisation sequences where operation scheduling can be specified, *(iii)* $INST-$short for instantaneous refers to online loads that are interactive and have minimal scheduling flexibility based on the restrictions/comfortability factor induced on Prosumer's lifestyle (*e.g.* entertainment devices/consoles, lighting, electric stove), and lastly *(iv)* $THRT-$are appliances whose energy consumption capacity can be controlled (*e.g.* PHEV charging rate, water heater, air condition). If given in a hierarchy level of load critical intensity, FX appliances will be ranked first, followed by $INST$, then $SHFT$ and last will be $THRT$.

$$LD = \{FX_u; u \in U, SHFT_v; v \in V, INST_w; w \in W, THRT_x; x \in X\} \tag{4.33}$$

$$LD(t, day) = \sum_{u\in U, v\in V, w\in W, x\in X} (FX_u + SHFT_v + INST_w + THRT_x)(t) \tag{4.34}$$

Suggested in [233], the demand loads in typical households can be classified using combinations of supervised and unsupervised learning techniques; K-means clustering and K-Nearest Neighbours (KNN) classification respectively. These learning models are trained to identify appliances' feature into different classes and determining its operations in steady

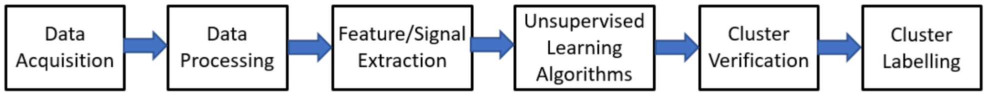

Fig. 4.17 Initialisation and classification processes of demand load appliances.

state. Assisted by current transducer installed at all appliances' live lines, it abstracts the current waveform signatures and compared against other without having signals being overlapped. In this sense, the appliances' current rating are recorded individually into the database and rendered into a single current versus time framework. Indeed, some may argue that utilising the current waveform extracted from Nanogrid's smart meter will be more cost effective. However, decomposing a single waveform signature into multiple features based on number of online appliances at a specified time frame will be complicated/impossible and also provide no significances when performing clustering avenues. The flowchart shown in Fig. 4.17 proposes the initialising sequence to establish a database for identification processes where deployment of hybridise KNN and K-means algorithms profiles the demand load current waveforms.

Employing the proposed algorithm as suggested in [233], it aims to cluster those low-voltage online appliances within the time frame t into respective FX, $INST$, $SHFT$, and $THRT$ classifications. KNN provides identification and labelling of unknown signal elements in a cluster that has common correlations from its nearest neighbour while K-means computes the cluster's centroid determining the system is in steady state. From the labelled clusters, it then grouped into respective load classification specified in Table 4.2 and compute the total load consumption capacity. It is important that the extracted current data points are not normalise reduce metric duplications and enhance segmentation performance.

Load Consumption Minimisation Curve Theorem

The criteria involves strategic scheduling of PSPG and demand load connections (targeting shift- and throttle-able loads) through load balancing theorem that bridges total load consumptions close to the objective curve. It aims to maximise PSPG utilisation that offers economic benefits by reducing downstream energy exchange at PCC when tariff is high or provide ancillary services during global peak demand loading at the next time stamp. Hence, the goal is to minimise online load capacity curve against desired at time t defined in (4.35)−(4.36) and offers scheduling prepositions (*i.e.* reschedule or shed) based on generation availability and electricity tariff (clearing price).

Table 4.2 Assignment of load classification based on KNN Cluster and K-means centroid.

KNN Cluster Label	Centroid Value (mean×var×avar)	Load Classification
Fridge	0.982×0.0289×0.0032	
Freezer	0.913×0.0209×0.0011	
Water DISP.	0.947×0.0098×0.0065	
TELECOM & Digital Network	0.033×0.0127×0.0024	*FX*
Security % Router Devices	0.099×0.0191×0.0038	
Water Pump & Living AUTOM.	2.344×0.0522×0.0137	
Washing Mach.	3.478×0.0822×0.0345	
Dish Washer	6.521×0.0594×0.0284	*SHFT*
Dryer	13.043×0.0403×0.0211	
Charging Device Port	0.867×0.0377×0.0056	
Lighting	0.217×0.0321×0.0156	
Entertainment consoles	0.867×0.0455×0.0092	*INST*
Kitchen appliances	0.146×0.0236×0.0149	
Smart LED TV	1.462×0.0317×0.0083	
Air-condition	7.234×0.0924×0.0726	
PHEV	5.112×0.0598×0.0501	*THRT*
Heating Unit	8.457×0.0818×0.0688	

$$\min \sum_{i=1}^{N} [P_{load_{i,t}}^{online} - P_{load_{i,t}}^{OBJ}]^2 \tag{4.35}$$

$$P_{load_t}^{online} = \left[P_{load_t}^{EST} + \left(P_{load_t}^{connect} - P_{load_t}^{disconnect}\right)\right] \tag{4.36}$$

where $P_{load_t}^{OBJ}$ and $P_{load_t}^{online}$ referred to the objective/desirable and actual/measured load consumption capacity at time t respectively. $P_{load_t}^{EST}$ is estimated consumption capacity at time t quantified using Gaussian distribution or any other forecasting technique. The *connect* and *disconnect* are loads that connected and disconnected during the load shifting intervals. Individually, *connect* and *disconnect* are separated into two operating definitions. In *connect*; *(i)* incremental of connected load appliances shifted into current time, t, from previous time intervals, $(t-i)$, and *(ii)* relations to the supposed loads that are scheduled to connect at time, t. (4.37) expresses the definition of *connect* loads in relation to time frame intervals:

$$P_{load_t}^{connect} = \sum_{i=1}^{t-1} \sum_{j=1}^{D} A_{j,i_t} P_{1,j} + \sum_{k=1}^{K-1} \sum_{i=1}^{t-1} \sum_{j=1}^{D} A_{j,i_{(t-1)}} P_{(1+k),j} \tag{4.37}$$

where A_{j,i_t} denotes the number of appliances type j shifted from time i to t. $P_{1,j}$ and $P_{(1+k),j}$ are the power consumption ratings at time stamp 1 and $(1+k)$ respectively for reciprocal appliance type j. K is the total consumption span for appliance type j.

Likewise, for *disconnect* loads as expressed in (4.37) defines; *(i)* the decremented load capacity at time, t, due for delayed scheduling connection event of appliances that were supposed to initiate connection at time stamp t, and *(ii)* load decrement at time t due to postponement in connection times of appliances that were supposed to start their consumption at time, $(t-i)$.

$$P_{load_t}^{disconnect} = \sum_{i=(t+1)}^{t+del} \sum_{j=1}^{D} A_{j_t,i} P_{1,j} + \sum_{k=1}^{K-1} \sum_{i=(t+1)}^{t+del} \sum_{j=1}^{D} A_{j_{(t-1)},i} P_{(1+k),j} \tag{4.38}$$

where $A_{j_t,i}$ refers to the number of appliances of type j delayed for connection from time stamp t to i and del implies maximum allowable time delay (*i.e.* 30mins).

The minimisation statement is subjected to two constraints in relations to the number of shifted appliances at time t. First constraint dictates that number of shifted appliances cannot be a negative value and must select at least one load type; $A_{j,i_t} > 0$; $\forall i, K, j)$. Second, the number of appliances from a time stamp cannot be more than the number of shiftable appliances at that time stamp;$\sum_{t=1}^{N} A_{j,i_t} \leq SHFT_i$.

Maximum Demand Loading

The term maximum demand (MD) refers to the contracted power consumption level at respective Nanogrid. Prosumers are to monitor their real-time consumption level as not to exceed the MD limit as penalties will be incurred into the electricity bill. MD value is the average instantaneous power consumption rating in W or VA during a predefined time interval, typically rated at 15mins. Through realisation of maximum MD limit and minimise demand factor, DF, they both can aid in scheduling shaving load sequence during peak demand loading. There are two approach in determining MD index; *(i)* Fixed window$-$computations are performed 4 times in an hour for intervals of every 15mins, or *(ii)* Sliding window$-$compute MD based on 15minutes and wait for a minute before recomputing the next MD interval. It will record 1 MD value from the last 15mins period.

The $P_{load_{t=15mins}}^{connect}$ will be compared against MD to ensure its consumption capacity is within the specified limit. In this sense, demand consumption assignment of each categorised appliance will be specified with Prosumer-defined diversity factor percentage, $DivF$, before computing the total MD. Meanwhile assignment of $DivF$ can be based on importance/impact against Prosumer's electricity usage lifestyle.

$$P^{MD}_{load_d}(t) = P^{non\text{-}CL}_{load_d}(t) * DivF_d(t) \ \ \forall d = \{appliance\} \tag{4.39}$$

$$\max P^{total}_{MD}(t) = \sum_{d=1}^{D} P^{MD}_{load_d}(t) \ \forall d = non\text{-}critical + \sum_{c=1}^{C} P^{CL}_{load}(t) \ \forall c = critical \tag{4.40}$$

$$\min DF(t) = \frac{MD}{P^{online}_{load}}(t) \tag{4.41}$$

where *CL* and *non-CL* are critical and non-critical load.

Forecasting of Local Generation (PSPG)

It is inevitable that having PSPG integrated into the EPS, uncertainty element of power generation can bring forth indeterministic exertions on scheduling downstream energy exchanged at Nanogrid PCC. Hence, supervised forecasting technique has become key in probabilistic quantifications of available local generations that can support energy demand at local or global level. It also aids in enhancing modelling of local energy management with better constraint jurisdictions in ordering ESS operations and scheduling for day-ahead administrations.

Here, it employs Extreme Learning Machine (ELM) algorithm [234, 235] and data mining processes (analytical information) to train neural network learning behaviour with regularised ensemble regression to achieve better universal approximation capabilities. The extracted data from the power generation devices provide analytical information that serves as some prognostic initiations on neural network learning. These forecasted PSPG generation data will strategically influence decisional making processes on adjusting non-critical load capacities and ESS usages to procure benefiting impacts on Prosumers and DSO-TSO.

The ELM architecture is separated into 3 layers; input, hidden, and output. These layers create a sequential sequence connected by weighted lines, bridging each layer's node to another as seen in Fig. 4.18a. Subsequently, it uses an ensemble approach which combines multiple ELMs as illustrated in Fig. 4.18b to enhance probabilistic consistency when compared to a single structured ELM performance. The input layer takes in samples of historical data, generation capacity and other relevant data that can influential the learning behaviour to achieve better forecast regression. The provided data can be structured in a multi-dimension matrix formation, taking more than a single variable (*i.e.* power, weather, month). The hidden layer, interlinking the input to output layer, transforms data into implicit

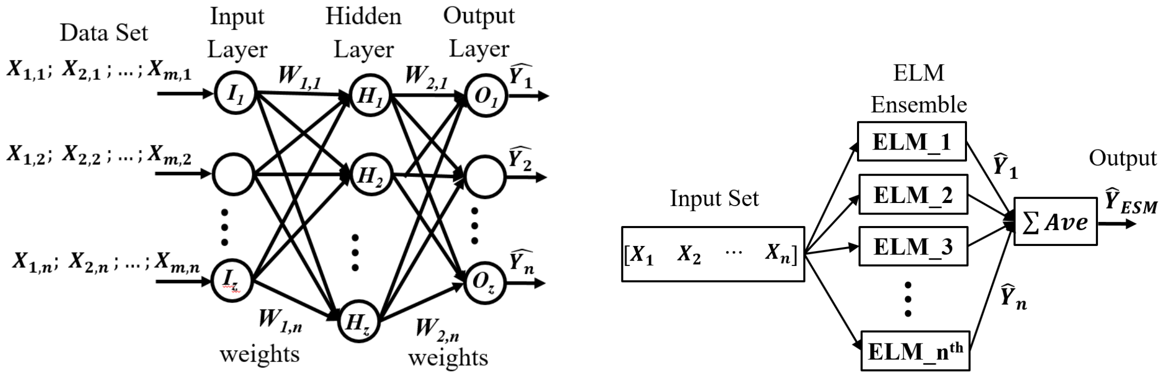

(a) Neural network. (b) Ensembled.

Fig. 4.18 Proposed ELM architecture.

knowledge where linguistic features are refined into correlation representations between input and output's objectives. All nodes in the hidden and output layers employ non-linear activation function to introduce non-linearity during the learning processes. The output layer produces the estimated/forecasted solution best structured in a single dimension matrix to avoid divergence.

In view of the weighted lines, they represent the correlation strength between nodes. For an instant, if weight connecting from node 1 of input layer to node 2 of hidden layer has larger magnitude than other weights which means node 1 has greater influence over node 2. These weights carry magnitude values that represent best fit estimation of its learning behaviour. Significantly, ELM performs a single iteration estimations adjusting only the weights connecting to the output layer. Thus, it reduces computational time as compared to other machine learning algorithm that requires iterative procedure when training the weights (*e.g.* gradient-descent based training schemes). Additionally, regularised factor, I/δ, and ensemble formation are incorporated to resolve performance inconsistency when dealt with different input or hidden layer sizes. (4.42) to (4.45) define derivations of ELM:

$$\begin{aligned} H[n,z] &= X\left[n_{sample}, m_{var}\right] * W_1[m, z_{hidden}] \\ z &= ((m+1)/2) + \sqrt{n} \end{aligned} \tag{4.42}$$

$$\begin{aligned} Y[n,1] &= g(H) * W_2[z,1] \\ g(H) &= 1/(1+e^{-H_{i,j}}) \\ W_2 &= H^{\dagger} * Y \end{aligned} \tag{4.43}$$

$$
\begin{aligned}
H^{\dagger} &= (H^T * H + (I/\delta))^{-1} * H^T \\
\min \hat{Y} - Y &= (H_{out} * W_2) - Y
\end{aligned}
\tag{4.44}
$$

$s.t.$

$$
\hat{Y} = \begin{cases} 0, & \hat{Y} < 0 \\ Y_{max}, & Ymax \leq \hat{Y} \\ \hat{Y}, & otherwise \end{cases}
\tag{4.45}
$$

where $W_{1,n}$ and initial $W_{2,n}$ matrices are a randomly assigned integer $(0 < x < 1)$. $g(.)$ employs a sigmoid-based activation function. X and Y are input and output matrices that have equal number of rows. H refers to the nodes in hidden layer matrix structured $[n \times z]$. I in regularised factor represents an identity matrix while δ is a real number proportionate to z (ideal). Y and $\hat{Y}$ denotes the actual and estimated output values. The goal is to achieve minimised $\hat{Y} - Y$ before stopping the learning process.

Subsequently, ensemble technique is employed by using multiple ELM architecture on the same input data and concatenate their output to find the average $\hat{Y}$. It aims to minimise root mean square deviation errors, $RMSD$, and enhance accuracy resolution against actual output, Y. Virtually, in ensuring forecasted results are not overfitted and data are not misinterpreted due to "noise" during the learning process, k-fold cross validation is employed. It increases predictive accuracy by minimising the training and testing sets errors against unseen data. Suggested in [236], it highlights the advantage in using k-fold approach as it splits predictive model into size of training and testing sets, and shuffles the data subset selections to gain interpretation accuracy.

$$
\hat{Y}_{ESM} = \frac{\sum_{i=1}^{N} \hat{Y}_i}{N}
\tag{4.46}
$$

$$
RMSD = \sqrt{\frac{\sum_{i=1}^{N} (\hat{Y}_i - Y_i)^2}{N}}
\tag{4.47}
$$

$$
E_k(\lambda) = \sum_{i \in k^{th}\ fold} (Y_i - \hat{Y}_i^{-k}(\lambda))^2
\tag{4.48}
$$

$$
CV(\lambda) = \frac{1}{K} \sum_{k=1}^{K} E_k(\lambda)
\tag{4.49}
$$

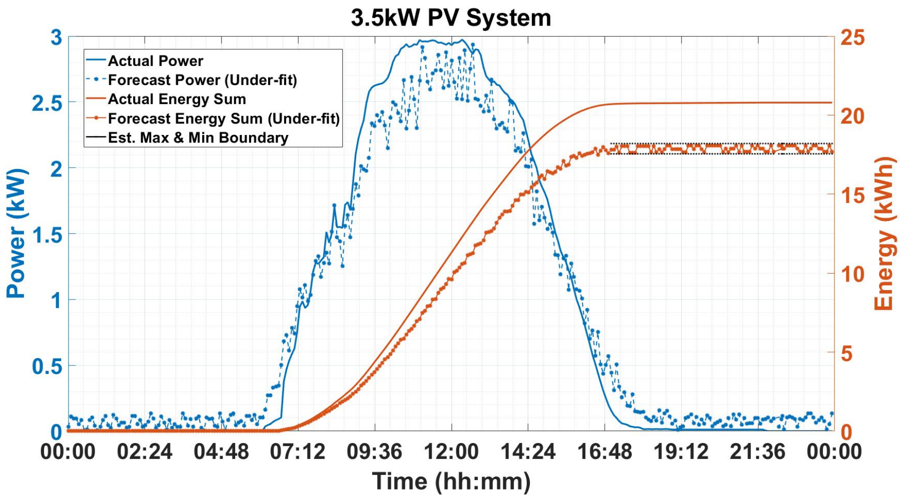

Fig. 4.19 Forecasting of 3.5kW PV system against actual data using ELM approach.

where estimated tuning parameter is λ, E_k consolidates the error between actual and estimated at respective folds which typically set to k=5 or 10. $CV(\lambda)$ depicts the cross validation error during iterative process when changing λ. Fig. 4.19 presents employment of ELM algorithm in forecasting 3.5kW PV system on a sunny day.

Ordering of Demand Capacity against Unit Commitment

Indeed, in the global aspect of the demand load consumption curve, DSO is responsible in satisfying EPS's equality constraint in real-time by scheduling thermal generation unit (TGU) loadings ahead of time. However, Prosumers can cooperatively manage ordering of energy downstream by limiting the rate of power capacity change within a specified time span. There are two methods for Prosumers to adhere/support the ramp-up (UR) and down-ramp (DR) constraints limited by the upstream TGUs; *(i)* compute the total maximum allowable generation from TGUs at time t (typical hourly rating) and equally portion out to Prosumers in the Community based on the contracted MD or superior bidding price defined in (4.56)−(4.59), or *(ii)* calculate the power mismatch at local level in each time interval and adjust respective TGUs loading capacity proportion to their maximum generation capacities expressed in (4.60)−(4.62). Meanwhile, TGU's loading and de-loading generation operations, it is constrained by ramp rate limits which restricts generation capacity given in a specified time interval. It also influence in shaping a smooth global demand curve profile that complies to baseline loading and avoids "Duck Curve" crises induced by local installation of PSPG-ESSs. Hence, comprehending TGU's ramp rate limits, Prosumers can better schedule respective demand load capacities in parallel with the UR and DR rates (assuming constant rate of change).

$$\Delta P_{TGU,i}^{INEQ}(t) = P_{load}^{demand}(t) - \left(\sum_{i=1}^{I} P_{TGU,i}(t) + \sum_{j=1}^{J} P_{ESS,j}^{MAX}(t) + \sum_{k=1}^{K} P_{RES,k}^{MAX}(t) \right) \tag{4.50}$$

$$\begin{cases} UR, & \Delta P_{TGU,i}^{INEQ}(t) > 0 \\ DR, & \Delta P_{TGU,i}^{INEQ}(t) < 0 \\ 0, & otherwise \end{cases} \tag{4.51}$$

The UR constraint dictates:

$$\begin{gathered} \Delta P_{TGU,i}^{ADJ}(t) = P_{TGU,i}^{SCHD}(t) - P_{TU,i}(t-1) \leq UR_i \ \forall generating\ units \\ \min\left[P_{TGU,i}(t-1) + UR_i; P_{TGU,i}(t-1) + \Delta P_{TGU,i}^{ADJ}(t) \right] \end{gathered} \tag{4.52}$$

$$\Delta P_{TGU,i}^{INEQ}(t) = \sum_{i=1}^{I} \Delta P_{TGU,i}^{ADJ}(t) \tag{4.53}$$

where $UR_i(t)$ is the ramp-up rate defined by individual thermal generating unit, i. $\Delta P_{TGU,i}^{INEQ}(t)$ refers to the global power mismatch between supply and demand which requires upstream TGUs to compensate.$\Delta P_{TGU,i}^{ADJ}(t)$ equates to the ordered power compensation rating for each TGU and $P_{TGU,i}^{SCHD}(t)$ is the scheduled power rating for each TGU at time, t. Likewise, derivations of DR limits the ramping down of respective TGU before it suffers losses due to excess generation against lower demand load capacity:

$$\begin{gathered} \Delta P_{TGU,i}^{ADJ}(t) = P_{TGU,i}^{SCHD}(t) - P_{TU,i}(t-1) \geq DR_i \ \forall generating\ units \\ \max\left[P_{TGU,i}(t-1) + DR_i; P_{TGU,i}(t-1) + \Delta P_{TGU,i}^{ADJ}(t) \right] \end{gathered} \tag{4.54}$$

$$\Delta P_{TGU,i}^{INEQ}(t) = \sum_{i=1}^{I} \Delta P_{TGU,i}^{ADJ}(t) \tag{4.55}$$

The following equations defines the proposed DR and UR limit mitigations at individual Prosumers:

$$P_{TGU,total}^{MAX}(t) = \sum_{i=1}^{I} \left(P_{TGU,i}(t-1) + UR_i\right); \text{ demand increase}$$
$$\text{or} \tag{4.56}$$
$$P_{TGU,total}^{MAX}(t) = \sum_{i=1}^{I} \left(P_{TGU,i}(t-1) + DR_i\right); \text{ demand decrease}$$

$$P_{tol}(t) = P_{TGU,total}^{MAX}(t) - P_{load,global}^{demand}(t-1) \tag{4.57}$$

$$\begin{aligned} \Delta P_{assgn}^{NG_i}(t) &= \frac{P_{tol}(t) * RR_1^{Class_1}}{No._{\text{Class1}}^{Prosumer}} \\ \Delta P_{assgn}^{NG_i}(t) &= \frac{P_{tol}(t) * RR_2^{Class_2}}{No._{\text{Class2}}^{Prosumer}} \\ &\;\;. \\ &\;\;. \\ \Delta P_{assgn}^{NG_i}(t) &= \frac{P_{tol}(t) * RR_N^{Class_N}}{No._{\text{ClassN}}^{Prosumer}} \end{aligned} \tag{4.58}$$

$s.t.$

$$RR_1^{Class_1} + RR_2^{Class_2} + ... + RR_N^{Class_N} = 1 \tag{4.59}$$

where $P_{tol}(t)$ is the threshold/tolerance of available power capacity at time t based on the maximum allowable ramp rate limit of all TGUs against the scheduled demand capacity from $(t-1)$ to t. $\Delta P_{assgn}^{Class_i}(t)$ denotes the available power capacity limit when Prosumer's consumption deviates from time $(t-1)$ to t at individual NGs. The intuition for $RR_i^{Class_i}$ are predefined by DSO on how the distribution of total available $P_{tol}(t)$ should be assigned to individual Prosumers. Either the assignment can be based on a priority hierarchical structure based on bidding price, Prosumer type and contribution, or equally portioned based on building size and its energy consumption trends.

Alternatively, the second approach proposes adjustment of power loading at each TGU proportional to its maximum generation at time t in relation to unit commitment strategy suggested in [237]. The decoupled supply from TGUs and demand load consumption of unit commitment sub-problems for individual Nanogrid are defined as:

$$SU(\lambda^t) = \max_{P_{i,t-1}^{TGU}+DR \leq P_{i,t}^{TGU} \leq P_{i,t-1}^{TGU}+UR} \sum_{t=1}^{T} \left[\lambda_t P_{i,t}^{TGU} u_{i,t}^{TGU} - C(P_{i,t}^{TGU}, u_{i,t}^{TGU}) - S(P_{i,t}^{TGU}) u_{i,t-1}^{TGU}\right] \tag{4.60}$$

where λ_t reflects marginal cost or clearing price of the electricity produced at time t compute by using Lagrangian function. $u_{i,t}^{TGU}$ indicates the unit commitment state of unit at time t, 0-OFF or 1-ON. $C(P_{i,t}^{TGU}, u_{i,t}^{TGU})$ expresses the generation cost of each TGU given at that specific power capacity. The TGU start-up cost of unit i is represented as $S(P_{i,t}^{TGU})$ derived in [237].

$$DU(\lambda^t) = \max_{P_{j,t}^{demand,min} \leq P_{j,t}^{demand} \leq P_{j,t}^{demand,max}} \sum_{t=1}^{T} \left[U(\alpha_{j,t}^{demand}, P_{j,t}^{demand}) - \lambda_t P_{j,t}^{demand}\right] \tag{4.61}$$

where $U(\alpha, P_j^{demand})$ denotes the Prosumer's utility function. Using $SU(\lambda^t)$ and $DU(\lambda^t)$, assignment of power adjustment for respective TGU against individual Nanogrid is as follows:

$$\Delta P_{assgn}^{NG_i}(t) = \frac{P_{TGU,i}^{MAX}(t) - P_{TGU,i}^{SCHD}(t)}{SU(\lambda^t) - DU(\lambda^t)} * \sum \left(P_{TGU,i}^{SCHD}(t) - P_{TGU,i}^{MEAS}(t)\right) \tag{4.62}$$

where $-P_{TGU,i}^{MEAS}(t)$ is the actual recorded generation capacity of TGU in real-time, satisfying the equality constraint of EPS.

Utilisation of Local Energy Storage System

It is inevitable that there will be instances where the global equality constraint between supply and demand fails to reach equilibrium state. Thus, power generation dependency on Retailers having to initiate TGUs in spinning reserve mode and overfitted management procured by DSO still serves as a viable resolution when dealing with TE-based demand curve profile. In this sense, involvements of ESS at local domain can provide instantaneous support, non-spinning reserve, on compensating any imbalance operation in EPS. However, utilisation of ESS requires strategical control measures where Prosumers can regain maximum leverage on return investments. Substantial reserve power pooling, incentive programme with highest cost value, and influential on market clearing prices are some avenues that ESS can provide during DSR operations. Prosumers need to realise that constant maximisation of ESS may not necessarily be an optimum TE solution.

$$P_{NG,i}^{ESS}(t) = P_{NG,i}^{PCC}(t) - P_{NG,i}^{demand}(t) + P_{NG,i}^{PSPG}(t) \tag{4.63}$$

$$ESS = \begin{cases} \text{charging}, & P_{NG}^{ESS} > 0 \\ \text{discharging}, & P_{NG}^{ESS} < 0 \\ \text{idle}, & P_{NG}^{ESS} > P_{MAX}^{ESS} \\ \text{idle}, & P_{NG}^{ESS} < P_{MIN}^{ESS} \end{cases} \tag{4.64}$$

$$PCC = \begin{cases} \text{downstream}, & P_{NG}^{PCC} > 0 \\ \text{upstream}, & P_{NG}^{PCC} < 0 \\ \text{islanded}, & P_{NG}^{PCC} = 0 \end{cases} \tag{4.65}$$

Conventionally, ordering of ESS's charging and discharging operations is regulated by the percentage of State-of-Charge (SOC) level. In addition, it uses to demarcate ESS's threshold regions; SOC$_m in\%$ denotes the $P_{ESS}^{reserve}$ or spinning reserve and SOC$_m ax\%$ refers to the maximum allowable charge, P_{ESS}^{max}. The SOC% levels at time t is defined as follows:

$$SOC\%(t) = SOC\%(t-1) + (\int_0^t \frac{1}{C_{batt}} dt) \tag{4.66}$$

$$C(t) = C(t-1) + [\Delta t * \frac{\eta_{batt}^{DP}}{V_{batt}(t)} * (P_{NG}^{PSPG}(t) - P_{NG}^{ESS}(t))] \tag{4.67}$$

$s.t.$

$$\begin{aligned} C(t)|_{t=0}&;\ \text{inital charge} \\ C(t)|_{t=N}&;\ \text{final charge} \\ C_{min} \leq C(t) &\leq C_{max} \end{aligned} \tag{4.68}$$

where $C(t)$ represent the battery's charge at time t. η_{batt}^{DP} denotes the efficiency of battery charging and discharging time with depreciation factor over time. V_{batt} measures the voltage level at battery terminal and C_{batt} is the electric charge passing through battery express in ampere an hour.

In gaining optimum utilisation of ESS, charging and discharging operations are synchronised with real-time electricity tariff or clearing prices. It serves as another pivotal mean for Prosumers to reschedule load consumption capacities in time, t, and PSPG to settle maximum profit margin.

$$\max Profit(t) = [Revenue - Expenses](t) \tag{4.69}$$

$$Profit(t) = \left(ET * \sum_{i=1}^{N} P_i^{TGU} + ET.P_{NG}^{PCC} \right)(t) - \left(ET.P_{NG}^{PCC} + \sum_{i=1}^{N} bid(P_i^{TGU}) \right)(t) \tag{4.70}$$

where ET reflects the wholesale electricity price and $bid(P_i^{TGU})$ is the bidding price in PMP for respective TGU i at time t. However, utilisation of PSPG requires further exploration into its credibility towards REM and PMP operations, and Prosumers' expectations on clearing market prices when contributing upstream generation. In this sense, DSOs have to rethink new incentive policy models that will value Prosumers' contributions toward DSR engagements.

In the efforts on invigorating TE developments, Feed-in tariff (FiT) policy was proposed to offer cost-based compensation for $PT\text{-}I$s as energy producers through stable long-term agreements/contracts (15-25 years period) with DSO. The contract is bounded with fixed bidding price that helps finance PSPG investments with certainty while adding more incentive programmes to fund FiT schemes [238]. Hence, to stimulate Prosumers' return investments, (4.71)–(4.74) maximises FiT policy revenue streams by predominating the wholesale electricity tariff [239].

$$\text{LCOE} = \frac{\sum_{n=0}^{N} C_n * (\frac{1+i}{1+d})^n}{\sum_{n=0}^{N} Q_n * (1-D)^n} \tag{4.71}$$

$$\begin{aligned} \max \sum_t [(P_i^{PSPG} * \rho_{LCOE}) + (P_{PCC}^{upstream} * \rho_{FiT}) - (P_{PCC}^{downstream} * \rho_{wholesale}) \\ -(P_{ESS}^{charge} * \rho_{wholesale}) + (P_{ESS}^{discharge} * \rho_{FiT})](\Delta t) \end{aligned} \tag{4.72}$$

subjected to:

$$0 \leq P_{PCC}^{upstream}(t) \leq P_{PSPG\text{-}ESS}^{excess}(t) \tag{4.73}$$

$$P_{PSPG\text{-}ESS}^{excess}(t) = \begin{cases} \left(P_{PSPG\text{-}ESS} - P_{load}^{online}\right)(t), & P_{PSPG\text{-}ESS}(t) > P_{load}^{online}(t) \\ 0, & otherwise \end{cases} \tag{4.74}$$

where the investment costs comprises from installations and deployment to maintenance fees of PSPG denote as C_n. The energy produced by PSPG, Q_n, in kilo-Watt hour which includes efficiency degradation factor, D, in percentage per annum after a year of installation. N reflects PSPG expected lifespan expressed in years while i and d refers to the inflation and discount rates offered annually. In (4.72), the profit margin is maximised by incorporating PSPG into the energy mix during Nanogrid operations. ρ_{LCOE} specify the real-time operating costs of PSPG based on levelised cost of electricity (LCOE). ρ_{FiT} is the promised electricity price offered by FiT policy and $\rho_{wholesale}$ is the wholesale electricity prices uniform across all Prosumers. P_{PSPG}^{excess} corresponds to the upstream power exchange at PCC, absorbed by the grid. P_{ESS}^{charge} and $P_{ESS}^{discharge}$ refer to the ordered power rating to charges and discharge ESS respectively. The charging and discharging operations is not restricted to $P_{PSPG}^{excess} > 0$ or $P_{NG}^{PSPG} > P_{load}^{demand}$.

In view of searching for an economically solution to harness maximum return on investments and performance index, economic assessment in contrast to the market operations is appraised. (4.75)−(4.78) further enhanced LCOE index by exploiting PSPG and ESS.

$$LCOE_{(PSPG+ESS)} = \frac{CE_{(PSPG+ESS)}}{E_{(PSPG+ESS)}} \tag{4.75}$$

$$CE_{(PSPG+ESS)} = LCOE_i * E_i;\ i = \{PSPG, ESS\} \tag{4.76}$$

sub (4.76) into (4.75)

$$LCOE_{(PSPG+ESS)} = \sum_{i=1}^{2} LCOE_i * \alpha_i \tag{4.77}$$

$$\begin{aligned} \alpha_i &= \frac{\beta_i * P_i}{\beta_{(PSPG+ESS)} * P_{(PSPG+ESS)}} \\ \beta_i &= [\frac{E_{ESS,in}}{E_{ESS,rated}} * \frac{\eta_i}{1+\eta_i}] \leq 50\%\ typically \end{aligned} \tag{4.78}$$

where $LCOE_{(PSPG+ESS)}$ equates the worth of electricity produced both PSPG and ESS in dollars and CE refers to the energy costs. Both E and α_i are energy generated by PSPG while β_i is the capacity factor of available energy storage in parallel to the charging and discharging rates. η_i reflects the efficiency of both PSPG and ESS.

In the case where high excess power generation from PSPG could be stored in ESS after compensating the load consumption capacity, Prosumers are resorted to selling surplus power at bidding price. Due to poor utilisation of ESS during high penetrations of PSPG, DSOs are forced to bring the electricity tariff price down as to avoid demand curve hitting below the baseline. Thus, (4.79)−(4.82) monitors large excess upstream generation during low demand loading.

$$E_{PSPG}^{utilise}(t) = \left(E_{PSPG} - E_{PCC}^{upstream}\right)(t) \tag{4.79}$$

$$E_{ESS}^{charge}(t) = UI * E_{PSPG}^{utilise}(t);\ UI \leq 1.0 \tag{4.80}$$

$$E_{(PSPG+batt)}(t) = (1 - UI) * \left(E_{ESS}^{discharge}(t) + \left(E_{PSPG}^{utilise}(t) - E_{ESS}^{charge}(t)\right)\right) \tag{4.81}$$

$$payoff = \begin{cases} 0.0, & E_{PSPG}^{upstream}(t) > E_{PSPG}^{upstream}(t-1) \\ 1.0, & otherwise \end{cases} \tag{4.82}$$

UI is the scalar factor for charging ESS based on available PSPG generation.

4.4.3 Characterisation of Agents in Nanogrid Area Network

Apart from the proposed flexi-edge computing infrastructure using Microsoft Azure IoT cloud described in Fig. 3.3 and 3.10, and multi-Agent control framework in proposed multi-layered DCF shown in Fig. 3.7 and 3.8 of Chapter 3.2, addition Agents are deployed focusing in NAN environment (Fig. 2.7a). It aims to tag Agents with respective communication devices and appliances in Nanogrid, and computation modules in Azure IoT Edge Device for aggregator. Deployment of these Agents will be labelled based on their roles and operational obligation domains in synchronise with aggregator's primary control functionalities. It aims to gain real-time authority and micro-manage individual appliances/devices in NAN using Agents of MAS provided by Azure IoT Edge Device as shown in Fig. 4.20.

Critical Load (CL) & non-Critical Load (non-CL) Agents

Both CL and non-CL Agents represents identity for all load entities. They are constantly communicating with PCCM and PCM Agents in governing online load consumption demographics by ordering scheduling routines at respective time intervals (*i.e.* shifting, shedding, throttling). The CL Agent comprises of FX and $INST$ classified loads while non-CL Agents assigned to $SHFT$ and $THRT$. Both CL and non-CL Agents are responsible in logging their

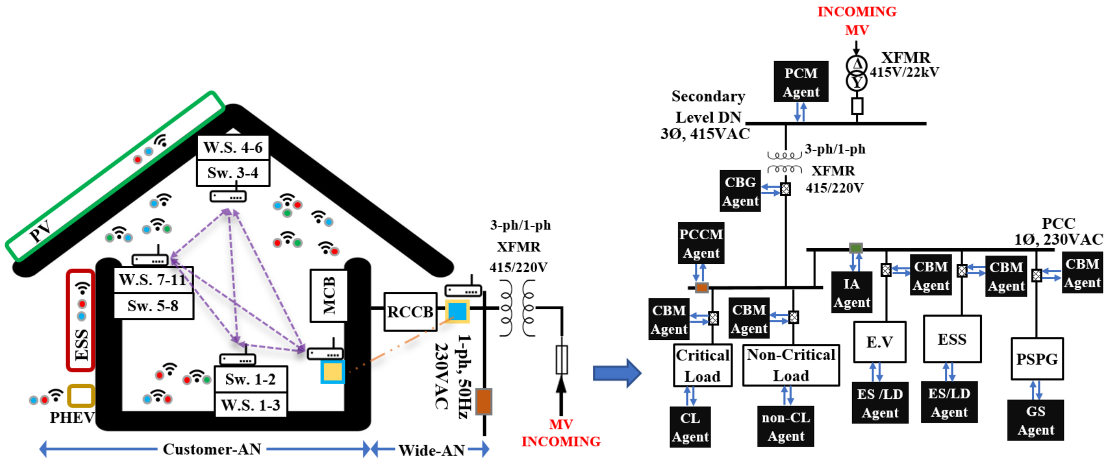

Fig. 4.20 Addition deployment of Agents in NAN for respective grid-tied appliances/devices.

load coupling status and consumption capacities. These data provide viable information when modelling local demand curve using Gaussian distribution function and classify them into respective classes using KNN and K-means clustering technique.

Point of Common Coupling Monitor (PCCM) Agent

PCCM Agent deals with comprehending Prosumer's energy management interests. It represents a single Nanogrid identifier within the Prosumer Community, governed by aggregators to schedule BTM DERs and controllable loads to gain maximum profit and local energy interests. It officiates all power transactions exchanged at PCC and monitor Nanogrid's operational reliability and stability that could affect DSR operations. PCCM Agent also programmed to interact with neighbouring NGs to initiate cooperative yet competitive management ruling in the PMP and DSR.

Circuit Breaker Grid (CBG) and Monitor (CBM) Agents

CBG and CBM Agents serve as the primary protection aggregator that aids in isolating abnormality events that transpired locally. The engagement of CBG Agent administers island mode operations, primarily executed when fault crises propagated downstream at PCC. While, CBM Agents coupled to individual grid-tied entities in Nanogrid, isolating devices/appliances (especially PSPG) if faulted episodes are transpired. Both Agents are responsible in curbing propagative faulted effects that could collapse the integrity of EPS or Nanogrid connectivity.

Power Condition Monitoring (PCM) Agent

Invigilate distribution network operations, securing operation reliability and regulating demand-supply equilibrium in Prosumer Community domain. PCM Agent functions as an aggregator that meditates demand-side operations between Prosumer and DSO in coordinating DER, DSR, and REM managements, focusing on modelling policies for efficient TE transactions. It schedules global load consumption curve ensuring "Duck Curve" crisis and unit commitment operations are in safe region. It also acquaint energy clearing price and officiate bidding in PMP by offering incentives and penalties to steer Prosumers towards fair-play bidding process and reliable EPS.

PSPG Agent

PSPG Agent represents identification for respective local integrated power generation resources (*i.e.* DC or AC-based technology). It monitors the frequency and voltage level of the devices, ensuring interoperability is achieved constantly. In the case of abnormality, instruction message will be transferred to CBM Agent to decouple the system.

Energy Storage/Load Device (ES/LD) Agent

ES/LD Agent represents a dual operating functions, typically ESS, that contributes either generation upstream or consume energy acting as a load ($THRT$). It monitors state-of-charge level and observes reserve power pooling capacity through strategic initiation of charging or discharging switching sequences.

Integrated Assets (IA) Agent

IA Agent is responsible in encapsulating operations of all integrated generation assets, PSPG. It governs power exchange management between PSPG and ESS by interacting closely with PCCM Agent. The computation required in IA Agent involves quantifying of generation availability generated by PSPG using forecasting technique and manage utilisation of ESS (charging or discharging rate) based on ahead scheduling and electricity tariffs at different time intervals.

4.4.4 Coordination and Functionality of Agents in NAN

Fig. 4.21a presents a systematised coordination of Agent's interactions in a collaborative network while, Table 4.3 describes the dataflow sequences of Agent's task protocols. The tasks involve Prosumer-centric directive commands shared across all online Agents to gain a cooperative commitments in directing Nanogrid's operations/managements. Utilising collaborative assignments, perceptive on Agent's ruling obligatory are made visible to neighbouring Agents in modelling cooperative solution through individual managerial avocations. In this sense, Agents are constantly broadcasting their individual findings to converge compounding resolutions before reaching to an agreement. Primitively, all contracted agreements concede prior settlements with PCCM Agent involving online CL Agent before advancing to other decision-making processes.

Subsequently, in view of forecasting PSPG generation and estimating load consumption curve, the Short-term Scheduler (STS) provides time span synchronism between all deployed Agents based on two-level scheduling approach; day-ahead and real-time scheduler as

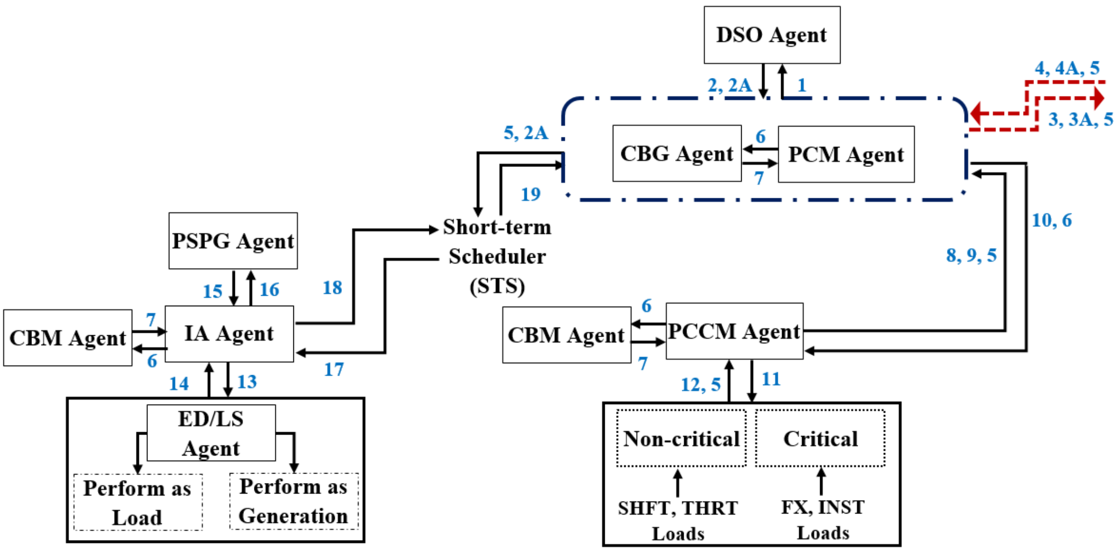

(a) Collaborative network: Agents of MAS in NAN.

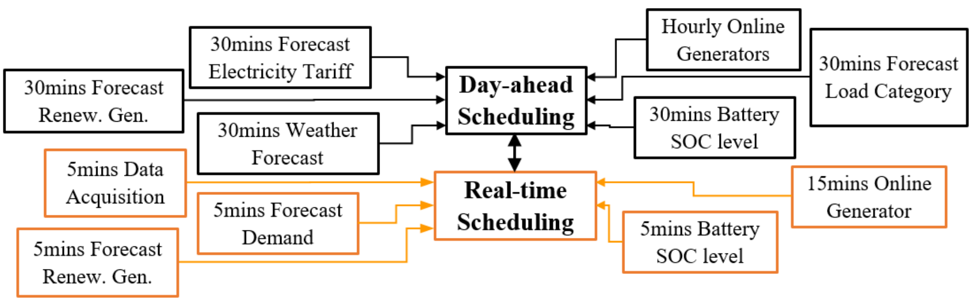

(b) Time-based allotment for respective Agents in NAN: Short-term scheduling (STS).

Fig. 4.21 Systematised coordination of Agents in collaborative network for NAN engagements.

Table 4.3 Interaction sequences of Agents and individual task assignments.

1	Record load profile & notifies state changes.	2,2A	Execute power transfer, Store Utility electricity prices.
3, 3A	Display load capacity, Request for power & bid electricity cost.	4, 4A	Display surplus generation capacity, Offer electricity cost.
5	Accept/Reject Proposal.	6, 10	Fault detected status, Load Shedding.
13	Instruct ES/LD Agent to perform charging or discharging operation.	8	Update power imparity call for new assets management strategy.
9	Provide anticipated load capacities, status of coupled CBs.	11	Proposed CB switching operations and update power availability.
12	Request and update online load capacity.	7	Status of CB.
16	Request for power generation.	15	Display and forecasts local power generation.
14	Monitor ES/LD SOC level & suggest storage operations (charge/ discharge).	17	Propose load balance management (load shedding & reserve for storage).
18	Renewable power generation profile, generator's start-up time & storage SOC level.	19	Compile summary of available power generations taking battery storage & electricity prices into considerations to PCM Agent.

shown in Fig. 4.21b. In day-ahead STS resolution, historical data are employed to estimate the system state. Whereas, real-time STS dictates instantaneous compensating responses, involving the integrity and efficiency of EPS operations when preserving demand-supply equilibrium. The approach in sizing STS results must adhere to over- and under-fitting constraints to avoid scheduling complications.

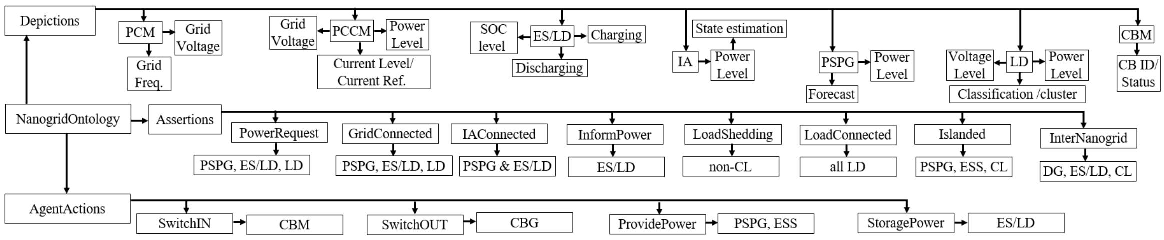

Fig. 4.22 Agents' real-time communication ontologies and control protocols in NAN.

Finally, strategic allocation of ontologies into Agents' communication directive is modelled to provide communal knowledge on structured commands rendered by Agents in cooperative domain. Hence, ontologies are coded information exchanged during Agents' interactions typically packaged with Agent's ID and a target action. Fig. 4.22 represents the proposed 'NanogridOntology' for participating Agents in IoT Azure Device Edge platform.

4.5 Proposed Prosumer-Centric Energy Management

Fig. 4.23 depicts a detailed operational flowchart of the proposed Prosumer-centric EMS with TE control features for individual Nanogrid. The architecture transacts day-ahead and real-time asset scheduling capabilities though adaptations of DCF and Agents of MAS to cooperatively negotiate in decision-making processes. The employed control features at respective DCF layers defined in Fig. 3.8 is utilised to procure optimal energy management settings and participation in the PMP based on Prosumer's interests at different time intervals (*i.e.* 60mins based on clearing market operations). The TE control scheme is separated into two computing domains; optimal scheduling of load consumptions with PSPG engagements, and joint bidding of market clearing pricing based on load serving entity.

The optimal load consumption scheduling approach employs reinforce Q-learning algorithm. When compared to other reinforcement learning technique (*i.e.* algorithms that uses neural network concept), it surfaces complications in solving DSR problems with multi-objective constraint implications especially satisfying supply-demand equilibrium. In addition, utilisation of neural network learning approach might have a redundancy effect as its search space is greatly reduced/restricted due to supply-demand constraint. Note that, forecasting of PSPG generation and load consumption capacity estimation are performed externally hence, neural network implementations in learning algorithm is no longer viable. Even though solving DSR problems requires continuous state or action space, Q-learning can stimulate such requirement by discretise the state space and have infinite number of states.

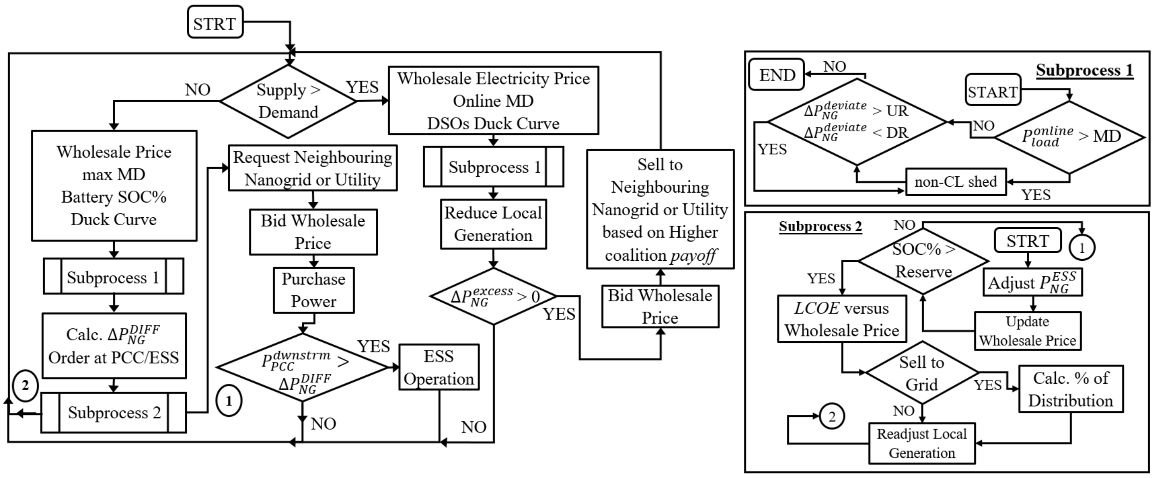

Fig. 4.23 Proposed TE-based energy management scheme in Nanogrid domain to support global DSR operations.

Hence, it does not commit in maximising over all state actions in order to evaluate a policy (meeting the operating constraints is the utmost priority).

On the contrary, in relations to PMP participations in bidding for market clearing prices, MADDPG algorithm is adopted to achieve a joint learning process with other NGs. It addresses the problem in joint determining of submitted energy bid, wholesale electricity prices, and electricity charging prices of REM for load consumption serving entity. The learning processes is in continuous state and action spaces where the energy bid and price (two actions) shared common objectives. Here, adaptation of neural network is necessary as it aids in learning the dynamic response of bid and price function from historical data to model wholesale market and Prosumers' collective acceptance behaviour correspondingly. In this sense, these response functions capture the joint temporal correlations of both clearing price outcomes and Prosumers' feedback to generate state transition samples without any cost incurment. Furthermore, the response function can direct choice of state in formulating Markov Decision Process (MDP).

The architecture and algorithms for both Q-learning and MADDPG have been modelled and defined in Chapter 3.6.1−3.6.5 to serve as the base model. Therefore, subsequent modelling focuses on defining MDP's action and state space, and learning policies.

4.5.1 Reinforce Q-Learning for Load Commitment with PSPG

The consumption load scheduling problem aims to minimise total billing costs consumed in a day based on various operating constraints. Considering that Prosumer has *m* number of loads and each day has 24 equal time intervals, k, hence, each load is modelled with five-tuple representation:

$$LOAD_j = (s_j, f_j, l_j, r_j, UDC_j);\ j \in J \tag{4.83}$$

where (s_j, f_j) reflects the operating threshold interval in bringing load j online. l_j refers to the total duration required for load j to remain in 'ON' state and r_j equates to the power rating in kW. When j^{th} load is brought online at s_j, it must remain in the same operating mode from s_j to $(s_j + l_j - 1)$. For an example; $LOAD_j = (3, 7, 2, 1)$ specify load j with $4kW$ rating is to be brought online any time in-between 3^{rd} to 7^{th} hour time slot for a duration of 2 hours. It aims to achieve optimal time allocation at which load j must be turn 'ON', subjected to other affiliated constraints. UDC_j is the unit delay costs introduce to apprehend usage interruptions in Prosumer's lifestyle due to 'ON' delay events. A low UDC_j denotes longer delay intervals which can be imposed to non-critical loads and vice versa.

Considering a Nanogrid transition from state $x_0 \to x_1$, it reflects an immediate reinforcement also known as cost, $C_0 = g(x_0, a_0, x_1)-$generally a random integer value. At any state, k, the Agent performs an action, $a_k \in A$ based on the system's attribute before moving to state, $x_{(k+1)}$ and the cost incurred is expressed as $g(x_k, a_k, x_{(k+1)})$. Hence, defined by the Markov property, the stochastic function is $x_{(k+1)} = f(x_k, a_k)$. Despite its model-free algorithm in Q-learning, its model can be estimated using transition probabilistic performance, $P^{a_k}_{x_k, x_{(k+1)}}$. To find the optimal sequence of action-state pairs, it is required to find maximised function of $E\sum_{N-1}^{k=1} \gamma g(x_k, a_k, x_{(k+1)})$ that is assisted by an optimal policy, π^*. In this sense, such decision-making problems can be solved using Q-learning algorithm despite having an unknown transition probabilistic. Using Q-value under policy π of Q-learning, $Q^{\pi}(x,a)$, the total expected reinforcement value, $E[]$, under optimal policy is defined as $\max Q^{\pi}(x,a) = E\sum_{k=0}^{T-1} \gamma g(x_k, a_k, x_{(k+1)})|x_0 = x, a_0 = a$. Here, ε-greedy algorithm for action selection is employed to select actions while learning. The greedy action is taken with probability (1-ε) where probability ε is a random action.

The reinforcement multi-objective Q-learning algorithm for load consumption commitment problem tasks to minimise Prosumer electricity bill considering existence of PSPG, ESS, and downstream generation exchanged at PCC:

$$\max_{u^k_{j,i}} E\left[\sum_{k=1}^{24}\sum_{i=1}^{3} C^k_i r_j u^k_{j,i}\right] \tag{4.84}$$

$s.t.$

$$\sum_{k=s_j}^{f_j} u_{j,i}^k = l_j \tag{4.85}$$

$$u_{j,i}^k = \begin{cases} 0, & k < s_j \\ 0, & k > f_j \\ u_{j,i}^k, & \text{otherwise} \end{cases} \tag{4.86}$$

where $i = 1$ refers to downstream generation, $i = 2$ is PV(PSPG), and $i = 3$ is ESS. $u_{j,i}^k$ reflects the load status being online or offline, 0=OFF and 1=ON at time slot k. In relation to the Q-learning states, $[x(1), x(2)]$; $x(1)$ refers to the present time slot and $x(2)$ is the total 'ON' state duration for load j. The action set is redefined into: $A = \{0, 1, 2, 3\}$. The action set reflects switching operation of load device; a=0 denotes load j is switched 'OFF'. a=1,2,3 is load brought online and supplied by grid, PV and ESS, respectively. In the case where a=2 or a=3, available power rating from PV and ESS will reduced at that present hour slot, k, and available power will be updated:

$$\begin{aligned} P_{PV}(k) &= P_{PV}(k-1) - r_j \\ P_{ESS}(k) &= P_{ESS}(k-1) - r_j \end{aligned} \tag{4.87}$$

The stochastic operation of PV generation is incorporated with a reward function:

$$g(x, a, x_{next}) = C_i^k r_j;\ a = 1, a = 2 \tag{4.88}$$

$$\begin{cases} \text{penalty}, & \text{if } \big(P_{PV}(k) < r_j \ \&\& \ a = 2\big) \\ \text{penalty}, & \text{if } \big(P_{ESS}(k) < r_j \ \&\& \ a = 3\big) \\ \text{penalty}, & \text{if } (f = x_{next}(1) \ \&\& \ x_{next}(2) < l) \\ UDC_j r_j, & \text{if } a = 0 \\ \text{reward}, & \text{otherwise} \end{cases} \tag{4.89}$$

The function of state transition is defined as follow:

$$\big[x_{(k+1)}(1), x_{(k+1)}(2)\big] = \big[x_k(1) + 1, x_k(2) + a'\big] \tag{4.90}$$

where a' depicts the next transition action for instant if a'=0 it defined that load j is offline and $a = 0 \rightarrow a' = 1$ refers to load j being brought online at time interval k taking its supply from the grid.

In the Q-learning iterative process, Q-values of different action-state pair are analysed until an optimal value is attained. Before engaging Q-value updates, forecasting of PV generation is performed based on historical data. Initialisation of each load j in 'OFF' state is assign with $Q^0(x,a) = 0$. Initialising from $[x(1),x(2)] = [s_j,0]$, the action taken is based on generation availability of PV or ESS with ε-greedy strategy before transiting into the next state which updates the Q-value and generation capacities. The process repeats in iterative approach until Q-value converges to a nearly stagnated value with small deviation error. After which perform $a_g = \arg\max_{a \in A} Q^{\pi*}(x,a)$ to retrieve at optimised action-state pair.

In addition to utilising PSPG operations in solving load consumption commitments, consideration of DSR operation constraints and reward payoff must be incorporated to better schedule online load capacities discussed in Chapter 4.4.2.

$$\begin{aligned} Q^{\pi}(x_k,a_k) &= E\sum_{k=0}^{T-1}\gamma g(x_k,a_k,x_{(k+1)})|x_0 = x, a_0 = a \\ Q^{\pi}(x_k,a_k) &= Q^{\pi}(x_k,a_k) + \sum_{c=1}^{C} R(x_k,a_k) \end{aligned} \tag{4.91}$$

where $R(x_k,a_k)$ is the newly introduced reward function that sums all payoff(s) from the listed DSR constraints, $c \in C$, based on current state-action pair. Fig. 4.24 illustrates the flowchart sequence in employing the proposed Q-learning algorithm in solving load commitment problem.

Payoff for Load Consumption Minimisation Curve

$$P_{tol} = \sum_{i=1}^{N}\left[P_{load_{i,t}}^{online} - P_{load_{i,t}}^{OBJ}\right]^2 \tag{4.92}$$

$$R(x_k,a_k) = \begin{cases} \text{reward}, & P_{tol}(t) \leq P_{tol}(t-1) \\ 0, & P_{tol}(t-1) < P_{tol}(t) < P_{tol}(t-1)*1.1 \\ \text{penalty}, & P_{tol}(t) \geq P_{tol}(t-1)*1.1 \end{cases} \tag{4.93}$$

where the reward assignment is dependant on how much the total online load capacity deviates from the objective. Hence, a threshold payoff is defined on based on the deviation

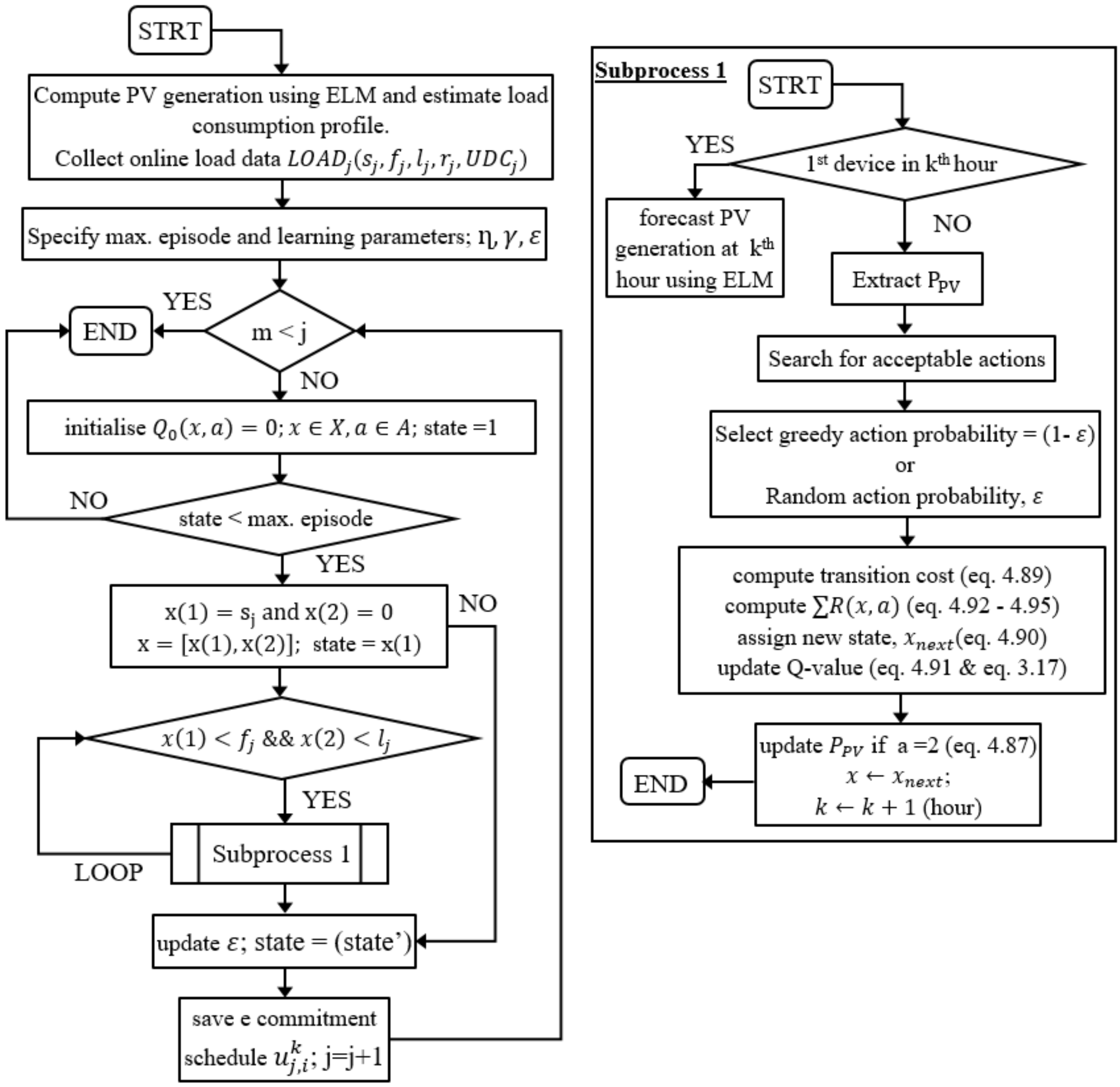

Fig. 4.24 Solving load commitment problems with PSPG and DSR operating constraints process flow using Q-learning approach.

intensity. It aims to improve the load consumption offset against desired from time $(t-1)$ to t based on the state and action pair sequences.

Payoff for Maximum Demand Loading

In MD criterion, assignment of penalty factor will be the greatest when compared to other constraint's payoff. Based on the contracted load demand capacity, DSO imposes high penalty factor into Prosumer's energy billing fees if DF drop below 1 as it implies Prosumer has poor scheduling of load commitment. The severity in DF negligence on DSR operations can result to 'Duck Curve' and unit commitment crises.

$$R(x_k, a_k) = \begin{cases} \text{penalty}, & DF(t) < 1.0 \\ \text{reward}, & DF(t) \geq 1.0 \end{cases} \tag{4.94}$$

Observing Unit Commitment Ramp Rate Limits

Likewise, in view of unit commitment's ramp-up and ramp-down limits against ordering of downstream energy exchanged at PCC, the imposed penalty is much greater due to unit commitment issues. TGU are resorted to be brought online but not generating any output power as it is put on spinning reserve mode to support sudden surge in demand curve. Such operation incurs higher operating costs.

$$R(x_k, a_k) = \begin{cases} \text{penalty}, & \Delta P^{NG_i}_{assign_{(t-1)\to t}} < \Delta P^{online}_{load_{(t-1)\to t}} \\ \text{reward}, & \Delta P^{NG_i}_{assign_{(t-1)\to t}} \geq \Delta P^{online}_{load_{(t-1)\to t}} \end{cases} \tag{4.95}$$

4.5.2 MADDPG Learning for Cooperative Pricing and Bidding of Load Serving Entity

Assume that a day has 24 interval, $T = \{0, ..., T-1\}$is decomposed into 1 hour intervals. The market participation involving buyer and seller need to submit their energy bid/offer at time, $(t-1)$, for t. Then, the wholesale market operator will generate the wholesale electricity price and also compiles energy purchases and sales that are successfully transacted at respective buyers and sellers, correspondingly. Meanwhile, the Load Serving Entity (LSE) also referred as the wholesale buyer determines the retail price for time interval t. Those purchase energy are resold at a different price to its customers in the REM. In response, Prosumers will adjust their load consumption capacities based on the price signals at time t.

In wholesale market model, let $S = \{s_1, ..., s_S\}$ reflects the set of sellers and $B = \{b_1, ..., b_B\}$ set for buyers. Each seller in the set, $s \in S$ submits an offer denoted by $f_t^s(.)$, which indicates the minimum price threshold at which seller agrees to sell at time t. Hence, $f_t^s(q_t^s)$ specifies minimum price at rated energy quantity. Likewise for buyer, $b \in B$, submits it maximum threshold bidding price expressed as $f_t^b(q_t^b)$. (4.96)–(4.98) defines the maximisation problem in solving social welfare cleared by ISO on wholesale market prices.

$$\max_{q_t^{s_1,b_1},\ldots,q_t^{s_S,b_B}} \sum_{b\in B}\int_0^{q_t^b} f_t^b(q)dq - \sum_{s\in S}\int_0^{q_t^s} f_t^s(q)dq \tag{4.96}$$

$s.t.$

$$\sum_{b\in B} q_t^b - \sum_{s\in S} q_t^s = 0 \Leftrightarrow \lambda_t \tag{4.97}$$

$$\left(q_t^{s_1},\ldots,q_t^{s_S},q_t^{b_1},\ldots,q_t^{b_B}\right) \in Q_t \tag{4.98}$$

where λ_t refers to the interchangeable variable affiliated to (4.97) and it reflects the power balance equation. Depending on the market clearing prices in time $t-1$, the feasible decision variable set is expressed as Q_t. For simplicity, q_t refers to the total transacted sales/purchases (*i.e.* $q_t = \sum_{b\in B} q_t^b = \sum_{s\in S} q_t^s$). (4.96)−(4.98) provide a cleared energy sales and purchase, and also wholesale prices for respective market participants. All are to receive levelised pricing that linked to λ_t. In an event of aggressive wholesale market engagements, the dominance of a single participant typically does not have any repercussions on the clearing price and also having a low marginal unit. In this sense, given λ_t, the cleared purchased energy for buyer b when it is in non-marginal state can be expressed as follows:

$$q_t^b = \arg\max_{q^b} q^b|_{f_t^b(q^b)\geq\lambda_t} \tag{4.99}$$

Whereas, in REM model, LSE participates as a buyer in wholesale market and bid for its purchased energy. Consider LSE is buyer b in wholesale market, it resells the purchased energy to a set of Prosumer in REM at a regulated price. Let v_t reflects the regulated price at time t interval and the corresponding energy purchased from wholesale is q_t^b. The Prosumer set is denoted as $C = \{c_1,\ldots,c_n\}$ served by LSE in REM. All Prosumers $c \in C$ will then respond to the price v_t by adjusting load consumption capacity, d_t^c. Hence, the sum of energy consumed by set of Prosumers at time interval t is expressed as $d_t = \sum_{c\in C} d_t^c$. Therefore, LSE aims to maximise its profit earned between consumption capacity against REM price defined (4.100) at individual time frame, limited to energy equilibrium constraint.

$$\max_{v_t,v_{(t+1)},\ldots\in[\overline{v},\underline{\mathrm{v}}]} E\left[\sum_{\tau=t}^{\infty}\gamma^{\tau-t}\left((v_\tau-\lambda_\tau)d_\tau-\phi_\tau(d_\tau,q_\tau^b)\right)\right] \tag{4.100}$$

where E is the expected operation and the discount factor for reduces future profit, $\gamma\in[0,1)$. A non-negative scalar function, $\phi_\tau(.,.)$. $\overline{v},\underline{\mathrm{v}}$ are upper and lower limit of the price range, respectively. λ_t and q_t^b are determined in the wholesale market defined in (4.96)−(4.98) while d_τ price is regulated by Prosumers through (4.101) and (4.102). The objective comprises of two elements; *(i)* quantify the profit earned from trading energy with LSE, and *(ii)* penalty cost induced when aggregated load consumption capacity diverges from purchased energy. The actual aggregated load consumption capacity, d_τ, only reflects those energies that have been paid to wholesale market operator and that is acquired from Prosumers.

Lastly, the PMP model receives a regulated price, v_t from LSE at each time interval t for $c \in C$. Following, Prosumers will adjust its load consumption capacity to gain maximum profit return. Let e_t^c reflects the energy capacity needs by Prosumer c at time t. Suggested in [240], the utility maximisation problem defined in (4.101)−(4.102) solves the optimal Prosumer action.

$$\max_{d_t^c \in D_t^c} \beta^c(e_t^c, d_t^c) - v_t d_t^c \tag{4.101}$$

$s.t.$

$$e_{(t+1)}^c = e_t^c + \eta_t^c(e_t^c - d_t^c) + \xi_t^c \tag{4.102}$$

where $\beta^c(.)$ refers to the benefit function which benefited Prosumer based on optimised energy needs and consumption capacity. $\eta_t^c \in [0,1]$ denotes the cache rate representing percentage of unsatisfied energy need criterion needed to be carried over to the next time interval. D_t^c represents the set of energy consumption that is feasible and ξ_t^c models the new incremental energy needs by assigning random variable.

Fig. 4.25 proposes the interactions of MADDPG's actor and critic components in executing joint learning processes for optimal bidding and pricing in the electricity market.

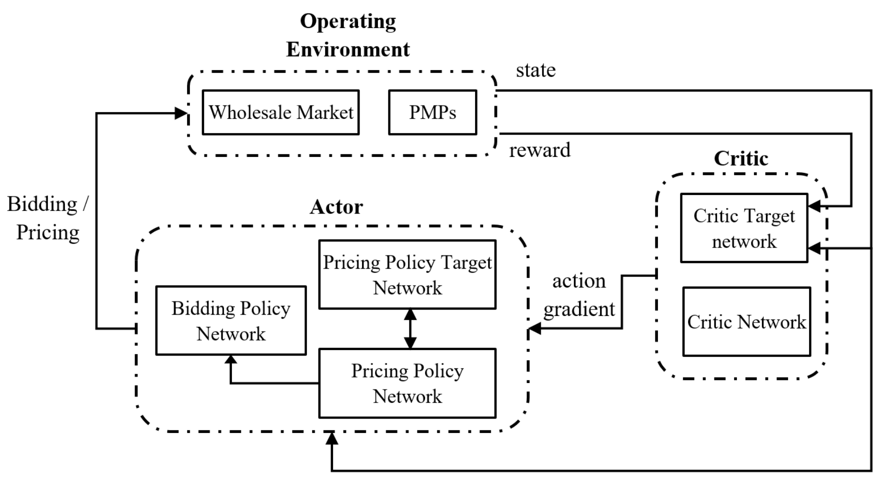

Fig. 4.25 Overview of critic and actor interactions on operating environment for joint bidding and pricing processes.

Dynamic Bidding and Pricing Response Functions

In the LSE domain, it determines the bid, f_t^b and price, v_t problems at time t. Assume that the bidding problem is characterised a vector parameter, ω_t, and let $\{\lambda_\tau, q_\tau\}_{(t-n_1)}^{(t-1)}$ represents the set of wholesale market clearing price from time $(t-n_1)$ to $(t-1)$. The model interactions between LSE and wholesale market operator is defined through (4.96)−(4.98) using n_1-order bidding response function denoted by $\psi(.)$:

$$(\lambda_t, q_t) = \psi\left(\{\lambda_\tau, q_\tau\}_{(t-n_1)}^{(t-1)}, \omega_t, t\%T\right) \tag{4.103}$$

where $t\%T$ is the time modulo for 1 day and the cleared energy price can be computed using (4.99). Given in the scenario where $n_1 = 0$, the wholesale clearing price is dependent on LSE's bidding price at current time t. ω_t must have a neutral impact on the clearing price outcome to procure a competitive wholesale market and hence, (4.103) models the dynamics of clearing price weightage. It also evolves the clearing price results in wholesale market to λ_t, q_t, q_t^b from $(t-1)$ clearing price based on its bid, ω_t. To accommodate a large bidding response from other market participants, n_1 needs to be large enough to include participants' actions. In consequence, the n_1-order bidding response function can comprehend the wholesale market dynamics. Subsequently, in aggregate energy consumption, d_t, n_2-order price response was employed to forgo its reliance on the complete Prosumer model defined in (4.100) and utilise real-time total consumption data instead. The n_2-order response price function, $\varphi(.)$, characterises joint behaviour of all Prosumer $c \in C$ as a set of problem in conjunction to (4.101).

$$d_t = \varphi\left(\{d_\tau, v\tau\}_{(t-n_2)}^{(t-1)}, v_t, t\%T\right) \tag{4.104}$$

Similarly, when $n_2 = 0$, the aggregate Prosumers' demand uses the price at current t interval. It can be seen that the response function for bidding and pricing are similar and have better learning capability based on data availability at LSE as compared to those complete wholesale market and Prosumer models.

Policies for Pricing and Bidding

The objective is to identify the joint bidding and pricing function, and LSE to solve the optimal bid and price values based on available data. As mentioned before, the parameters related to the wholesale market operations (*i.e.* $\omega_\tau, \lambda_\tau, q_\tau \ \forall \ \tau \leq (t-1)$) are to be made available to LSE at time $(t-1)$ interval. In addition, information made available in view of

REM domain includes $v_\tau, d_\tau \; \forall \; \tau \leq (t-1)$. Therefore, aggregating the informations, $I_{(t-1)}$, together is as follows:

$$I_{(t-1)} = \{\omega_\tau, \lambda_\tau, q_\tau, v_\tau, d_\tau\}; \; \forall \; \tau \leq (t-1) \tag{4.105}$$

Subsequently, the coupled bid ω_t and price v_t are required to solve jointly from $I_{(t-1)}$ for time interval t. In order to procure a competitive but yet uniform pricing market, it is optimal that the bidding and pricing policies are defined separately before mapping into the joined bid and price response function, $I_{(t-1)} \rightarrow [\omega_\tau, v_\tau]$. It allows efficient decision-making adversaries based on common information utilisation.

In the uniform pricing market, the price will be cleared if the bidding price is lower than λ_t. Moreover, to gain minimised penalty inducements due to energy mismatch between purchase capacity and total consumption (aggregated) in real-time, it is wise to bid the exact amount of energy as the aggregated energy consumption. In a competitive and uniform pricing market, for any v_t, λ_t will not affect ω_t. Hence, $q^b_\tau = d_\tau$ is to be defined by finding the optimal ω_t that maximises profit return expressed in (4.100). Eventually, it is essential to find optimal price v_t in REM and establish bid from v_t. Hence ,the deterministic pricing policy, $\pi(.)$, that maps $I_{(t-1)}$ to v_t is give as follows:

$$v_t = \pi(I_{(t-1)}) \tag{4.106}$$

and its bidding policy, $\mu(.)$, that maps $I_{(t-1)}$ and v_t to ω_t is:

$$\omega_t = \mu(I_{(t-1)}, v_t) \tag{4.107}$$

where assuming that the bid price, ω_t, comprises of two components; bidding price, ω^P_t, expressed as W/MWh, and bid capacity, ω^q_t, in MWh. Hence, to achieve optimal bidding policy, μ^*, ω^P_t set to v_t and ω^q_t equates to the aggregated energy consumption attained from the price response function, φ.

Formulation of Markov Decision Process

Formulation of MDP property is modelled to represent the joined bidding and pricing problem. First, it defines the state at time interval t:

$$s_t = \left(\{\lambda_\tau, q_\tau\}^{t-1}_{(t-n_1)}, \{d_\tau, v_\tau\}^{t-1}_{(t-n_2)}, t\%T \right) \tag{4.108}$$

The actions set at time interval t is $a_t = v_t$. ω_t is formed from v_t through a set of deterministic procedure derived in Chapter 4.5.2. Both action and state spaces are in continuous domain. Using (4.103) and (4.104), $s_t, a_t, s_{(t+1)}$ can be determined. Nevertheless, the state transition probability function remains foreign for LSE as it can only be defined if all market participants' parameters are provided. Hence, to mitigate such issue, the pricing and bidding policies can be redefined as:

$$v_t = \pi(s_t) \tag{4.109}$$

$$\omega_t = \mu(s_t, v_t) \tag{4.110}$$

As the objective in joint bidding and pricing problem is to maximise LSE profit, the reward, r_t, serves as an indication for profit margin received by LSE at time interval t:

$$r_t = (v_t - \lambda_t)d_t - \phi_t(d_t, q_t^b) \tag{4.111}$$

Subsequently, the Q function under price and bid policy at respective state-action pair can be modelled to compute the expected return expressed as $Q^{\pi,\mu}(s_t, a_t)$. Further derivation and subsequent implementation of MADDPG are already explained in Chapter 3.6.5.

Actor and Critic Neural Network

The supervised actor network is a fully connected feed forward structure comprising two hidden layer of 100 and 50 neuron nodes, respectively. The nodes employ exponential linear unit [241] activation function to gain accelerated training process as compared when using rectified linear unit. Whereas, the output layer has 24 unit nodes programmed with hyperbolic tangent activation function. The loss function uses mean squared error and also 12 regulariser with hyper-parameter tuned to 0.1, avoiding over-fitting crisis on training data set. It employs Adam optimiser to reap its advantage over computation speed and robustness, and also a learning rate of 0.0001.The neural network is trained under 4000 epochs.

Meanwhile, the critic network takes in two input state space, similar to actor network, and the other action space from actor network. The output generates a scalar value for every action-state input pairs. The first hidden layer of actor network is shared with critic's first hidden layer of state space input comprising of 100 neuron nodes. It helps in the network's training processes as the features extracted from the state space are useful for both actor and critic network. The second hidden layer comprising of 50 neuron nodes is employed for the

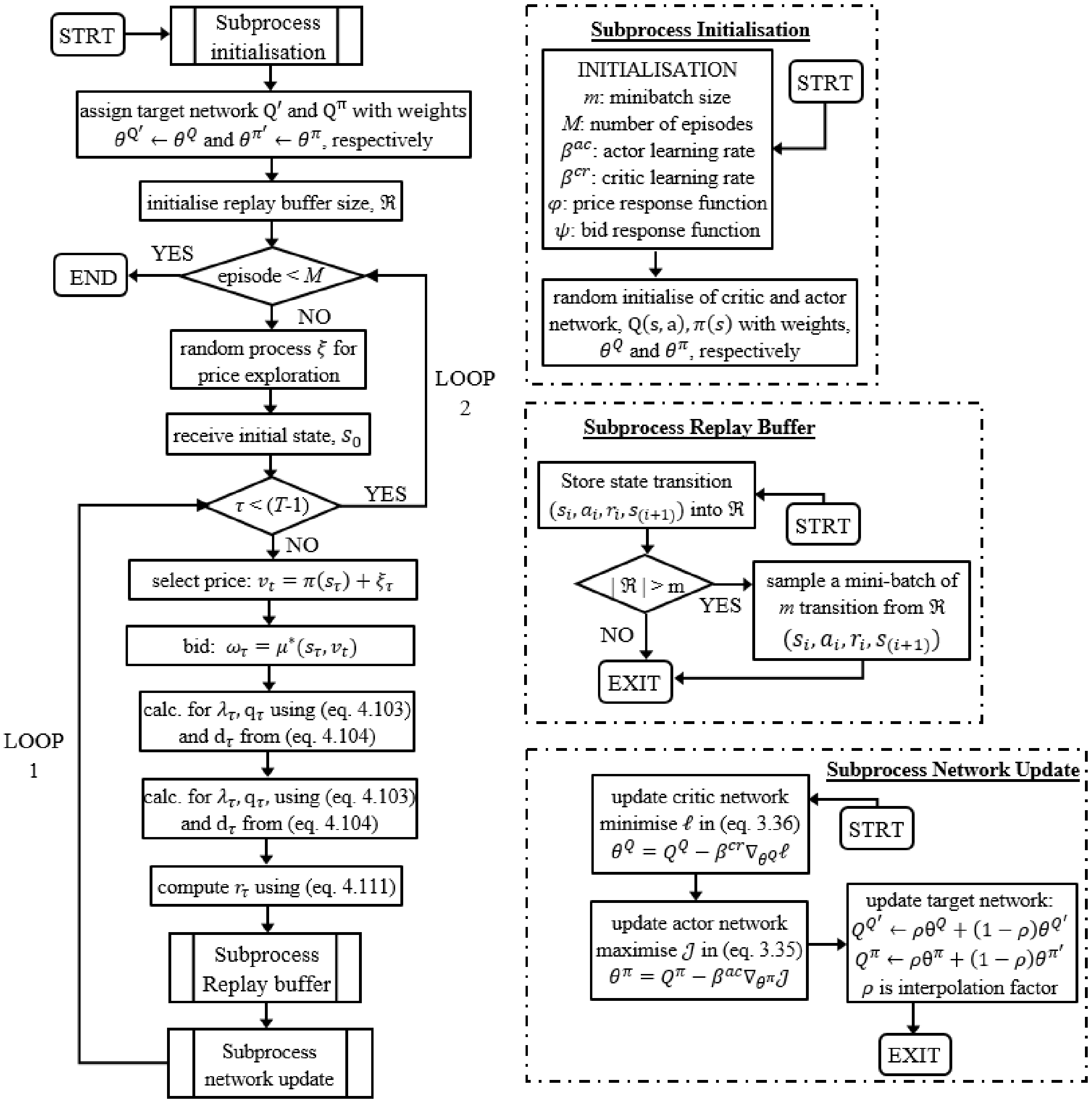

Fig. 4.26 Solving joint bidding and pricing of LSE in electricity market operations using MADDPG learning technique.

action space input. An additional hidden layer is introduced comprising of 25 neuron nodes. The neuron nodes in the hidden layer uses an exponential linear unit as the activation function while the output layer omits out the use of activation function. Similar to actor network, critic employs 0.001 learning rate and uses Adam optimiser for training the network's weights. It also specify that 12 regulariser with hyper-parameter set to 0.1 is engaged.

Fig. 4.26 illustrates the flowchart sequence in employing MADDPG learning algorithm in solving joint bidding and pricing in the electricity market.

4.6 Case Studies: Findings and Results

Investigations were performed in analysing two case studies; *(i)* deployment of Prosumer-centric EMS based on TE functions in a single Nanogrid domain, and *(ii)* operations of multiple NGs in a Prosumer Community environment and analyse their socio-economical impacts on cooperative-competitive DSR operations and market participations. Both case studies evaluate Prosumers as primary (lead) energy regulator in the DSR domain−distributing majority of the managerial processes and intelligences at low-voltage level participants (Prosumer). Such undertaking upgrades distributed energy actors at low-voltage level as RDSOs, having greater jurisdictions in securing their energy consumption and generation interests while optimising response in scheduling DSR resources for the provision of grid services. Moreover, operational and cost benefit analyses for DSO-TSO in TE system implementation are also reviewed to comprehend transactional business model and value realisations in policy and wholesale market design and unit-commitment operations for transactive and flexible DSR engagements.

Analytical analyses are biased towards engagements of PT-Is in Prosumer Community as to better comprehend TE value which also verifies the proposed reinforced-CDL learning intelligences for Prosumer-centric EMS. Evaluations involves cooperative yet competitive bidding operations in PMP and optimal utilisation of PSPG that can influence demand curve demographics at the global level. In addition, having Prosumers to subscribe into various transactive value programs/contracts issued by DSO, analyses were conducted to view Prosumers' responses toward superior incentive payouts and how it influence energy exchange at NGs' PCC (*i.e.* downstream consumption and upstream generation) and energy clearing price profiles.

The proposed NGs are modelled in MATLAB simulation environment and connect to Microsoft Azure in the cloud guided in [241, 242] to utilise Azure's IoT edge device and artificial intelligence modules. The MATLAB will be running as a deployment reference architecture, a virtual machine in Azure cloud controlling through a remote desktop connection. However, due to licensing (free), the number of connected interactive devices is limited (1 device). Hence, the simulation uses excel spreadsheet containing real-time performance data of devices (*i.e.* load appliances, PSPG). The data are taken from [108] to profile Prosumer's energy consumption and generation trends.

4.6.1 TE Operations of Single Nanogrid System: Residential

A 24-hours simulation analyses were conducted on a residential environment (single-phase 220VAC, 50Hz, short-circuit current of 71$Amps$) labelled NG-1 of Prosumer-type I, PT-I, shown in Fig. 4.27. Here, the PT-I creates a full-pledge Nanogrid system as shown in Fig. 4.27 where it comprises of PV-based PSPG, an ESS that is connected at the PV's inverter (DC-link), a PHEV charging point, and a back-up diesel-based generator. The specifications of listed devices/appliances are given in Table 4.4. The integrated systems' performance are sampled at every 5mins intervals. The collected energy consumption and PV power generation data are recorded during summer.

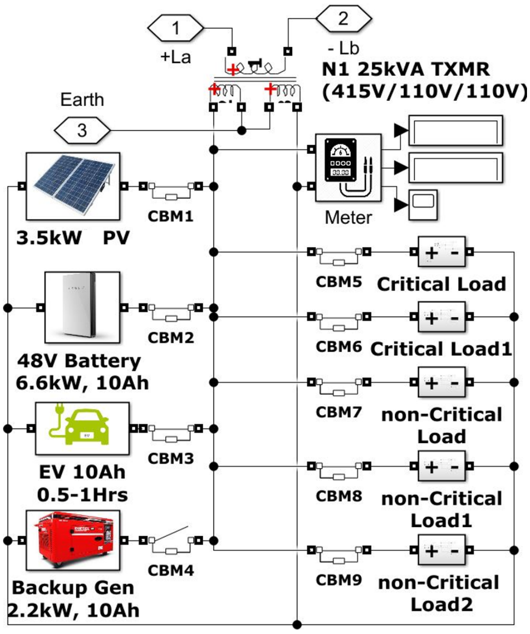

Fig. 4.27 Residential-base Prosumer, Nanogrid-1, operating in full-pledge mode.

Table 4.4 Listing of appliances/device ratings in NG-1 coupled to the grid.

Device System	Ratings	Model
PV	3.5kWh	PV Panel: ABB PVI-3.6kW
		Inverter: ABB UNO DM
ESS	48V 6.6kW,10Ah	ABB: REACT 2
PHEV	10Ah−half charge 0.5-1HR	Hyundai IONIQ Electric
Charc. Pt (PHEV)	800V_{DC}−fast charging	Delphi SiC Inverter
Back-up diesel gen.	2.2kW, 10Ah	PowerFriend

First, Fig. 4.28a presents the results attained from forecasting PV available generation against the actual data. Using the proposed ELM algorithm with an ensemble approach and day-ahead historical data of actual output generation for the past year, it can be seen that the day-ahead forecasted generation is much underrated. The ELM's learning behaviour was deliberately attuned with under-fit regularisation index to reduce the risk of overgeneration prediction that may have negative influence on other scheduling processes. From the result,

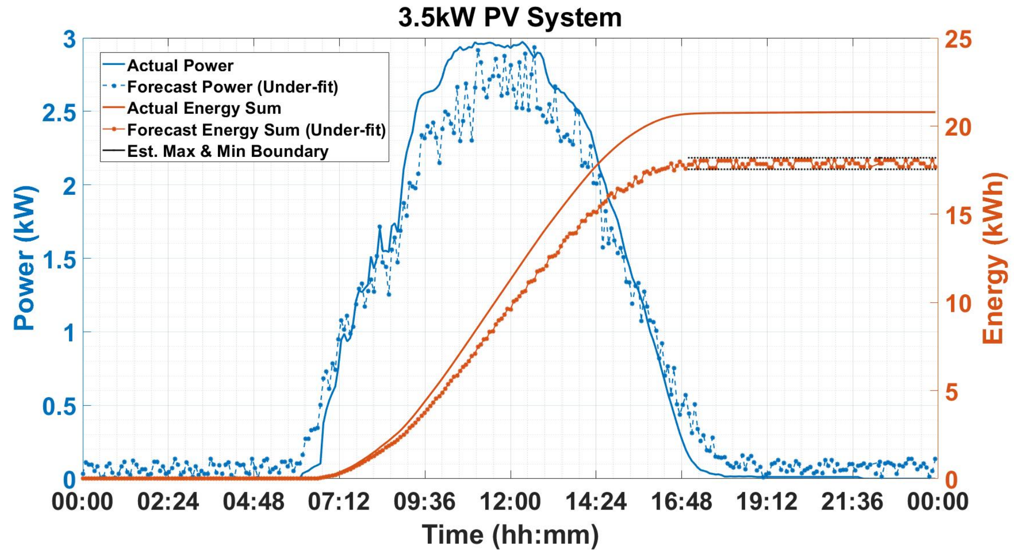

(a) 3.5kW PV system output power generation: forecasted versus actual.

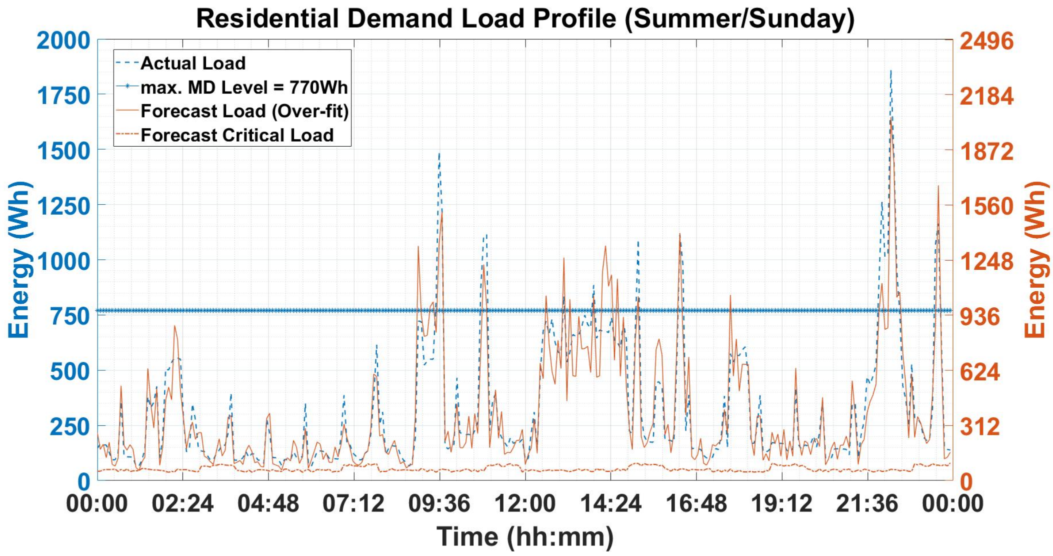

(b) Energy consumption of online critical load: forecasted versus actual.

Fig. 4.28 Performance in forecasting available PV generation and critical load consumption capacities sampled at 5mins intervals.

it also deduce that the demand side response will have a large power dip at noon due to large PV generation penetration (bell-shaped curve). Therefore, phenomenon such as 'Duck Curve' crises is transpired which create unit commitment issues and demand curve dipping below baseline requirement.

On the contrary, Fig. 4.28a exhibits results in forecasting day-ahead energy consumptions profile with over-fit regularisation criterion. In DSO point of view, overfitting regression model is well suited in forecasting total consumption capacity as power deviations rendered by instantaneous load could be represented along the time domain. However, in Prosumer perspective, the load consumption profile requires an additional load classification segregation to identify non-critical loads for scheduling purposes using the proposed clustering and identifying algorithms (KNN & K-means). After which ELM algorithm is employed to forecast respective load classes. In relation to the Gaussian distribution function approach in estimating load consumption profile, it is incorporated into the ELM's training set to serve as a viable influence during the testing phase. Notably, the critical load capacity can also used to recognise network's baseline load. Table 4.5 presents the 24-hours forecasted load consumption (30mins interval) in Nanogrid-1 ciphered into critical and non-critical load classes.

Table 4.5 Forecasted results of load consumption capacity consumed by Nanogrid-1 separated into critical and non-critical load (30mins intervals).

(HRS)	(Wh)		(HRS)	(Wh)		(HRS)	(Wh)	
Time	non-crit.	crit.	Time	non-crit.	crit.	Time	non-crit.	crit.
00:00 -	213	524	08:00 -	223	561	16:00 -	1077	2335
01:00	302	665	09:00	155	306	17:00	452	892
01:00 -	217	596	09:00 -	1550	3994	17:00 -	190	375
02:00	507	1127	10:00	1197	2822	18:00	960	2054
02:00 -	969	2211	10:00 -	409	882	18:00 -	749	1759
03:00	384	857	11:00	1022	2391	19:00	297	727
03:00 -	111	246	11:00 -	397	919	19:00 -	203	519
04:00	224	517	12:00	239	520	20:00	358	734
04:00 -	141	377	12:00 -	404	846	20:00 -	264	755
05:00	251	485	13:00	1173	2837	21:00	225	470
05:00 -	64	178	13:00 -	1213	3007	21:00 -	404	911
06:00	189	480	14:00	1397	3096	22:00	760	1954
06:00 -	188	448	14:00 -	1585	4018	22:00 -	2306	5082
07:00	211	477	15:00	1099	2690	23:00	897	2158
07:00 -	90	226	15:00 -	649	1454	23:00 -	403	959
08:00	503	1051	16:00	851	1747	23:59	924	2237

ELM forecasting technique is also employed in estimating the electricity price tariff for Prosumers, PMP, in relations to wholesale and LSE electricity market. Here, the regression model employs neither over- nor under-fit regularisation to gain optimal curve fitting between actual and forecasted. It aids in scheduling day-ahead charging and discharging operations of ESS SOC% level to better accommodate shifting of load consumption capacities into low price tariffs regions or supported by ESS during peak tariffs. Table 4.6 presents the performance index of ELM algorithm based on a 2 years training and 1 year testing datasets. In addition, STS Agent will retrieve all forecasted data and generate a timed-based predicament report seen in Table 4.7, suggesting plausible alarming or abnormal exposures during operations defined by Prosumer.

Fig. 4.29a exhibits the energy profile exchanged at PCC against load consumption and PV generation of Nanogrid-1. Here, Prosumer does not employ any means of intelligent scheduling, neither shifting of non-critical load nor charging and discharging sequences for ESS. Nevertheless, an unambiguous governance of energy transactions between PV generation and ESS; *(i)* charge ESS from PV's excess generation provided that SOC is less than 90% limited to power ramp-rate constraint, *(ii)* exhaust ESS to meet load consumption capacity with PV generation when SOC is greater than 10% limited to power ramp-rate constraint. Here, the initial SOC of ESS is set at 0% and due to optimal sizing of ESS

Table 4.6 Forecasting performance index.

Agent	Accuracy (RMSE)	Std. Deviation (σ)
STS 2e10.8 < δ < 2e11.05 15 < ESM < 25 Computing Time: 0.323s	Elec. Price: 2.162 ES Capacity: 2.044 Load Profiling: 4.135	0.134 0.062 1.088
non-CL (over-fit) 2e8.1 < δ < 2e8.7 15 < ESM < 25 Computing Time: 0.177s	Load Capacity: 3.091 Large ΔP^{shift} Detection: 2.523	0.119 0.038
GS (under-fit) 2e12.7 < δ < 2e13.1 15 < ESM < 25 Computing Time: 0.525s	Generation Availability: 2.337	0.065
@PCC 2e10.8 < δ < 2e11.05 15 < ESM < 25 Computing Time: 0.318s	Reserve Capacity: 2.061 Gen. Pooling: 1.915	0.078 0.111

Table 4.7 Alarm Report generated by STS Agent: forecasting alarming events or operation violations.

ΔP_{shift}	PV Op.	max MD	Batt. Charge	Elec. Price
01:20-02:10	Sunny	02:05-02:10	08:30-08:55	Tier 1
08:55-09:00	ClearSky	08:55-09:00	09:55-10:30	00:10-08:25
09:30-09:45	Sunrise:	09:20-09:40	10:55-11:00	Base:$1.086e-4
10:40-11:00	06:10	10:45-10:50	11:15-12:25	00:30-00:55(EX)
12:30-12:35	High PEN.:	12:30-12:35		Tier 2
13:00-13:20	09:30-13:40	13:05-13:15		08:30-14:20
13:50-14:10	Sunset:	13:50-13:55		Base:$1.102e-4
14:25-14:40	18:05	14:10-14:35		09:30-10:25(EX)
15:00-15:15		15:05-15:10		14:00-14:15(EX)
15:30-15:55		16:20-16:25		Tier 3
16:10-16:40		17:50:17:55		14:20-00:00
17:40-17:50		21:55-22:30		Base:$1.246e-4
19:30-19:35		23:25-23:35		20:00-21:25(EX)
22:10-22:25				
23:30-23:45				

against PV installation and demand load, exchange of upstream generation at PCC was not necessary. There are three instances where Nanogrid was operating in islanded operation ($0W$ downstream energy exchange at PCC); $0811-0849$, $1024-1041$, and $1123-1212$. The analyses also profiles the electricity and fixed LCOE tariffs to view Prosumer's online load contributions during peak price period.

From the load consumption profile seen in Fig. 4.29a, Fig. 4.29b identifies large downstream energy deviation instances exchanged at PCC which interjects unit commitment issues for PGRs when dealing with TGUs (ramping rate limit). Moreover, the load consumption curve is compared against the maximum MD limit. Overall, the results have shown poor energy management performance as Nanogrid-1 contributes; *(i)* Duck Curve phenomenon to transpire and the global demand curve falls below baseline at noon, *(ii)* utilisation of PSPG is not optimal as large percentage of load consumption capacity throughout the day falls in the high electricity price tariff region, *(iii)* events of large power demand shift were seen during the two peak period where PV generation is inactive and ESS is depleted, *(iv)* plausible divergence in supply-demand equilibrium as ramping rate limits could not match Prosumer's large load consumption shift within time t, *(v)* high operating costs was induced due to unitary dependency on downstream energy exchange after $1720hrs$ at which electricity prices is at highest throughout the day, *(vi)* multiple violations of $\max MD_{total}$ were exposed hence, penalties will be imposed to Prosumer at a large fee.

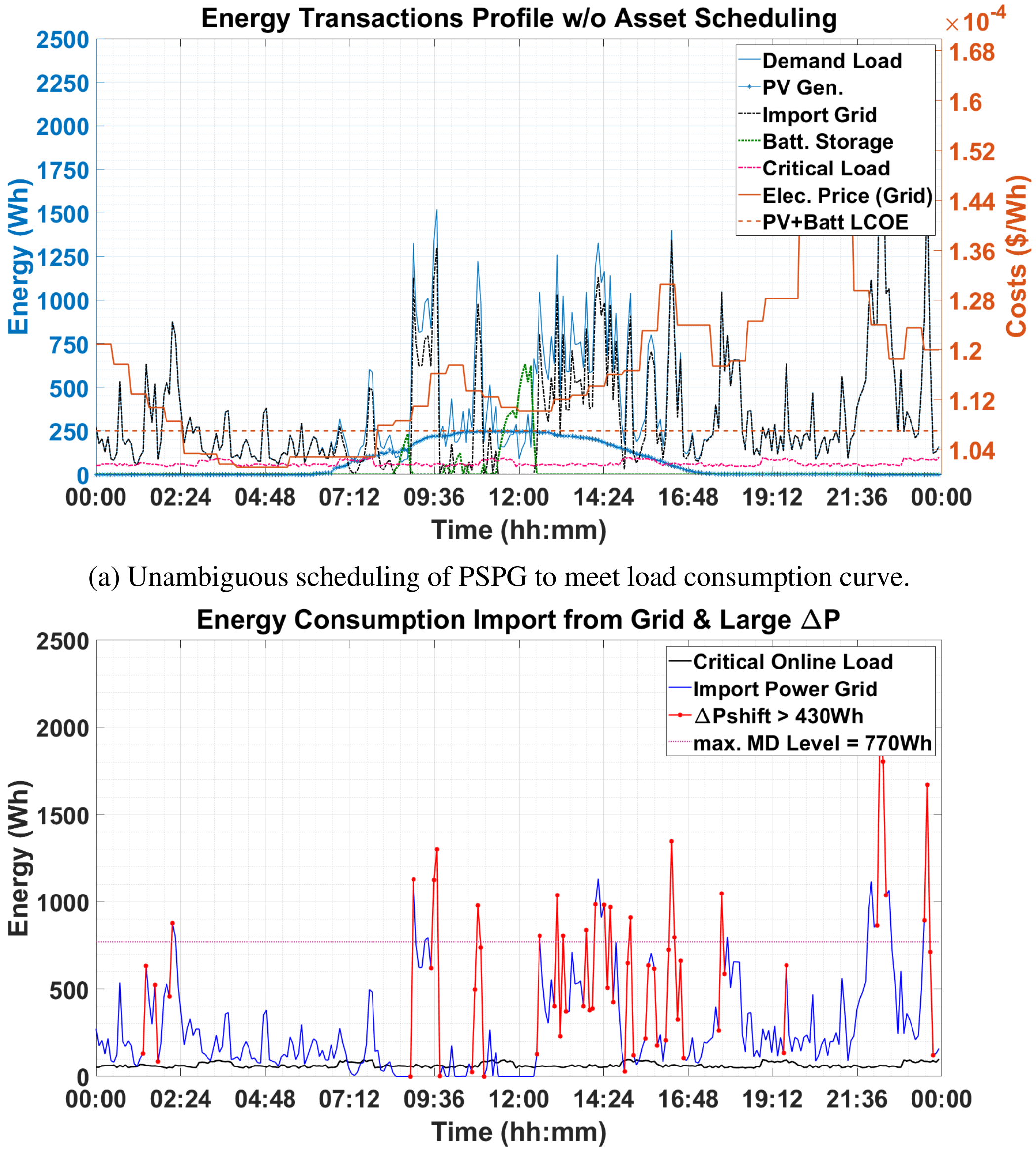

(a) Unambiguous scheduling of PSPG to meet load consumption curve.

(b) Identifying MD violations and large power demand shift.

Fig. 4.29 Overview of Nanogrid-1 energy transactions using 'dumb' management control scheme and its impact on DSR based on 5mins intervals.

In contrast, subsequent results depict energy transactions of Nanogrid-1 governed by the proposed Prosumer-centric EMS that observes TE value and functions. Similarly, performance evaluations are appraised based on its ability to learn and cipher optimal managerial response for Prosumer's electrification interests and demand-side management regulatory. Using the same PV generation and load consumption profiles, Fig. 4.30 and 4.31 present the impact on Prosumer's load consumption curve being shed at respective time t and shifted to another time period and management of ESS charging and discharging sequences with an initial 0% SOC. The learning algorithm abled to maintain at least 75% of Prosumer's non-critical load at respective time intervals and secure a minimal baseline load by ordering a minimum downstream power exchange of $1.2kW$. Fig. 4.32 shows the learning regression response and Agent's search space in locating optimality when solving DSR constraints and minimise Prosumer's operating costs.

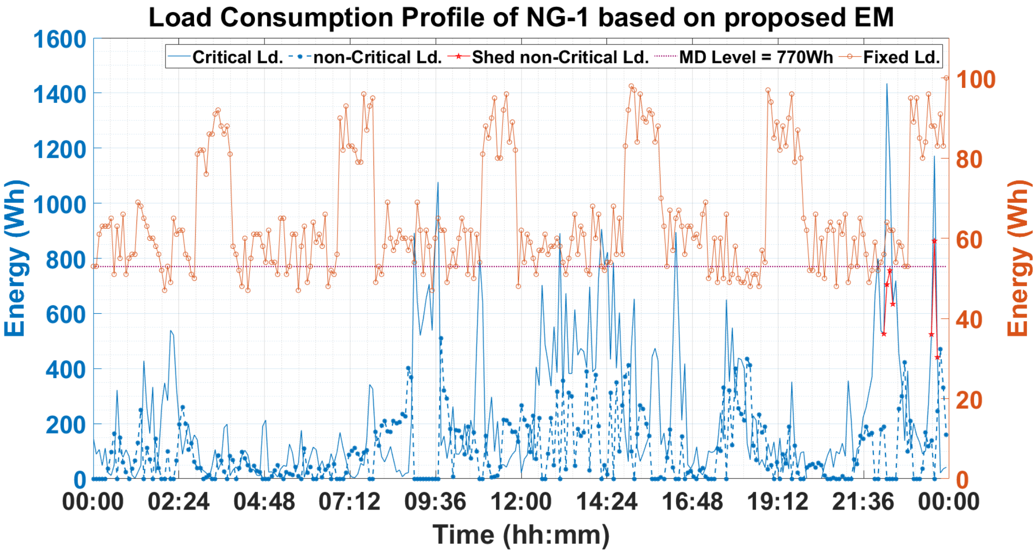

(a) Power exchange transactions at PCC and scheduling of non-critical loads.

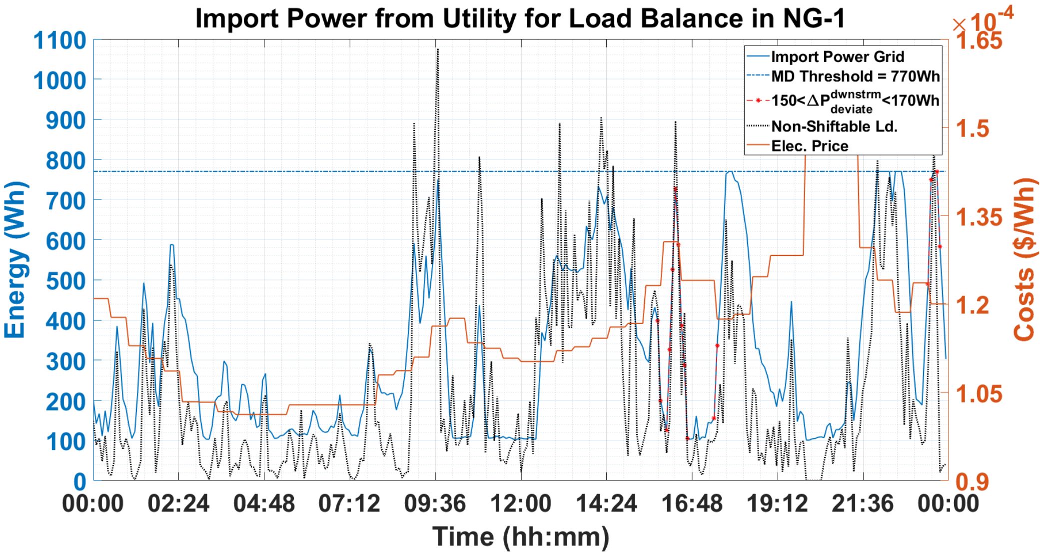

(b) Identifying MD violations and large downstream power deviations.

Fig. 4.30 Profiling power exchange at Nanogrid-1 PCC based on Prosumer-centric EMS intelligence that observes TE function and DSR constraints based on 5mins intervals.

Fig. 4.30a demonstrates the impact on online load consumption curve upon performing load shifting and shedding of non-critical loads at time t. An interval rate of half-an-hour was imposed on the shifting sequence search space to limit redistribution of shiftable loads into another time frame$-$maintain integrity of Prosumer's energy usage interests. Such constraints promote low shedding percentage and protect Prosumer's serviceability on non-critical load and yet rendered a bargained electricity billing. In this sense, exploitation of load shedding solutions or rescheduling beyond the time-stamp threshold (30mins) is minimised resulting in sub-optimal operating costs and plausible violations in response to DSR constraints. The results spotted two instances where non-critical load consumption was shed for a duration of 10 and 5mins, respectively (highlighted with red line). Almost $600Wh$ of the non-critical load capacity was shed despite after performing load shifting and atone ESS at maximum discharging rate, primarily to curb ordering of downstream energy capacity below the $\max MD$ limit.

Meanwhile, Fig. 4.30b focuses on the responses of energy exchange at PCC to meet supply-demand equilibrium in $NG1$. A significant improvements was redeemed in securing $\Delta E^{Deviate}(t)$ capping at less than $170Wh$ at time t to $(t+1)$ intervals, advocating levelised demand shift deviations in correspond to the upstream generator's (TGUs) ramp-rate limits. Such undertaking allows DSO to have greater flexibility in addressing unit commitment issues and evade from overestimated spinning reserve dilemma that could incur high operating costs. Moreover, the energy consumption ordered from the grid complies religiously with the $\max MD$ limit and baseline load criterion. However, significance in mitigating Duck Curve crisis was minimal as the learning trajectory was biased towards local managerial interests$-$directed to ordain reduced energy billing and shift peak consumption levels to low tariff regions. Greedy-based load scheduling and allocation administrations were recognised when ordering charging and discharging sequence of ESS. Likewise, shiftable load are constantly shifted to the next or previous allowable (30mins) time frame which result in constant energy backlog or advance scheduling, respectively. In consequence, Prosumer may face higher operating costs at time t as larger load consumption than the supposed capacity was introduce into a more expensive electricity tariff as compared to $(t-1)$. It was recorded that Prosumer has to pay 3% more despite adding incentives for preserving $\max MD$ level and $\Delta E^{Deviate}(t)$ thresholds.

Fig. 4.31 depicts the operations of ESS with a $184Wh$ charging and $180Wh$ discharging rate for every 5mins with 0% SOC at initial state. Supported by the Alarm Report generated by STS Agent seen in Table 4.7, ESS is programmed to anticipate charging and discharging operations to gain optimal operating costs at time, $(t+1)$ interval. Utilisation fo ESS

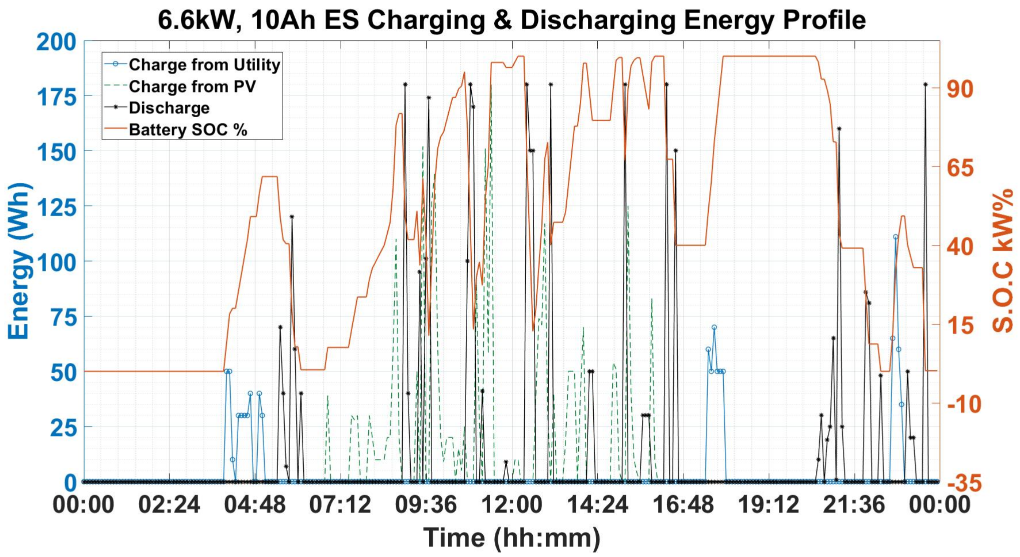

Fig. 4.31 Charging & discharging sequence of ESS using Prosumer-centric intelligence and TE functions at fixed LCOE, 1.22e-4 \$/Wh.

correspond in parallel with the electricity tariff curve (a 3-tier price regions), allocation of PV excess generation, and peak load consumption episodes. Dominantly, the operations of ESS are to compensate large inclination or declination of $\Delta P_{grid}^{Deviate}$ capacities, and support ordering of downstream energy exchange at PCC below max MD limit. Moreover, the assigned ES Agent limits excess utilisation of ESS by limiting a minimum SOC level threshold at 15% for spinning reserve operation. However, it can be seen that there were two episodes where ESS's SOC% drops below the defined threshold at 0550*hrs* and 2200*hrs*. The ES Agent is granted to bypass the constraint, only if two of these conditions were met; *(i)* discharge energy to accommodate large PV generation, and *(ii)* to evade from day highest electricity tariff by reducing ordering of downstream energy and increase ESS generation to support load consumption. Nevertheless, both instances did not raise any alarming concerns in regards to operating reserve as the network has a back-up generator to be brought online if islanding is required to recover from service interruption. Furthermore, the load consumption capacity at time $(t+1)$ declined towards the baseline load level allowing maximum ordering energy from grid.

Through incentive programmes for MD regulation, Prosumer are rewarded with compensated electricity billing that can help to offset losses when having higher load capacity than supposed being shifted into high tariff regions. As compared to conventional energy management proceedings [201, 243, 122, 173], the managerial intelligence focuses on load shedding and shifting into spotted regions where tariffs are low, depriving Prosumers from

Table 4.8 Operating cost comparisons based on $91kWh$ energy consumption.

Constraints	24hrs Operating Costs (Inclu. LCOE) (≈$, Std. Dev.<0.087)
Propose *max MD*	10.108
W/O *max MD*	8.776
W/O *max MD* W/ Penalty	9.918
Propose W/ *max MD* W/ Incentives	9.519
Δ Pshift > 250kWh W/ Penalty	10.203
Δ Pshift < 150kWh W/ Incentive	9.931
Proposed Δ Pshift W/ Incentive	9.702
Propose ES Size: 2.2kWh (LCOE: $1.20e-4)	9.479
ES Size: 3.0kWh (LCOE: $1.636e-4)	9.221
ES Size: 3.8kWh (LCOE: $2.072e-4)	9.914
ES Size: 2.0kWh (LCOE: $1.090e-4)	9.765

increasing load consumptions during peak periods. However, such innovation may not be pragmatic as Prosumers are forced to restrict its daily electricity usage and peak demand profile will shift which results in high electricity tariff at the shift time interval. Therefrom, imposing higher penalty premium for $\max MD$ violators can curb smooth demand curve trajectory at $(t+1)$ which then assists DSO in better scheduling of unit commitments. The penalty payouts can be portioned out as incentive for $\max MD$ abider as seen in Table 4.8.

Supplementarily, finding the optimal sizing for ESS installation against PV system and load consumption trends can influence Nanogrid's operating cost. From the results seen in Fig. 4.31, there are instances where ESS is charged through ordering of energy from grid and the corresponding tariff it is not deterministically cheap. Therefore, bidding strategy for charging/discharging sequence gets complicated when taking ESS size constraints into consideration for optimal scheduling of ESS utilisation. Alternatively, such crises can be rectified by monitoring Agent's cooperative reward responses where penalty assignment are posed when IA Agent is forced to exhaust ESS during low electricity tariff to contain high PV penetration at time $(t+1)$ or restricted discharge rate when servicing peak load consumptions. These are some indications that the ESS size is not accustom to the energy attributes of Nanogrid system. In addition, economic evaluation on LCOE for excess PSPG generation to be sold upstream may not be able to compensate the investments made in maintaining PSPG (oversized). Therefore, optimal sizing of PSPG proof to be a viable aspect in striking a balance between engaging an oversized ESS to gain maximum incentive but provoke very low return on investment while undersized ESS has high return on investment ratio but lose out on all the incentive payouts or worst penalties as seen in Table 4.8.

The Agents' Q-Learning probabilistic regression in localising optimal operating costs in cooperative tendency is presented in Fig. 4.32a based on predefined learning parameters listed in Table 4.9. Its objective is to attune Agents' learning curve to achieve optimal energy billing for Prosumer by cooperatively addressing all TE functions in DCF and operation of PSPG

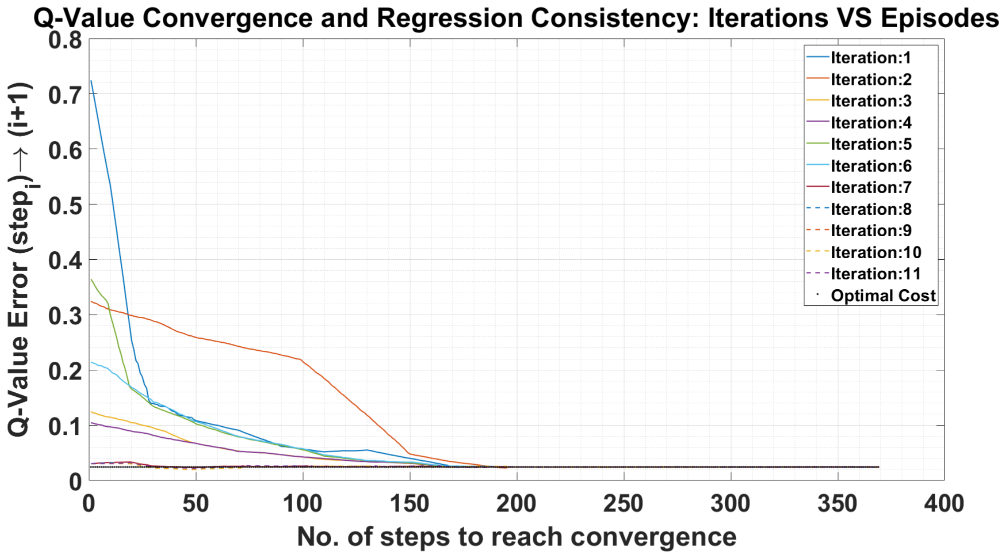

(a) Converging Q-value.

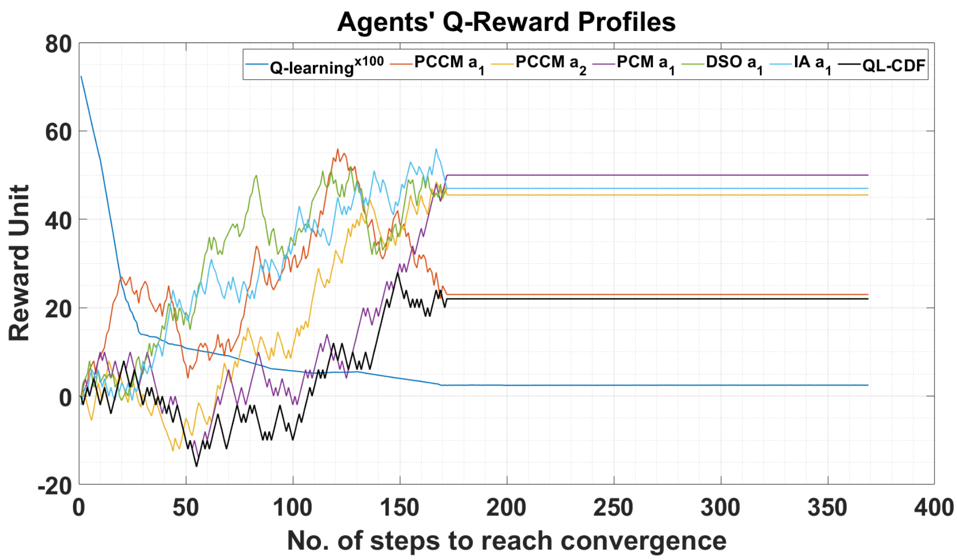

(b) Individual Agent's reward unit.

Fig. 4.32 Q-Learning in DCF learning regressions and reward assignments.

Table 4.9 Parameters for Q-learning Reward System.

Constants	Tuned values
ε	0.25
α	0.76
β	0.03

Agent Rewarding System
Initialise each Agent & QL-DCF Reward = 0;
IF:Agent satisfy constraint = +2;
ELSE IF:Agent fall in-between the constraint's threshold = 0;
ELSE IF:Agent fails to satisfy constraint = -3;
ELSE IF:Participating Agents converged a solution)
-Agents complied Cooperative Tendency in DCF = +2;)
-Agents neglected Cooperative Tendency in DCF = 0;)
ELSE: Reward = -1;

against DSR constraints. In the Agents' auctioning processes, penalty and reward values were assigned to respective Agents' state-action pair sequences and indeed, cooperative tendency based on centralised critic has better energy management response as compared to unambiguous administrations for a single Nanogrid operations. The results also showed that a three tier reward function should be employed to avoid stagnation in the Agents' learning trajectories. Through assignments of penalty with a negative value and reward with positive, the consolidated result could not provide a descriptive quantification on Agents' learning performance and sometime misleading. Hence, a three tier reward structure is introduced to represent degree of severity; positive value for reward, within a specified threshold with is 0, and penalty with a negative value. Such implementation helps Prosumer to view respective Agent's negotiation learning performances in the cooperative state-action pair assignments. The results exhibits a successful learning process where the Q-value able to converge and locate uniform global minima for Nanogrid's operating costs. As expected, the learning search space improves in proportionate to the number of iterations conducted. Thus, to reduce computational intensive and time in recognising solution-optimality, it suggests to run iteration order between 7 and 9 is sufficient.

Fig. 4.32b presents the Agents' reward payoffs during cooperative tendency. The payoffs uses positive, neutral, and negative rewards on the action-state pair in searching for optimal Nanogrid's energy billing and DSR mitigations. The reward unit provide information on which Agent(s) is being compromised (trade-off) to gain optimal resolution in cooperative tendency environment. However, using three tier reward function, the small learning rate is needed to provide bidding relaxation on Q-value regression and reach convergence.

4.6.2 TE Operations of Prosumer Community: Commercial & Residential

In this section, operations of four aggregated NGs were modelled, $NG\text{-}1 - NG\text{-}4$, as shown in Fig. 4.33 involving residential- and commercial-based buildings. It aims to analyse performances of cooperative energy management strategies on trading and market operations in view of TE functions. The Agents' learning search space is now extended will larger scaled serviceability constraints, extending managerial processes with respect to other neighbouring NGs. Thus, reliance on electricity pool market for DSO and PCM Agent is no longer restricted to a single bonded PCCM Agent. PCM Agent required to interact closely with all PCCM Agents to gain information from IA Agent in recognising excess generation flowing upstream that is ready for disposal at time $(t+1)$, excluding available operating reserve capacity. Hence, modelling of spinning reserve market model is also ventured to ensure DSR is stable during energy interrupted crises. The Prosumer-centric EMS employs the proposed MADDPG for joint bidding in the electricity market using decentralised critic function. Respective Nanogrid will then perform Q-learning technique using the regulated critic function to cipher local state-action pair sequences.

The electricity tariff oriented PCM Agents is separated into two authorities; *(i))* classical marginal pricing (MP) determined by DSO Agent during any electrification transactions occurs between wholesale and REM/LSE operators, *(ii)* bid-as-request (BAR) pricing where forward bilateral contracts are negotiated between Prosumers in PMP. Fig. 4.34 profiles the energy prices of wholesale and retail in summer under MADDPG reinforce learning algorithm based on 30mins intervals. An observation was concurred that the price curves for both market domains have similar trends due to the cumulative reward which is much dependent on the price difference. Subsequently, bidding quantities and the load consumption capacity of aggregated NGs through MADDPG reinforce learning and baseline policies are presented in Fig. 4.35. The baseline policy has a constant electricity tariff of \$35MWh. Here, Prosumers in PMP have direct access to the wholesale market assuming that LSE neglects profiteering avenues and furthermore, compliance for electricity pool policies were involved in view of Market Rules for competing regulations and codes of practices.

Two observations were performed where first LSE seek to profit from Prosumers which results in higher electricity price tariff for REM when compared against wholesale price. It

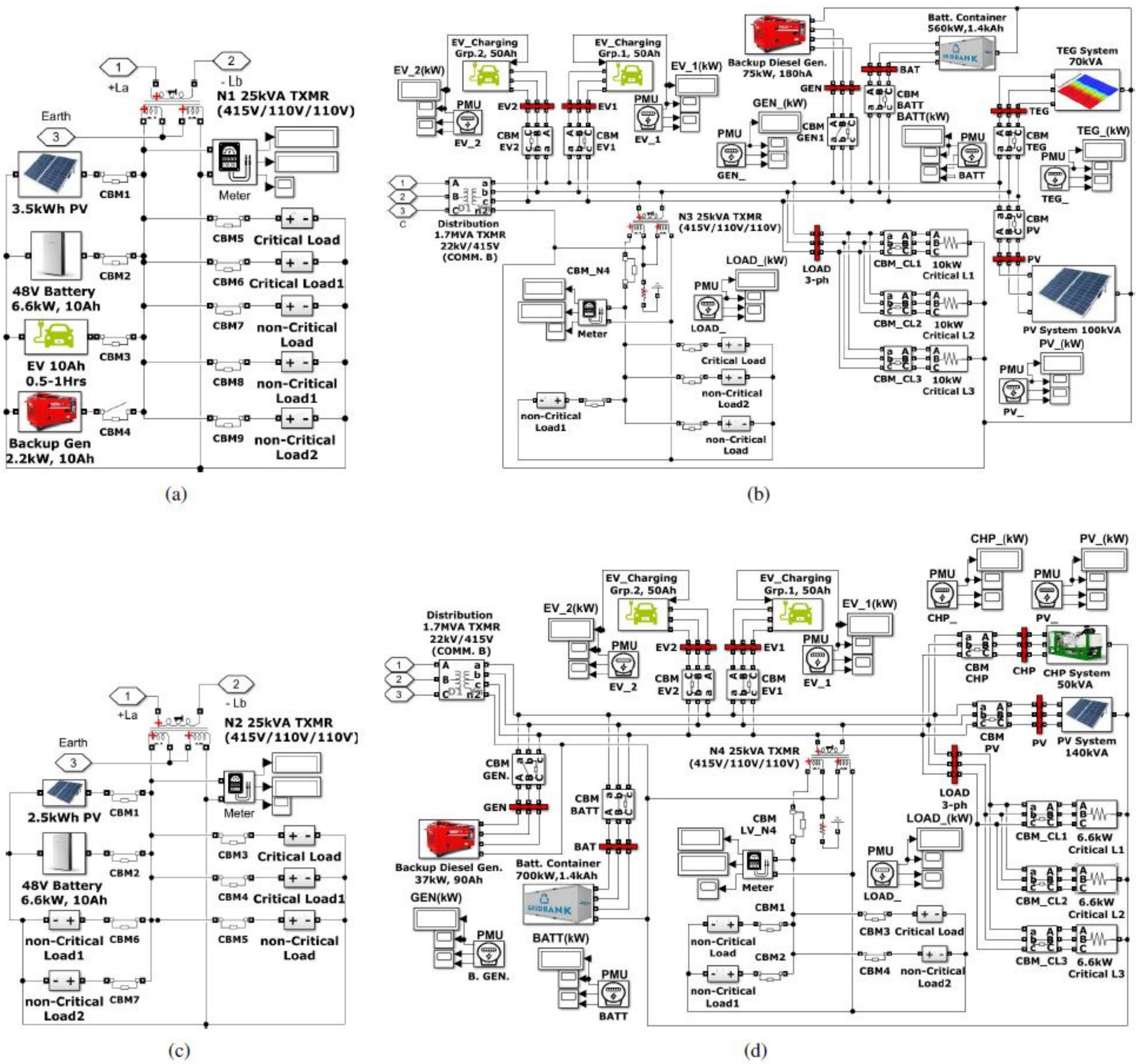

Fig. 4.33 Electrical network configuration and PSPG installation of NG-1 to NG-4 coupled to $22kVAC$ medium-voltage distribution network. (a) NG-1−Single-phase Residential network operating at $220VAC$, $50Hz$, pole mounter XFMR, (b) NG-3−Three- and single-phase Commercial Building (Hospital) network operating $415VAC$ and $220VAC$, $50Hz$ network system, respectively coupled to a lone distribution MV sub-station, (c) NG-2−Single-phase Residential network network operating at $220VAC$, $50Hz$, pole mounter XFMR, (d) NG-4−Three- and single-phase Commercial Building (Industrial) network operating $415VAC$ and $220VAC$, $50Hz$ network system, respectively coupled to a shared distribution MV sub-station.

aims to maximise it profit margin but yet a reduced load consumptions profile generated by the aggregated NGs was observed as compared to the scenario where Prosumers have direct access to wholesale market. Second, in reference to the baseline load consumption policy,

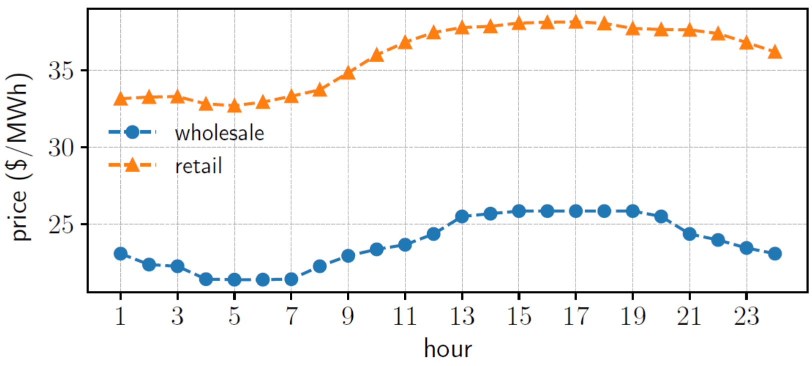

Fig. 4.34 Typical energy prices in retail and wholesale market under MADDPG policy during summer.

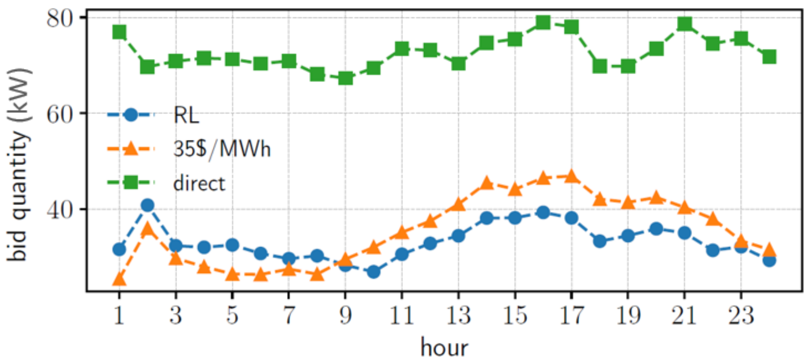

(a) Bidding of energy quantity Bid in summer under MADDPG reinforce learning policy, a baseline policy that endorses constant price of $35*MWh*, and direct access into wholesale market.

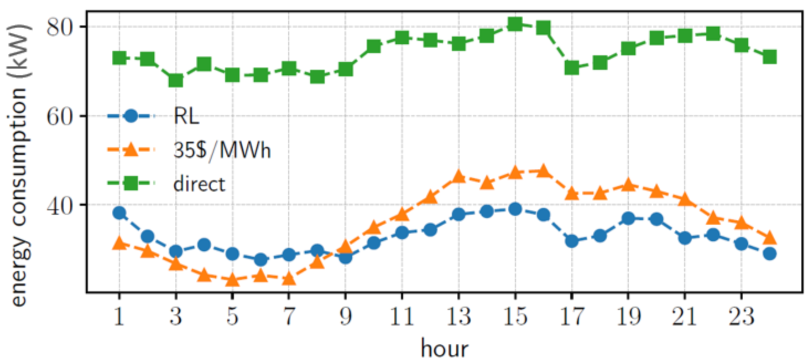

(b) Total aggregated energy consumptions in summer under MADDPG reinforce learning policy, a baseline policy that endorses constant price of $35*MWh*, and direct access into wholesale market.

Fig. 4.35 Wholesale electricity price tariff under different learning policies.

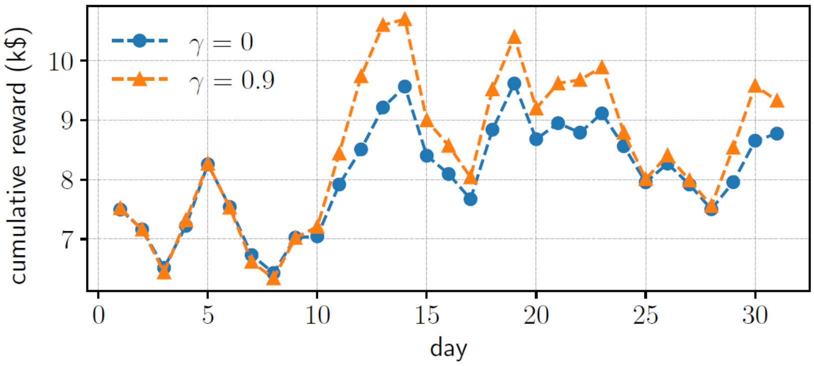

Fig. 4.36 Cumulative reward profile based on two sets of discount factor.

the aggregated Nanogrid's energy consumption capacity rendered by MADDPG reinforce learning has lower variance which maps a smoother demand curve.

Mentioned earlier, considerations in long-term behaviour has better influence on the decision-making processes as compared to short-term in which future reward is neglected. To comprehend better, comparisons were conducted on the cumulative reward using MADDPG reinforce learning with $\gamma = 0.9$ and, $\gamma = 0$ for short-term learning policy as shown in Fig. 4.36. The results demonstrates that learning policy set with $\gamma = 0.9$ has superior reward unit which justifies successful modelling of joint bidding and pricing algorithm as Markov Decision Process problem.

Subsequently, based on the bid quantities and aggregated load consumption capacity, Prosumers have to cooperatively manage the global demand curve by performing strategic load scheduling at individual Nanogrid. In addition, Prosumers must observe TE function constraints that will add value during DSR operations and impede Duck Curve crisis. Here, assuming that the bidding and selling of excess energy can be transacted between PtP, Fig. 4.37 presents auctioning processes at time t; limited to energy transactions listed in Table 4.10. Fig. 4.37a records Nanogrid's excess generations that is ready to be deployed upstream while Fig. 4.37b displays successful bidding and selling of excess generation between PtP at respective time t. All selling electricity prices are rated similar to the electricity tariff in REM. Figure 4.37c profiles the Utility's energy generation managed by DSO where its constraints were bounded by a baseline load of $8.2kWh$, $maxMD$ capped at $62.8kWh$, and preserved $\Delta P_{Deviate}$ less than $3.5kWh$.

In relations to the energy attributes at respective NGs, various self-driven trading models conspired by Prosumers were observed during the bidding and selling of excess energy among PtP. The characteristics of these trading functions are user-specified conditions, generally influenced by Prosumers' expectancies in TE value which allows better profit margins

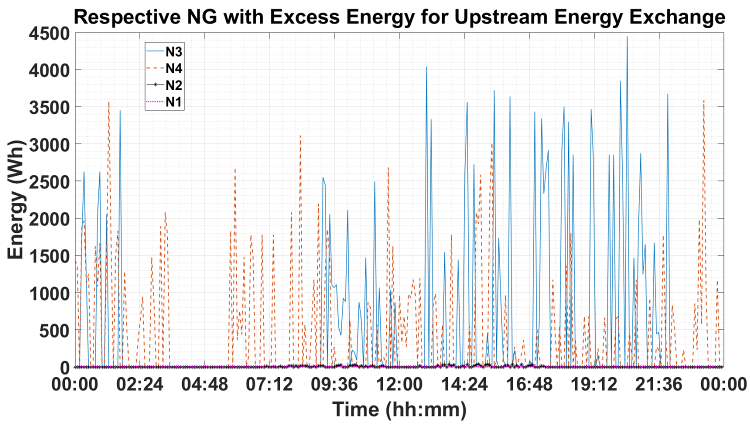

(a) Excess energy capacity available for selling or buying between PtP or DSO.

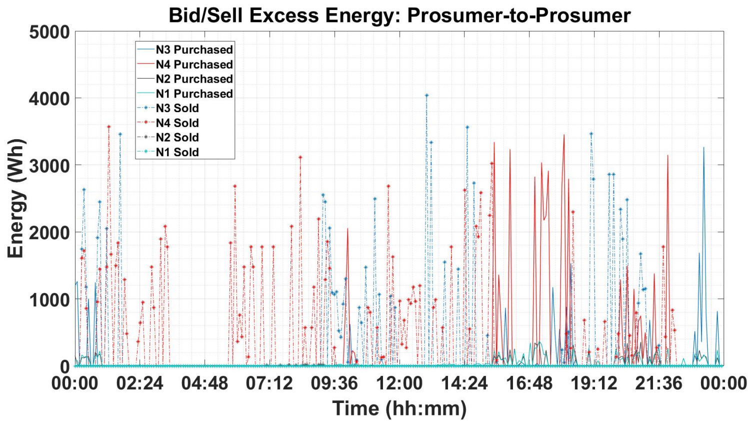

(b) Completed energy sharing transactions between PtP or selling back to Grid.

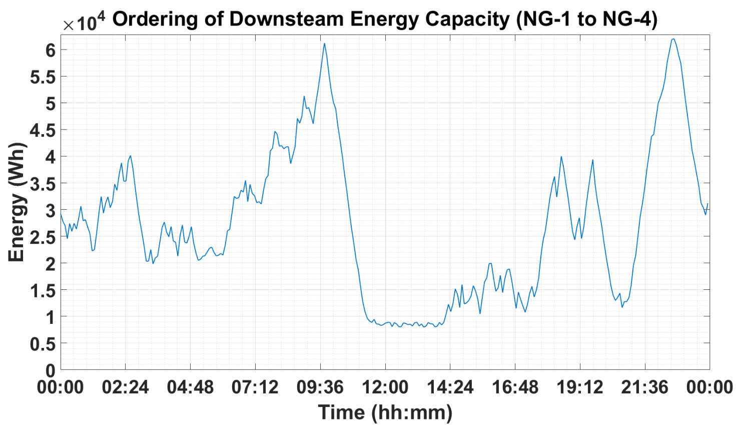

(c) Aggregated load consumption capacity ordered from grid (downstream energy supply).

Fig. 4.37 Exchange of excess energy between PtP in Prosumer Community.

Table 4.10 PtP Permissible energy transaction engagements: read row then column.

	Residential	Commercial	DSO
Residential	no	no	yes
Commercial	yes	yes	yes
DSO	yes	yes	nil

through wholesale market operation and prices. For instances, the operational objectives for respective NGs is as follows:

1. NG-3−targets to model a discharge scheduling strategy from ESS to service peak demand period during high electricity price tariff. It aims to take market dominance by auctioning a marginal cheaper price to lure PCCM Agents' of other neighbouring NGs to opt their purchase of energy from Retailers.

2. NG-4−prioritises operations of global TE function that helps DSOs in scheduling better DSR operations. It suppresses Duck Curve crisis and rectifying confrontations of large energy deviation stress that could violate supply-demand in gaining equilibrium and unit commitment issues at upstream. Hence, it employs a relaxed auctioning strategy at the lowest price rate threshold and hopes to gain return on investment by wagering on incentives payouts.

3. NG-2−adopts an oversized PSPG accompanied with intense load shedding criterion motivated to drive energy usage sustainability and averts from participating in the bidding processes ($<$islanding).

4. NG-1−active participant in the PMP market, seeking opportunities for PtP energy trading sequences. Adopts an undersized PSPG and steep load consumption demographics.

From the above energy management behaviour, DSO spotted the need for policy implementation in market monopolism is important to secure bilateral trading at minimal. In consequence, liberations in PtP energy trading yet to receive great attentions, restricting Residential(s) engaging in direct bidding processes and also discourage NGs from setting-up large PSPG that could impose safety threads in living community. Hence, in practice, DSO and EMO dominate the DSR and market operation, serving as mediators when coordinating PtP energy trading. Whereas, Commercial-based Prosumers are contracted to sell power level at $\min - \max$ thresholds of $<1MW$ and $>10MW$, asserting generation certainty for DSO

Table 4.11 Comparisons of earned profit margin between single-bounded and aggregated energy management approach.

	Single EM ($ per day)	Joint EM ($ per day)
NG-1	9.479	8.725
Incentives Payout	0.482	0.351
LCOE losses	0.028	0.019
NG-2	9.257	8.873
Incentives Payout	0.385	0.401
LCOE losses	0.244	0.181
NG-3	88.646	86.158
Incentives Payout	1.273	2.706
LCOE losses	1.599	1.233
NG-4	85.691	85.829
Incentives Payout	2.572	3.932
LCOE losses	1.828	4.720

to positively schedule unit-commitment problem and constraints to anticipate peak- and off-peak demand loading.

Table 4.11 provides comparative analyses on Nanogrid's profit margins earned based on above mentioned auctioning strategies. NG-3 received favourable profit margin and low operating costs through profiteering from other bidders during the trading processes. Whereas, NG-4 experienced small marginal losses based on small and fixed incentive payouts rated at $\$0.03kWh$ across all TE services. NG-2 managed to reach at a break-even point despite limited contributions in the bidding process and rely energy exchange from grid to compensate LCOE from its PSPG. NG-1 gained superior profit margin as compared to other NGs encompassing incentive payouts and successfully schedule/bid its peak load consumption at low electricity tariff.

4.6.3 Comparisons with other Reinforcement Learning Approach

To evaluate the proposed Prosumer-centric EMS, performance comparisons for Prosumer Community engagements were presented to view managerial superiority in addressing DSR operations and maximising TE values. Despite unique modelling of energy management strategies (*i.e.* unparalleled problem and objective statements), aspirations to trim Prosumer's operating costs based on optimal scheduling of PSPG demand curve curtailment are in common. Prosumers' are driven to gain profiteering incentive payouts and perform shifting/shedding of load consumption capacity into low electricity tariff region while adhering to DSR constraints in real-time. Accordingly, to appraised individual control performances, four evaluation indices are proposed; Market Clearing Incentives (MCI), Penalty Costs imposed on grid participant (PC), Operation Costs Consistency (OCC), and Load Shifting Factor (LSF).

$$MCI = \frac{\sum_{i=1}^{10}(Profit_{bid} + Incentive_{grid})(t,i)}{10} \tag{4.112}$$

$$PC = \frac{\sum_{i=1}^{10}(Penalty_{grid} + LCOE_{loss})(t,i)}{10} \tag{4.113}$$

$$OCC = \sqrt{\frac{\sum_{i=1}^{10}\left(cost(t,i) - \frac{\sum_{i=1}^{10} cost(t,i)}{10}\right)^2}{10}} \tag{4.114}$$

$$LSF = \min\left(\frac{shifted_{load}}{total_{load}}(t_{1hr},1),\ \dots,\frac{shifted_{load}}{total_{load}}(t_{1hr},10)\right) * 100\% \tag{4.115}$$

where i refers to the number of iterations performed by the discrete computation at time, t. OCC quantifies solution consistency by weighing operating costs standard deviation at respective time t intervals. PC computes the total costing for penalties (violations) submitted by Utility at time t. LSF measures the load consumption capacity shifted at time t_{1hr} for an hour. Smaller LSF depicts greater conservation of Prosumer(s) energy usage lifestyle, and MCI evaluates the total of profit margin and incentives received at time t (including PSPG LCOE revenues).

Hierarchical Energy Management System

Peigen Tian [244] proposes an energy management system based on hierarchical status (HEMS). It conducts a two-level hierarchical optimisation approach at distribution level to administrate Prosumer Community operations. The hierarchy is separated into two phase optimisation; *(i)* forecast day-ahead PSPG output generation, schedules charging and discharging power capacity for ESS, and load demand curve based on $1hr$ time intervals. In addition, optimal power exchanged at PCC were deduced, monitoring power generated from upstream generators and Community's PSPGs. *(ii)* perform mixed-integer linear programming (MILP) to solve multi objective TE functions defined in Chapter 4.4.2 and 4.5.1 with demand-side constraints. Linearised approximation is fused into modelling the objective function to achieve operating constraints that are implicit.

Table 4.12 Performances of different EM methodologies against proposed on DSR operations.

	Proposed			
	NG-1	NG-2	NG-4	NG-3
Ops. Costs ; OCC	\$8.725 ; 1.591	\$8.873 ; 1.858	\$85.829 ; 2.267	\$86.158 ; 1.772
PC ; OCC	\$0.019 ; 0.661	\$0.181 ; 0.348	\$4.720 ; 0.369	\$1.233 ; 0.535
LSF	5.629%	4.138%	5.038%	3.812%
MCI ; OCC	\$0.773 ; 1.032	\$0.565 ; 0.579	\$4.582 ; 1.265	\$3.721 ; 1.186
	HEMS [244]			
	NG-1	NG-2	NG-4	NG-3
Ops. Costs ; OCC	\$8.943 ; 4.104	\$9.004 ; 3.726	\$86.117 ; 3.883	\$86.749 ; 3.274
PC ; OCC	\$0.397 ; 3.161	\$0.541 ; 2.926	\$4.828 ; 3.374	\$5.162 ; 3.145
LSF	21.736%	15.288%	19.638%	16.825%
MCI ; OCC	\$0.894 ; 2.590	\$0.726 ; 2.342	\$3.638 ; 2.689	\$4.221 ; 2.911
	SSEMS[245]			
	NG-1	NG-2	NG-4	NG-3
Ops. Costs ; OCC	\$8.842 ; 1.240	\$9.047 ; 1.536	\$86.265 ; 1.219	\$86.769 ; 1.681
PC ; OCC	\$0.054 ; 0.728	\$0.318 ; 0.819	\$4.669 ; 0.743	\$1.382 ; 0.725
LSF	6.522%	4.614%	4.895%	4.254%
MCI ; OCC	\$0.704 ; 0.811	\$0.497 ; 0.725	\$3.884 ; 0.870	\$3.176 ; 1.132

Scenario-based Stochastic Energy Management System

Jingshuang Shen [245] proposes a scenario-based stochastic energy maangemtnt system (SSEMS) for Prosumer Community operations. It utilises and consider electricity pool market when scheduling its shiftable loads to maximise profit margin. A two level stochastic optimisation approach was employed to mitigate uncertainties and risk-constrained elements instigated from integrated PSPGs. The first level gathers historical information on economic operation scheme based on the forecasted data using deviation compensator. While, the second level solves scheduling of shiftable load units in real-time using Monte Carlo scenario-based. It also suggests to infuse risk management into formulating objective functions using conditional values to reduce risks of misinterpreted profit margin. The formulation in defining maximum profit margin during operation defined in (4.69)−(4.70) will be replaced in accordance to [245].

Performance Evaluation Results

Table 4.12 compares the energy management performance between the proposed Prosumer-centric maximising TE value against HEMS and SSEMS.

Results attained in using HEMS shown detrimental impacts in solving optimal operating costs due to weak competencies in containing large multi-constraints based on discrete-time search space when using MILP. Furthermore, in LSF, the results has shown unsatisfactory value as the algorithm focuses on elevating operating cost at an expense of shedding high percentage of online shiftable loads. It provides sub-optimal solutions in rescheduling shiftable loads given at a larger timespan of $1hr$ causing its load capacity to recede. The proposed MILP shows weakness in cooperative optimisation which impose high penalty when mitigating demand-side constraints. It fails to adhere ramping rate limit constraint, $\Delta E^{deviate}$, and Duck Curve crisis becomes apparent causing propagative violations in other TE functions. Nevertheless, to improve performance index, author could introduce cooperative strategies into MILP as suggested in [246] where predictive control model is incorporated to better solve DSR operations using rewarding schemes.

In view of SSEMS performances, the attained results are comparable against proposed due to its large continual search space in generating numerous scenarios for uncertain parameter representations. It employs Latin hypercube sampling technique which reduces algebraic computation time without compensating resolution of the optimised results. However, the suggested risk management model proposed a heavily penalised factor on electricity price market to compensate weak forecasting of uncertainties under the normal distribution curve. In consequence, quantification of profit margin is guaranteed despite changes in variability.

4.7 Findings

A proposed clustering technique, expectation-maximisation Gaussian mixture model, ciphers Prosumer(s) in a Community based on their energy attributes. The algorithm has successfully provide informative information for Prosumer(s) in monitoring their energy contributions in the distribution network and how they fair against others. Likewise, aggregators also gained better jurisdictions in scheduling clusters' with high excess generation and high load consumption capacity to compensate each other. Aggregator is tasked to serve as a secondary DERMS operator at a Community level, where its energy management intelligences are fixed based on a specified energy attribute. Aggregator required to identify partnering clusters and procure a communal solution that could benefit Prosumers in respective cluster.

In the TE management, a self-directed nano-biased Prosumer-centric EMS is proposed to facilitate optimal utilisation of Prosumers' PSPG against load consumption capacity and electricity price tariffs. It fuses decentralised demand-side operating constraints into local TE function while interoperating Prosumers' energy usage interests. Furthermore, Prosumer's involvements in the REM is also considered when modelling the proposed control intelligences. Here, the Prosumer-centric EMS employs Q-learning reinforcement learning approach to solve for optimum scheduling of PSPG and power exchange capacities, and provides BTM BERMS solution for Prosumer at low-voltage level based on individual subscribed business proposal and services. The Q-learning algorithm, centralised critic policy, ciphers local energy attribute based on strategic scheduling of PSPG operations and local controllable load. Whereas, in the joined bidding and pricing of electricity price in REM, it uses MADDPG due to its decentralised critic policy that provides CDL relations. Results deliver positive and comparable energy management performances when benchmarked against other methodologies based on the proposed aggregated Prosumer Community network.

4.8 Summary

In this chapter, realisations in Prosumer Community engagements for transactive managerial proceedings serve as a viable concoction when employing aggregators to deal with decentralised demand-side operating constraints and meeting Prosumers' energy business model and PSPG utilisation interests. Having high penetrations of DERs at low-voltage level, generation companies are exponentially faced with unit-commitment uncertainties which causes difficulties in coordinating demand-supply equilibrium. The demand load curve profiles are no longer predictive and upstream energy generations from distribution network are constantly causing Duck Curve and baseline load crises. Hence, to mitigate such predicaments in securing power quality, DERMS, and DSR operations while maximising TE values, Prosumers are offered with BTM DERMS proposal governed by aggregators to bring DSR managements and optimum local operating costs closer to the low-voltage level. Such proposal relief DSO-TSO from orchestrating nano-manage avenues for individual Prosumer and focuses more as a policy maker that relaxes competitive-playing electricity market and establish congestion management.

DSO-Aggregators need to rethink new innovations that allow managerial proceeding to be conducted from the top (primary-side distribution network) and yet having full appreciation on Prosumers' energy attributes. Therefore, this chapter proposes two avenue in gaining full access into demand-side management despite liberating Prosumers in attuning their energy attributes based on individual socio-economical interests. It involves clustering of Prosumers into a Community based on their energy attributes for better demand curve jurisdiction and designing a Prosumer-centric EMS that comprehends operating constraints and also maximising TE values.

However, potentials in energy market monopolism can arise during bidding in REM. Prosumer(s) are liberalised to model their constraints requirements based on individual interests causing MADDPG learning processes to be blinded and lead to ill-defined competition rules. Hence, DSO-TSO as policy maker, need to revise Market Ruling in REM by introducing new policies and regulatory to ensure Prosumer's interests when auctioning is transparent to create a competitive trading environment for all energy actors.

Chapter 5

Local Protection Relay System for Low-Voltage DER Installation

This chapter proposes a real-time solution for in-house OMS that diagnose and isolate fault interruptions materialised from local PSPG. The idea is to bring outage analysis closer into the low-voltage level where high penetration of BTM DERs are installed. Rather than being used as a management function, it serves more as an outage protection system for local use (*i.e.* Nanogrid EPS domain) that can help aggregators in Prosumer Community power distribution planning. The proposed controller is not only limited to detect local fault intrusions but also isolating Nanogrid to operate in island mode when fault transpired from upstream (*i.e.* Utility). Such implementation provides an add-on service into existing ADMS for low profile building operators to monitor on-going isolation processes targeting a specific faulted PSPG autonomously. It relieves RDSO from ADMS complications and intense search space computations when pinpointing fault source contributed by BTM PSPG.

5.1 Problem Descriptions

Having BTM DER installations at low-voltage level, service interruption due to weak ride-through compliance or undetected high-impedance fault crisis can propagate distribution network to collapse. Hence, despite maturity in modelling TE system and management, efficient DSR operations and power quality ancillary services, and reserve & wholesale market participation, realisation towards accrediting early detection by localising and profiling fault crises in Nanogrid need further recognitions. It is advantageous to both Prosumers and aggregator to adopt decentralised Outage Management System (OMS) with early fault detection capability to isolate PSPG in times of fault crises before it propels upstream and affects the integrity of distribution network even during blackstart.

Favourable methodologies in relations to diagnosing fault interruptions transpired in the distribution network have shown significant advancements. Superior control features in repressing fault crises and method in profiling fault attributes using heuristic algorithms are common avenues in transacting restoration and isolation proceedings as suggested in [220–222]. However, employment of such approach may not be suitable when dealing with a search space that aggrandises proportionally to Prosumer existences. Worst, it could potentially developed into malicious unified modelling of objective statements that will conceive divergence [223, 247]. Therefore, encompassing fault managements in Nanogrid perspective provides better jurisdiction towards preceding fault interruptions as it relieves aggregator and accredit Prosumer to coordinate local fault episodes locally.

5.2 Contributions

Prosumers can contribute into the ADMS operations (*i.e.* OMS) by adopting the proposed fault protection relay system designed to mitigate fault events that could transpire frequently when operating these BTM DERs. Fault infiltrations are inevitable when dealing with PSPG−inverter malfunction causing frequency synchronisation issue at PCC or fault mishaps induced by anomalous current or voltage transients [248, 249]. The classical approach in detecting fault current is commonly expressed through predetermining the phase current magnitude threshold and assessing its phase-shift deviation factor using Phasor Measurement Unit (PMU). These fault qualities are commonly referred as fault level described in MVA (nominal voltage into fault current ratings) or short-circuit current, I_{SC} (current rating at secondary-side divide network impedance). The advantage in adopting MVA method; *(i)* does not need to recalculate impedance ratings for one voltage to another, *(ii)* forgoes the need to select and convert a common MVA base, *(iii)* uses whole number when doing computation hence providing a more deterministic identification in fuzzy system (avoid transitional zone). Till to date, prepositions for fault diagnostic analysis involves detecting, identifying and locating fault transients. With technological advancement, fault analysis have exploits various technique such as follows:

- *Signal processing & feature extraction techniques* to amplify accuracy resolution and accelerate sampling rate capabilities.

- *Utilising novel recording and sensory devices* to measure factual data collections and remote monitoring.
- Deploy *wide-area coverage communication network & Cloud data storage* for data transfer and computational.
- Adopting *Heuristic algorithm, them being supervised or unsupervised* techniques to cipher multi-objective domains in decentralised or centralised architecture.
- Increase awareness in *special class fault*; High-impedance or arc-fault.

From synthesising above-mentioned pointers, a customised Nanogrid fault diagnostic algorithm is proposed uniquely for Prosumers engagements. A revised Directional Overcurrent Current Relay (DOCR) devise is redesigned to serve as a protection mechanism in resolving fault interruptions developed locally or externally in reference to PCC. It innovates to exploit Fuzzy Logic (FL) intelligent system and create knowledge from line-current magnitude transients, symmetrical-sequence components, and network's relative phase angle deviations to interpret fault synopsis.

5.3 Proposed Fault Diagnostic Framework

Fig. 5.1 illustrates the workflow of proposed Fuzzy Logic Directional Overcurrent Current Relay (FL DOCR) in diagnosing fault attributes. The FL DOCR control operations is divided into four phases: *(i)* initiate communication and data acquisition with Frequency Disturbance Recorders (FDR) which is coupled before the circuit breaker of each individual PSPG and devise coupled at Nanogrid PCC, *(ii)* compute the six Conditional Correlate Coefficients (COC), δ_0-δ_5, and assigned to FL as inputs for fuzzification and create FL expert knowledge library, *(iii)* execute FL decision builder to decompose input into output report stating fault identity and current directional flow, and *(iv)* trigger respective circuit breakers to isolate faulted region.

5.3.1 Data Acquisition and Feature Extraction Processes

The engagement of FL DOCR is heavily dependent on data acquisition processes involving rate of sampling and resolution of data sensitivity. It is a data driven operating model where the output performances in profiling fault attributes synchronises with data acquisition from PMU and FDR. Utilising the proposed Nanogrid Area Network mentioned in Chapter 2.4.3

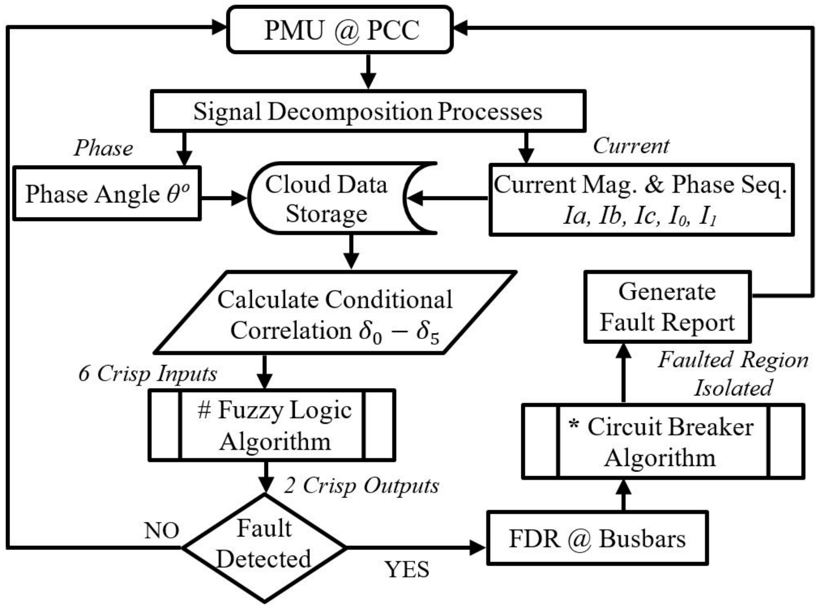

Fig. 5.1 Workflow of the proposed control sequences for FL DOCR.

and Azure IoT edge device, PMU and FDR communication connection will be established seen in Fig. 5.2. It aims to create a single client host communication between Frequency Monitoring Network (FNET) [250] and Azure IoT cloud to create a FL DOCR module that exchange real-time data logging and send command control to actuators (circuit breaker) for execution. FNET is a separate cloud domain that is to design at a low cost generally to serve as a deployable wide-area frequency measurement system with high dynamic accuracy. It employs high resolute e-corder sampler to perform definite preprocessing aptitudes when decoding sampled signals into digital. When dealing sensitive frequency-based data acquisition sampling rate, such as signal processing exertions, FNET deemed to have greater superiority in extending into a wide-area network system when compared to Azure IoT cloud. Despite running FL DOCR operations in two separate wide-area domains (Azure IoT and FNET), efforts in integrating them at shared cloud point is proposed to create as single host client that is stackable for other wide-area systems under the compliance to IEEE C37.118 communication standards. FNET is programmed to record measurements of line current magnitudes, and phasor readings at respective symmetrical components to cipher phase-shift angles and frequency deviations in sync with GPS-synchronised timestamps. PMU is solely designed to have greater sampling rate and enhanced filtering ability that enables higher order harmonics measurements as compared to FDRs (up to 49^{th} order).

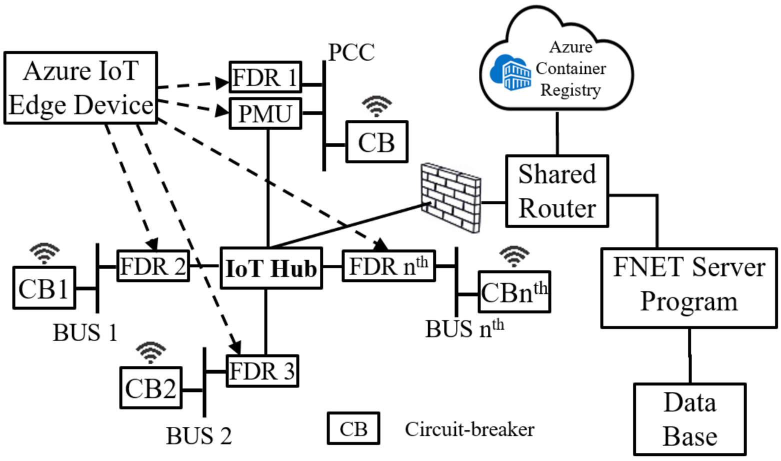

Fig. 5.2 Hybridised FNET & Azure IoT cloud for wide area network with low recording discrepancies and high sampling rate.

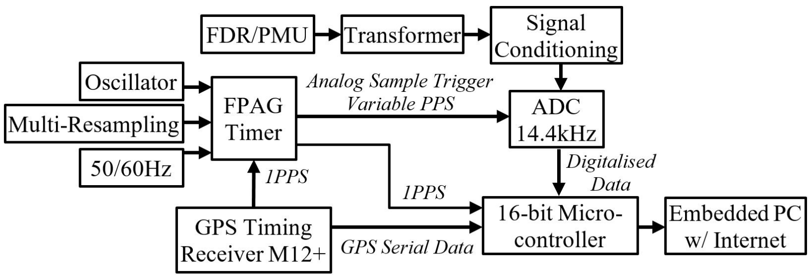

Fig. 5.3 GPS-based timing subsystem.

The design architecture of FDR and PMU are typically equipped with a Digital Signal Processor (DSP) rated with very high oscillator frequency, serve as the computational building blocks in sampling and converting analogue signals into digital (ADC) interpretations. In addition, a field programmable gate array (timing module architecture), is coupled to execute precision sampling timestamps that synchronises with the received data between GPS and ADC signals. Fig. 5.3 demonstrates the framework of GPS-based timing subsystem programmed to sample 1 pulse per second (1PPS). The 1PPS signal is then distributed to time microprocessor in propagating trigger pulses for ADC.

Subsequently, the ADC signals are quantise using Discrete Fourier Transform (DFT) algorithm to recast into continuous-time signals—equally sampled discrete-frequency data sets using moving average algorithm. The resultant magnitude and phase angle signals estimation is as follows:

$$f(t) = \frac{a_0}{2} + \sum_{n=1}^{\infty} a_n \cos(n\omega t) + b_n \sin(n\omega t) \tag{5.1}$$

$s.t.$

$$\begin{aligned} |H_n| &= \sqrt{a_n^2 + b_n^2} \\ \angle H_n &= atan\left(\frac{a_n}{b_n}\right) \end{aligned} \tag{5.2}$$

where $a_n = \frac{2}{T}\int_{t-T}^{t} f(t)\cos(n\omega t)dt$; $b_n = \frac{2}{T}\int_{t-T}^{t} f(t)\sin(n\omega t)dt$ and $T = \frac{1}{fundemental\,freq.}$

The execution commands for circuit breakers will be controlled by Azure IoT Edge device.

5.3.2 Fuzzy Logic Architecture

To highlight deployment applicability for industrial-based controller, FL implementation serve as a promising solution in deciphering and apprehending fault interruptions during Nanogrid operations. Here, modelled FL DOCR algorithm ensure versatility in detecting fault interruptions for both DC-based or AC-based PSPG operations. Fig. 5.4 presents the Fuzzy Interface System that is equipped with fuzzy reasoning algorithm. Furthermore, an aerial perspective of the fault's attributes contains autonomous diagnostical commands to aid Nanogrid regain its stability.

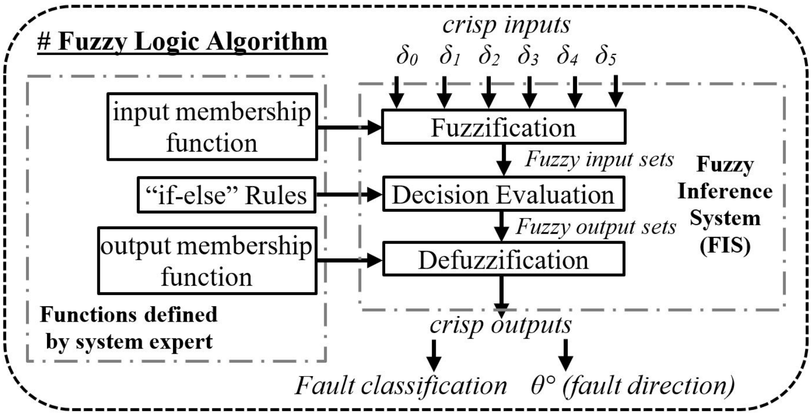

Fig. 5.4 Architecture of the engaged Fuzzy Logic controller.

In reference to Fig. 5.4, the Fuzzy Inference System (FIS) comprises of three sequential computations; fuzzification, fuzzy rule evaluation, and defuzzification. Following explains each of their processes.

Fuzzification

Fuzzification is a processes that translates crisp inputs (real integer) of FL input into fuzzy input, ordained by the membership function peculiarity. By reserving descriptive labelling

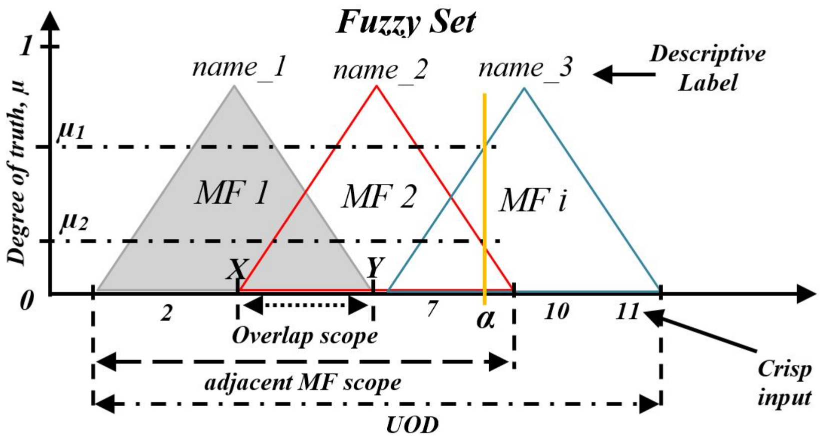

Fig. 5.5 Designing of fuzzy sets and respective complements.

and compositional dimensions for respective Membership Functions (MF), labelled fuzzy input sets are joined based on the relativity construe of individual crisp input in contrast to respective MF's domain. Using overlap trapezoidal-shaped MFs as shown in Fig. 5.5, the crisp input's degree of truth is weighed against its bearing peculiarity along the Universe Of Discourse, UOD. UOD is strategically modelled with predefined demarcations that sets regional regions using multi-level MFs to associate corresponding representations. Each of the multi-level MFs will infer affiliated 3ϕ short-circuit current magnitudes. Following suggests guidelines in defining input MFs of a fuzzy set:

$$\text{overlap ratio} = \frac{overlap\ scope}{adj.MF\ scope} \leq 1 \tag{5.3}$$

$$\text{overlap robustness} = \frac{\int_X^Y (\mu 1 + \mu 2)dx}{2(Y - X)} \leq 1 \tag{5.4}$$

Fuzzy Rule Evaluation

With fuzzified input sets, decision-making processes are then administered by employing Mamdani fuzzy rule-based system defined in (5.5). Fuzzy evaluation can be regarded as the expert knowledge that able to perceive any applied applications. Having the fuzzified input set and labelled MFs, the system then proceed in mapping out respective linguistic terms based on the fittest active rule. Each of the active rules contains 'if-else' conditional statement as knowledge embodiment providing reasoning evaluations to infer degree of truth. Based on the intensity of truth, the input sets are assigned into respective labels. The 'if' statement is referred as the elastic condition that captures knowledge while 'then'

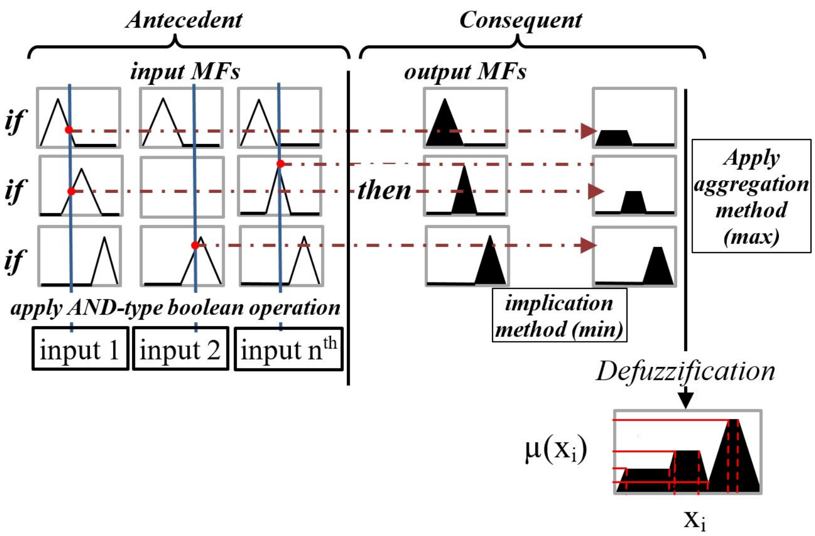

Fig. 5.6 Employing fuzzy rule evaluation on the fuzzy input sets.

proffer a conclusive linguistic variable. The labelled input sets undergoes valuation processes that employs Boolean operator *AND* to infer consequence through weighing the minimum intersection defined as follows:

$$MAMD(x,y) = \bigvee_{i=1}^{n} (A_i(x) \& B_i(y)) \tag{5.5}$$

where x is A_1 or A_2 and y is B_1 or $B_2,\ldots$.

$$\mu_{A \bigcap B} = min(\mu_A(x), \mu_B(x)) \tag{5.6}$$

where $\mu_(A,B)$ is the intersection points from $2MFs$.

Defuzzification

In the defuzzification process, it transpose fuzzy output/consequent into crisp output sets. It suggests Center of Gravity *COG* approach when averaging out a single crisp output value from the aggregated MFs. The output MFs are assigned to being singleton, decreasing computational intensity on the micro-processor. (5.7) and Fig.5.6 demonstrates how the singleton-based *COG* computes the crisp output value.

$$COG = (\sum_{i=1}^{n} x_i * \mu(x_i)) / \sum_{i=1}^{n} \mu(x_i) \tag{5.7}$$

5.3.3 Formulating Conditional Correlation as Crisp Inputs

Computation of linguistic crisp inputs, δ, are defined to represent the fault interruption attributes based on the measurements recorded by PMU. The formulated crisp inputs are designed to engender fault uniqueness between symmetrical and unsymmetrical fault paradigm. Customarily, in Shunt fault events creates a low impedance path causing high inrush current at respective affected lines. Furthermore, as FL DOCR is installed at low-voltage network, a uniform fault level is made suitable for all NGs regardless of its PSPG installation size as the short-circuit current is governed by pole transformer at full load. Therefore, the proposed correlation coefficients, δ_0-δ_4, expresses fault current magnitude and amplify various fault discreteness in relations to the sampled single-phase current profile. Similarly, in a three-phase Nanogrid network connecting to the medium-voltage level, the short-circuit current can be measured based on the sub-station transformer operating at full load. δs in equations (5.8) and (5.12) addresses individual tasks in segregating fault composites into detection and classifications.

$$\delta_0 = \begin{cases} 1, & MVA_{grid} \geq V_{norm} * I_{fault}\,(surge) \\ 1, & \leq 0.7 * I_{ref}\,(sag) \\ 0, & \text{otherwise} \end{cases} \tag{5.8}$$

$$\delta_1 = \frac{I_a - I_b}{\max(I_a, I_b, I_c)} \tag{5.9}$$

$$\delta_2 = \frac{I_b - I_c}{\max(I_a, I_b, I_c)} \tag{5.10}$$

$$\delta_3 = \frac{I_c - I_a}{\max I_a, I_b, I_c} \tag{5.11}$$

$$\delta_4 = \frac{0.333[I_a + I_b + I_c]}{0.333(I_a + [\exp^{j2\pi/3} * I_b] + [(\exp^{j2\pi/3})^2 * I_c])} \tag{5.12}$$

where: I_a, I_b, I_c is the single phase current magnitude

δ_0 denotes the presence of fault being detected [0,1] in the electrical network. δ_1-δ_3 expresses which of the three-phase lines (*i.e.* L_A, L_B, and L_C) is faulted or any other line combinations. Based on the magnitude intensity contributed by the respective coefficients, it flags faulted lines. δ_4 reveals the existence of line to ground fault through sequence components interpretations. Subsequently, using Fortescue theorem, it estimates the fault current directional flow/migration (*i.e.* upstream or downstream). The polarity of shifted phase angle induced by fault can be acquired using synchrophasor−current potential differences at the installed busbar. In reverse or upstream fault, F_{rev}, the fault current, I_{rev}, flows from the grid to the lowest potential point:

$$I_{rev} = V_{grid}/V_{G\_F} \tag{5.13}$$

where $_{G\_F}$ denotes grid to fault point. Likewise, for downstream or forward fault, F_{fwd}, fault current, I_{fwd}, flows from source to the lowest potential point:

$$I_{fwd} = V_{grid}/V_{S\_F} \tag{5.14}$$

where $_{S\_F}$ expresses generation source to fault. In practise, impedance ratings of Z_{G_F} and Z_{S_F} are not known. Hence, taking the assumptions that transmission lines are purely inductive, the impedance value found in (5.13)−(5.14) are typically negative imaginary values in the current phasor diagram [251]. Therefore, pre-fault current, I_{pre_F}, is expressed as follows:

$$I_{pre\_F} = (V_S - V_{grid})/Z_{S\_G} \tag{5.15}$$

where $_{S\_G}$ refers generation source to grid and therefore, the pre-fault current detected by circuit breaker, *CB*, with reference to I_{rev} is:

$$CB_{trigger} = I_{pre\_CB,rev} = I_{pre\_F} - (V_{grid}/Z_{G\_F}) \tag{5.16}$$

and pre-fault current with respect to I_{fwd} is:

$$CB_{trigger} = I_{pre\_CB,fwd} = I_{pre\_F} + (V_{grid}/Z_{S\_F}) \tag{5.17}$$

On the contrary, current phasor diagram, $I_{pre\_CB,rev}$, contributes a positive magnitude whereas, $I_{pre\_CB,fwd}$, yields a negative magnitude defined in (5.16)−(5.17). An additional crisp input, δ_5, is introduced to apprehend fault current directional flow using phase shift deviation defined in (5.18). A negative δ_5 is reverse fault direction and vice versa.

$$\delta_5 = \theta_F - \theta_{pre\_F} \tag{5.18}$$

Table 5.1 Crisp inputs for input membership functions, $\delta_0 - \delta_5$.

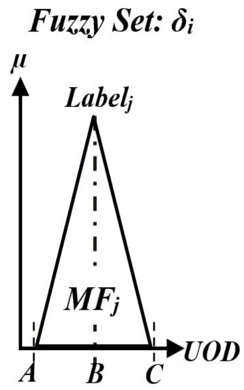

MF_j	$Label_j$	A	B	C
Fuzzy Set: δ_0				
1	No Fault	-0.1	0.0	0.1
2	Fault	0.9	1.0	1.1
Fuzzy Set: $\delta_1 - \delta_3$				
1	Low	-1	-0.56	-0.1
2	Medium	-0.15	0.125	0.4
3	High	0.1	0.55	1.0
Fuzzy Set: δ_4				
1	Low	-2.0	0.1	1.0
2	High	-0.01	1.0	3.0
Fuzzy Set: δ_5				
1	Negative	-180	-90	0
2	Positive	-1e-1	90	180

5.3.4 Modelling of Input Membership Functions and Decision Rules

The modelled MFs that are strategically placed along UOD spectrum, demarcated into sections to represents fault levels, *MVA*, of Nanogrid. Individual MFs will then be labelled to characterise fault current intensities which later used to correlate the calculated *COCs* during the fuzzification process. Subsequently, development the expert fuzzy-knowledge is proposed to detect fault interruptions and provide definite categorisation of fault genres based on the truth values of input membership. Details given in Table 5.1, mixtures of dual- and triplet-level fuzzifiers were employed into designing the input MFs for respective crisp input.

Subsequently, those fuzzified antecedents undergoes a decisional evaluation processes to generate a single consequent which corresponds to an output MF. The fuzzy rule uses *AND*-type fuzzy operator for all fuzzified input sets and 'if-then' conditional statement to verify the entire fuzzy set as a successful candidate. Table 5.2 and 5.3 are listed predefined fuzzy rules to cipher fault peculiarity and determine fault current migrations based on the calculated crisp input sets.

If the fuzzified input lingers in-between MF's boundaries (transitional zone), fuzzy overlay reasoning will be activated to cipher fittest assignment to a distinct MF. Therefore, a

Table 5.2 Fuzzy rule evaluations for fault current migrations.

$$\boldsymbol{IF}\ \overbrace{\delta_5}^{Antecedents}\ \boldsymbol{THEN}\ \overbrace{\text{Fault Current Migration}}^{Consequent}$$

No.	δ_5	Fault Current Migration
1	Positive	Forward
2	Negative	Reverse

Table 5.3 Fuzzy rule evaluations for fault classification.

$$\boldsymbol{IF}\ \overbrace{\delta_0 \wedge \delta_1 \wedge \delta_2 \wedge \delta_3 \wedge \delta_4}^{Antecedents}\ \boldsymbol{THEN}\ \overbrace{\text{Fault Type}}^{Consequent}$$

No.	δ_0	δ_1	δ_2	δ_3	δ_4	Fault Type
1	Fault	High	Medium	Low	High	$L_A - G$
2	Fault	Low	High	Medium	High	$L_B - G$
3	Fault	Medium	Low	High	High	$L_C - G$
4	Fault	Medium	Medium	Low	Low	$L_A - L_B$
5	Fault	Low	Medium	Medium	Low	$L_B - L_C$
6	Fault	Medium	Low	Medium	Low	$L_C{}^{\vee}L_A$
7	Fault	Medium	Medium	Low	High	$L_A{}^{\vee}L_B - G$
8	Fault	Low	Medium	Medium	High	$L_B{}^{\vee}L_C - G$
9	Fault	Medium	Low	Medium	High	$L_C{}^{\vee}L_A - G$
10	Fault	Medium	Medium	Medium	Low	$L_A{}^{\vee}L_B{}^{\vee}L_C$
11	High	Medium	Medium	Medium	High	$L_A{}^{\vee}L_B{}^{\vee}L_C - G$

triangular-based pivotal MF is opted to coordinate graphical depiction of fault level capacity expressed by the normalised fault currents, I_A, I_B, I_C *or* I_0, I_1, and also the angle deviations, θ_t, θ_{t-1} from $(t-1)$ to t (t = time when fault is detected).

5.3.5 Proposed Output Membership Function and Defuzzification

The *COG*-based defuzzification processes transpose fuzzy output into crisp values containing fault type and fault current directional flow information. Meanwhile, separated into two output fuzzy sets, the output membership functions provide details on fault attributes and fault current migration. Similar to input, the output MFs undergoes *AND*-type implication method to cipher valid/true consequents.

Whereas, Table 5.4 equates respective crisp output magnitudes for affiliate fault identities while Table 5.5 ordained the directional fault current consequents. To achieve better segregation accuracies, stringent axioms is implemented when designing the output MFs; *(i)* use

Table 5.4 Output membership functions, fault classifier fuzzy set.

Fuzzy Set: Fault Class

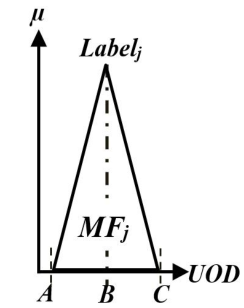

MF_j	$label_j$	A	B	C
1	$L_A - G$	6.5	7	7.5
2	$L_B - G$	4.5	5	5.5
3	$L_C - G$	2.5	3	3.5
4	$L_A - L_B$	63.5	64	64.5
5	$L_B - L_C$	65.5	66	66.5
6	$L_C - L_A$	60	60.5	61
7	$L_A - L_B - G$	76.57	76.87	77.57
8	$L_B - L_C - G$	96.5	97	97.5
9	$L_C - L_A - G$	94.5	95	95.5
10	$L_A - L_B - L_C$	73.5	74	74.5
11	$L_A - L_B - L_C$	82	82.5	83

Table 5.5 Output membership functions, fault current migrations.

Fuzzy Set: Fault Orientation

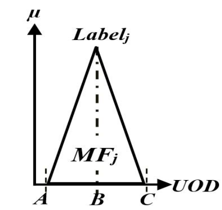

MFj	Labelj	A	B	C
1	Reverse	-180	-90	-1.00E-05
2	Forward	1.00E-06	90	180

triangular-based MF for steady response, *(ii)* have small overlap ratios, and *(iii)* limit UOD spectrum boundaries to reduce data processing glitches. Afterwards, the output fuzzy sets are truncated using min function to trim output MFs to align itself with the degree of truth.

5.3.6 Locating Faulted Region & Circuit Breaker Operation

The computation in localising and isolating faulted regions requires strategical countermeasures as to maximise its appreciations in casting the exact fault location. Extracting faulted current directional flow data at targeted FDRs and PMU, deterministic triggering of specific circuit breakers can be initiated to isolate faulted region as shown in Fig. 5.7. The proposed CB algorithm only implies if the buses of Nanogrid electrical is numbered in a sequential order from left to right. Given its credibility, it is safe to suggest that the Nanogrid PCC will serve as the referencing point against other busbars.

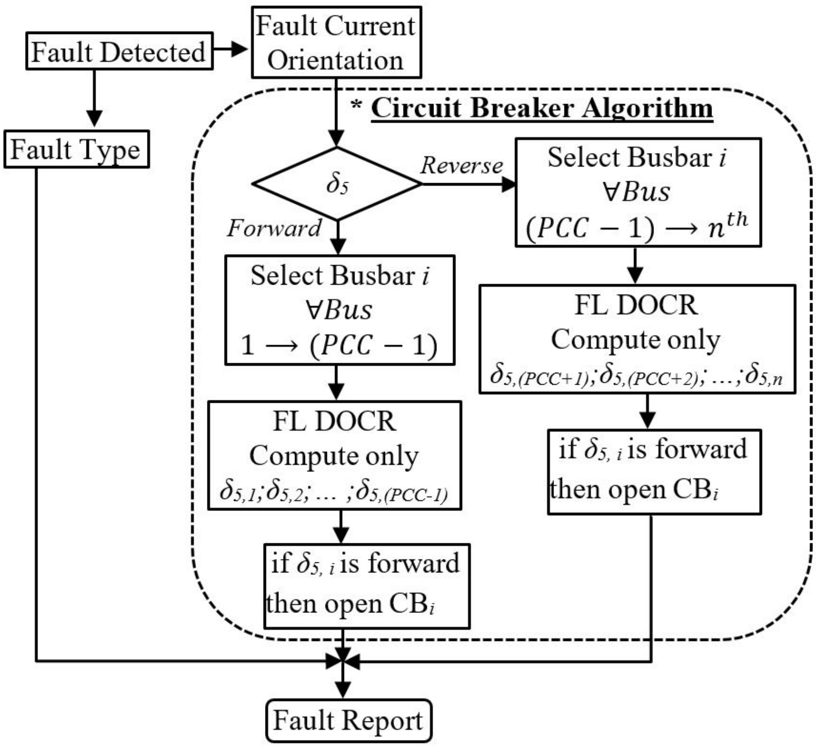

Fig. 5.7 Triggering of circuit breaker to regain network stability.

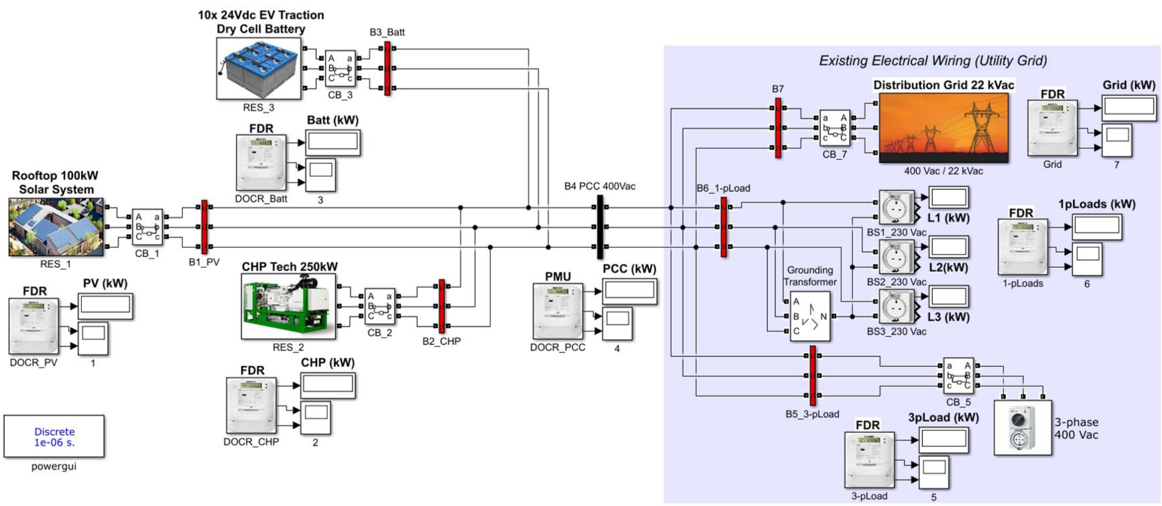

Fig. 5.8 Testbed model of the 7-BUS Nanogrid system, PARKROYAL Hotel, modelled in MATLAB.

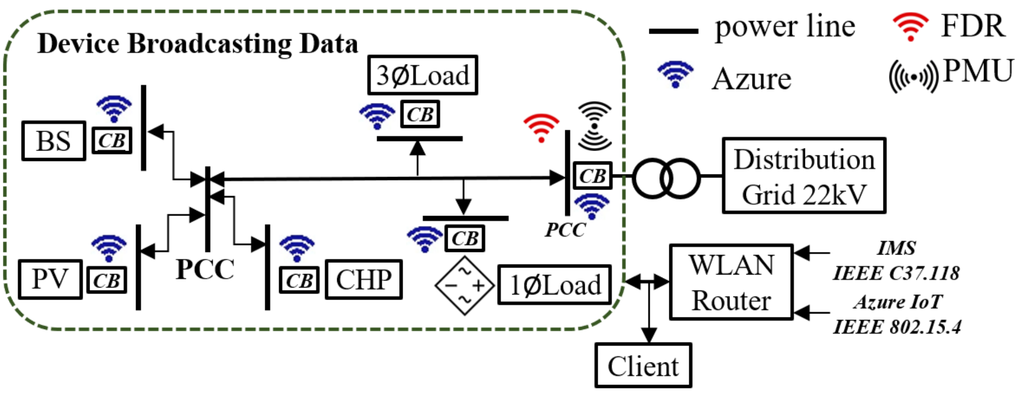

Fig. 5.9 Distribution of communication & networking infrastructure in PARKROYAL Hotel.

5.4 Proposed Testbed Model and Operation Results

A proposed Nanogrid testbed system inspired from Singapore's first eco-friendly hotel, PARKROYAL, presented in Fig. 5.8. The building's demand load consumptions are estimated to consume 30.4% lesser energy as compared against the Environment Sustainability of Building requirements. In the day, having high humidity index, its demand was recorded with an average of $0.85kWh/m^2$ [252]. Table 5.6 lists the installed PSPG in Nanogrid coupled to the $22kV$ distribution network. The demand loads are characterised into two categories; single-phase domestic appliances rated at $230VAC$, and three-phase rated at $400VAC$ for operating heavy rotatory machines (*i.e.* lift, escalator, washing machine).

Fig. 5.9 exhibits the CB control system and communication framework established in Nanogrid. While, Fig. 5.10 displays the overview operational sequence of FL DOCR deployed at every busbar. These two coexisted systems are managed centrally in Azure client server to mitigate fault interruptions and generate a single optimal solution to regain network's stability. The three-phase medium-voltage distribution network is rated at $22kVAC$, $50Hz$, and short-circuit ratio (X/R) of 7. The voltage is then stepped down to $400VAC$ at Nanogrid PCC busbar which then connects PSPG. All PSPG elements are coupled to the three-phase busbar and regulated by individual power inverter−synchronising at $50Hz$. In relations to the single-phase installations, an earthing transformer (zig-zag grounding banks) is coupled. It provides a grounding system for connected appliances with ground current isolation source for zero sequence current.

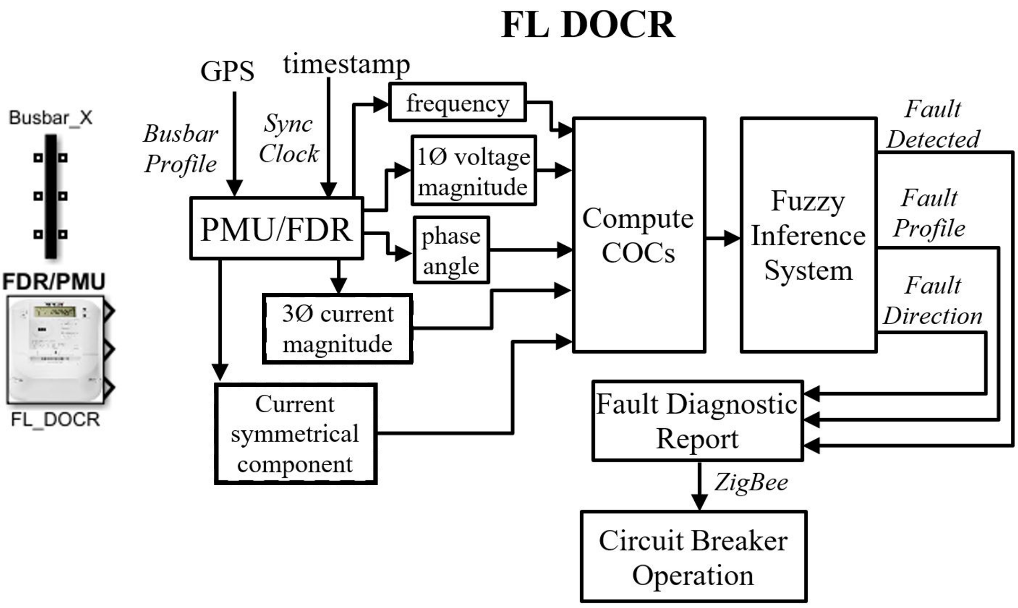

Fig. 5.10 Propose FL DOCR model.

Table 5.6 Equipment ratings and specifications.

Component	Ratings
Grid 2500MVA S.C. level	X/R=7; 22kVAC(RMS); 50Hz
Y-Y Grid XRMR (T1)	1MVA; 50Hz; 400V/22kV
Grounding XRMR	50kVA; 50Hz; 400VAC(RMS)
Photovoltaic System	100kW; 500VDC; 45deg; 1000W/m2
CHP Microturbine	250kVA; 50Hz; 8poles; 575VAC(RMS)
EV Traction Dry Cell Battery	10x24VDC; 150Ah
1x 3-p Load	500kW; 400VAC(RMS); 50Hz
3x 1-p Load	3x10kW; 230VAC(RMS)

5.4.1 Case Study: In Normal Condition

The performance of FL DOCR during Nanogrid operation in normal condition has shown full synchronicity at PCC and respective busbars. The results seen in Table 5.7 presents the readings collected from the proposed FL DOCR system during no fault interruption. Having Nanogrid running at full load capacity and PSPG generating at 0% loading, the short circuit (SC) current, I_F, is rated approximately at 1850A. The short-circuit level serves as a guideline for aggregator to ensure network is not overloaded. Thus, subsequent case studies are programmed to operated at 50% loading of load consumptions.

Table 5.7 Results generated by FL DOCR controller in normal condition diagnosis.

Readings abstracted @ PCC Busbar 4						
Instn. Volt. (VRMS)	t<0.162s: 360VAC ; t>0.163s:400VAC					
THD (%)	1.134					
Exported Power (kW)	$389.39 < P_{DER} < 390.13$					
Symm. Cmpnent. (A)	+Seq: 975,		-Seq: 0.5,		0Seq: 3.09e-7	
Line Magnitude (A)	$Line_A$: 975,		$Line_B$: 975,		$Line_C$: 975	
Phase Angle (deg)	$Line_A$: +30.13,		$Line_B$: -89.93,		$Line_C$: +150.08	
Crisp Inputs	δ_0: 0,	δ_1: 0,	δ_2: 0,	δ_3: 0,	δ_4: 0,	δ_5: 0
Crisp Output	50					
Fault Migration (deg)	Phase Shift: 0deg					
Fault Report	Alarm Flagged: None					
CB Triggered	None					

5.5 Nanogrid Operations in Faulted Conditions

To investigate proposed FL DOCR credibility and performances in providing fault diagnosis proceedings, three proposed case studies were presented. The objective is to analyse FL DOCR responses in early detection during fault interruptions. First, analyses were conducted in detecting and categorising all 11-types of fault intrusions autonomously. Second, random fault injections were generated along Nanogrid electrical network to appraise FL DOCRs' efficiency in localising fault origins. Third, review on optimal placement of FL DOCR units were discussed to curtail installation costs against operational reliability.

5.5.1 Detecting & Classifying Fault Intrusions

Fault injections were introduced at the $22kVAC$ distribution network, inferring that an external fault crisis in generated. Moreover, to address dynamic fault interruptions transpired for operations in coupling AC- and DC-based PSPG, analyses on low and high impedance fault ratings were too executed to ensure versatility in FL DOCRs' performance. In addition, interjections of external noise amplifications were interpolated, simulating data misinterpretations during communication between measuring devices and cloud server. The results presented in Table 5.8−5.11 are observations gathered based on a single deployment of FL DOCR system (both PMU and FDR) embedded at PCC busbar while the remaining busbars were FDR-based FL DOCR. The Nanogrid system was simulated for 10sec with fault initiated at 1.8sec (regain stability after $0.3secs$ due to initial transient) without circuit breaker operations.

Table 5.8 Fault detection and classification for single line-to-ground.

Fault	$L_A - G$	$L_B - G$	$L_C - G$
Ground *ohm*		0.001 - 0.01	
Crip Inputs Fault 0.1*ohms* Std.Deviation: 0.183	δ_0: 1 δ_1: 0.515 δ_2: 0.27 δ_3: -0.865 δ_4: 0.395 δ_5: -15.8 t=14.3° (t-1)=30.1° Reverse	δ_0: 1 δ_1: -0.832 δ_2: 0.457 δ_3: 0.375 δ_4: 1.6 δ_5: -10.56 t=19.6° (t-1)=30.1° Reverse	δ_0: 1 δ_1: 0.375 δ_2: -0.831 δ_3: 0.458 δ_4: 1.6 δ_5: -10.52 t=19.6° (t-1)=30.1° Reverse
Crip Inputs Fault 0.1*ohms* Std.Deviation: 0.212	δ_0: 1 δ_1: 0.417 δ_2: 0.275 δ_3: -0.693 δ_4: 2.29 δ_5: -0.83 t=29.8° (t-1)=30.1° Reverse	δ_0: 1 δ_1: -0.78 δ_2: 0.52 δ_3: 0.265 δ_4: 0.395 δ_5: -0.25 t=29.75° (t-1)=30° Reverse	δ_0: 1 δ_1: 0.265 δ_2: -0.78 δ_3: 0.515 δ_4: 0.395 δ_5: -0.2 t=29.9° (t-1)=30.1° Reverse
Crisp Output Detection Classify Accuracy Δfreq.	7.25 0.0244-0.0325s 0.0692-0.0820s 97.89-98.25% 3.286-6.822Hz	5.35 0.0217-0.0381s 0.0630-0.0785s 98.59-99.1% 9.176-14.678Hz	3.45 0.0358-0.0382s 0.0736-0.0801s 98.88-99.25% 10.254-15.14Hz

Conclusively, FL DOCR has acquired 100% success rate in profiling all 11-types of fault genres and also comprehend the fault current migration at PCC busbar. Having identification accuracy resolution begins at 96.67%, with signal-to-noise ratio of approximately 50, FL DOCR conceived the status of fault interruptions within 120*ms* or less. Noticeably, at high impedance fault paradigm, the attained frequency deviations were at minimal. It concludes that those proposed fault detection algorithms that solely depends on frequency response will fail when deploying into a DC-based PSPG. Expectedly, the migration of fault current dictates in reverse orientation where fault current discharges from the grid to PCC busbar. Overall, respective fault peculiarities have reached convergence predefined by FL's expert knowledge and the permutations offered by crisp input magnitudes.

Table 5.9 Fault detection and classification for two line-to-ground fault.

Fault	$L_A - L_B - G$	$L_B - L_C - G$	$L_C - L_A - G$
Ground *ohm*		0.001 - 0.01	
Crisp Inputs Fault 10*ohms* Std.Deviation: 0.189	δ_0: 1 δ_1: 0.319 δ_2: 0.114 δ_3: -0.434 δ_4: 1.1 δ_5: -29.5 t=2.3° (t-1)=31.8° Reverse	δ_0: 1 δ_1: -0.434 δ_2: 0.319 δ_3: 0.114 δ_4: 1.1 δ_5: -29.5 t=2.3° (t-1)=31.8° Reverse	δ_0: 1 δ_1: 0.114 δ_2: -0.433 δ_3: 0.319 δ_4: 1.1 δ_5: -29.5 t=2.3° (t-1)=31.8° Reverse
Crisp Inputs Fault 10*ohms* Std.Deviation: 0.257	δ_0: 1 δ_1: 0.189 δ_2: 0.092 δ_3: -0.355 δ_4: 0.902 δ_5: -0.41 t=31.39° (t-1)=31.8° Reverse	δ_0: 1 δ_1: -0.355 δ_2: 0.189 δ_3: 0.092 δ_4: 0.902 δ_5: -0.41 t=31.39° (t-1)=31.8° Reverse	δ_0: 1 δ_1: 0.092 δ_2: -0.355 δ_3: 0.189 δ_4: 0.902 δ_5: -0.41 t=31.39° (t-1)=31.8° Reverse
Crisp Outputs	25.08	33.15	71.4
Detection	0.02440-0.00320s	0.0218-0.0323s	0.0352-0.0388s
Classify	0.0749-0.0822s	0.0692-0.0768s	0.0776-0.0812s
Accuracy	96.67-97.1%	97.9-98.73%	97.98-98.12%
Δfreq.	6.286-6.822Hz	10.176-14.678Hz	11.254-15.14Hz

5.5.2 Locating Faulted Region & Triggering of Circuit Breakers

Besides detecting and profiling fault's attributes, second case study offers realisations in employing fault current orientations at relevant busbars to command triggering operations of CBs suggested in Chapter 5.3.6. Two distinctive locations were introduced with fault as shown in Fig. 5.11.

Subsequently, integrations of 6 more FDR devices were installed at other busbars to localise fault current directional migrations centered at the PCC busbar. Line-to-ground and line-to-line fault paradigms were the selected, induced at two separate regions, Fault 1 locate at PV system [F1 (PV)] and Fault 2 at 3-phase load [F2 (3Ø Load)]. The motives are to validate FL DOCR system in locating fault origins and trigger relevant CBs autonomously in

Table 5.10 Fault detection and classification for line-to-line fault.

Fault	$L_A - L_B$	$L_B - L_C$	$L_C - L_A$
Ground *ohm*		0.001 - 0.01	
Crip Inputs Fault 0.1*ohms* Std.Deviation: 0.223	δ_0: 1 δ_1: 0.352 δ_2: 0.275 δ_3: -0.626 δ_4: 1.7^{-8} δ_5: -25.9 t=5.9° (t-1)=31.8° Reverse	δ_0: 1 δ_1: -0.626 δ_2: 0.351 δ_3: 0.275 δ_4: 1.1^{-8} δ_5: -25.9 t=5.9° (t-1)=31.8° Reverse	δ_0: 1 δ_1: 0.275 δ_2: -0.626 δ_3: 0.351 δ_4: 2.7^{-8} δ_5: -25.9 t=5.9° (t-1)=31.8° Reverse
Crip Inputs Fault 10*ohms* Std.Deviation: 0.283	δ_0: 1 δ_1: 0.277 δ_2: 0.152 δ_3: -0.457 δ_4: 0.9^{-4} δ_5: -0.45 t=31.35° (t-1)=31.8° Reverse	δ_0: 1 δ_1: -0.457 δ_2: 0.277 δ_3: 0.152 δ_4: 0.9^{-4} δ_5: -0.45 t=31.35° (t-1)=31.8° Reverse	δ_0: 1 δ_1: 0.152 δ_2: -0.457 δ_3: 0.277 δ_4: 0.9^{-4} δ_5: -0.45 t=31.35° (t-1)=31.8° Reverse
Crisp Output Detection Classify Accuracy Δfreq.	63.01 0.0341-0.00388s 0.0692-0.0820s 97.9-98.3% 2.316-5.571Hz	64.50 0.0348-0.0405s 0.0630-0.0785s 97.2-99.1% 8.18-12.276Hz	60.13 0.0312-0.0346s 0.0736-0.0801s 97.98-98.75% 2.988-10.19Hz

correspond to the fault's current directional flow seen in Fig. 5.11. Assisted by the FDR's synchrophasor at busbars, fault current migration using phase-shift deviations at t (t= fault detected) is broadcast and isolation proceeding is executed. In the following analyses, all fault occurrences are introduced at 1.8sec of the simulation time. Results displaying FL DOCR's time responses in triggering selected CB defined by delegated FDR's synchrophasor and its post-fault transient riposte.

Based on both test case studies in locating fault origins, F1 (PV) and F2 (3Ø Load), Table 5.12 and 5.13 have displayed decisive results in contrasting fault current migrating upstream or downstream. Furthermore, spot-on CB triggering was rendered, isolating faulted busbar. Indeed, there are instances where FL DOCR generates false interpretations of the fault's attribute right after CB is triggered. Such instances caused by transitional transient (frequency

Table 5.11 Fault detection and classification for three line-to-line and to-ground fault.

Fault	$L_A - L_B - L_C$	$L_A - L_B - L_C - G$
Ground *ohm*	0.001 - 0.01	
Crisp Inputs	δ_0: 1	δ_0: 1
Fault 0.1*ohms*	δ_1: 1.01^{-3}	δ_1: 0.98^{-2}
Std.Deviation:	δ_2: 0.86^{-3}	3.22^{-3}
0.257	δ_3:0.78^{-3}	δ_3:1.2^{-3}
	δ_4: 7.5^{-9}	δ_4: 1.73
	δ_5: -46.14	δ_5: -64.44
	t=16.04°	t=32.34°
	(t-1)=30.1°	(t-1)=30.1°
	Reverse	Reverse
Crisp Inputs	δ_0: 1	δ_0: 1
Fault 10*ohms*	δ_1:0.25^{-2}	1.22^{-4}
Std.Deviation:	δ_2: 1.32^{-4}	δ_2: 2.16^{-5}
0.223	δ_3: -5^{-3}	δ_3: 4.21^{-4}
	δ_4: 5.52^{-8}	δ_4:0.886
	δ_5: -0.68	δ_5: -0.48
	t=29.42°	t=29.62°
	(t-1)=30.1°	(t-1)=30.1°
	Reverse	Reverse
Crisp Outputs	73.97	82.37
Detection	0.0434-0.0472s	0.0451-0.0496s
Classify	0.0677-0.0829s	0.0693-0.0822s
Accuracy	97.15-97.59%	97.33-98.04%
Δfreq.	9.45-11.25Hz	12.95-14.25Hz

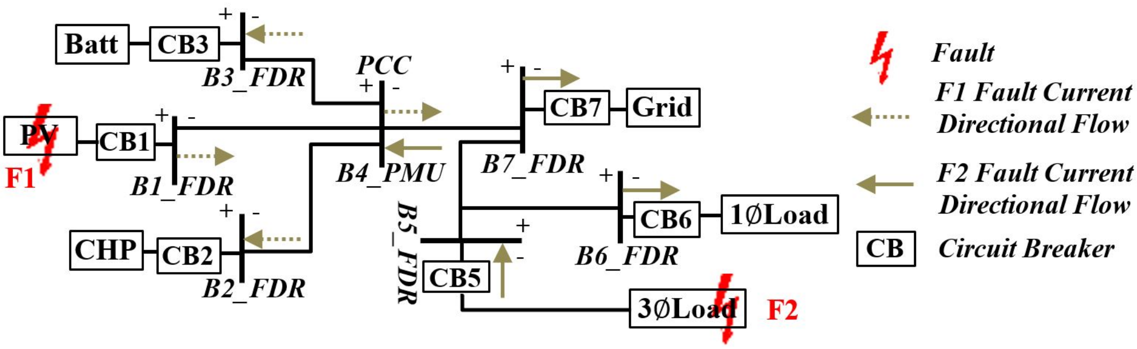

Fig. 5.11 Testbed system with 2 interjected fault locations.

Table 5.12 Fault current directional flow and circuit breaker operation for F1.
Fault at Location 1, F1 (PV System)

$L_A - G$ Fault Std. Deviation 0.211			
Busbar 4 PCC (PMU)	CB Activated Busbars (FDRs)		
Line Current Mag. (A)	Busb. 1	Busb. 2	Busb. 3
L_A:1.07^4; L_B:2755; L_C:620	Fault	Fault	Fault
0Seq.:3035; +Seq.:4580	Direc.:	Direc.:	Direc.:
δ_0:1, δ_1:0.74, δ_2:0.20	Forward	Reverse	Reverse
δ_3:-0.94, δ_4:0.71, δ_5:133.4°	δ_5:169.65°	δ_5:-11.6°	δ_5:-3.53°
Detected Direction Forward	CB Open	-	-
t:163.8°, (t-1):30.4°; 6.2ms	6.65ms		
Accuracy: 99.27%	Regain stability: 75.3ms		
$L_A - L_B - L_C$ Fault Std. Deviation 0.142			
Busbar 4 PCC (PMU)	CB Activated Busbars (FDRs)		
Line Current Mag. (A)	Busb. 1	Busb. 2	Busb. 3
L_A:1.8^4; L_B:1.8^4; L_C:1.8^4	Fault	Fault	Fault
0Seq.:653; +Seq.:1.27^4	Direc.:	Direc.:	Direc.:
δ_0:1, δ_1:1.1^{-4}, δ_2:0.94^{-4}	Forward	Reverse	Reverse
δ_3:0.9^{-4}, δ_4:0.0514, δ_5:108.14°	δ_5:125.8°	δ_5:-46.7°	δ_5:-28.9°
Detected Direction Forward	CB Open	-	-
t:138.54°, (t-1):30.4°; 4.982ms	8.83ms		
Accuracy: 97.62%	Regain stability: 89.77ms		

and voltage) picked up during triggering of CB to isolating fault. In this sense, it forces FL DOCR to coincidently pick up other fault criterion during shedding of load or generation before settling towards nominal operating current level (steady-state). Nevertheless, FL DOCR algorithm did not diverge and regain 100% accuracy through rapid detection of phase shift deviations defined by δ_5. Elected CBs were activated within less than 10*ms* shown in Fig. 5.12. Comprehensively, FL DOCR and Circuit Breaker algorithms provide comprehensive fault diagnosis for Nanogrid operations. Nanogrid is able to regain stability within a time span of 100ms from fault interventions.

5.6 Challenges in Minimising use of FDRs

Inherently, it is trivial to install FDR and PMU units on all existing busbars for large cascaded distribution network as costing will be an issue. In opposition, taking compromising measures in instrumenting a single monitoring FDR unit installed only at PCC busbar propagate much

Table 5.13 Fault current directional flow and circuit breaker operation for F2. Fault at Location 2, F2 (3Ø Load)

$L_A - G$ Fault Std. Deviation 0.209			
Busbar 4 PCC (PMU)	CB Activated Busbars (FDRs)		
Line Current Mag. (A)	Busb. 5	Busb. 6	Busb. 7
L_A:3172; L_B:1720; L_C:635	Fault	Fault	Fault
0Seq.:1760; +Seq.:1004	Direc.:	Direc.:	Direc.:
δ_0:1, δ_1:0.475, δ_2:0.324	Forward	Reverse	Reverse
δ_3:-0.8, δ_4:1.753, δ_5:-10.75°	δ_5:-19.54°	δ_5:7.88°	δ_5:31.06°
Detected Direction Reverse	CB Open	-	-
t:19.05°, (t-1):29.8°; 4.87ms	7.51ms		
Accuracy: 98.79%	Regain stability: 78.23ms		
$L_A - L_B - L_C$ Fault Std. Deviation 0.168			
Busbar 4 PCC (PMU)	CB Activated Busbars (FDRs)		
Line Current Mag. (A)	Busb. 5	Busb. 6	Busb. 7
L_A:883; L_B:884; L_C:886	Fault	Fault	Fault
0Seq.:884.2; +Seq.:884.0	Direc.:	Direc.:	Direc.:
δ_0:1, δ_1:-3.9^{-3}, δ_2:2.1^{-3}	Forward	Reverse	Reverse
δ_3:2.4^{-3}, δ_4:1.0, δ_5:-44.95°	δ_5:-39.43°	δ_5:39.52°	δ_5:16.65°
Detected Direction Reverse	CB Open	-	-
t:-15.2°, (t-1):29.75°; 6.2ms	7.68ms		
Accuracy: 97.67%	Regain stability: 81.15ms		

turmoil in navigating the exact faulted region. Some may argue that implementations of heuristic or unsupervised learning algorithm can aid in solving collective problem statement with multi-dimensional constraints during fault interventions effectively. However, such implementations impose high risk of divergence when PSPG integrations are not accounted for, creating uncertainty in the search space domain. Furthermore, centralised learning approach for whole distribution network could not possibly provide early detection services for particular Nanogrid at low-voltage level.

Design solely for Nanogrid engagements, it is acceptable for FL DOCR system to maximise installation of FDRs at all busbars due to its affordability as compared to PMU. It also provide absolute control in rendering fault diagnostical proceedings centrally. Nevertheless, studies on optimal placement of FDR units and minimising its quantity are still an open research problem till to date.

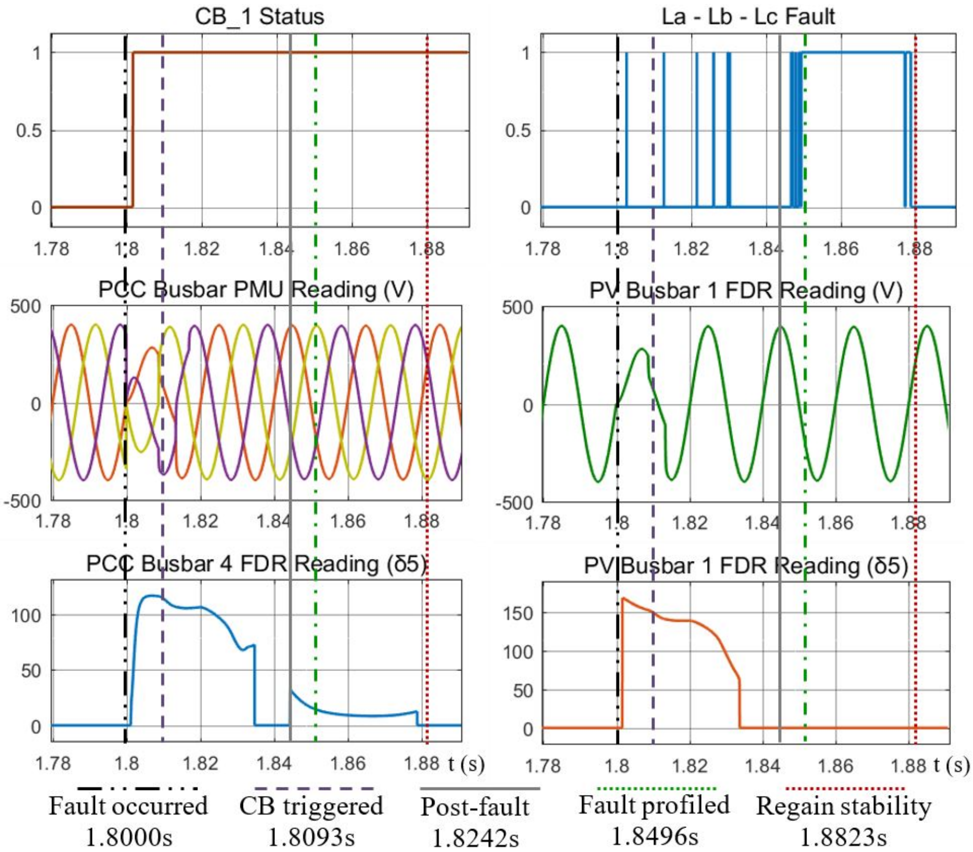

Fig. 5.12 FL DOCR transient from fault intervened to CB operation, $L_A - L_B - L_C$ fault.

5.7 Benchmarking & Discussions

To appraise performances of FL DOCR, analytical comparisons were made against; (i) continuous hidden markov model (CHMM) [253], (ii) phasor-measurement-unit-based state estimation processes (PMU-based state estimation) [254], and (iii) simple current-based directional relay (CDR) [255]. To render fair assessment, same test cases were adopted when testing respective fault diagnostic algorithms; detecting, classifying and locating fault crisis interrupted during grid-tied operations.

H. Jiang introduces CHMM approach to diagnose fault interventions using machine learning and signal decomposition algorithms in a grid level perspective. A hybrid computational algorithm that descries frequency and voltage variation features through matching pursuit Gaussian atom dictionary while contouring maps of faulted area using machine learning signal repository were proposed.

Subsequently, M. Pignati focuses on exhibiting unique time determinism and high refresh rate during time-critical to boost PMU's synchronisation accuracy in appraising faulted line

Table 5.14 Efficiency in fault detection and classification performance rates.

Method	Detection	Classify Accuracy @SNR 40dB
CHMM	100%	99.1%
900ms (detect, profiled & locate faulted region)		
PMU-based	100%	84.65%
122ms (detect & profiled)		
CDR	100%	95%
15ms (discern fault direction) 218ms (detect & profiled)		
FL DOCR	100%	97.04-99.5%
5ms (fault detected) 10ms (discern fault direction) 82ms (fault profiled) 92.8ms (grid regain stability)		

empathies. A parallel synchrophasor-based state estimator was suggested to characterize different augmented topology to seize floating bus fault scenarios. Decisions in setting appropriate state estimator provides accurate metric solutions which computes sum of the weighted measurement residual.

Finally, H.J. Ashtiani addresses the flaws in adopting existing directional relays which fails to provide factual interpretations on the current directional flow status during fault interventions. Implementing of fault direction discrimination through exploiting sign of imaginary part of post-fault current profile was enforced. Utilisation of moving data window and DFT, high estimation resolutions are attained to cipher post-fault current phasor unit.

Table 5.14 summaries the results of four different approaches in detecting and classifying fault genres. Surpassingly, all methods abled to preserve sufficient tolerance percentage in providing credible solutions even in low *SNR* situations. Furthermore, all proposed algorithms adopted signal decomposition technique which filtrates undesirable noises and preserves signal's attributes. In relations to early detection or time response (average), the results had shown that FL DOCR may not be as responsive (lag by 13.8*ms*) when compared to PMU-based approach. However, when dealing with cost and computation efforts/stress, FL DOCR employ primitive learning algorithm that will in-turn have cheaper computation costs. Moreover, PMU-based only provide detection and profiling of fault attributes hence justifies for having faster response time.

Table 5.15 Consistency assessment in comprehending faulted location.

CHMM	100%
PMU-based state estimation	96.28%
CDR	99%
FL DOCR	100%

Likewise, Table 5.15 lists the consistency performances of respective approaches when generating a comprehensive fault synopsis report. Evaluations were weighed based on percentage of accuracy given at 100^{th} sets of solutions based on arbitrary fault assertions at random locations. The proposed algorithm has rendered positive results against other schemes however, such comparisons may bring forth biasness as the size of network implementation differs from each other. Regardless, in the near future, monopolism in decentralised conceptions are trending for high penetration of distributed generations at low-voltage level. Hence, fault detection and restoration could adopt decentralised administrations, relieving aggregator and liberalising nano-managing frameworks. Imminently, centralised control algorithm in regulating large bus network evokes divergences, high computational stress, or data misalignments issues. Thus, endorsing FL DOCR in Nanogrid administrations proffers Prosumers to self-contain and officiate fault crisis independently. Such undertaking bridges cohesiveness between aggregator and Prosumers in mitigating fault crisis from escalating upstream. Nevertheless, all mentioned methodologies have common objectives and intents towards modelling fault diagnostic schemas.

5.8 Summary

This chapter highlights potential in fault interruptions transpired by Prosumers' PSPG during operations. Moreover, due to alarming responses in integrating DERs at low-voltage level, the operational integrity of distribution network is exposed to upstream fault current. In this sense, due to generation uncertainty and mismatch of supply-demand equilibrium induced by high excess energy generations from NGs flowing upstream, unsynchronised frequency levels will enact and operating voltage at Nanogrid PCC will exponentially swell. Therefore, aggregator is constantly challenged when tasks to micro-manage individual Prosumer's PSPG when localising fault interruptions.

In conjunction to personalised ruling of EMS proceedings for Nanogrid operations, OMS can also be liberated onto Prosumers without the interventions of aggregator. The proposed FL DOCR is solely designed to provide Prosumer's PSPG with early fault detection and isolation protocols that could save EPS's integrity from cascading failure effect (even with blackstart if fault is not isolated). The intelligence in FL DOCR uses fuzzy logic algorithm and current magnitude attributes at Nanogrid PCC to generate fault diagnostic with its objective to isolate the faulted region/PSPG autonomously. Moreover, dependency of time synchronisation between FDR and FL DOCR are unaffiliated therefore, it assert portability for any Nanogrid operations. Whereas, FL DOCR and FNET provide supportive fault localising information when external fault is detected. Aggregators can exploit FNET to map those decentralised FL DOCRs which flagged *external fault* and pinpoint towards the saturate faulted region along the distribution network before dispatching restoration protocol.

As FL DOCR adopts a data driven intelligence system, its performances was evaluated based on low signal-to-noise ratio acquisition to simulate external disturbances when recording measurements. Surpassingly, FL DOCR demonstrates high fault detection accuracy index with $\frac{1}{4}$ of a cycle in response time. It also provide comprehensive analyses of the fault interruption; detection of fault, nature of fault, origin of fault, and perform isolation of the fault. Additionally, FL DOCR's comprehensiveness in assenting stacking problem statement for other provisional operations in ADMS can be augmented to solve post-fault problems such as execution of restoration or operations in islanded mode.

Chapter 6

Conclusions and Future Works

6.1 Conclusions

This dissertation discusses penetration of PSPGs at low-voltage level and maturity in EMS and ADMS for Transactive Energy managerial suite. Power grid operators, policy makers, industrial partners, and investors are working closely to formulate viable solutions that can maximise TE values in view of market policies and operational Standards for secured demand-side and power quality managements. However, devising a laudable and effective TE system and control, initiated trajectories must reach common consensus on the decisions and actions taken.

Therefore, decentralised intelligent systems and information & communications technology infrastructure were proposed to create a safe Prosumer-centric energy trading environment that observes levelled playing field benefitting for all participating actors. The major contributions are summarised as follows:

1. *Chapter 2*−Nanostructuring distribution network to mathematical model Nanogrid system. Nanogrid models are introduced with PSPG and simulation was validated to critic system interoperability. Based on Prosumers' Community settings, investigations were conducted to analyse PSPG impacts on load demand consumption curve and how they have influence DSR operations based on ineffective control proceedings. Results have shown detrimental effect on grid's integrity where violations in unit-commitment scheduling and Duck Curve crises were trivial. Moreover, Prosumers suffered very low return on investment and PSPG operations had a negative impact on its daily energy billing (higher) due to poor scheduling of charging and discharging of ESS. In this chapter, it also models NAN and MultiCloud fogging for coalition computing

capability in a decentralised environment. The aim it to impart edge computing ability at respective Nanogrid, where intelligent system can execute individualism when managing Prosumer's energy usage interests while apprehending operating constraints of external parties at a global level (DSR ruling).

2. *Chapter 3*—Focuses in distributed control organisation intelligent computing coordination in distribution network. A multi-layered DCF was proposed to assign energy actors with corresponding control functions at respective layer. The DCF is encapsulate by an IoT cloud infrastructure, Microsoft Azure, that has edge computing capability. Hence, a flexi-edge computing configuration is proposed to fused COSAP and Azure as the comprehensive IoT edge device. It observes data-sharing privacy and security, and employ modular-based intelligence that is stackable for Prosumer while establishing communication with other actors in the distribution network. In addition, modelling of intelligent system using reinforcement learning was proposed. The objective is to create an algorithm that provoke cooperativeness but yet competitive when executing decision-making processes. Testing of the AMI and system intelligent were validated to serve as a proof of concept for TE management deployment. Results have shown comprehensive performance in various test cases where Prosumers are able to cooperate in meeting optimal global objectives with competitive edge to satisfy local interests.

3. *Chapter 4*—Proposes two avenues in which Aggregator-Prosumer can gain full access in DSR management despite liberating Prosumers in attuning their energy attributes based on individual socio-economical interests. It involves clustering of Prosumers into a Community based on their energy attributes for better demand curve jurisdiction. A proposed clustering technique, EM-GMM, ciphers Prosumer(s) in a Community based on their energy attributes. The algorithm has successfully provide informative information for Prosumer(s) in monitoring their energy contributions in the distribution network and how they fair against others. Likewise, aggregator also gained better jurisdictions in scheduling clusters' with high excess generation and high load consumption capacity to compensate each other. These clusters are to find corresponding partners to procure a communal solution that could benefit Prosumers in respective cluster. A self-directed nano-biased Prosumer-centric EMS is proposed to facilitate optimal utilisation of Prosumers' PSPG against load consumption capacity and electricity price tariffs. It redefines the complex decentralised DSR operating constraints into local TE function while interoperating Prosumers' energy usage interests. Here, the

Prosumer-centric EMS employs Q-learning reinforcement learning approach to model Prosumer's energy control system. The Q-learning algorithm, centralised critic policy, is employed to solve local energy attribute based on strategic scheduling of PSPG operation and demand load. Whereas, in the joined bidding and pricing of electricity price in REM, it uses MADDPG due to its decentralised critic policy that provides CDL relations. Results deliver positive and comparable energy management performances when benchmarked against other methodologies based on the proposed aggregated NGs network. However, potentials in energy market monopolism can arise during bidding in REM. Hence, DSO-TSO as policy maker, need to revise Market Ruling in REM by introducing new policies and regulatory to ensure Prosumer's interests when auctioning is transparent to create a competitive trading environment for all energy actors.

4. *Chapter 5*—Highlights potential in fault interruptions transpired by Prosumers' PSPG during operations. Moreover, due to alarming responses in integrating DERs at low-voltage level, the operational integrity of distribution network is exposed to upstream fault current. In conjunction to personalised ruling of EMS proceedings for Nanogrid operations, protection relay system as an add-on service to OMS can also be liberated onto Prosumers. The proposed FL DOCR is solely designed to provide Prosumer's PSPG with early fault detection and isolation protocols that could save EPS's integrity from cascading failure effect (even with blackstart if fault is not isolated). As FL DOCR adopts a data driven intelligence system, its performances was evaluated based on low signal-to-noise ratio acquisition to simulate external disturbances when recording measurements. Surpassingly, FL DOCR demonstrates high fault detection accuracy index with $\frac{1}{4}$ of a cycle in response time. It also provide comprehensive analyses of the fault interruption; detection of fault, nature of fault, origin of fault, and perform isolation of the fault. Additionally, FL DOCR's comprehensiveness in assenting stacking problem statement for other provisional operations in ADMS can be augmented to solve post-fault problems such as execution of restoration or operations in islanded mode.

6.2 Future Works

The proposed future directions for this research involves two prepositions that can be modelled into a unified monitoring and control system:

1. *Power converter design* to secure interoperability regulations involving frequency/voltage *ride-through and support* at low-voltage level for PSPG integrations.

2. *Islanding operation* intelligence where control features involve PSPG operating in *isochronous mode and conduct load shedding protocols* to secure Nanogrid supply-demand equilibrium when islanded.

In view of higher penetration level in DERs, it expands stronger coupling between grid Power Quality (PQ) and inverter role. In this sense, the role of inverter in regulating/supporting PQ exponentially increase in islanding applications or experiencing zero ordering of energy generation from upstream−from grid-following to grid-forming. Without the support or strength from the grid to maintain voltage and frequency, inverter regulating control capabilities, and transient & load following responses have greater impact in influencing PQ. Thus, initiative for inverter with control features that resolves; *(i)* low-voltage ride-through, *(ii)* voltage and frequency support, and *(iii)* ramp rates, can minimise negative impact in providing stability compensation. The inverter's controller aims to take isochronous and droop operation mode regulating at fixed output, voltage and frequency. These control features were designed to accommodate the newly revised IEEE Standard for interconnection and interoperability of DERs with associated EPS interfaces, IEEE 1547-2018. Investigations and proposed ride-through controls have been explored and published listed in the publication section labelled "other papers". These works are still in the early stage of implementation and on-going hence, not included in the dissertation.

Meanwhile, in islanding operations, Prosumers are able to self-sustain by meeting local load consumption capacities using local PSPG or neighbouring Nanogrids. Such intentional islanding can introduce benefitting operations in securing system resiliency. However, unintentionally islanding too can be formed if neighbouring NGs or primary-side of distribution network consist of grid-following DERs and loads in isolation by a circuit breaker. Hence, uncoordinated protection (voltage/frequency) control may deviate out of phase with grid thus creating risk of asynchronous reclosure. In addition, it may also operate without the awareness of network operator posing risks to personnels who are working on the field. Therefore, islanding detection methods (*i.e.* passive inverter-resident, active inverter-resident, and non-inverter-resident [256]) can aid in resolving such issues. Likewise, preliminary research have been conducted however not comprehensively conclusive. Published work can be referred to the publication section labelled "other papers".

The above listed research directions/areas do have promising contributions in lieu of Transactive Energy applications that focuses activities at the low-voltage level.

Appendix A

System Design, Specifications, Performance Analyses for Chapter 2

Taking reference to the Nanogrid systems seen in Fig. 2.13, further explorations into modelling of BTM DERs and corresponding inverters in the household and commercial building environment were analysed to view operational behaviour and data specification respectively in MATLAB. Here, it assumes that all Prosumers adopts identical BTM DER configuration and sizes installed at respective Nanogrid for modelling simplicity. However, power generation responses/performances for solar PV will differ based on geographical location and weather input. In this sense, it also will influence available energy storage at respective ESS.

A.1 Nanogrid: Domestic Household

In this section, it reveals system modelling and responses of BTM DER assets in the domain of full-pledge Prosumer; solar PV ($5kW$), ESS ($240V$, $35Ah$, $8.4kWh$), and PHEV ($375V$, $248.1Ah$, $100kWh$) system. The solar PV system adopts grid-tied configuration where it has its independent inverter system (non-hybrid) decoupled from battery storage to gain better flexibility in retrofitting storage size considering PHEV and Utility energy exchange operations. Moreover, ESS can extend its utilisation for other ancillary services at distribution level (feeder-based) rather than focused only for local Nanogrid usage.

Figure A.1a presents the BTM solar PV system coupled to the LV distribution network. It uses total of 15 SunPower 305E PV panels that are connected in array; 3 parallel by 5 series. It uses buck-boost converter with MPPT Fractional Open Circuit Voltage (MPPT-FOCV) controller [257, 258] to secure "near" maximum active power transference from PV and held output voltage constant at $500V$. Meanwhile, a Full Bridge Neutral Point Clamped (FB-NPC) inverter with SPWM Linear Current Control Loop (SPWM-LCCL) controller [259, 260] is coupled to the single-phase LV network with synchronised voltage-frequency attributes. Fig. A.2 presents solar PV system performance under a controlled environment coupled to the LV distribution network where it receives constant $1000W/m^2$ at 32deg. Overall, the solar PV system efficiency is measured at $90.26\%_{AVE}$ as losses induced by both converters, output active power comparison between solar PV MPPT and generation at grid. Likewise, to simulate deployment practicability, the input data for irradiance and temperature of solar PV is imported from *PVOutput.org* where it has an archive of many live solar PV across countries sampled at 5mins intervals for 24 hours as shown in Fig. A.3. Moreover, the proposed testbed distribution network uses three type of PV power generation efficiency in view of weather conditions for respective Prosumers. It is assigned based on feeder/region to simulate geographical distribution of PV performances.

Meanwhile, detailed modelling of independent inverter BTM ESS coupled to the LV distribution network is presented in Fig. A.4. Here, conventional bidirectional buck-boost and full-bridge inverter were employed to legislate two-way energy transfer from and to battery. The lithium-ion battery cell operates at $24V$ with $35Ah$ rated current capacity and set to have 38% of initial SOC. Its charging voltage ranges from 17-22V with maximum charging current of $18.9A@20V$ and discharging voltage of 12-20V with maximum discharge current at $23.3A@14V$. Fig. A.4b illustrates the battery response curve of a single cell with respect to time. Here, a passive battery management controller is designed based on measured SOC level against power difference between demand load capacity and solar PV generation: P(ESS) = P(LOAD) - P(PV) subject to 20%<SOC<80% else charging/discharging at idle state. If P(ESS) is positive, battery is operating in discharging mode limited to its maximum discharging current rate and vice versa when P(ESS) is negative. Any excess energy unattended by battery with be absorbed by or supplied to Utility. Lastly, Fig. A.4c presents the battery charging and discharging performances through switching from load to power source. The overall ESS efficiencies are rated at $96.61\%_{AVE}$ and $91.37\%_{AVE}$ during charging/discharging respectively, measured between battery storage and energy trading at grid.

A.2 Nanogrid: Commercial Building

Similar solar PV and ESS design configurations were adopted for commercial building Nanogrid environment. The differences are; solar PV and ESS have larger generation and storage capacity, and the control design for Voltage Source Converter (VSC) at grid-side uses Virtual Oscillator Controller (VOC) [261, 262] suitable for 3-phase grid-following operation and is coupled to the 3-phase $415Vac$, $50Hz$ LV distribution network. Figures A.5-A.6 presents the performances of solar PV and ESS, under the same observations made in Chapter A.1. The solar PV system efficiency is measured at $91.08\%_{AVE}$ as losses induced by both converters, output active power comparison between solar PV MPPT and generation at grid. The lithium-ion battery cell operates at $24V$ with $20Ah$ rated current capacity and set to have 38% of initial SOC. Here, total of 70 battery cells were configured in 10 rows (series) by 7 column (parallel) connection to generate $336kWh$, $1.4kAh$ ESS. Its charging voltage ranges from 15-20V with maximum charging current of $11.8A@18V$ and discharging voltage of 12-16V with maximum discharge current at $14.1A@14V$. The overall ESS efficiencies are rated at $90.77\%_{AVE}$ and $91.03\%_{AVE}$ during charging/discharging respectively, measured between battery storage and energy trading at grid.

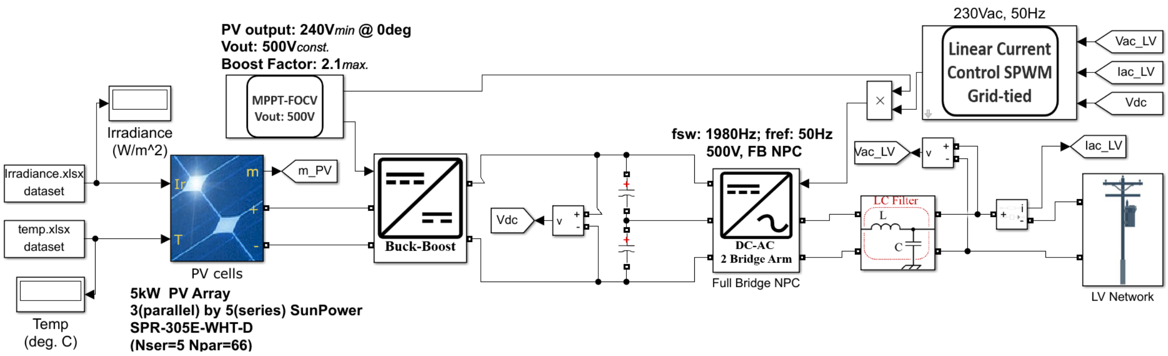

(a) $5kW$ solar PV system coupled to the $230V_{AC}$, $50Hz$, single-phase LV network.

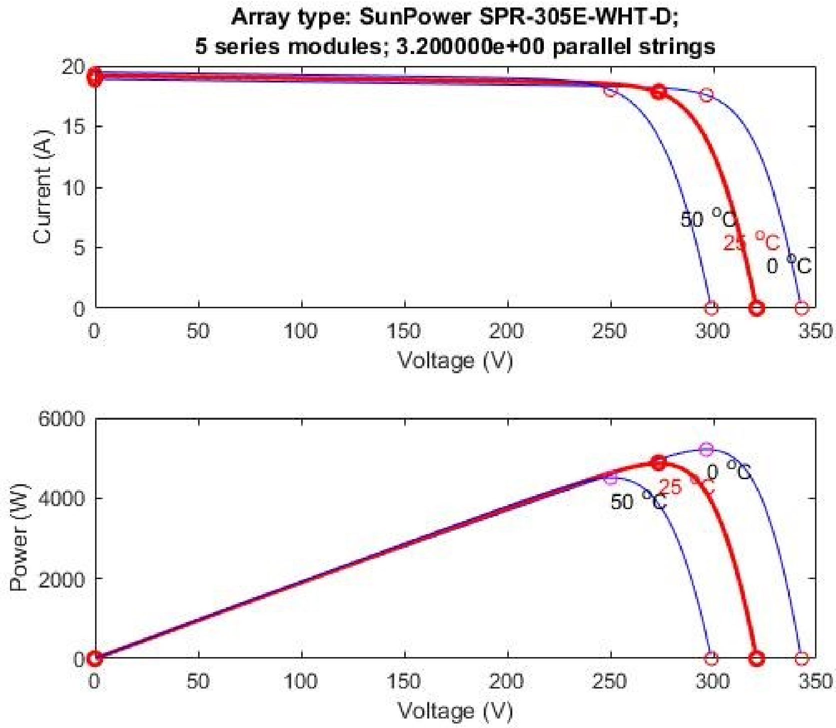

(b) P-V and V-I characteristics of PV in array configuration, 3 parallel by 5 series.

Fig. A.1 Proposed BTM $5kW$ solar PV system for domestic household.

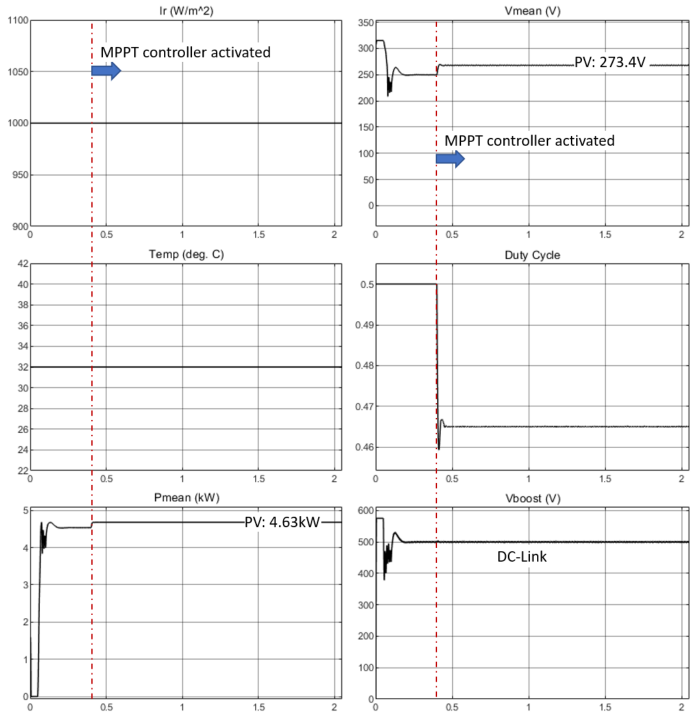

(a) Responses at DER-side, DC-DC boost converter with MPPT control.

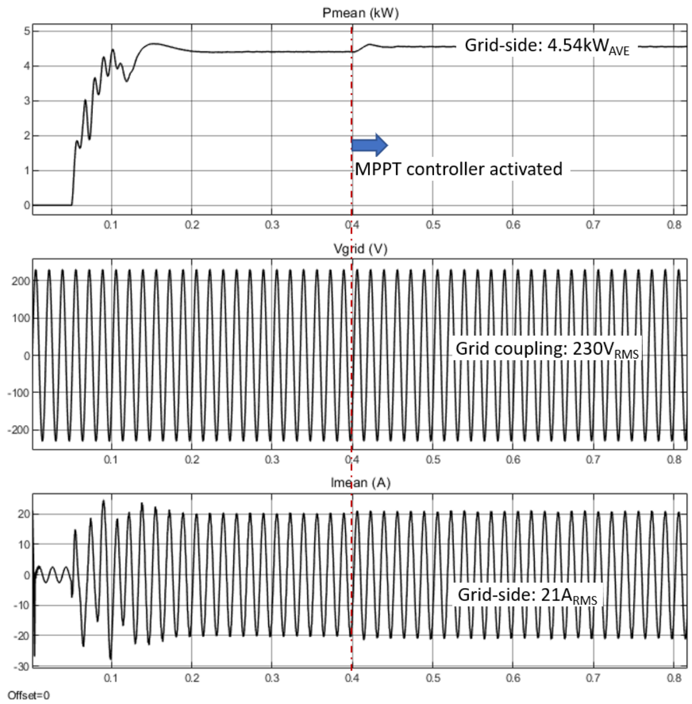

(b) Responses at grid-side, DC-AC VSC with SPWM-LCCL control.

Fig. A.2 BTM 5kW solar PV system grid-following performances in controlled environment.

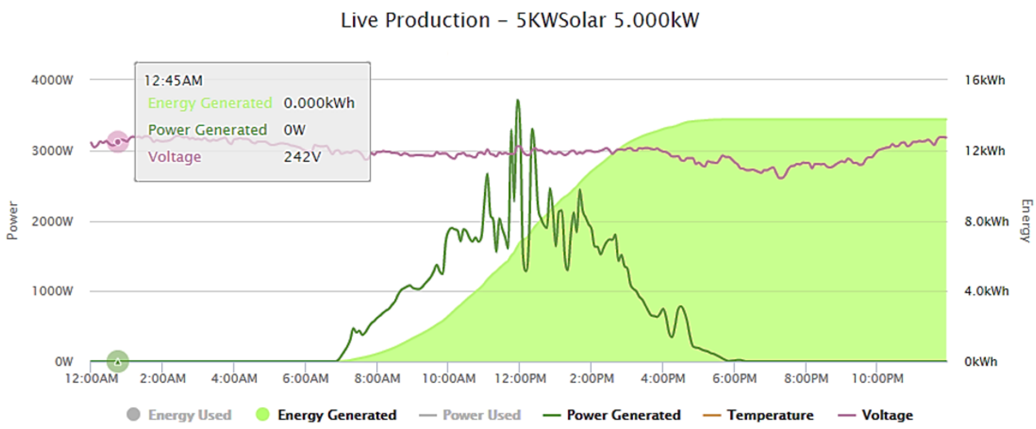

(a) Cloudy.

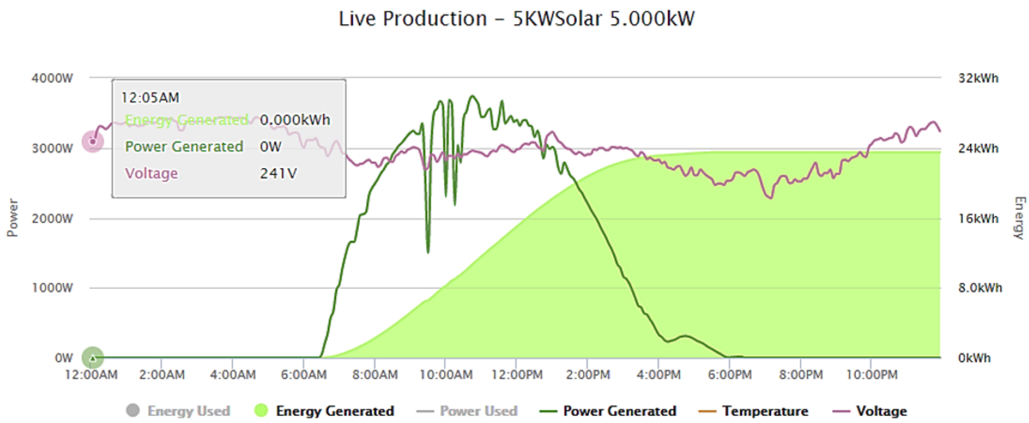

(b) Sunny.

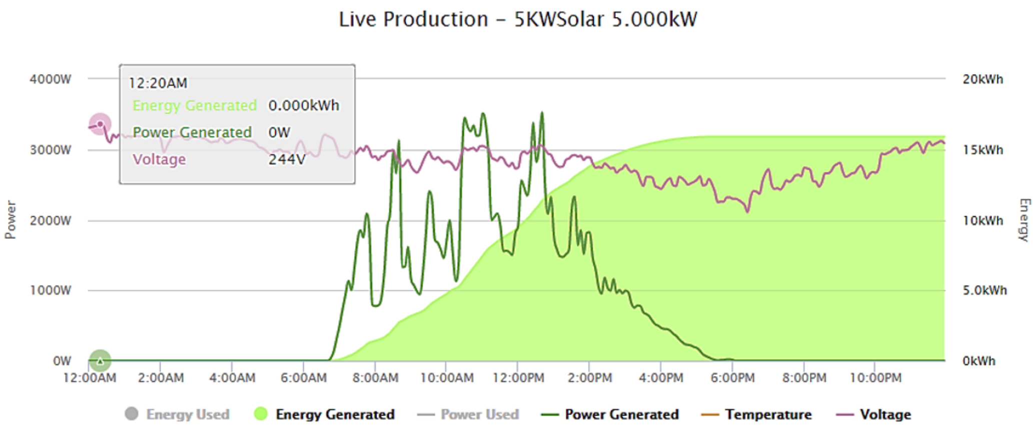

(c) Moving clouds.

Fig. A.3 $5kW$ solar PV power generation under different weather conditions.

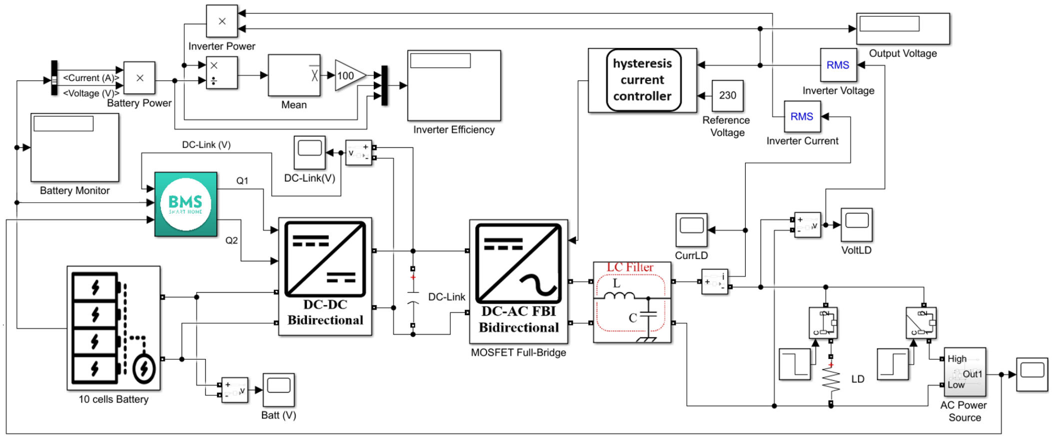

(a) $10x$ $24V$, $35Ah$ battery cells series connected coupled to the $230V_{AC}$, $50Hz$, single-phase LV network.

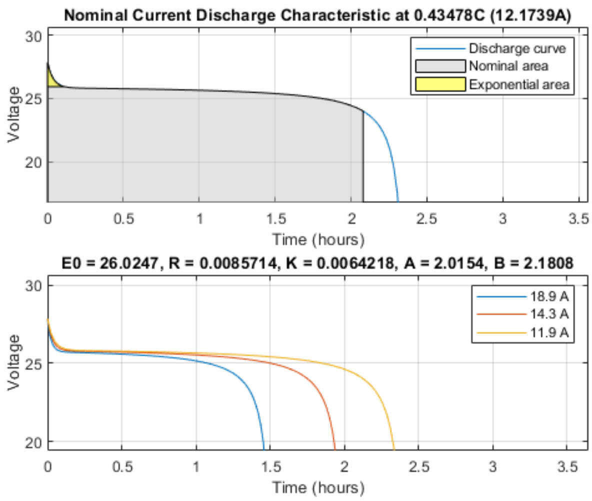

(b) Response curve of a single battery cell, $24V$, $35Ah$.

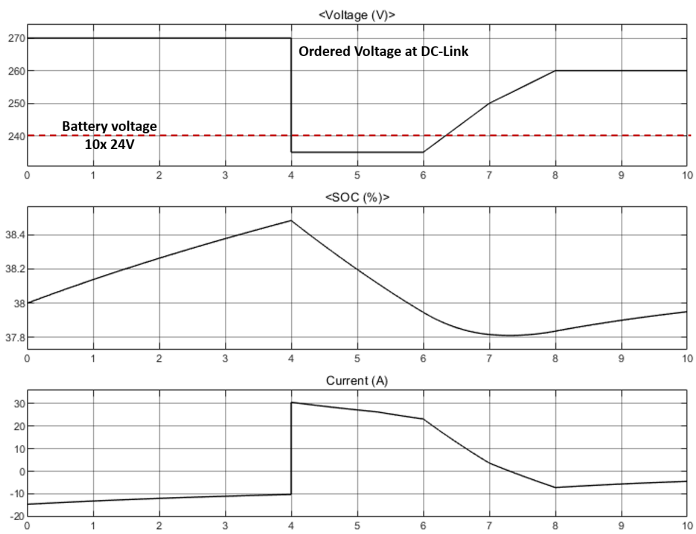

(c) Charging and discharging rates of $8.4kWh$ ESS; $240V$, $35Ah$.

Fig. A.4 Proposed BTM $8.4kWh$ ESS for domestic household.

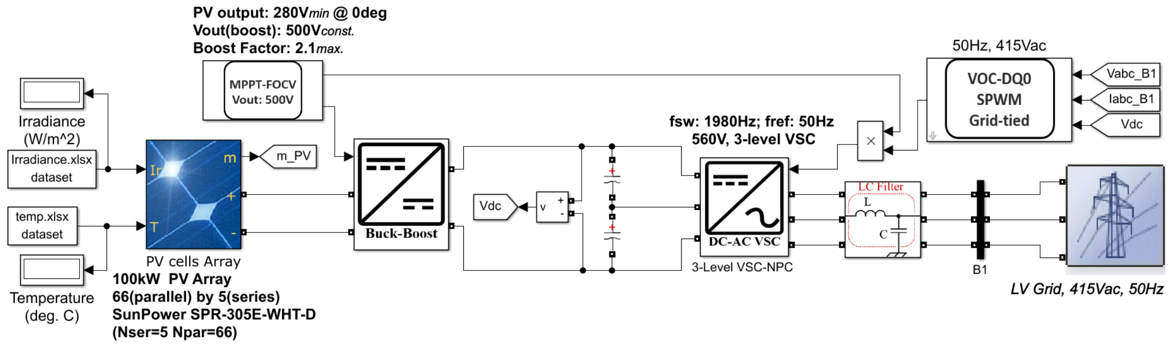

(a) 100kW solar PV system coupled to the 415V_{AC}, 50Hz, three-phase LV network.

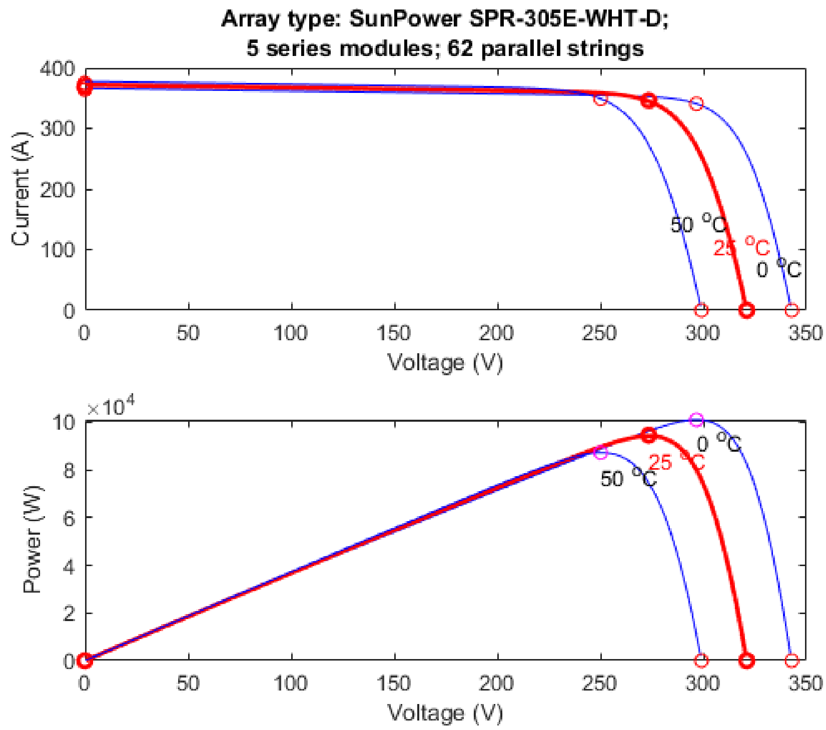

(b) P-V and V-I characteristics of PV in array configuration, 66 parallel by 5 series.

Fig. A.5 Proposed BTM 100kW solar PV system for commercial building.

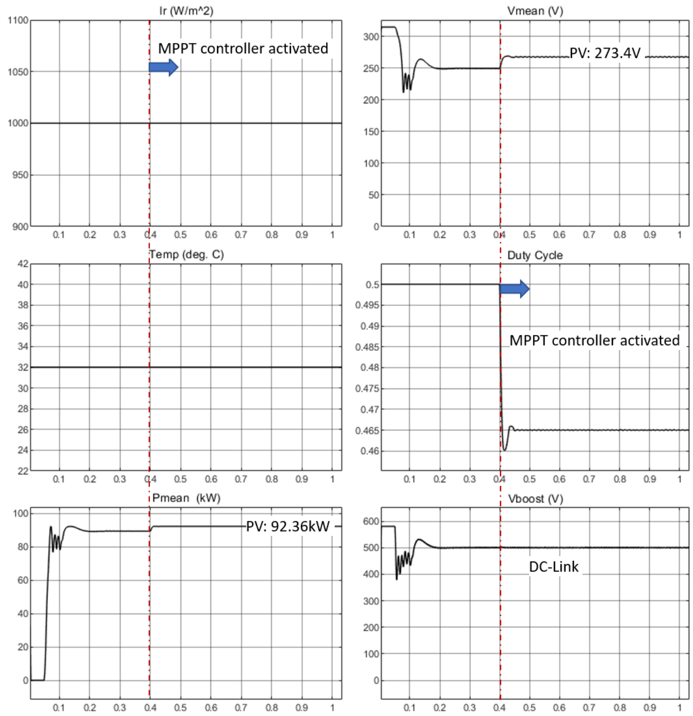

(a) Responses at DER-side, DC-DC boost converter with MPPT control.

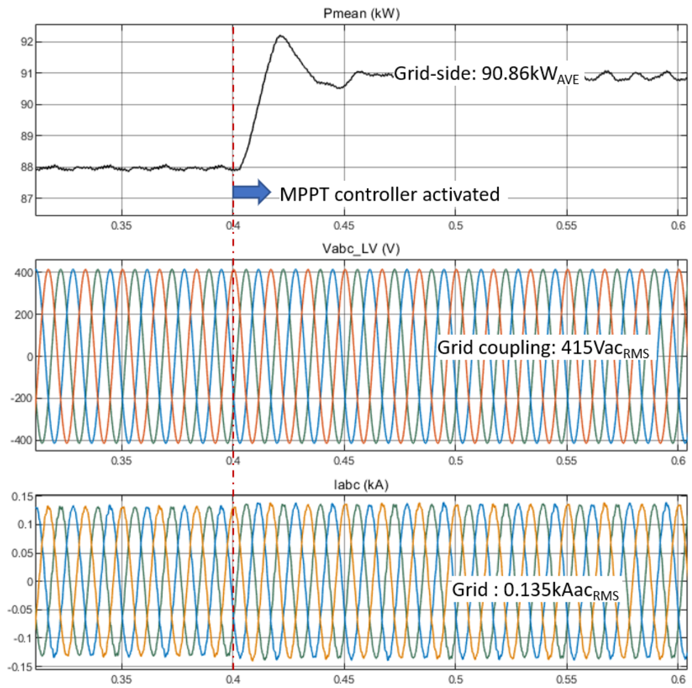

(b) Responses at grid-side, DC-AC VSC with VOC control.

Fig. A.6 BTM 100kW solar PV system grid-following performances in controlled environment.

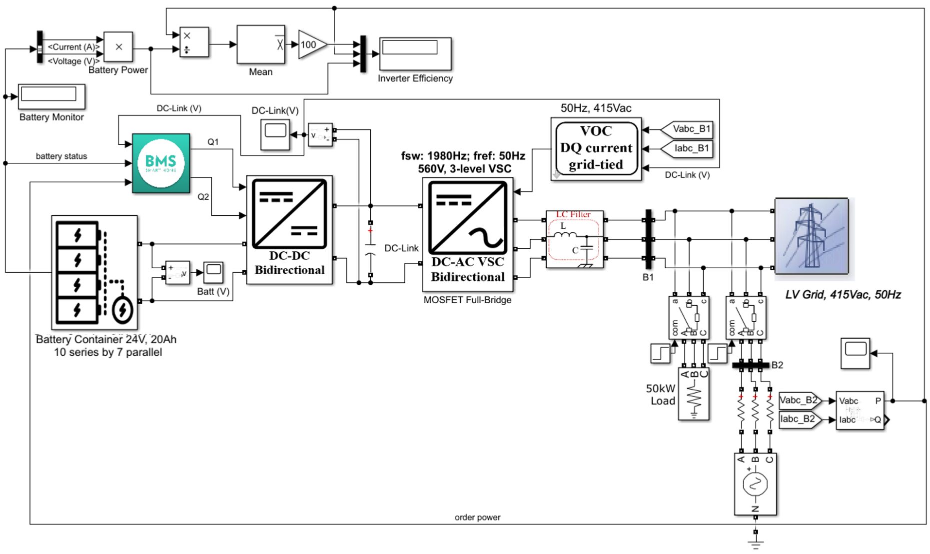

(a) 10 series and 7 parallel $24V$, $20Ah$ battery cells configuration coupled to the $415V_{AC}$, $50Hz$, three-phase LV network.

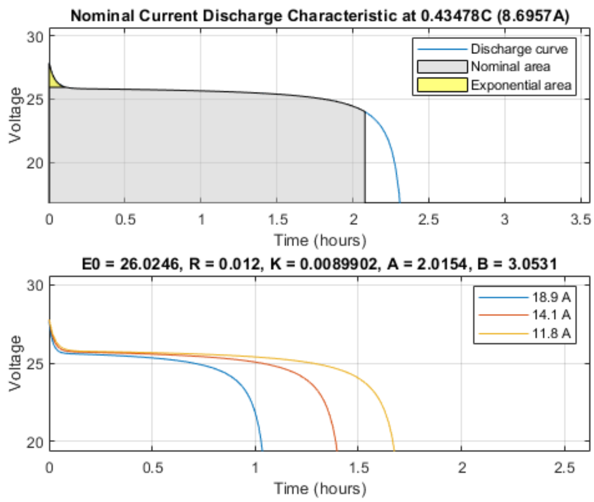

(b) Response curve of a single battery cell, $24V$, $20Ah$.

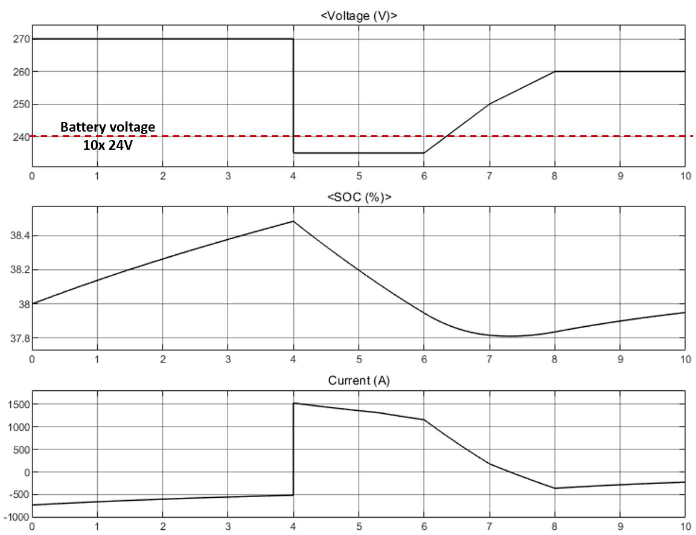

(c) Charging and discharging rates of $336kWh$ ESS; $240V$, $1.4kAh$.

Fig. A.7 Proposed BTM $336kWh$ ESS for commercial building.

Appendix B

Proof-of-Lemma for Chapter 3

B.1 Derivation of State-Value Function

Given the state, s, and policy, π, the value is:

$$V^p i(s) = \mathbb{E}\left[\sum_{k=0}^{\infty} \alpha^k r_{t+k+1} | s_t = s\right] \tag{B.1}$$

Using Bellman concept, expression for V state-value function:

$$V^\pi(s) = \sum_{a \in A} \pi(a|s) \sum_{s' \in S} P(s'|s,a) \left[R(s,a,s') + \alpha V^\pi(s')\right] \tag{B.2}$$

Proving Bellman equation:

$$V^\pi(s) = \mathbb{E}_\pi \left[\sum_{k=0}^{\infty} \alpha^k r_{t+k+1} | s_t = s\right] \tag{B.3}$$

$$V^\pi(s) = \mathbb{E}_\pi \left[r_{t+1} + \alpha \sum_{k=0}^{\infty} \alpha^k r_{t+k+2} | s+t = s\right] \tag{B.4}$$

$$\begin{aligned} V^\pi(s) = &\sum_{a \in A} \pi(a_t = a|s_t = s) \sum_{s' \in S} P(s_{t+1} = s'|s_t = s, a_t = a) \\ &\times \left(R(s,a,s') + \alpha \sum_{k=0}^{\infty} \alpha r_{t+k+2} | s_t = s, a_t = a, a_{t+1} = s'\right) \end{aligned} \tag{B.5}$$

$$V^\pi(s) = \sum_{a \in A} \pi(a|s) \sum_{s' \in S} P(s'|s,a) \left[R(s,a,s') + \alpha V^\pi(s')\right] \tag{B.6}$$

$$V^{\pi}(s) = \sum_{a \in A} \pi(a|s) \sum_{s' \in S} P(s'|s,a) \left[R(s,a) + \alpha V^{\pi}(s')\right] \tag{B.7}$$

Redefine from V to Q function:

$$Q^{\pi}(s,a) = \sum_{s' \in S} P(s'|s,a) \left[R(s,a,s') + \alpha V^{\pi}(s')\right] \tag{B.8}$$

Therefore, the Bellman equation of Q action-value function is:

$$Q^{\pi}(s,a) = \sum_{s' \in S} P(s'|s,a) \left[R(s,a,s') + \alpha \sum_{a' \in A} \pi(a'|s') Q^{\pi}(s',a')\right] \tag{B.9}$$

B.2 Optimal Action-Value Function of State-Value Function

Similarly, the optimal Q action-value function is defined by searching optimum policy:

$$Q^{*}(s,a) = \max_{\pi} Q^{\pi}(s,a) \tag{B.10}$$

$s.t.$

$$Q^{*}(s,a) = \mathbb{E}\left[r_{t+1} + \alpha V^{*}(s_{t+1}) | s_t = s, a_t = a\right] \tag{B.11}$$

$$V^{*}(s) = \max_{a \in A} Q^{*}(s,a) \tag{B.12}$$

Proof:

$$V^{*}(s) = \max_{a} \mathbb{E}_{\pi^*}\left[\sum_{k=0}^{\infty} \alpha^k r_{t+k+1} | s_t = s, a_t = a\right] \tag{B.13}$$

$$V^{*}(s) = \max_{a} \mathbb{E}_{\pi^*}\left[r_{t+1} + \alpha \sum_{k=0}^{\infty} \alpha^k r_{t+k+2} | s_t = s, a_t = a\right] \tag{B.14}$$

$$V^{*}(s) = max_a \mathbb{E}_{\pi^*}\left[r_{t+1} + \alpha V^{*}(s_{t+1}) | s_t = s, a_t = a\right] \tag{B.15}$$

$$V^{*}(s) = \max_{a} \sum_{s' \in S} P(s'|s,a) \left[R(s,a,s') + \alpha V^{*}(s')\right] \tag{B.16}$$

$$Q^*(s,a) = \mathbb{E}\left[r_{t+1} + \alpha \max_{a'} Q^*(s_{t+1},a')|s_t = s, a_t = a\right] \tag{B.17}$$

$$Q^*(s,a) = \sum_{s' \in S} P(s'|s,a)\left[R(s,a,s') + \alpha \max_{a} Q^*(s',a')\right] \tag{B.18}$$

For any Markov Decision Processes the existence of an optimal policy:

$$\pi^* \geq \pi;\ \forall\ \pi \tag{B.19}$$

However, there could be multiple of optimal policies and all gained optimal value function:

$$V^{\pi^*}(s) = V^*(s);\ \forall\ s \tag{B.20}$$

$$Q^{\pi^*} = (s,a) = Q^*(s,a);\ \forall\ s,a \tag{B.21}$$

Nevertheless, there is always a deterministic optimal policy for any Markov Decision Process problem.

B.3 Derivation of Policy Gradient Theorem

Computation of policy gradient is dependent on the actions determined by policies, π_θ, and the state stationary distribution which follows the target selection behaviour (determined indirectly by π_θ). Being that the state is unknown, it is difficult to estimate its impact on the state distribution based on the updated policy.

Thus, policy gradient theorem provides a reformation on object derivative function and avoid derivative of the state distribution $d^\pi(.)$. The gradient computation,$\nabla_\theta J(\theta)$, isgreatly simplified:

$$\nabla_\theta J(\theta) = \nabla_\theta \sum_{s \in S} d^\pi(s) \sum_{a \in A} Q^\pi(s,a)\pi + \theta(a|s) \tag{B.22}$$

$$\nabla_\theta J(\theta) \propto \sum_{s \in S} d^\pi(s) \sum_{a \in A} Q^\pi(s,a)\nabla_\theta \pi_\theta(a|s) \tag{B.23}$$

Proof of theorem starts with finding the derivative of state value function:

$$\nabla_\theta V^\pi(s) = \nabla_\theta \left(\sum_{a\in A} \pi_\theta(a|s) Q^\pi(s,a) \right) \tag{B.24}$$

$$\nabla_\theta V^\pi(s) = \sum_{a\in A} \left(\nabla_\theta \pi_\theta(a|s) Q^\pi(s,a) + \pi_\theta(a|s) \nabla_\theta Q^\pi(s,a) \right) \tag{B.25}$$

$$\nabla_\theta V^\pi(s) = \sum_{a\in A} \left(\nabla_\theta \pi_\theta(a|s) Q^\pi(s,a) + \pi_\theta(a|s) \nabla_\theta \sum_{s',r} P(s',r|s,a)(r + V^\pi(s')) \right) \tag{B.26}$$

$$\nabla_\theta V^\pi(s) = \sum_{a\in A} \left(\nabla_\theta \pi_\theta(a|s) Q^\pi(s,a) + \pi_\theta(a|s) \sum_{s',r} P(s',r|s,a) \nabla_\theta V^\pi(s')) \right) \tag{B.27}$$

$$\nabla_\theta V^\pi(s) = \sum_{a\in A} \left(\nabla_\theta \pi_\theta(a|s) Q^\pi(s,a) + \pi_\theta(a|s) \sum_{s} P(s'|s,a) \nabla_\theta V^\pi(s') \right) \tag{B.28}$$

Perform iteration for future state $V^\pi(s')$. To rewrite the above equations that excludes Q-value function, $\nabla_\theta Q^\pi(s,a)$ by assigning it into the objective function, $J(\theta)$. Starting from a random state:

$$\nabla_\theta J(\theta) = \nabla_\theta V^\pi(s_0) \tag{B.29}$$

Let $\eta(s) = \sum_{k=0}^{\infty} \rho(s_0 \to s, k)$:

$$\nabla_\theta J(\theta) = \sum_s \sum_{k=0}^{\infty} \rho^\pi(s \to s, k) \phi(s) = \sum_s \eta(s) \phi(s) \tag{B.30}$$

Then normalise $\eta(s), s \in S$ to be a probability distribution:

$$\nabla_\theta J(\theta) = \left(\sum_s \eta(s) \right) \sum_s \frac{\eta(s)}{\sum_s \eta(s)} \phi(s) \tag{B.31}$$

Set $\sum_s \eta(s)$ constant:

$$\nabla_\theta J(\theta) \propto \sum_s \frac{\eta(s)}{\sum_s \eta(s)} \phi(s) \tag{B.32}$$

$$\nabla_\theta J(\theta) = \sum_s d^\pi(s) \sum_a \nabla_\theta \pi_\theta(a|s) Q^\pi(s,a) \tag{B.33}$$

where $d^\pi(s) = \frac{\eta(s)}{\sum_s \eta(s)}$ is stationary distribution.

Appendix C

Proof-of-Lemma for Chapter 4

C.1 Mixture Model

The approach in mixture model is to provide modelling assumptions of an analysed data set to have multimodal distribution. Typically, using a uni-model distribution (*i.e.* Gaussian) technique, a set of data can be modelled assuming that only one specified observation is analysed. After which maximum likelihood estimation is used to estimate distribution parameters; mean and variance. However, taking the assumption of that each sample come from the same distribution is too rigid and dose not provide intuitive sense about the sample.

Therefore, a multi-model distribution also known as mixture model provides a conscientious avenue when designing complex structured data. Assuming that a collective of data X, $\{X_1, X_2, ..., X_n\}$ and each sample, X_i is taken from K mixture component. Associated to a random variable, X_i, is a label of $Z_i \in \{1, ..., K\}$ where X_i come from. Z_i's are sometimes referred as latent variables. Hence, using the concept in law of total probability, the marginal probability of X_i is as follows:

$$p(X_i = x) = \sum_{k=1}^{K} P(X_i = x|Z_i = k)P(Z_i = k) \tag{C.1}$$

$s.t.$

$$\pi_k = P(Z_i = k) \tag{C.2}$$

where π_k is referred as mixture weights which represents the probability in which X_i belong to in the K mix. Mixture proportions are absolute integer values where the sum of π_k equates to 1:

$$\sum_{k=1}^{K} \pi_k = 1 \tag{C.3}$$

Meanwhile, the mixture component expressed as $P(X_i|Z_i = k)$ represents distribution of X_i with the assumption that X_i was extracted from k.

In the case of discrete random variables, the mixture component can be denote as any Probability Mass Function (PMF), $p(.|Z_k)$. Whereas for random variable in continuous, it uses Probability Density Function (PDF), $f(.|Z_k)$. (C.4) and (C.5) defines both the corresponding PMF and PDF for mixture model.

$$p(x) = \sum_{k=1}^{K} \pi_k p(x|Z_k) \tag{C.4}$$

$$f_x(x) = \sum_{k=1}^{K} \pi_k f_{x|Z_k}(x|Zk) \tag{C.5}$$

Based on the observed independent sample of $X_1, ..., X_n$ from mixture k and the mixture proportion vector, $\pi = (\pi_1, ..., \pi_K)$ therefore, the likelihood can be expressed as follow:

$$L(\pi) = \prod_{i=1}^{n} P(X_i|\pi) = \prod_{i=1}^{n} \sum_{k=1}^{K} P(X_i|Z_i = k)\pi_k \tag{C.6}$$

C.2 Validate Performance of Proposed Testbed Systems using Existing Methodologies

Prior operational validations of existing methods on simulated Microgrid testbed system are presented to ensure credibility when performing comparative studies. Two existing methodologies were selected to analyse socio-economic superiority and setbacks in respective proposed energy management system; hierarchical [244] and scenario-based stochastic [245]. Fig. C.1 represents the simulation environment, consisting of 5 Nanogrids, where the component ratings are approximately modelled close-to the proposed systems in [244] and [245] to validate methodology synchronisation. On a side note, the modelled VPP-NG5 (IPP) uses hybrid inverter that integrates ESS and solar PV farm at the DC-link before coupling to the VSC-based inverter.

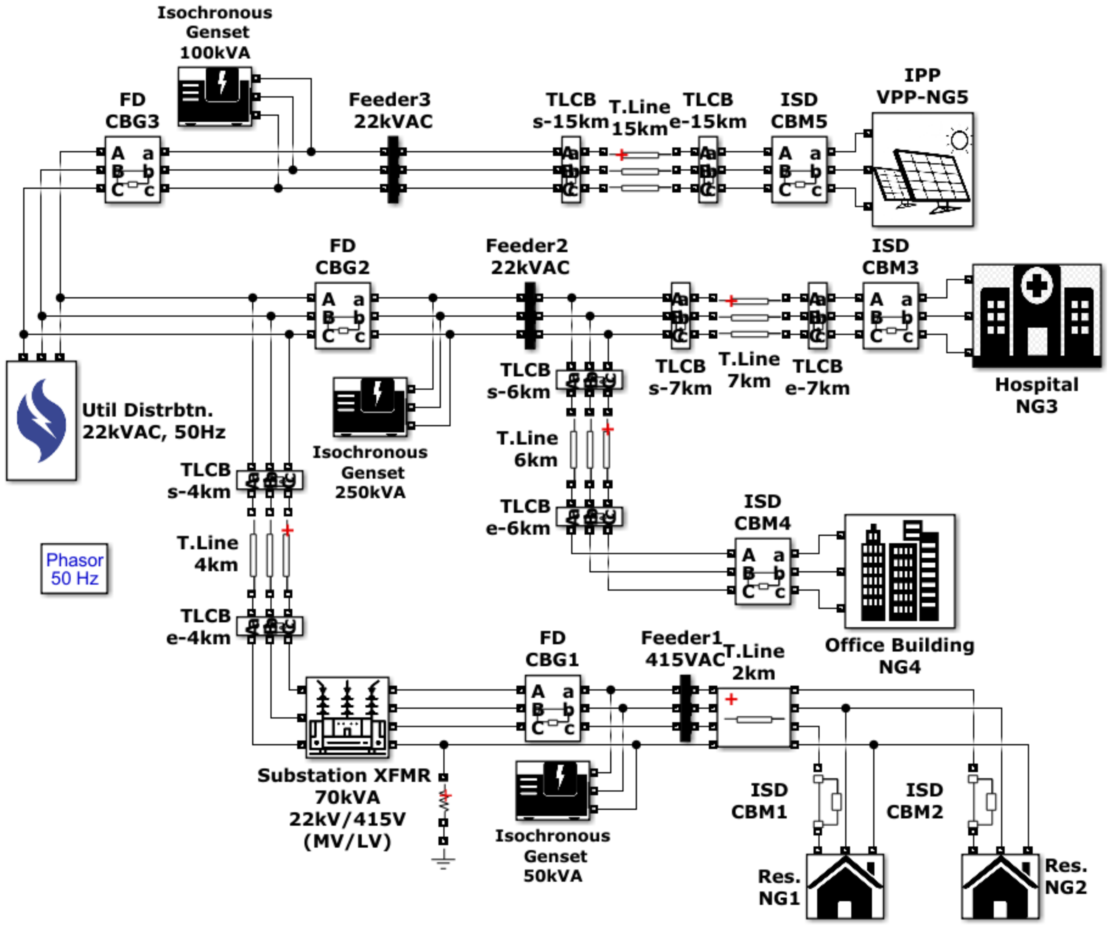

Fig. C.1 Proposed Prosumer Community Microgrid Testbed System consisting 2 residential homes (NG1, NG2), office commercial building (NG4), hospital commercial building (NG3), and IPP solar PV farm (NG5).

C.2.1 Hierarchical Energy Management System

Modelling of each component (*i.e.* DER capacity size, operation characteristics) in respective Nanogrids are based on the specifications suggested by [244] (Microgrid settings) hence, rationality of Nanogrid operating environment and BTM DER sizes may not be logical. However, it presents comparative simulated environment between the proposed and [244] for methodology validation purposes. Table C.1 lists the operating conditions of respective components that correspond to [244] and note that the installed isochronous generator at individual feeders will not be utilised as it is assumed that DERs are in grid-following mode. The objective is to deploy hierarchical EMS control architecture for Nanogrid engagements proposed in Fig. C.2b by scaling down Microgrid operation suggested in [244], Fig. C.2a. To synchronise operating attributes between Nanogrid and Microgrid Community, matching of

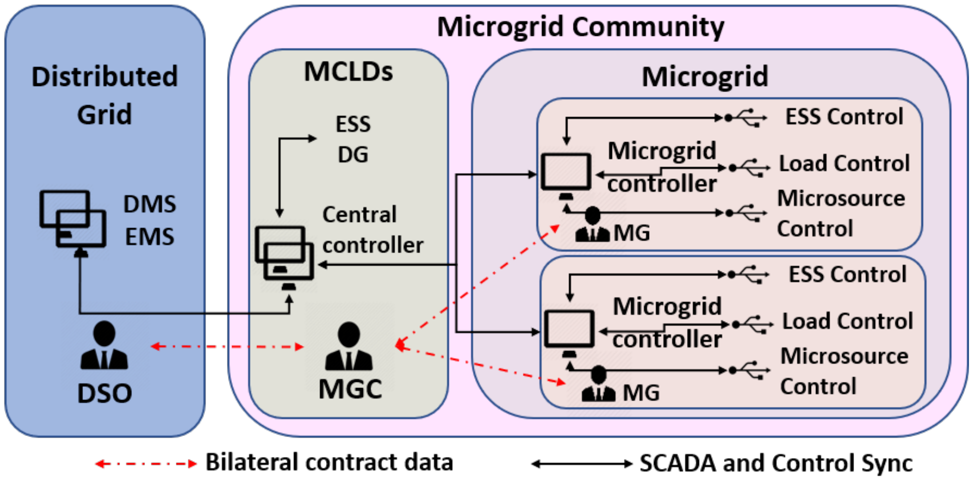

(a) Microgrid Community environment.

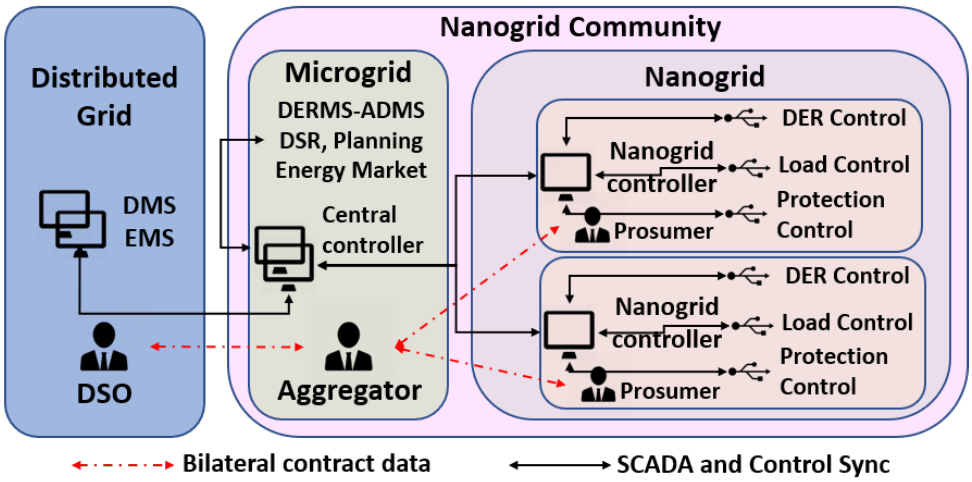

(b) Proposed Nanogrid Community environment.

Fig. C.2 Scaling down Microgrid Community control architecture for Nanogrid Community operations using hierarchical EMS methodology.

available power generation and demand load profile trends are validated as shown in Fig. C.3. Figure C.3a visualises the total DER power generation and consumption of the Nanogrid Community, monitored at distribution grid PCC, while Fig. C.3b scopes down into respective Nanogrids. Likewise, a similar trend was recorded where energy surplus and shortage was high during the day and nightfall respectively. The PV generation from Nanogrid 1, 2, and 4 exceeded the load consumption capacity due to it oversized ESS as compared to Nanogrid 3. Following presents the impact on using hierarchical EMS at respective Nanogrids and profiles their power exchange at PCC. There are two-part investigation processes for hierarchical EMS realisation as suggested; lower and upper level optimisation.

Lower Level EMS

The lower level schedules the local usage of ESS in the Nanogrid domain based on the constraints of available PV generation, maintenance cost coefficient, and power price. It then determines the required downstream or upstream power exchanged at PCC as seen in Fig. C.4a. A positive power rating implies that the Nanogrid need to purchase purchases power from upstream to meet local demand capacity, it being from other Nanogrids or Utility, while negative value expresses available excess power ready to be sold. A trend was observed

Table C.1 Installed DER ratings and performance index for respective Nanogrid.

Nanogrid	**NG1 Resd. (full-pledge)**	**NG2 Resd. (full-pledge)**	**NG3 Comm. (hospital)**	**NG4 Comm. (office)**	**NG5 IPP. (VPP)**
ESS (kWh)	57	71	75	91	200
Conv. config.	indept.	indept.	indept.	indept.	hybrid
DC-DC Controller	buck-boost (BMS-Volt.)	buck-boost (BMS-Volt.)	buck-boost (BMS-Volt.)	buck-boost (BMS-Volt.)	buck-boost (BMS-Volt.)
DC-AC Controller	FBI (hysterisis)	FBI (hysterisis)	VSI (VOC-DQ0)	VSI (VOC-DQ0)	shared PV –
CH/DCH limit (kW)	-50,50	-50,50	-50,50	-50,50	-200,200
SOC limit	20-80%	20-80%	20-80%	20-80%	20-80%
SOC init.	50%	50%	50%	50%	50%
Time-of-use power price (yuan/kWh)	Price Time	0.35 24:00 $\sim$ 0600	0.55 11:00 $\sim$ 13:00 17:00 $\sim$ 18:00 21:00 $\sim$ 23:00	0.85 07:00 $\sim$ 10:00 14:00 $\sim$ 16:00 19:00 $\sim$ 20:00	
Maintenance cost coeff. (yuan/kWh)	k_{ess}=0.027	k_{ess}=0.027	k_{ess}=0.027	k_{ess}=0.027	k_{ess}=0.027
ON & OFF time (repeat)	T_{ON}=1hr (strt) T_{OFF}=1hr	T_{ON}=1hr (strt) T_{OFF}=1hr	T_{ON}=1hr (strt) T_{OFF}=1hr	T_{ON}=1hr (strt) T_{OFF}=1hr	T_{ON}=1hr (strt) T_{OFF}=1hr
PV (kW)	5	5	30	30	100
Conv. config.	indept.	indept.	indept.	indept.	hybrid
DC-DC Controller	buck-boost MPPT-FOCV	buck-boost MPPT-FOCV	buck-boost MPPT-FOCV	buck-boost MPPT-FOCV	shared ESS –
DC-AC Controller	FBI (linear curr.)	FBI (linear curr.)	VSI (VOC-DQ0)	VSI (VOC-DQ0)	VSI (VOC-DQ0)
Maintenance cost coeff. (yuan/kWh)	k_{PV}=0.016	k_{ess}=0.016	k_{ess}=0.016	k_{ess}=0.016	k_{ess}=0.016

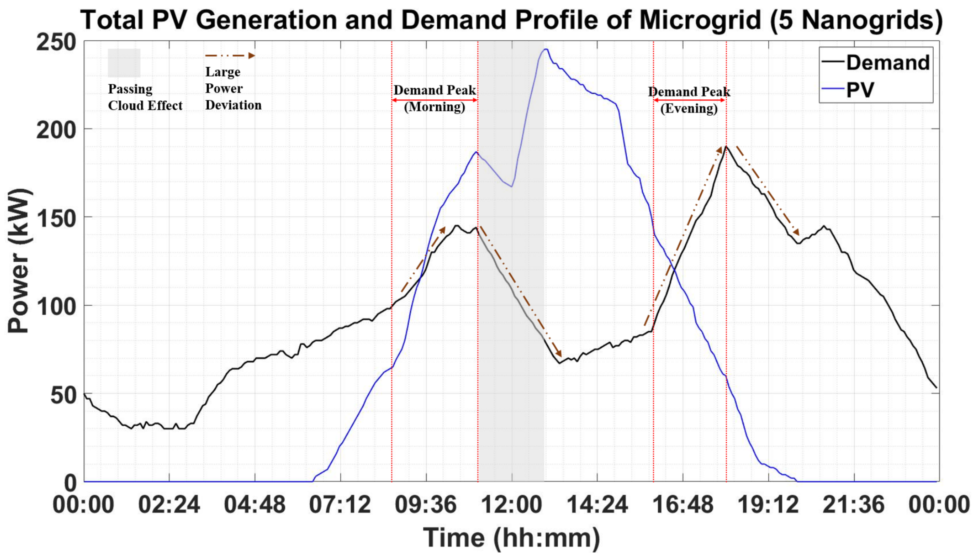

(a) Total PV generation and demand load capacity (5 Nanogrids).

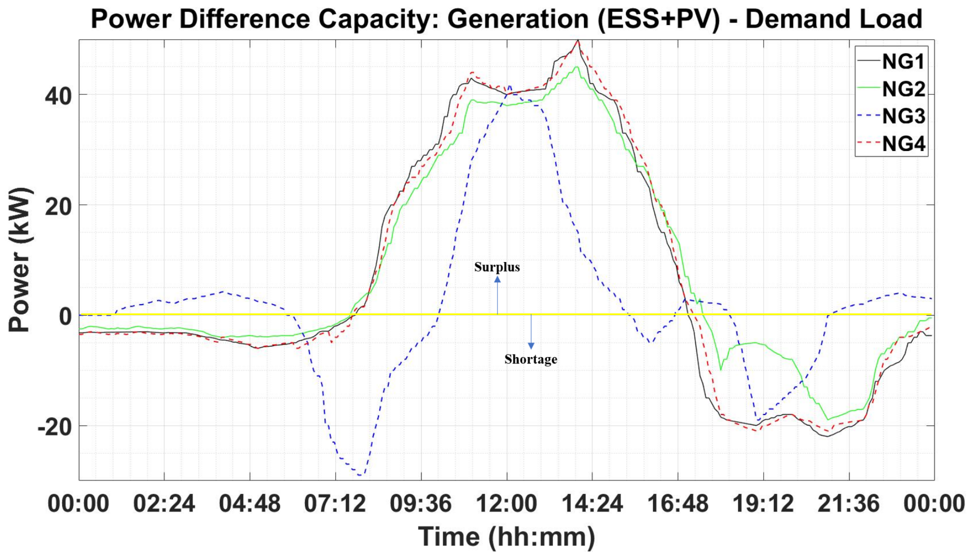

(b) Power difference between available generation (*i.e.* $ESS + PV$) and demand load capacity.

Fig. C.3 Profiling DER contributions against consumptions in Nanogrid Community.

during the day where all Nanogrids have scheduled to sell excess power upstream to minimise operational cost and higher return on investments.

Table C.2 presents the results attained from respective Nanogrids using three performance quantifiers, in lieu to Fig. C.4a; (i) total amount of energy exchanged at PCC, (ii) the costs gained/incurred for the amounted exchanged energy, and (iii) operating costs in a day (24hrs operation). The total earning solely represents the amount of money obtained from selling the surplus energy upstream (negative value) or paid for the exchanged energy to meet its

Table C.2 Total operation costs & profit margins gained from the scheduled exchanged energy.

Nanogrid	NG1	NG2	NG3	NG4
Total exchanged energy ($\|kWh\|$)	23	40	59	92
Earning from exchanged energy (*RMB* yuan)	-22.4	-27.7	129.4	-195.86
Paid operating costs (*RMB* yuan)	10.7	16.3	28.1	15.9
Profit/Loss margin (*RMB* yuan)	-11.7	-11.4	157.5	-179.9

local demand consumption capacity (positive value), excluding the operational costs incurred when utilising local DERs. The results shown a decreased in profit when compared to [244] as the proposed testbed system considers transmission losses and efficiency of inverters for DERs. Meanwhile, Fig. C.4b presents operation of ESS charging/discharging capacity for Nanogrid 3 and 4. Despite Nanogrid 3 is supported by ESS, it can be seen that majority of the duration is dependent on other Nanogrids or Utility to satisfy its load capacity as compared to Nanogrid 4. Mark at approximately 10:00-12:00 and 22:00-24:00, the algorithm suggests to charge ESS in order to reach normal range of SOC. Moreover, to gain maximum profit margin, ESS was discharged at 10:00–11:00 and 15:00–17:00 to sell excess power upstream as the electricity tariff was all time high. Similar power exchange and ESS operations is scheduled for Nanogrid 4 where from 10:00–12:00, ESS is charging to reach healthy SOC level however, it has larger contribution towards upstream generation due to its oversized ESS and low load consumption capacity unlike Nanogrid 3.

Upper Level EMS

Indeed investigations in [244] highlighted four Microgrid configuration modes and optimisation strategy however, following present results gathered for Microgrid operating in scenario 1 as it assumes Nanogrid operates in grid-following mode; Nanogrids does not operate in islanded and total demand consumptions will be supported by Utility. In this sense it is assumed that Microgrid operations will not be interrupted by fault and isochronous generators will not be considered in the upper level EMS.

For upper level EMS, analyses were focused into Nanogrid 5 (IPP) providing demand load support to Nanogrid 1 to 4 and view its power exchange and ESS charging/discharging power reference to meet demand capacity and SOC charge level of ESS as shown in Fig. C.5a. At 00:00-06:00, ESS in Nanogrid 5 purchases power from Utility to maintain ESS SOC level. The resulted EMS shown that Nanogrid 5 also delivers excess generation upstream due to high penetration of solar PV between 14:00-16:00 and benefited from the high electricity

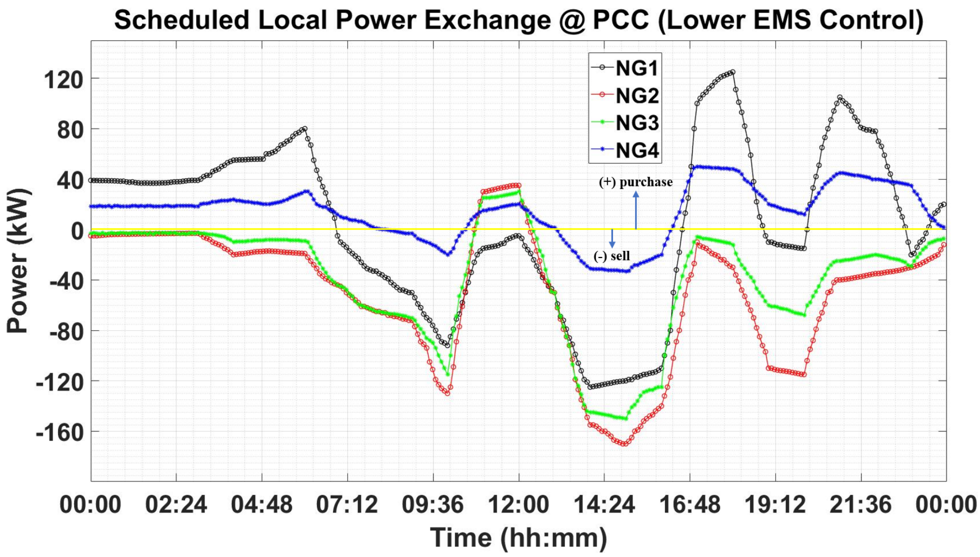

(a) Power exchanged, upstream and downstream.

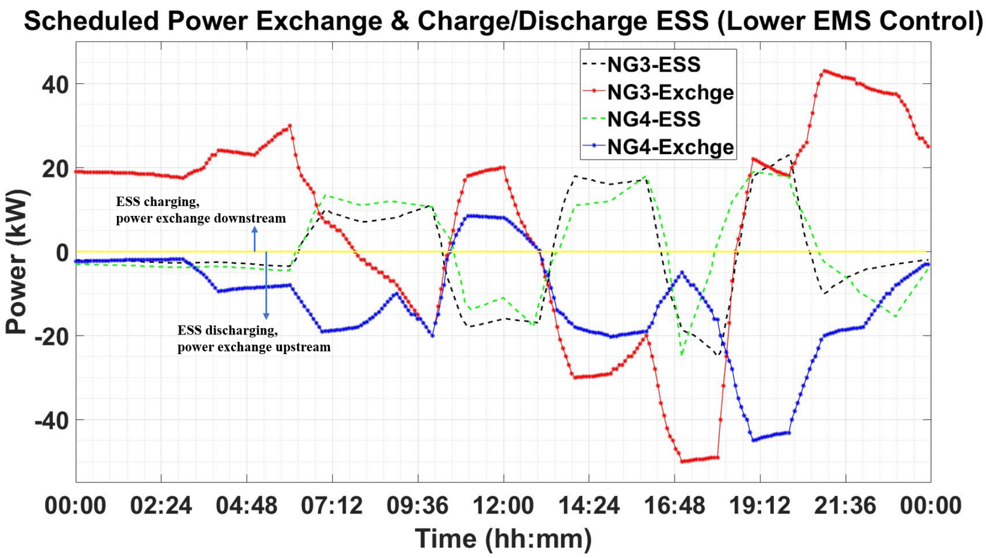

(b) Nanogrid 3 & 4 power exchange and ESS charging/discharging capacity.

Fig. C.4 Scheduled ESS and power exchange using lower level EMS algorithm for local optimum operating costs.

tariff for greater return on investments. Furthermore, Fig. C.5b presents the SOC curve index of Nanogrid 5 ESS in a day where it is limited to between 0.2–0.8 for charging/discharging operations. Moreover, the upper level EMS constraint defined that the ESS SOC index level must levelled above 0.5 at the end of day to contribute demand capacity from 00:00-06:00. Nanogrid 5 gained a profit of -318*RMB* yuan in selling surplus energy to Utility before distributing power back to the Nanogrids.

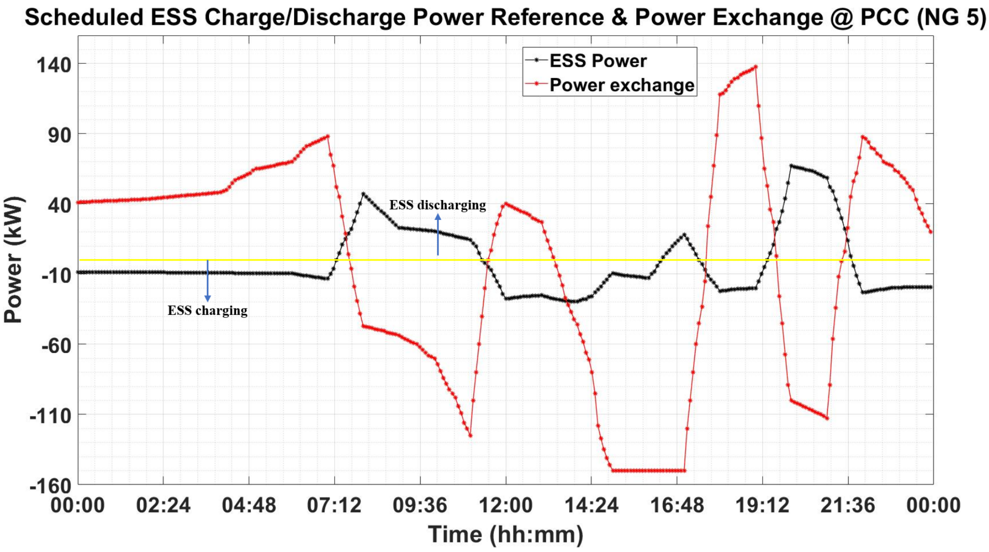

(a) Power exchange and ESS power contribution at PCC.

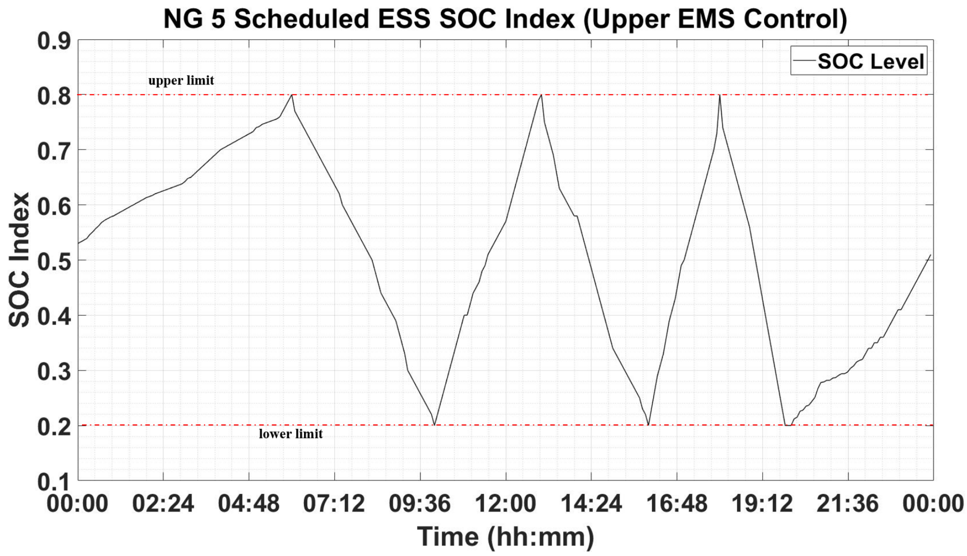

(b) SOC index level.

Fig. C.5 Scheduled ESS and power exchange in Nanogrid 5 for global optimum operating costs using upper level EMS.

Findings

The results attained from the proposed hierarchical EMS showed similar trends as presented in [244] however, the obtained optimised operating costs depreciated by approximately 13% due to; (i) consideration to transmission line losses when transporting power upstream, (ii) non-ideal power inverter efficiencies thus, experiencing depreciated power rating harvested from solar PV and charging/discharging power reference from ESS, and (iii) transmission charges which reduces received incentive payout. Moreover, optimised management in battery utilisation was rigid as it was programmed to sequentially discharge and charge power upon reaching maximum and minimum limit of SOC level and performed full charging or discharging operations without considering subsequent ESS state at $(t+i)$. Consequently, such operations can increase maintenance costs and depreciate battery state of health at an alarming speed.

Meanwhile, several observations were noticed when using hierarchical EMS against demand-side planning optimisation and unit commitment problem based on DER penetration in low-voltage level. Suggested in [244], the hierarchical EMS focuses in minimising operating costs where the lower level maximises operations of ESS and selling surplus energy upstream to gain greater return on investment while the upper level has similar objective but constrained to respective Nanogrids EMS interests which supports further operating costs curtailment at global level. Indeed, the results showed positive operating costs index where the EMS algorithm promotes upstream power exchange. However, it poses complications at DSO perspective where Duck Curve crisis, power level falling below the baseload criterion (overgeneration), and uncertainty in unit-commitment problem is guaranteed. Such predicaments can be solved through several prepositions; *(i)* employ Nanogrid 5 (IPP) to render ancillary services by storing these excess power into its local ESS and maximise power contribution during peak period, *(ii)* DSO needs to anticipate with optimum scheduling of unit-commitments for possible zero generation, *(iii)* greater incentives for participation in the $(N+1)$ redundancy (reserve) market for system resiliency to reduce upstream generation, *(iv)* promote peer-to-peer power trading based on profiling power consumption demographic of neighbouring Nanogrids and model optimum EMS operations accordingly, and (v) and local EMS must participate in DSR and load shedding to support unit-commitment and Duck-Curve problems.

C.2.2 Scenario-based Stochastic Energy Management System

In [245], the authors proposes a novel EMS method for a Microgrid operation which schedules DER-ESS and controllable loads based on generation uncertainty to minimise its operating costs/billings. It also assumes that the Microgrid takes part in the pool market and actively respond to electricity prices for maximum profit margin. A risk-constrained scenario-based stochastic programming framework using conditional value at risk method is suggested to address various uncertainties generated by RES, market prices, and customers' load consumption profiles. The algorithm is modelled in a double layered stochastic optimisation; *(i)*

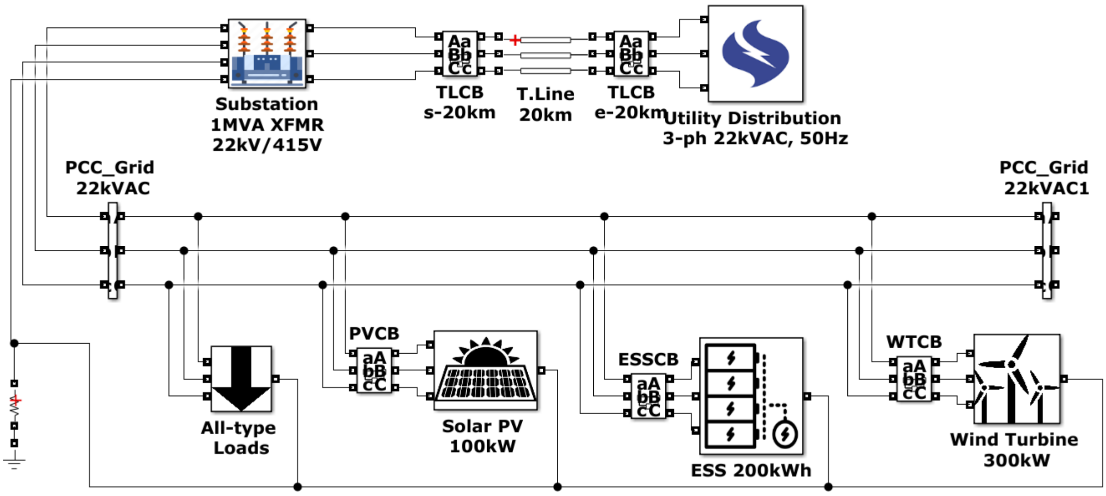

Fig. C.6 Proposed Microgrid testbed system comprising aggregated controllable loads, solar PV, ESS, and wind turbine system.

first layer−submit hourly optimum bidding to the day-ahead market based on the forecasted data (economic operation), and *(ii)* second layer−optimally schedule uncertain resources using scenario-based stochastic from their data (maximise profit). It aims to provide DER management services benefitting to customers, aggregators, and VPP owners. In addition, it acknowledge that the calculated profit margin will be at risk due to significant resource uncertainty in scenario-based stochastic programs hence, introduce risk management in the proposed objective functions.

The proposed optimisation algorithm focused at the global perspective of energy management, aggregator as energy service provider (Microgrid), which accumulates all DERs-ESSs resources and load where the power exchange trading and market participation transacts between Microgrid as a single EPS entity and Utility. In this sense, Fig. C.6 presents the testbed Microgrid system involving a $100kW$ solar PV, $200kWh$ ESS, $300kW$ wind turbine, and all-types loads (*i.e* fixed and controllable). It is assumed that the controllable load is not more than 50% of the total demand load at any time suggested in [263] as a rule of thumb. Meanwhile, the solar PV, wind turbine generation, and total demand load capacity for 24hr duration (1hr intervals) is forecasted based on [264] as shown in Fig. C.7a. Likewise, the forecasted electricity prices seen in Fig. C.7b is also adopted from [263]. The power generation profiles seen in Fig. C.7 are based on a ratio estimated solar PV irradiance and wind speed for the testbed system to gain similar power generation tends as suggested in [245]. Moreover, it specifies several operation constraints; *(i)* ESS charging/discharging ramp rates are limited to $50kW$ for each hour intervals, *(ii)* the maximum power exchange upstream/downstream is capped to $800kW$, *(iii)* the expected operation profit includes risk management limits, *(iv)*

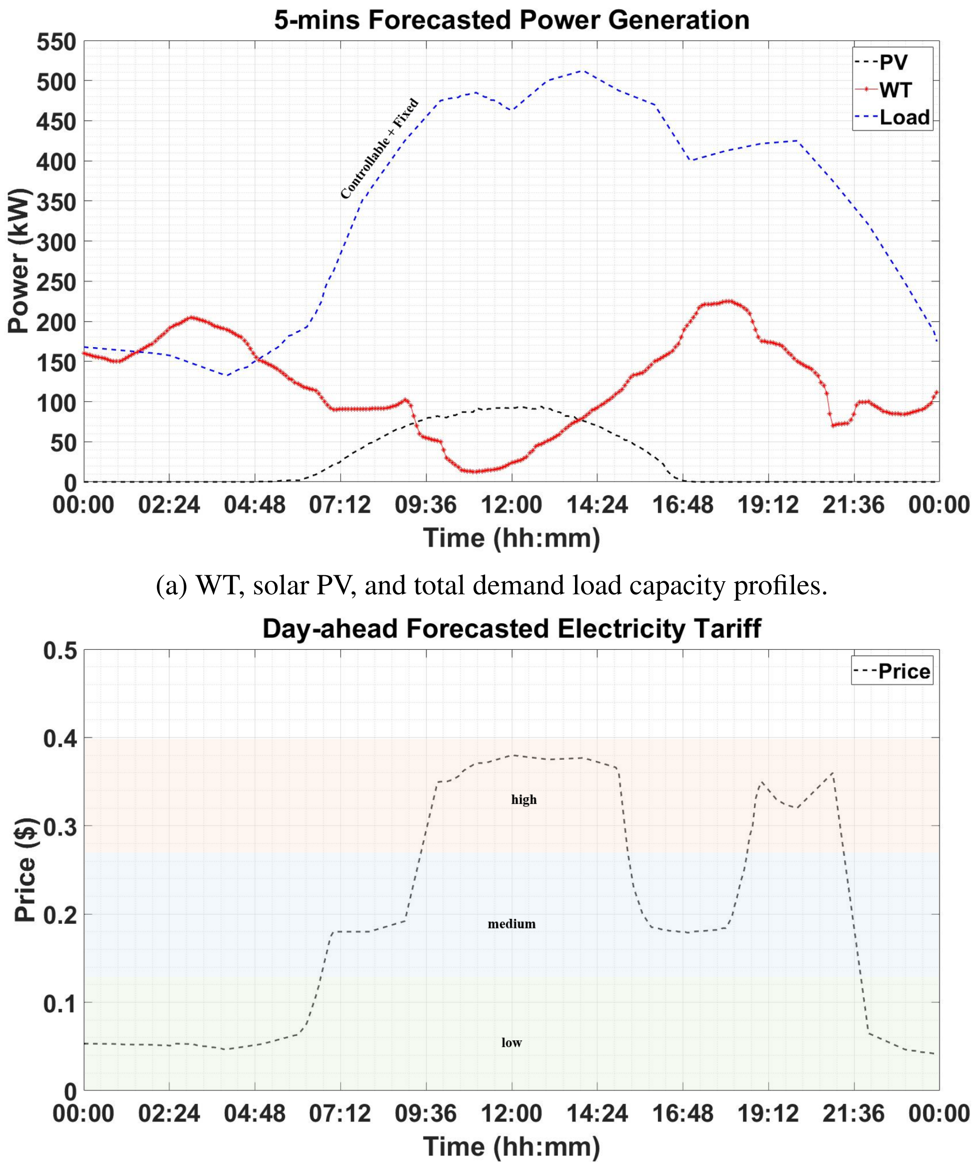

(a) WT, solar PV, and total demand load capacity profiles.

(b) Day-ahead electricity prices.

Fig. C.7 24Hrs forecasted data of resources defined in testbed system.

power converter configuration and efficiency for respective resources will adopt ratings listed in Table C.1, and (v) the maximum profit objective function do includes the sum of maintenance costs defined by a constant coefficient for solar PV:$k_{PV} = 0.027$,WT: $k_{WT} = 0.013$,and ESS: $k_{ESS} = 0.027$, $\sum OM(P) = k_i * P$.

Schedule Day-Ahead Microgrid Operations using Forecasted Data

Fig. C.8 illustrates the day-ahead scheduled resources for DERMS and controllable load consumptions driven by price-incentive model based on the forecasted power generation data of PV and WT, demand load capacity, and electricity tariff without considering stochastic optimisation for uncertainties. The trends in scheduling DERMS, load shifting, and power exchange between Utility pivoted on the electricity prices by identifying high and low regions for each hour intervals to meet the desired total 24Hrs demand load capacity.

The results highlights three scheduling performances; *(i)* power exchanged capacity to Microgrid where positive indicates downstream (*i.e.* purchase) and negative is upstream (*i.e.* sell), *(ii)* ESS power exchanged at PCC where positive value depicts the power discharging capacity and vice versa for negative, and lastly *(iii)* load transfer defines the increase/decrease in demand power shifted into that particular time stamp where negative value represents increase in load capacity by that much while positive value decreases. Observations showed that the power exchange from Utility fluctuates severely. Such trend is typical for a price-driven EMS model as it purchases large power capacity from Utility during low or medium electricity price regions seen at 06:00-10:00 and 16:00-18:00 and reduces load consumption capacities during high price seen at 08:00-12:00 and 14:00-15:00 where it maximises use of local resources to support the reduced load capacity (*i.e.* load shifting).

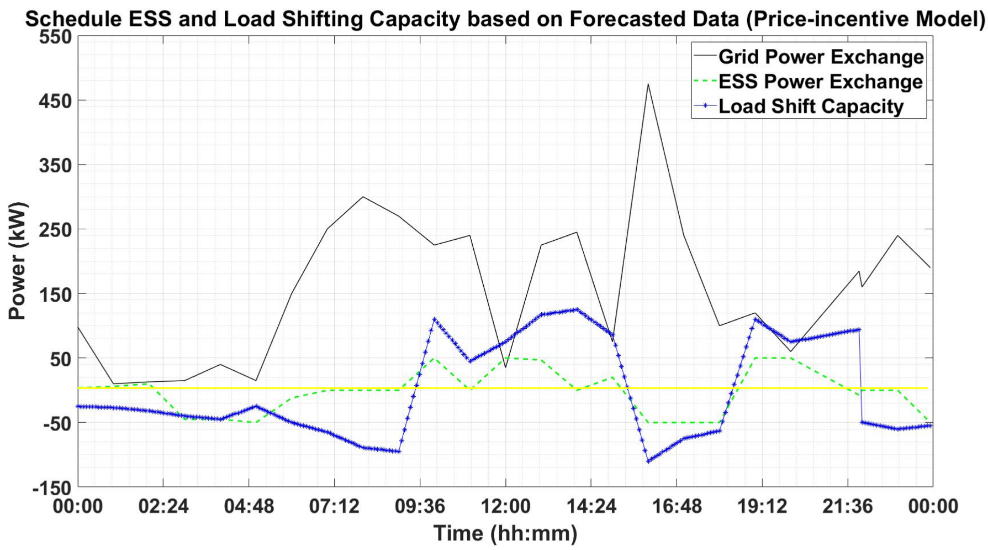

Fig. C.8 Scheduling day-ahead DERMS and controllable load capacity based on price-incentive model and forecasted data.

Bidding and Selling Strategies based on Scenario-based Electricity Prices

Similar scheduling investigations as Chapter C.2.2 were performed using the forecasted data however, the algorithm includes several scenarios representing the uncertainty parameters generated by Monte Carlo simulation into profiling PV, WT, load, and electricity price trends. Using Monte Carlo Latin Hypercube Sampling (LHS) approach, we generated 2000 scenarios and deployed scenario-based stochastic programming to solve optimum Microgrid

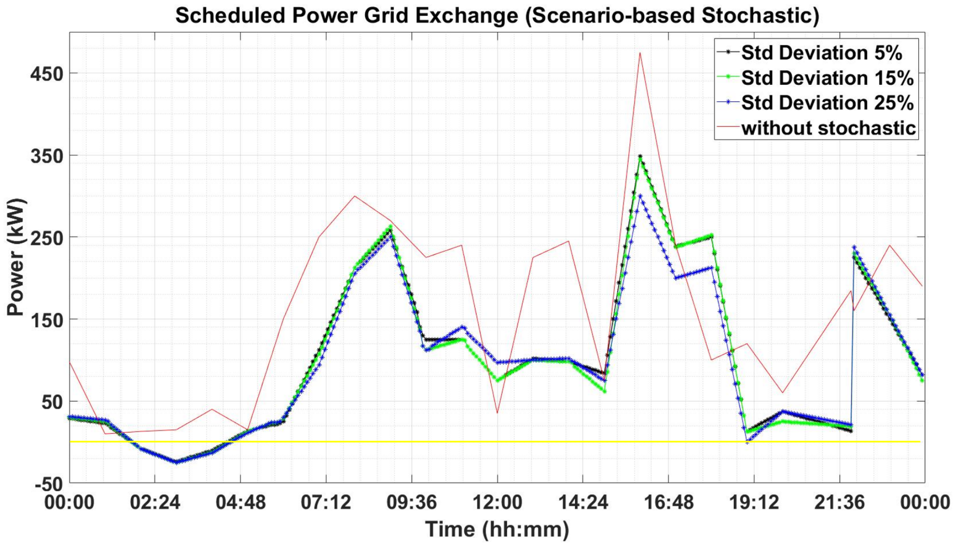

(a) Price standard deviation effects.

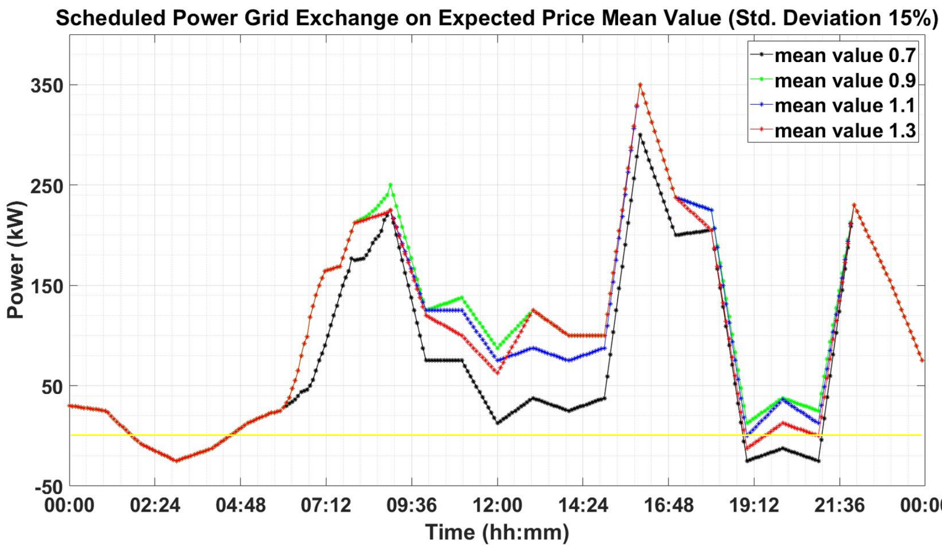

(b) Expected price mean value effects.

Fig. C.9 Power exchange management responses between Utility using scenarios-based to generate uncertainties.

Table C.3 Effects of price standard deviations on profit and CVaR.

Price Std. Deviation	Profit ($)	CVaR ($)
0.05	644.567	311.345
0.1	660.352	311.108
0.15	681.478	308.234
0.2	693.360	311.948
0.25	728.775	302.122

operations (*i.e.* maximum profit) that considers uncertainty circumstances. It is assumed that the forecasted electricity price errors are distributed normally with standard deviation ranges from 5% to 25% hence, Fig. C.9a presents the results of power exchange with Utility. It aimed to reduce power exchange fluctuations as compared to results attained in Fig. C.8. Likewise, less fluctuation index was recorded for standard deviations are less than 15% and power exchange rating decrease dramatically as standard deviation increases more than 25%.

Meanwhile, Fig. C.9b presents scheduled power purchase and sale strategy based on the expected electricity price mean values against standard deviation of 15%. Minimal power deviation were observed during 01:00-06:00 and 20:00-24:00 regardless of increase or decease in the expected electricity price mean value. Table C.3 compiles the profit and conditional value at risk based on price standard deviations.

Lastly, investigations into available percentage for load shifting to enhance demand response management was discussed to view impacts on scheduling strategy for power

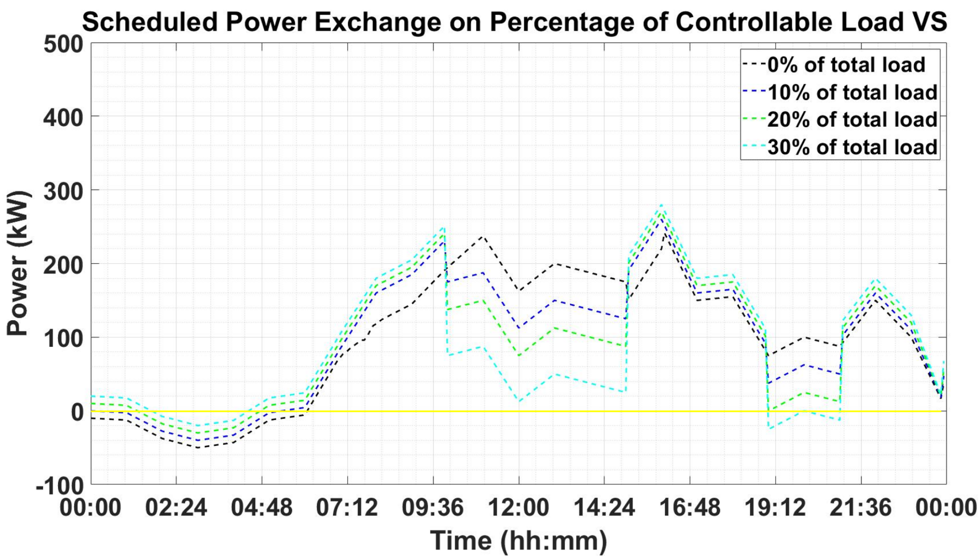

Fig. C.10 Scheduled power exchange responses against controllable load percentage available for shifting.

Table C.4 Effects of available controllable load percentages on Microgrid profit & CVaR.

Controllable Load/Total demand (%)	Profit ($)	CVaR ($)
0%	622.699	286.611
10%	645.502	291.188
20%	659.141	310.774
30%	674.272	328.948

exchange between Utility. The result seen in Fig. C.10 depicts that as the percentage for controllable load increases, the power exchange has greater power fluctuations however, it improves DSR crises by reducing load consumption during peak periods (*i.e.* 10:00-15:00) and increases during non-peak periods (*i.e.* 01:00-06:00). In this sense, Microgrid can gain better profit margin by shifting controllable load to other periods during peak and provide surplus power upstream at high electricity prices. Table C.4 presents the relationship between profit and CVaR against percentage of available controllable load capacity.

Findings

The results have shown similar performance trends when using the proposed testbed system seen in Fig. C.6 against the scenario-based stochastic EMS proposed in [245]. It analysed Microgrid operations that considered risk management to deal with uncertainty resources (*i.e.* DER, demand load capacity) and electricity prices in real-time. It proposed using forecasted data for day-ahead scheduling that involves controllable load management to address DSR crisis and strategic power exchange with Utility to maximise its profit margin. Moreover, it uses Monte Carlo LHS simulation to generate several scenarios to represent uncertain parameters and takes forecast errors into consideration. Indeed, the attained results showed lower profit and CVaR values due to several factors; *(i)* power converter efficiency for DERs are approximately 92% whereas [245] only considered battery efficiency, *(ii)* power losses (*i.e.* 10% loss) in the AC transmission line hence, power exchanged capacities are lower, and *(iii)* the proposed objective function for maximum profit includes maintenance costs of DERs (*i.e.* k_{ESS}, k_{PV}, k_{WT}).

Contrarily, the suggested optimisation approach for EMS serves at a Microgrid level, suitable for aggregators in gaining optimised DERMS. However, it lacks considerations in Prosumer engagements and securing individual energy business model interests as a constraint. How can scenario-based stochastic EMS serves at a Nanogrid level which latter used to render global yet cooperative solutions? Moreover, the uncertainty in DSR management and profit margin can be improved if Microgrid participates in the reserve market, supporting power quality management for DER penetrations.

Appendix D

Proof-of-Lemma for Chapter 5

D.0.1 Fault Level *MVA*

Calculation for fault MVA and current in steady-state condition:

Per unit short circuit current;

$$I^{SC}_{p.u.} = \frac{P.U.\text{voltage at fault location}}{P.U.X_{equiv.}} \tag{D.1}$$

Fault level per unit (MVA);

$$\sqrt{3}P.U.\text{fault current} \times P.U.\text{source voltage} \tag{D.2}$$

$$\text{Fault } MVA = \frac{\text{base } MVA}{P.U.X_{equiv.}} MVA \tag{D.3}$$

$$I_{SC} = \frac{\text{base } MVA \times 10^3}{\sqrt{3} \times \text{base } kV} \tag{D.4}$$

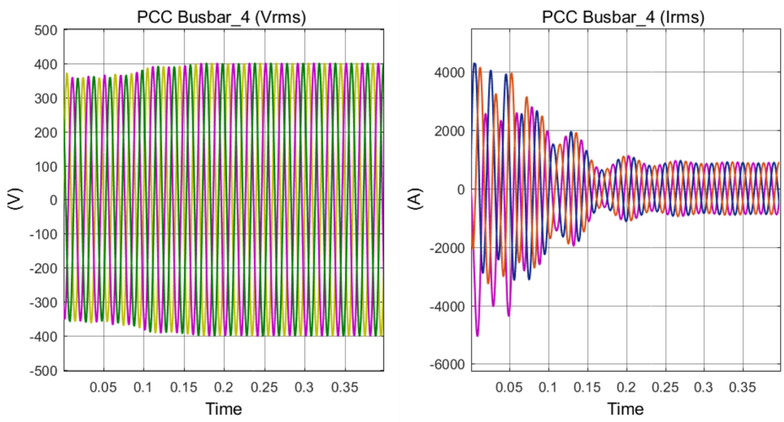

(a) Instantaneous voltage (RMS).

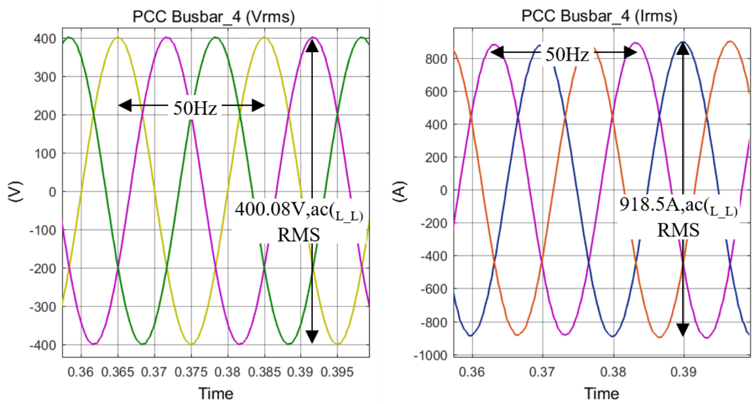

(b) Frequency (Hz).

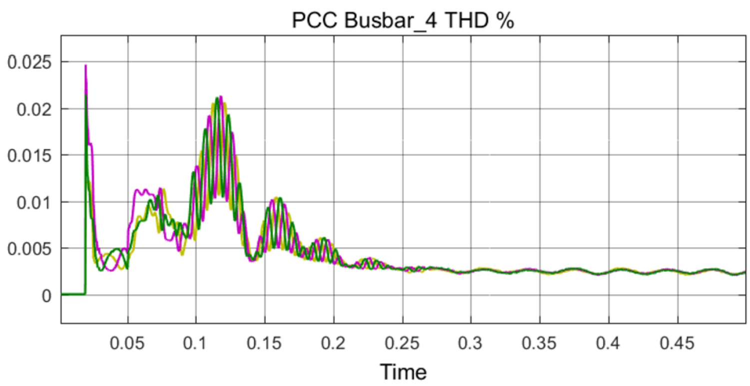

(c) THD%.

Fig. D.1 Instantaneous voltage and current transient at PCC busbar 4.

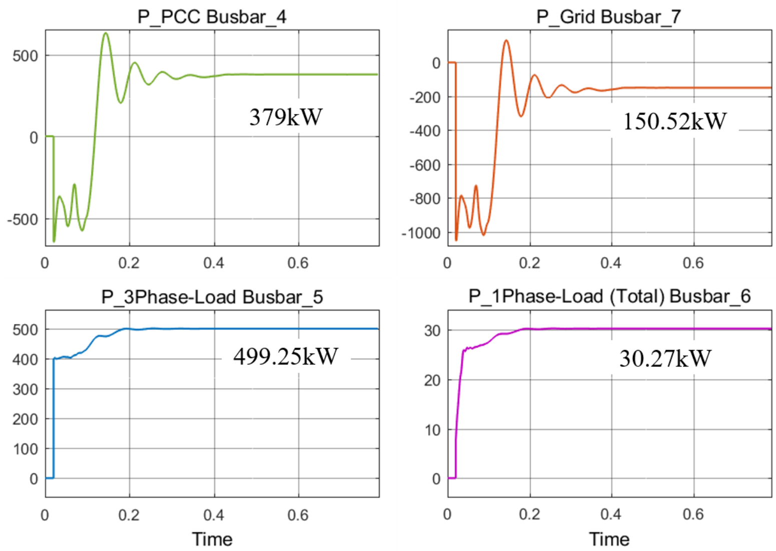

Fig. D.2 Power flow distribution at PCC (kW).

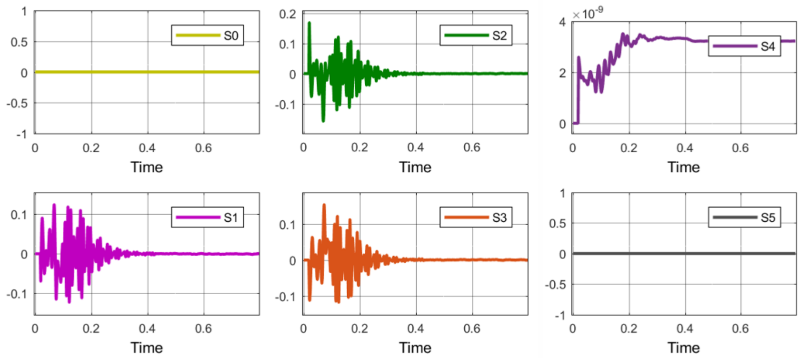

Fig. D.3 Crisp inputs for fuzzy inference system.

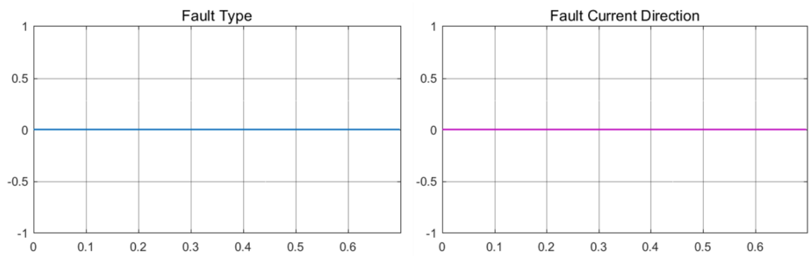

Fig. D.4 Crisp outputs from fuzzy inference system.

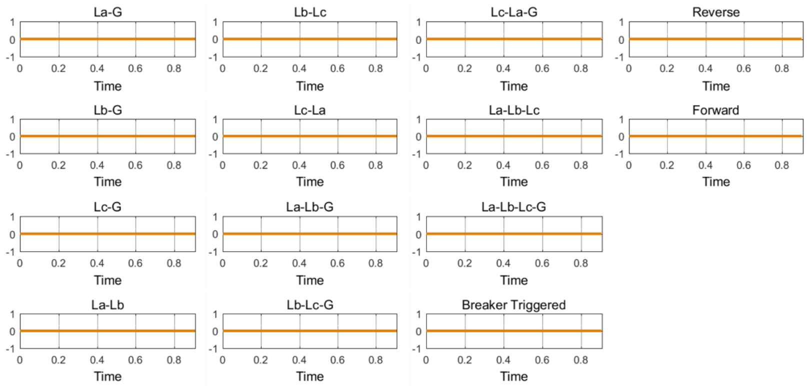

Fig. D.5 FL DOCR fault diagnostic report.

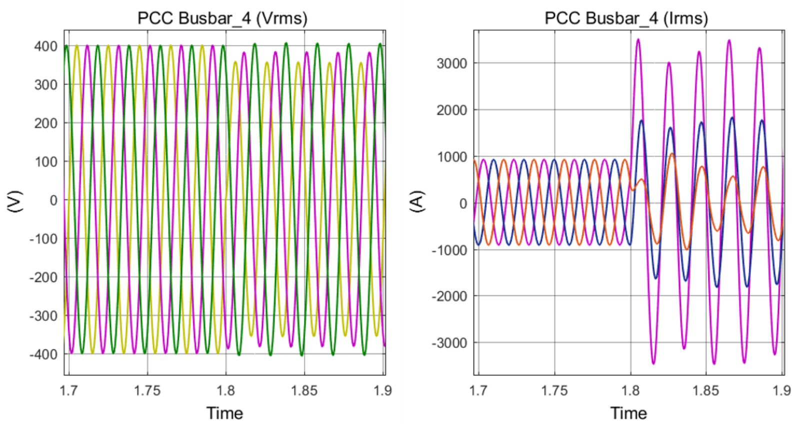

Fig. D.6 PMU voltage (left) and current (right) measurement at Busbar_4 during L_A-G fault interruption.

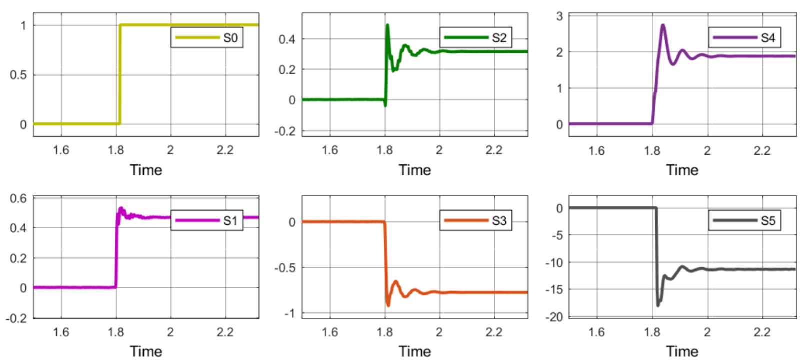

Fig. D.7 Crisp inputs (COCs) for fuzzy inference system, L_A-G.

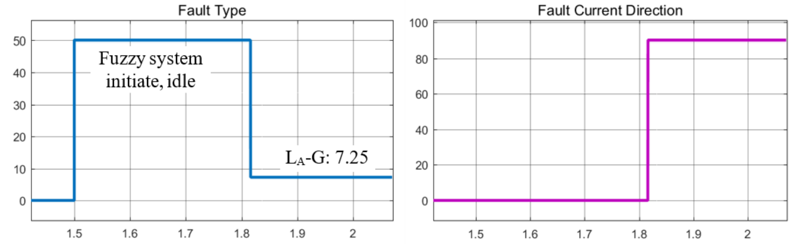

Fig. D.8 Fuzzy inference crisp outputs, L_A-G fault interruption.

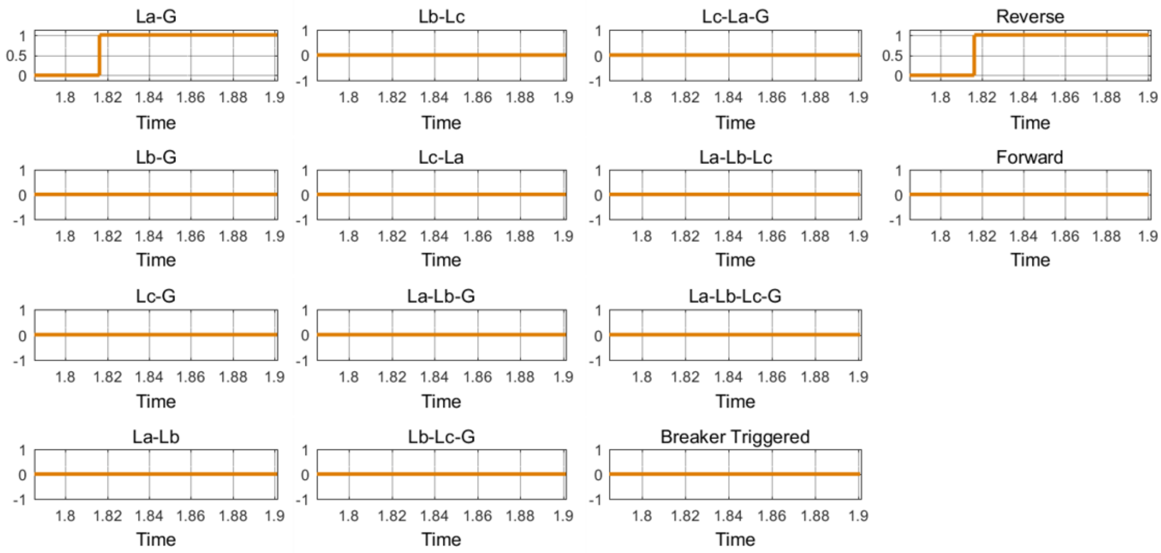

Fig. D.9 FL DOCR fault diagnostic report, L_A-G.

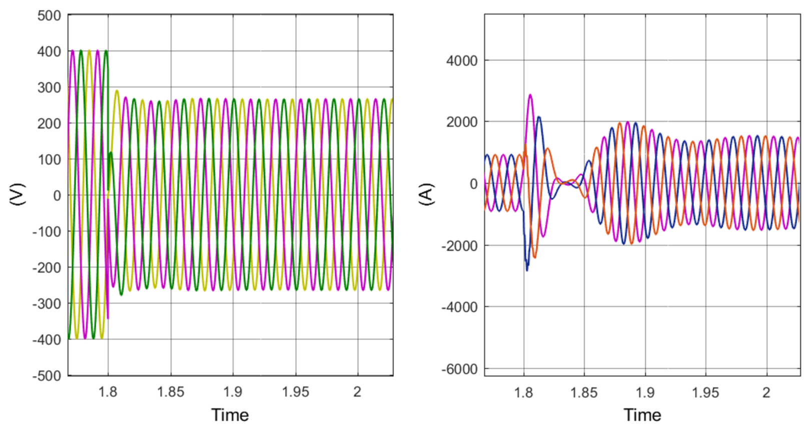

Fig. D.10 PMU voltage (left) and current (right) measurement at Busbar_4 during L_A-L_B-L_C fault interruption.

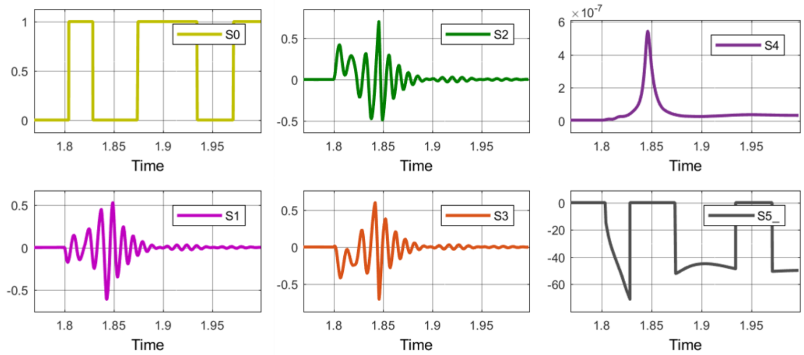

Fig. D.11 Crisp inputs (COCs) for fuzzy inference system, L_A-G.

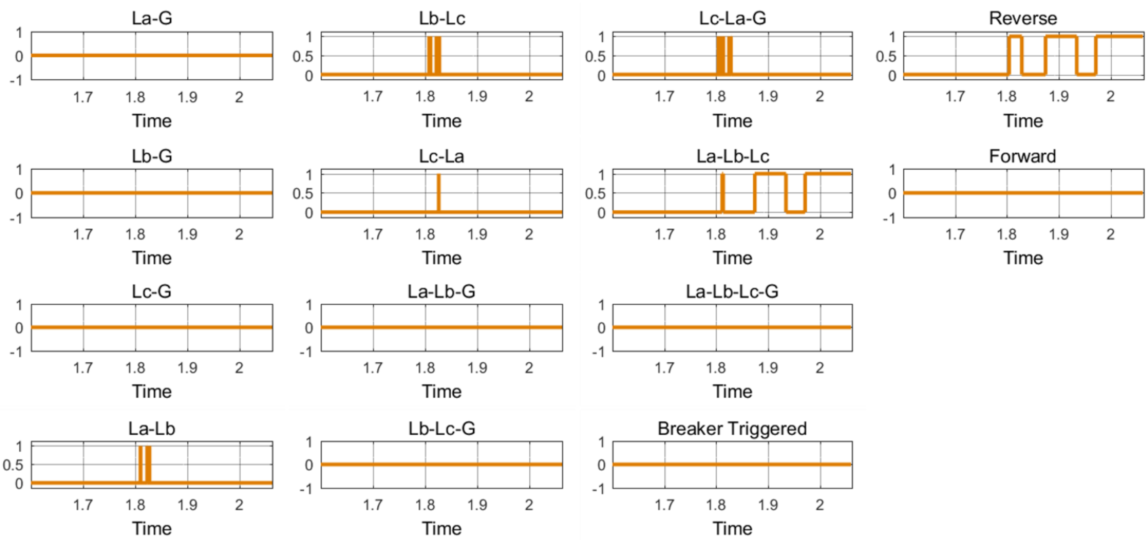

Fig. D.12 FL DOCR fault diagnostic report, L_A-G.

References

[1] L. Castanheira, G. Ault, M. Cardoso, J. McDonald, J. B. Gouveia, and Z. Vale, "Coordination of transmission and distribution planning and operations to maximise efficiency in future power systems," in *2005 International Conference on Future Power Systems*, pp. 5 pp.–5, 2005.

[2] C. Ward and W. Hung, "Electrical transmission system planning/operation-managing change and uncertainty," in *IEE Colloquium on Pipes vs Wires - The Interaction Between Gas and Electricity Transmission Systems (Ref. No. 1999/146)*, pp. 2/1–211, 1999.

[3] D. Shirmohammadi, B. Wollenberg, A. Vojdani, P. Sandrin, M. Pereira, F. Rahimi, T. Schneider, and B. Stott, "Transmission dispatch and congestion management in the emerging energy market structures," *IEEE Transactions on Power Systems*, vol. 13, no. 4, pp. 1466–1474, 1998.

[4] W. Dolega, "The role of transmission system operator in the context of energy security the case of poland," in *2010 Modern Electric Power Systems*, pp. 1–6, 2010.

[5] J. Tesseron, "Mission: Reliability," *IEEE Power and Energy Magazine*, vol. 6, no. 1, pp. 42–48, 2008.

[6] J. Han and A. Papavasiliou, "The impacts of transmission topology control on the european electricity network," *IEEE Transactions on Power Systems*, vol. 31, no. 1, pp. 496–507, 2016.

[7] S. Henry, P. Panciatici, and A. Parisot, "Going green: Transmission grids as enablers of the transition to a low-carbon european economy," *IEEE Power and Energy Magazine*, vol. 12, no. 2, pp. 26–35, 2014.

[8] R. M. M. Pereira, C. M. M. Ferreira, J. A. D. Pinto, and F. P. M. Barbosa, "Influence of the under load tap changers on the dynamic voltage collapse of an electric power system," in *39th International Universities Power Engineering Conference, 2004. UPEC 2004.*, vol. 3, pp. 1106–1110 vol. 2, 2004.

[9] G. Zhang, X. Guo, M. Swider, and M. Marwali, "Transmission constraint relaxation and pricing in the new york electricity market," in *2018 North American Power Symposium (NAPS)*, pp. 1–6, 2018.

[10] K. Sayler, S. M. Halpin, J. Valenzuela, and C. S. Park, "Pricing transmission congestion to alleviate system stability constraints in bulk power planning," in *Thirty-Sixth*

Southeastern Symposium on System Theory, 2004. Proceedings of the, pp. 261–265, 2004.

[11] N. A. Laway and H. O. Gupta, "A method for adaptive coordination of overcurrent relays in an interconnected power system," in *1993 Fifth International Conference on Developments in Power System Protection*, pp. 240–243, 1993.

[12] A. Ozdemir, M. Bagriyanik, I. Ilisu, O. Gul, A. Kaypmaz, and Y. Akkaya, "Impacts of protection system misoperation on the reliability of turkish national power transmission system," in *2011 International Conference on Advanced Power System Automation and Protection*, vol. 1, pp. 619–623, 2011.

[13] W. Shao, Y. Li, Y. Liu, and Xiaowei Zhang, "Non-fault detection for single-phase reclosure of transmission lines based on fault location," in *2011 IEEE Power Engineering and Automation Conference*, vol. 2, pp. 421–424, 2011.

[14] D. del Rio, I. Gurutzeaga, H. Solar, A. Beriain, A. Rezola, I. Velez, and R. Berenguer, "Variable-length transmission lines for self-healing systems and reconfigurable millimeter-wave integrated circuits," in *2017 32nd Conference on Design of Circuits and Integrated Systems (DCIS)*, pp. 1–5, 2017.

[15] H. Saboori, M. Mohammadi, and R. Taghe, "Virtual power plant (vpp), definition, concept, components and types," in *2011 Asia-Pacific Power and Energy Engineering Conference*, pp. 1–4, 2011.

[16] M. Lv, S. Lou, B. Liu, Z. Fan, and Z. Wu, "Review on power generation and bidding optimization of virtual power plant," in *2017 International Conference on Electrical Engineering and Informatics (ICELTICs)*, pp. 66–71, 2017.

[17] J. M. Xu, Y. Sun, Q. Sun, and J. W. Ma, "A comprehensive evaluation index system of virtual power plant participating in power coordination and optimal dispatching," in *2018 IEEE International Conference on Applied Superconductivity and Electromagnetic Devices (ASEMD)*, pp. 1–2, 2018.

[18] J. Yang, Q. Zheng, J. Zhao, X. Guo, and C. Gao, "Control strategy of virtual power plant participating in the system frequency regulation service," in *2017 4th International Conference on Systems and Informatics (ICSAI)*, pp. 324–328, 2017.

[19] S. R. Dabbagh and M. K. Sheikh-El-Eslami, "Risk assessment of virtual power plants offering in energy and reserve markets," *IEEE Transactions on Power Systems*, vol. 31, no. 5, pp. 3572–3582, 2016.

[20] H. Nezamabadi and M. Setayesh Nazar, "Arbitrage strategy of virtual power plants in energy, spinning reserve and reactive power markets," *IET Generation, Transmission Distribution*, vol. 10, no. 3, pp. 750–763, 2016.

[21] A. Mnatsakanyan and S. W. Kennedy, "A novel demand response model with an application for a virtual power plant," *IEEE Transactions on Smart Grid*, vol. 6, no. 1, pp. 230–237, 2015.

[22] I. P. I. T. S. T. Force, "Managing the new grid," tech. rep., Quanta Technology, USA, July 2018.

[23] C. Vartanian, R. Bauer, L. Casey, C. Loutan, D. Narang, and V. Patel, "Ensuring system reliability: Distributed energy resources and bulk power system considerations," *IEEE Power and Energy Magazine*, vol. 16, no. 6, pp. 52–63, 2018.

[24] K. Manickavasagam, "Intelligent energy control center for distributed generators using multi-agent system," *IEEE Transactions on Power Systems*, vol. 30, no. 5, pp. 2442–2449, 2015.

[25] R. T. Guttromson, "Modeling distributed energy resource dynamics on the transmission system," *IEEE Transactions on Power Systems*, vol. 17, no. 4, pp. 1148–1153, 2002.

[26] I. J. Perez-Arriaga, "The transmission of the future: The impact of distributed energy resources on the network," *IEEE Power and Energy Magazine*, vol. 14, no. 4, pp. 41–53, 2016.

[27] J. Arai, K. Iba, T. Funabashi, Y. Nakanishi, K. Koyanagi, and R. Yokoyama, "Power electronics and its applications to renewable energy in japan," *IEEE Circuits and Systems Magazine*, vol. 8, no. 3, pp. 52–66, 2008.

[28] J. S. Horton, B. Prince, A. M. Sasson, W. T. Wynne, F. Trefny, F. Cleveland, and J. T. Robinson, "Advances in energy management systems," *IEEE Power Engineering Review*, vol. PER-6, pp. 50–50, Aug 1986.

[29] F. Maghsoodlou, R. Masiello, and T. Ray, "Energy management systems," *IEEE Power and Energy Magazine*, vol. 2, pp. 49–57, Sep. 2004.

[30] F. F. Wu, K. Moslehi, and A. Bose, "Power system control centers: Past, present, and future," *Proceedings of the IEEE*, vol. 93, pp. 1890–1908, Nov 2005.

[31] K. Ghoshal, "Distribution automation: Scada integration is key," *IEEE Computer Applications in Power*, vol. 10, no. 1, pp. 31–35, 1997.

[32] C. T. Lindeberg and W. R. Block, "Project planning for ems and scada systems," *IEEE Computer Applications in Power*, vol. 6, no. 4, pp. 40–45, 1993.

[33] A. A. Sallam and O. P. Malik, *Scada Systems and Smart Grid Vision*, pp. 469–493. 2011.

[34] R. H. Simpson, "Power system data base management," *IEEE Transactions on Industry Applications*, vol. 37, pp. 153–157, Jan 2001.

[35] J. C. Van Gorp, "Enterprising energy management," *IEEE Power and Energy Magazine*, vol. 2, pp. 59–63, Jan 2004.

[36] M. Lobur, S. Tkachenko, and O. Khnykin, "Researching and creation of scada system," in *2011 11th International Conference The Experience of Designing and Application of CAD Systems in Microelectronics (CADSM)*, pp. 371–372, 2011.

[37] Rajeev Kumar, M. L. Dewal, and Kalpana Saini, "Utility of scada in power generation and distribution system," in *2010 3rd International Conference on Computer Science and Information Technology*, vol. 6, pp. 648–652, 2010.

[38] P. Guha Thakurta, J. Maeght, R. Belmans, and D. Van Hertem, "Increasing transmission grid flexibility by tso coordination to integrate more wind energy sources while maintaining system security," *IEEE Transactions on Sustainable Energy*, vol. 6, no. 3, pp. 1122–1130, 2015.

[39] S. Perkin, C. Hamon, R. Kristjansson, H. Stefansson, and P. Jensson, "Framework for trajectory-based probabilistic security assessment of power systems," *IET Generation, Transmission Distribution*, vol. 13, no. 7, pp. 1088–1094, 2019.

[40] "Ieee approved draft recommended practice for conducting load-flow studies of industrial and commercial power systems," *IEEE P3002.2/D9, September 2017*, pp. 1–82, 2018.

[41] A. Monticelli and F. F. Wu, "Observability analysis for orthogonal transformation based state estimation," *IEEE Transactions on Power Systems*, vol. 1, no. 1, pp. 201–206, 1986.

[42] P. C. Wong, Z. Huang, Y. Chen, P. Mackey, and S. Jin, "Visual analytics for power grid contingency analysis," *IEEE Computer Graphics and Applications*, vol. 34, no. 1, pp. 42–51, 2014.

[43] K. Iba, H. Suzuki, K. . Suzuki, and K. Suzuki, "Practical reactive power allocation/operation planning using successive linear programming," *IEEE Transactions on Power Systems*, vol. 3, no. 2, pp. 558–566, 1988.

[44] Z. Wu, J. Ding, Q. H. Wu, Z. Jing, and J. Zheng, "Reserve constrained dynamic economic dispatch with valve-point effect: A two-stage mixed integer linear programming approach," *CSEE Journal of Power and Energy Systems*, vol. 3, no. 2, pp. 203–211, 2017.

[45] M. Tuffaha and J. T. Gravdahl, "Dynamic formulation of the unit commitment and economic dispatch problems," in *2015 IEEE International Conference on Industrial Technology (ICIT)*, pp. 1294–1298, 2015.

[46] M. Q. Wang, H. B. Gooi, S. X. Chen, and S. Lu, "A mixed integer quadratic programming for dynamic economic dispatch with valve point effect," *IEEE Transactions on Power Systems*, vol. 29, no. 5, pp. 2097–2106, 2014.

[47] M. Farsadi, H. Hosseinnejad, and T. S. Dizaji, "Solving unit commitment and economic dispatch simultaneously considering generator constraints by using nested pso," in *2015 9th International Conference on Electrical and Electronics Engineering (ELECO)*, pp. 493–499, 2015.

[48] B. M. S. Muhammad Ramadan, T. Logenthiran, R. T. Naayagi, and C. Su, "Hybridization of genetic algorithm and priority list to solve economic dispatch problems," in *2016 IEEE Region 10 Conference (TENCON)*, pp. 1467–1470, 2016.

[49] R. Hoffman, R. C. Young, B. Vishnubhatla, B. Ganesan, R. Johnson, and F. Tempel, "The energy scheduling and accounting package for the grant county pud scada/agc system," in *[Proceedings] Conference Papers 1991 Power Industry Computer Application Conference*, pp. 134–139, 1991.

[50] H. Mohammadnezhad-Shourkaei, A. Abiri-Jahromi, and M. Fotuhi-Firuzabad, “Incorporating service quality regulation in distribution system maintenance strategy,” *IEEE Transactions on Power Delivery*, vol. 26, pp. 2495–2504, Oct 2011.

[51] H. Farzin, M. Fotuhi-Firuzabad, and M. Moeini-Aghtaie, “Role of outage management strategy in reliability performance of multi-microgrid distribution systems,” *IEEE Transactions on Power Systems*, vol. 33, pp. 2359–2369, May 2018.

[52] D. F. Hall, “Outage management systems as integrated elements of the distribution enterprise,” in *2001 IEEE/PES Transmission and Distribution Conference and Exposition. Developing New Perspectives (Cat. No.01CH37294)*, vol. 2, pp. 1175–1177 vol.2, 2001.

[53] I. S. Baxevanos and D. P. Labridis, “Implementing multiagent systems technology for power distribution network control and protection management,” *IEEE Transactions on Power Delivery*, vol. 22, no. 1, pp. 433–443, 2007.

[54] N. Singh, E. Kliokys, H. Feldmann, R. Kussel, R. Chrustowski, and C. Joborowicz, “Power system modelling and analysis in a mixed energy management and distribution management system,” *IEEE Transactions on Power Systems*, vol. 13, no. 3, pp. 1143–1149, 1998.

[55] Z. Ullah, G. Mokryani, F. Campean, and Y. F. Hu, “Comprehensive review of vpps planning, operation and scheduling considering the uncertainties related to renewable energy sources,” *IET Energy Systems Integration*, vol. 1, no. 3, pp. 147–157, 2019.

[56] Jun Yu and S. X. Wang, “A study of ercot real-time energy market price,” in *2006 IEEE Power Engineering Society General Meeting*, pp. 6 pp.–, 2006.

[57] Z.-f. Tan, H.-h. Li, L.-w. Ju, and Q.-k. Tan, “Joint scheduling optimization of virtual power plants and equitable profit distribution using shapely value theory,” *Mathematical Problems in Engineering*, vol. 2018, 2018.

[58] D. Thomas, M. Iain, and G. Dale, “Virtual power plants leveraging energy flexibility in regional markets,” *CIRED - Open Access Proceedings Journal*, vol. 2017, no. 1, pp. 2939–2943, 2017.

[59] Y. Wang, X. Ai, Z. Tan, L. Yan, and S. Liu, “Interactive dispatch modes and bidding strategy of multiple virtual power plants based on demand response and game theory,” *IEEE Transactions on Smart Grid*, vol. 7, no. 1, pp. 510–519, 2016.

[60] M. Farhoodnea, A. Mohamed, H. Shareef, and H. Zayandehroodi, “Power quality impact of renewable energy based generators and electric vehicles on distribution systems,” *Procedia Technology*, vol. 11, pp. 11–17, 2013.

[61] Y. Wu and J. Hong, “A literature review of wind forecasting technology in the world,” in *2007 IEEE Lausanne Power Tech*, pp. 504–509, 2007.

[62] M. U. Yousuf, I. Al-Bahadly, and E. Avci, “Current perspective on the accuracy of deterministic wind speed and power forecasting,” *IEEE Access*, vol. 7, pp. 159547–159564, 2019.

[63] M. Cerjan, I. Krželj, M. Vidak, and M. Delimar, "A literature review with statistical analysis of electricity price forecasting methods," in *Eurocon 2013*, pp. 756–763, July 2013.

[64] H. Nezamabadi and M. Setayesh Nazar, "Arbitrage strategy of virtual power plants in energy, spinning reserve and reactive power markets," *IET Generation, Transmission Distribution*, vol. 10, no. 3, pp. 750–763, 2016.

[65] T. D. Towada, "Green data center and virtual power plant," Mar. 19 2009. US Patent App. 12/197,088.

[66] Anuradha M. Annaswamy and Massoud Amin, "Ieee vision for smart grid controls: 2030 and beyond," *IEEE Vision for Smart Grid Controls: 2030 and Beyond*, pp. 1–168, 2013.

[67] H. Nezamabadi and M. Setayesh Nazar, "Arbitrage strategy of virtual power plants in energy, spinning reserve and reactive power markets," *IET Generation, Transmission Distribution*, vol. 10, no. 3, pp. 750–763, 2016.

[68] A. Baringo, L. Baringo, and J. M. Arroyo, "Day-ahead self-scheduling of a virtual power plant in energy and reserve electricity markets under uncertainty," *IEEE Transactions on Power Systems*, vol. 34, no. 3, pp. 1881–1894, 2019.

[69] J. Romero Aguero and A. Khodaei, "Grid modernization, der integration utility business models - trends challenges," *IEEE Power and Energy Magazine*, vol. 16, no. 2, pp. 112–121, 2018.

[70] B. Olek and M. Wierzbowski, "Local energy balancing and ancillary services in low-voltage networks with distributed generation, energy storage, and active loads," *IEEE Transactions on Industrial Electronics*, vol. 62, no. 4, pp. 2499–2508, 2015.

[71] S. P. Burger, J. D. Jenkins, S. C. Huntington, and I. J. Perez-Arriaga, "Why distributed?: A critical review of the tradeoffs between centralized and decentralized resources," *IEEE Power and Energy Magazine*, vol. 17, no. 2, pp. 16–24, 2019.

[72] M. D. Ilic, R. Jaddivada, and M. Korpas, "Interactive protocols for distributed energy resource management systems (derms)," *IET Generation, Transmission Distribution*, vol. 14, no. 11, pp. 2065–2081, 2020.

[73] D. Pudjianto, C. Ramsay, and G. Strbac, "Virtual power plant and system integration of distributed energy resources," *IET Renewable Power Generation*, vol. 1, no. 1, pp. 10–16, 2007.

[74] A. Maitra, T. Hubert, J. Wang, R. Singh, N. Kang, X. Lu, J. Reilly, A. Pratt, and S. Veda, "Dms advanced applications for accommodating high penetrations of ders and microgrids," *CIRED - Open Access Proceedings Journal*, vol. 2017, no. 1, pp. 2236–2240, 2017.

[75] K. Furukawa, D. Katoh, and T. Onishi, "Next generation scada system for distribution network with large amounts of renewable energy," in *2012 China International Conference on Electricity Distribution*, pp. 1–5, 2012.

[76] A. Nagarajan and R. Ayyanar, “Design and strategy for the deployment of energy storage systems in a distribution feeder with penetration of renewable resources,” *IEEE Transactions on Sustainable Energy*, vol. 6, no. 3, pp. 1085–1092, 2015.

[77] Yue Shi, Zhan Shen, and M. E. Baran, “A decentralized volt/var optimization scheme for smart distribution systems,” in *2016 IEEE Power Energy Society Innovative Smart Grid Technologies Conference (ISGT)*, pp. 1–5, 2016.

[78] A. Fazio, G. Fusco, and M. Russo, “Smart der control for minimizing power losses in distribution feeders,” *Electric Power Systems Research*, vol. 109, p. 71–79, 04 2014.

[79] B. Kroposki, P. K. Sen, and K. Malmedal, “Selection of distribution feeders for implementing distributed generation and renewable energy applications,” *IEEE Transactions on Industry Applications*, vol. 49, no. 6, pp. 2825–2834, 2013.

[80] B. Kroposki, P. K. Sen, and K. Malmedal, “Optimum sizing and placement of distributed and renewable energy sources in electric power distribution systems,” *IEEE Transactions on Industry Applications*, vol. 49, no. 6, pp. 2741–2752, 2013.

[81] M. Khorasany, Y. Mishra, and G. Ledwich, “Two-step market clearing for local energy trading in feeder-based markets,” *The Journal of Engineering*, vol. 2019, no. 18, pp. 4775–4779, 2019.

[82] M. D. Ilic, R. Jaddivada, and M. Korpas, “Interactive protocols for distributed energy resource management systems (derms),” *IET Generation, Transmission Distribution*, vol. 14, no. 11, pp. 2065–2081, 2020.

[83] N. Blaauwbroek, P. H. Nguyen, M. J. Konsman, H. Shi, R. I. G. Kamphuis, and W. L. Kling, “Decentralized resource allocation and load scheduling for multicommodity smart energy systems,” *IEEE Transactions on Sustainable Energy*, vol. 6, no. 4, pp. 1506–1514, 2015.

[84] B. Liang, W. Liu, L. Sun, Z. He, and B. Hou, “An aggregated model for energy management considering crowdsourcing behaviors of distributed energy resources,” *IEEE Access*, vol. 7, pp. 145757–145766, 2019.

[85] L. Bai, J. Wang, C. Wang, C. Chen, and F. Li, “Distribution locational marginal pricing (dlmp) for congestion management and voltage support,” *IEEE Transactions on Power Systems*, vol. 33, no. 4, pp. 4061–4073, 2018.

[86] A. P. S. Meliopoulos, E. Polymeneas, Z. Tan, R. Huang, and D. Zhao, “Advanced distribution management system,” *IEEE Transactions on Smart Grid*, vol. 4, no. 4, pp. 2109–2117, 2013.

[87] K. Dehghanpour, Z. Wang, J. Wang, Y. Yuan, and F. Bu, “A survey on state estimation techniques and challenges in smart distribution systems,” *IEEE Transactions on Smart Grid*, vol. 10, no. 2, pp. 2312–2322, 2019.

[88] N. D. Popović, D. S. Popović, and I. Seskar, “A novel cloud-based advanced distribution management system solution,” *IEEE Transactions on Industrial Informatics*, vol. 14, no. 8, pp. 3469–3476, 2018.

[89] J. Giri, "Proactive management of the future grid," *IEEE Power and Energy Technology Systems Journal*, vol. 2, pp. 43–52, June 2015.

[90] A. J. D. Rathnayaka, V. M. Potdar, T. Dillon, O. Hussain, and S. Kuruppu, "Goal-oriented prosumer community groups for the smart grid," *IEEE Technology and Society Magazine*, vol. 33, no. 1, pp. 41–48, 2014.

[91] R. Dashti and S. Afsharnia, "Decisions, decisions: An asset management—based distribution system framework," *IEEE Power and Energy Magazine*, vol. 12, pp. 96–108, May 2014.

[92] G. Schonwalder, "Power to the people?: What it means to the changing energy landscape [in my view]," *IEEE Power and Energy Magazine*, vol. 16, pp. 76–72, Jan 2018.

[93] J. Lin, C. Wan, Y. Song, R. Huang, X. Chen, W. Guo, Y. Zong, and Y. Shi, "Situation awareness of active distribution network: Roadmap, technologies, and bottlenecks," *CSEE Journal of Power and Energy Systems*, vol. 2, pp. 35–42, Sep. 2016.

[94] J. Giri, "Proactive management of the future grid," *IEEE Power and Energy Technology Systems Journal*, vol. 2, pp. 43–52, June 2015.

[95] M. H. K. Tushar and C. Assi, "Volt-var control through joint optimization of capacitor bank switching, renewable energy, and home appliances," *IEEE Transactions on Smart Grid*, vol. 9, no. 5, pp. 4077–4086, 2018.

[96] J. Ospina, N. Gupta, A. Newaz, M. Harper, M. O. Faruque, E. G. Collins, R. Meeker, and G. Lofman, "Sampling-based model predictive control of pv-integrated energy storage system considering power generation forecast and real-time price," *IEEE Power and Energy Technology Systems Journal*, vol. 6, no. 4, pp. 195–207, 2019.

[97] F. Li, J. W. Marangon-Lima, H. Rudnick, L. M. Marangon-Lima, N. P. Padhy, G. Brunekreeft, J. Reneses, and C. Kang, "Distribution pricing: Are we ready for the smart grid?," *IEEE Power and Energy Magazine*, vol. 13, pp. 76–86, July 2015.

[98] F. Rahimi and A. Ipakchi, "Using a transactive energy framework: Providing grid services from smart buildings," *IEEE Electrification Magazine*, vol. 4, no. 4, pp. 23–29, 2016.

[99] D. Forfia, M. Knight, and R. Melton, "The view from the top of the mountain: Building a community of practice with the gridwise transactive energy framework," *IEEE Power and Energy Magazine*, vol. 14, pp. 25–33, May 2016.

[100] A. Khazaee, H. H. Safa, M. Ghasempour, and M. K. Moghaddam, "Experience of ami system implementation in mashhad: the green project of faham," *CIRED - Open Access Proceedings Journal*, vol. 2017, no. 1, pp. 2752–2755, 2017.

[101] S. S. Osterholt, "Aep ohio: Working to build a smarter grid," *IEEE Power and Energy Magazine*, vol. 14, pp. 22–26, Sep. 2016.

[102] N. D. Popović, D. S. Popović, and I. Seskar, "A novel cloud-based advanced distribution management system solution," *IEEE Transactions on Industrial Informatics*, vol. 14, pp. 3469–3476, Aug 2018.

[103] F. Bouhafs, M. Mackay, and M. Merabti, "Links to the future: Communication requirements and challenges in the smart grid," *IEEE Power and Energy Magazine*, vol. 10, pp. 24–32, Jan 2012.

[104] C. Mouradian, D. Naboulsi, S. Yangui, R. H. Glitho, M. J. Morrow, and P. A. Polakos, "A comprehensive survey on fog computing: State-of-the-art and research challenges," *IEEE Communications Surveys Tutorials*, vol. 20, pp. 416–464, Firstquarter 2018.

[105] P. Basanta-Val, N. C. Audsley, A. J. Wellings, I. Gray, and N. Fernández-García, "Architecting time-critical big-data systems," *IEEE Transactions on Big Data*, vol. 2, pp. 310–324, Dec 2016.

[106] P. Basanta-Val, "An efficient industrial big-data engine," *IEEE Transactions on Industrial Informatics*, vol. 14, pp. 1361–1369, April 2018.

[107] L. Gu, D. Zeng, P. Li, and S. Guo, "Cost minimization for big data processing in geo-distributed data centers," *IEEE Transactions on Emerging Topics in Computing*, vol. 2, pp. 314–323, Sep. 2014.

[108] Pecan Street, ""energy data of pecan street"." [Online]. Available from: https://www.pecanstreet.org/dataport/access/, 2018. Accessed 29 June 2019.

[109] K. Kok and S. Widergren, "A society of devices: Integrating intelligent distributed resources with transactive energy," *IEEE Power and Energy Magazine*, vol. 14, pp. 34–45, May 2016.

[110] K. Kotilainen, P. Järventausta, and P. Aalto, "Prosumer centric co-creation in smart grid innovation ecosystem," in *2016 IEEE Innovative Smart Grid Technologies - Asia (ISGT-Asia)*, pp. 884–889, Nov 2016.

[111] K. Kotilainen, M. Sommarberg, P. Järventausta, and P. Aalto, "Prosumer centric digital energy ecosystem framework," in *Proceedings of the 8th International Conference on Management of Digital EcoSystems*, pp. 47–51, ACM, 2016.

[112] M. Kubli, M. Loock, and R. Wüstenhagen, "The flexible prosumer: Measuring the willingness to co-create distributed flexibility," *Energy policy*, vol. 114, pp. 540–548, 2018.

[113] K. Kotilainen, S. J. Mäkinen, P. Järvetausta, A. Rautiainen, and J. Markkula, "The role of residential prosumers initiating the energy innovation ecosystem to future flexible energy system," in *2016 13th International Conference on the European Energy Market (EEM)*, pp. 1–5, June 2016.

[114] Y. Hamdaoui and A. Maach, "Dynamic balancing of powers in islanded microgrid using distributed energy resources and prosumers for efficient energy management," in *2017 IEEE International Conference on Smart Energy Grid Engineering (SEGE)*, pp. 155–161, Aug 2017.

[115] J. Pitt, A. Diaconescu, and A. Bourazeri, "Democratisation of the smartgrid and the active participation of prosumers," in *2017 IEEE 26th International Symposium on Industrial Electronics (ISIE)*, pp. 1707–1714, June 2017.

[116] A. J. D. Rathnayaka, V. M. Potdar, T. Dillon, O. Hussain, and S. Kuruppu, "Goal-oriented prosumer community groups for the smart grid," *IEEE Technology and Society Magazine*, vol. 33, pp. 41–48, Spring 2014.

[117] A. J. D. Rathnayaka, V. M. Potdar, and S. J. Kuruppu, "An innovative approach to manage prosumers in smart grid," in *2011 World Congress on Sustainable Technologies (WCST)*, pp. 141–146, Nov 2011.

[118] K. Fabisz, A. Filipowska, T. Hossa, and R. Hofman, "Profiling of prosumers for the needs of energy demand estimation in microgrids," in *2014 5th International Renewable Energy Congress (IREC)*, pp. 1–6, March 2014.

[119] A. J. D. Rathnayaka, V. M. Potdar, T. S. Dillon, O. K. Hussain, and E. Chang, "A methodology to find influential prosumers in prosumer community groups," *IEEE Transactions on Industrial Informatics*, vol. 10, pp. 706–713, Feb 2014.

[120] Y. Parag, "Beyond energy efficiency: A 'prosumer market'as an integrated platform for consumer engagement with the energy system," *Eur. Counc. Energy Effic. Econ. Summer Study*, vol. 1, pp. 15–23, 2015.

[121] Y. Parag and B. K. Sovacool, "Electricity market design for the prosumer era," *Nature energy*, vol. 1, no. 4, p. 16032, 2016.

[122] S. Choi and S. Min, "Optimal scheduling and operation of the ess for prosumer market environment in grid-connected industrial complex," *IEEE Transactions on Industry Applications*, vol. 54, pp. 1949–1957, May 2018.

[123] N. Gensollen, V. Gauthier, M. Becker, and M. Marot, "Stability and performance of coalitions of prosumers through diversification in the smart grid," *IEEE Transactions on Smart Grid*, vol. 9, pp. 963–970, March 2018.

[124] O. Ellabban and H. Abu-Rub, "Smart grid customers' acceptance and engagement: an overview," *Renewable and Sustainable Energy Reviews*, vol. 65, pp. 1285–1298, Nov 2016.

[125] A. Moreno-Munoz, F. Bellido-Outeirino, P. Siano, and M. Gomez-Nieto, "Mobile social media for smart grids customer engagement: Emerging trends and challenges," *Renewable and Sustainable Energy Reviews*, vol. 53, pp. 1611–1616, Jan 2016.

[126] C. Büscher and P. Sumpf, ""trust" and "confidence" as socio-technical problems in the transformation of energy systems," *Energy, Sustainability and Society*, vol. 5, p. 34, Dec 2015.

[127] S. Teufel and B. Teufel, "Crowd energy information security culture - security guidelines for smart environments," in *2015 IEEE International Conference on Smart City/SocialCom/SustainCom (SmartCity)*, pp. 123–128, Dec 2015.

[128] S. Teufel and B. Teufel, "The crowd energy concept," *Journal of electronic science and technology*, vol. 12, pp. 263–269, Sept 2014.

[129] X. Cheng, R. Zhang, and L. Yang, "Consumer-centered energy system for electric vehicles and the smart grid," *IEEE Intelligent Systems*, vol. 31, pp. 97–101, May 2016.

[130] Y. Cai, T. Huang, E. Bompard, Y. Cao, and Y. Li, "Self-sustainable community of electricity prosumers in the emerging distribution system," *IEEE Transactions on Smart Grid*, vol. 8, pp. 2207–2216, Sep. 2017.

[131] A. Nowak, A. Rychwalska, and J. Szamrej, "Social, psychological and technological determinants of energy use," *IEEE Technology and Society Magazine*, vol. 33, pp. 42–47, Fall 2014.

[132] P. Shamsi, H. Xie, A. Longe, and J. Joo, "Economic dispatch for an agent-based community microgrid," *IEEE Transactions on Smart Grid*, vol. 7, pp. 2317–2324, Sep. 2016.

[133] G. Prinsloo, A. Mammoli, and R. Dobson, "Participatory smartgrid control and transactive energy management in community shared solar cogeneration systems for isolated rural villages," in *2016 IEEE Global Humanitarian Technology Conference (GHTC)*, pp. 352–359, Oct 2016.

[134] A. Zibelmen, "Reving up the energy vision in new york: Seizing the opportunity to create a cleaner, more resilient, and affordable energy system," *IEEE Power and Energy Magazine*, vol. 14, pp. 18–24, May 2016.

[135] K. P. Kathryne Cleary and K. Rennert, *Clean Energy Standards*, vol. Issue Brief 19-01 of *RFF research and policy engagement*. Washington, D.C, United States: Resources for the Future, 2019-01.

[136] Gopal K. Sarangi, "Green energy finance in india: Challenges and solutions," 2018.

[137] STATE OF NEW YORK PUBLIC SERVICE COMMISSION, "In the matter of regulation and oversight of distributed energy resource providers and products," 2017.

[138] Eric O'Shaughnessy, Jenny Heeter, Julien Gattaciecca, Jenny Sauer, Kelly Trumbull, and Emily Chen, "Community choice aggregation: Challenges, opportunities, and impacts on renewable energy markets," 2019.

[139] STATE OF NEW YORK DEPARTMENT OF PUBLIC SERVICE, "Staff whitepaper on future community distributed generation compensation," 2018.

[140] Public Service Commission of Maryland, "Report on the status of net energy metering in the state of maryland," 2018.

[141] Orange and Roackland Utilities, Inc., "2018 distribution system implementation plan," 2018.

[142] Galen L. Barbose, Charles A. Goldman, Ian M. Hoffman, Megan Billingsley, "The future of utility customer-funded energy efficiency programs in the united states: Projected spending and savings to 2025," 2013.

[143] National Environment Agency, "Application guidelines for the assessment and accreditation of energy services companies under the esco accreditation scheme," 2018.

[144] European Parliamentary Research Service, "Ethical aspects of cyber-physical systems," 2016.

[145] U.S. Department of Energy, "Customer acceptance, retention, and response to time-based rates from the consumer behavior studies," 2016.

[146] J. Park, H. Lee, and D. Kim, "Challenges for utility with energy prosumer in korea," *CIRED - Open Access Proceedings Journal*, vol. 2017, no. 1, pp. 2632–2634, 2017.

[147] R. K. Naha, S. Garg, D. Georgakopoulos, P. P. Jayaraman, L. Gao, Y. Xiang, and R. Ranjan, "Fog computing: Survey of trends, architectures, requirements, and research directions," *IEEE Access*, vol. 6, pp. 47980–48009, 2018.

[148] K. Yeow, A. Gani, R. W. Ahmad, J. J. P. C. Rodrigues, and K. Ko, "Decentralized consensus for edge-centric internet of things: A review, taxonomy, and research issues," *IEEE Access*, vol. 6, pp. 1513–1524, 2018.

[149] Y. Guan, J. Shao, G. Wei, and M. Xie, "Data security and privacy in fog computing," *IEEE Network*, vol. 32, pp. 106–111, Sep. 2018.

[150] S. N. Shirazi, A. Gouglidis, A. Farshad, and D. Hutchison, "The extended cloud: Review and analysis of mobile edge computing and fog from a security and resilience perspective," *IEEE Journal on Selected Areas in Communications*, vol. 35, pp. 2586–2595, Nov 2017.

[151] B. Nordman, K. Christensen, and A. Meier, "Think globally, distribute power locally: The promise of nanogrids," *Computer*, vol. 45, pp. 89–91, Sep. 2012.

[152] I. Cvetkovic, *Modeling, Analysis and Design of Renewable Energy Nanogrid Systems*. PhD thesis, Virginia Tech, 2010.

[153] J. Kubalik, P. Tichy, R. Sindelar, and R. J. Staron, "Clustering methods for agent distribution optimization," *IEEE Transactions on Systems, Man, and Cybernetics, Part C (Applications and Reviews)*, vol. 40, pp. 78–86, Jan 2010.

[154] Y. Wang, Q. Chen, T. Hong, and C. Kang, "Review of smart meter data analytics: Applications, methodologies, and challenges," *IEEE Transactions on Smart Grid*, vol. 10, pp. 3125–3148, May 2019.

[155] S. Chen, H. Wen, J. Wu, W. Lei, W. Hou, W. Liu, A. Xu, and Y. Jiang, "Internet of things based smart grids supported by intelligent edge computing," *IEEE Access*, vol. 7, pp. 74089–74102, 2019.

[156] H. El-Sayed, S. Sankar, M. Prasad, D. Puthal, A. Gupta, M. Mohanty, and C. Lin, "Edge of things: The big picture on the integration of edge, iot and the cloud in a distributed computing environment," *IEEE Access*, vol. 6, pp. 1706–1717, 2018.

[157] J. Lloret, J. Tomas, A. Canovas, and L. Parra, "An integrated iot architecture for smart metering," *IEEE Communications Magazine*, vol. 54, pp. 50–57, December 2016.

[158] F. Ye, Y. Qian, and R. Q. Hu, *Big Data Analytics and Cloud Computing in the Smart Grid*. IEEE, 2017.

[159] J. Baek, Q. H. Vu, J. K. Liu, X. Huang, and Y. Xiang, "A secure cloud computing based framework for big data information management of smart grid," *IEEE Transactions on Cloud Computing*, vol. 3, pp. 233–244, April 2015.

[160] A. Ghosal and M. Conti, "Key management systems for smart grid advanced metering infrastructure: A survey," *IEEE Communications Surveys Tutorials*, pp. 1–1, 2019.

[161] Energy Systems Division, "Expand device capability with multiprotocol bluetooth and zigbee connectivity." [Online]. Available from: https://www.silabs.com/whitepapers/expand-device-capability-with-multiprotocol-bluetooth-and-zigbee-connectivity, April 2018. Accessed 29 Jan 2019.

[162] Y. Li, X. Huang, and S. Wang, "Multiple protocols interworking with open connectivity foundation in fog networks," *IEEE Access*, vol. 7, pp. 60764–60773, 2019.

[163] F. Aalamifar and L. Lampe, "Cost-efficient qos-aware data acquisition point placement for advanced metering infrastructure," *IEEE Transactions on Communications*, vol. 66, pp. 6260–6274, Dec 2018.

[164] F. Aalamifar and L. Lampe, "Optimized data acquisition point placement for an advanced metering infrastructure based on power line communication technology," *IEEE Access*, vol. 6, pp. 45347–45358, 2018.

[165] K. S. Swarup and S. Yamashiro, "Unit commitment solution methodology using genetic algorithm," *IEEE Transactions on Power Systems*, vol. 17, pp. 87–91, Feb 2002.

[166] B. M. S. Muhammad Ramadan, T. Logenthiran, R. T. Naayagi, and C. Su, "Hybridization of genetic algorithm and priority list to solve economic dispatch problems," in *2016 IEEE Region 10 Conference (TENCON)*, pp. 1467–1470, Nov 2016.

[167] B. M. S. M. Ramadan, T. Logenthiran, R. T. Naayagi, and C. Su, "Accelerated lambda iteration method for solving economic dispatch with transmission line losses management," in *2016 IEEE Innovative Smart Grid Technologies - Asia (ISGT-Asia)*, pp. 138–143, Nov 2016.

[168] J. Meus, K. Poncelet, and E. Delarue, "Applicability of a clustered unit commitment model in power system modeling," *IEEE Transactions on Power Systems*, vol. 33, pp. 2195–2204, March 2018.

[169] P. Pourbeik, S. E. Williams, J. Weber, J. Sanchez-Gasca, J. Senthil, S. Huang, and K. Bolton, "Modeling and dynamic behavior of battery energy storage: A simple model for large-scale time-domain stability studies," *IEEE Electrification Magazine*, vol. 3, pp. 47–51, Sep. 2015.

[170] J. Zhang, S. Ci, H. Sharif, and M. Alahmad, "Modeling discharge behavior of multicell battery," *IEEE Transactions on Energy Conversion*, vol. 25, pp. 1133–1141, Dec 2010.

[171] R. Torabi, A. Gomes, and F. Morgado-Dias, “The duck curve characteristic and storage requirements for greening the island of porto santo,” in *2018 Energy and Sustainability for Small Developing Economies (ES2DE)*, pp. 1–7, July 2018.

[172] Energy Market Authority Singapore, “Price information.” [Online]. Available from: https://www.emcsg.com/marketdata/priceinformation, Aug 2019. Accessed 29 Jan 2019.

[173] L. Cheng and T. Yu, “Game-theoretic approaches applied to transactions in the open and ever-growing electricity markets from the perspective of power demand response: An overview,” *IEEE Access*, vol. 7, pp. 25727–25762, 2019.

[174] R. K. Varma and E. M. Siavashi, “Enhancement of solar farm connectivity with smart pv inverter pv-statcom,” *IEEE Transactions on Sustainable Energy*, vol. 10, pp. 1161–1171, July 2019.

[175] R. K. Varma and E. M. Siavashi, “Pv-statcom: A new smart inverter for voltage control in distribution systems,” *IEEE Transactions on Sustainable Energy*, vol. 9, pp. 1681–1691, Oct 2018.

[176] H. Han, X. Hou, J. Yang, J. Wu, M. Su, and J. M. Guerrero, “Review of power sharing control strategies for islanding operation of ac microgrids,” *IEEE Transactions on Smart Grid*, vol. 7, pp. 200–215, Jan 2016.

[177] A. Esmaeilian and M. Kezunovic, “Prevention of power grid blackouts using intentional islanding scheme,” *IEEE Transactions on Industry Applications*, vol. 53, pp. 622–629, Jan 2017.

[178] Y. Li, P. Zhang, W. Li, J. N. Debs, D. A. Ferrante, D. J. Kane, S. N. Woolard, R. Kalbfleisch, K. B. Bowes, and A. J. Kasznay, “Nondetection zone analytics for unintentional islanding in a distribution grid integrated with distributed energy resources,” *IEEE Transactions on Sustainable Energy*, vol. 10, pp. 214–225, Jan 2019.

[179] X. He, H. Geng, R. Li, and B. C. Pal, “Transient stability analysis and enhancement of renewable energy conversion system during lvrt,” *IEEE Transactions on Sustainable Energy*, pp. 1–1, 2019.

[180] H. Kong and B. Zhang, “A novel ferroresonance and single-phase earth fault recognition method based on correlation analysis,” in *2014 14th International Conference on Environment and Electrical Engineering*, pp. 426–430, May 2014.

[181] V. P. Singh, N. Kishor, and P. Samuel, “Distributed multi-agent system-based load frequency control for multi-area power system in smart grid,” *IEEE Transactions on Industrial Electronics*, vol. 64, pp. 5151–5160, June 2017.

[182] A. Nassaj and S. M. Shahrtash, “An accelerated preventive agent based scheme for postdisturbance voltage control and loss reduction,” *IEEE Transactions on Power Systems*, vol. 33, pp. 4508–4518, July 2018.

[183] F. D. Kanellos, E. M. Volanis, and N. D. Hatziargyriou, “Power management method for large ports with multi-agent systems,” *IEEE Transactions on Smart Grid*, vol. 10, pp. 1259–1268, March 2019.

[184] W. Kang, M. Chen, B. Li, F. Chen, W. Lai, H. Lin, and B. Zhao, "Distributed reactive power control and soc sharing method for battery energy storage system in microgrids," *IEEE Access*, vol. 7, pp. 60707–60720, 2019.

[185] A. Dorri, S. S. Kanhere, and R. Jurdak, "Multi-agent systems: A survey," *IEEE Access*, vol. 6, pp. 28573–28593, 2018.

[186] K. P. Birman, Jie Chen, E. M. Hopkinson, R. J. Thomas, J. S. Thorp, R. Van Renesse, and W. Vogels, "dcovercoming communications challenges in software for monitoring and controlling power systems," *Proceedings of the IEEE*, vol. 93, no. 5, pp. 1028–1041, 2005.

[187] A. N. Bikos and N. Sklavos, "Lte/sae security issues on 4g wireless networks," *IEEE Security Privacy*, vol. 11, no. 2, pp. 55–62, 2013.

[188] S. Bera, S. Misra, and J. J. P. C. Rodrigues, "Cloud computing applications for smart grid: A survey," *IEEE Transactions on Parallel and Distributed Systems*, vol. 26, no. 5, pp. 1477–1494, 2015.

[189] J. Li, Z. Bao, and Z. Li, "Modeling demand response capability by internet data centers processing batch computing jobs," *IEEE Transactions on Smart Grid*, vol. 6, no. 2, pp. 737–747, 2015.

[190] X. Li, J. Wan, H. Dai, M. Imran, M. Xia, and A. Celesti, "A hybrid computing solution and resource scheduling strategy for edge computing in smart manufacturing," *IEEE Transactions on Industrial Informatics*, vol. 15, no. 7, pp. 4225–4234, 2019.

[191] J. Ren, Y. Guo, D. Zhang, Q. Liu, and Y. Zhang, "Distributed and efficient object detection in edge computing: Challenges and solutions," *IEEE Network*, vol. 32, pp. 137–143, November 2018.

[192] Z. M. Fadlullah, F. Tang, B. Mao, N. Kato, O. Akashi, T. Inoue, and K. Mizutani, "State-of-the-art deep learning: Evolving machine intelligence toward tomorrow's intelligent network traffic control systems," *IEEE Communications Surveys Tutorials*, vol. 19, pp. 2432–2455, Fourthquarter 2017.

[193] N. Kato, Z. M. Fadlullah, B. Mao, F. Tang, O. Akashi, T. Inoue, and K. Mizutani, "The deep learning vision for heterogeneous network traffic control: Proposal, challenges, and future perspective," *IEEE Wireless Communications*, vol. 24, pp. 146–153, June 2017.

[194] T. Suganuma, T. Oide, S. Kitagami, K. Sugawara, and N. Shiratori, "Multiagent-based flexible edge computing architecture for iot," *IEEE Network*, vol. 32, pp. 16–23, Jan 2018.

[195] T. Oide, T. Abe, and T. Suganuma, "Cosap: Contract-oriented sensor-based application platform," *IEEE Access*, vol. 5, pp. 8261–8275, 2017.

[196] B. Predić, Z. Yan, J. Eberle, D. Stojanovic, and K. Aberer, "Exposuresense: Integrating daily activities with air quality using mobile participatory sensing," in *2013 IEEE International Conference on Pervasive Computing and Communications Workshops (PERCOM Workshops)*, pp. 303–305, March 2013.

[197] D. Loghin, L. Ramapantulu, and Y. M. Teo, "Towards analyzing the performance of hybrid edge-cloud processing," in *2019 IEEE International Conference on Edge Computing (EDGE)*, pp. 87–94, 2019.

[198] X. Xu and M. Tang, "A new approach to the cloud-based heterogeneous mapreduce placement problem," *IEEE Transactions on Services Computing*, vol. 9, no. 6, pp. 862–871, 2016.

[199] M. Pau, E. Patti, L. Barbierato, A. Estebsari, E. Pons, F. Ponci, and A. Monti, "A cloud-based smart metering infrastructure for distribution grid services and automation," *Sustainable Energy, Grids and Networks*, vol. 15, pp. 14–25, 2018.

[200] D. Forfia, M. Knight, and R. Melton, "The view from the top of the mountain: Building a community of practice with the gridwise transactive energy framework," *IEEE Power and Energy Magazine*, vol. 14, pp. 25–33, May 2016.

[201] P. Palensky and D. Dietrich, "Demand side management: Demand response, intelligent energy systems, and smart loads," *IEEE Transactions on Industrial Informatics*, vol. 7, pp. 381–388, Aug 2011.

[202] W. Liu, J. Zhan, and C. Y. Chung, "A novel transactive energy control mechanism for collaborative networked microgrids," *IEEE Transactions on Power Systems*, vol. 34, pp. 2048–2060, May 2019.

[203] F. Rahimi, A. Ipakchi, and F. Fletcher, "The changing electrical landscape: End-to-end power system operation under the transactive energy paradigm," *IEEE Power and Energy Magazine*, vol. 14, pp. 52–62, May 2016.

[204] I. Lorscheid, "Learning agents for human complex systems," in *2014 IEEE 38th International Computer Software and Applications Conference Workshops*, pp. 432–437, July 2014.

[205] R. S. Sutton and A. G. Barto, "Reinforcement learning: An introduction," *IEEE Transactions on Neural Networks*, vol. 9, pp. 1054–1054, Sep. 1998.

[206] Y. Liang, W. Wei, and C. Wang, "A generalized nash equilibrium approach for autonomous energy management of residential energy hubs," *IEEE Transactions on Industrial Informatics*, pp. 1–1, 2019.

[207] J. Xu, Z. Hou, W. Wang, B. Xu, K. Zhang, and K. Chen, "Feedback deep deterministic policy gradient with fuzzy reward for robotic multiple peg-in-hole assembly tasks," *IEEE Transactions on Industrial Informatics*, vol. 15, pp. 1658–1667, March 2019.

[208] C. Szepesvari, *Algorithms for Reinforcement Learning*. Morgan & Claypool, 2010.

[209] D. P. Bertsekas, "Value and policy iterations in optimal control and adaptive dynamic programming," *IEEE Transactions on Neural Networks and Learning Systems*, vol. 28, pp. 500–509, March 2017.

[210] D. P. Bertsekas, "Value and policy iterations in optimal control and adaptive dynamic programming," *IEEE Transactions on Neural Networks and Learning Systems*, vol. 28, pp. 500–509, March 2017.

[211] S. Paul and L. Vig, "Deterministic policy gradient based robotic path planning with continuous action spaces," in *2017 IEEE International Conference on Computer Vision Workshops (ICCVW)*, pp. 725–733, Oct 2017.

[212] E. İlhan and A. . Etaner-Uyar, "Monte carlo tree search with temporal-difference learning for general video game playing," in *2017 IEEE Conference on Computational Intelligence and Games (CIG)*, pp. 317–324, Aug 2017.

[213] I. Grondman, L. Busoniu, G. A. D. Lopes, and R. Babuska, "A survey of actor-critic reinforcement learning: Standard and natural policy gradients," *IEEE Transactions on Systems, Man, and Cybernetics, Part C (Applications and Reviews)*, vol. 42, pp. 1291–1307, Nov 2012.

[214] Z. Wang, H. Li, and C. Chen, "Incremental reinforcement learning in continuous spaces via policy relaxation and importance weighting," *IEEE Transactions on Neural Networks and Learning Systems*, pp. 1–14, 2019.

[215] K. Arulkumaran, M. P. Deisenroth, M. Brundage, and A. A. Bharath, "Deep reinforcement learning: A brief survey," *IEEE Signal Processing Magazine*, vol. 34, pp. 26–38, Nov 2017.

[216] D. Silver, G. Lever, N. Heess, T. Degris, D. Wierstra, and M. Riedmiller, "Deterministic policy gradient algorithms," 2014.

[217] L. Lv, S. Zhang, D. Ding, and Y. Wang, "Path planning via an improved dqn-based learning policy," *IEEE Access*, vol. 7, pp. 67319–67330, 2019.

[218] H. Qie, D. Shi, T. Shen, X. Xu, Y. Li, and L. Wang, "Joint optimization of multi-uav target assignment and path planning based on multi-agent reinforcement learning," *IEEE Access*, pp. 1–1, 2019.

[219] Y. Grandvalet and Y. Bengio, "Entropy regularization," *Semi-supervised learning*, pp. 151–168, 2006.

[220] R. Nishant, T. S. H. Teo, and M. Goh, "Energy efficiency benefits: Is technophilic optimism justified?," *IEEE Transactions on Engineering Management*, vol. 61, no. 3, pp. 476–487, 2014.

[221] M. Alahmad, M. F. Zulfiqar, H. Hasna, H. Sharif, E. Sordiashie, and N. A. Aljuhaishi, "Green and sustainable technologies for the built environment," in *2011 Developments in E-systems Engineering*, pp. 521–526, 2011.

[222] A. Guerrisi, M. Martino, and M. Tartaglia, "Energy saving in social housing: An innovative ict service to improve the occupant behaviour," in *2012 International Conference on Renewable Energy Research and Applications (ICRERA)*, pp. 1–6, 2012.

[223] A. Domijan, O. Hancock, and C. Maytrott, "A study and evaluation of power electronic based adjustable speed motor drives for air conditioners and heat pumps with an example utility case study of the florida power and light company," *IEEE Transactions on Energy Conversion*, vol. 7, no. 3, pp. 396–404, 1992.

[224] Dua, Dheeru and Graff, Casey, “"UCI machine learning repository-individual household electric power consumption data set".” [Online]. Available from: https://archive.ics.uci.edu/ml/datasets/individual+household+electric+power+consumption, 2017. Accessed 29 June 2019.

[225] A. Kumar, A. R. Singh, Y. Deng, X. He, P. Kumar, and R. C. Bansal, “A novel methodological framework for the design of sustainable rural microgrid for developing nations,” *IEEE Access*, vol. 6, pp. 24925–24951, 2018.

[226] T. Morstyn, B. Hredzak, and V. G. Agelidis, “Control strategies for microgrids with distributed energy storage systems: An overview,” *IEEE Transactions on Smart Grid*, vol. 9, pp. 3652–3666, July 2018.

[227] A. Habib, A. Arshad, and R. Khan, “Distributed renewable energy under the guidance of price autonomous operation technology,” *Smart Grid and Renewable Energy*, vol. 8, no. 10, p. 305, 2017.

[228] P. Almeida, L. Kane, M. Collins, C. Breaden, E. Davidson, and G. Ault, “Implementing optimisation functionality on network management platforms for new dso business models,” *CIRED-Open Access Proceedings Journal*, vol. 2017, no. 1, pp. 2779–2782, 2017.

[229] A. Saint-Pierre and P. Mancarella, “Active distribution system management: A dual-horizon scheduling framework for dso/tso interface under uncertainty,” *IEEE Transactions on Smart Grid*, vol. 8, pp. 2186–2197, Sep. 2017.

[230] Y. G. Yohanis, J. D. Mondol, A. Wright, and B. Norton, “Real-life energy use in the uk: How occupancy and dwelling characteristics affect domestic electricity use,” *Energy and Buildings*, vol. 40, no. 6, pp. 1053–1059, 2008.

[231] C. Palmborg, “Social habits and energy consumption in single-family homes,” *Energy*, vol. 11, no. 7, pp. 643–650, 1986.

[232] C. Mullaly, “Home energy use behaviour: a necessary component of successful local government home energy conservation (lghec) programs,” *Energy Policy*, vol. 26, no. 14, pp. 1041–1052, 1998.

[233] Y. T. Quek, W. L. Woo, and T. Logenthiran, “Dc equipment identification using k-means clustering and knn classification techniques,” in *2016 IEEE Region 10 Conference (TENCON)*, pp. 777–780, Nov 2016.

[234] I. Ahmad, M. Basheri, M. J. Iqbal, and A. Rahim, “Performance comparison of support vector machine, random forest, and extreme learning machine for intrusion detection,” *IEEE Access*, vol. 6, pp. 33789–33795, 2018.

[235] Y. Jiang, Y. Yang, Q. Wu, X. Chi, and J. Miao, “Research on predicting the short-term output of photovoltaic (pv) based on extreme learning machine model and improved similar day,” in *2019 IEEE Innovative Smart Grid Technologies - Asia (ISGT Asia)*, pp. 3691–3695, May 2019.

[236] T. Wong and N. Yang, "Dependency analysis of accuracy estimates in k-fold cross validation," *IEEE Transactions on Knowledge and Data Engineering*, vol. 29, pp. 2417–2427, Nov 2017.

[237] Y. Zhang, X. Han, B. Xu, L. Zhang, D. Sun, X. Miao, and J. Jiang, "Unit commitment considering demand response behavior based on utility maximization," in *2017 IEEE Conference on Energy Internet and Energy System Integration (EI2)*, pp. 1–6, Nov 2017.

[238] N. D. Doulamis, A. D. Doulamis, and E. Varvarigos, "Virtual associations of prosumers for smart energy networks under a renewable split market," *IEEE Transactions on Smart Grid*, vol. 9, pp. 6069–6083, Nov 2018.

[239] T. Georgitsioti, N. Pearsall, and I. Forbes, "Simplified levelised cost of the domestic photovoltaic energy in the uk: the importance of the feed-in tariff scheme," *IET Renewable Power Generation*, vol. 8, pp. 451–458, July 2014.

[240] B. Kim, Y. Zhang, M. van der Schaar, and J. Lee, "Dynamic pricing and energy consumption scheduling with reinforcement learning," *IEEE Transactions on Smart Grid*, vol. 7, pp. 2187–2198, Sep. 2016.

[241] John Fluet, MathWorks, "How to run matlab in the cloud with microsoft azure." [Online]. Available from: https://www.mathworks.com/videos/how-to-run-matlab-in-the-cloud-with-microsoft-azure-1542633563140.html, April 2019. Accessed 9 June 2019.

[242] John Fluet, MathWorks, "Github-matlab on microsoft azure." [Online]. Available from: https://github.com/mathworks-ref-arch/matlab-on-azure, April 2018. Accessed 9 June 2019.

[243] S. Grijalva and M. U. Tariq, "Prosumer-based smart grid architecture enables a flat, sustainable electricity industry," in *ISGT 2011*, pp. 1–6, Jan 2011.

[244] P. Tian, X. Xiao, K. Wang, and R. Ding, "A hierarchical energy management system based on hierarchical optimization for microgrid community economic operation," *IEEE Transactions on Smart Grid*, vol. 7, pp. 2230–2241, Sep. 2016.

[245] J. Shen, C. Jiang, Y. Liu, and X. Wang, "A microgrid energy management system and risk management under an electricity market environment," *IEEE Access*, vol. 4, pp. 2349–2356, 2016.

[246] D. Mcnair, D. Phelan, and L. Coleman, "Voices of experience: Insights into advanced distribution management systems," *US Department of Energy: Washington, DC, USA*, 2015.

[247] A. S. Dobakhshari and A. M. Ranjbar, "A wide-area scheme for power system fault location incorporating bad data detection," *IEEE Transactions on Power Delivery*, vol. 30, no. 2, pp. 800–808, 2015.

[248] E. Lee, C. Choi, and P. Kim, "Intelligent handover scheme for drone using fuzzy inference systems," *IEEE Access*, vol. 5, pp. 13712–13719, 2017.

[249] Y. W. Kerk, K. M. Tay, and C. P. Lim, "An analytical interval fuzzy inference system for risk evaluation and prioritization in failure mode and effect analysis," *IEEE Systems Journal*, vol. 11, no. 3, pp. 1589–1600, 2017.

[250] L. Wang, J. Burgett, J. Zuo, C. C. Xu, B. J. Billian, R. W. Conners, and Y. Liu, "Frequency disturbance recorder design and developments," in *2007 IEEE Power Engineering Society General Meeting*, pp. 1–7, June 2007.

[251] P. Jena and A. K. Pradhan, "Directional relaying during single-pole tripping using phase change in negative-sequence current," *IEEE Transactions on Power Delivery*, vol. 28, no. 3, pp. 1548–1557, 2013.

[252] Y. Li, "Singapore's building greenery: A strategy to respond to urban heat island effect," 2016.

[253] H. Jiang, J. J. Zhang, W. Gao, and Z. Wu, "Fault detection, identification, and location in smart grid based on data-driven computational methods," *IEEE Transactions on Smart Grid*, vol. 5, no. 6, pp. 2947–2956, 2014.

[254] M. Pignati, L. Zanni, P. Romano, R. Cherkaoui, and M. Paolone, "Fault detection and faulted line identification in active distribution networks using synchrophasors-based real-time state estimation," *IEEE Transactions on Power Delivery Pwrd*, vol. 32, no. EPFL-ARTICLE-218391, pp. 381–392, 2017.

[255] H. J. Ashtiani, H. Samet, and T. Ghanbari, "Simple current-based algorithm for directional relays," *IET Generation, Transmission & Distribution*, vol. 11, no. 17, pp. 4227–4237, 2017.

[256] H. Kobayashi and K. Takigawa, "Statistical evaluation of optimum islanding preventing method for utility interactive small scale dispersed pv systems," in *Proceedings of 1994 IEEE 1st World Conference on Photovoltaic Energy Conversion - WCPEC (A Joint Conference of PVSC, PVSEC and PSEC)*, vol. 1, pp. 1085–1088 vol.1, Dec 1994.

[257] P. Das, "Maximum power tracking based open circuit voltage method for pv system," *Energy Procedia*, vol. 90, pp. 2–13, 2016.

[258] D. Baimel, S. Tapuchi, Y. Levron, and J. Belikov, "Improved fractional open circuit voltage mppt methods for pv systems," *Electronics*, vol. 8, no. 3, p. 321, 2019.

[259] L. Hassaine and M. R. Bengourina, "Control technique for single phase inverter photovoltaic system connected to the grid," *Energy Reports*, vol. 6, pp. 200–208, 2020.

[260] S. M. Cherati, N. A. Azli, S. M. Ayob, and A. Mortezaei, "Design of a current mode pi controller for a single-phase pwm inverter," in *2011 IEEE Applied Power Electronics Colloquium (IAPEC)*, pp. 180–184, 2011.

[261] M. Zarif and M. Monfared, "Step-by-step design and tuning of voc control loops for grid connected rectifiers," *International Journal of Electrical Power & Energy Systems*, vol. 64, pp. 708–713, 2015.

[262] M. Liserre*, F. Blaabjerg, and A. Dell'Aquila, "Step-by-step design procedure for a grid-connected three-phase pwm voltage source converter," *International journal of electronics*, vol. 91, no. 8, pp. 445–460, 2004.

[263] M. M. Sahebi, E. A. Duki, M. Kia, A. Soroudi, and M. Ehsan, "Simultanous emergency demand response programming and unit commitment programming in comparison with interruptible load contracts," *IET Generation, Transmission Distribution*, vol. 6, no. 7, pp. 605–611, 2012.

[264] M. Mao, P. Jin, N. D. Hatziargyriou, and L. Chang, "Multiagent-based hybrid energy management system for microgrids," *IEEE Transactions on Sustainable Energy*, vol. 5, no. 3, pp. 938–946, 2014.